Hydroelementation of Elemental Phosphorus: Direct Routes to Monophosphines

Dissertation

Zur Erlangung des Doktorgrades der Naturwissenschaften

Dr. rer. nat.

an der Fakultät Chemie und Pharmazie der Universität Regensburg

vorgelegt von:

Jose Ricardo Cammarata Paredes

aus Barinas, Venezuela

Regensburg, Juni 2024

Der experimentelle Teil der vorliegenden Arbeit wurde in der Zeit zwischen Juni 2020 und Juni 2024 unter Anleitung von Prof. Dr. Robert Wolf am Institut für Anorganische Chemie der Universität Regensburg angefertigt.

Die Arbeit wurde angeleitet von:		Prof. Dr. Robert Wolf
Promotionsgesuch eingereicht am:		03.06.2024
Tag der mündlichen Prüfung:		01.08.2024
Promotionsausschuss:	Vorsitz	Apl. Prof. Dr. Rainer Müller
	Erstgutachter	Prof. Dr. Robert Wolf
	Zweitgutachter	Prof. Dr. Manfred Scheer
	Dritter Prüfer	Prof. Dr. Frank-Michael Matysik

A mis padres

Prologue

This doctoral thesis reports on the development of efficient methods for the preparation of industrially and academically relevant monophosphorus compounds directly from elemental phosphorus, *via* radical-mediated hydroelementation reactions. Chapter 1 provides an overview of key recent academic reports on the organofunctionalisation of white phosphorus (P_4), highlighting direct and catalytic transformations into P_1 compounds. Chapter 2 describes the hydrostannylation of P_4, a simple and effective 'one-pot' method for the synthesis of a wide range of organic and inorganic monophosphorus compounds directly from P_4, mediated by the classical radical reagent tri-*n*-butyltin hydride (Bu_3SnH). In addition, Chapter 2 also reports the facile and efficient recycling and ultimately even catalytic use of the organotin reagent, thereby avoiding the generation of significant Sn-containing waste. Chapter 3 describes the preparation of a variety of P_1 compounds directly from the bench-stable allotrope *red* phosphorus (P_{red}) following analogous hydrostannylation reactions. Chapter 4 provides comprehensive mechanistic insights into the hydrostannylation of P_4, obtained through a collaborative effort that combined DFT calculations and *in situ* ^{31}P NMR reaction monitoring. Chapter 5 describes experimental and computational studies of the reactivity of lighter and less toxic hydrogermane and hydrosilane homologues of organotin hydrides (R_3EH, E = Ge or Si) towards P_4, which could also be employed to directly transform P_4 into useful P_1 compounds, in a simple 'one-pot' fashion. Finally, Chapter 6 gives a summary of the results described in this thesis and provides a short outlook.

Table of Contents

1 Organofunctionalisation of Elemental Phosphorus: Recent Advances in Direct and Catalytic P–C Bond Formation

Abstract:

Organophosphorus compounds have a wide range of applications, including as pharmaceuticals, photoinitiators, flame retardants, and numerous others. However, these compounds are produced industrially through hazardous and wasteful multi-step processes starting from white phosphorus (P_4), which remains their sole industrial precursor. Recently, dedicated academic efforts have been made to develop strategies that could overcome such limitations. This chapter provides an overview of the key recent advances in the organofunctionalisation of P_4, with a particular focus on direct transformations into monophosphorus compounds, and relevant strategies that might facilitate the preparation of these compounds in a 'one-pot' manner.

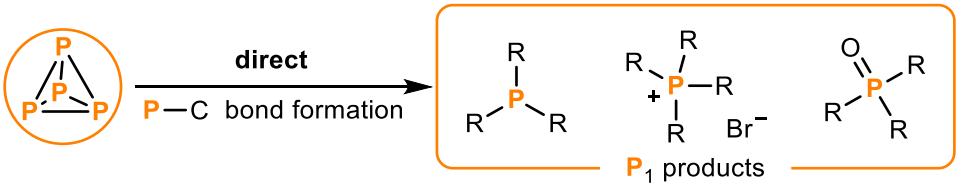

[a] Jose Cammarata wrote the chapter, which was proofread by Daniel J. Scott and Robert Wolf.

1.1 Introduction

Phosphorus is a ubiquitous element, present both within and around humanity. It plays a crucial role in nature as a key building block of DNA and of the cellular energy carrier ATP.[1–3] Additionally, phosphorus-containing compounds are present in a wide range of products, including fertilisers, insecticides, detergents, foodstuffs, battery electrolytes, and pharmaceuticals.[1–3] Elemental phosphorus can exist in three main allotropes: white, red and black phosphorus.[1,4,5] These are not found in nature, but instead phosphorus is widely encountered in its fully oxidised state (P^V) as phosphate minerals. White phosphorus, P_4, is by far the most reactive and industrially relevant allotrope of the element. Currently, its production is estimated to occur on a scale of above one million tons per year by reduction of phosphate rock (apatite, $Ca_{10}(PO_4)_6(X)_2$, X = OH, F, Cl, or Br). In this process a mixture of apatite, quartz sand (SiO_2) and coke (C) is heated at around 1500 °C in an electric arc furnace to yield the desired P_4 (Scheme 1, top).[1–4,6–8] The majority of the global supply of white phosphorus is utilised in the production of high-purity phosphoric acid, which is used in the manufacture of high-quality fertiliser, foodstuffs, beverages and other dairy products.[3,8] Additionally, P_4 also serves as the primary synthetic precursor for nearly all organophosphorus compounds worldwide. However, the industrial preparation of the valuable organophosphorus derivatives from P_4 typically involves a multistep process that begins with its oxidation using toxic chlorine gas (Cl_2) to produce the highly corrosive PCl_3, which can be further oxidized to generate similarly reactive (and hazardous) electrophiles such as PCl_5 and $POCl_3$. Subsequent treatment of these chlorinated intermediates with suitable nucleophiles leads to the formation of the desired compounds *via* chloride substitution (Scheme 1).[9,10] Notably, the final products usually do not contain the reactive P−Cl bonds formed in the first step, resulting in the generation of stoichiometric amounts of chlorinated waste.[10] An alternative route for the preparation of P_1 compounds is the acid-catalysed or alkali-mediated disproportionation of P_4 to generate PH_3,[11,12] which can be used as a starting material for the synthesis of alkylphosphines and phosphonium salts through the addition of alkenes or carbonyl compounds to the P−H bonds (Scheme 1).[9,12] However, this approach also suffers from similar limitations, as it is a multistep process that requires the manipulation of a flammable and highly toxic intermediate (PH_3) and generates stoichiometric by-products, such as phosphorus oxyacid derivatives during the disproportionation reaction, although it should be noted that these by-products have independent value of their own.[12]

Therefore, the development of new, simple, and environmentally benign strategies for the preparation of valuable organophosphorus compounds is highly desirable from both a safety and a sustainability standpoint. Some recent approaches have targeted alternative routes that could bypass the use of P_4 as the source of P atoms by using phosphate derivatives instead.[8,13–17] Nevertheless, P_4 currently remains as the only industrially viable precursor for the preparation of relevant P-containing compounds. Consequently, several research groups have been keen to

investigate the highly attractive direct transformations of P_4, which would avoid the hazards and inefficiencies associated with current industrial multi-step processes (Scheme 1, right). However, such reactions are extremely challenging, as they require the complete cleavage of the six P−P bonds of the P_4 tetrahedron and the formation of up to 16 new P−E bonds in a controlled and selective manner.[10] The term organophosphorus compounds (OPCs) encompasses a diverse range of phosphorus compounds bearing at least one organic substituent (e.g. phosphites, phosphoric acid esters). This chapter focuses on P_1 organophosphorus compounds bearing P−C bonds, which represent the main focus of the subsequent chapters of this thesis.

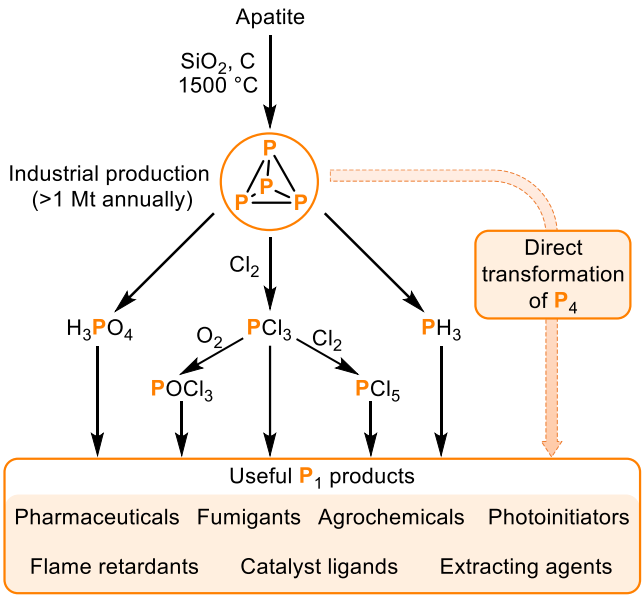

Scheme 1. Overview of current industrial processes for the production of useful monophosphorus compounds and the explored direct transformation of P_4 as an alternative route.

1.2 Direct transformation of P_4 into monophosphorus compounds

In order to facilitate the direct conversion of P_4 into useful monophosphorus compounds, a considerable amount of research effort has been directed towards elucidating the fundamental reactivity of P_4. Thus, many main group element species and transition-metal compounds have been studied for the activation and degradation of P_4, as highlighted in several useful and dedicated reviews.[6,18–24] This section will therefore only highlight a selection of the most significant and recent breakthroughs in the direct functionalisation of P_4 into P_1 organophosphorus compounds, as well as relevant related methodologies that could, in principle, be extended to this end in a 'one-pot' fashion.[25,26]

1.2.1 Nucleophilic functionalisation of P_4

Since the first report from Rauhut *et al.* in 1963 (Scheme 2),[27,28] the activation of P_4 with nucleophiles (e.g. organolithium reagents,[29] organozinc reagents,[30] carbenes[31])[20] has been well established. Nevertheless, such reactions have generally been associated with poor yields and selectivity.[20] Consequently, alternative approaches have been pursued to achieve nucleophilic transformations that could proceed in a more selective and productive manner.[20,29]

Particularly, the group of Zhang has demonstrated that treatment of P_4 with organo-*di*-lithium reagents (e.g. 1,4-dilithio-1,3-butadienes) promotes the selective construction of P−C bonds through cooperative nucleophilic attack of two C−Li bonds.[29,32] Recently, they reported the preparation of phosphafluorenyl lithium derivatives directly from P_4 in a one-pot reaction with different biphenyl dilithio reagents.[33] Notably, it was demonstrated that such compounds can serve as key intermediates in the preparation of a variety of organophosphorus compounds (Scheme 2.b).[29,33,34] However, these transformations suffer from very poor P atom economy, as at least 1.0 equivalent of P_4 is required in the reaction, but only one out of the four available P atoms is incorporated into the final products. The remaining three phosphorus atoms are lost as polyphosphide "LiP_3" by-products. Moreover, the need for a *di*-lithium reagent represents an inherent limitation to the scope of this methodology.

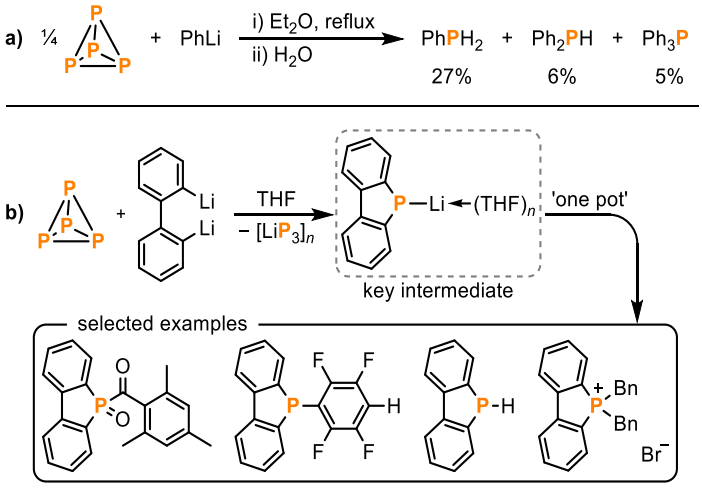

Scheme 2. Selected examples of the reaction of P_4 with organo-*mono*-lithium (a) and organo-*di*-lithium (b) reagents, the latter are used for the preparation of phosphafluorene derivatives directly from P_4.

1.2.2 Electrochemical oxidative cyanation of P_4

A further, example of the reactivity of P_4 with nucleophiles has been recently reported by the group of Liu.[35] The authors developed an efficient synthesis of the dicyanophosphide anion salt $[Li(dioxane)_x][P(CN)_2]$ by direct electrochemical activation of P_4 in the presence of hydrogen cyanide (HCN) and lithium cyanide (LiCN). Although the preparation of salts of the anion $[P(CN)_2]^-$ directly from P_4 was originally reported by Schmidpeter in 1985 (Scheme 3a),[36,37] the new method represents a significant advance over the previously reported synthetic routes, which suffer from very poor P atom economy, with only 1/16 of the P atoms previously being incorporated into the desired product. The electrochemical activation of P_4 was achieved upon its reaction in an undivided electrochemical cell at a constant 4 V potential with HCN and LiCN, both generated in situ to avoid the direct use of the toxic HCN gas, through the combination of Me_3SiCN and LiOH and elimination of $(Me_3Si)_2O$ (Scheme 3b, c). Subsequent work-up with dioxane afforded the salt $[Li(dioxane)_x][P(CN)_2]$ in excellent yields (92%, although this was reduced to 55% upon upscaling from 0.125 mmol to 5.0 mmol P_4). Furthermore, treatment of the

isolated salt with carbenes, organolithium and organodilithium reagents resulted in the formation of phosphinidene, cyclophosphane and phospholide derivatives in good to excellent yields (Scheme 3d).[35] It is important to note that while in principle feasible, the preparation of these academically relevant P_1 products was not investigated in a 'one-pot' manner, with the salt $Li(dioxane)_x][P(CN)_2]$ being the only product strictly prepared directly from P_4. Moreover, this methodology is limited by the use of highly toxic reagents, although it successfully demonstrates the potential of electrochemical strategies for the activation of P_4.[38]

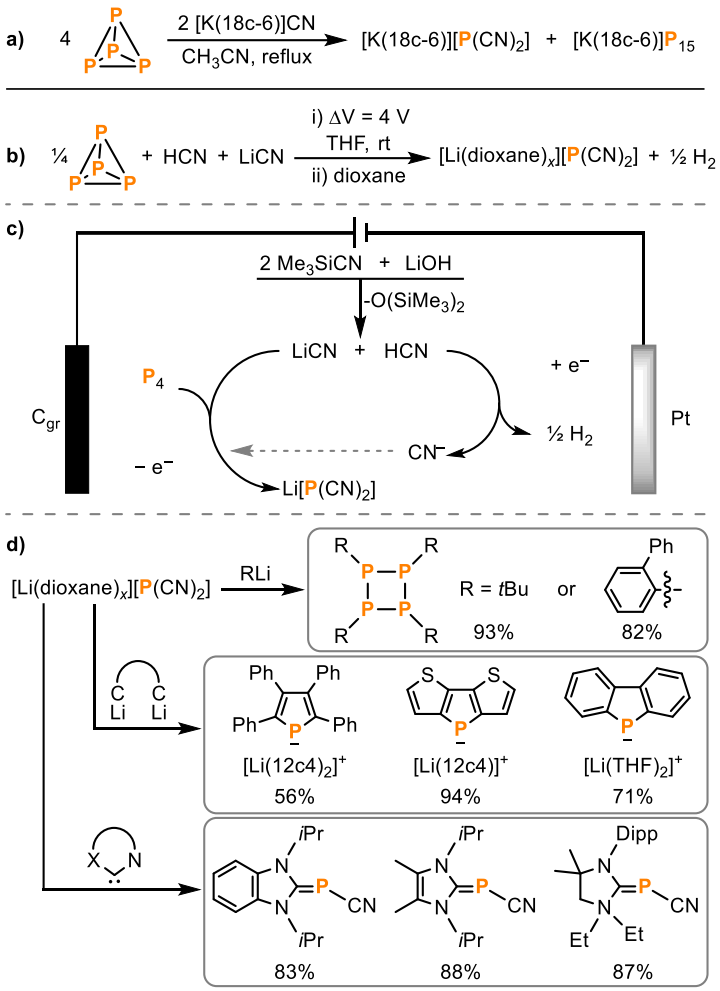

Scheme 3. a) Previous route for the direct synthesis of $[P(CN)_2]^-$ from P_4. b) Synthesis of $[Li(dioxane)_x][P(CN)_2]$ by electrochemical activation of P_4. c) Schematic of the electrochemical system. d) Products accessible from the isolated salt.

1.2.3 Functionalisation of P_4 by oxidative onioation

As part of the ongoing efforts to develop a viable and accessible alternative to the conventional PCl_3, the Weigand group reported in 2022 the preparation of P_1 transfer reagents directly from P_4 *via* a process they have termed "oxidative onioation".[39] This methodology involves the reaction of P_4 with a suitable nitrogen-centred Lewis base and an oxidising Lewis acid, such as DMAP (4-dimethylamiopyridinio) and $Ph_3As(OTf)_2$, respectively, resulting in the formation of the triflate salt $[(DMAP)_3P](OTf)_3$ in excellent yields. Analogous results were obtained from the reaction of P_4 with $[PhI(DMAP)_2](OTf)_2$, thus avoiding the use of the toxic arsenic-based reagent.

Moreover, the respective byproducts of these transformations Ph_3As and PhI can be isolated and regenerated to the initial oxidants. Remarkably, the base-stabilised P_1 transfer reagent $[(DMAP)_3P](OTf)_3$ can be treated with a broad range of nucleophiles, enabling the selective and quantitative formation of a variety of industrially relevant monophosphorus compounds (Scheme 4, right). Although the 'one-pot' preparation of such compounds was not investigated in this report, it seems feasible to extend this sequential reaction to a potential direct transformation. Furthermore, the authors demonstrated the potential for a closed synthetic cycle involving the efficient recovery and recycling of both the oxidants and the DMAP-based by-products (Scheme 4, left).[39] It should be noted, however, that this is currently a multi-step methodology that relies on the stoichiometric use of relatively elaborate reagents.

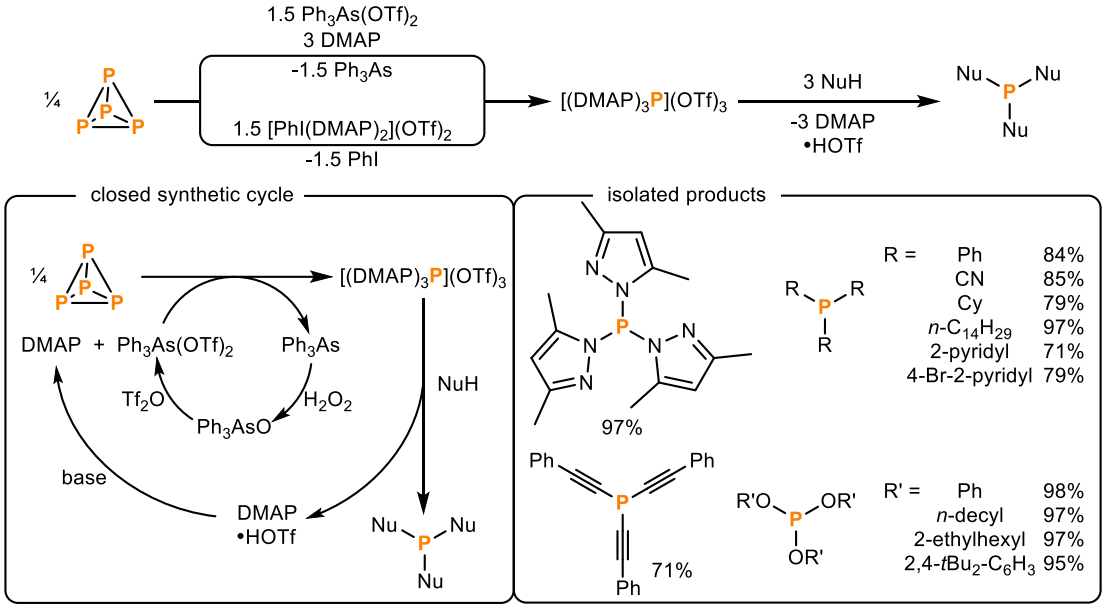

Scheme 4. Oxidation of P_4 into the P_1 transfer reagent $[(DMAP)_3P](OTf)_3$, and subsequent reaction with nucleophiles to afford P_1 products (right) in a potential closed synthetic cycle (left).

1.2.4 Transition-metal-mediated functionalisation of P_4 into P_1 compounds

Many efforts in academia have focused on stepwise, transition-metal-mediated transformations of P_4, where the molecule is first activated through metal coordination, and the coordinated P_n moiety is then reacted further with a suitable organic reagent.[6,18–24] Nevertheless, while the initial activation steps have been subjected to thorough investigation, examples of the subsequent functionalisation steps and release of the desired monophosphorus compounds remain scarce.[40,41] However, a recent report from the Scheer group illustrates this approach using the widely studied pentaphosphaferrocene $[Cp^*FeP_5]$ ($Cp^* = \eta^5\text{-}C_5Me_5$), first synthesised by Scherer in 1987,[42] as a mediator for the preparation of asymmetrically substituted tertiary phosphines.[43] The authors demonstrate that nucleophilic addition to the cyclo-P_5 ring upon reaction with an organolithium reagent RLi (R = Me, *t*Bu, Ph), followed by treatment of the resulting $[Cp^*Fe(\eta^4\text{-}P_5R)]^-$ species with an electrophile R′X (R′ = Me, *i*Pr; X = Br, I), leads to the selective formation of the 1,1-diorgano-substituted complex $[Cp^*Fe(\eta^4\text{-}P_5RR')]$. Subsequent addition of a second

organometallic nucleophile R″M (KBn, *n*BuLi, MeLi) releases the asymmetric phosphines RR′R″P (R ≠ R′ ≠R″), with the formation of the anionic *cyclo*-P_4 complex $[Cp^*FeP_4]^-$ as the metal-based byproduct (Scheme 5). Notably, this approach allows the preparation of phosphines with a variety of different substitution patterns. Moreover, the authors described the preparation of a representative phosphine (Me_2PBn) in 'one-pot' from $[Cp^*FeP_5]$ through the sequential addition of the relevant reagents, with no intermediate purification or solvent changes being necessary. Additionally, it was demonstrated that for this particular case, following the separation of the phosphine product by distillation, the starting material $[Cp^*FeP_5]$ could be regenerated in the same reaction vessel, upon the addition of P_4 to the residual byproduct $[Cp^*FeP_4]^-$ and heating at 275 °C, thus extending this sequential reaction to a closed synthetic cycle, with KP_5 as a side product (Scheme 5).[43] This methodology, however, requires multiple steps and high temperatures, and suffers from poor P atom economy.

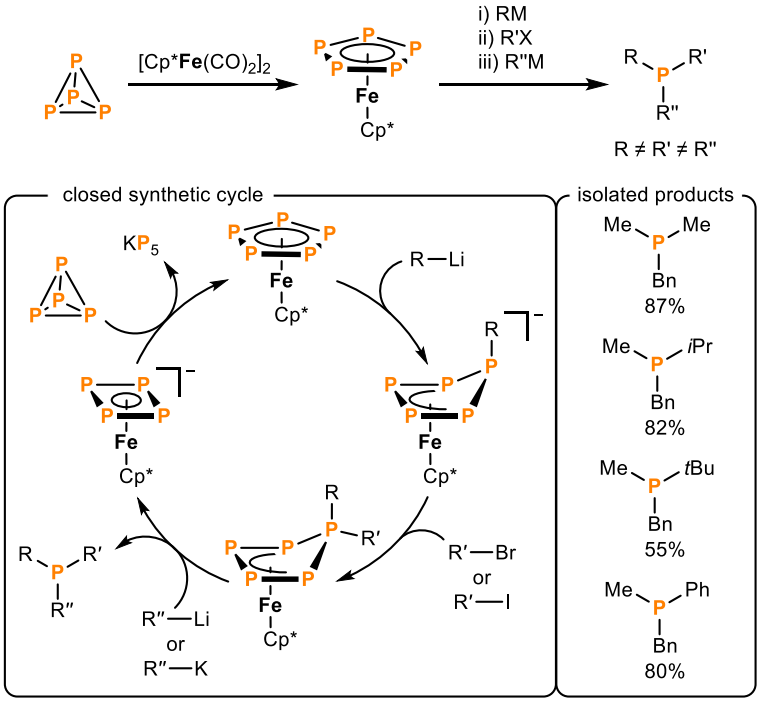

Scheme 5. Synthesis of tertiary phosphines mediated by $[Cp^*FeP_5]$.

1.2.5 Radical functionalisation of white phosphorus

An unusual approach that is particularly relevant to this doctoral thesis and which has gained increasing attention over the past five years is the functionalisation of P_4 by a free radical mechanism. In this method, free radicals induce successive homolytic P–P bond cleavage reactions, resulting in the stepwise degradation of the P_4 molecule through multiple polyphosphorus intermediates (Scheme 6).[20,24–26]

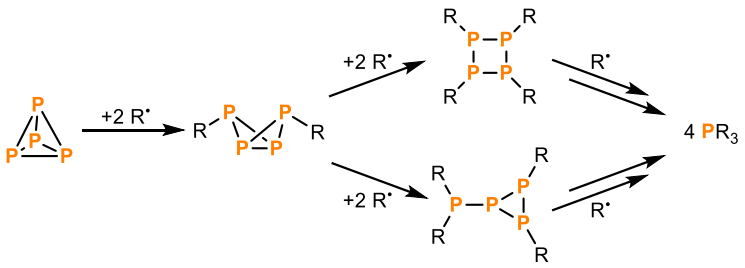

Scheme 6. Potential radical-based mechanism for the degradation of P_4 into monophosphorus compounds.

Barton and Zhu's pioneering work in 1993 demonstrated that the use of P_4 as a radical trap for carbon-centred radicals could be an effective strategy for the generation of organophosphorus compounds. The authors described the preparation of phosphonic acids by reacting P_4 with alkyl radicals generated by photolysis of pyridine thione oxycarbonyl esters (Barton's PTOC esters) with white light in a CH_2Cl_2/CS_2 solvent mixture (Scheme 7, Method A).[44] Notably, a subsequent report by the same group demonstrated that the same transformation could be efficiently achieved by replacing the solvent mixture with THF and without irradiation (Scheme 7, Method B).[45] Mechanistic investigations revealed that the key radicals (R•) can be generated from PTOC esters either by photolysis (Method A) or in the presence of a radical species. In particular, $[P_4O_2]^•$ was proposed to initiate the radical chain reaction, as it can be formed from the reaction of P_4 with traces of oxygen (Method B). In addition, a tetraphosphetane $[R_2P_4(SPy)_2]$ was proposed as a potential intermediate in the degradation of P_4, formed after formal addition of two PTOC ester fragments.[45] A significant drawback of both methods, however, is their low P-atom economy, needing the use of eight (Method A) or four equivalents (Method B) of phosphorus atoms (derived from two and one equivalents of P_4, respectively) to generate the final P_1 product.

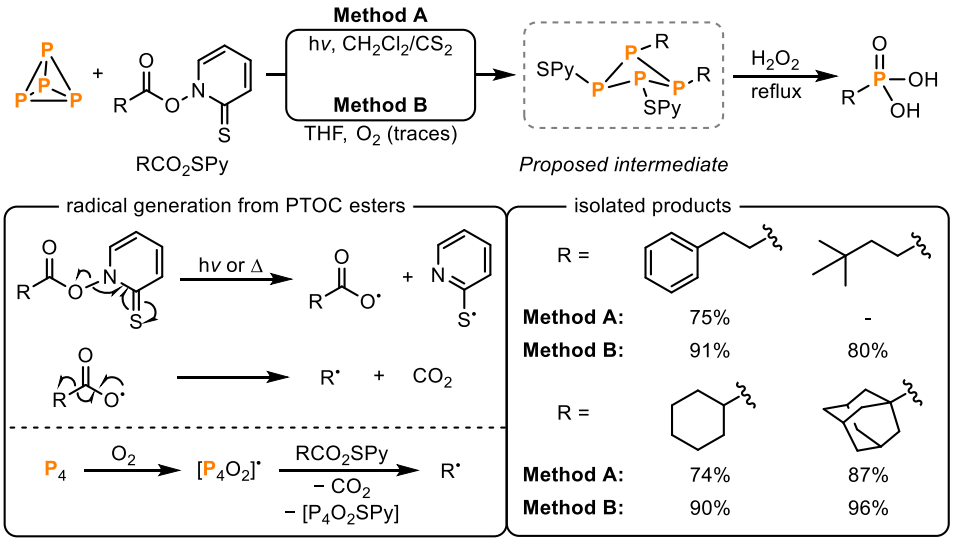

Scheme 7. Synthesis of phosphonic acids by reaction of P_4 with alkyl radicals generated from Barton's PTOC esters. For ease of comparison the yields are reported with respect to the PTOC esters.

Building on this seminal work nearly two decades later, in 2010 Cossairt and Cummins reported the use of a Ti(III) complex [Ti(N[*t*Bu]Ar)$_3$] (Ar = 3,5-$C_6H_3Me_2$), in the stoichiometric halogen radical abstraction from main group element halides RX (RX = PhBr, CyBr, Me_3SiI, Ph_3SnCl). This process resulted in the formation of the respective Ti(IV) halide species and the generation of the corresponding radicals (R•), which would then react with P_4 to afford valuable tertiary phosphines (Scheme 8).[46]

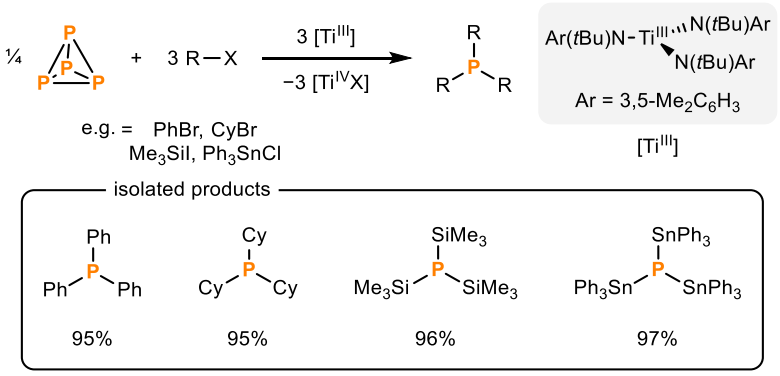

Scheme 8. Radical synthesis of tertiary phosphines directly from P_4, mediated by a Ti(III) complex.

Furthermore, in an extension of this work, Cummins and co-workers subsequently reported that samarium(II) halides can also be used as reductants in a similar fashion, for the reaction of P_4 with fluorous alkyl and aryl iodides to afford the respective trialkylphosphines and triarylphosphines in moderate to good yields (Scheme 9).[47]

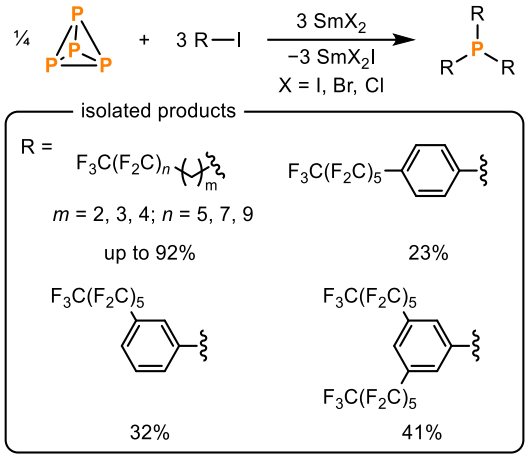

Scheme 9. Radical synthesis of fluorous trialkyl- and triarylphosphines directly from P_4, mediated by Sm(II) halides.

A breakthrough on the direct and catalytic functionalisation of P_4, was published by Wolf and co-workers in 2019.[48] Remarkably, valuable triarylphosphines and tetraarylphosphonium salts were obtained directly from P_4 upon treatment with aryl iodides and triethylamine in the presence of an iridium-based photocatalyst and blue-LED irradiation (455 nm). Mechanistic investigations suggest that initial photoexcitation of the photocatalyst (PC), followed by reductive quenching with triethylamine, results in the formation of a reduced species ($PC^{\bullet-}$) which subsequently reduces the aryl iodides in a single electron transfer step, thereby generating the key aryl radicals

(Ar•). These carbon-centred radicals are then proposed to directly react with P_4, leading to the successive cleavage of its P–P bonds and ultimately to the sequential formation of the P_1 compounds $ArPH_2$, Ar_2PH, Ar_3P, and $[Ar_4P]I$ (Scheme 10).[48] Notably, the steric and electronic nature of the aryl iodide substrate exhibits a marked influence on the formation of either the triarylphosphines or tetraarylphosphonium salts, with the former being favoured by bulky and/or electron-deficient arenes. Moreover, a follow-up on this strategy was reported by the same group one year later, describing the replacement of the precious transition metal iridium photocatalyst by the inexpensive organic photocatalyst 3DPAFIPN (2,4,6-tris(diphenylamino)-5-fluoroisophthalonitrile; Scheme 10).[49] Nevertheless, further dedicated mechanistic evaluations of the photocatalytic arylation of P_4 revealed the complexity of this transformation, with a variety of competing side reactions being relevant to the overall course of the reaction.[50]

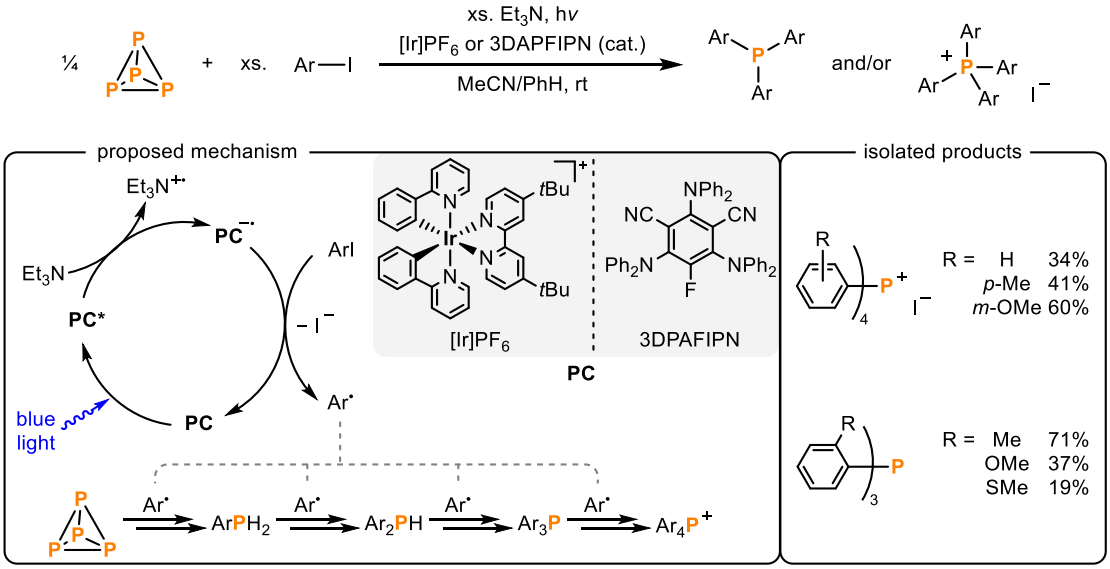

Scheme 10. Direct photocatalytic arylation of P_4 into arylphosphines and phosphonium salts.

A more recent publication by the Wolf group demonstrated that analogous arylation of P_4 could also be achieved using inexpensive and abundant aryl chlorides as precursors, thus overcoming a significant limitation of the previous transformation, which was restricted to aryl iodides due to the chemical inertness of the former.[51] Notably, inspired by previous work from the Wenger group,[52] the reduction of different aryl chlorides was possible following a light-driven process mediated by the photoreductant TDAE (tetrakis(dimethylamino)ethylene) in acetone under UV light irradiation (365 nm), generating the key aryl radicals (Ar•) which then react directly with P_4 to ultimately form the desired aryl phosphines and phosphonium salts (Scheme 11). Although this methodology offers a valuable proof-of-principle, it is important to note that it suffers from the need for an excess of both aryl chlorides and TDAE to obtain the final products in good yields.

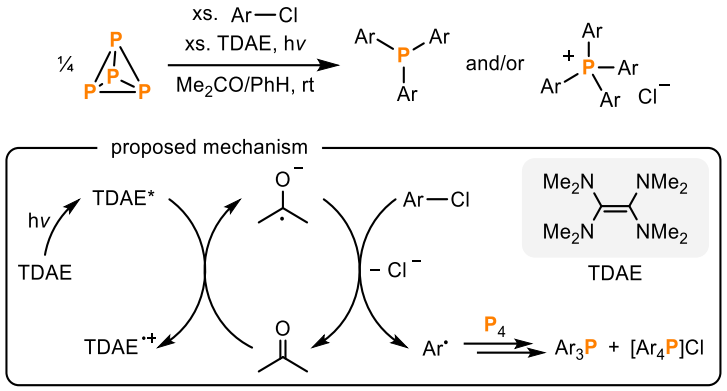

Scheme 11. Photochemical functionalisation of P_4 using aryl chlorides and TDAE as an organic photoreductant.

More recently, related strategies targeting relevant alkyl-substituted monophosphorus compounds have also been described by other groups. In 2022, the group of Tang reported the preparation of di- and trialkyl phosphine oxides directly from P_4 following a photoinduced alkylation process.[53] This methodology relies on the successive generation of alkyl radicals from aliphatic carboxylic acid *N*-hydroxyphthalimide (NHPI) esters, in the presence of Hantzsch ester (HE, 1,4-dihydropyridine-3,5-di-carboxylate) as a sacrificial electron donor, substoichiometric amounts of NaI as an electron transfer reagent and irradiation with blue light (450–470 nm), to afford the desired P_1 products after oxidation under air (Scheme 12a).

Later, Zhang and co-workers demonstrated that photochemically generated benzyl radicals can react with P_4 to give tetrabenzyl phosphonium salts in moderate to good yields.[54] The authors reported the activation and reactivity towards P_4 of benzyl bromides substituted with electron-donating groups upon irradiation with blue light (456 nm) in the presence of Hantzsch ester and *N*,*N*-diisopropylethylamine (DIPEA). In addition, by adding catalytic amounts of both the metal complex Cp_2TiCl_2 and the photocatalyst 4CzIPN (1,2,3,5-tetrakis(carbazole-9-yl)-4,6-dicyanobenzene), efficient activation of substrates bearing strong electron-withdrawing groups was achieved in a cooperative catalytic system, broadening the range of substrates for this transformation (Scheme 12b).[54] Furthermore, the same research group reported the reaction of P_4 with α-bromo esters using $Ir(ppy)_3$ (ppy = 2-phenylpyridine) as a photocatalyst, NaOAc as base, and blue LED irradiation (456 nm) to prepare a variety of phosphoryltriacetates in moderate yields.[55] Mechanistic investigations suggest that following a photoredox catalytic process, analogous to that described by Wolf and coworkers (see above), a tetrasubstituted phosphonium salt intermediate is generated. Subsequent elimination of HBr and an alkyne then forms the desired product (Scheme 12c).[55]

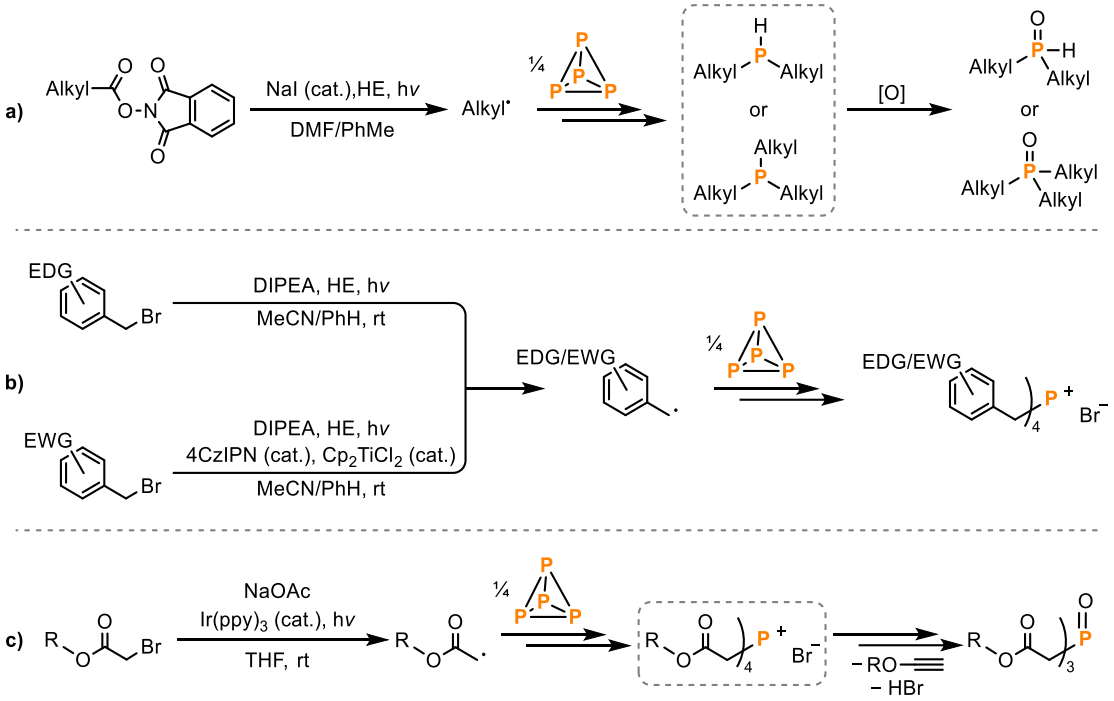

Scheme 12. Photoinduced preparation of alkyl-substituted monophosphorus compounds directly from P_4 upon reactions with alkyl radicals generated from NHPI esters (a), benzyl bromide derivatives (b) and α-bromo esters (c).

1.3 Conclusion and Outlook

Building on long-standing and dedicated academic efforts to study the reactivity of white phosphorus, a rapidly growing field of research has emerged with the aim of developing direct and even catalytic methods for the efficient functionalisation of P_4 into useful monophosphorus compounds. A number of independent investigations have been recently published describing alternative methodologies, including the direct nucleophilic functionalisation of P_4, electrochemical approaches, and transition-metal-mediated transformations. Although these strategies remain as proof-of-principle approaches that cannot yet replace or even compete with the efficiency of current industrial procedures, they represent a significant advance towards the development of more benign methods for the preparation of these ubiquitous compounds. Remarkably, the radical-mediated degradation of P_4 has attracted increasing attention since the report on the first photocatalytic P_4 arylation procedure by Wolf and co-workers in 2019, as a promising avenue for the preparation of organophosphorus compounds. Various approaches have been explored for the efficient generation of carbon-centred radicals, which can then react with P_4 in a controlled manner to afford a variety of P_1 compounds. Nevertheless, these systems have so far required elaborate strategies involving highly complex mechanisms to access the necessary radical intermediates, thereby limiting their practicality and potential scope of their implementation. Hence, alternative methodologies that favour the formation of radicals in a simpler and more accessible manner would be highly beneficial.

Motivated by these insights, the primary focus of the work presented in this doctoral thesis is the development of direct routes to useful monophosphorus compounds. Particularly, methods involving the radical-mediated hydroelementation of elemental phosphorus are described.

1.4 References

[1] D. E. C. Corbridge, *Phosphorus. Chemistry, Biochemistry and Technology*, Elsevier, **2000**.

[2] W. Schipper, *Eur. J. Inorg. Chem.* **2014**, 1567–1571.

[3] A. R. Jupp, S. Beijer, G. C. Narain, W. Schipper, J. C. Slootweg, *Chem. Soc. Rev.* **2021**, *50*, 87–101.

[4] M. Scheer, G. Balázs, A. Seitz, *Chem. Rev.* **2010**, *110*, 4236–4256.

[5] X. Ye, M. Qi, M. Chen, L. Zhang, J. Zhang, *Adv. Mater. Interfaces* **2023**, *10*, 2201941.

[6] B. M. Cossairt, N. A. Piro, C. C. Cummins, *Chem. Rev.* **2010**, *110*, 4164–4177.

[7] H. Diskowski, T. Hofmann, *Ullmann's Encycl. Ind. Chem.* **2012**, *26*, 725–746.

[8] S. P.-M. Ung, C.-J. Li, *RSC Sustain.* **2023**, *1*, 11–37.

[9] J. Svara, N. Weferling, T. Hofmann, *Ullmann's Encycl. Ind. Chem.* **2012**, *27*, 20–50.

[10] M. Caporali, M. Serrano-Ruiz, M. Peruzzini, in *Chem. beyond Chlorine* (Eds.: P. Tundo, L.N. He, E. Lokteva, C. Mota), Springer International Publishing, **2016**, pp. 97–136.

[11] G. Bettermann, W. Krause, G. Riess, T. Hofmann, *Ullmann's Encycl. Ind. Chem.* **2012**, *27*, 1–18.

[12] T. M. Hood, S. Lau, R. L. Webster, *J. Am. Chem. Soc.* **2022**, *144*, 16684–16697.

[13] T. Schneider, K. Schwedtmann, J. Fidelius, J. J. Weigand, *Nat. Synth.* **2023**, *2*, 972–979.

[14] F. Zhai, T. Xin, M. B. Geeson, C. C. Cummins, *ACS Cent. Sci.* **2022**, *8*, 332–339.

[15] M. B. Geeson, C. C. Cummins, *ACS Cent. Sci.* **2020**, *6*, 848–860.

[16] M. B. Geeson, P. Ríos, W. J. Transue, C. C. Cummins, *J. Am. Chem. Soc.* **2019**, *141*, 6375–6384.

[17] M. B. Geeson, C. C. Cummins, *Science* **2018**, *359*, 1383–1385.

[18] L. Giusti, V. R. Landaeta, M. Vanni, J. A. Kelly, R. Wolf, M. Caporali, *Coord. Chem. Rev.* **2021**, *441*, 213927.

[19] C. M. Hoidn, D. J. Scott, R. Wolf, *Chem. Eur. J.* **2021**, *27*, 1886–1902.

[20] J. E. Borger, A. W. Ehlers, J. C. Slootweg, K. Lammertsma, *Chem. Eur. J.* **2017**, *23*, 11738–11746.

[21] M. Caporali, L. Gonsalvi, A. Rossin, M. Peruzzini, *Chem. Rev.* **2010**, *110*, 4178–4235.

[22] V. A. Milyukov, Y. H. Budnikova, O. G. Sinyashin, *Russ. Chem. Rev.* **2005**, *74*, 781–805.

[23] M. Peruzzini, L. Gonsalvi, A. Romerosa, *Chem. Soc. Rev.* **2005**, *34*, 1038–1047.

[24] N. A. Giffin, J. D. Masuda, *Coord. Chem. Rev.* **2011**, *255*, 1342–1359.

[25] D. J. Scott, *Angew. Chem. Int. Ed.* **2022**, *61*, e2022050.

[26] Y. Liu, X. Chen, B. Yu, *Chem. Eur. J.* **2023**, *29*, e202302142.

[27] M. M. Rauhut, A. M. Semsel, *J. Org. Chem.* **1963**, *28*, 471–473.

[28] M. M. Rauhut, A. M. Semsel, *J. Org. Chem.* **1963**, *28*, 473–477.

[29] J. Hu, W. Liu, W. X. Zhang, *Phosphorus, Sulfur Silicon Relat. Elem.* **2022**, *197*, 398–407.

[30] D. G. Yakhvarov, Y. S. Ganushevich, O. G. Sinyashin, *Mendeleev Commun.* **2007**, *17*, 197–198.

[31] O. Back, G. Kuchenbeiser, B. Donnadieu, G. Bertrand, *Angew. Chem. Int. Ed.* **2009**, *48*, 5530–5533.

[32] L. Xu, Y. Chi, S. Du, W. Zhang, Z. Xi, *Angew. Chem. Int. Ed.* **2016**, *128*, 9333–9336.

[33] J. Hu, Z. Chai, W. Liu, Z. Huang, J. Wei, W. X. Zhang, *Sci. China Chem.* **2022**, *65*, 322–327.

[34] J. Hu, Z. Chai, W. Liu, J. Wei, Z. J. Lv, W. X. Zhang, *Green Synth. Catal.* **2023**, *4*, 330–333.

[35] Y. Mei, Z. Yan, L. L. Liu, *J. Am. Chem. Soc.* **2022**, *144*, 1517–1522.

[36] A. Schmidpeter, F. Zwaschka, *Angew. Chem. Int. Ed.* **1977**, *16*, 704–705.

[37] A. Schmidpeter, G. Burget, F. Zwaschka, W. S. Sheldrick, *Z. Anorg. Allg. Chem.* **1985**, *527*, 17–32.

[38] D. G. Yakhvarov, E. V. Gorbachuk, O. G. Sinyashin, *Eur. J. Inorg. Chem.* **2013**, 4709–4726.

[39] M. Donath, K. Schwedtmann, T. Schneider, F. Hennersdorf, A. Bauzá, A. Frontera, J. J. Weigand, *Nat. Chem.* **2022**, *14*, 384–391.

[40] P. Barbaro, M. Peruzzini, J. A. Ramirez, F. Vizza, *Organometallics* **1999**, *18*, 4237–4240.

[41] S. Hauer, T. M. Horsley Downie, G. Balázs, K. Schwedtmann, J. J. Weigand, R. Wolf, *Angew. Chem. Int. Ed.* **2024**, *63*, e202317170.

[42] O. J. Scherer, T. Brück, *Angew. Chem. Int. Ed.* **1987**, *26*, 59–59.

[43] S. Reichl, E. Mädl, F. Riedlberger, M. Piesch, G. Balázs, M. Seidl, M. Scheer, *Nat. Commun.* **2021**, *12*, 1–9.

[44] D. H. R. Barton, J. Zhu, *J. Am. Chem. Soc.* **1993**, *115*, 2071–2072.

[45] D. H. R. Barton, R. A. V. Embse, *Tetrahedron* **1998**, *54*, 12475–12496.

[46] B. M. Cossairt, C. C. Cummins, *New J. Chem.* **2010**, *34*, 1533–1536.

[47] S. K. Ghosh, C. C. Cummins, J. A. Gladysz, *Org. Chem. Front.* **2018**, *5*, 3421–3429.

[48] U. Lennert, P. B. Arockiam, V. Streitferdt, D. J. Scott, C. Rödl, R. M. Gschwind, R. Wolf, *Nat. Catal.* **2019**, *2*, 1101–1106.

[49] P. B. Arockiam, U. Lennert, C. Graf, R. Rothfelder, D. J. Scott, T. G. Fischer, K. Zeitler, R. Wolf, *Chem. Eur. J.* **2020**, *26*, 16374–16382.

[50] R. Rothfelder, V. Streitferdt, U. Lennert, J. Cammarata, D. J. Scott, K. Zeitler, R. M. Gschwind, R. Wolf, *Angew. Chem. Int. Ed.* **2021**, *60*, 24650–24658.

[51] M. Till, V. Streitferdt, D. J. Scott, M. Mende, R. M. Gschwind, R. Wolf, *Chem. Commun.* **2022**, *58*, 1100–1103.

[52] F. Glaser, C. B. Larsen, C. Kerzig, O. S. Wenger, *Photochem. Photobiol. Sci.* **2020**, *19*, 1035–1041.

[53] F. Chen, M. Bai, Y. Zhang, W. Liu, X. Huangfu, Y. Liu, G. Tang, Y. Zhao, *Angew. Chem.* **2022**, *61*, e202210334.

[54] X. Huangfu, W. Liu, H. Xu, Z. Wang, J. Wei, W. X. Zhang, *Inorg. Chem.* **2023**, *62*, 12009–12017.

[55] Y. Chen, W. Liu, X. Huangfu, J. Wei, J. Yu, W. X. Zhang, *Chem. Eur. J.* **2024**, *30*, e202302289.

2 Synthesis of Monophosphines Directly from White Phosphorus[a,b]

Abstract:

Monophosphorus compounds are of enormous industrial importance due to the crucial roles they play in applications including pharmaceuticals, photoinitiators, and ligands for catalysis, among many others. White phosphorus (P_4) is the key starting material for the preparation of all such chemicals. However, current production depends upon indirect and inefficient, multi-step procedures. Here, we report a simple, effective 'one-pot' synthesis of a wide range of organic and inorganic monophosphorus species directly from P_4. Reduction of P_4 using tri-*n*-butyltin hydride and subsequent treatment with various electrophiles affords compounds that are of key importance for the chemical industry, and requires only mild conditions and inexpensive, easily handled reagents. Crucially, we also demonstrate facile and efficient recycling and ultimately even catalytic use of the tributyltin reagent, thereby avoiding the formation of significant Sn-containing waste. Accessible, industrially relevant products include the fumigant PH_3, the reducing agent hypophosphorous acid, and the flame-retardant precursor tetrakis(hydroxymethyl)phosphonium chloride.

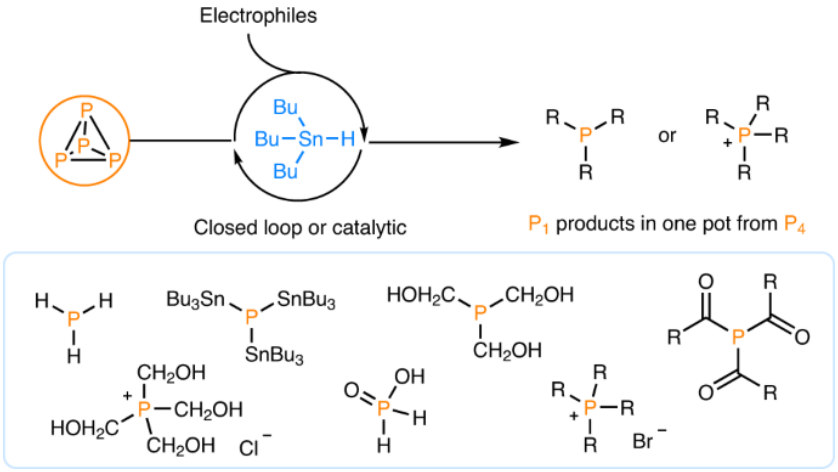

[a] Reproduced with permission from: D. J. Scott, J. Cammarata, M. Schimpf and R. Wolf, *Nat. Chem.* **2021**, *13*, 458–464.

[b] Daniel J. Scott developed the hydrostannylation procedure of P_4 reported in Section 2.2.1, and performed mechanistic studies described in Section 2.4.1. Daniel J. Scott and Jose Cammarata together investigated the functionalisation of the crude hydrostannylphosphine mixture into final P_1 products (Section 2.2.2). Jose Cammarata developed the synthesis, isolation, and purification of products at increased scale (Section 2.4.2) as well as the recovery and recycling of Bu_3Sn-based byproducts (Sections 2.2.3 and 2.4.3). Daniel J. Scott and Maximilian Schimpf developed the catalytic synthesis of THPC (Sections 2.2.4 and 2.4.4). Daniel J. Scott wrote the manuscript with contributions from Jose Cammarata. The manuscript was reviewed and edited by Robert Wolf. Daniel J. Scott and Robert Wolf supervised and directed the project.

2.1 Introduction

White phosphorus (P_4) is one of the most important synthetic feedstocks for the modern chemical industry[1] and is produced on a scale of more than 10^6 tons per year. The pyrophoric nature of P_4 and its hazardous and energy-intensive synthesis from phosphate ores have prompted recent academic efforts to bypass this compound and instead use phosphate materials directly as synthetic precursors.[2-4] Other researchers have emphasized the need to develop more sustainable routes for the recycling and reuse of P-containing materials, which are otherwise lost as environmentally-hazardous wastes.[2,5,6] However, despite these efforts, P_4 remains the only industrially viable precursor from which to prepare the vast majority of monophosphorus compounds, which find applications ranging from pharmaceuticals to chemical catalysts.[7-9] Unfortunately, state-of-the-art industrial methods for the synthesis of these useful P_1 species rely on indirect and correspondingly inefficient multi-step processes. The most common route (Scheme 1a) involves oxidation of P_4 by toxic Cl_2 gas to generate extremely corrosive PCl_3.[10] Treatment with suitable nucleophiles then provides the desired products *via* substitution of chloride, with concomitant generation of chloride-containing waste. Alternatively, some P_1 products can be generated by hydrophosphination of unsaturated organic compounds using PH_3 gas. However, industrial-scale preparation of PH_3 involves acid-catalysed or alkali-mediated disproportionation of P_4, which demands harsh reactions conditions and produces phosphorus oxyacid derivatives as stoichiometric byproducts (Scheme 1a).[10]

Recognition of the deficiencies of current routes for generating P_1 products has prompted a strong desire to discover reactions that are capable of transforming P_4 into these useful compounds directly, bypassing the need for isolation and manipulation of potentially hazardous intermediates.[11-13] Unfortunately, such reactions are highly challenging, as they demand the complete and controlled cleavage of all six P–P bonds of the P_4 tetrahedron, alongside similarly orderly formation of up to 16 new P–E bonds. As a result, methods for the direct functionalisation of P_4 remain exceedingly rare.[14-24] The few known examples typically require highly forcing conditions and/or undesirable reagents (such as alkali metal reductants or elaborate transition metal – even precious metal – complexes) to ensure that the reactions are driven to completion, severely limiting their scope and practicality.

We describe herein a simple, efficient, 'one-pot' synthesis of various valuable and industrially relevant monophosphorus species from P_4 using only commonly available reagents (Scheme 1b). The ubiquitous reducing agent tri-*n*-butyltin hydride (Bu_3SnH) provides clean access to stannyl-substituted monophosphines in a process that is both very mild and highly versatile, being compatible with either photoinitiation or common chemical radical initiators.[25-27] The product phosphines can be treated with organic and inorganic electrophiles to directly furnish commercially relevant P_1 products. Furthermore, we show that the key Bu_3Sn moiety can be readily recycled, and even employed catalytically, thereby mitigating any problems that might

arise from formation of stoichiometric Sn-containing waste. Accessible products include PH_3 (used as a fumigant, a reagent in the microelectronics industry, and a precursor to other organophosphorus compounds),[10] hypophosphorous acid (used industrially as a reducing agent and synthetic intermediate),[9,10,28] the tetrabenzylphosphonium salt $[Bn_4P]Br$ (a Wittig chemistry precursor),[29] and the phosphonium salt tetrakis(hydroxymethyl)phosphonium chloride (THPC, an important precursor to flame-retardant materials).[9,30]

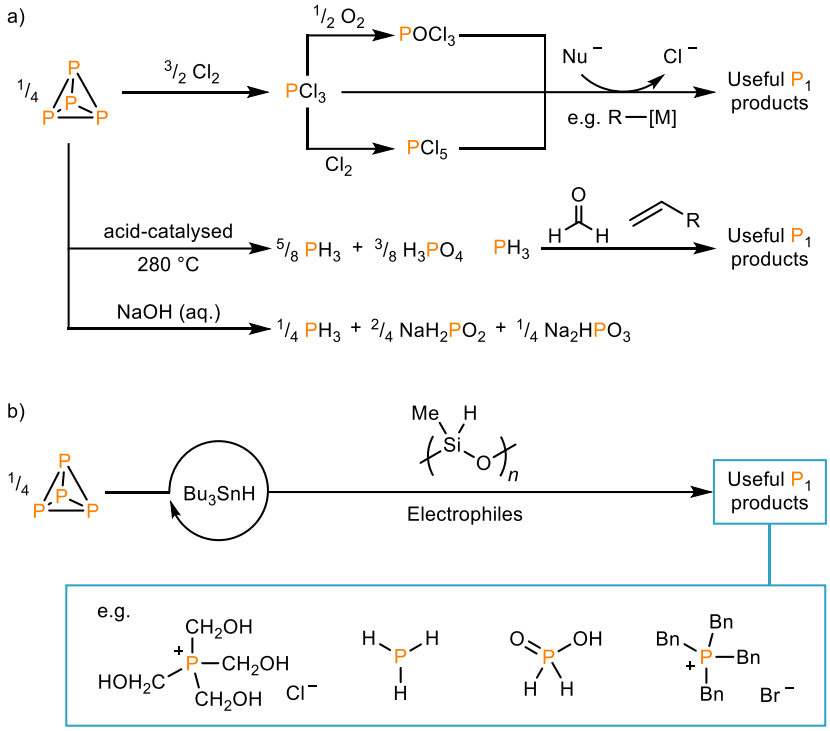

Scheme 1. Strategies for the transformation of P_4 into monophosphorus products. a) Current state-of-the-art methods, which involve either oxidation with Cl_2 (to generate PCl_3, which may be oxidized further to PCl_5 or $POCl_3$) and subsequent reaction with nucleophiles, or base-induced or acid-catalysed disproportionation to form PH_3, which is then used for hydrophosphination of unsaturated substrates. b) The strategy reported here, in which hydrostannylation of P_4 using Bu_3SnH is followed by reaction with electrophiles in a 'one-pot' fashion. The Bu_3SnH-derived by-products can be recovered and used to regenerate Bu_3SnH in a closed synthetic loop, using polymethylhydrosiloxane as a cheap and benign terminal reductant.

2.2 Results and Discussion

2.2.1 Hydrostannylation of P_4

The reactivity of P_4 towards radical reagents potentially provides a viable route for the preparation of P_1 products. However, in the few examples that have been reported to date, the elaborate strategies required to selectively access the necessary radical intermediates have severely limited their practicality and scope.[17-22] We reasoned that the inexpensive, commercially available radical source Bu_3SnH could serve as a convenient reagent for breaking apart the P_4 molecule, since Bu_3SnH readily generates formal $H^{\bullet}$ and $Bu_3Sn^{\bullet}$ radicals upon photolysis or thermolysis in the presence of a radical initiator.[31-34]

In an initial experiment, Bu_3SnH and P_4 were combined in a 6:1 molar ratio in PhMe at room temperature. Gratifyingly, $^{31}P\{^1H\}$ NMR spectroscopic monitoring of the mixture showed clear

consumption of P_4 over the course of several days, with concomitant appearance of new upfield resonances at −288.7 and −324.9 ppm (major), and −242.0 and −346.4 ppm (trace), which collectively correspond to the products $(Bu_3Sn)_nPH_{3-n}$ (n = 0-3, vide infra). Control experiments showed negligible reactivity when the reaction was repeated in the dark, suggesting a light-driven reaction. Indeed, when the reaction was performed under blue LED irradiation complete consumption of P_4 was observed within 18 h (Scheme 2 and Figures S1-4). Nearly identical product distributions were observed in various other common organic solvents (*n*-hexane, PhH, Et_2O, THF, DME; Figure S5) and an analogous outcome was also observed for the equivalent reaction of P_4 with Ph_3SnH (see Section 2.4.1.3 for full details).[35]

The signal observed at −242.0 ppm is consistent with the formation of minor PH_3 (**1**),[3] while the remaining resonances are assigned to the formation of new products Bu_3SnPH_2 (**2**; −288.7 ppm),[36] $(Bu_3Sn)_2PH$ (**3**; −324.9 ppm) and $(Bu_3Sn)_3P$ (**4**; −346.4 ppm).[19] The observed upfield chemical shifts agree with previously reported stannyl phosphines,[37] and the presence of P–Sn and P–H bonds is confirmed by observation of $^{117/119}$Sn satellites and multiplicity in the proton-coupled ^{31}P spectra, respectively (Figures S2 and S3).[16,38,39] The products obtained are consistent with complete, stoichiometric hydrostannylation of all six P–P bonds of P_4, as shown in Scheme 2a. The observed preference for Bu_3SnPH_2 and $(Bu_3Sn)_2PH$ over PH_3 and $(Bu_3Sn)_3P$ is probably kinetic in origin (see Section 2.4.1.4) and may be attributable to steric factors that would disfavor installation of multiple Bu_3Sn moieties on a single P atom. The major products can be separated by distillation under high vacuum (105 °C, 10^{-2} mbar, see Section 2.4.1.4) to give Bu_3SnPH_2 (**2**; 31%) and $(Bu_3Sn)_2PH$ (**3**; 45%, typically containing ~10% Bu_3SnPH_2/$(Bu_3Sn)_3P$) as colourless oils. Both are indefinitely stable when stored at −35 °C but undergo noticeable scrambling of their H and Bu_3Sn ligands within a few days at room temperature, or more rapidly at elevated temperature (hence the minor impurities observed in samples of $(Bu_3Sn)_2PH$ isolated by distillation). Notably, however, all three of the stannylated phosphines are highly stable in the presence of hydroxylic species such as H_2O or alcohols. They are even moderately stable in the presence of O_2 and can be exposed to air overnight at ambient temperature without significant decomposition (see Section 2.4.1.5). This stands in stark contrast to other common "P^{3-}" synthons such as $P(SiMe_3)_3$ and represents a considerable practical advantage.[15]

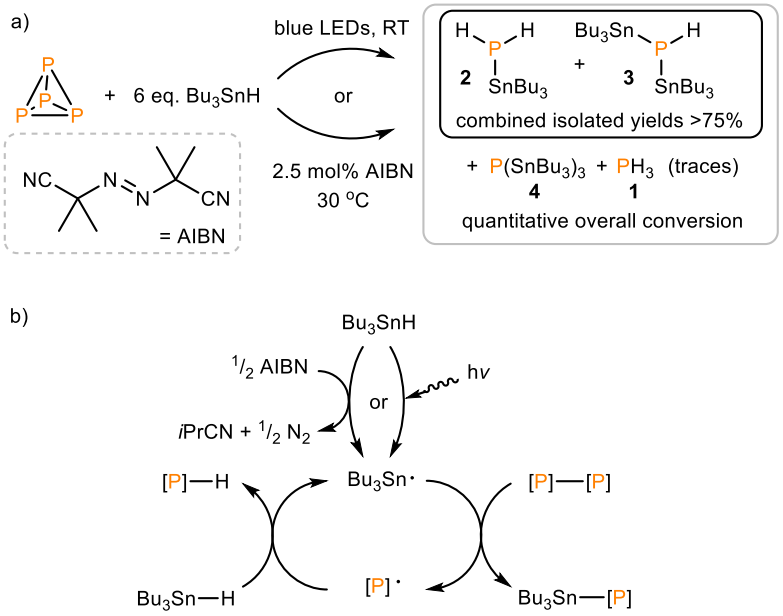

Scheme 2. Hydrostannylation of P_4. a) Stoichiometric reaction of P_4 with Bu_3SnH to give products $(Bu_3Sn)_xPH_{3-x}$ (x = 0–3), initiated by either light or a chemical radical initiator. b) a plausible radical chain mechanism for P_4 hydrostannylation, where [P]–[P] represents a generic P–P bond. AIBN (azobis(isobutyronitrile)) loading (mol%) is defined per P atom.

The precise mechanism of the P_4 hydrostannylation reaction remains under investigation. Nevertheless, the use of light as an initiator clearly suggests a radical process, as radical chain reactions mediated by Bu_3SnH are well established.[31-34] A plausible mechanism is therefore outlined in Scheme 2b, in which each P–P bond is cleaved through initial attack of a $Bu_3Sn^{\bullet}$ radical (for example, generated by photoelectron catalysis; see Section 2.4.1.2),[40-42] followed by abstraction of $H^{\bullet}$ by the resulting P-centred radical from another equivalent of Bu_3SnH, to regenerate $Bu_3Sn^{\bullet}$ and continue the radical chain. Based on the proposed mechanism, it should also be possible to initiate hydrostannylation through use of a chemical (rather than photochemical) radical source. Indeed, addition of 2.5 mol% per P atom of the thermally activated radical initiator azobis(isobutyronitrile) (AIBN) was found to induce similarly efficient $(Bu_3Sn)_xPH_{3-x}$ formation over a comparable timeframe in the dark, with only very gentle heating (shorter reaction times could be used at higher temperatures; see Section 2.4.1.6).[43] Comparable results were observed at more elevated temperatures using the related radical initiator 1,1'-azobis(cyclohexanecarbonitrile) (ACN; see Section 2.4.1.7).[44] Similarly, addition of the stable radical 2,2,6,6-tetramethylpiperidinyloxyl (TEMPO) also led to slow hydrostannylation in the dark at room temperature (Section 2.4.1.8; see also Sections 2.4.1.9-2.4.1.11 for discussion of reactions involving excess TEMPO).[45] $^{31}P\{^1H\}$ NMR spectroscopic analysis of reaction mixtures at partial conversion revealed no resonances attributable to intermediate structures (see Section 2.4.1.1 for examples). However, we note that other P–P bonded species such as P_2Ph_4 and cyclo-P_5Ph_5 were also efficiently hydrostannylated under identical conditions (Sections 2.4.1.13 and 2.4.1.14),[46] suggesting that analogous H/Bu_3Sn-substituted oligophosphorus structures are plausible.

2.2.2 Functionalisation of $(Bu_3Sn)_xPH_{3-x}$

As with other phosphines, the P_4 hydrostannylation products $(Bu_3Sn)_xPH_{3-x}$ (x = 1-3) were expected to display nucleophilic character at P. To confirm this, the reactions of the major isolated products Bu_3SnPH_2 (**2**) and $(Bu_3Sn)_2PH$ (**3**) with pivaloyl chloride (*t*BuC(O)Cl) were investigated. It was anticipated that these could provide access to acyl-phosphorus linkages, which are a key structural motif in many industrially employed photoinitiators.[47] Although both the P–Sn and P–H bonds of the starting phosphines are potentially reactive, in this case the reactions were seen to lead to mild cleavage of the P–Sn bonds only. The reaction of Bu_3SnPH_2 (**2**) with 1 equiv. *t*BuC(O)Cl was observed by $^{31}P\{^1H\}$ NMR spectroscopy to lead to the formation of a single major species, which was identified as the primary acyl phosphine *t*BuC(O)PH_2 (**5**; Scheme 3, path (iii) and Section 2.4.2.1) and could be isolated as a spectroscopically clean solution by simple trap-to-trap distillation.[48] Similarly, reactions with $(Bu_3Sn)_2PH$ (**3**) sequentially gave the *mono*- and *bis*-acyl phosphines *t*BuC(O)P(H)$SnBu_3$ and [*t*BuC(O)]$_2$PH as the major products (**6** and **7**, respectively; Scheme 3 paths (iv) and (v), and Section 2.4.2.2).[49]

P–Sn bond cleavage could also be accomplished through addition of a Brønsted acid (Section 2.4.2.3), leading to formation of PH_3, which is employed industrially as a fumigant, in the synthesis of semiconductors, and as a precursor to many other P_1 chemicals.[10] Because, in this case, the same product was produced from both starting materials, it was possible to combine P_4 hydrostannylation and subsequent acidification into a simple one-pot procedure, producing PH_3 (**1**) directly and with high efficiency (Scheme 3 (vi)).

Transformation of only the P–H bonds of the hydrostannylation products could also be achieved. Reacting Bu_3SnPH_2 (**2**) or $(Bu_3Sn)_2PH$ (**3**) with Bu_3SnOMe led to selective formation of the fully stannylated phosphine $(Bu_3Sn)_3P$ (**4**), thereby completing the set of isolable phosphines $(Bu_3Sn)_xPH_{3-x}$ (x = 1-3). The same product is again produced from both starting materials, and it was possible to combine P_4 hydrostannylation and subsequent functionalisation into a simple one-pot procedure in which **4** was isolated in excellent yield (85%) without the need for isolation of any intermediates (Scheme 3(vii) and Section 2.4.2.4).

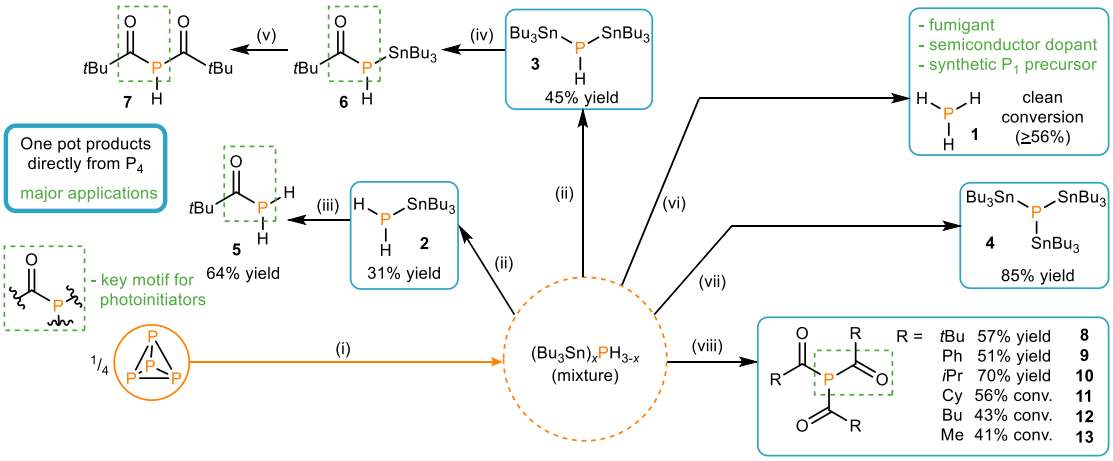

Scheme 3. Functionalisation of phosphines $(Bu_3Sn)_xPH_{3-x}$ and direct, 'one-pot' functionalisation of P_4. Equivalents (equiv.) are defined per P atom. (i) Hydrostannylation of P_4 using Bu_3SnH (from P_4: 1.5 equiv. Bu_3SnH, PhMe, 455 nm LEDs, room temperature (RT), 16 h). (ii) Preparative separation of Bu_3SnPH_2 (**2**) and $(Bu_3Sn)_2PH$ (**3**) (from crude $(Bu_3Sn)_xPH_{3-x}$: distillation, ~105 °C, 10^{-2} mbar). (iii) Monoacylation of Bu_3SnPH_2 (**2**) using *t*BuC(O)Cl (from Bu_3SnPH_2: 0.95 equiv. *t*BuC(O)Cl, PhMe, dark, RT, 16 h). (iv) Monoacylation of $(Bu_3Sn)_2PH$ (**3**) using *t*BuC(O)Cl (from $(Bu_3Sn)_2PH$: 1 equiv. *t*BuC(O)Cl, C_6D_6, RT). (v) Double acylation of $(Bu_3Sn)_2PH$ (**3**) using *t*BuC(O)Cl (from $(Bu_3Sn)_2PH$: 2 equiv. *t*BuC(O)Cl, C_6D_6, RT). (vi) One-pot, selective transformation of P_4 into PH_3 (**1**) (from crude $(Bu_3Sn)_xPH_{3-x}$: 10 equiv. HCl (4.0 M in 1,4-dioxane), RT, 1 h). (vii) One-pot synthesis of $(Bu_3Sn)_3P$ (**4**) (from P_4: 1.5 equiv. Bu_3SnH, 1.5 equiv. Bu_3SnOMe, PhMe, 455 nm LEDs, RT, 16 h, then –PhMe, 100 °C, 16 h). (viii) One-pot synthesis of triacylphosphines $P(C(O)R)_3$ (**8**–**13**) (from P_4: 1.6 equiv. Bu_3SnH, PhMe, 455 nm LEDs, RT, 16 h, then 4 equiv. RC(O)Cl, 1.5 equiv. potassium bis(trimethylsilyl)amide (KHMDS) (R=*t*Bu, Ph) or NEt_3 (R=*i*Pr, Cy, Bu, Me), PhMe, dark, RT, 16 h).

In the above reactions Bu_3SnPH_2 and $(Bu_3Sn)_2PH$ behave as formal sources of "$[H_2P]^-$", "$[HP]^{2-}$", "$[Bu_3SnP]^{2-}$" and "$[(Bu_3Sn)_2P]^-$". Also of great interest, however, are reactions in which these phosphines react as simple "P^{3-}" synthons. Thus, repeating their acylation using *t*BuC(O)Cl (vide supra) in the presence of a suitable base led to successful cleavage of both P–Sn and P–H bonds, and clean formation of the tertiary product $P(C(O)tBu)_3$ (**8**).[50] Again, because the same compound is produced regardless of the starting phosphine, it was possible to access this species in an efficient, one-pot manner directly from P_4, and this reaction could be easily generalised to a variety of other acid chlorides substrates (RC(O)Cl, R = Ph, *i*Pr, Cy, Bu, Me; **9**–**13**; Scheme 3(viii) and Sections 2.4.2.5-2.4.2.10).[51]

Alternatively, in situ treatment of the hydrostannylation products with benzyl bromide (BnBr) under gentle heating led to selective formation of the corresponding fully alkylated phosphonium salt, $[Bn_4P]Br$ (**14**), which is a precursor for useful Wittig chemistry (Scheme 4(ii) and Section 2.4.2.11).[29] As for the previous acylation reactions, in the absence of base the formation of **14** is proposed to proceed through functionalisation of P–Sn bonds only,[52] with P–H bonds ultimately sequestered in the form of PH_3 (Scheme S2, Section 2.4.2.12). In the presence of base, productive functionalisation of the P–H bonds could also be achieved, leading to very efficient incorporation of P (Scheme 4(iii)). An analogous reaction using EtBr could also be used to obtain the ethyl-substituted salt $[Et_4P]Br$ (**15**; Scheme 4(iv) and Section 2.4.2.13; for further reactions with organic halide substrates see Sections 2.4.2.14-2.4.2.16).

Formaldehyde is also a suitable C-centred electrophile for reaction with the crude hydrostannylation product mixture.[53] Such reactions result in hydroxymethyl-substituted phosphines, which have specific industrial importance. Most notably, salts of the tetrakis(hydroxymethyl)phosphonium cation, $[(HOCH_2)_4P]X$ (THPC, X = Cl; THPS, X = ½SO_4) are used to prepare flame retardant materials through the PROBAN process (THPC).[9] They are also employed as microbicides for water treatment (THPS), and as precursors to other valuable P_1 chemicals via extrusion of CH_2O.[30] Treatment of the in situ generated $(Bu_3Sn)_xPH_{3-x}$ mixture with paraformaldehyde in EtOH provided good conversion to the parent phosphine $(HOCH_2)_3P$ (THP, **16**), which is conventionally produced by dealkylation of THPC,[9] and is also used as a synthetic P_1 precursor, as well as a water-soluble ligand for transition metals.[54] This could be isolated directly (Scheme 4(v) and Section 2.4.2.17), or quenched with HCl to furnish THPC (**17**) in one-pot and good yield following a simple work-up (Scheme 4(vi) and Section 2.4.2.18). Notably, excellent yields of THPC were also obtained when the initial hydrostannylation step was performed in EtOH in the presence of paraformaldehyde, or when hydrostannylation was achieved using AIBN instead of light (82% and 87% yield, respectively; Sections 2.4.2.19 and 2.4.2.20). The latter procedure could conveniently be used to prepare THPC on over gram scale (3.3 g, 87%; Section 2.4.2.21). Alternatively, quenching THP through exposure to air provided direct access to the corresponding phosphine oxide $(HOCH_2P)_3PO$ (THPO, **18**), also in good isolated yield (Scheme 4(vii) and Section 2.4.2.22). Like THPC, THPO has been used for the preparation of flame-retardant materials.[55]

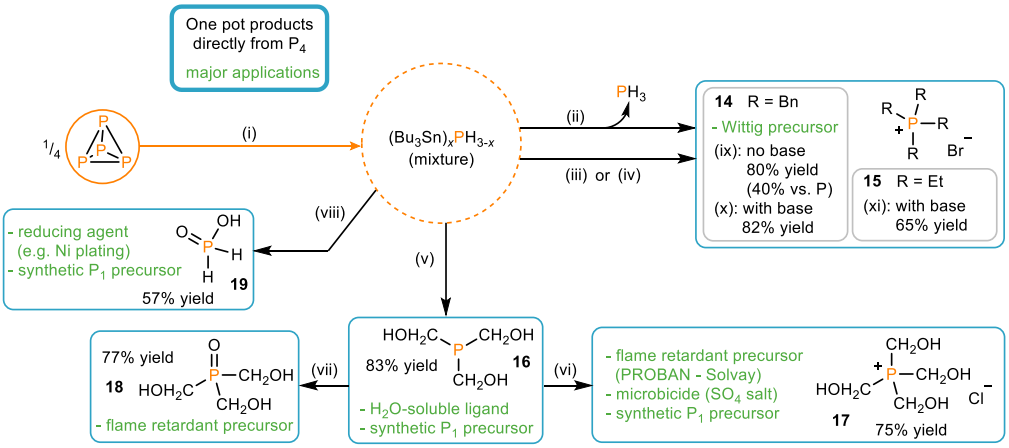

Scheme 4. Further direct, 'one-pot' functionalisation of P_4. Equivalents are defined per P atom. (i) Hydrostannylation of P_4 using Bu_3SnH (from P_4: 1.5 equiv. Bu_3SnH, PhMe, 455 nm LEDs, RT, 16 h). (ii) One-pot synthesis of $[Bn_4P]Br$ (**14**), without base (from P_4: 1.6 equiv. Bu_3SnH, PhMe, 455 nm LEDs, RT, 16 h, then 10 equiv. BnBr, 60 °C, 3 days). (iii) One-pot synthesis of $[Bn_4P]Br$ (**14**), with base (from P_4: 1.6 equiv. Bu_3SnH, PhMe, 455 nm LEDs, RT, 16 h, then 10 equiv. BnBr, 1 equiv. KHMDS, 60 °C, 3 days). (iv) One-pot synthesis of $[Et_4P]Br$ (**15**), with base (from P_4: 1.6 equiv. Bu_3SnH, PhMe, 455 nm LEDs, RT, 16 h, then 5 equiv. EtBr, 2 equiv. KHMDS, 100 °C, 3 days). (v) One-pot synthesis of $(HOCH_2)_3P$ (THP, **16**) (from P_4: 1.6 equiv. Bu_3SnH, 3 equiv. paraformaldehyde, EtOH, 455 nm LEDs, RT, 16 h). (vi) One-pot synthesis of $[(HOCH_2)_4P]Cl$ (THPC, **17**) (from P_4: 1.6 equiv. Bu_3SnH, PhMe, 455 nm LEDs, RT, 16 h, then –PhMe, EtOH, 12.5 equiv. paraformaldehyde, RT, 16 h, then 10 equiv. HCl (4.0 M in 1,4-dioxane), RT, 2 h). (vii) One-pot synthesis of $(HOCH_2)_3PO$ (THPO, **18**) (from crude THP: PhMe/H_2O, air, 90 °C, 16 h). (viii) One-pot synthesis of $H_2P(O)OH$ (HPA, **19**) (from P_4: 1.6 equiv. Bu_3SnH, PhMe, 455 nm LEDs, RT, 16 h, then 10 equiv. H_2O_2 (35% aq.), RT, 30 min, then H_2O, 2.5 equiv. HCl (4.0 M in 1,4-dioxane)).

Oxidation of the $(Bu_3Sn)_xPH_{3-x}$ mixture in the absence of paraformaldehyde was also investigated, and treatment with H_2O_2 was found to selectively furnish partially oxidised hypophosphorous acid ($H_2P(O)OH$, HPA, **19**) after work-up (Scheme 4(viii) and Section 2.4.2.23), alongside minor amounts (<10%) of the known HPA oxidation product $HP(O)(OH)_2$. By comparison, direct oxidation of P_4 using peroxide reagents is known to be much less selective.[56] HPA is another important P_1 precursor, used to prepare phosphinic acid derivatives (for example, Cyanex, used in metal separation processes),[9] and is also employed industrially as a reductant (for example, for electroless Nickel plating).[28]

2.2.3 Regeneration and recycling of the tri-*n*-butyl reagent

Having established the ability of Bu_3SnH to efficiently mediate the direct transformation of P_4 into various useful and industrially relevant monophosphorus species, we became interested in the possibility of recovering and/or recycling the key Bu_3Sn moiety.[57] Such recycling would bypass any net formation of Sn-containing waste and could also provide a first step towards the development of catalytic reactions, which are all but unknown for P_4 (vide infra).[21-24] Fortunately, the Bu_3Sn moiety is relatively robust, and in the above reactions is ultimately incorporated into a by-product of the type Bu_3SnX (X = OR or halide, R = Bu_3Sn or alkyl) that is easily separated from the target product. For example, Bu_3SnCl (**20**) could be recovered in high yield and with minimal effort from the syntheses of THPC and HPA by a simple extraction procedure after the reaction mixture was quenched with HCl (Scheme 5a). Transformation of Bu_3SnCl into Bu_3SnH is well established and can be achieved by various means (either directly or via facile hydrolysis or alcoholysis to Bu_3SnOR), commonly with near-quantitative conversions and excellent isolated yields (up to 95%).[58] Combination of any of these methods with the above reactions thus provides a simple and efficient synthetic cycle that does not produce any stoichiometric Sn-containing by-products (Scheme 5b).

Although any known method could be employed for the regeneration of Bu_3SnH, especially attractive is the reaction of Bu_3SnOR under mild conditions with polymethylhydrosiloxane (PMHS), a benign, stable and inexpensive polymeric reductant (Scheme 5c).[59,60] In particular, it was anticipated that use of such a gentle method might allow generation of Bu_3SnH to be combined with subsequent P_4 functionalisation in a single reaction step (in a similar manner to Bu_3SnH-mediated reduction of some organic substrates),[61] further simplifying the synthetic cycle. Indeed, hydrostannylation of P_4 could be successfully achieved upon replacement of Bu_3SnH with a mixture of Bu_3SnOMe or $(Bu_3Sn)_2O$ and PMHS (Sections 2.4.3.1-2.4.3.3).

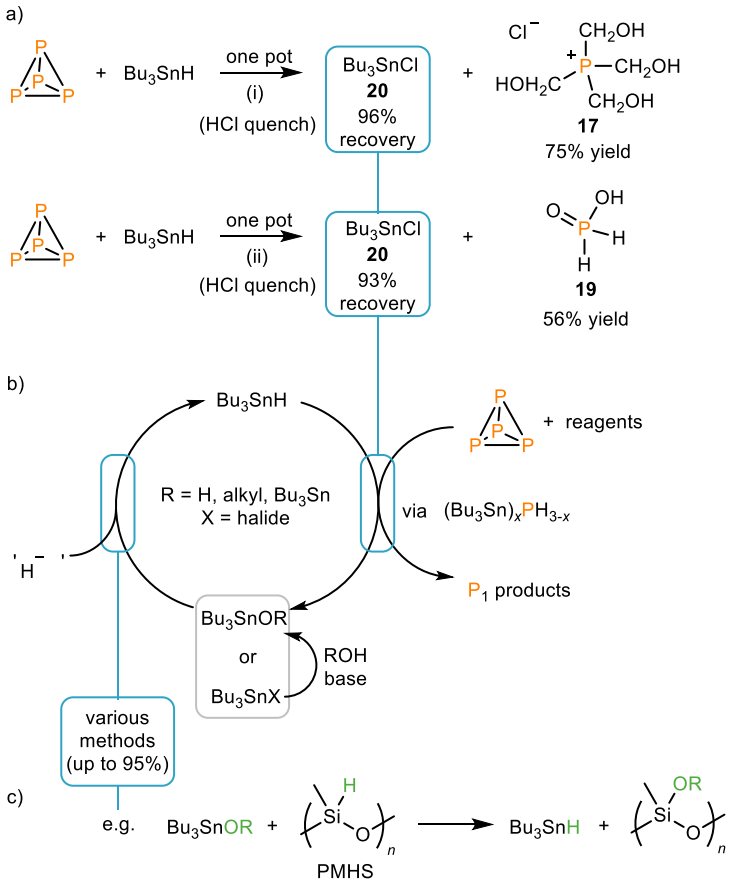

Scheme 5. Recycling of the Bu_3Sn moiety. a) Recovery of Bu_3SnCl from the syntheses of THPC and HPA. b) An outline 'Bu_3Sn-neutral' synthetic cycle for transformation of P_4 into monophosphorus species, through reduction of recovered Bu_3Sn derivatives with hydride sources.[58] c) A specific example of regeneration of Bu_3SnH using PMHS as a hydride source. Conditions (equiv. are defined per P atom): (i) from P_4: 1.6 equiv. Bu_3SnH, PhMe, 455 nm LEDs, RT, 16 h, then –PhMe, EtOH, 12.5 equiv. paraformaldehyde, RT, 16 h, then 10 equiv. HCl (4.0 M in 1,4-dioxane), RT, 2 h; (ii) from P_4: 1.6 equiv. Bu_3SnH, PhMe, 455 nm LEDs, RT, 16 h, then 10 equiv. H_2O_2 (35% aq.), RT, 30 min, then H_2O, 2.5 equiv. HCl (4.0 M in 1,4-dioxane).

These tandem reactions could be fed directly into subsequent steps, as illustrated by the synthesis of THPC, which was isolated in one-pot and excellent yields starting from both Bu_3SnOMe and $(Bu_3Sn)_2O$ (Scheme 6a,b and Sections 2.4.3.4 and 2.4.3.5). The Bu_3SnCl by-product of the latter reaction could again be separated from the target product by simple extraction, alongside PMHS-derived by-products. In fact, it was found that this 'crude' Bu_3SnCl could be employed directly as a Bu_3Sn source for further P_4 functionalisation, without the need for separation of the pure compound. Thus, after simple stirring over aqueous Na_2CO_3 (to convert back to $(Bu_3Sn)_2O$) this unpurified material was added to a fresh reaction mixture, ultimately yielding a new batch of THPC in good yield (albeit reduced somewhat relative to the first 'cycle'; Scheme 6c and Sections 2.4.3.5 and 2.4.3.6).

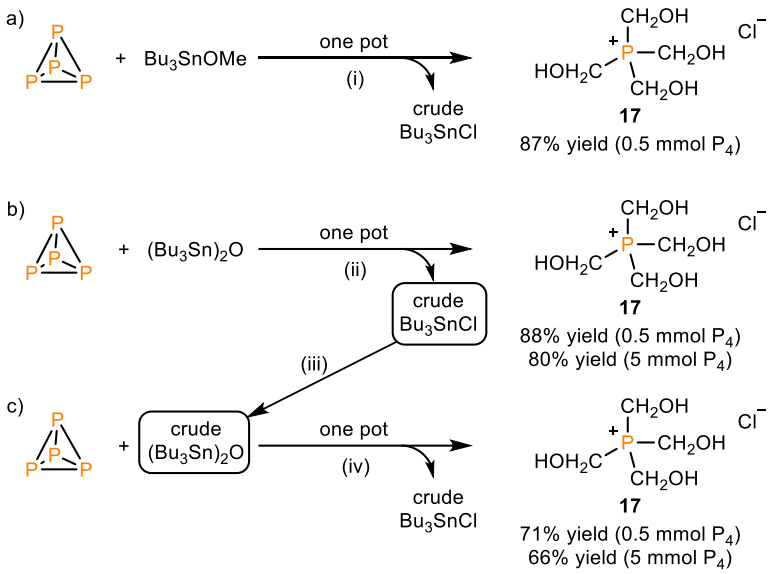

Scheme 6. Synthesis of THPC via in situ generation of Bu_3SnH. One-pot synthesis of THPC (**17**) starting directly from P_4 and Bu_3SnOMe (a) or $(Bu_3Sn)_2O$ (b). c) Direct recycling of the Bu_3Sn moiety without re-isolation of any intermediate Bu_3SnX. Conditions (equiv. are defined per P atom): (i) from P_4: 2 equiv. Bu_3SnOMe, 2 equiv. PMHS, PhMe, 455 nm LEDs, RT, 16 h, then –PhMe, EtOH, 12.5 equiv. paraformaldehyde, RT, 16 h, then 10 equiv. HCl (4.0 M in 1,4-dioxane), RT, 2 h; (ii) from P_4: 1 equiv. $(Bu_3Sn)_2O$, 5 mol% ACN, 2 equiv. PMHS, PhMe, dark, 80 °C, 3 days, then –PhMe, EtOH, 12.5 equiv. paraformaldehyde, RT, 16 h, then 10 equiv. HCl (4.0 M in 1,4-dioxane), RT, 2 h; (iii) from crude Bu_3SnCl: sat. Na_2CO_3 (aq.), RT, 16 h; (iv) from P_4: 1 equiv. crude $(Bu_3Sn)_2O$, 5 mol% ACN, 2 equiv. PMHS, PhMe, dark, 80 °C, 3 days, then –PhMe, EtOH, 12.5 equiv. paraformaldehyde, RT, 16 h, then 10 equiv. HCl (4.0 M in 1,4-dioxane), RT, 2 h.

2.2.4 Catalytic use of the tri-*n*-butyl reagent

Having established the viability of a synthetic cycle that is closed in Bu_3Sn, attention was finally turned to the development of a catalytic process.[61] Such reactions represent a long-standing but almost entirely unmet goal in the field of P_4 activation.[21-24] Reducing the amount of the Bu_3SnX reagent employed should also further minimize any risks associated with its use. Gratifyingly, the formation of THP en route to THPC could be achieved using only a catalytic quantity (8.25 mol% per P atom) of Bu_3SnOMe, with turnover numbers (TONs) greater than 10 achievable after only minor modification of the stoichiometric procedures (Scheme 7 and Sections 2.4.4.1 and 2.4.4.2, see Scheme S4 for an outline catalytic cycle). Only one other example of catalytic P–C bond formation from P_4 is known, which is strictly limited to P–C(aryl) bonds.[21,22]

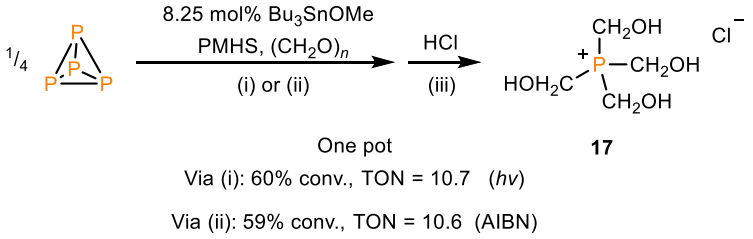

Scheme 7. Synthesis of THPC (**17**) via catalytic transformation of P_4 into THP (**16**). Turnover numbers (TONs) are calculated from the measured conversion (conv.) to THPC and factor in the 1:6 stoichiometry of the P_4 hydrostannylation reaction, as described in Sections 2.4.4.1 and 2.4.4.2. Conversion and TON values are based on an average of two runs. Catalyst/initiator loadings (mol%) and molar equiv. are defined per P atom. Conditions: (i) 8.3 mol% Bu_3SnOMe, 4 equiv. PMHS, 8.3 equiv. paraformaldehyde, EtOH/PhH (2:1), 365 nm LEDs, RT, 65 h; (ii) 8.3 mol% Bu_3SnOMe, 8 equiv. PMHS, 8.3 equiv. paraformaldehyde, 8.3 mol% AIBN, EtOH/PhH (2:1), 60 °C, 65 h; (iii) 3.3 equiv. HCl (4.0 M in 1,4-dioxane), RT, 1 h.

2.3 Conclusion and Outlook

We have developed a practical, versatile method for the direct transformation of P_4 into useful monophosphorus species, mediated by the readily-available triorganotin(IV) moiety Bu_3Sn. This method can be used to prepare diverse monophosphorus compounds, which are of clear industrial relevance in areas such as flame retardants, photoinitiators and fumigants. Both organic and inorganic phosphorus products are accessible in a 'one-pot' manner without the need for wasteful or time-consuming isolation of intermediates, and the reactions require only inexpensive, commercially available reagents. Importantly, facile recovery and recycling of the Bu_3Sn moiety has been achieved, which prevents the formation of substantial Sn-containing waste. Indeed, the Bu_3Sn moiety may even be employed in a truly catalytic fashion, as illustrated for the synthesis of the important industrial precursor THPC. This catalytic use of the tri-*n*-butyltin reagent further minimises any risks associated with the use of organotin compounds. The use of a p-block element catalyst to produce a highly useful organophosphorus compound was previously unknown, and our results thus suggest that the conspicuous shortage of catalytic methods of the transformation of P_4 can be overcome. Although our research has so far focused on commercially available butyl-substituted tin derivatives, the practical and conceptual simplicity of the approach described herein promises ready extension to a much wider range of radical sources, potentially even including those based on other p-block elements. We therefore anticipate that the reported method will have a major impact on the future synthesis of monophosphorus compounds in laboratory and industrial settings.

2.4 Supporting Information

General Information

Unless stated otherwise, all reactions and manipulations were performed under an N_2 atmosphere (< 0.1 ppm O_2, H_2O) through use of MBraun Unilab and GS MEGA Line gloveboxes, and standard Schlenk line techniques. All glassware was oven-dried (160 °C) overnight prior to use. PhH and DME were distilled from Na/benzophenone and stored over molecular sieves (3 Å). MeCN was distilled from CaH_2 and stored over molecular sieves (3 Å). *n*-Pentane was distilled from Na and stored over K. *n*-Hexane was purified using an MBraun SPS-800 system and stored over K. PhMe, Et_2O and THF were purified using an MBraun SPS-800 system and stored over molecular sieves (3 Å). EtOH was degassed and dried by standing over at least three sequential batches of molecular sieves (3 Å). C_6D_6 was distilled from K and stored over molecular sieves (3 Å). CD_3CN, CD_3OD and D_2O were used without purification. All reagents and starting materials were purchased from major suppliers. Liquids were degassed (if not supplied under inert atmosphere) but were otherwise used as supplied, unless stated otherwise. Bu_3SnH was supplied containing 0.05% BHT as stabilizer and was used as received. Bu_3SnOMe and PMHS were degassed and stored over molecular sieves (3 Å). PhBr was distilled and degassed. $(Bu_3Sn)_2O$, NEt_3 and BnBr were distilled, degassed, and stored over molecular sieves (3 Å). H_2O_2 (ca. 35%) was used as supplied. Solids were dried under vacuum (with the exception of paraformaldehyde and Na_2CO_3) but otherwise used as supplied, unless stated otherwise. P_4 was sublimed prior to use. P_5Ph_5 was prepared in accordance with the literature.[62]

NMR spectra were recorded at room temperature on Bruker Avance 400 (400 MHz) spectrometers and were processed using Topspin 3.2. Chemical shifts, δ, are reported in parts per million (ppm); ^{1}H NMR and ^{13}C NMR shifts are reported relative to $SiMe_4$ and were referenced internally to residual solvent peaks, while ^{31}P and ^{119}Sn NMR shifts were referenced externally to 85 % H_3PO_4 (aq.) and $SnMe_4$ (90% in C_6D_6), respectively. Except where stated otherwise, integrals for $^{31}P\{^{1}H\}$ and ^{31}P spectra are provided for the purposes of qualitative comparison only, and should not be considered quantitatively accurate. The abbreviations s, d, t, q, m are used to indicate singlets, doublets, triplets, quartets and multiplets, respectively.

Mass spectrometry was performed by the analytical department of the University of Regensburg using Jeol AccuTOF GCX and Agilent Q-TOF 6540 UHD spectrometers.

Reactions driven by light were performed using apparatus that has been illustrated in a previous publication,[21] in which reaction vessels are illuminated from beneath by LEDs while placed in a metal block through which cooling water is constantly circulated to maintain near-ambient temperature.

2.4.1 Hydrostannylation of P_4

2.4.1.1 Hydrostannylation of P_4 using Bu_3SnH under blue LED irradiation (0.01 mmol scale)

To a 10 mL, flat-bottomed, stoppered tube were added PhMe (500 µL), P_4 (0.01 mmol, as a stock solution in 79.6 µL PhH) and Bu_3SnH (16.1 µL, 0.06 mmol). The tube was sealed, placed in a water-cooled block to maintain near-ambient temperature, and irradiated with blue light (455 nm (±15 nm), 3.2 V, 700 mA, Osram OSLON SSL 80) for 18 h. The resulting mixture was analysed by ^{1}H, $^{31}P\{^{1}H\}$, ^{31}P and $^{119}Sn\{^{1}H\}$ NMR spectroscopy, as shown in Figures S1-4, below.

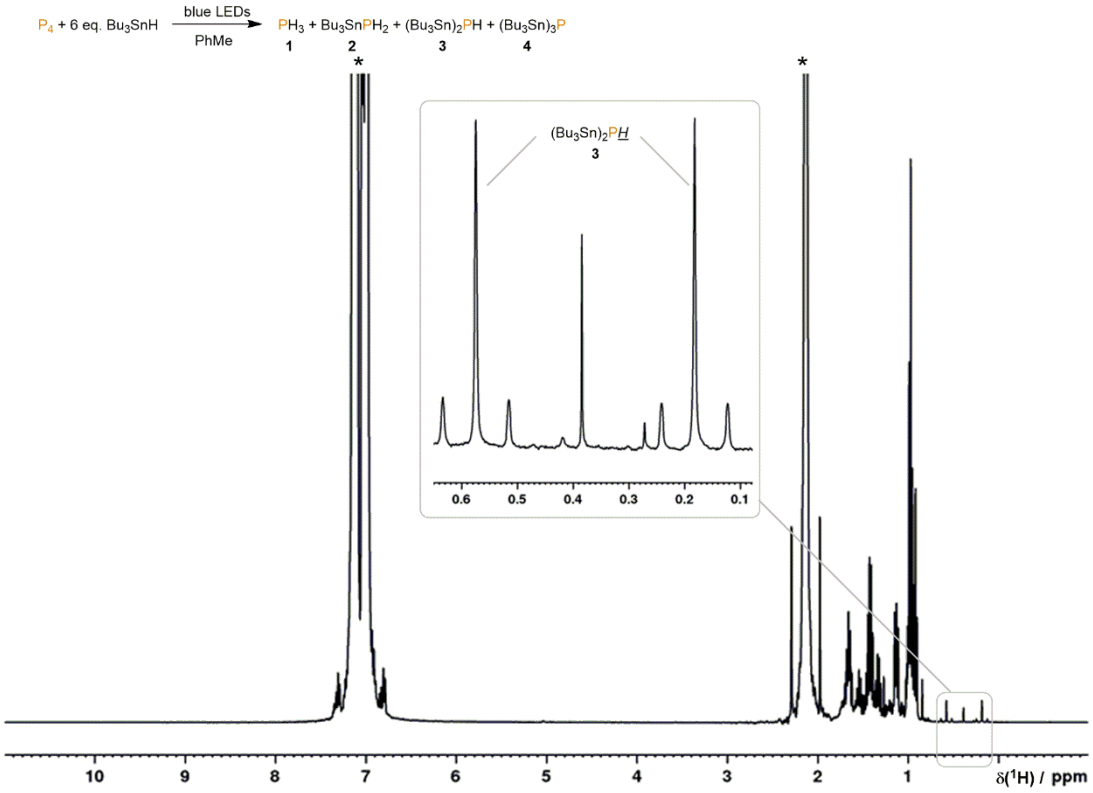

Figure S1. ^{1}H NMR spectrum for the photoreaction of P_4 with 6 eq. Bu_3SnH. The reaction was performed in PhMe and driven by 455 nm LED irradiation for 18 h prior to acquisition. Solvent resonances are marked with an asterisk and are truncated for clarity. The inset shows an expansion of the doublet resonance with $^{117/119}Sn$ satellites attributed to the PH moiety of $(Bu_3Sn)_2PH$ (**3**).

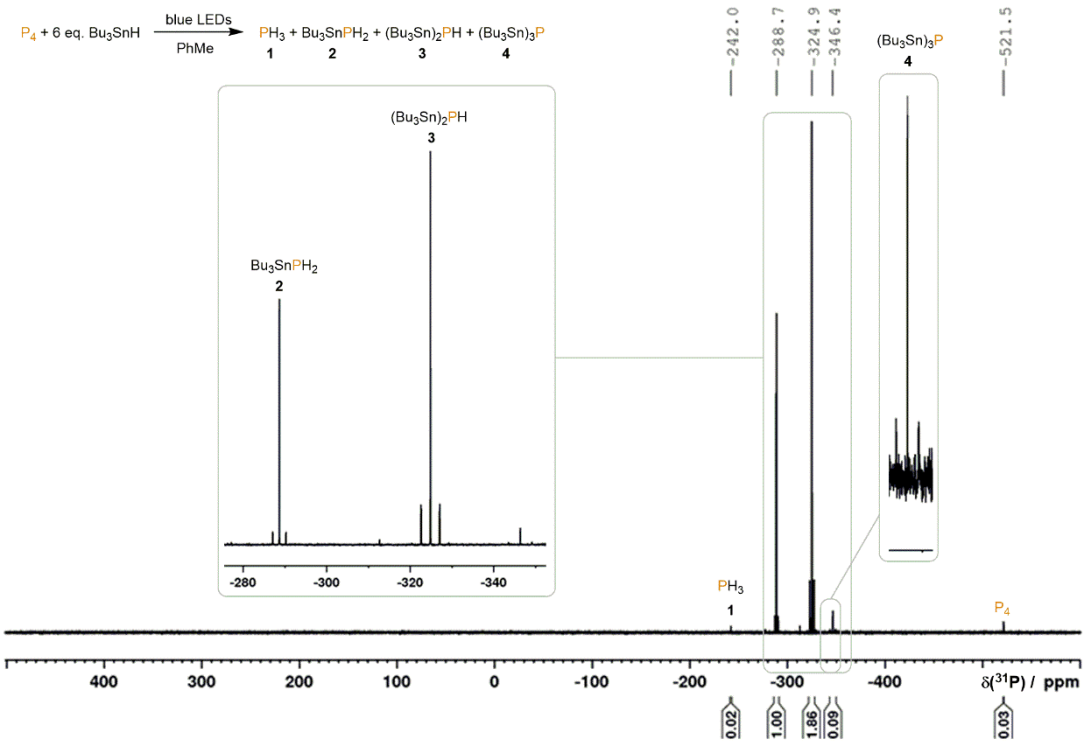

Figure S2. $^{31}P\{^{1}H\}$ NMR spectrum for the photoreaction of P_4 with 6 eq. Bu_3SnH. The reaction was performed in PhMe and driven by 455 nm LED irradiation for 18 h prior to acquisition. The insets show expansions of the signals attributed to Bu_3SnPH_2 (**2**) and $(Bu_3Sn)_2PH$ (**3**), and to $(Bu_3Sn)_3P$ (**4**), highlighting the presence of $^{117/119}Sn$ satellites.

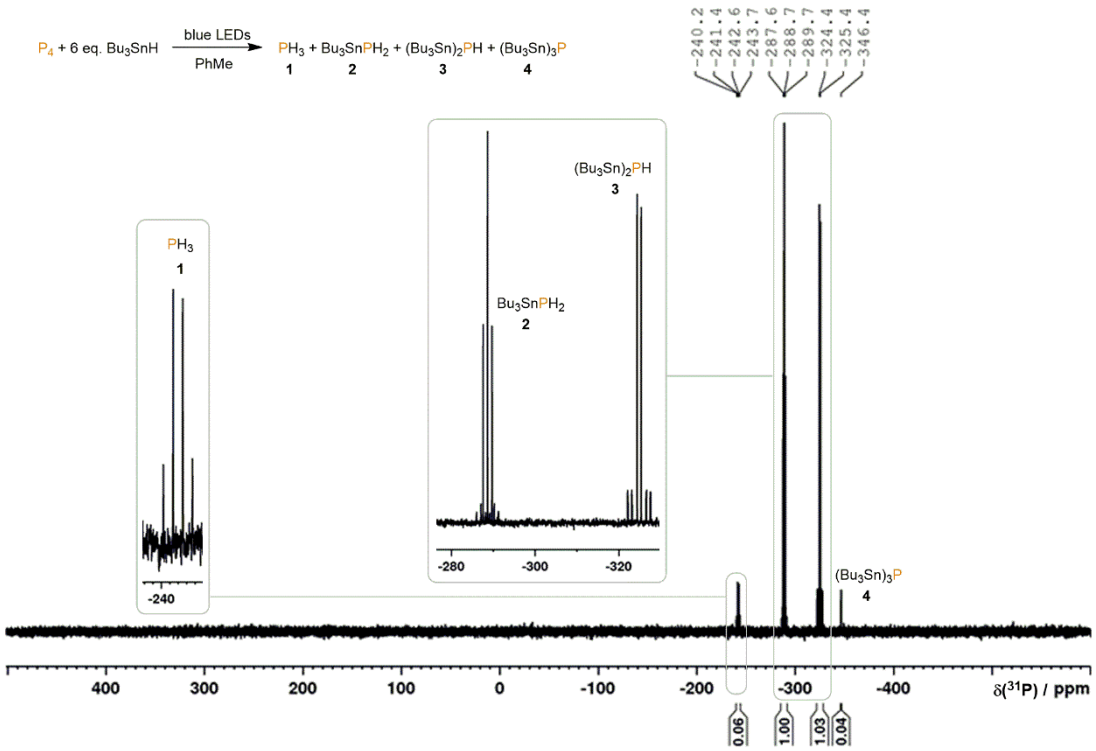

Figure S3. ^{31}P NMR spectrum for the photoreaction of P_4 with 6 eq. Bu_3SnH. The reaction was performed in PhMe and driven by 455 nm LED irradiation for 18 h. In this case, the reaction was performed in a sealed NMR tube fitted with a J. Young valve, to avoid loss of PH_3 (**1**) during manipulation. The insets show expansions of the signals attributed to PH_3 (**1**), and to Bu_3SnPH_2 (**2**) and $(Bu_3Sn)_2PH$ (**3**), highlighting their multiplicity due to $^{1}J(^{31}P\text{-}^{1}H)$ couplings.

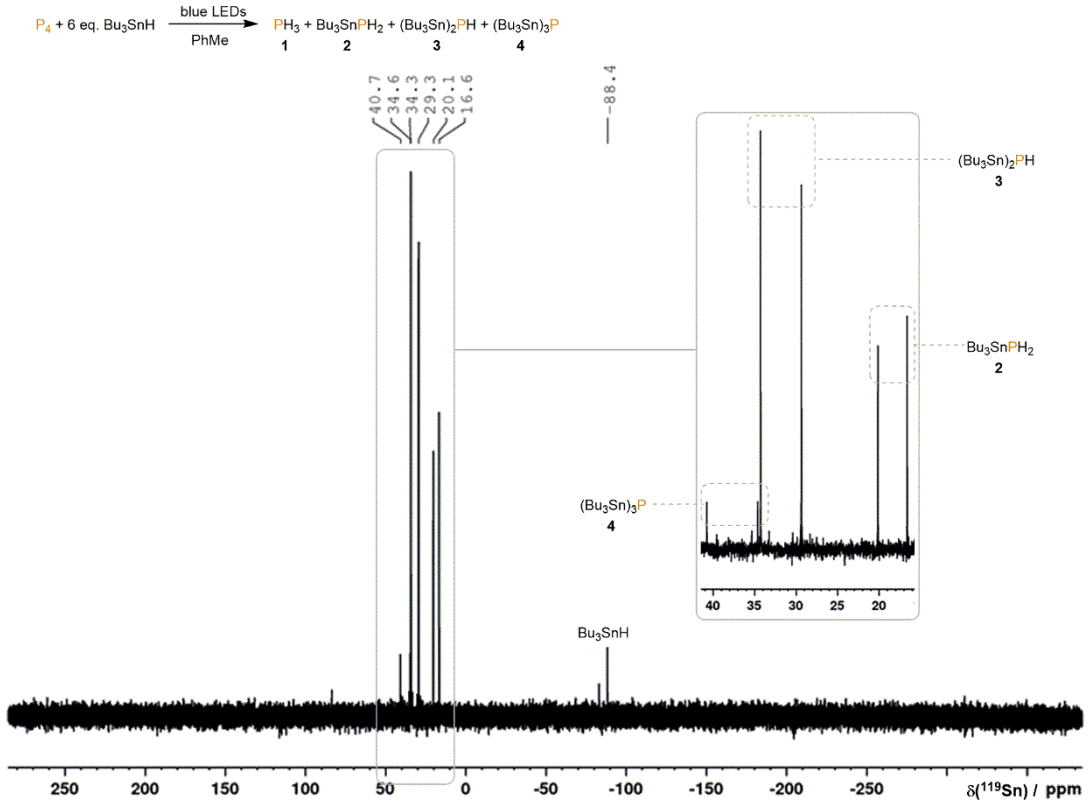

Figure S4. $^{119}Sn\{^{1}H\}$ NMR spectrum for the photoreaction of P_4 with 6 eq. Bu_3SnH. The reaction was performed in PhMe and driven by 455 nm LED irradiation for 18 h prior to acquisition. The inset highlights the doublets attributed to Bu_3SnPH_2 (**2**), $(Bu_3Sn)_2PH$ (**3**) and $(Bu_3Sn)_3P$ (**4**).

Of the four product resonances observed in the $^{31}P\{^{1}H\}$ spectrum, the most downfield is readily identified as belonging to PH_3 (**1**) on the basis of both chemical shift (–242.0 ppm) and the characteristic quartet splitting (with large $^{1}J(^{31}P\text{-}^{1}H)$ = 186.5 Hz) of the corresponding signal in the proton-coupled ^{31}P spectrum.[3] The remaining signals are consistent with the products $(Bu_3Sn)_xPH_{3-x}$ (x = 1-3; **2-4**, respectively), with larger x leading to increasingly upfield resonances. These assignments are consistent with the upfield chemical shifts reported for similar triorganotin-substituted phosphines,[37] with the multiplicities observed in the corresponding proton-coupled ^{31}P spectrum (as well as the magnitude of the $^{1}J(^{31}P\text{-}^{1}H)$ coupling constants), with the presence and relative intensities of observed $^{117/119}Sn$ satellites (as well as the magnitude of the corresponding coupling constants), and with the absence of any observable $^{31}P\text{-}^{31}P$ couplings. Spectra for analogous reactions performed using *n*-hexane, PhH, Et_2O, THF or DME in place of PhMe gave very similar NMR spectra. For illustration, the $^{31}P\{^{1}H\}$ spectra are shown in Figure S5, below.

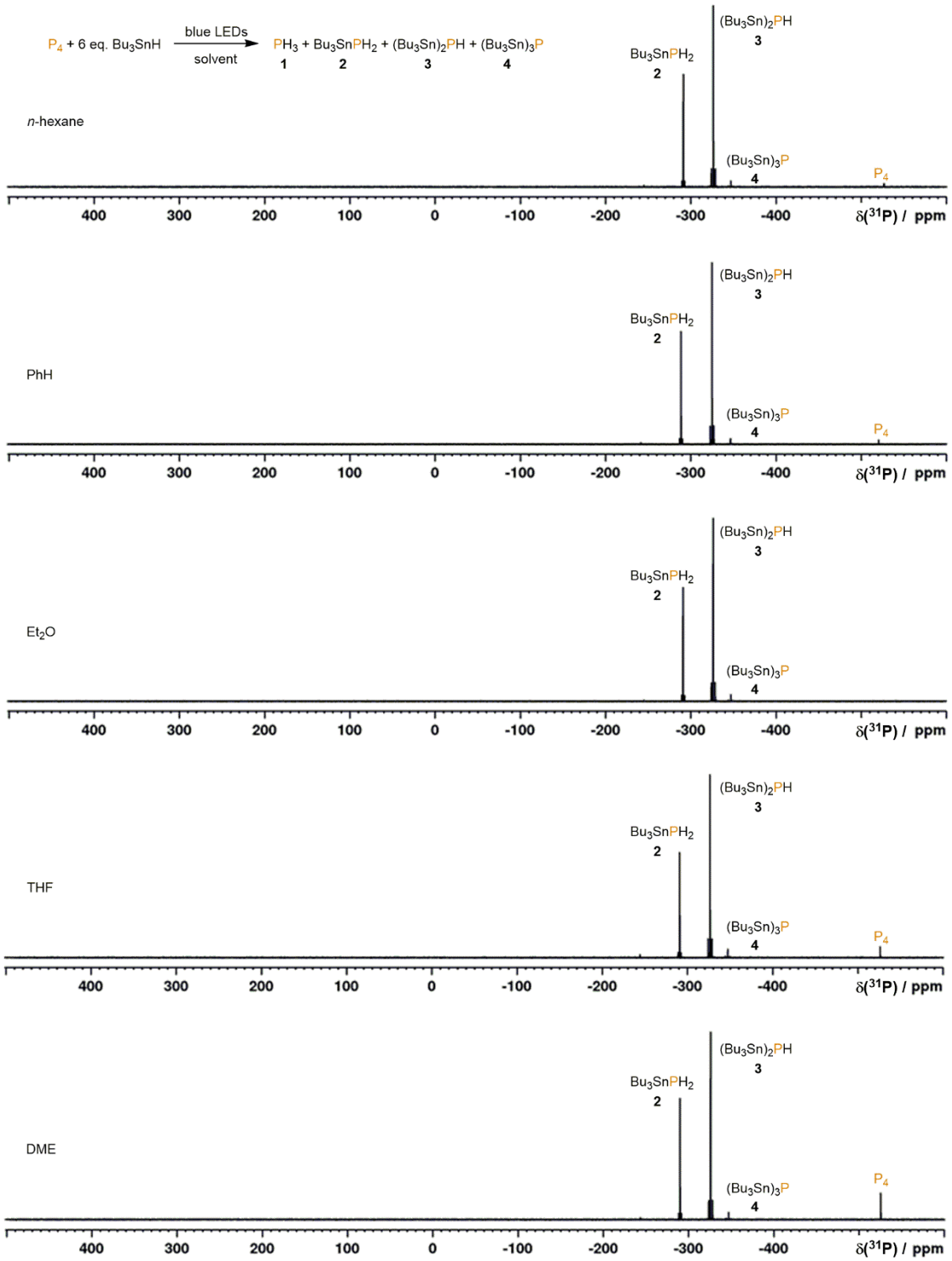

Figure S5. $^{31}P\{^{1}H\}$ NMR spectra for the photoreaction of P_4 with 6 eq. Bu_3SnH in various solvents. Reactions were otherwise identical to the example given in this section and were driven by 455 nm LED irradiation for 20 h.

2.4.1.2 Effect of wavelength on the hydrostannylation of P_4 using Bu_3SnH and LED irradiation (0.01 mmol scale)

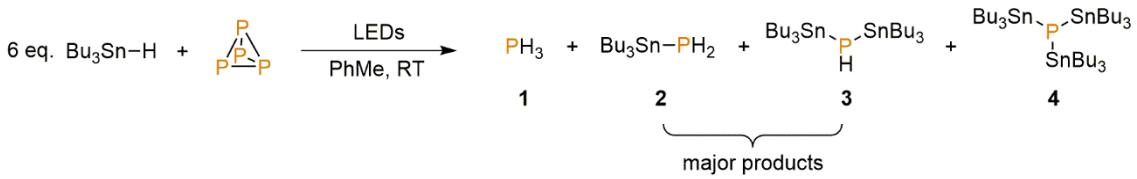

To 10 mL, flat-bottomed, stoppered tubes were added PhMe (500 µL), P_4 (0.01 mmol, as a stock solution in 86.0 µL PhH) and Bu_3SnH (16.1 µL, 0.06 mmol). The tubes were sealed, placed in a water-cooled block to maintain near-ambient temperature, and irradiated with blue light (455 nm (±15 nm), 3.2 V, 700 mA, Osram OSLON SSL 80) or near UV (365 nm) or green (528 nm) light of comparable intensity, for 45 minutes. The resulting mixtures were analysed by $^{31}P\{^1H\}$ spectroscopy, as shown in Figure S6, below.

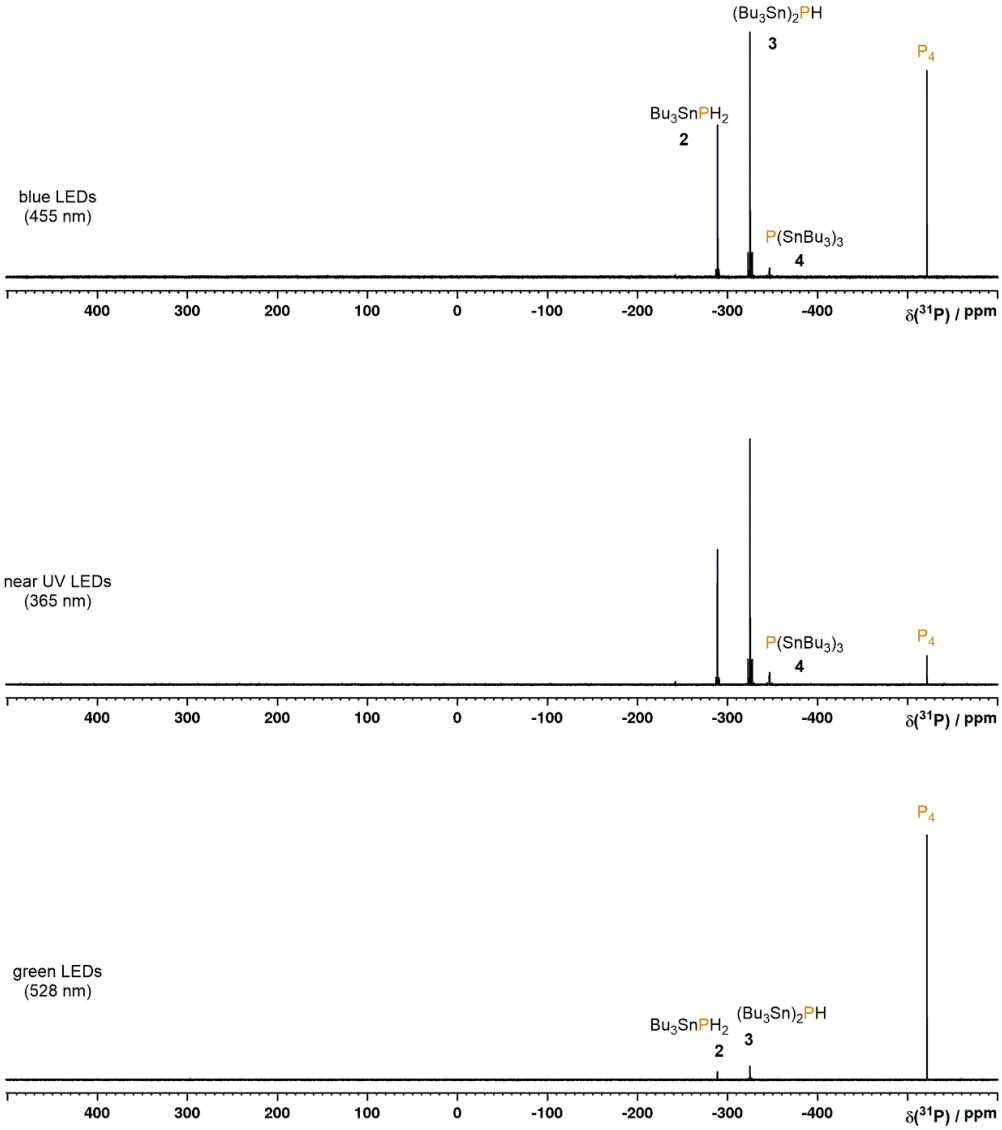

Figure S6. $^{31}P\{^1H\}$ NMR spectra for the reaction of P_4 and 6 eq. Bu_3SnH in PhMe, driven by LED irradiation at various wavelengths for 45 minutes.

The spectra clearly show that faster reactivity is observed using near UV LEDs than blue LEDs, which in turn give a significantly faster reaction than green LEDs. Based on these observations, as well as on the fact that none of the reaction components absorbs light appreciably in the visible region (including in the combined reaction mixture; Figure S7), we speculate that the observed photoreaction may not be driven by blue light *per se*, but rather by trace amounts of higher energy light being generated by the LED apparatus. Alternatively, Nakajima, Nemoto and colleagues have recently suggested that heavy atom-containing compounds may sometimes undergo direct S_0 to T_n photoexcitation at visible wavelengths, even if no appreciable absorption is observed at these frequencies in standard UV-vis experiments.[63]

Note also that, despite partial conversions, the spectra do not display any resonances other than those for the final products and starting material, suggesting an absence of stable intermediate products.

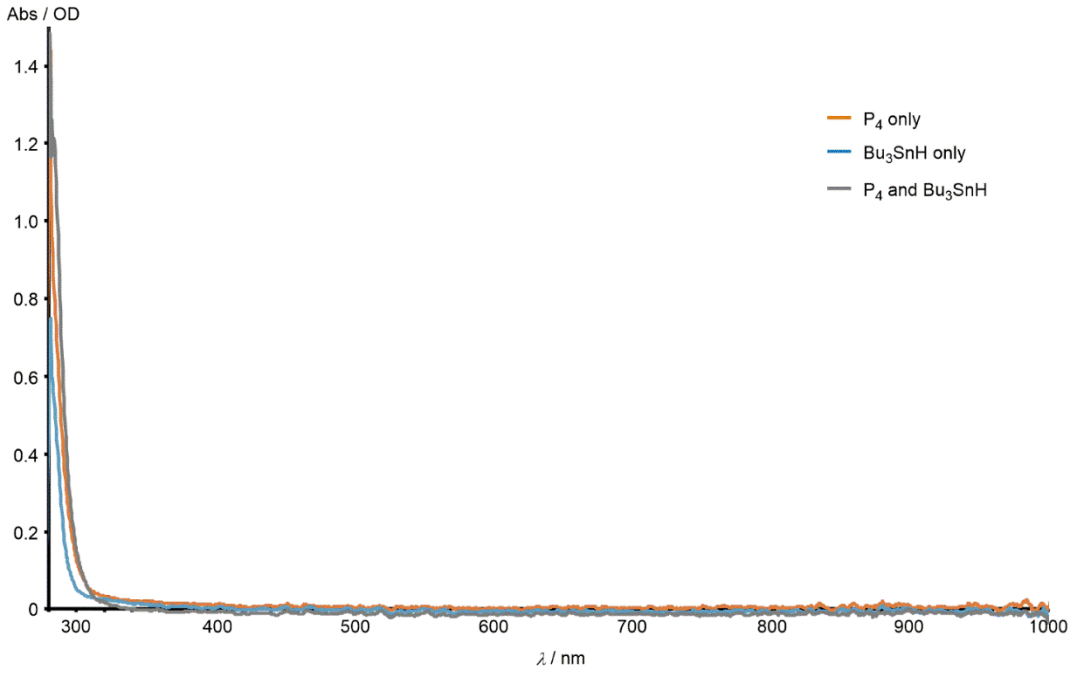

Figure S7. UV-vis spectra for solutions of P_4 (0.02 M) and/or Bu_3SnH (0.12) in PhMe. These concentrations correlate to those typically used in P_4 hydrostannylation reactions.

The precise mechanism(s) for initial photochemical generation of $Bu_3Sn\cdot$ radicals in this reaction (as indicated in Figure 2b) is a topic of ongoing investigation. However, previous studies into light-driven hydrostannylation reactions have suggested that initiation can proceed *via* initial photoinduced electron transfer from the relatively electron-rich tin hydride moiety to an electron-deficient substrate,[42] and an analogous pathway may be operative in this case, for example as illustrated in Scheme S1, below.

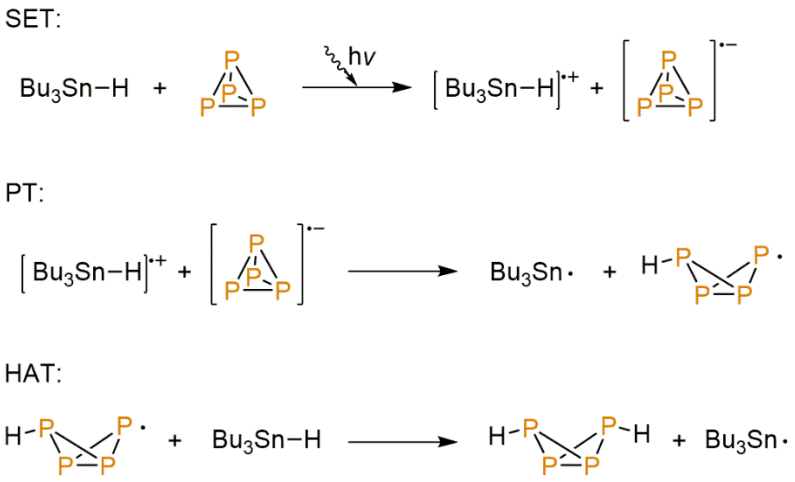

Scheme S1. A possible mechanism by which $Bu_3Sn\cdot$ radicals might be formed upon photoirradiation of a combination of Bu_3SnH and P_4, through a combination of photinduced single electron transfer (SET), proton transfer (PT) and hydrogen atom transfer (HAT) steps. Alternatively, the initial SET and PT steps could occur as a single, concerted, photoinduced HAT step.

2.4.1.3 Hydrostannylation of P_4 using Ph_3SnH under blue LED irradiation

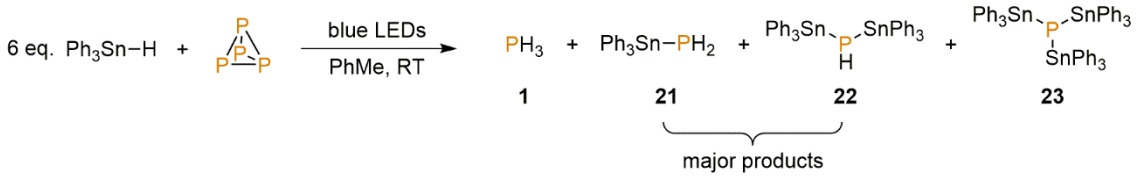

To a 10 mL, flat-bottomed, stoppered tube were added PhMe (500 µL), P_4 (0.01 mmol, as a stock solution in 77.4 µL PhH) and Ph_3SnH (21.1 mg, 0.06 mmol). The tube was sealed, placed in a water-cooled block to maintain near-ambient temperature, and irradiated with blue light (455 nm (±15 nm), 3.2 V, 700 mA, Osram OSLON SSL 80) for 18 h. The resulting mixture was analysed by ^{1}H, $^{31}P\{^{1}H\}$, ^{31}P and $^{119}Sn\{^{1}H\}$ NMR spectroscopy, as shown in Figures S8-11, below.

Compared to the analogous reaction using Bu_3SnH (Figures S2 and S3), a more appreciable amount of unreacted P_4 was seen to remain at the end of the reaction, although it remains a minor component of the mixture. Analysis of the $^{119}Sn\{^{1}H\}$ spectrum suggests this is probably due to competing generation of the distannane Sn_2Ph_6,[64-66] which could arise through dimerisation of $Ph_3Sn^{\bullet}$ radicals. Alternatively, this could be due to direct reaction of Ph_3SnH with stannylated (oligo)phosphorus species to generate new Sn–Sn and P–H bonds. Such reactions have precedent in the literature,[67] and are expected to be more facile for Ph_3SnH than Bu_3SnH. It must be noted, however, that direct addition of a further 6 eq. of Ph_3SnH at the end of the reaction was not observed to lead to any change in the $^{31}P\{^{1}H\}$ NMR spectrum of the product mixture, even after 24 h (similarly, no change was observed upon addition of further Bu_3SnH to the analogous reaction mixture produced using Bu_3SnH). The final reaction products $(Ph_3Sn)_xPH_{3-x}$ (x = 1, **21**; x = 2, **22** ; x = 3, **23**) thus do not seem to participate in such reactivity (at least under the relevant reaction conditions).

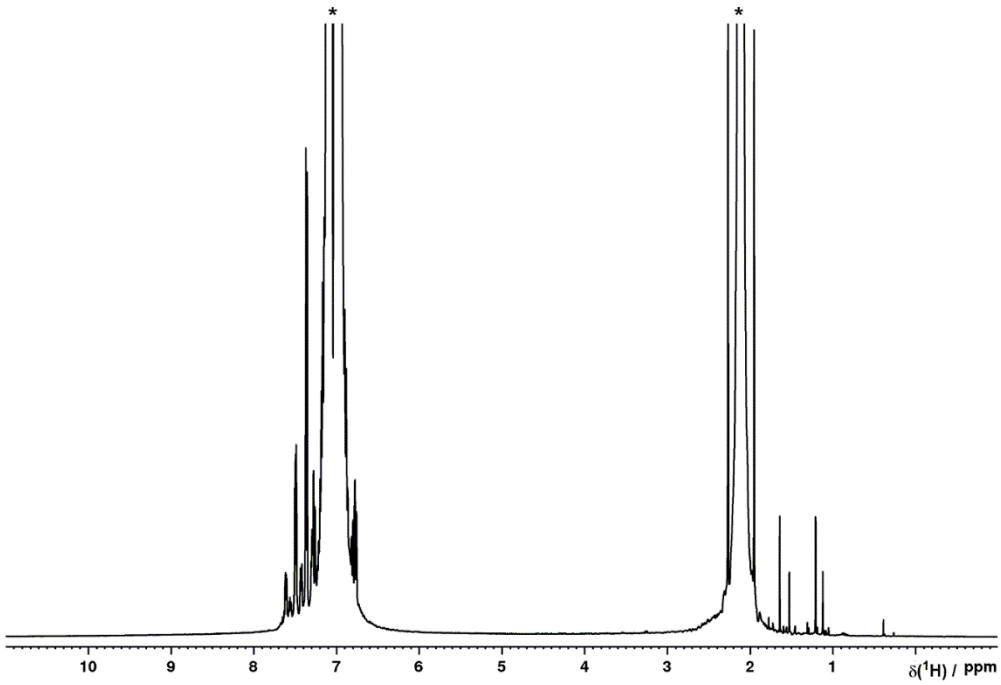

Figure S8. ^{1}H NMR spectrum for the reaction of P_4 and 6 eq. Ph_3SnH in PhMe, driven by 455 nm LED irradiation for 18 h. Solvent resonances (*) truncated for clarity.

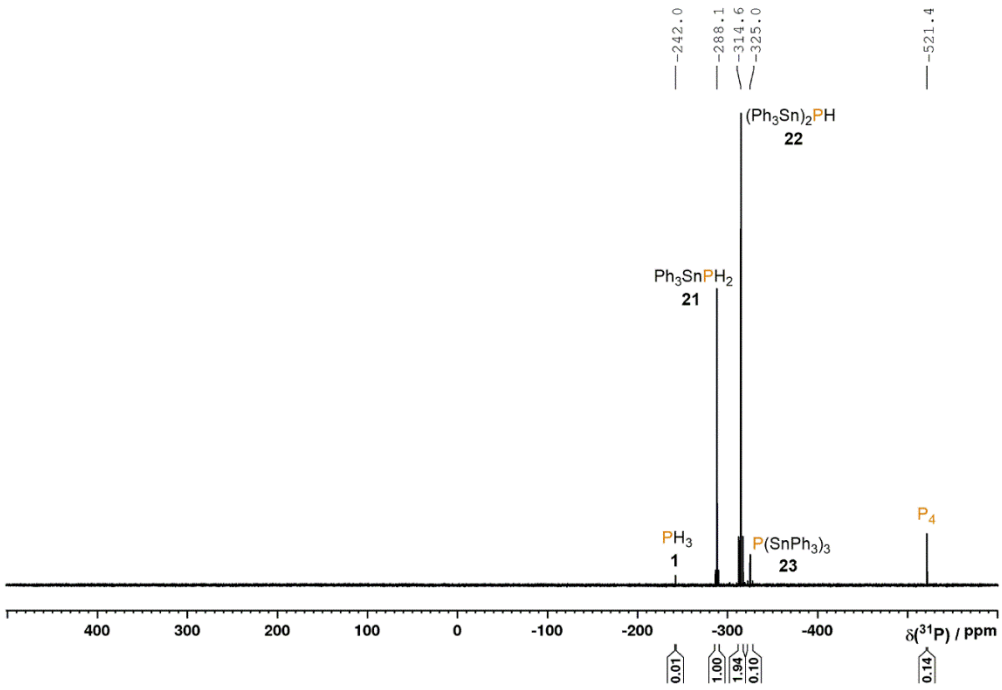

Figure S9. $^{31}P\{^{1}H\}$ NMR spectrum for the reaction of P_4 and 6 eq. Ph_3SnH in PhMe, driven by 455 nm LED irradiation for 18 h.

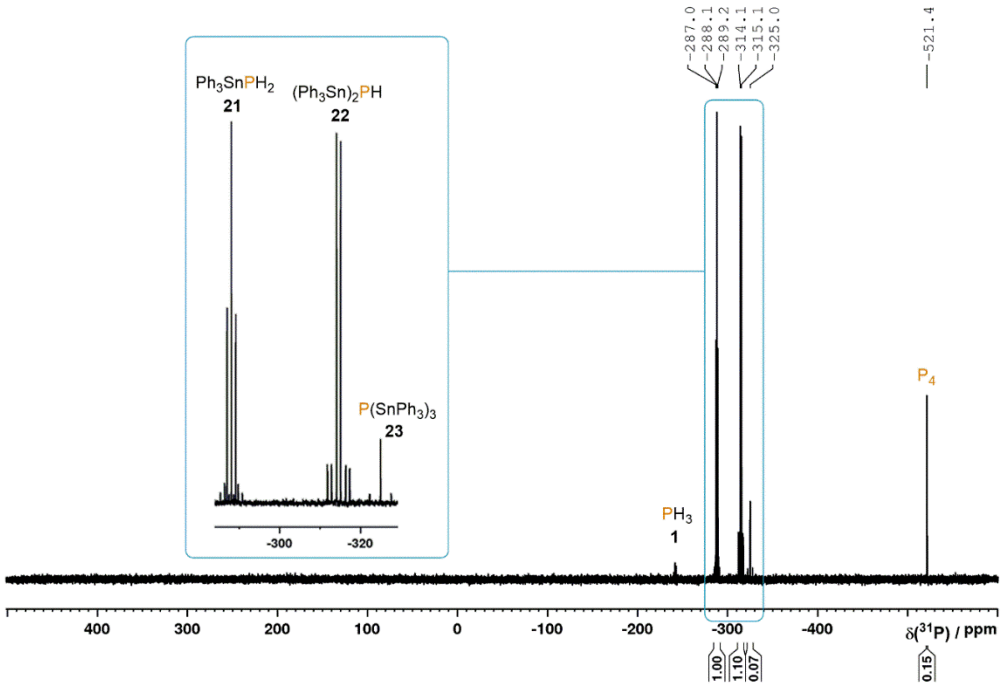

Figure S10. ^{31}P NMR spectrum for the reaction of P_4 and 6 eq. Ph_3SnH in PhMe, driven by 455 nm LED irradiation for 18 h.

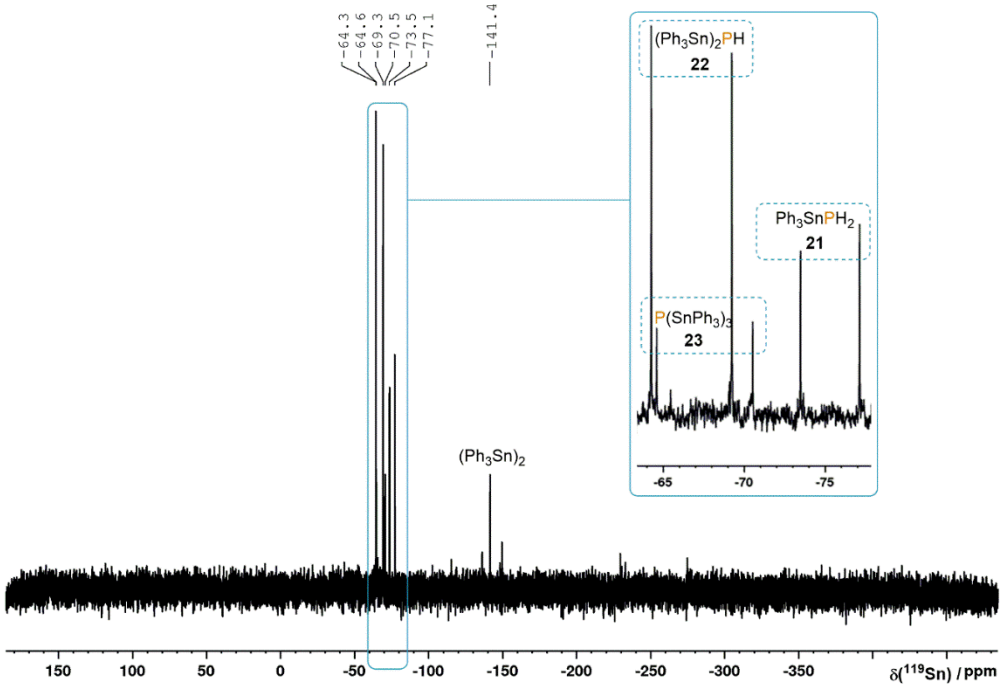

Figure S11. $^{119}Sn\{^1H\}$ NMR spectrum for the reaction of P_4 and 6 eq. Ph_3SnH in PhMe, driven by 455 nm LED irradiation for 18 h.

Table 1. Selected NMR parameters for compounds $(Ph_3Sn)_xPH_{3-x}$ (extracted from Figures S9-11).

	Ph_3SnPH_2 (**21**)	$(Ph_3Sn)_2PH$ (**22**)	$P(SnPh_3)_3$ (**23**)
$\delta(^{31}P)$ / ppm	–288.1	–314.6	–325.0
$\delta(^{119}Sn)$ / ppm	–75.3	–66.8	–67.6
$^1J(^{31}P\text{-}^1H)$ / Hz	173	162	-
$^1J(^{119}Sn\text{-}^{31}P)$ / Hz	545	741	883

2.4.1.4 Hydrostannylation of P_4 using Bu_3SnH under blue LED irradiation (0.5 mmol scale), and isolation and stability of Bu_3SnPH_2 (2) and $(Bu_3Sn)_2PH$ (3)

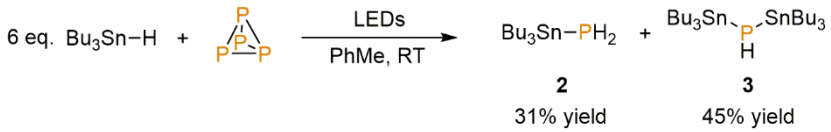

To a 50 mL flat-bottomed Schlenk tube were added P_4 (61.5 mg, 0.5 mmol) and PhMe (25 mL). After stirring to obtain a homogeneous solution Bu_3SnH was added (801 µL, 3.0 mmol). The resulting homogeneous, colourless solution was stirred under irradiation with blue LED light (7X Osram OSLON SSL80, 455 nm (±15 nm), 20.3 V 1000mA) for 18 h, during which time the Schlenk tube was placed in a block cooled by circulating water to maintain near-ambient temperature. Following removal of PhMe under vacuum, the major reaction products were separated by distillation under vacuum (*ca.* 105 °C, 10^{-2} mbar). Bu_3SnPH_2 (**2**) was collected as the volatile fraction (200 mg, 31%) as a colourless oil. $(Bu_3Sn)_2PH$ (**3**) remained as the non-volatile fraction (555 mg, 45%), which was also collected as a colourless oil.

The $(Bu_3Sn)_2PH$ (**3**) isolated in this manner is typically found to be *ca.* 90% pure (as assessed by $^{31}P\{^1H\}$ NMR spectroscopy), containing minor amounts of Bu_3SnPH_2 (**2**) and/or $P(SnBu_3)_3$ (**4**). Note that the yields and purities obtained for the individual major products are highly dependent on the conditions (temperature and duration) used during the distillation step. If performed too slowly, or at especially high temperature, significant scrambling of the substituents on the P atoms can be observed. This leads to reduced purity of the $(Bu_3Sn)_2PH$ product, due to increased contamination with $P(SnBu_3)_3$. At the same time, this can increase the yield of isolated Bu_3SnPH_2 (which remains clean if kept cold), as more of this compound is formed during scrambling of $(Bu_3Sn)_2PH$. To obtain good yields and purities of both products it is recommended to use as high a vacuum as possible during distillation. For example, using a significantly higher vacuum of *ca.* 10^{-5} mbar allows for a significantly lower distillation temperature (*ca.* 70 °C).

Slow scrambling (over the course of several days) is also observed at room temperature for isolated samples of both products (which suggests that these are kinetic products of the hydrostannylation reaction, with the thermodynamic products being PH_3 and $P(SnBu_3)_3$, presumably due to loss of the former as a gas). However, both are stable for extended periods (at least several months) if stored at –35 °C.

*For Bu_3SnPH_2 (**2**):*

^{1}H NMR (400 MHz, 300 K, C_6D_6): δ = 1.63-1.41 (2H, m), 1.38-1.22 (2H, m), 1.07-0.84 ppm (5H, m). **$^{31}P\{^1H\}$ NMR** (121 MHz, 300 K, C_6D_6): δ = –288.4 ppm (s). **^{31}P NMR** (121 MHz, 300 K, CD_3CN) : δ = –288.4 ppm (t, $^1J(^{31}P\text{-}^1H)$ = 171 Hz). **$^{119}Sn\{^1H\}$** (149 MHz, 300 K, C_6D_6) δ = 18.2 ppm (d, $^1J(^{31}P\text{-}^{119}Sn)$ = 522 Hz). **$^{13}C\{^1H\}$ NMR** (101 MHz, 300 K, C_6D_6): δ = 29.4 (s), 27.1 (s), 13.5 (s) 11.8 ppm (d, $J(^{31}P\text{-}^{13}C)$ = 3.5 Hz).

Analysis of Bu_3SnPH_2 by mass spectrometry has thus far only revealed molecular ion peaks attributable to $(Bu_3Sn)_2PH$ (see below), which we attribute to rapid scrambling in the instrument during the experiment. Similar NMR data have been reported previously for the related compound Me_3SnPH_2.[36]

*For $(Bu_3Sn)_2PH$ (**3**):*

^{1}H NMR (400 MHz, 300 K, C_6D_6): δ = 1.84-1.53 (12H, m), 1.53-1.33 (12H, m), 1.32-1.04 (12H, m), 1.02-0.86 (18H, m), 0.43 ppm (1H, d, $^1J(^{31}P\text{-}^1H)$ = 158 Hz). **^{31}P{^{1}H} NMR** (121 MHz, 300 K, C_6D_6): δ = –324.8 ppm (s). **^{31}P NMR** (121 MHz, 300 K, CD_3CN) : δ = –324.8 ppm (d, $^1J(^{31}P\text{-}^1H)$ = 158 Hz). **^{119}Sn{^{1}H}** (149 MHz, 300 K, C_6D_6) δ = 31.7 ppm (d, $^1J(^{31}P\text{-}^{119}Sn)$ = 731 Hz). **^{13}C{^{1}H} NMR** (101 MHz, 300 K, C_6D_6): δ = 29.5 (d, $J(^{31}P\text{-}^{13}C)$ = 0.9 Hz), 27.4 (s), 13.6 (s), 13.2 ppm (d, $J(^{31}P\text{-}^{13}C)$ = 0.9 Hz). **MS** (EI, PhMe): *m/z* = 612.2053 (M^+).

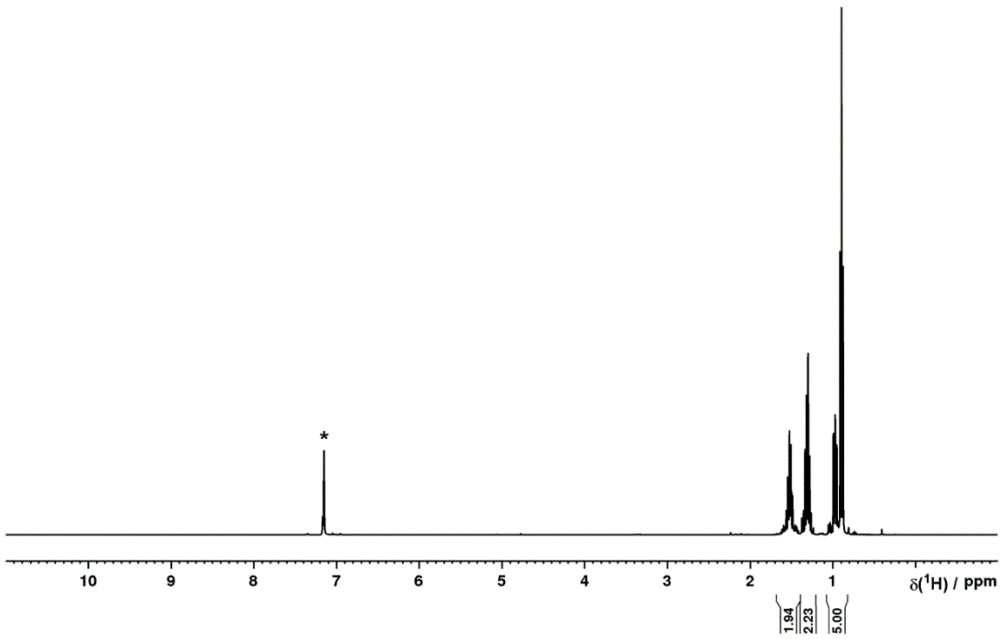

Figure S12. ^{1}H NMR spectrum of Bu_3SnPH_2 (**2**) in C_6D_6 (*).

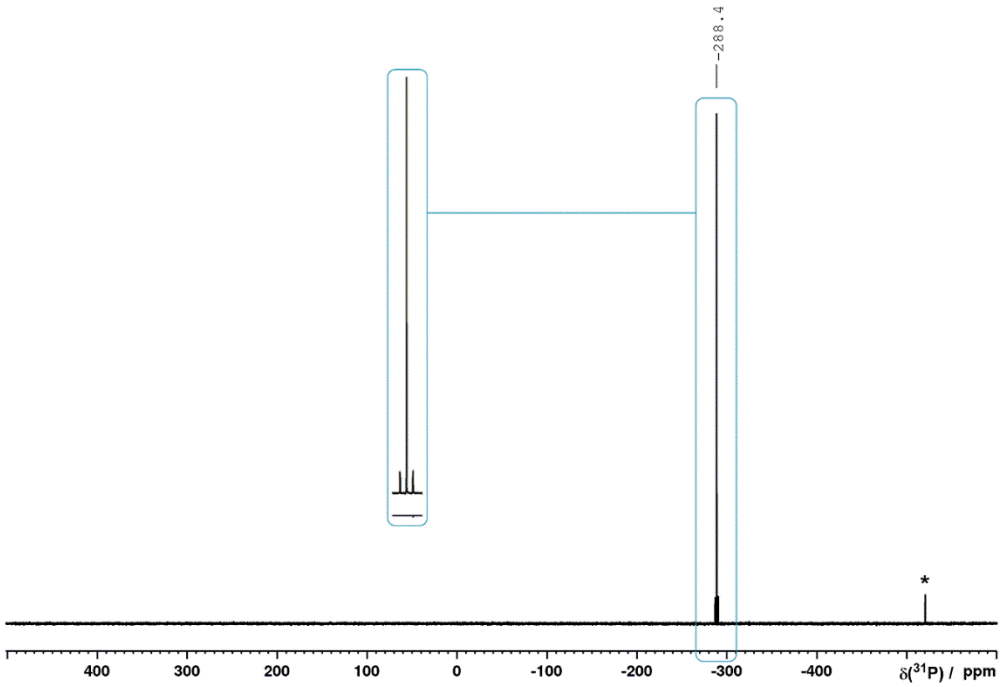

Figure S13. $^{119}Sn\{^{1}H\}$ NMR spectrum for the reaction of P_4 and 6 eq. Ph_3SnH in PhMe, driven by 455 nm LED irradiation for 18 h.

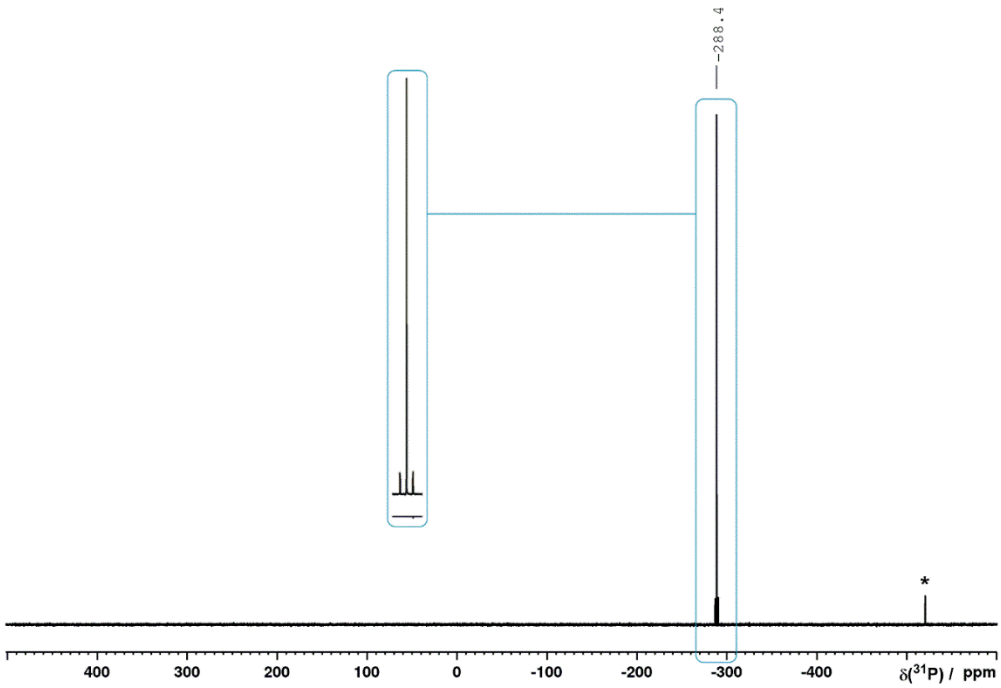

Figure S14. $^{31}P\{^{1}H\}$ NMR spectrum of Bu_3SnPH_2 (**2**) in C_6D_6 (*trace residual P_4).

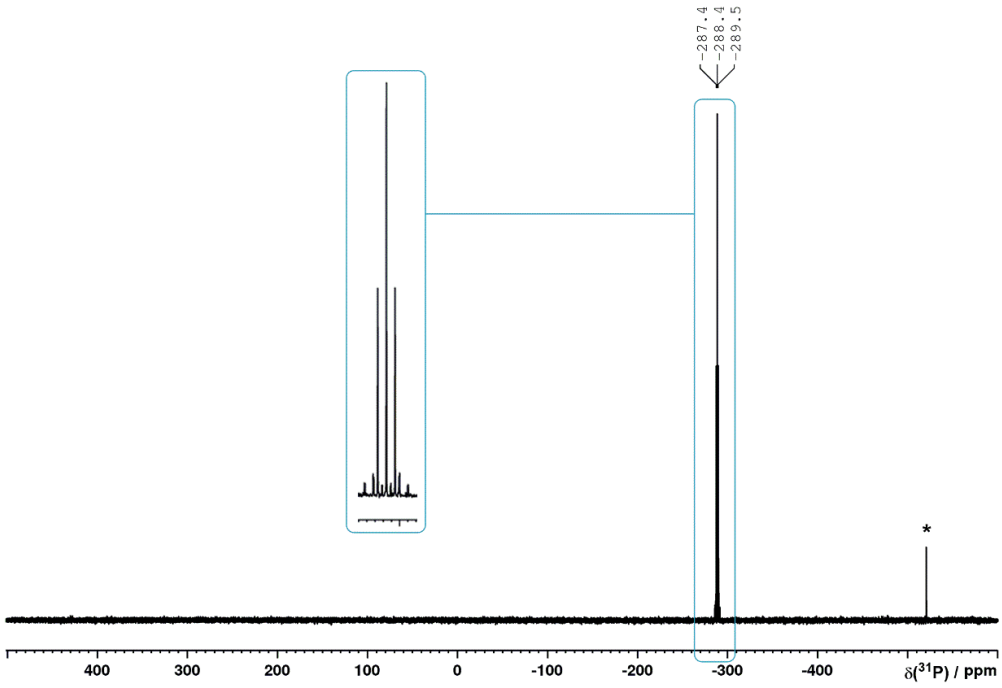

Figure S15. ^{31}P NMR spectrum of Bu_3SnPH_2 (**2**) in C_6D_6 (*trace residual P_4).

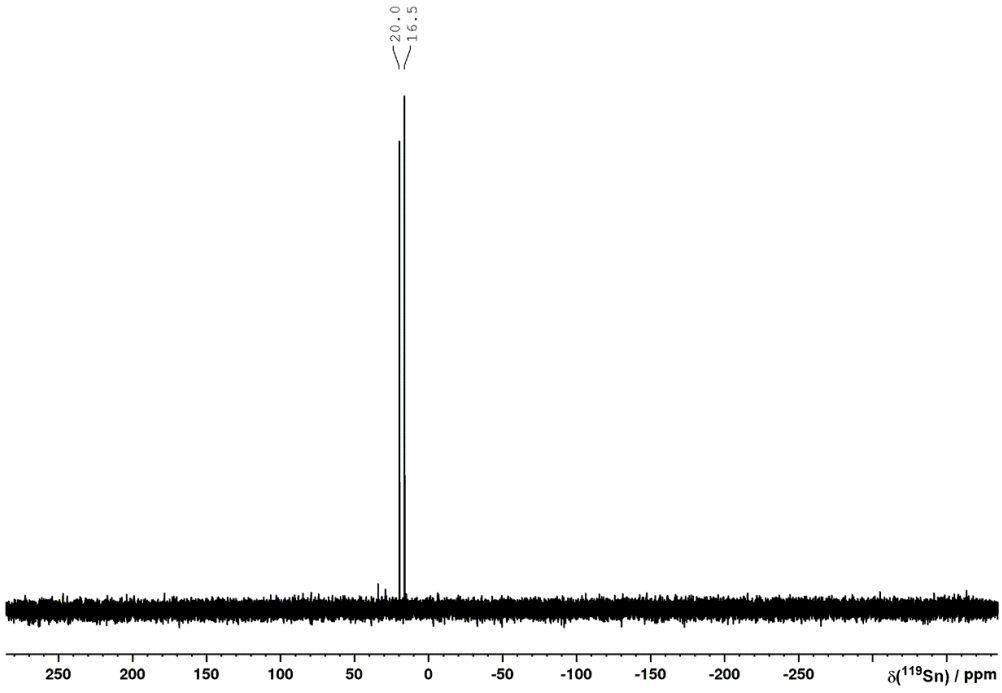

Figure S16. $^{119}Sn\{^1H\}$ NMR spectrum of Bu_3SnPH_2 (**2**) in C_6D_6.

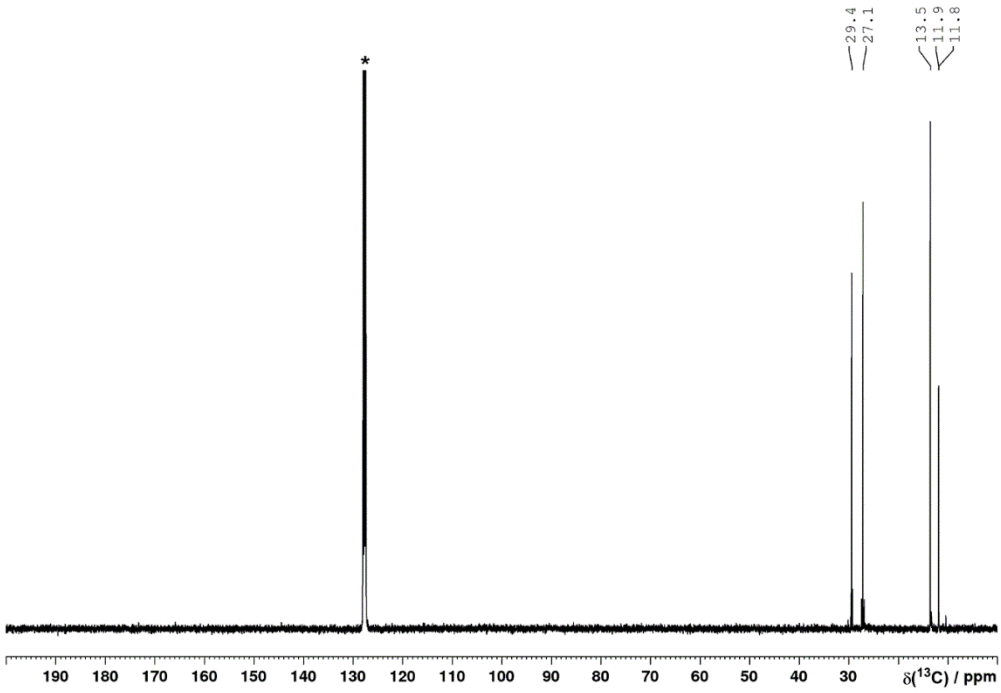

Figure S17. $^{13}C\{^{1}H\}$ NMR spectrum of Bu_3SnPH_2 (**2**) in C_6D_6. Solvent resonance (*) truncated for clarity.

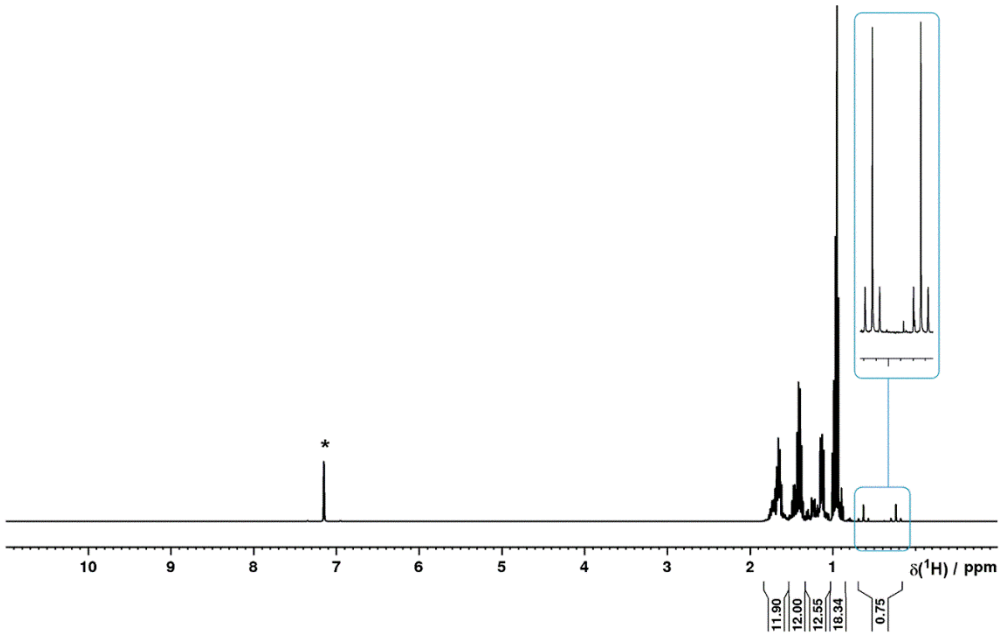

Figure S18. ^{1}H NMR spectrum of $(Bu_3Sn)_2PH$ (**3**) in C_6D_6 (*).

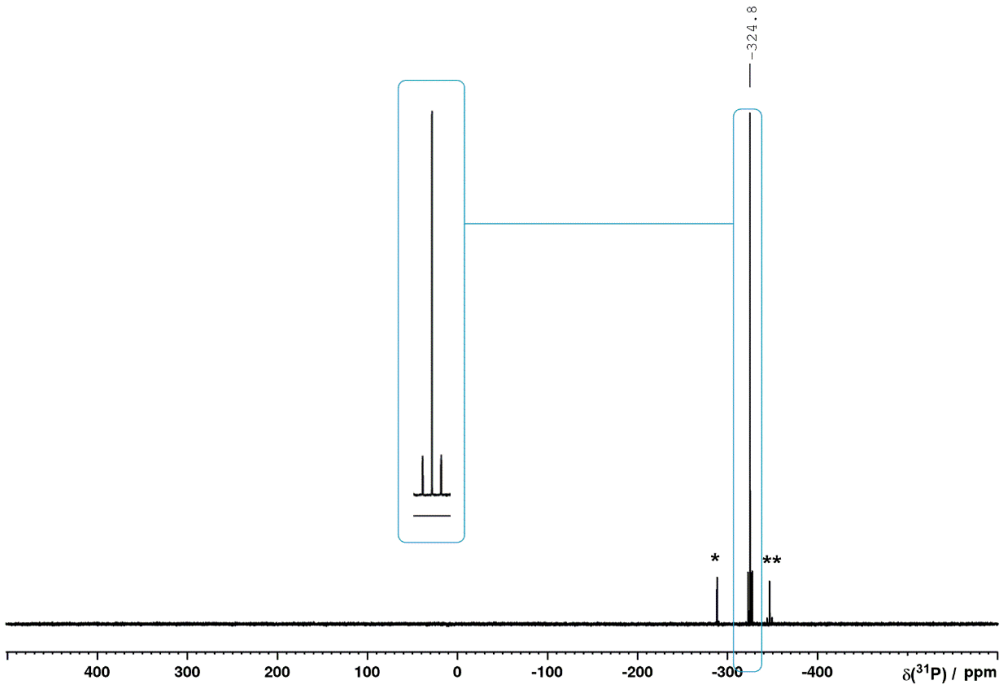

Figure S19. $^{31}P\{^{1}H\}$ NMR spectrum of $(Bu_3Sn)_2PH$ (**3**) in C_6D_6, also containing minor Bu_3SnPH_2 (*) and $P(SnBu_3)_3$ (**).

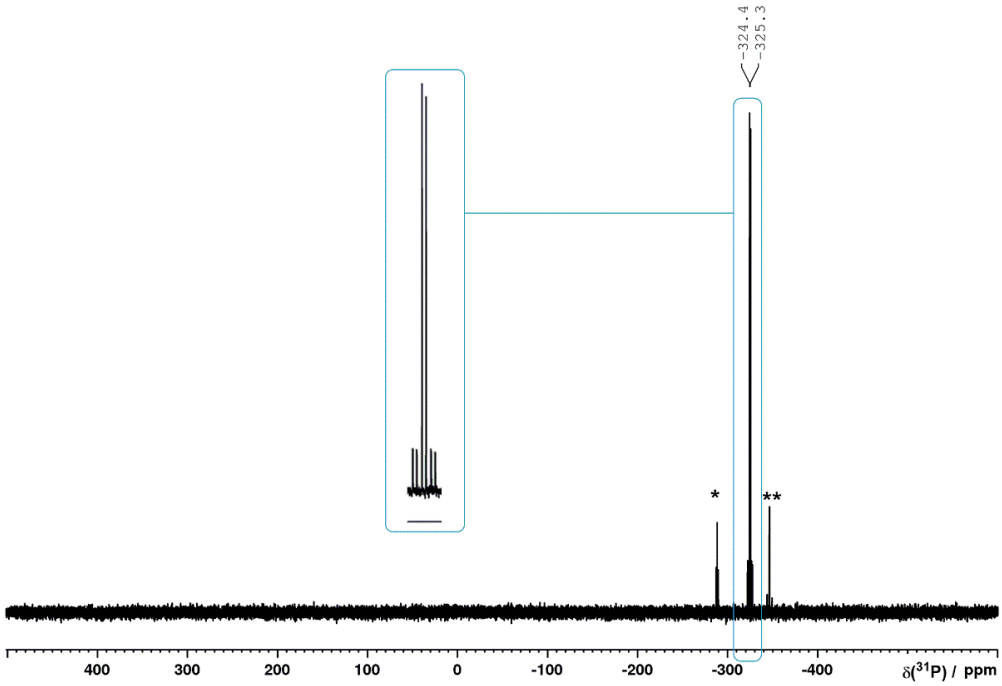

Figure S20. ^{31}P NMR spectrum of $(Bu_3Sn)_2PH$ (**3**) in C_6D_6, also containing minor Bu_3SnPH_2 (*) and $P(SnBu_3)_3$ (**).

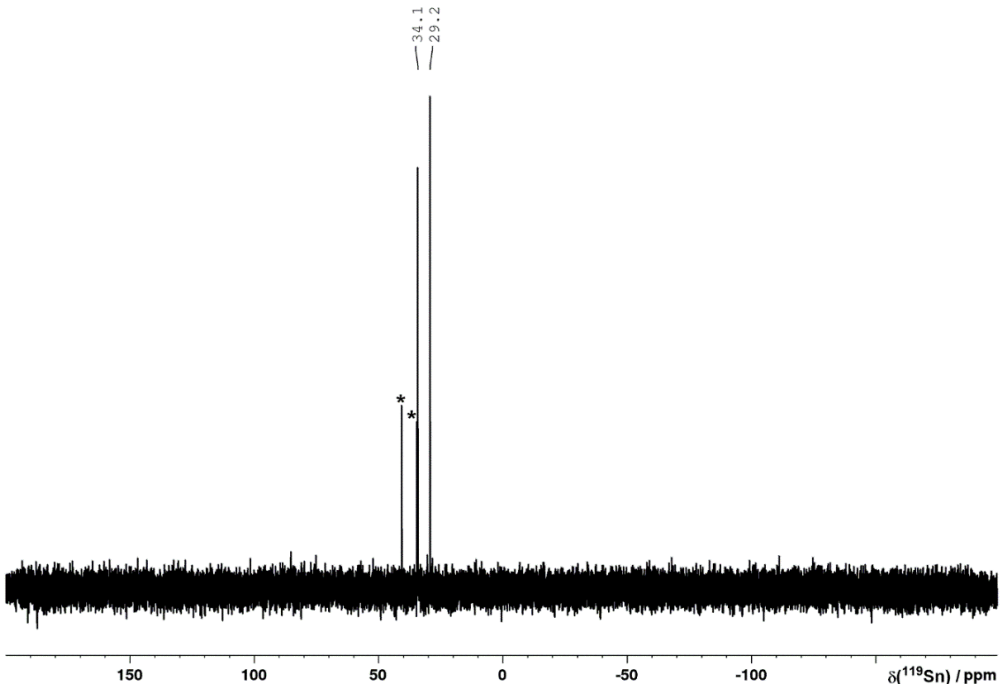

Figure S21. $^{119}Sn\{^{1}H\}$ NMR spectrum of $(Bu_3Sn)_2PH$ (**3**) in C_6D_6, also containing minor $P(SnBu_3)_3$ (*).

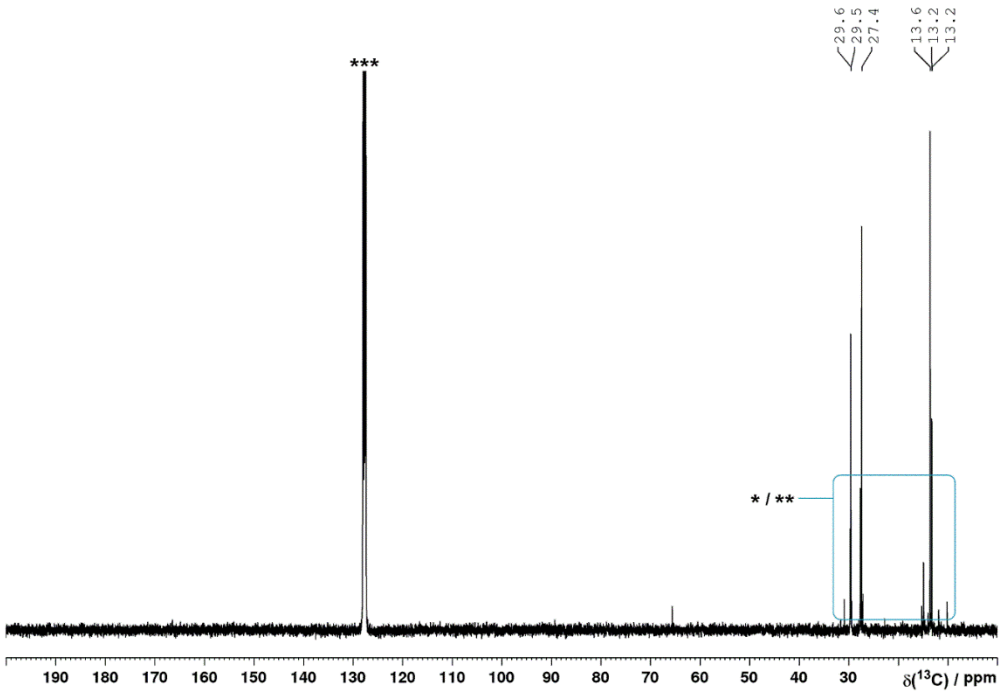

Figure S22. $^{13}C\{^{1}H\}$ NMR spectrum of $(Bu_3Sn)_2PH$ (**3**) in C_6D_6, also containing minor Bu_3SnPH_2 (*) and $P(SnBu_3)_3$ (**). Solvent resonance (***) truncated for clarity.

2.4.1.5 Air-stability of the products $(Bu_3Sn)_xPH_{3-x}$ (x = 1-3)

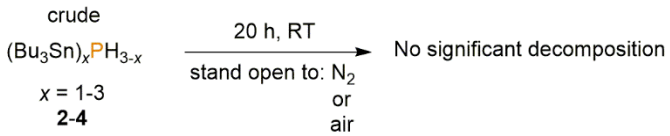

To a pair of 10 mL, flat-bottomed, stoppered Schlenks were added PhMe (500 µL), P_4 (0.01 mmol, as a stock solution in 86.0 µL PhH) and Bu_3SnH (16.1 µL, 0.06 mmol). The tubes was sealed,

placed in a water-cooled block to maintain near-ambient temperature, and irradiated with blue light (455 nm (±15 nm), 3.2 V, 700 mA, Osram OSLON SSL 80) for 18 h. Volatiles were then removed under vacuum to give identical colourless oils. One Schlenk was back-filled with dry N_2 and sealed. The other was back-filled with air and left open to the atmosphere. Both tubes were left to stand for 20 h. Dry, degassed PhMe (500 µL) was then added to both, followed by Ph_3PO (0.02 mmol, as a stock solution in 245 µL MeCN) to act as in internal standard for $^{31}P\{^1H\}$ NMR spectroscopy. The resulting solutions were analysed by $^{31}P\{^1H\}$ NMR spectroscopy, as shown in Figure S23, below. The spectra show no appreciable difference between the two samples, indicating that the Bu_3Sn-substituted phosphine products are all appreciably air-stable.

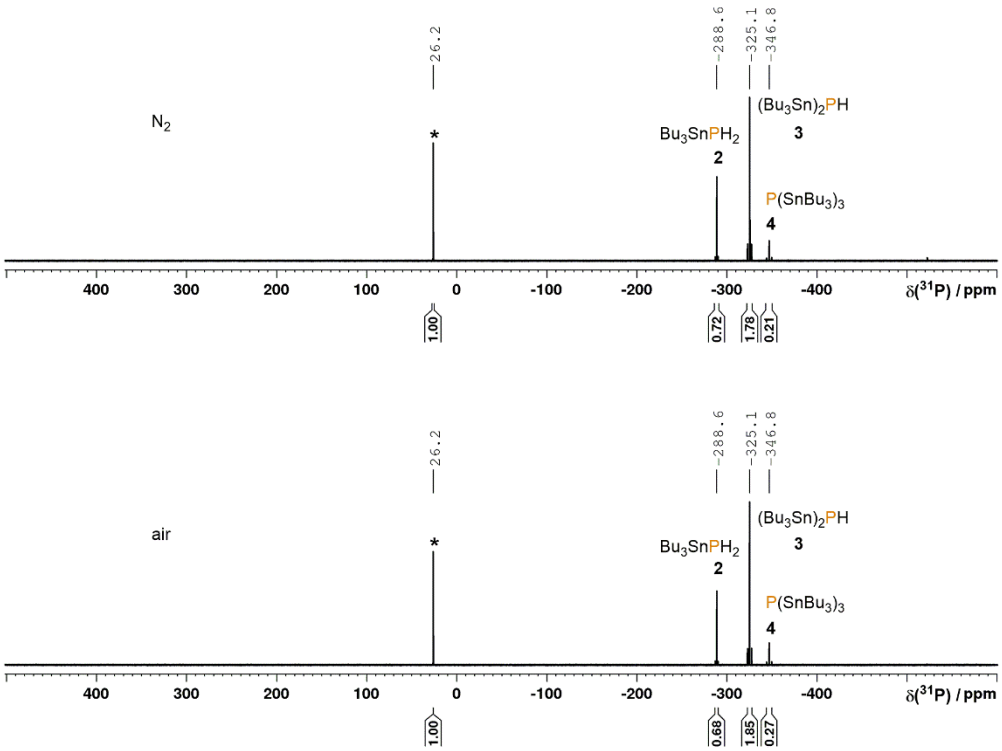

Figure S23. $^{31}P\{^1H\}$ NMR spectra in PhMe of a crude P_4 hydrostannylation mixture, after standing neat overnight under N_2 or under air. Spectra acquired in PhMe, also containing Ph_3PO (*) as an internal standard.

2.4.1.6 Hydrostannylation of P_4 using Bu_3SnH initiated by AIBN (0.01 mmol scale)

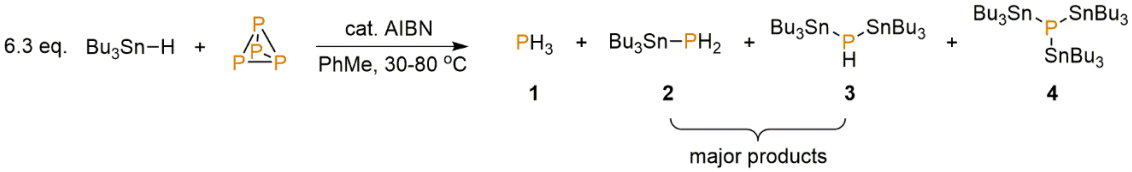

To a 10 mL, flat-bottomed, stoppered tube were added PhMe (500 µL), P_4 (0.01 mmol, as a stock solution in 77.4 µL PhH), AIBN (0.001 mmol, as a stock solution in 49.3 µL PhH) and Bu_3SnH (16.9 µL, 0.063 mmol). The tube was sealed, wrapped in Al foil to exclude light, and heated to 30 °C for 18 h. The resulting mixture was analysed by $^{31}P\{^1H\}$ NMR spectroscopy, as shown in Figure S24, below.

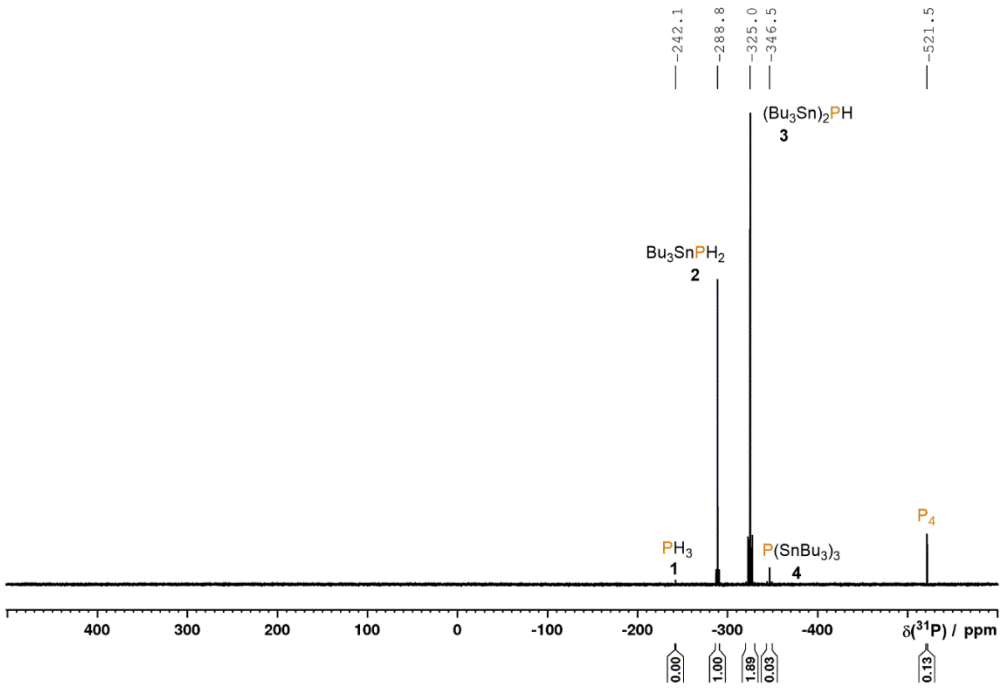

Figure S24. $^{31}P\{^{1}H\}$ NMR spectrum for the reaction of P_4 and 6.3 eq. Bu_3SnH in PhMe, driven by AIBN initiation (2.5 mol% per P) at 30 °C for 18 h.

Otherwise equivalent reactions could be driven to completion with shorter reaction times or reduced catalyst loadings by using elevated temperatures (Figures S25-28).

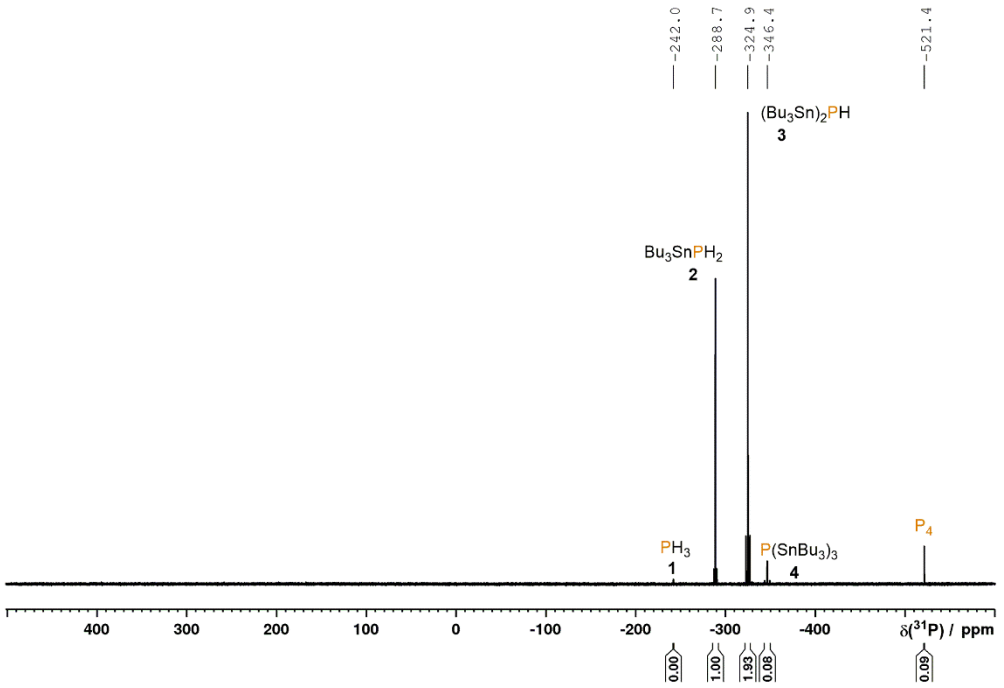

Figure S25. $^{31}P\{^{1}H\}$ NMR spectrum for the reaction of P_4 and 6.3 eq. Bu_3SnH in PhMe, driven by AIBN initiation (2.5 mol% per P) at 60 °C for 2 h.

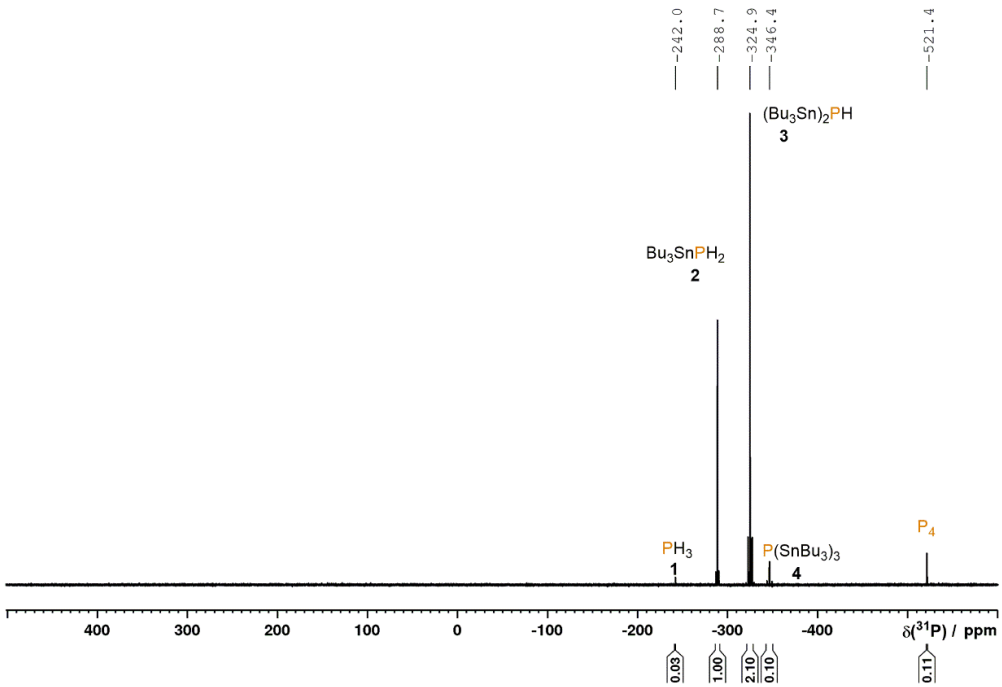

Figure S26. $^{31}P\{^{1}H\}$ NMR spectrum for the reaction of P_4 and 6.3 eq. Bu_3SnH in PhMe, driven by AIBN initiation (2.5 mol% per P) at 80 °C for 1 h.

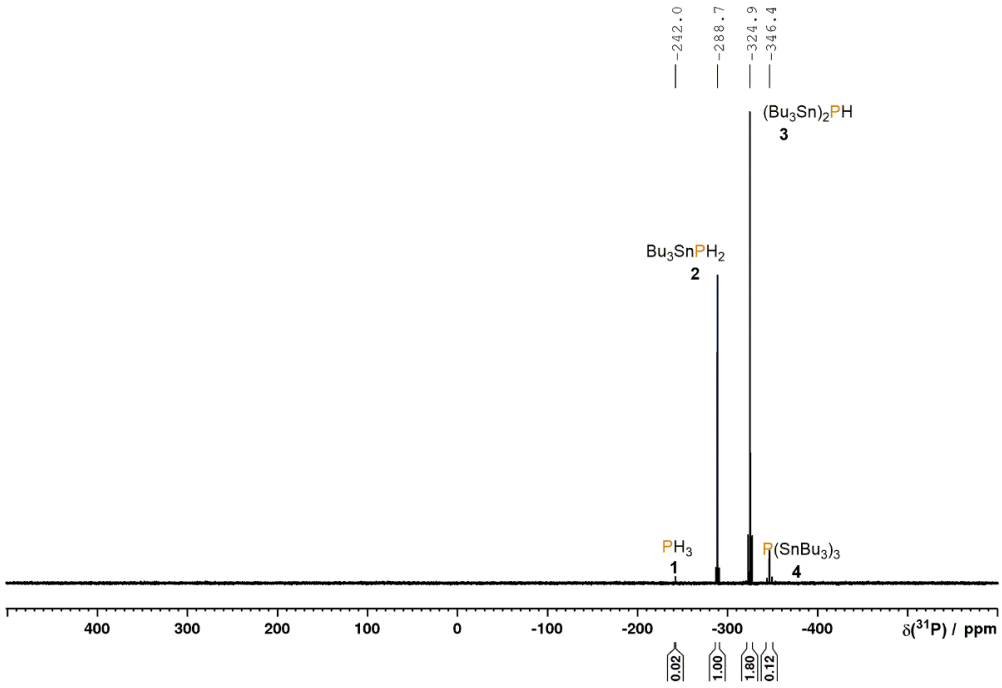

Figure S27. $^{31}P\{^{1}H\}$ NMR spectrum for the reaction of P_4 and 6.3 eq. Bu_3SnH in PhMe, driven by AIBN initiation (0.25 mol% per P) at 60 °C for 19 h.

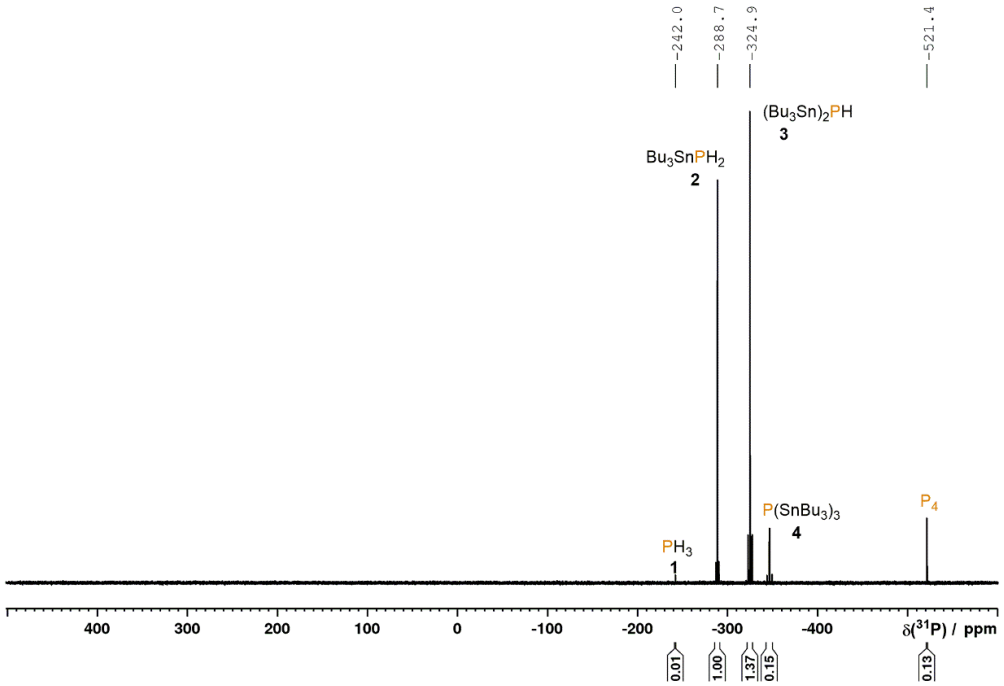

Figure S28. $^{31}P\{^{1}H\}$ NMR spectrum for the reaction of P_4 and 6.3 eq. Bu_3SnH in PhMe, driven by AIBN initiation (0.025 mol% per P) at 80 °C for 18 h.

2.4.1.7 Hydrostannylation of P_4 using Bu_3SnH initiated by ACN (0.01 mmol scale)

To a 10 mL, flat-bottomed, stoppered tube were added PhMe (500 µL), P_4 (0.01 mmol, as a stock solution in 86.0 µL PhH), ACN (1.2 mg, 0.005 mmol) and Bu_3SnH (26.9 µL, 0.1 mmol). The tube was sealed, wrapped in Al foil to exclude light, and heated to 60 °C for 16 h. The resulting mixture was analysed by $^{31}P\{^{1}H\}$ NMR spectroscopy, as shown in Figure S29, below.

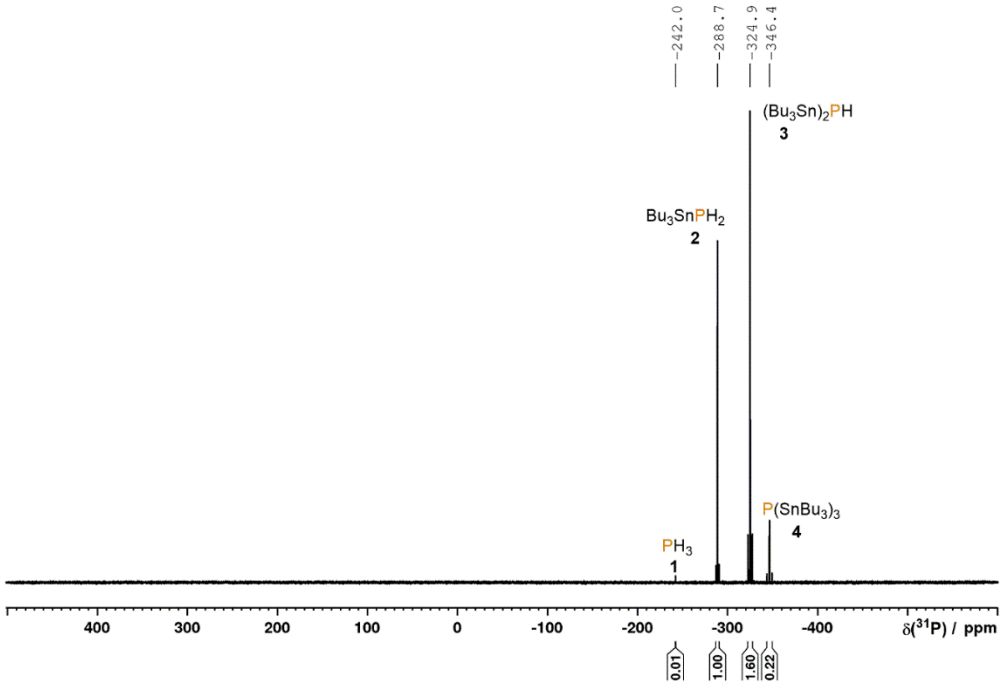

Figure S29. $^{31}P\{^{1}H\}$ NMR spectrum for the reaction of P_4 and 10 eq. Bu_3SnH in PhMe, driven by ACN initiation at 60 °C for 16 h.

2.4.1.8 Hydrostannylation of P_4 using Bu_3SnH initiated by TEMPO and attempted hydrostannylation in the presence of a catalytic amount of galvinoxyl (0.01 mmol scale)

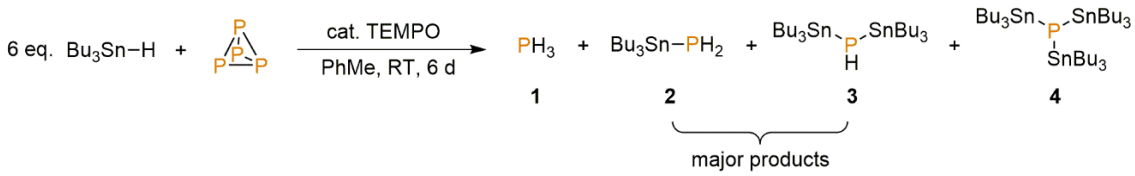

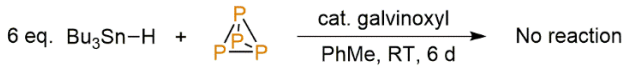

To a 10 mL, flat-bottomed, stoppered tube were added PhMe (500 µL), P_4 (0.01 mmol, as a stock solution in 86.0 µL PhH), TEMPO (1.6 mg, 0.01 mmol) and Bu_3SnH (16.1 µL, 0.06 mmol). The tube was placed in a sealed, opaque container to exclude light, and stirred at RT for 6 d. The resulting mixture was analysed by $^{31}P\{^{1}H\}$ NMR spectroscopy, as shown in Figure S30, below.

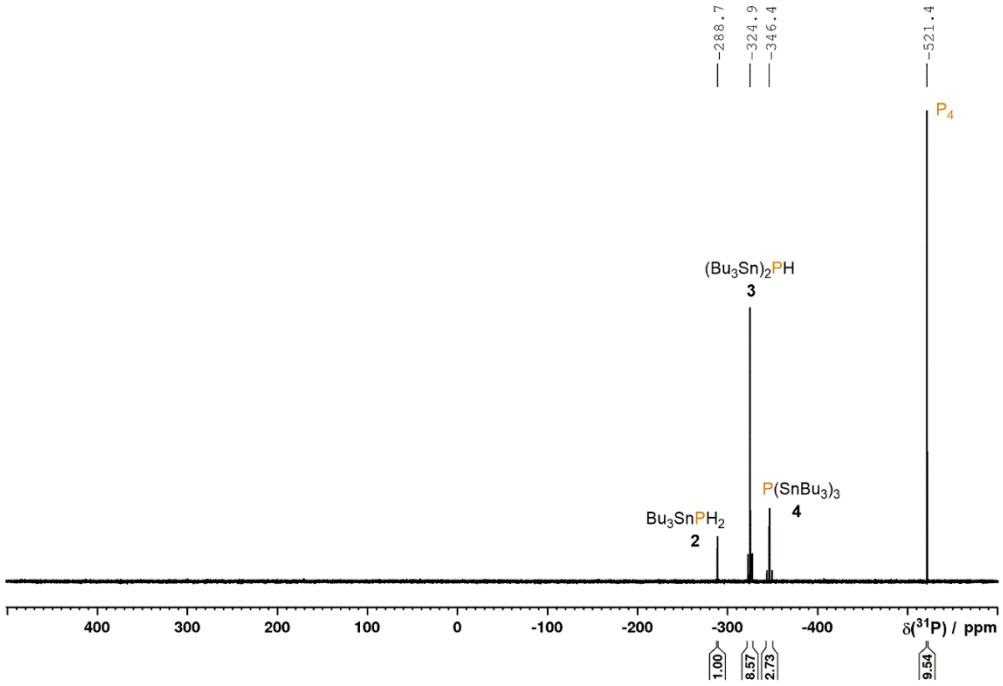

Figure S30. $^{31}P\{^{1}H\}$ NMR spectrum for the reaction of P_4 and 6 eq. Bu_3SnH in PhMe, driven by TEMPO initiation at RT for 6 d.

An analogous reaction was also performed using galvinoxyl (4.2 mg, 0.01 mmol) in place of TEMPO. The resulting $^{31}P\{^{1}H\}$ spectrum did not indicate any P_4 hydrostannylation (Figure S31).

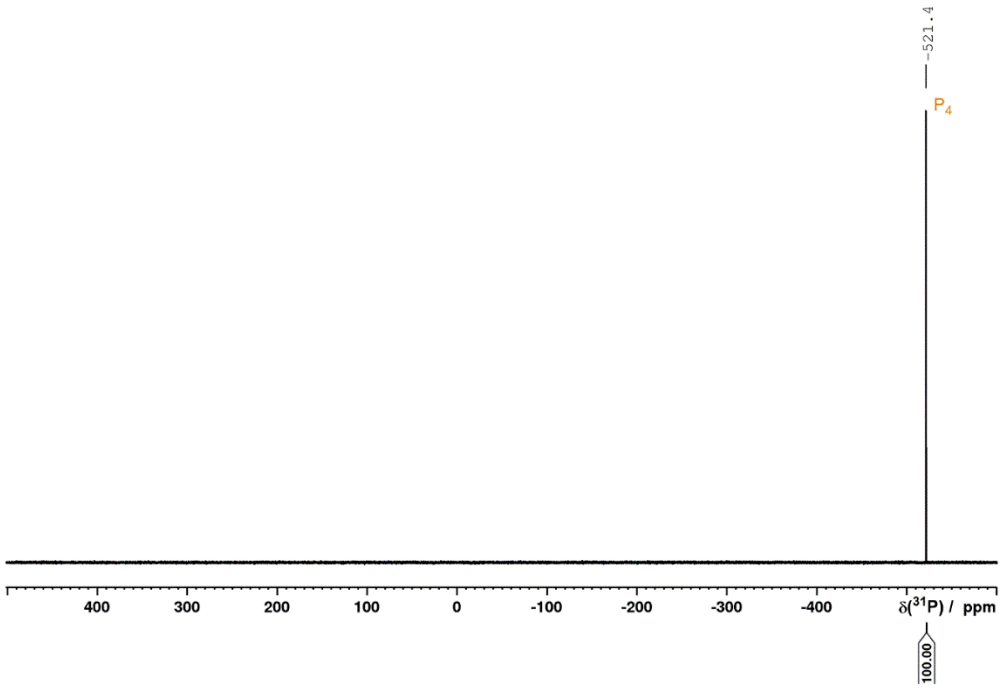

Figure S31. $^{31}P\{^{1}H\}$ NMR spectrum for the attempted reaction of P_4 and 6 eq. Bu_3SnH in PhMe, in the presence of a catalytic amount of galvinoxyl at RT for 6 d.

2.4.1.9 Inhibition by TEMPO of hydrostannylation of P_4 using Bu_3SnH under blue LED irradiation

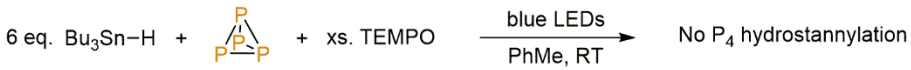

To a 10 mL, flat-bottomed, stoppered tube was added PhMe (500 µL), TEMPO (0.2 mmol, 31.3 mg), P_4 (0.01 mmol, as a stock solution in 86.0 µL PhH) and Bu_3SnH (16.1 µL, 0.06 mmol). The tube was sealed, placed in a water-cooled block to maintain near-ambient temperature, and irradiated with blue light (455 nm (±15 nm), 3.2 V, 700 mA, Osram OSLON SSL 80) for 18 h. The resulting mixture was analysed by ^{1}H, $^{31}P\{^{1}H\}$ and $^{119}Sn\{^{1}H\}$ NMR spectroscopy, as shown in Figures S32-34, below.

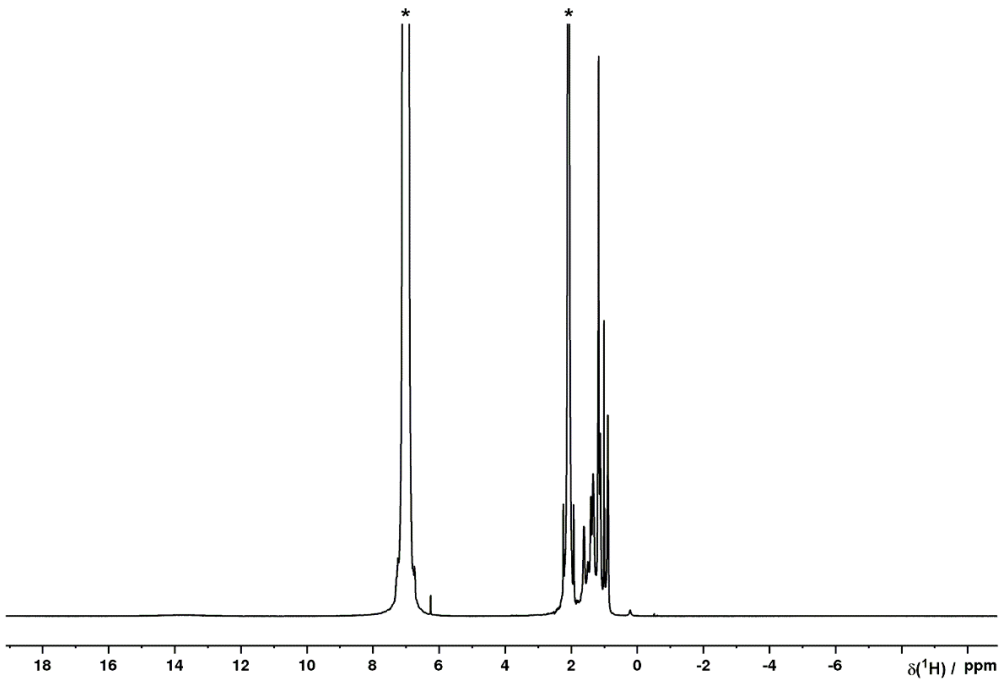

Figure S32. ^{1}H NMR spectrum for the reaction of P_4 and 6 eq. Bu_3SnH in the presence of 20 eq. TEMPO in PhMe, driven by 455 nm LED irradiation for 18 h. Solvent resonances (*) truncated for clarity.

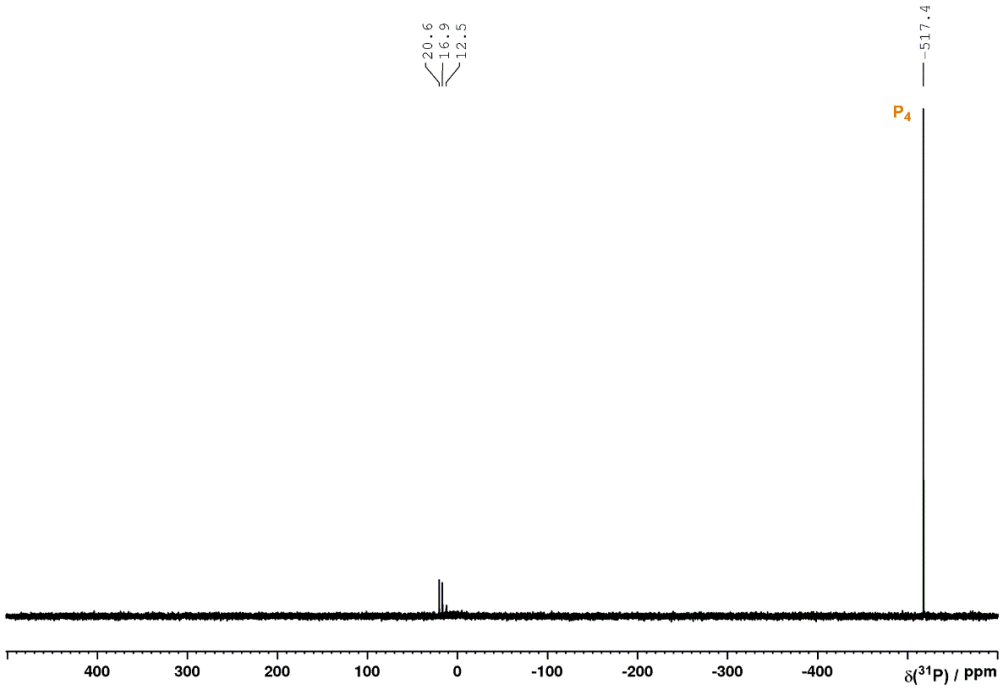

Figure S33. $^{31}P\{^{1}H\}$ NMR spectrum for the reaction of P_4 and 6 eq. Bu_3SnH in the presence of 20 eq. TEMPO in PhMe, driven by 455 nm LED irradiation for 18 h.

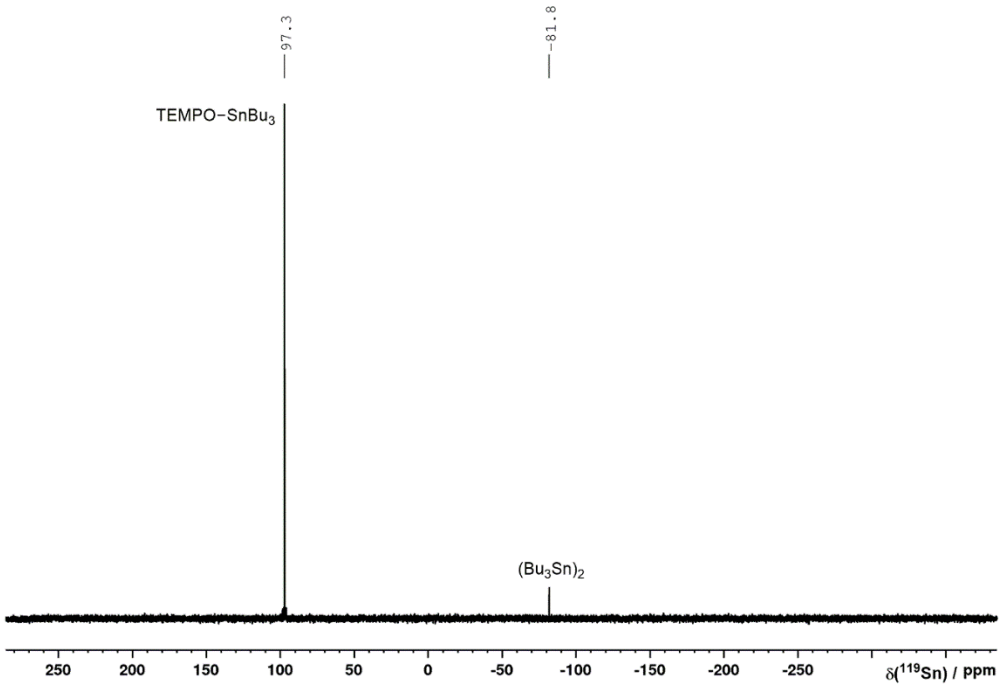

Figure S34. $^{119}Sn\{^{1}H\}$ NMR spectrum for the reaction of P_4 and 6 eq. Bu_3SnH in the presence of 20 eq. TEMPO in PhMe, driven by 455 nm LED irradiation for 18 h.

The spectra clearly show that the addition of TEMPO has an inhibitory effect on the P_4 hydrostannylation reaction that would be observed in its absence. The $^{31}P\{^{1}H\}$ spectrum indicates that the P_4 starting material is the only significant P-containing compound present, with no formation of the phosphines $(Bu_3Sn)_xPH_{3-x}$. The ^{1}H NMR spectrum shows full consumption of Bu_3SnH (through disappearance of the hydride resonance that would otherwise be observed at

ca. 5 ppm), and the single major $^{119}Sn\{^{1}H\}$ resonance is consistent with formation of TEMPO–$SnBu_3$.[68]

These observations are fully consistent with the mechanism proposed in Scheme 2 (see Section 2.2.1), with TEMPO trapping the initially formed $Bu_3Sn^{\bullet}$ radicals before they can appreciably propagate the productive radical chain. Nevertheless, it should be noted that control experiments in which the above procedure was repeated in the dark (i.e. in the absence of any deliberate source of initiation) showed an essentially identical outcome (Figures S35 and S36). This indicates that TEMPO is able to react directly with Bu_3SnH (presumably *via* initial H atom abstraction to form TEMPO–H, and subsequent trapping of $Bu_3Sn^{\bullet}$ by a second equivalent of TEMPO), and that this reaction proceeds to completion within the timeframe of the experiment. These results should therefore be interpreted with appropriate caution.

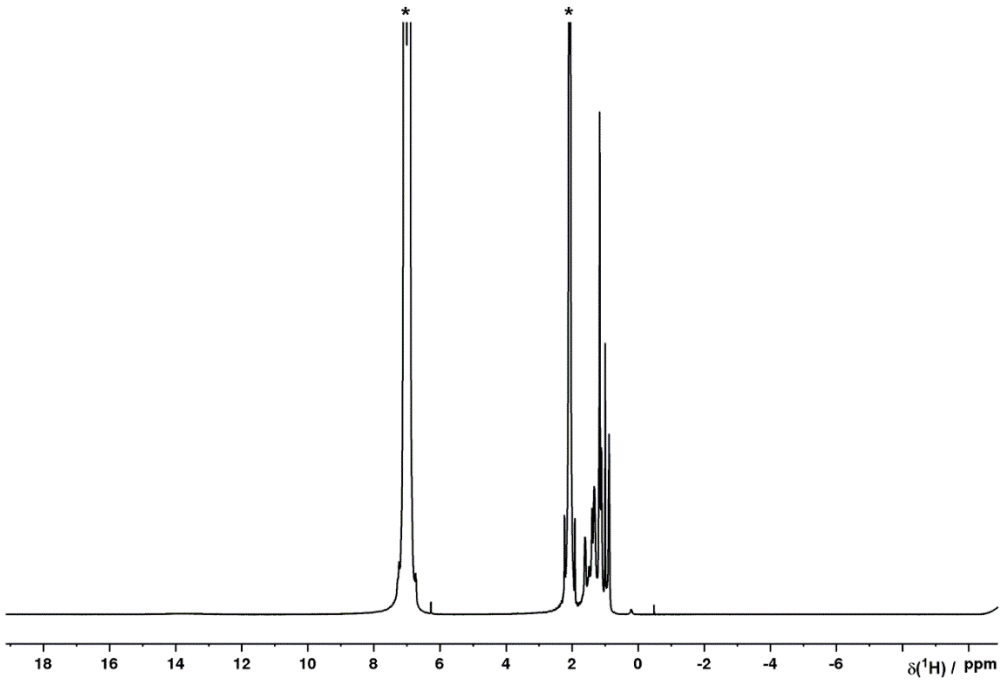

Figure S35. ^{1}H NMR spectrum for the reaction between P_4, 6 eq. Bu_3SnH and 20 eq. TEMPO in PhMe, stirred in the dark for 18 h. Solvent resonances (*) truncated for clarity.

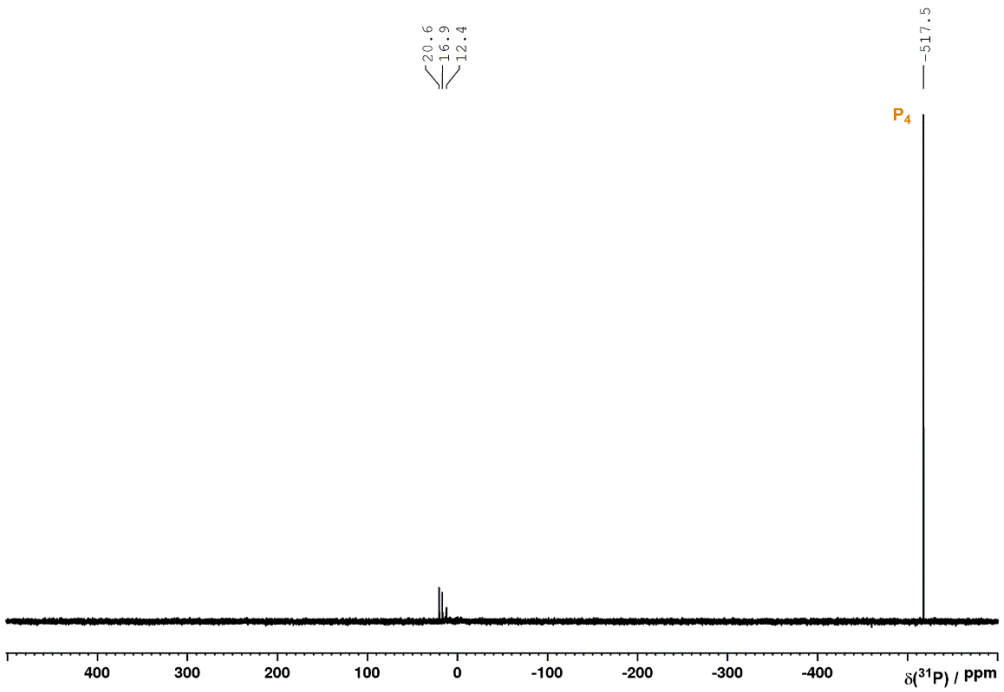

Figure S36. $^{31}P\{^{1}H\}$ NMR spectrum for the reaction between P_4, 6 eq. Bu_3SnH and 20 eq. TEMPO in PhMe, stirred in the dark for 18 h.

For the sake of completeness, it should also be noted that TEMPO appears to react directly with the phosphines $(Bu_3Sn)_xPH_{3-x}$ that are the usual products of the P_4 hydrostannylation reaction. This is illustrated when TEMPO (20 eq. relative to initial P_4) is added at the conclusion of the blue light-driven hydrostannylation reaction (as described in Section 2.4.1.1) instead of at the start, and the resulting mixture is stirred for 20 h at room temperature (identical results are obtained when this second step is performed under 455 nm irradiation, or in the dark). $^{31}P\{^{1}H\}$ NMR analysis of the final product mixture shows full consumption of $(Bu_3Sn)_xPH_{3-x}$ (with the exception of a small amount of $P(Bu_3Sn)_3$, Figure S37), and formation of a new major product characterized by a resonance at 17.0 ppm that has not yet been identified (this resonance does not split in the proton-coupled ^{31}P spectrum but appears to possess $^{117/119}Sn$ satellites, with $J(^{31}P\text{-}^{119}Sn)$ = 49 Hz, which is smaller than would be expected for a ^{1}J coupling).

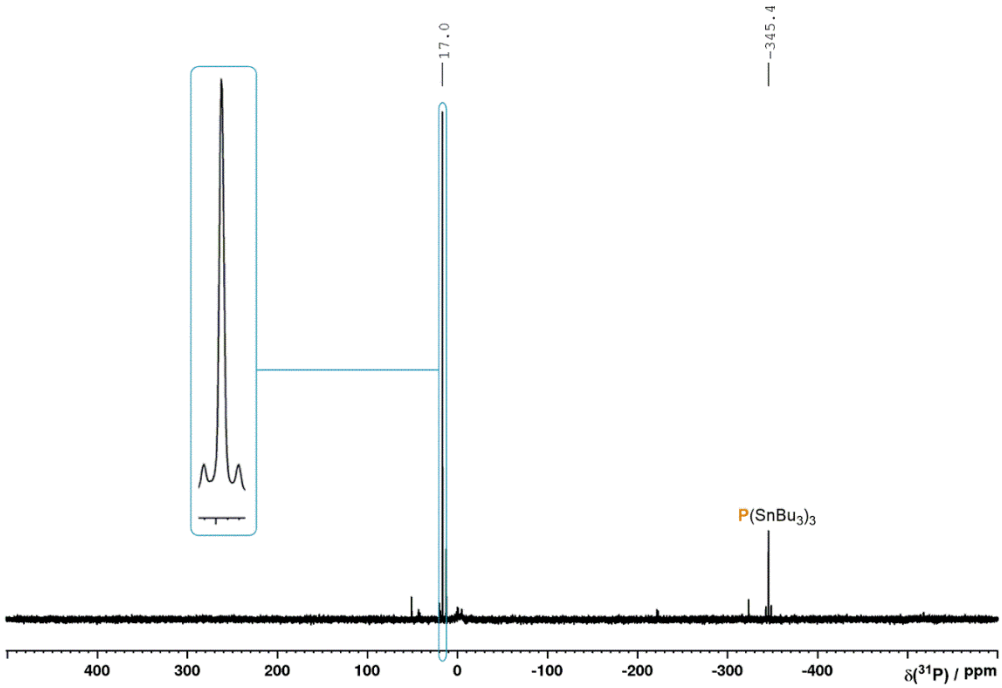

Figure S37. $^{31}P\{^{1}H\}$ NMR spectrum for the reaction of P_4 and 6 eq. Bu_3SnH in PhMe, driven by 455 nm LED irradiation for 18 h, followed by addition of TEMPO (20 eq.) and stirring at room temperature for 20 h.

2.4.1.10 Inhibition by TEMPO of hydrostannylation of P_4 using Bu_3SnH initiated by AIBN

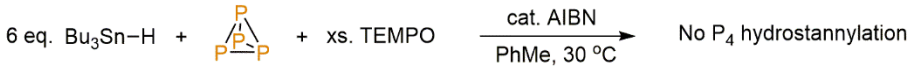

To a 10 mL, flat-bottomed, stoppered tube was added PhMe (500 µL), TEMPO (0.2 mmol, 31.3 mg), P_4 (0.01 mmol, as a stock solution in 93.9 µL PhH), AIBN (0.001 mmol, as a stock solution in 49.3 µL PhH) and Bu_3SnH (16.9 µL, 0.063 mmol). The tube was sealed, wrapped in Al foil to exclude light, and heated to 30 °C for 19 h. The resulting mixture was analysed by ^{1}H and $^{31}P\{^{1}H\}$ NMR spectroscopy, as shown in Figures S38 and S39, below.

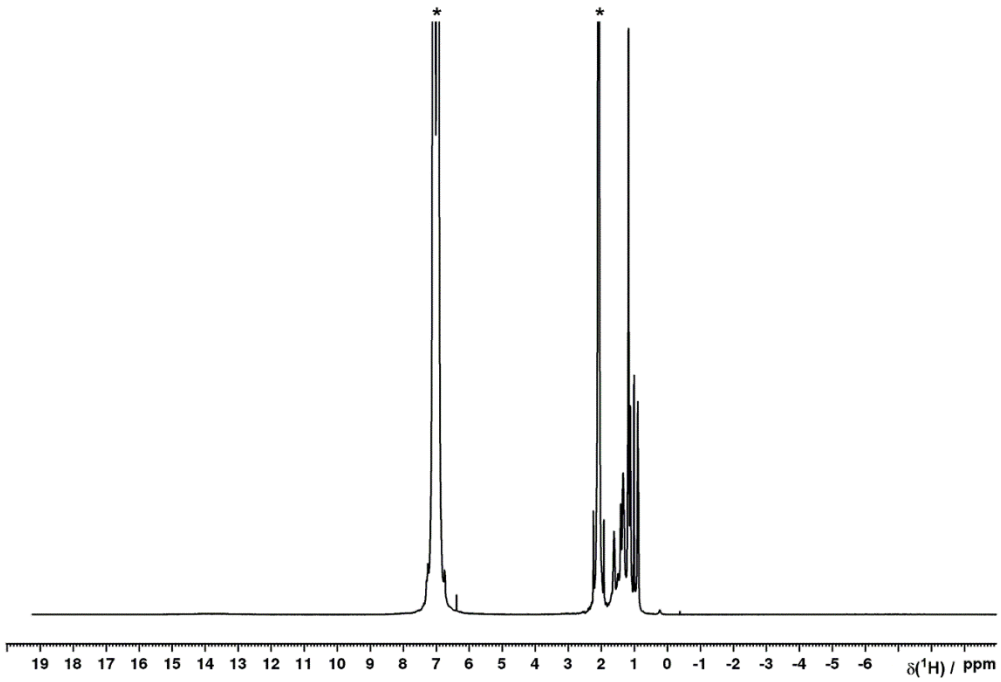

Figure S38. ^{1}H NMR spectrum for the reaction of P_4 and 6 eq. Bu_3SnH in the presence of 20 eq. TEMPO in PhMe, driven by AIBN initiation at 30 °C for 19 h. Solvent resonances (*) truncated for clarity.

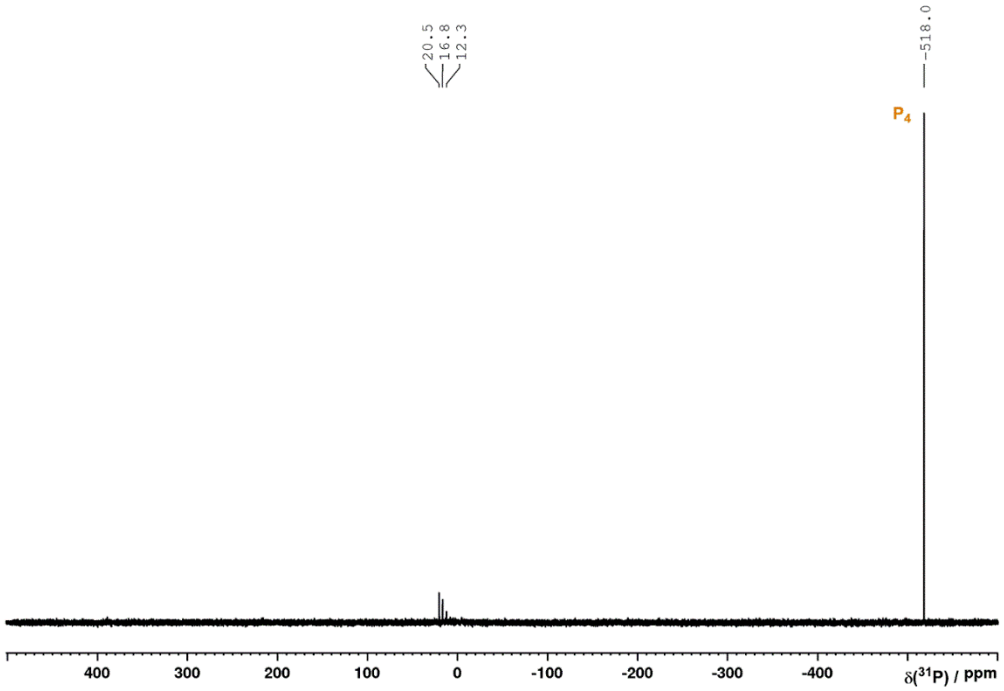

Figure S39. $^{31}P\{^{1}H\}$ NMR spectrum for the reaction of P_4 and 6 eq. Bu_3SnH in the presence of 20 eq. TEMPO in PhMe, driven by AIBN initiation at 30 °C for 19 h.

The spectra show that, as for the analogous light-driven reaction (Section 2.4.1.9), the addition of excess TEMPO effectively inhibits P_4 stannylation. These results should be interpreted with caution for the same reasons, however.

2.4.1.11 Inhibition by galvinoxyl of hydrostannylation of P_4 using Bu_3SnH under blue LED irradiation

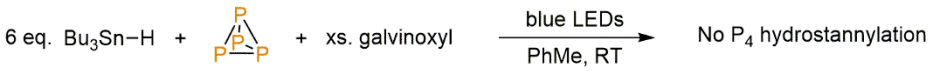

To a 10 mL, flat-bottomed, stoppered tube was added PhMe (500 µL), galvinoxyl (0.2 mmol, 84.3 mg), P_4 (0.01 mmol, as a stock solution in 93.9 µL PhH) and Bu_3SnH (16.1 µL, 0.06 mmol). The tube was sealed, placed in a water-cooled block to maintain near-ambient temperature, and irradiated with blue light (455 nm (±15 nm), 3.2 V, 700 mA, Osram OSLON SSL 80) for 19 h. The resulting mixture was analysed by ^{1}H and $^{31}P\{^{1}H\}$ NMR spectroscopy, as shown in Figures S40 and S41, below.

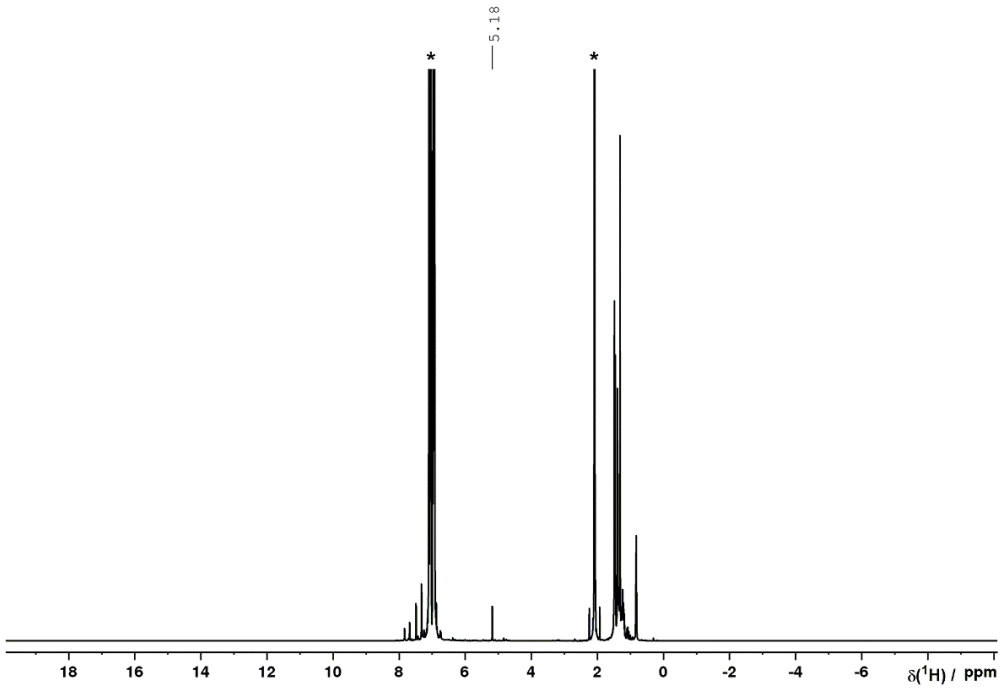

Figure S40. ^{1}H NMR spectrum for the reaction of P_4 and 6 eq. Bu_3SnH in the presence of 20 eq. galvinoxyl in PhMe, driven by 455 nm LED irradiation for 19 h. Solvent resonances (*) truncated for clarity.

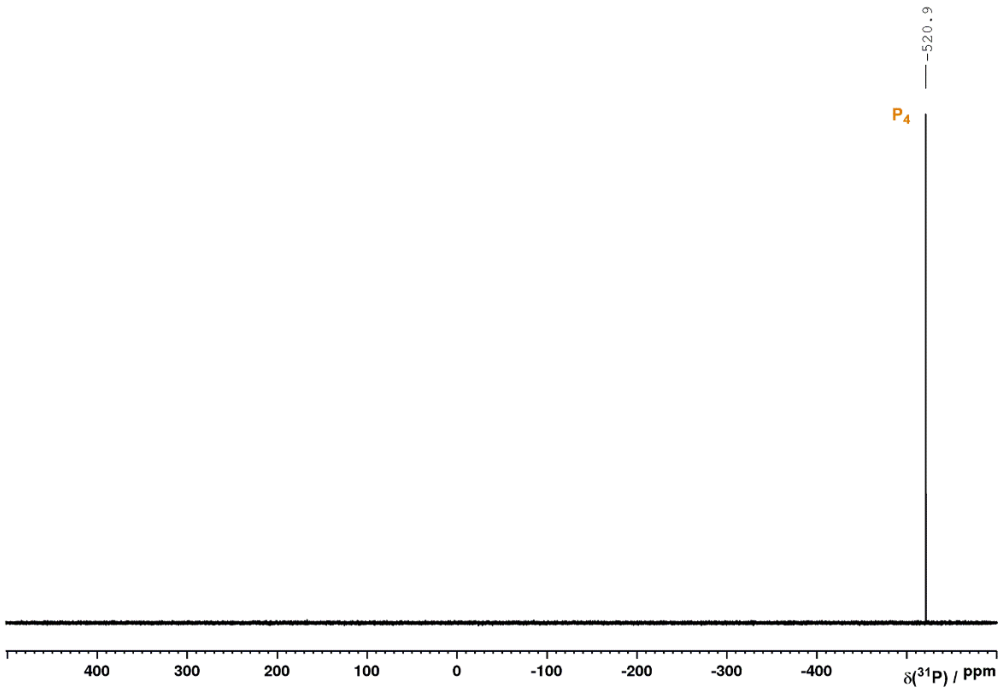

Figure S41. $^{31}P\{^{1}H\}$ NMR spectrum for the reaction of P_4 and 6 eq. Bu_3SnH in the presence of 20 eq. galvinoxyl in PhMe, driven by 455 nm LED irradiation for 19 h.

As with TEMPO (Section 2.4.1.9), the spectra clearly show that addition of galvinoxyl has an inhibitory effect on P_4 hydrostannylation, with the $^{31}P\{^{1}H\}$ spectrum again showing P_4 as the only P-containing compound. The same caution should be used when interpreting these results, however.

Control experiments in which the above procedure is repeated in the dark give a very broad, paramagnetic feature in the ^{1}H spectrum that overlaps with the expected location of the diagnostic $Bu_3Sn\underline{H}$ resonance (Figures S42 and S43). Nevertheless, the sharp signal expected for this starting material is not observed, which suggests that (as with TEMPO) it is consumed by direct reaction with the stable radical even in the absence of another source of initiation. Note that while a reasonably sharp feature can be observed at 5.15 ppm, this is *ca.* 0.15 ppm downfield from the chemical shift observed for the $Bu_3Sn\underline{H}$ resonance in closely related spectra (for example, during analysis of the attempted galvinoxyl-mediated hydrostannylation of P_4 described in Section 2.4.1.8, the $Bu_3Sn\underline{H}$ resonance was observed at 4.99 ppm), and given also the lack of obvious $^{1}J^{117/119}Sn$ satellites or $J(^{1}H\text{-}^{1}H)$ couplings, this signal is presumed to arise from a galvinoxyl-derived product (a similar resonance is also easily resolved in Figure S40).

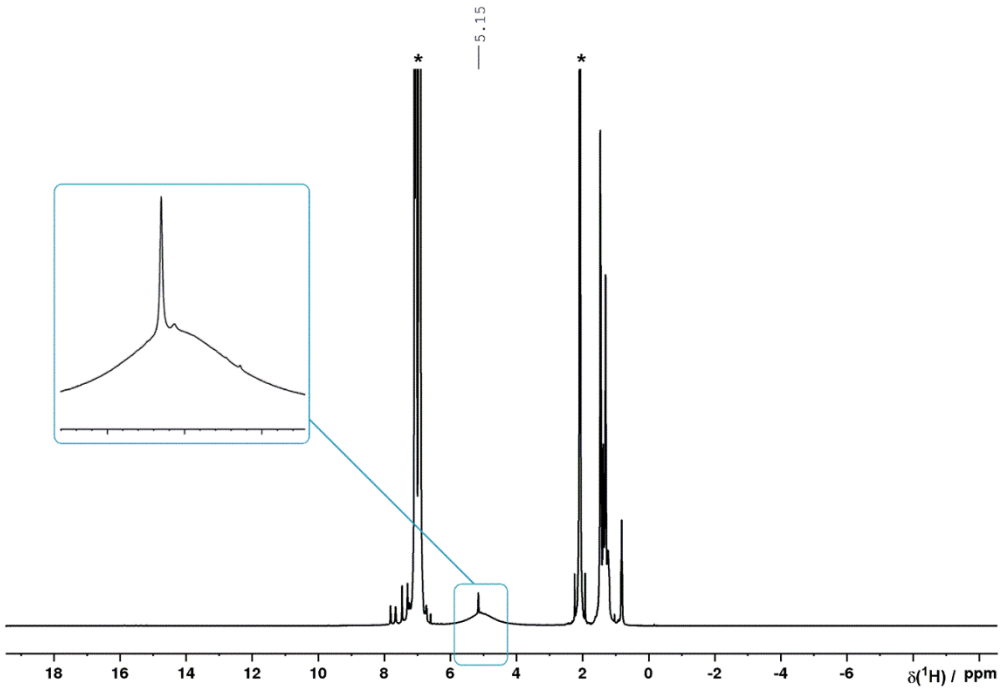

Figure S42. ^{1}H NMR spectrum for the reaction between P_4, 6 eq. Bu_3SnH and 20 eq. galvinoxyl in PhMe, stirred in the dark for 19 h. Solvent resonances (*) truncated for clarity.

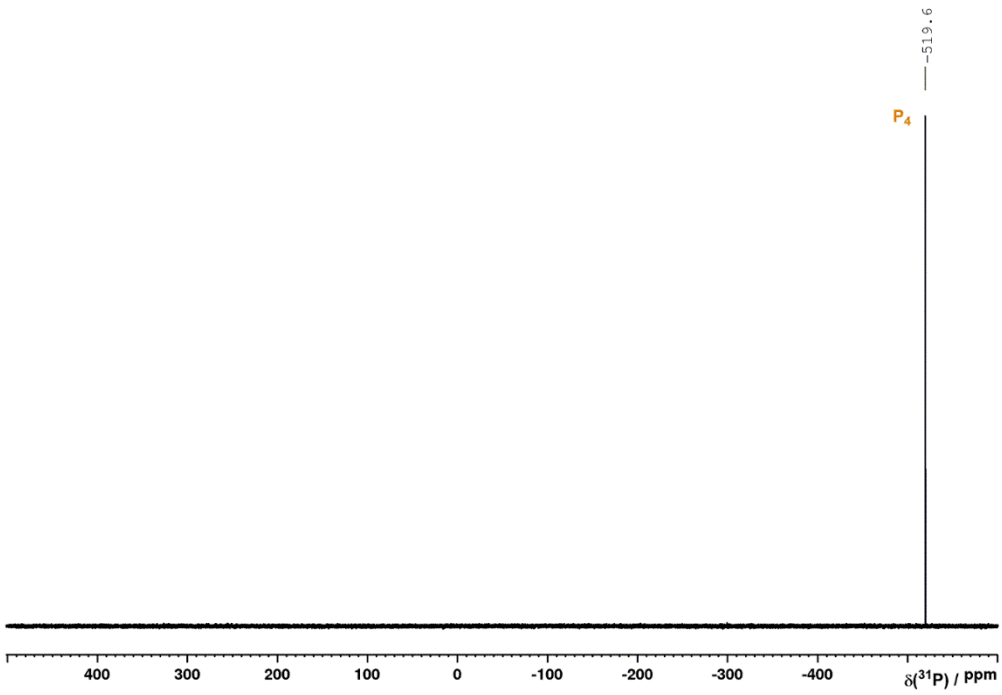

Figure S43. $^{31}P\{^{1}H\}$ NMR spectrum for the reaction between P_4, 6 eq. Bu_3SnH and 20 eq. galvinoxyl in PhMe, stirred in the dark for 19 h.

For the sake of completeness, it should also be noted that, like TEMPO, galvinoxyl appears to react directly with the phosphines $(Bu_3Sn)_xPH_{3-x}$ that are the usual products of the P_4 hydrostannylation reaction. This is illustrated when galvinoxyl (20 eq. relative to initial P_4) is added at the conclusion of the blue light-driven hydrostannylation reaction (as described in

Section 2.4.1.1) instead of at the start, and the resulting mixture is stirred for 21 h at room temperature (comparable results are obtained when this second step is performed under 455 nm irradiation, or in the dark). $^{31}P\{^{1}H\}$ NMR analysis of the final product mixture shows full consumption of $(Bu_3Sn)_xPH_{3-x}$. Unlike the analogous case using TEMPO, no major $^{31}P\{^{1}H\}$ product resonances can be observed in the range between ±500 ppm, which may suggest the formation of unidentified, paramagnetic products.

2.4.1.12 Inhibition by galvinoxyl of hydrostannylation of P_4 using Bu_3SnH initiated by AIBN

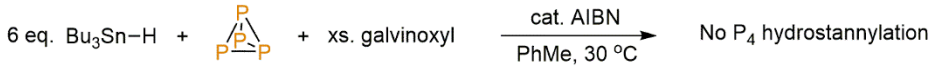

To a 10 mL, flat-bottomed, stoppered tube was added PhMe (500 µL), galvinoxyl (0.2 mmol, 84.3 mg), P_4 (0.01 mmol, as a stock solution in 93.9 µL PhH), AIBN (0.001 mmol, as a stock solution in 49.3 µL PhH) and Bu_3SnH (16.9 µL, 0.063 mmol). The tube was sealed, wrapped in Al foil to exclude light, and heated to 30 °C for 19 h. The resulting mixture was analysed by ^{1}H and $^{31}P\{^{1}H\}$ NMR spectroscopy, as shown in Figures S44 and S45, below.

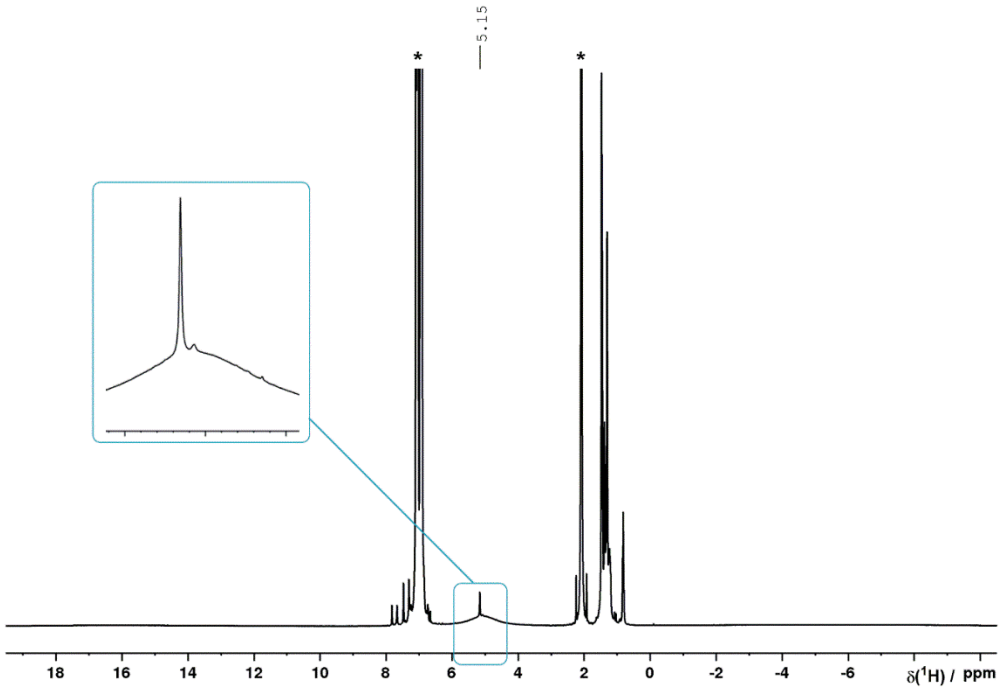

Figure S44. ^{1}H NMR spectrum for the reaction of P_4 and 6 eq. Bu_3SnH in the presence of 20 eq. galvinoxyl in PhMe, driven by AIBN initiation at 30 °C for 19 h. Solvent resonances (*) truncated for clarity.

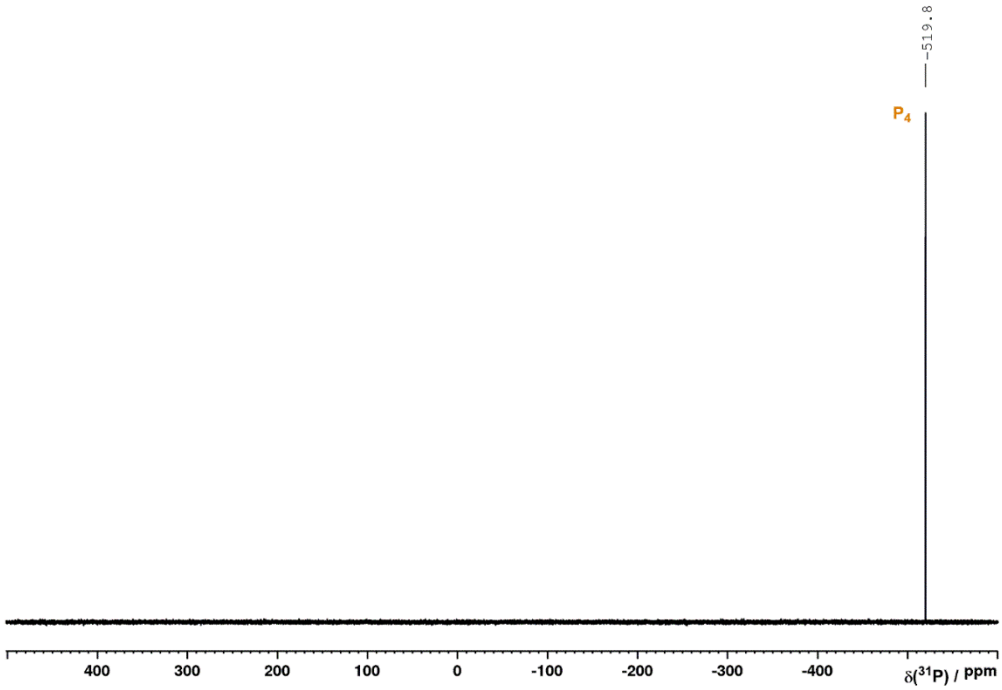

Figure S45. $^{31}P\{^{1}H\}$ NMR spectrum for the reaction of P_4 and 6 eq. Bu_3SnH in the presence of 20 eq. alvinoxylg in PhMe, driven by AIBN initiation at 30 °C for 19 h.

The spectra show that, as for the analogous light-driven reaction (Section 2.4.1.11), the addition of excess galvinoxyl effectively inhibits P_4 stannylation. These results should be interpreted with caution for the same reasons, however.

2.4.1.13 Hydrostannylation of P_2Ph_4 using Bu_3SnH under blue LED irradiation (0.02 mmol scale)

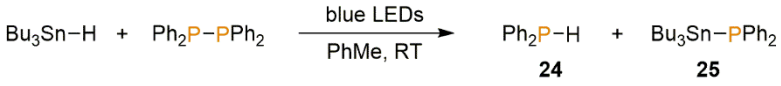

To a 10 mL, flat-bottomed, stoppered tube were added PhMe (500 µL), P_2Ph_4 (7.4 mg, 0.02 mmol) and Bu_3SnH (5.4 µL, 0.02 mmol). The tube was sealed, placed in a water-cooled block to maintain near-ambient temperature, and irradiated with blue light (455 nm (±15 nm), 3.2 V, 700 mA, Osram OSLON SSL 80) for 20 h. The resulting mixture was analysed by ^{1}H, $^{31}P\{^{1}H\}$ and ^{31}P NMR spectroscopy, as shown in Figures S46-48, below.

The $^{31}P\{^{1}H\}$ spectrum reveals full consumption of the starting material and formation of two new resonances with roughly equal intensity. The more downfield signal at –40.0 ppm splits into a doublet in the ^{1}H-coupled ^{31}P spectrum with a large $^{1}J(^{31}P\text{-}^{1}H)$ coupling constant of 215 Hz, consistent with formation of Ph_2PH (**24**).[69] The more upfield signal at –55.3 ppm remains a singlet in the ^{1}H-coupled ^{31}P spectrum, but shows $^{117/119}Sn$ satellites in both spectra with large $^{1}J(^{117}Sn\text{-}^{1}H)$ and $^{1}J(^{119}Sn\text{-}^{1}H)$ coupling constants of 645 Hz and 675 Hz, respectively, and is consistent with formation of Ph_2PSnBu_3 (**25**).[70]

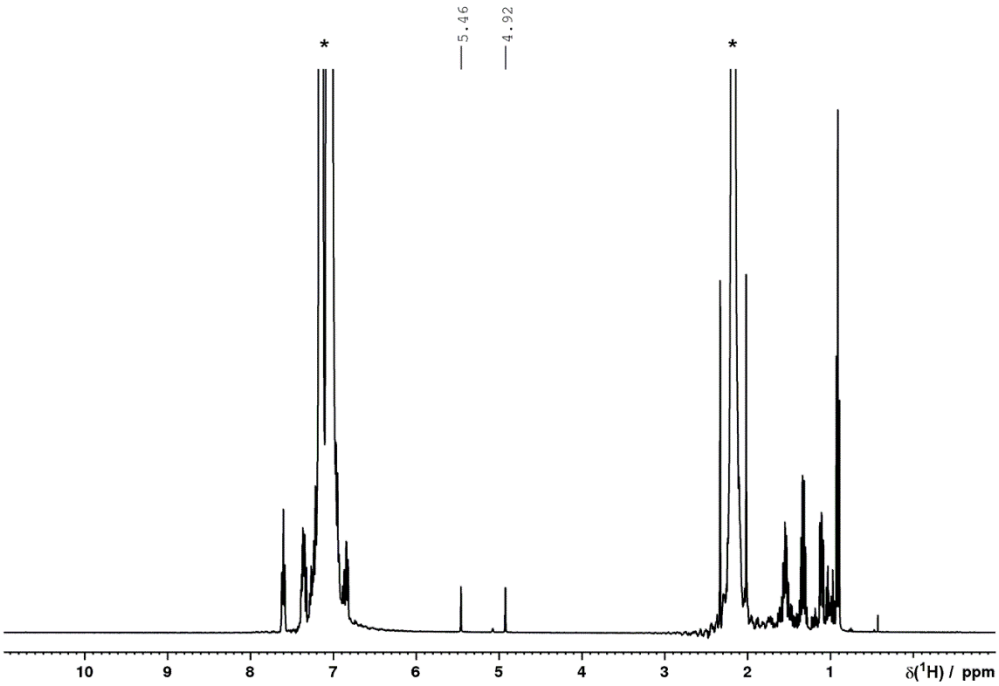

Figure S46. ^{1}H NMR spectrum for the reaction of P_2Ph_4 and 1 eq. Bu_3SnH in PhMe, driven by 455 nm LED irradiation for 20 h. Solvent resonances (*) truncated for clarity.

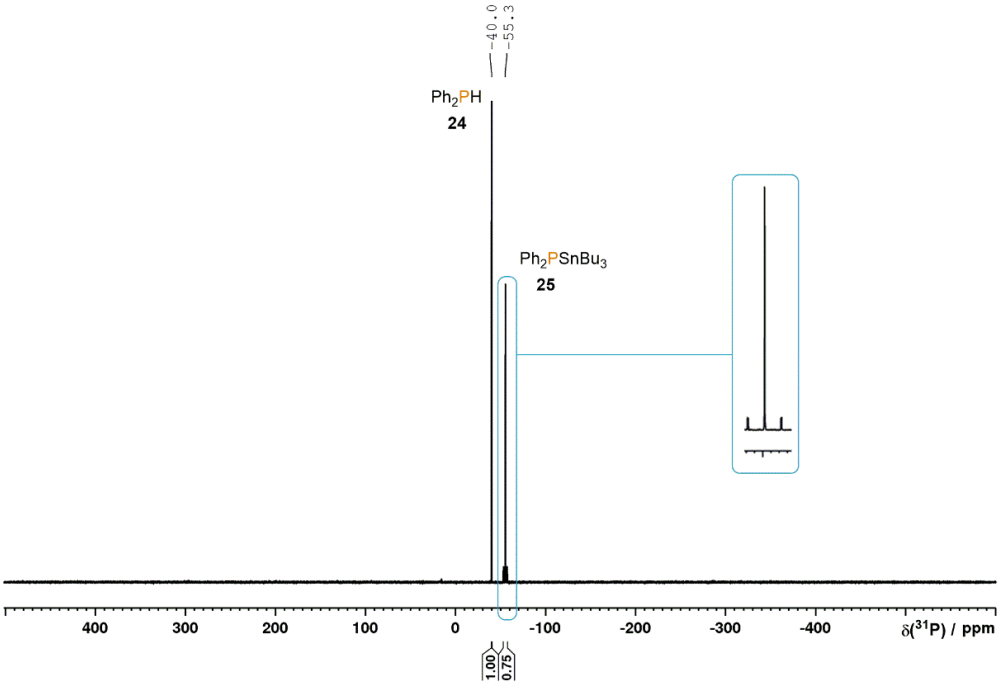

Figure S47. $^{31}P\{^{1}H\}$ NMR spectrum for the reaction of P_2Ph_4 and 1 eq. Bu_3SnH in PhMe, driven by 455 nm LED irradiation for 20 h.

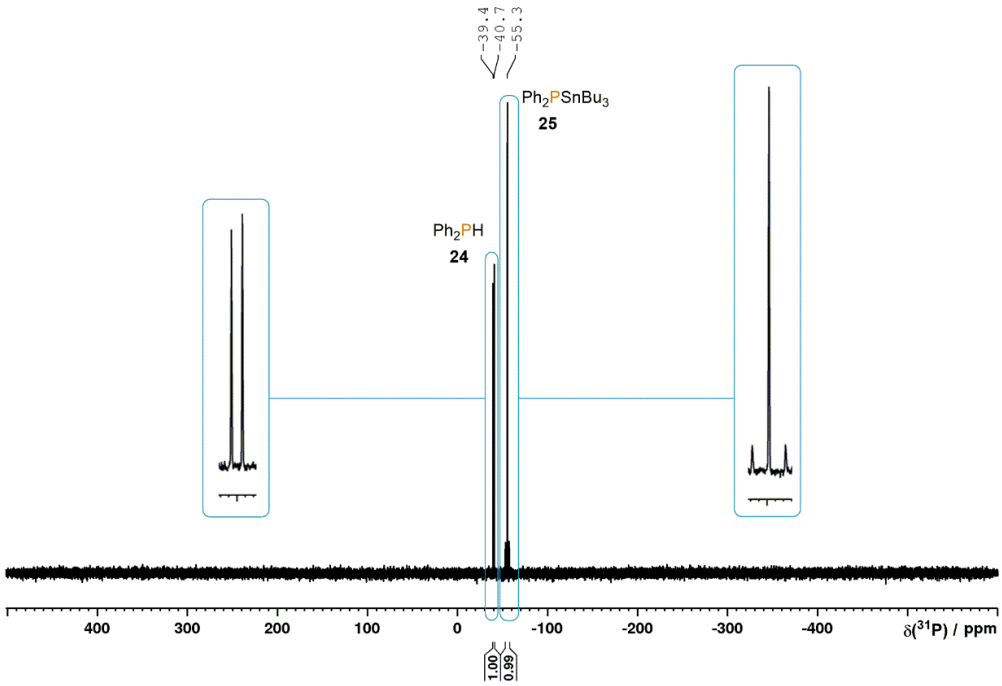

Figure S48. ^{31}P NMR spectrum for the reaction of P_2Ph_4 and 1 eq. Bu_3SnH in PhMe, driven by 455 nm LED irradiation for 20 h.

2.4.1.14 Hydrostannylation of P_5Ph_5 using Bu_3SnH under blue LED irradiation (0.008 mmol scale)

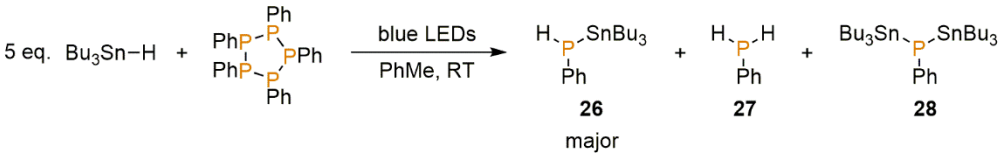

To a 10 mL, flat-bottomed, stoppered tube were added PhMe (500 µL), P_5Ph_5 (4.3 mg, 0.008 mmol) and Bu_3SnH (10.8 µL, 0.04 mmol). The tube was sealed, placed in a water-cooled block to maintain near-ambient temperature, and irradiated with blue light (455 nm (±15 nm), 3.2 V, 700 mA, Osram OSLON SSL 80) for 18 h. The resulting mixture was analysed by ^{1}H, ^{31}P{^{1}H} and ^{31}P NMR spectroscopy, as shown in Figures S49-51, below.

The ^{31}P{^{1}H} spectrum reveals full consumption of the starting material and formation of one major new resonance, alongside two more minor resonances with roughly equal intensity.

The major signal at –148.3 ppm splits into a doublet in the ^{1}H-coupled ^{31}P spectrum with a large $^{1}J(^{31}P\text{-}^{1}H)$ coupling constant of 188 Hz. It also displays $^{117/119}$Sn satellites in both spectra with large $^{1}J(^{117}Sn\text{-}^{1}H)$ and $^{1}J(^{119}Sn\text{-}^{1}H)$ coupling constants of 578 Hz and 604 Hz, respectively. This signal is therefore assigned to the product $PhP(H)SnBu_3$ (**26**; the related $PhP(H)SnMe_3$ has been reported previously).[71] Of the minor resonances, the more downfield signal at –123.5 ppm splits into a triplet in the ^{1}H-coupled ^{31}P spectrum with a large $^{1}J(^{31}P\text{-}^{1}H)$ coupling constant of 198 Hz, consistent with formation of $PhPH_2$ (**27**).[72] The more upfield-shifted signal at –167.9 ppm remains a singlet in the ^{1}H-coupled ^{31}P spectrum, but shows $^{117/119}$Sn satellites in both spectra with

large $^{1}J(^{117}\text{Sn-}^{1}\text{H})$ and $^{1}J(^{119}\text{Sn-}^{1}\text{H})$ coupling constants of 769 Hz and 804 Hz, respectively. This signal is therefore assigned to $PhP(SnBu_3)_2$ (**28**).

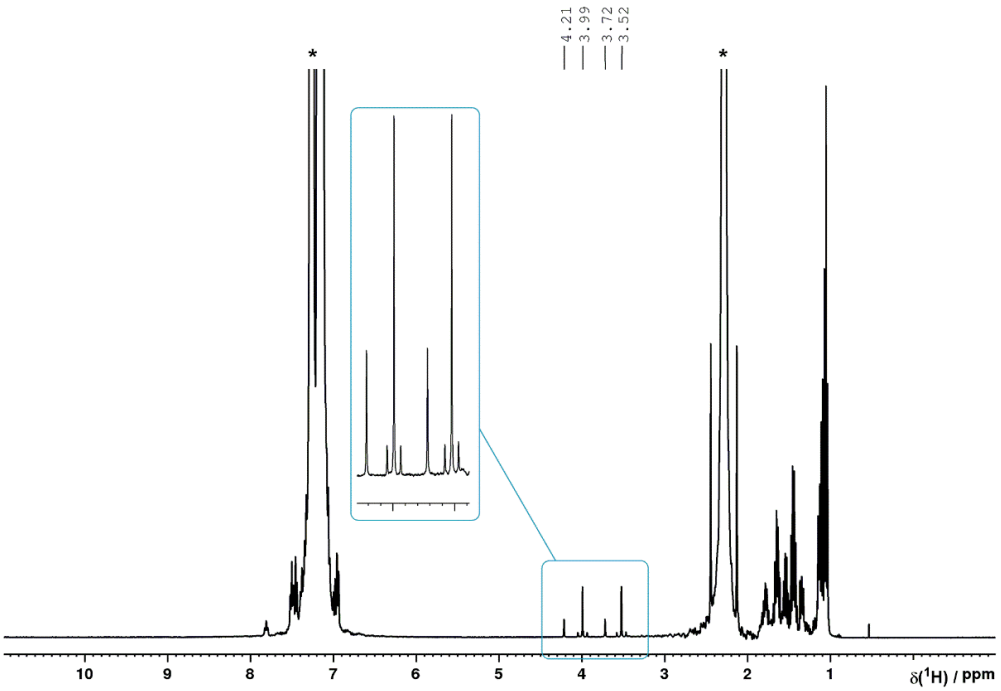

Figure S49. ^{1}H NMR spectrum for the reaction of P_5Ph_5 and 5 eq. Bu_3SnH in PhMe, driven by 455 nm LED irradiation for 18 h. Solvent resonances (*) truncated for clarity.

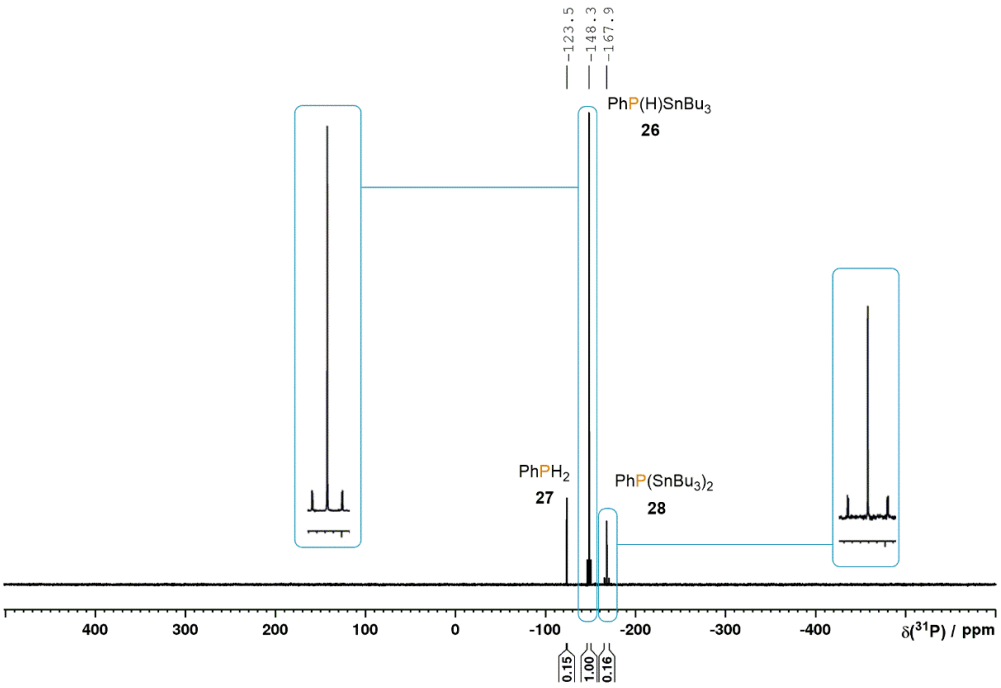

Figure S50. $^{31}P\{^{1}H\}$ NMR spectrum for the reaction of P_5Ph_5 and 5 eq. Bu_3SnH in PhMe, driven by 455 nm LED irradiation for 18 h.

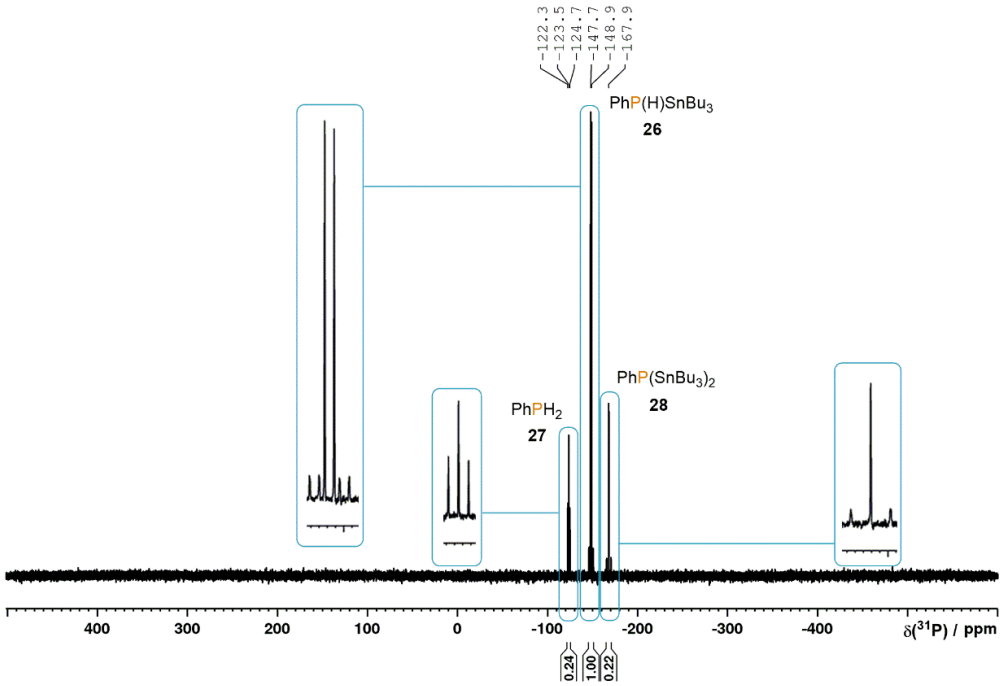

Figure S51. ^{31}P NMR spectrum for the reaction of P_5Ph_5 and 5 eq. Bu_3SnH in PhMe, driven by 455 nm LED irradiation for 18 h.

2.4.2 Synthesis and Isolation of Products Derived from $(Bu_3Sn)_xPH_{3-x}$

2.4.2.1 Synthesis and quantification of *t*BuC(O)PH_2 (5)

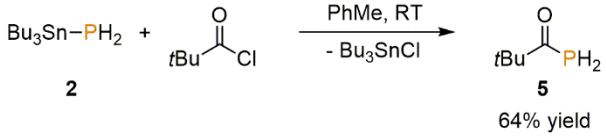

2 **5**

64% yield

*Note: The product tBuC(O)PH_2 (**5**) was found to be light-sensitive. During the preparation, handling and characterisation described below, great care was taken to exclude ambient light as far as possible.*

In a 10 mL stoppered tube were combined Bu_3SnPH_2 (16.2 mg, 0.05 mmol), PhMe (500 µL), and tBuC(O)Cl (5.8 µL, 0.048 mmol). The tube was immediately and thoroughly wrapped in Al foil, and the reaction mixture was stirred at room temperature for 16 h. Following trap-to-trap distillation (RT, ca. 10^{-2} mbar, receiving vessel cooled in liquid nitrogen), the product was obtained as a colourless solution. In order to assess the yield, Ph_3PO (9.4 mg, 0.034 mmol) was added, and the resulting mixture was analysed by ^{1}H, ^{31}P{^{1}H}, ^{31}P and ^{13}C{^{1}H} NMR spectroscopy. Quantitative relative integration of the Ph_3PO and tBuC(O)PH_2 resonances in the ^{31}P NMR spectrum (using D1 = 30 s; T_1 = 5.8 s for tBuC(O)PH_2) indicated a yield of 64% (0.031 mmol).

^{1}H NMR (400 MHz, 300 K, PhMe): δ = 3.49 (2H, d, $^1J(^{31}P\text{-}^1H)$ = 215 Hz), 0.84 ppm (9H, s). **^{31}P{^{1}H} NMR** (121 MHz, 300 K, PhMe): δ = –122.9 ppm (s). **^{31}P NMR** (121 MHz, 300 K, PhMe): δ = –122.9 ppm (t, $^1J(^{31}P\text{-}^1H)$ = 215 Hz). **^{13}C{^{1}H} NMR** (101 MHz, 300 K, PhMe): δ = 225.0 (d, $J(^{31}P\text{-}^{13}C)$ = 40.9 Hz), 48.9 (d, $J(^{31}P\text{-}^{13}C)$ = 22.3 Hz), 25.9 ppm (d, $J(^{31}P\text{-}^{13}C)$ = 3.0 Hz). NMR data are consistent with previous reports.[48]

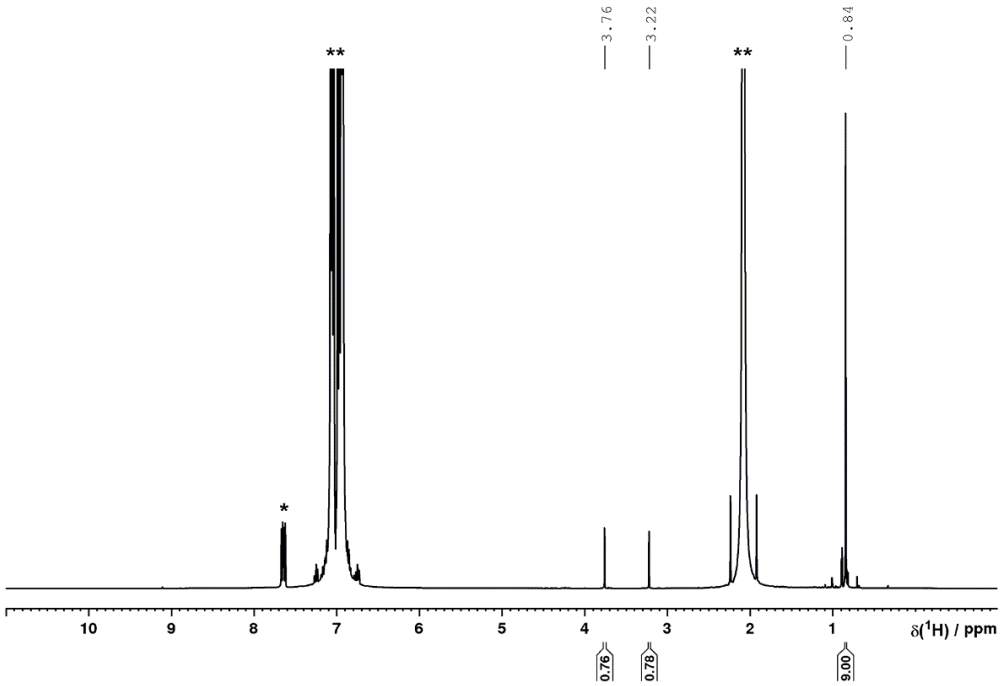

Figure S52. ^{1}H NMR spectrum of a solution of *t*BuC(O)PH_2 (**5**) in PhMe, also containing Ph_3PO (*). Solvent resonances (**) truncated for clarity.

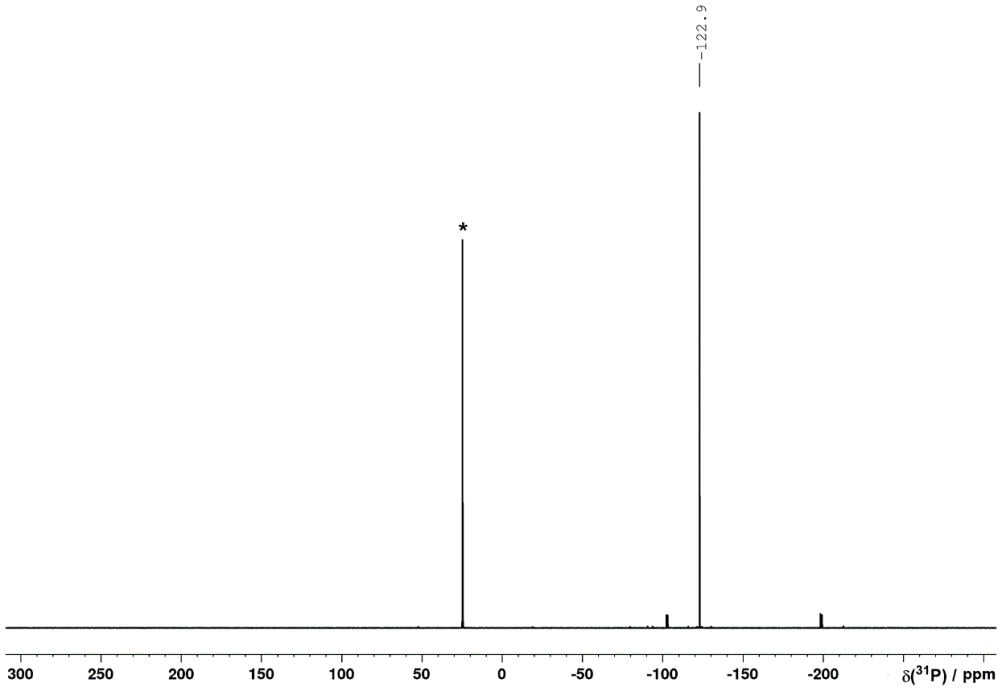

Figure S53. $^{31}P\{^{1}H\}$ NMR spectrum of a solution of *t*BuC(O)PH_2 (**5**) in PhMe, also containing Ph_3PO (*).

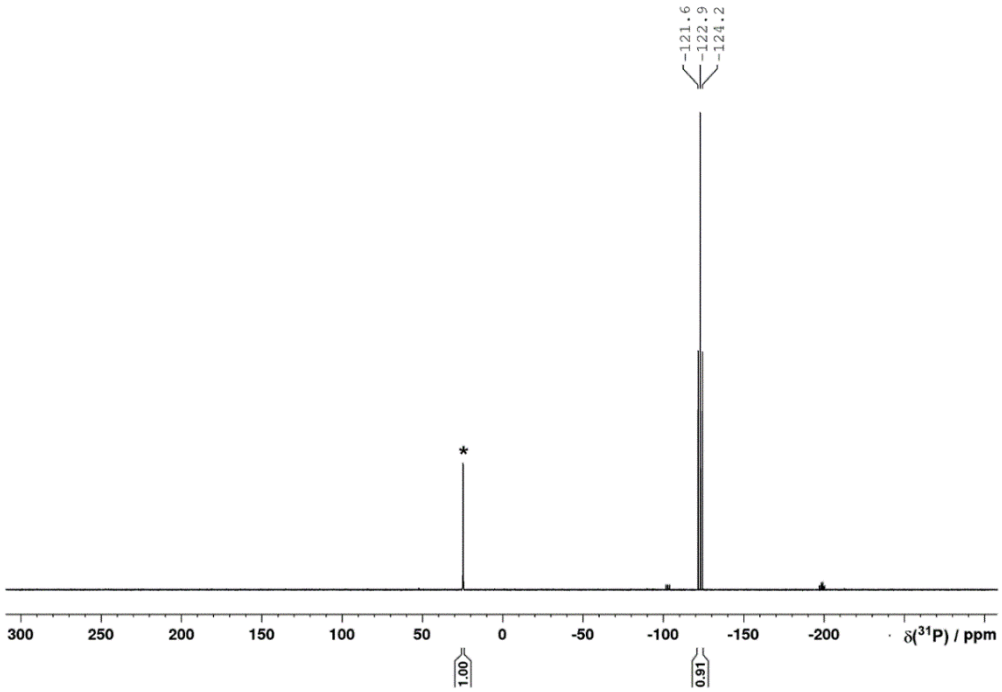

Figure S54. ^{31}P NMR spectrum of a solution of *t*BuC(O)PH_2 (**5**) in PhMe, also containing Ph_3PO (*).

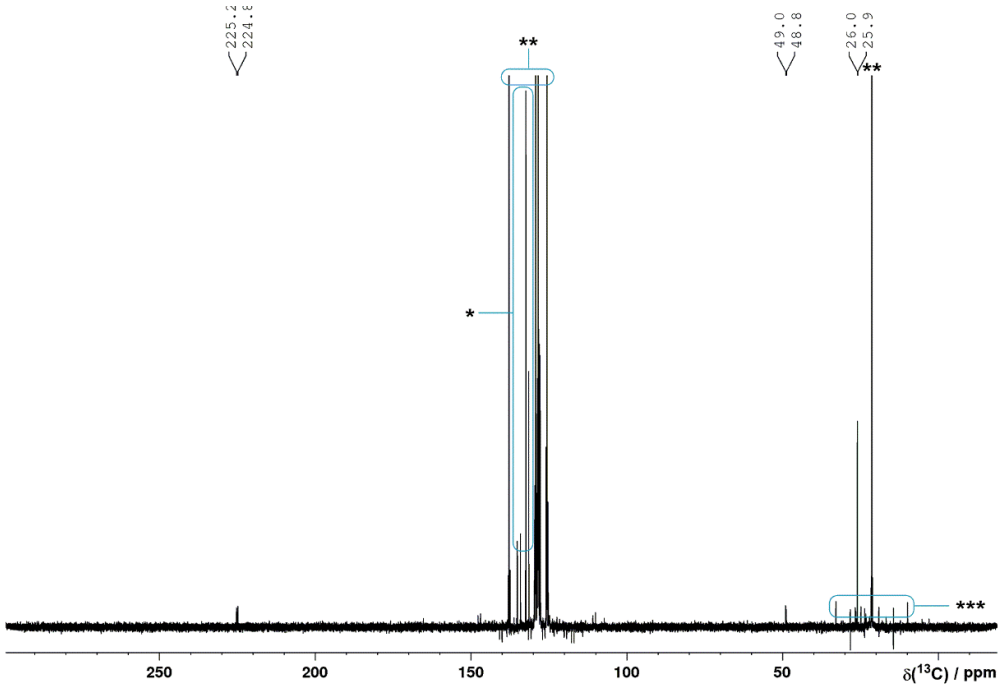

Figure S55. $^{13}C\{^1H\}$ NMR spectrum of a solution of *t*BuC(O)PH_2 (**5**) in PhMe, also containing Ph_3PO (*). Solvent resonances (**) truncated for clarity (***decoupling artefacts).

2.4.2.2 Single and double acylation of $(Bu_3Sn)_2PH$ (3)

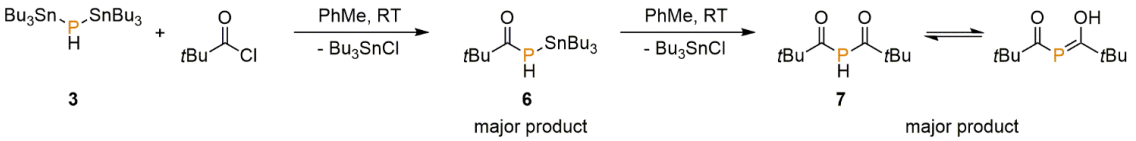

To a stirred solution of $(Bu_3Sn)_2PH$ (**3**, 30.6 mg, 0.05 mmol) in C_6D_6 (500 μL) was added *t*BuC(O)Cl (6.2 μL, 0.05 mmol). The resulting mixture was then analysed by ^{1}H, $^{31}P\{^{1}H\}$ and ^{31}P NMR spectroscopy, as shown in Figures S56-58, below.

The $^{31}P\{^{1}H\}$ spectrum clearly indicates formation of a single major species, characterised by a singlet resonance at –140.4 ppm, with $^{117/119}Sn$ satellites ($^{1}J(^{119}Sn\text{-}^{31}P)$ = 553 Hz), and which splits into a doublet in the ^{31}P spectrum ($^{1}J(^{31}P\text{-}^{1}H)$ = 193 Hz). Given the very similar chemical shift to *t*BuC(O)PH_2, this species can confidently be assigned as *t*BuC(O)P(H)$SnBu_3$ (**6**). Several minor product resonances can also be observed. Those at 52.2 ppm and –36.5 ppm are consistent with previous reports of the two tautomeric forms of the doubly-acylated product $HP(C(O)tBu)_2$ (**7**),[49] and the signal at –122.3 ppm can similarly be assigned to *t*BuC(O)PH_2 (**5**; Section 2.4.2.1). The unassigned signal at –125.2 ppm, which has $^{117/119}Sn$ satellites ($^{1}J(^{119}Sn\text{-}^{31}P)$ = 700 Hz) but remains a singlet in the ^{31}P spectrum, is attributed to *t*BuC(O)$P(SnBu_3)_2$, by analogy with *t*BuC(O)PH_2 and *t*BuC(O)P(H)$SnBu_3$. Finally, the signal arising at 10.2 ppm is assumed to be due to formation of $Bu_3SnP(C(O)tBu)_2$, based on the chemical shift (between the two tautomers of $HP(C(O)tBu)_2$), $^{117/119}Sn$ satellites ($^{1}J(^{119}Sn\text{-}^{31}P)$ = 547 Hz), and lack of splitting in the ^{31}P spectrum.

When the reaction was repeated using 2 eq. *t*BuC(O)Cl under otherwise identical conditions (Figures S59-61), the double acylation product **7** (in equilibrium with its tautomer) was observed to be the major product in the $^{31}P\{^{1}H\}$ spectrum, alongside minor $Bu_3SnP(C(O)tBu)_2$ and *t*BuC(O)$P(H)_x(SnBu_3)_{2-x}$ (x = 0-2).

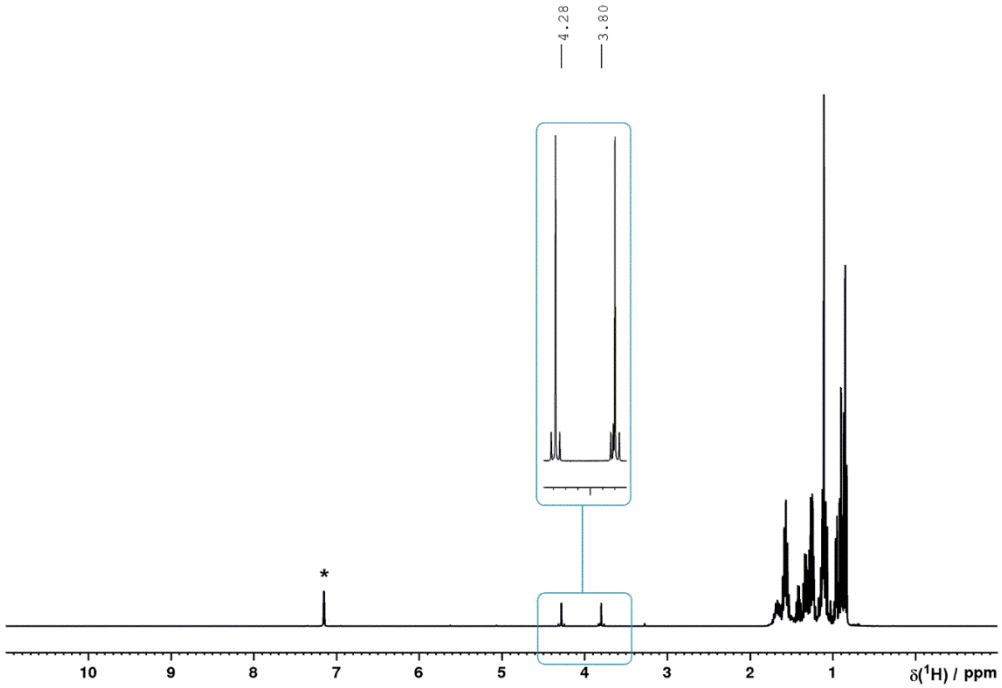

Figure S56. ^{1}H NMR spectrum for the reaction of $(Bu_3Sn)_2PH$ (**3**) with 1 eq. *t*BuC(O)Cl in C_6D_6 (*).

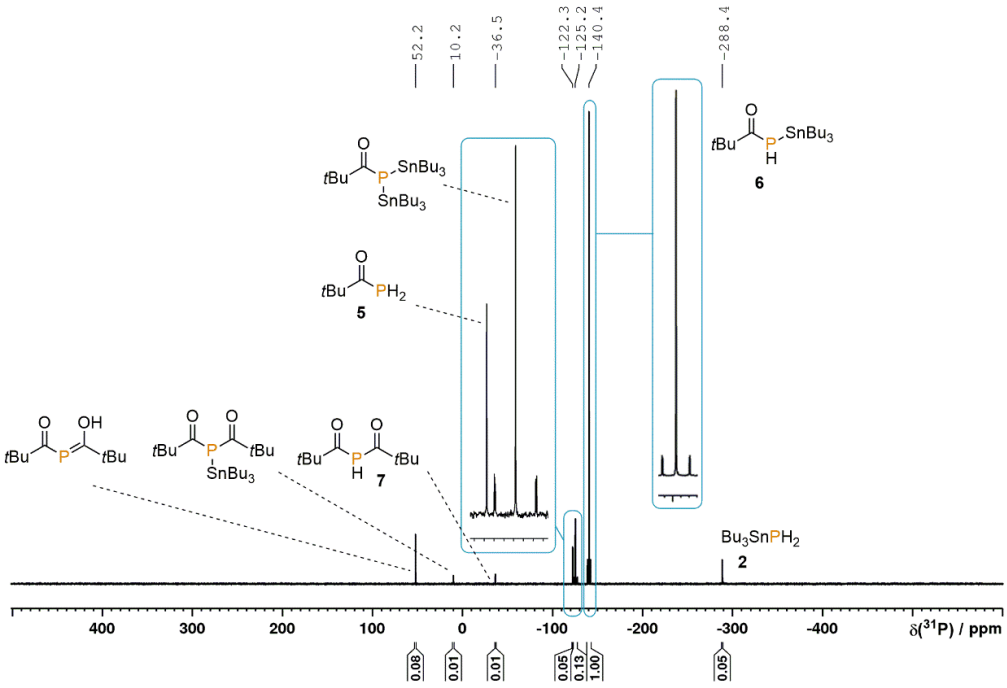

Figure S57. $^{31}P\{^{1}H\}$ NMR for the reaction of $(Bu_3Sn)_2PH$ (**3**) with 1 eq. *t*BuC(O)Cl in C_6D_6.

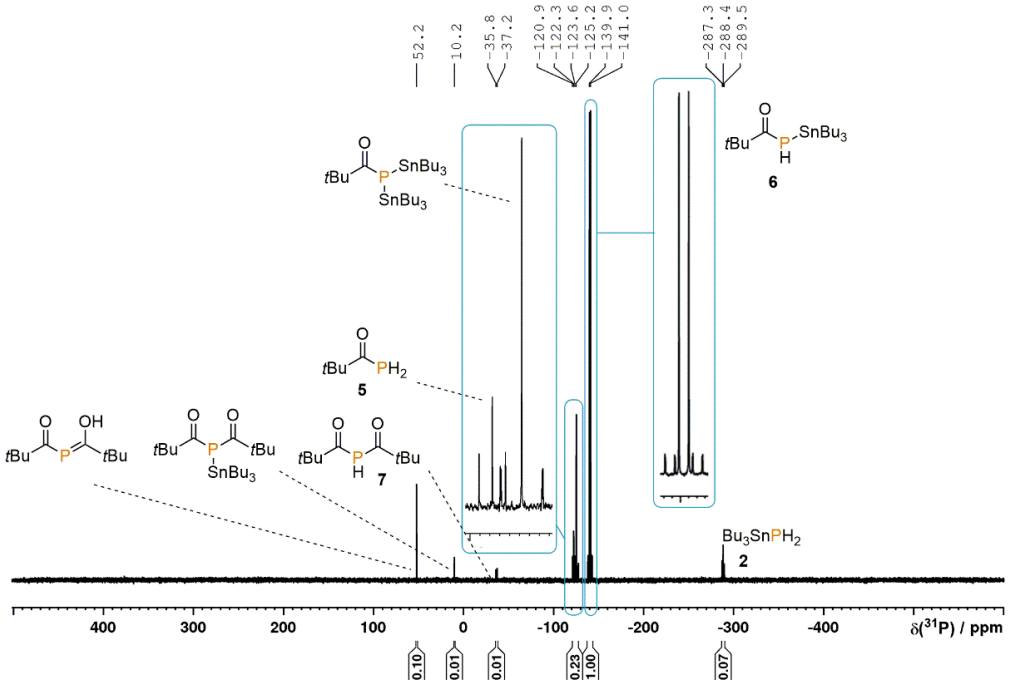

Figure S58. ^{31}P NMR spectrum for the reaction of $(Bu_3Sn)_2PH$ (**3**) with 1 eq. *t*BuC(O)Cl in C_6D_6.

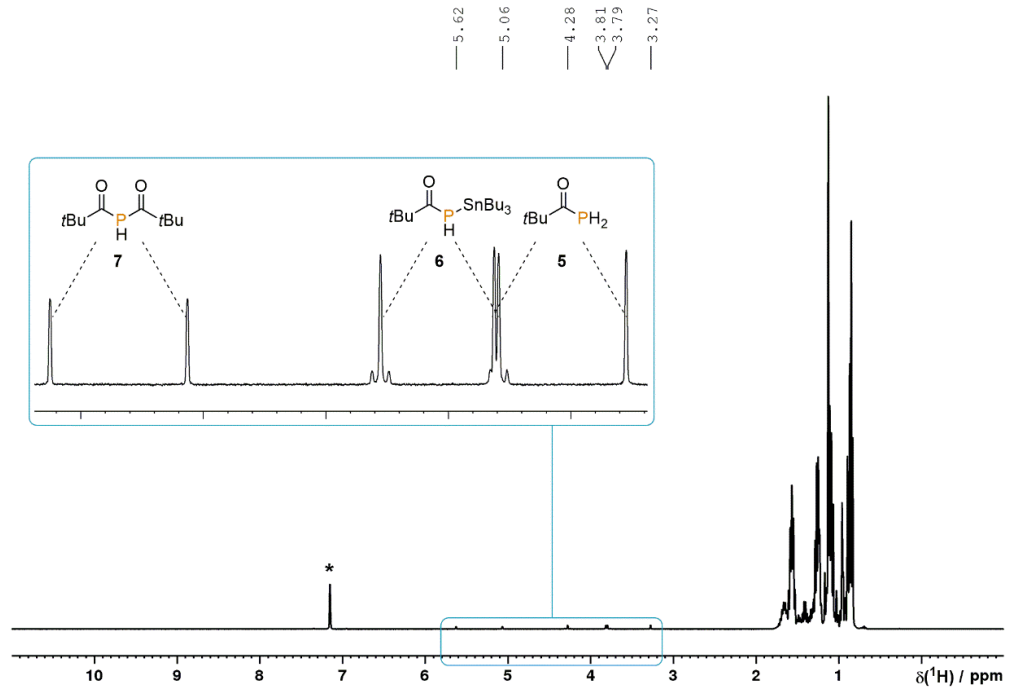

Figure S59. ^{1}H NMR spectrum for the reaction of $(Bu_3Sn)_2PH$ (**3**) with 2 eq. *t*BuC(O)Cl in C_6D_6 (*).

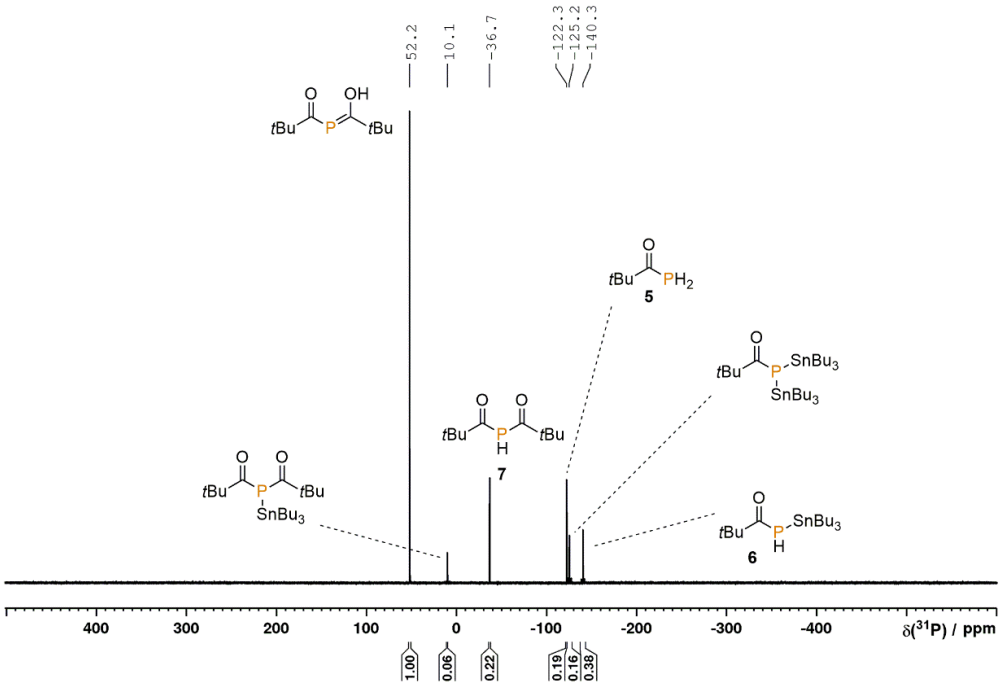

Figure S60. $^{31}P\{^{1}H\}$ NMR for the reaction of $(Bu_3Sn)_2PH$ (**3**) with 2 eq. *t*BuC(O)Cl in C_6D_6.

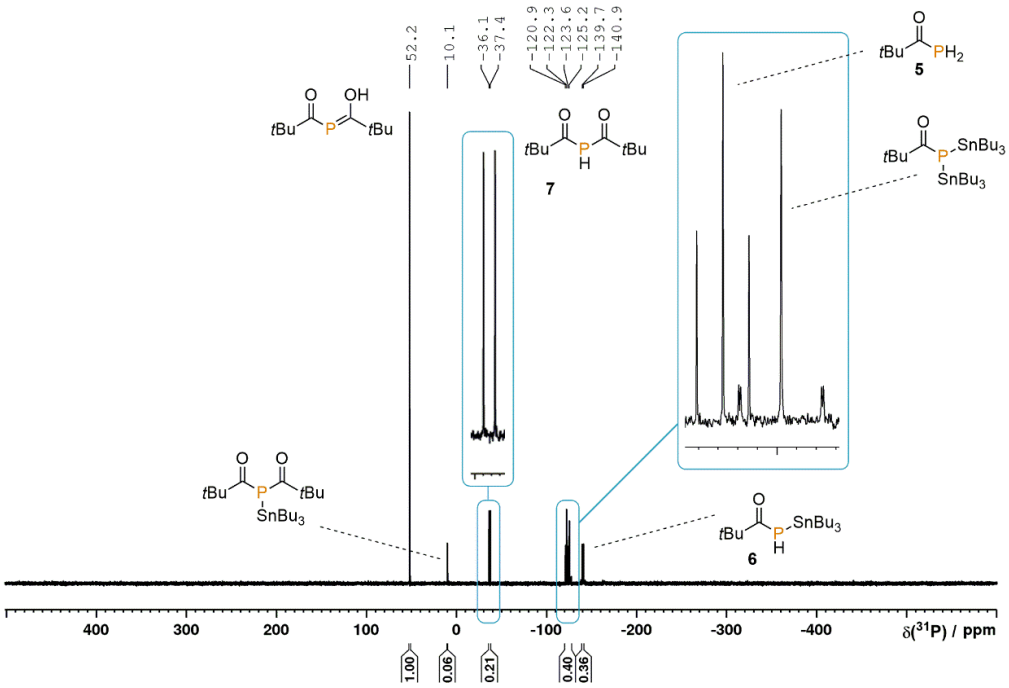

Figure S61. ^{31}P NMR spectrum for the reaction of $(Bu_3Sn)_2PH$ (**3**) with 2 eq. *t*BuC(O)Cl in C_6D_6.

2.4.2.3 Synthesis and quantification of PH_3 (1)

To an NMR tube fitted with a J. Young valve were added PhMe (500 µL), P_4 (0.01 mmol, as a stock solution in 77.4 µL PhH), Ph_3PO (14.2 mg, 0.051 mmol) and Bu_3SnH (16.1 µL, 0.06 mmol). The NMR tube was sealed, placed in thermal contact with a water-cooled block to maintain near-ambient temperature (by placing in a water-filled, flat-bottomed glass tube, which was in turn placed in the block and wrapped in Al foil), and irradiated with blue light (455 nm (±15 nm), 3.2 V, 700 mA, Osram OSLON SSL 80) for 17 h. The resulting colourless solution was frozen by placing the NMR tube in a bath of liquid nitrogen, and HCl (0.4 mmol, 4.0 M in 1,4-dioxane) was added (while still maintaining an inert atmosphere). The NMR tube was sealed and its contents were then thawed, agitated briefly, and analysed by ^{1}H, $^{31}P\{^{1}H\}$ and ^{31}P NMR spectroscopy. The resulting spectra indicated clean conversion to PH_3,[3] as shown in Figures S62-64, below.

In order to accurately quantify the amount of PH_3 in solution, a proton-coupled ^{31}P spectrum was acquired with a 20 s delay between scans (which was confirmed to be > 5 x T_1), and the intensity of the PH_3 resonance was integrated relative to that of Ph_3PO (which had been added specifically to act as an internal standard). This indicated 56% of the theoretical maximum conversion to PH_3 (Figure S65), which provides a lower bound for the actual conversion (this value does not include any PH_3 present in the NMR tube headspace).

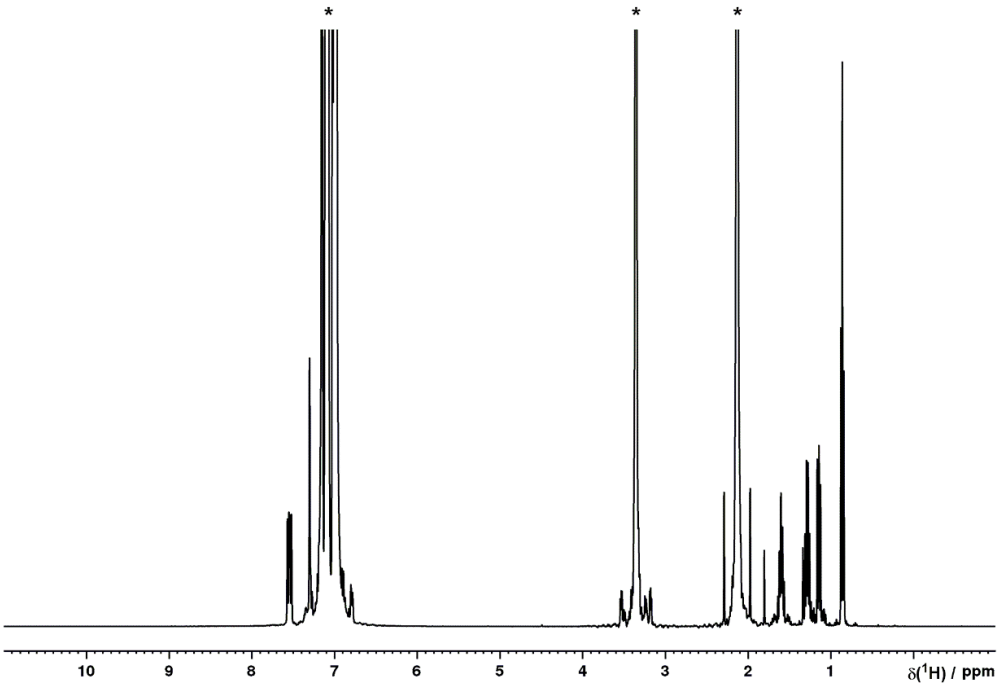

Figure S62. ^{1}H NMR spectrum of a solution of PH_3 (**1**) generated *via* hydrostannylation of P_4 in PhMe, followed by acidification. Solvent resonances (*) truncated for clarity.

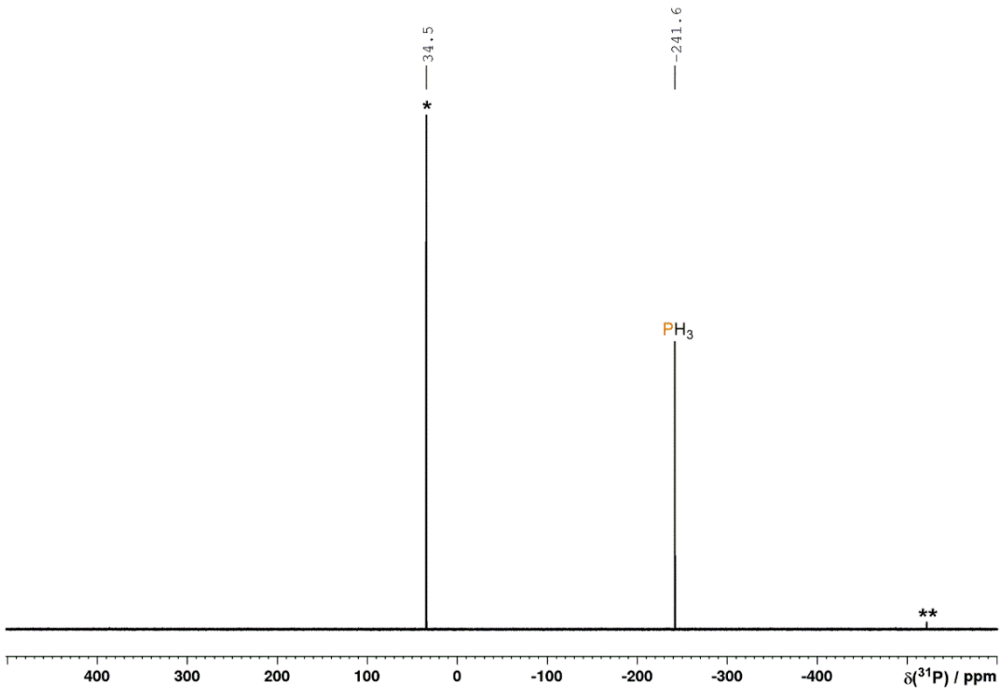

Figure S63. $^{31}P\{^{1}H\}$ NMR spectrum of PH_3 (**1**) generated *via* hydrostannylation of P_4 in PhMe, followed by acidification, in the presence of Ph_3PO (*) as an internal standard (** trace residual P_4).

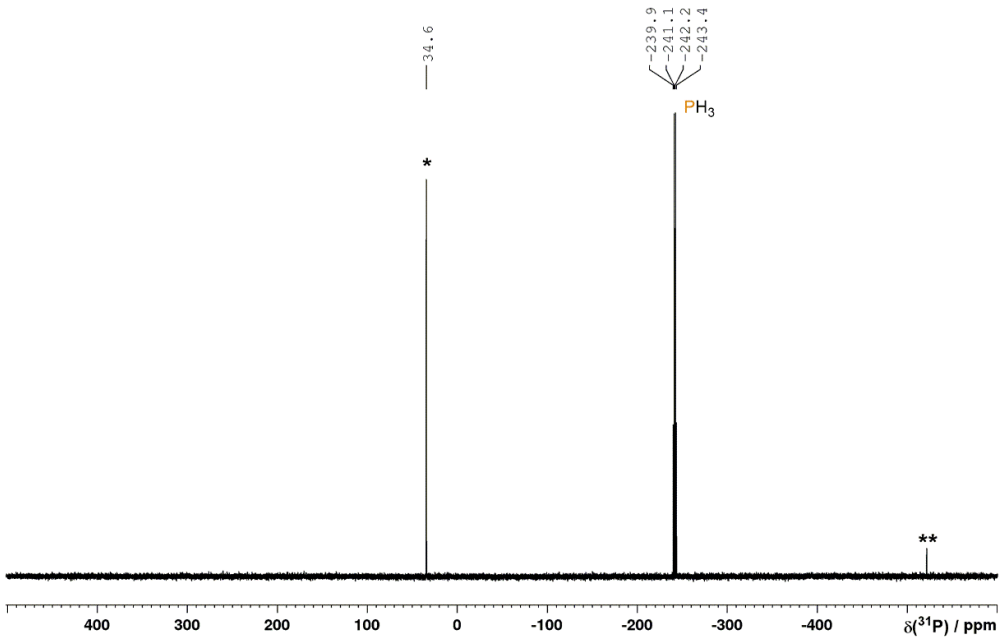

Figure S64. ^{31}P NMR spectrum of PH_3 (**1**) generated *via* hydrostannylation of P_4 in PhMe, followed by acidification, in the presence of Ph_3PO (*) as an internal standard (** trace residual P_4).

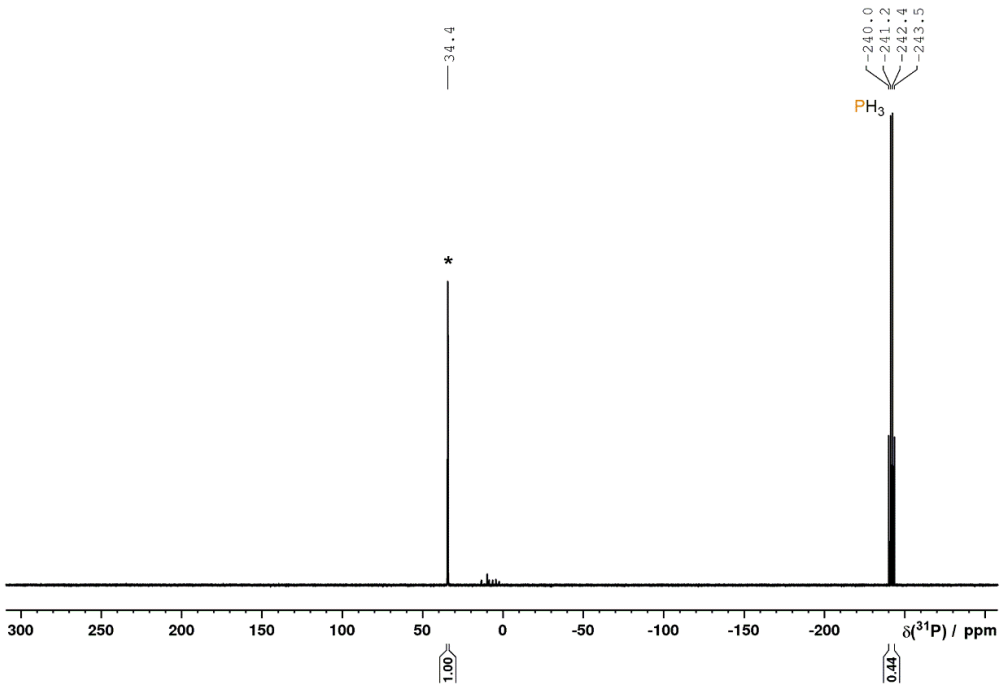

Figure S65. Quantitative ^{31}P NMR spectrum (D1 = 20 s) of PH_3 (**1**) generated *via* hydrostannylation of P_4 in PhMe, followed by acidification, in the presence of Ph_3PO (*) as an internal standard.

2.4.2.4 Synthesis and isolation of $P(SnBu_3)_3$ (4)

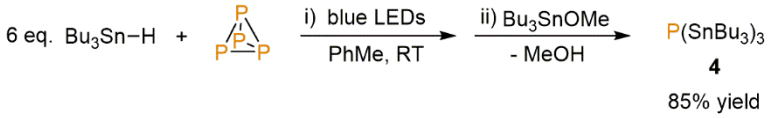

To a 50 mL, flat-bottomed Schlenk tube were added P_4 (61.9 mg, 0.5 mmol) and PhMe (25 mL). After stirring to obtain a homogeneous solution, Bu_3SnH (807 µL, 3.0 mmol) and Bu_3SnOMe (864 µL, 3.0 mmol) were added. The resulting colourless, homogeneous mixture was stirred in a water-cooled block (to maintain near-ambient temperature) and irradiated with blue light (7X Osram OSLON SSL80, 455 nm (±15 nm), 20.3 V 1000 mA) for 16 h. Following removal of volatiles under vacuum, the resulting yellowish oil was stirred at 100 °C for 16 h. After distillation under vacuum (*ca.* 105 °C, 10^{-2} mbar), the product was obtained as a colourless oil (1.53 g, 85%). **^{1}H NMR** (400 MHz, 300 K, C_6D_6): δ = 1.81-1.61 (2H, m), 1.51-1.40 (2H, m), 1.1-1.13 (2H, m), 0.98 ppm (3H, t, $^3J(^1H\text{-}^1H)$ = 7.3 Hz). **^{31}P{^{1}H} NMR** (121 MHz, 300 K, C_6D_6): δ = –346.5 ppm (s). **^{31}P NMR** (121 MHz, 300 K, C_6D_6): δ = –346.5 ppm (s). **^{119}Sn{^{1}H}** (149 MHz, 300 K, C_6D_6) δ = 37.6 ppm (d, $^1J(^{31}P\text{-}^{119}Sn)$ = 912 Hz, $^2J(^{119}Sn\text{-}^{117}Sn)$ = 279 Hz). **^{13}C{^{1}H} NMR** (101 MHz, 300 K, C_6D_6): δ = 29.7 (d, $J(^{31}P\text{-}^1H)$ = 1.4 Hz), 27.6 (s), 14.9 (d, $J(^{31}P\text{-}^1H)$ = 3.7 Hz), 13.5 ppm (s). **MS** (LIFDI, PhMe): *m*/*z* = 900.2518 (M^+). $P(SnBu_3)_3$ has been referenced in one previous paper of which we are aware, but no synthetic procedure or characterisation data appear to have been reported.[73] Nevertheless, the above ^{31}P NMR data are similar to those reported previously for the related compound $P(SnPh_3)_3$.[19]

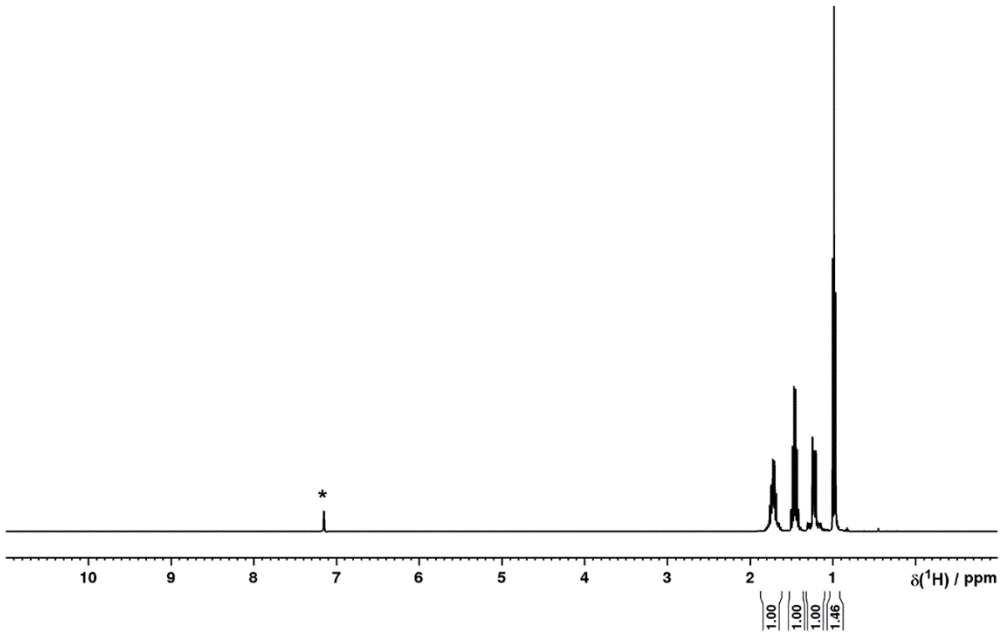

Figure S66. ^{1}H NMR spectrum of $P(SnBu_3)_3$ (**4**) in C_6D_6 (*).

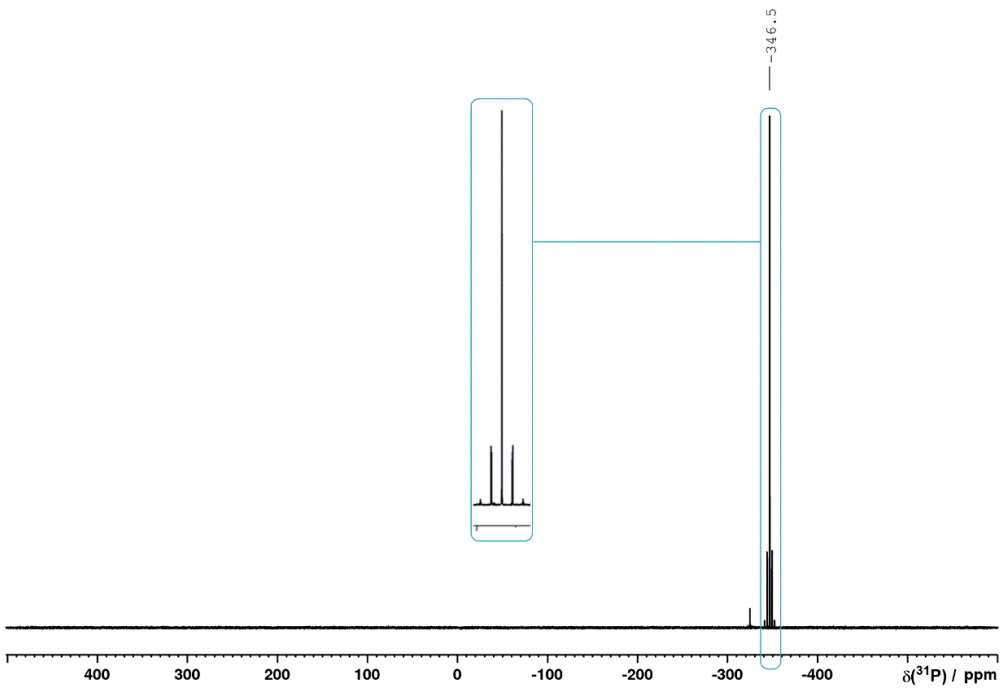

Figure S67. $^{31}P\{^{1}H\}$ NMR spectrum of $P(SnBu_3)_3$ (**4**) in C_6D_6.

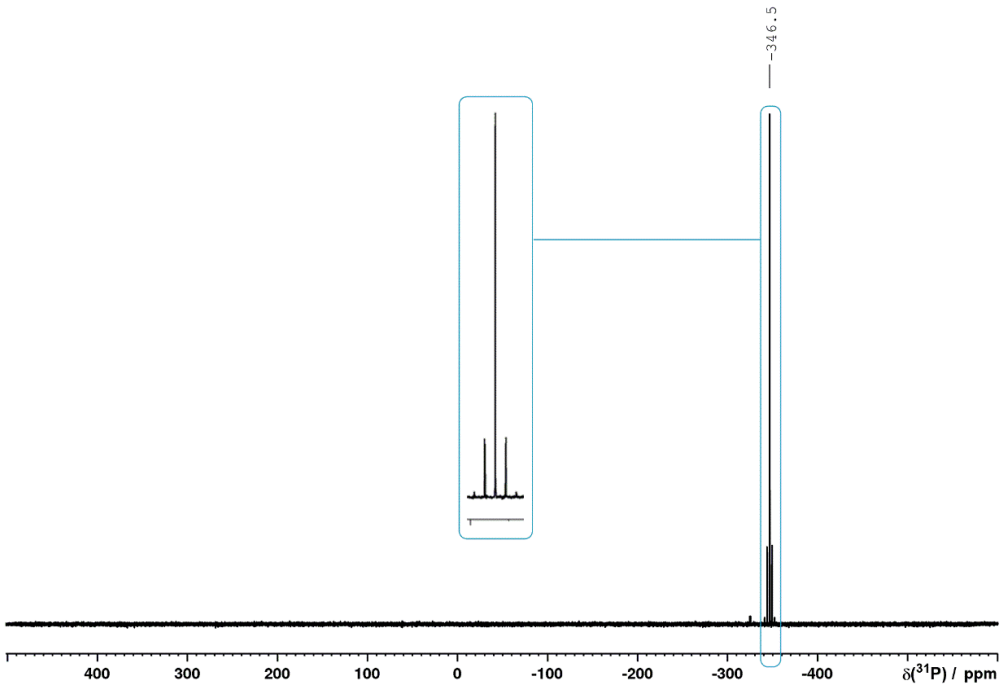

Figure S68. ^{31}P NMR spectrum of $P(SnBu_3)_3$ (**4**) in C_6D_6.

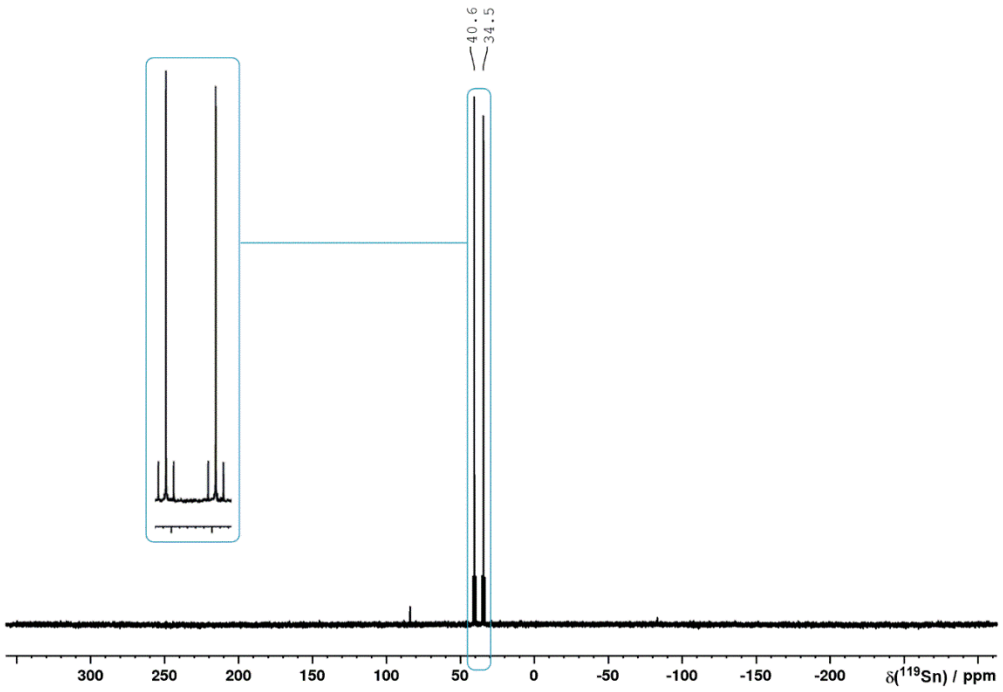

Figure S69. $^{119}Sn\{^1H\}$ NMR spectrum of $P(SnBu_3)_3$ (**4**) in C_6D_6.

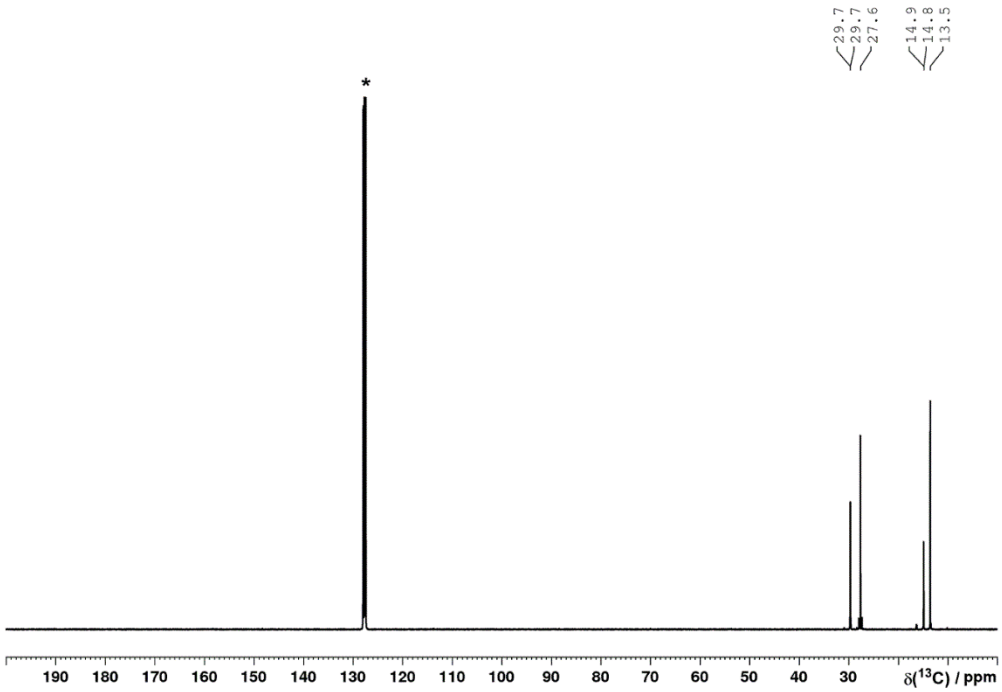

Figure S70. $^{13}C\{^{1}H\}$ NMR spectrum of $P(SnBu_3)_3$ (**4**) in C_6D_6 (*).

2.4.2.5 Synthesis and isolation of P(C(O)*t*Bu)$_3$ (8)

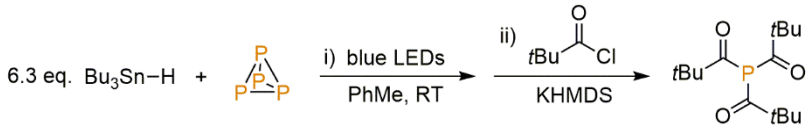

8

57% yield

To a 50 mL flat-bottomed Schlenk were added P_4 (62.0 mg, 0.5 mmol) and PhMe (25 mL). After stirring to obtain a homogeneous solution Bu_3SnH was added (847 µL, 3.15 mmol). The resulting colourless solution was stirred under irradiation with blue LED light (7X Osram OSLON SSL80, 455 nm (±15 nm), 20.3 V 1000mA) for 22 h, during which time the Schlenk tube was placed in a block cooled by circulating water to maintain near-ambient temperature. *t*BuC(O)Cl (979 µL, 8.0 mmol) and KHMDS (599 mg, 3.0 mmol) were added, the Schlenk tube was immediately and thoroughly wrapped in Al foil to exclude any ambient light, and the reaction mixture was stirred at room temperature for 16 h. The resulting light yellow suspension was filtered, and volatiles were removed under vacuum. The remaining white residue was recrystallized from n-hexane at –35 °C, to afford the desired product as colourless needles (325 mg, 57%).

^{1}H NMR (400 MHz, 300 K, C_6D_6): δ = 1.07 ppm (s). **^{31}P{^{1}H} NMR** (121 MHz, 300 K, C_6D_6): δ = 51.6 ppm (s). **^{31}P NMR** (121 MHz, 300 K, C_6D_6): δ = 51.6 ppm (s). **^{13}C{^{1}H} NMR** (101 MHz, 300 K, C_6D_6): δ = 221.3 (d, $^{1}J(^{31}P\text{-}^{1}H)$ = 47.9 Hz), 49.7 (d, $^{2}J(^{31}P\text{-}^{1}H)$ = 30.3 Hz), 25.4 ppm (d, $^{3}J(^{31}P\text{-}^{1}H)$ = 3.7 Hz). **MS** (APCI, PhMe): *m*/*z* = 304.2044 ($[M+NH_4]^+$). NMR data are consistent with previous reports.[50]

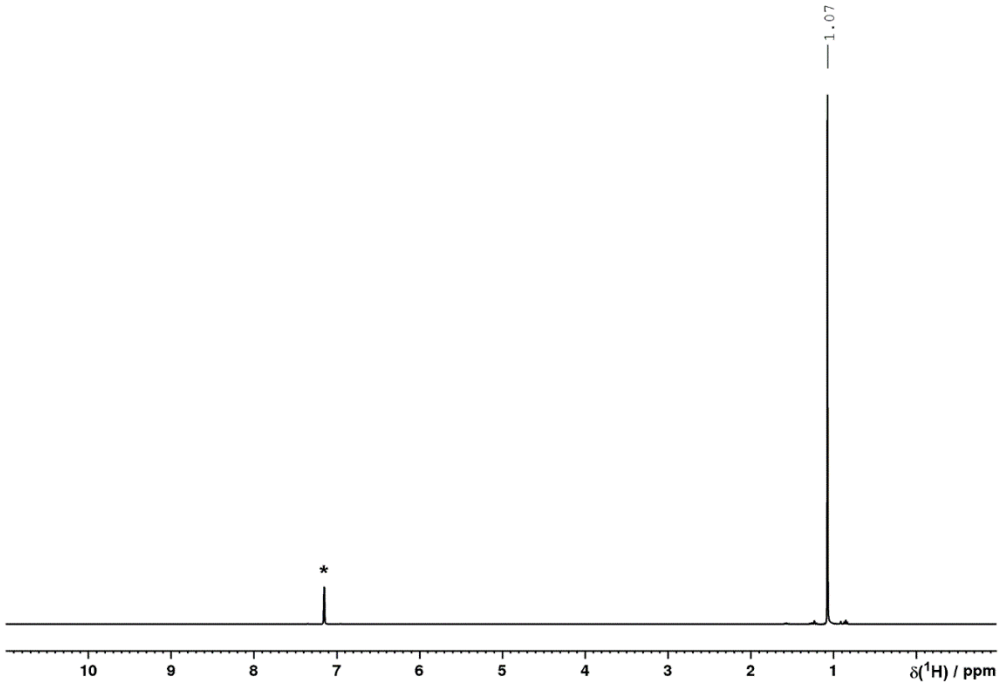

Figure S71. ^{1}H NMR spectrum of $P(C(O)tBu)_3$ (**8**) in C_6D_6 (*).

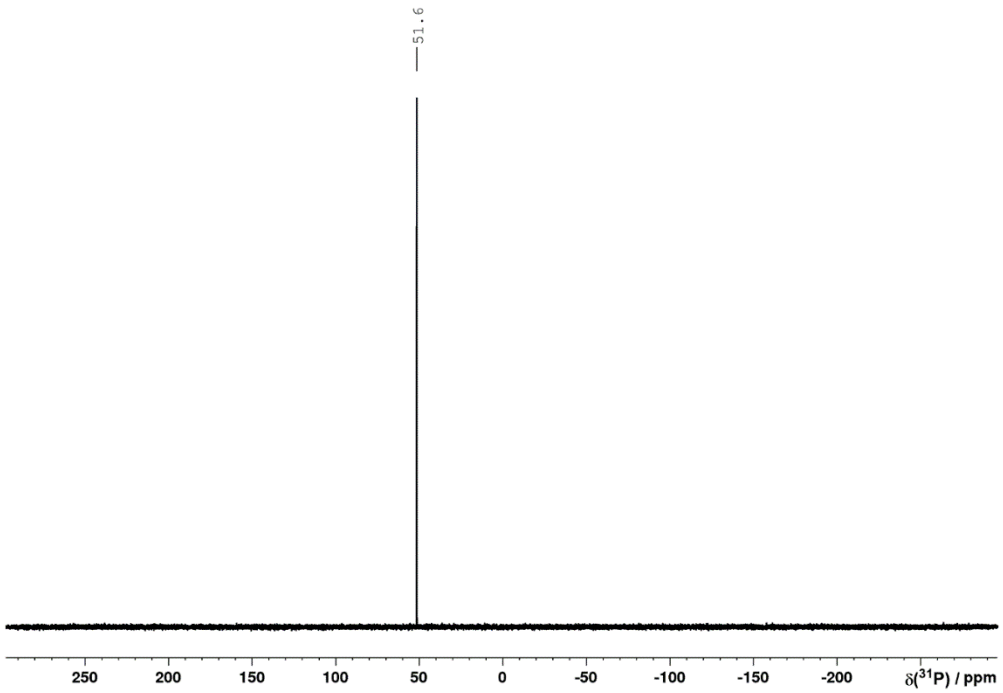

Figure S72. $^{31}P\{^{1}H\}$ NMR spectrum of $P(C(O)tBu)_3$ (**8**) in C_6D_6.

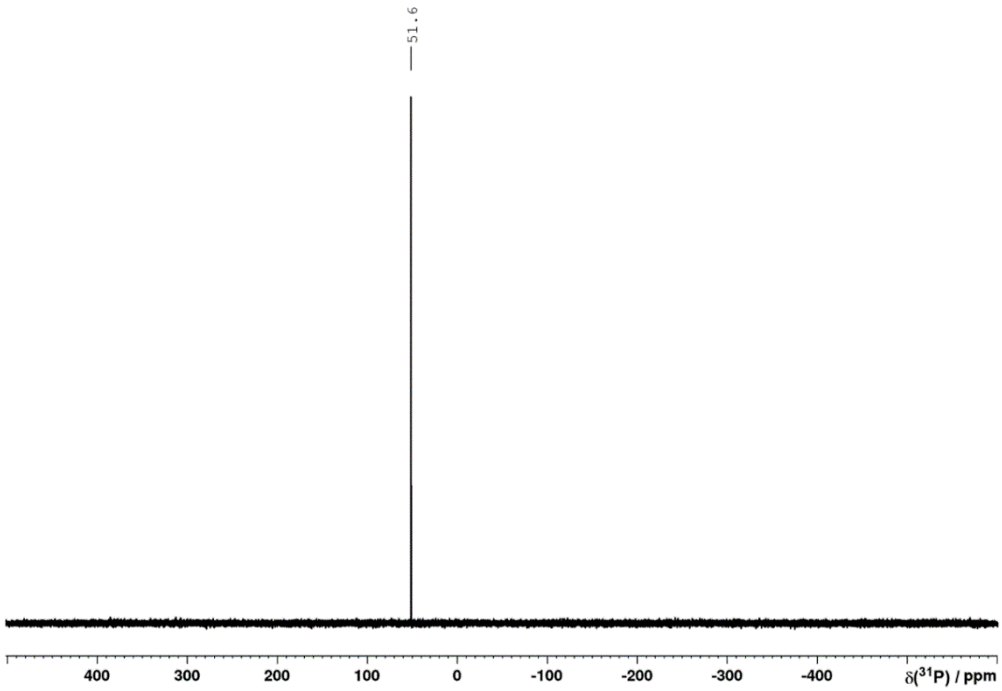

Figure S73. ^{31}P NMR spectrum of P(C(O)*t*Bu)$_3$ (**8**) in C_6D_6.

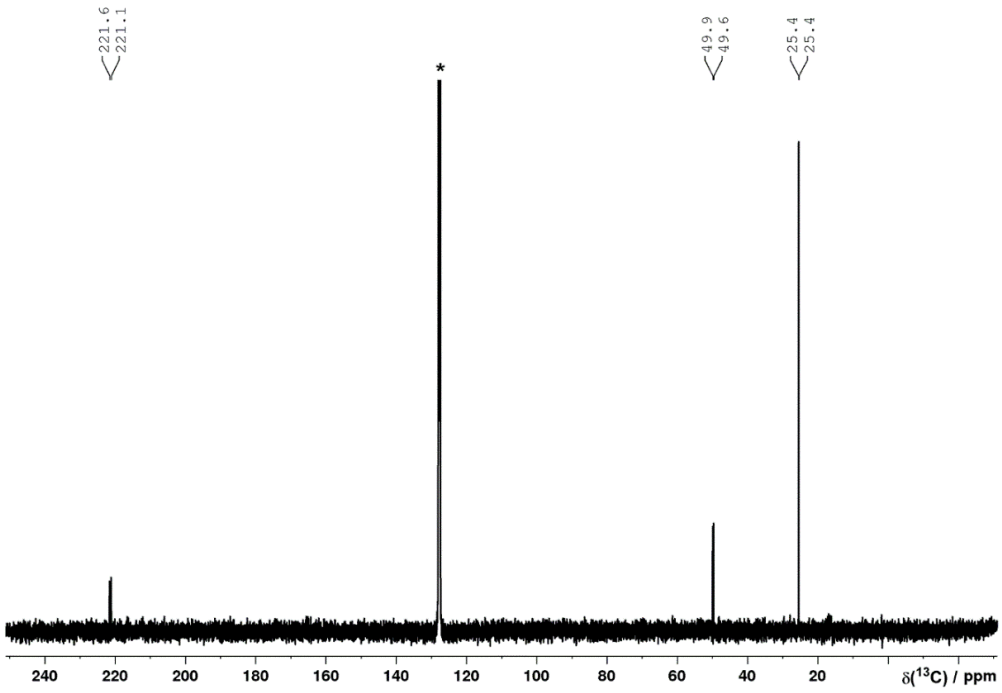

Figure S74. $^{13}C\{^1H\}$ NMR spectrum of P(C(O)*t*Bu)$_3$ (**8**) in C_6D_6. Solvent resonance (*) truncated for clarity.

2.4.2.6 Synthesis and isolation of $P(C(O)Ph)_3$ (9)

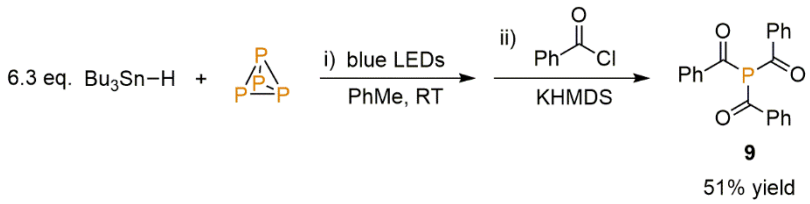

To a 50 mL flat-bottomed Schlenk tube were added P_4 (62.0 mg, 0.5 mmol) and PhMe (25 mL). After stirring to obtain a homogeneous solution Bu_3SnH was added (847 µL, 3.15 mmol). The resulting colourless solution was stirred under irradiation with blue LED light (7X Osram OSLON SSL80, 455 nm (±15 nm), 20.3 V 1000mA) for 22 h, during which time the Schlenk tube was placed in a block cooled by circulating water to maintain near-ambient temperature. PhC(O)Cl (929 µL, 8.0 mmol) and KHMDS (599 mg, 3.0 mmol) were added, and the reaction mixture was stirred at room temperature for 16 h. The resulting yellow suspension was filtered, volatiles were removed under vacuum, and the remaining solid was washed with *n*-hexane (4 x 20 mL). The remaining yellow residue was recrystallized from THF/*n*-hexane at –35 °C, to afford the desired product as yellow needles (355 mg, 51%).

^{1}H NMR (400 MHz, 300 K, C_6D_6): δ = 7.98 ppm (2H, m), 7.03 ppm (1H, tt, $^3J(^1H\text{-}^1H)$ =7.3 Hz, $^5J(^1H\text{-}^1H)$ =1.4 Hz), 6.96 ppm (2H, m). **^{31}P{^{1}H} NMR** (121 MHz, 300 K, C_6D_6): δ = 54.4 ppm (s). **^{31}P NMR** (121 MHz, 300 K, C_6D_6): δ = 54.4 ppm (s). **^{13}C{^{1}H} NMR** (101 MHz, 300 K, C_6D_6): δ = 205.8 (d, $J(^{31}P\text{-}^1H)$ = 32.9 Hz), 140.9 (d, $J(^{31}P\text{-}^1H)$ = 35.2 Hz), 133.9 (d, $J(^{31}P\text{-}^1H)$ = 1.4 Hz), 129.0 (d, $J(^{31}P\text{-}^1H)$ = 8.0 Hz), 128.9 ppm (d, $J(^{31}P\text{-}^1H)$ = 0.8 Hz). **MS** (ESI, PhMe): *m*/*z* = 347.0840 ($[M+H]^+$). NMR data are consistent with previous reports.[74]

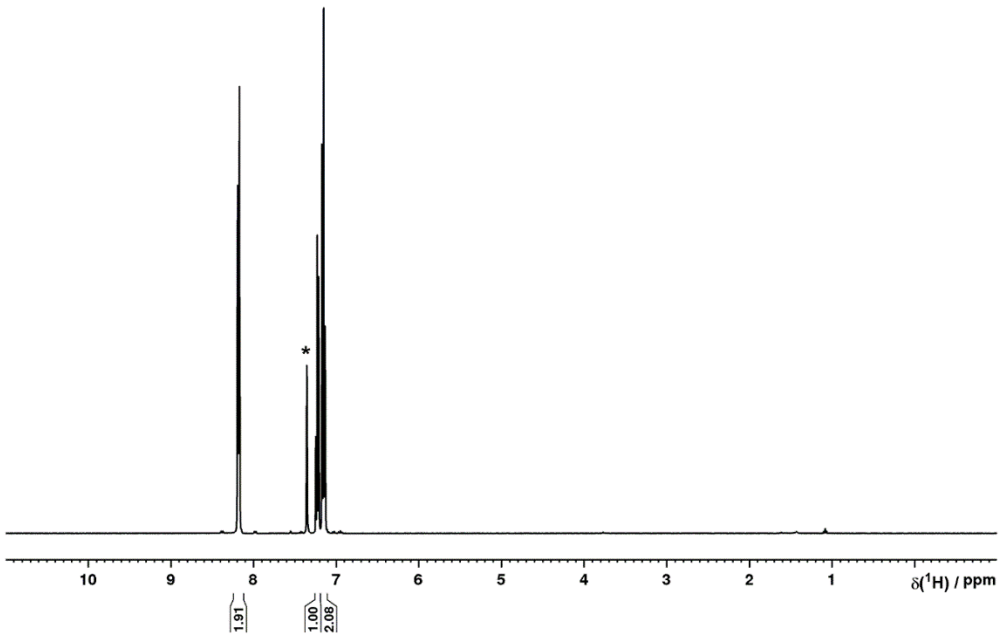

Figure S75. ^{1}H NMR spectrum of $P(C(O)Ph)_3$ (**9**) in C_6D_6 (*).

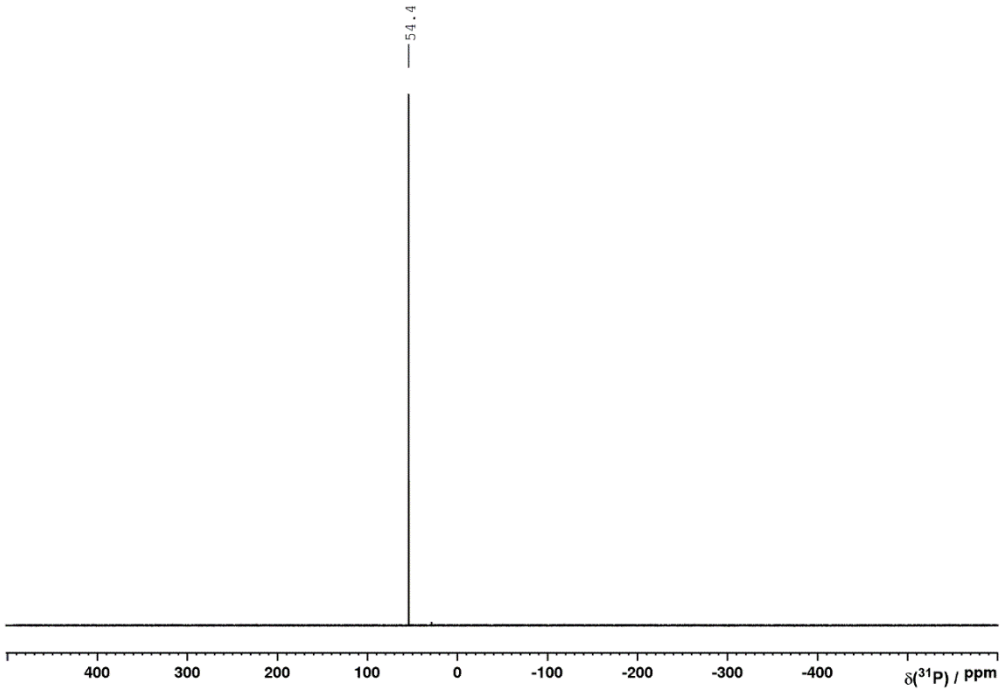

Figure S76. $^{31}P\{^{1}H\}$ NMR spectrum of $P(C(O)Ph)_3$ (**9**) in C_6D_6.

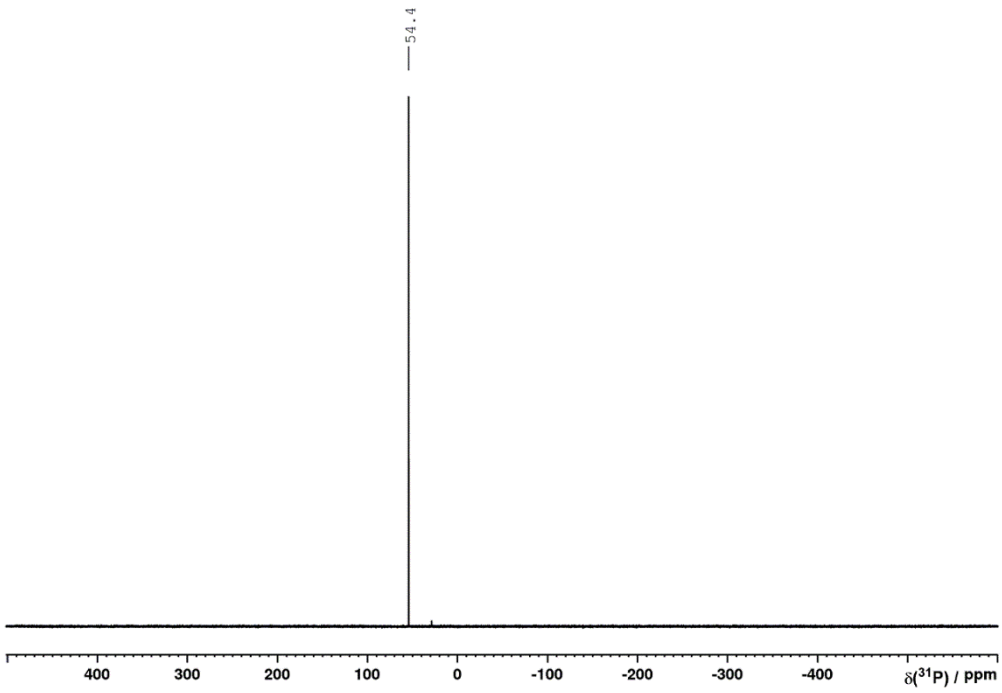

Figure S77. ^{31}P NMR spectrum of $P(C(O)Ph)_3$ (**9**) in C_6D_6.

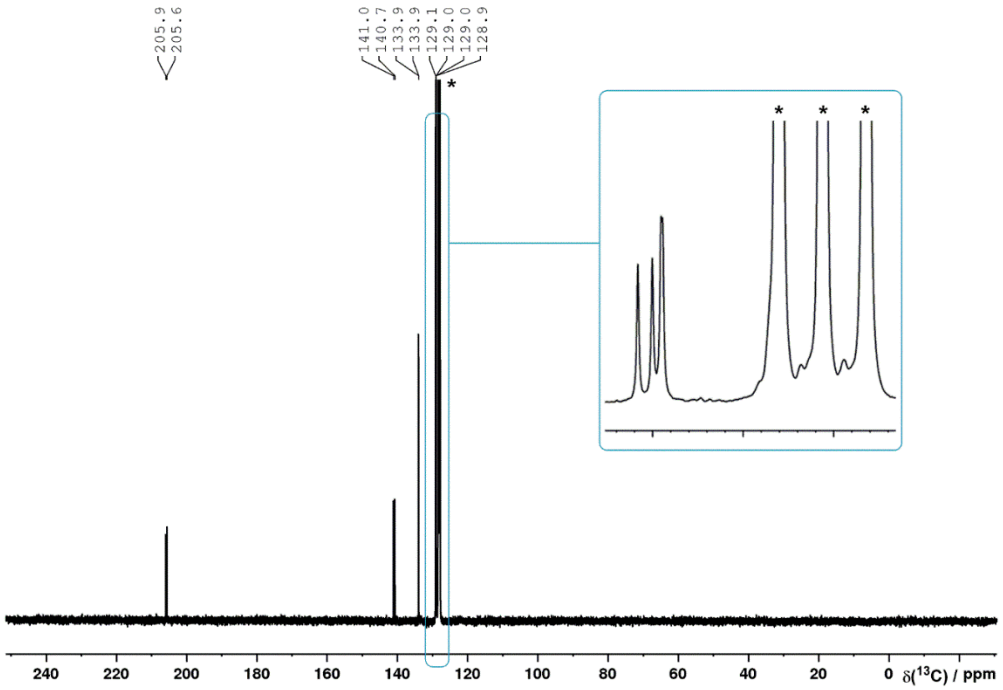

Figure S78. $^{13}C\{^{1}H\}$ NMR spectrum of $P(C(O)Ph)_3$ (**9**) in C_6D_6. Solvent resonance (*) truncated for clarity.

2.4.2.7 Synthesis and isolation of P(C(O)*i*Pr)$_3$ (10)

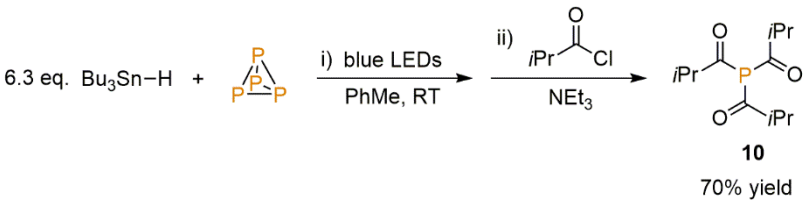

10

70% yield

To a 50 mL flat-bottomed Schlenk tube were added P_4 (62.0 mg, 0.5 mmol) and PhMe (25 mL). After stirring to obtain a homogeneous solution Bu_3SnH was added (847 µL, 3.15 mmol). The resulting colourless solution was stirred under irradiation with blue LED light (7X Osram OSLON SSL80, 455 nm (±15 nm), 20.3 V 1000mA) for 22 h, during which time the Schlenk tube was placed in a block cooled by circulating water to maintain near-ambient temperature. *i*PrC(O)Cl (838 µL, 8.0 mmol) and NEt_3 (418 µL, 3.0 mmol) were added, and the reaction mixture was stirred at room temperature for 16 h. The resulting light yellow suspension was evaporated to dryness, and the remaining solid was extracted with *n*-hexane (3 x 20 mL). The combined extracts were again evaporated to dryness, and the remaining residue was distilled under vacuum (*ca*. 45 °C, 10^{-5} mbar) to afford the desired product as a yellowish oil (341 mg, 70%).

^{1}H NMR (400 MHz, 300 K, C_6D_6): δ = 3.17 ppm (1H, septet, $^{3}J(^{1}H\text{-}^{1}H)$ = 6.9 Hz), 1.03 ppm (6H, d, $^{3}J(^{1}H\text{-}^{1}H)$ = 6.9 Hz). **$^{31}P\{^{1}H\}$ NMR** (121 MHz, 300 K, C_6D_6): δ = 54.1 ppm (s). **^{31}P NMR** (121 MHz, 300 K, C_6D_6): δ = 54.1 ppm (s). **$^{13}C\{^{1}H\}$ NMR** (101 MHz, 300 K, C_6D_6): δ = 219.6 (d, $^{1}J(^{31}P\text{-}^{1}H)$ = 49.6 Hz), 46.6 (d, $^{2}J(^{31}P\text{-}^{1}H)$ = 31.1 Hz), 17.8 ppm (d, $^{3}J(^{31}P\text{-}^{1}H)$ = 3.8 Hz). **MS** (APCI, PhMe): *m*/*z* = 245.1304 ($[M+H]^+$).

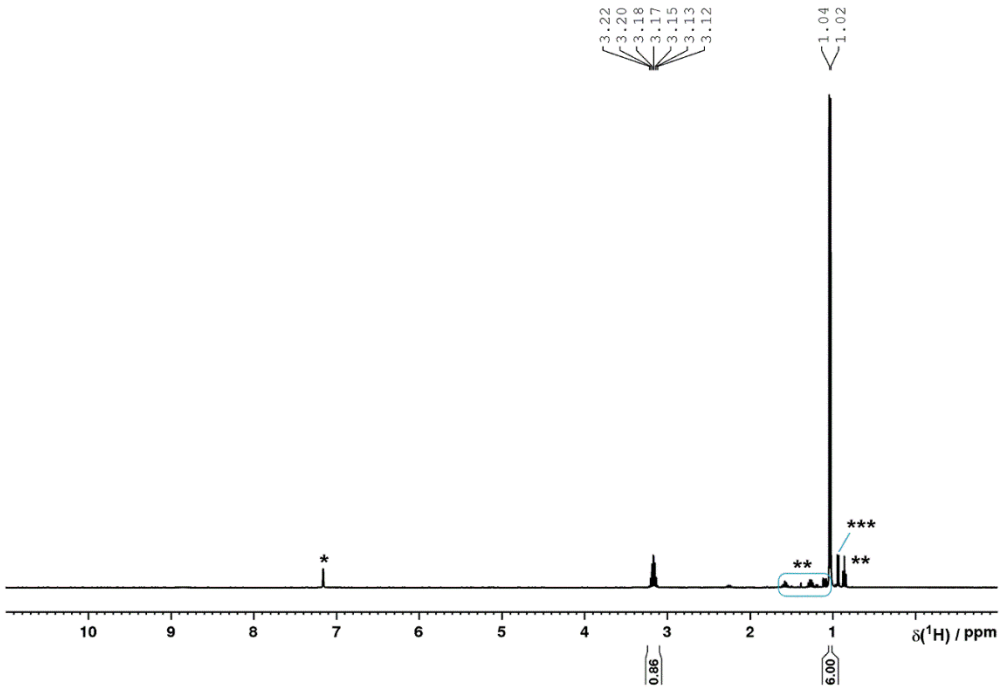

Figure S79. ^{1}H NMR spectrum of $P(C(O)iPr)_3$ (**10**) in C_6D_6 (*solvent, **minor Bu_3SnCl, ***unidentified minor impurity).

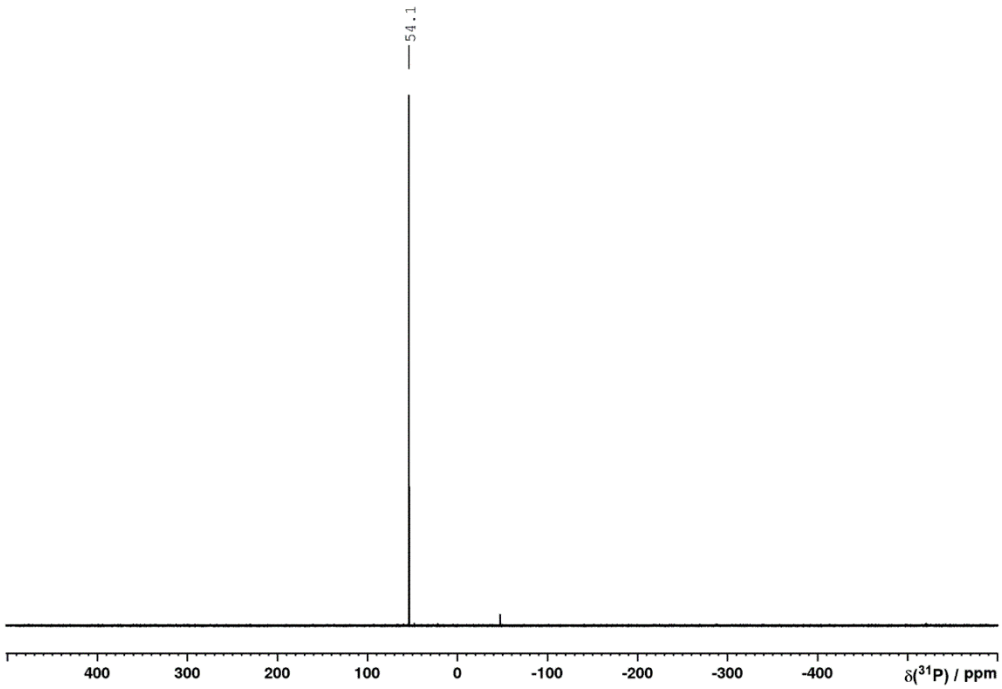

Figure S80. $^{31}P\{^{1}H\}$ NMR spectrum of $P(C(O)iPr)_3$ (**10**) in C_6D_6.

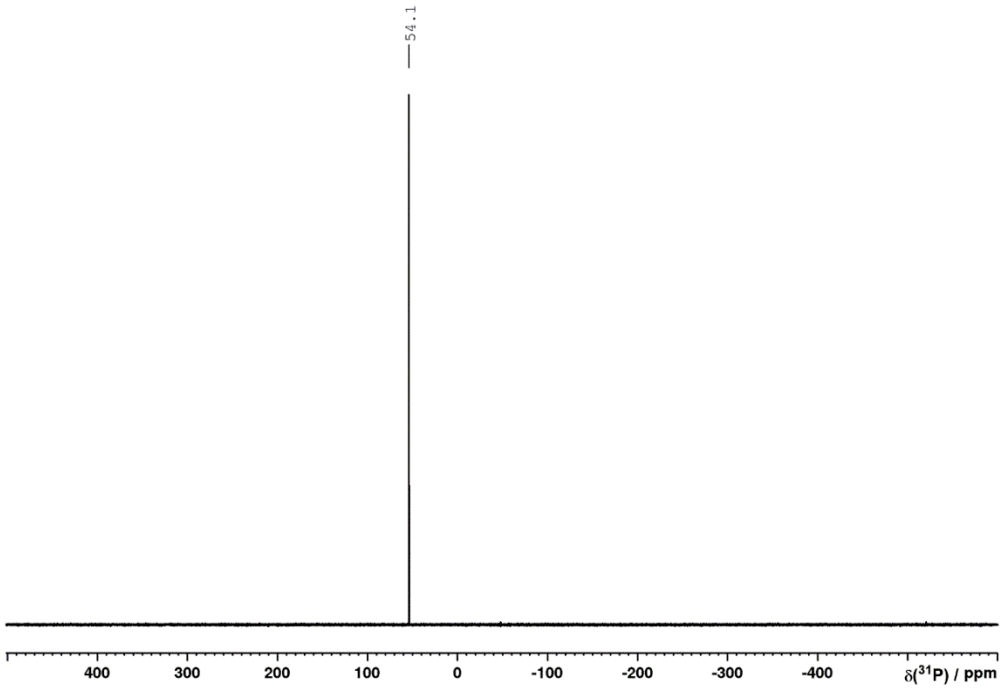

Figure S81. ^{31}P NMR spectrum of $P(C(O)iPr)_3$ (**10**) in C_6D_6.

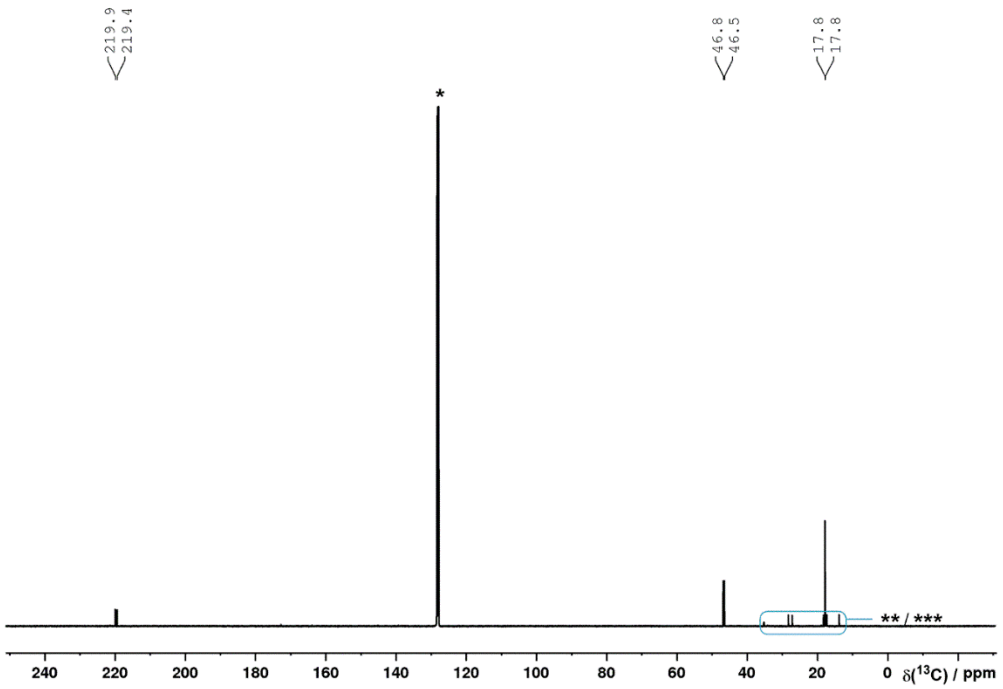

Figure S82. $^{13}C\{^1H\}$ NMR spectrum of $P(C(O)iPr)_3$ (**10**) in C_6D_6. Solvent resonance (*) truncated for clarity (**minor Bu_3SnCl, ***unidentified minor impurity).

2.4.2.8 Synthesis and quantification of $P(C(O)Cy)_3$ (11)

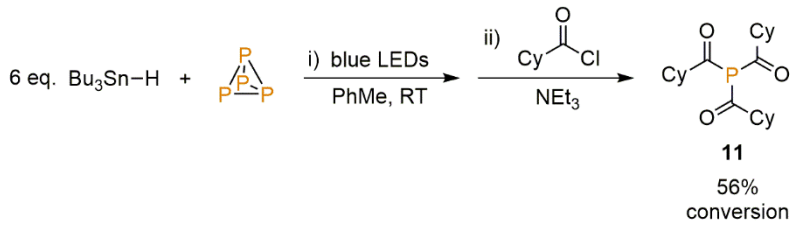

To a 10 mL, flat-bottomed, stoppered tube were added PhMe (500 µL), P_4 (0.01 mmol, as a stock solution in 77.4 µL PhH) and Bu_3SnH (16.1 µL, 0.06 mmol). The resulting colourless solution was stirred under irradiation with blue LED light (455 nm (±15 nm), 3.2 V, 700 mA, Osram OSLON SSL 80) for 18 h, during which time the tube was placed in a block cooled by circulating water to maintain near-ambient temperature. CyC(O)Cl (21.4 µL, 0.16 mmol) and Et_3N (8.4 µL, 0.06 mmol) were added, and the reaction mixture was stirred at room temperature for 16 h. Ph_3PO (13.1 mg, 0.047 mmol) was added, and the resulting mixture was analysed by ^1H, $^{31}P\{^1H\}$ and ^{31}P NMR spectroscopy (Figures S83-85). Conversion to $P(C(O)Cy)_3$ (56%) was determined using quantitative $^{31}P\{^1H\}$ spectroscopy (D1 = 22 s, Figure S86), by relative integration of the resonances assigned to Ph_3PO and $P(C(O)Cy)_3$.

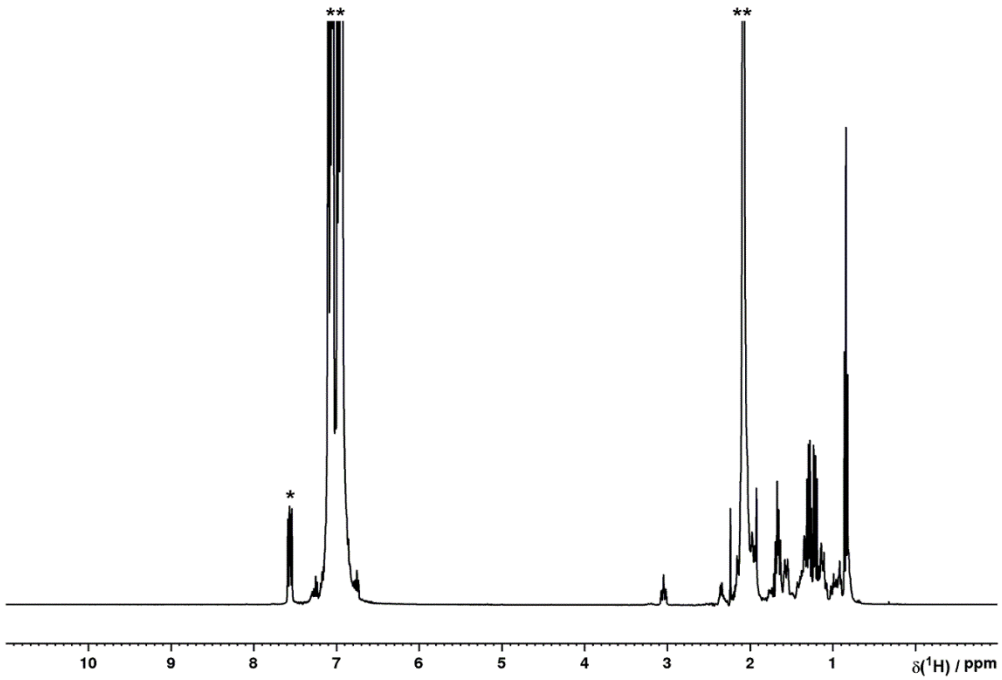

Figure S83. ^1H NMR spectrum of $P(C(O)Cy)_3$ (**11**) generated *via* hydrostannylation of P_4 in PhMe followed by acylation, in the presence of Ph_3PO (*) as an internal standard. Solvent resonances (**) truncated for clarity.

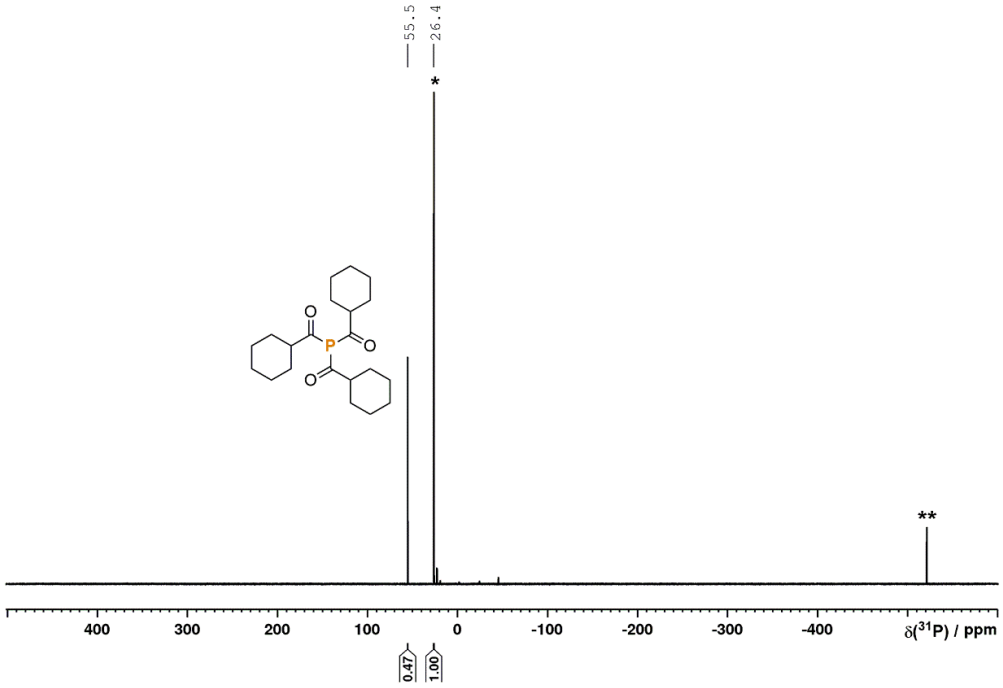

Figure S84. $^{31}P\{^{1}H\}$ NMR spectrum of $P(C(O)Cy)_3$ (**11**) generated *via* hydrostannylation of P_4 in PhMe followed by acylation, in the presence of Ph_3PO (*) as internal standard (**minor residual P_4).

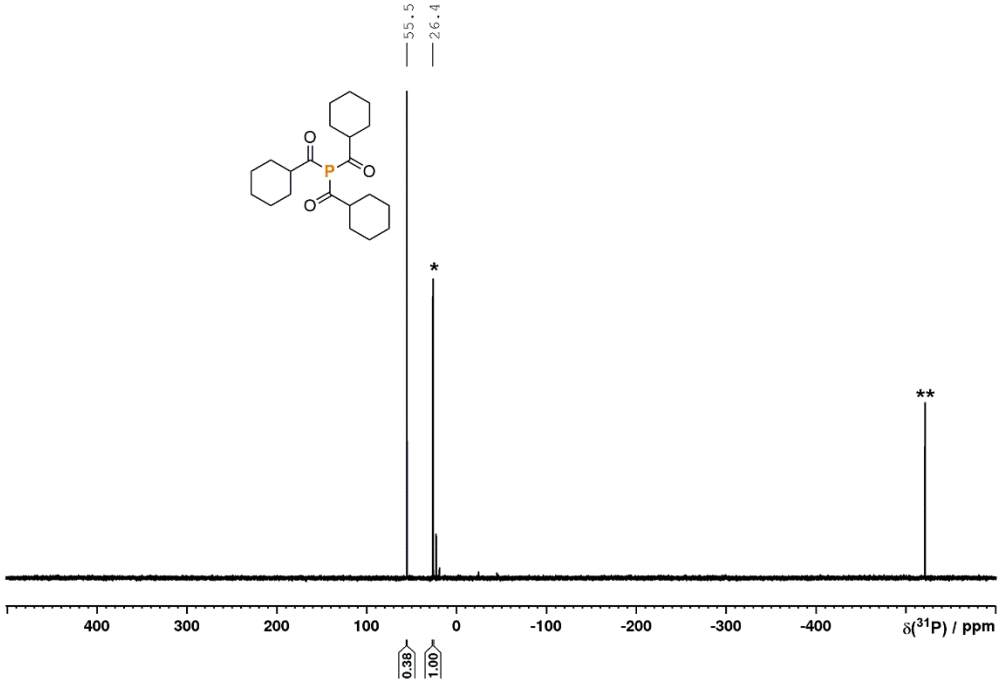

Figure S85. ^{31}P NMR spectrum of $P(C(O)Cy)_3$ (**11**) generated *via* hydrostannylation of P_4 in PhMe followed by acylation, in the presence of Ph_3PO (*) as an internal standard (**minor residual P_4).

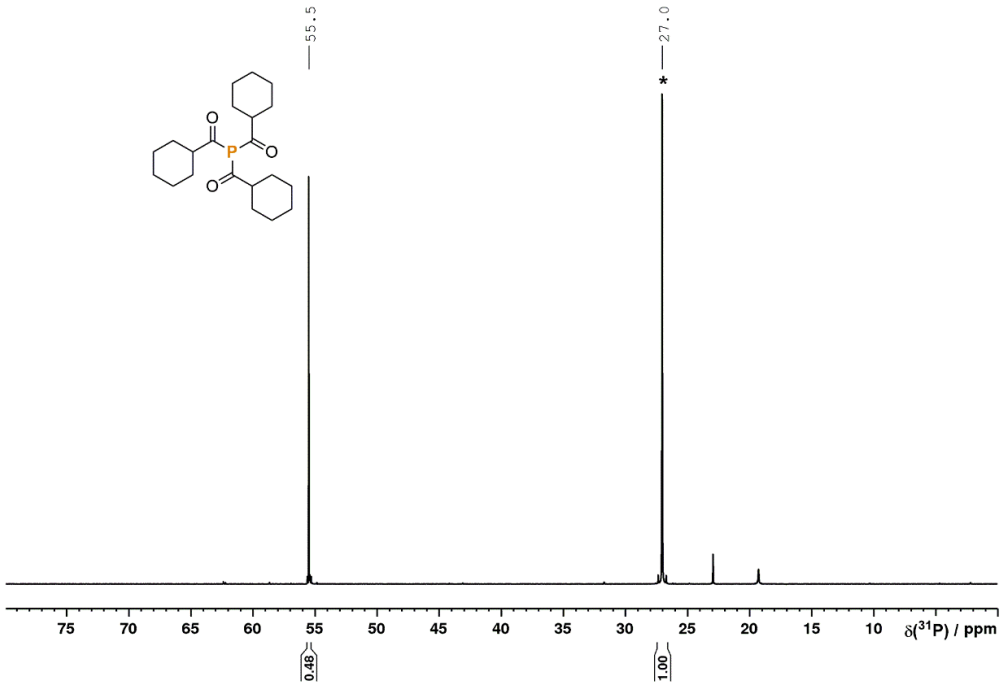

Figure S86. Quantitative $^{31}P\{^{1}H\}$ NMR spectrum (D1 = 22 s) of $P(C(O)Cy)_3$ (**11**) generated *via* hydrostannylation of P_4 in PhMe followed by acylation, in the presence of Ph_3PO (*) as an internal standard.

2.4.2.9 Synthesis and quantification of $P(C(O)Bu)_3$ (12)

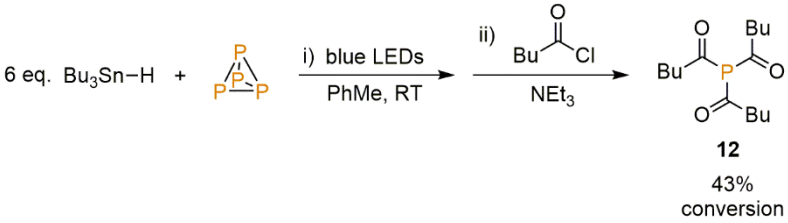

To a 10 mL, flat-bottomed, stoppered tube were added PhMe (500 µL), P_4 (0.01 mmol, as a stock solution in 77.4 µL PhH) and Bu_3SnH (16.1 µL, 0.06 mmol). The resulting colourless solution was stirred under irradiation with blue LED light (455 nm (±15 nm), 3.2 V, 700 mA, Osram OSLON SSL 80) for 18 h, during which time the tube was placed in a block cooled by circulating water to maintain near-ambient temperature. BuC(O)Cl (19.0 µL, 0.16 mmol) and Et_3N (8.4 µL, 0.06 mmol) were added, and the reaction mixture was stirred at room temperature for 16 h. Ph_3PO (13.0 mg, 0.047 mmol) was added, and the resulting mixture was analysed by ^{1}H, $^{31}P\{^{1}H\}$ and ^{31}P NMR spectroscopy (Figures S87-89). Conversion to $P(C(O)Bu)_3$ (43%) was determined using quantitative $^{31}P\{^{1}H\}$ spectroscopy (D1 = 22 s, Figure S90), by relative integration of the resonances assigned to Ph_3PO and $P(C(O)Bu)_3$.

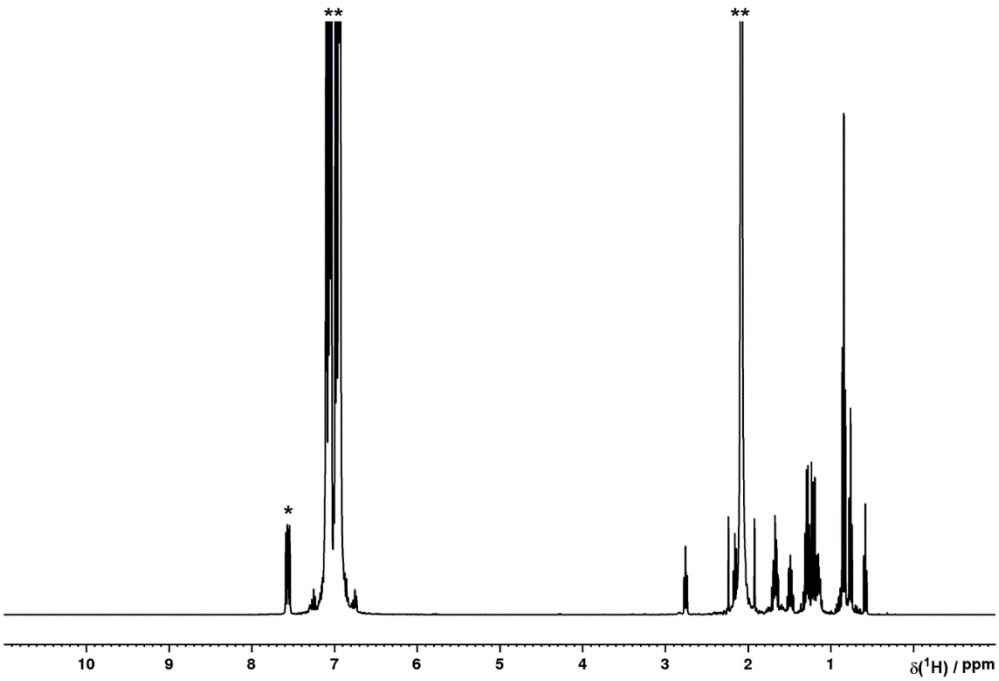

Figure S87. ^{1}H NMR spectrum of $P(C(O)Bu)_3$ (**12**) generated *via* hydrostannylation of P_4 in PhMe followed by acylation, in the presence of Ph_3PO (*) as an internal standard. Solvent resonances (**) truncated for clarity.

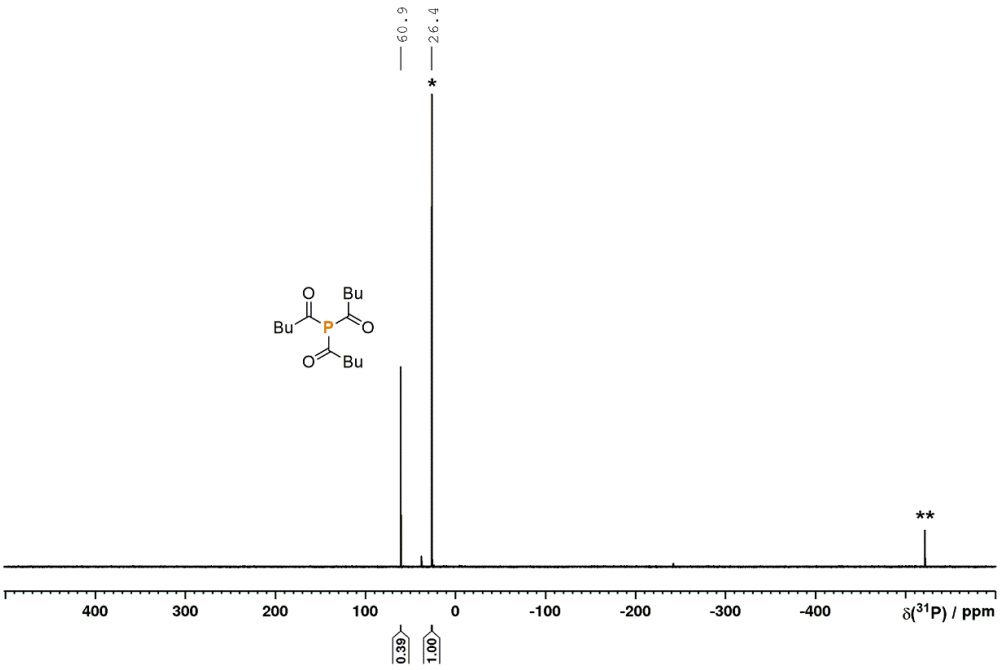

Figure S88. $^{31}P\{^{1}H\}$ NMR spectrum of $P(C(O)Bu)_3$ (**12**) generated *via* hydrostannylation of P_4 in PhMe followed by acylation, in the presence of Ph_3PO (*) as internal standard (**minor residual P_4).

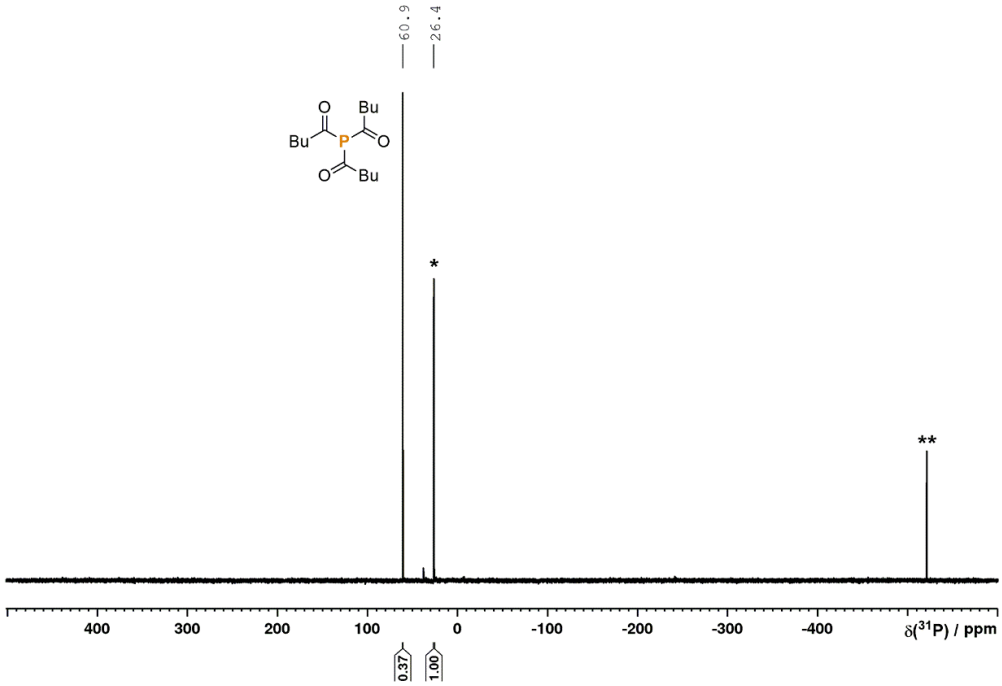

Figure S89. ^{31}P NMR spectrum of $P(C(O)Bu)_3$ (**12**) generated *via* hydrostannylation of P_4 in PhMe followed by acylation, in the presence of Ph_3PO (*) as an internal standard (**minor residual P_4).

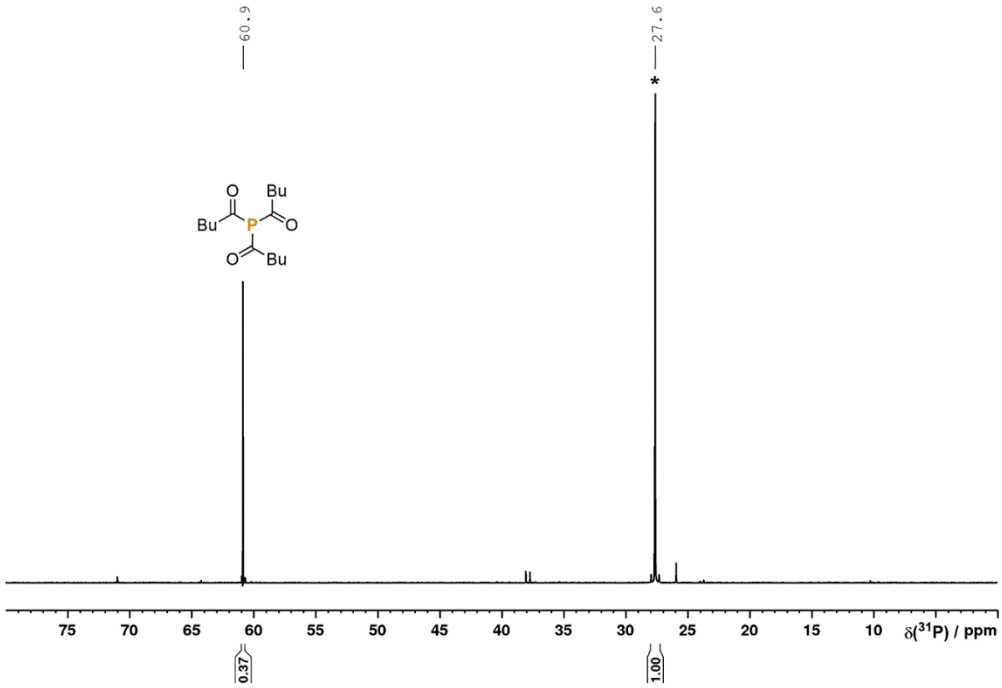

Figure S90. Quantitative $^{31}P\{^1H\}$ NMR spectrum (D1 = 22 s) of $P(C(O)Bu)_3$ (**12**) generated *via* hydrostannylation of P_4 in PhMe followed by acylation, in the presence of Ph_3PO (*) as an internal standard.

2.4.2.10 Synthesis and quantification of $P(C(O)Me)_3$ (13)

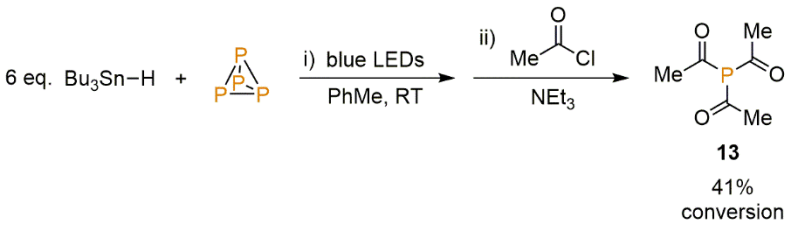

To a 10 mL, flat-bottomed, stoppered tube were added PhMe (500 µL), P_4 (0.01 mmol, as a stock solution in 77.4 µL PhH) and Bu_3SnH (16.1 µL, 0.06 mmol). The resulting colourless solution was stirred under irradiation with blue LED light (455 nm (±15 nm), 3.2 V, 700 mA, Osram OSLON SSL 80) for 18 h, during which time the tube was placed in a block cooled by circulating water to maintain near-ambient temperature. MeC(O)Cl (11.4 µL, 0.16 mmol) and Et_3N (8.4 µL, 0.06 mmol) were added, and the reaction mixture was stirred at room temperature for 16 h. Ph_3PO (10.6 mg, 0.038 mmol) was added, and the resulting mixture was analysed by ^1H, $^{31}P\{^1H\}$ and ^{31}P NMR spectroscopy (Figures S91-93). Conversion to $P(C(O)Me)_3$ (41%) was determined using quantitative $^{31}P\{^1H\}$ spectroscopy (D1 = 22 s, Figure S94), by relative integration of the resonances assigned to Ph_3PO and $P(C(O)Me)_3$.

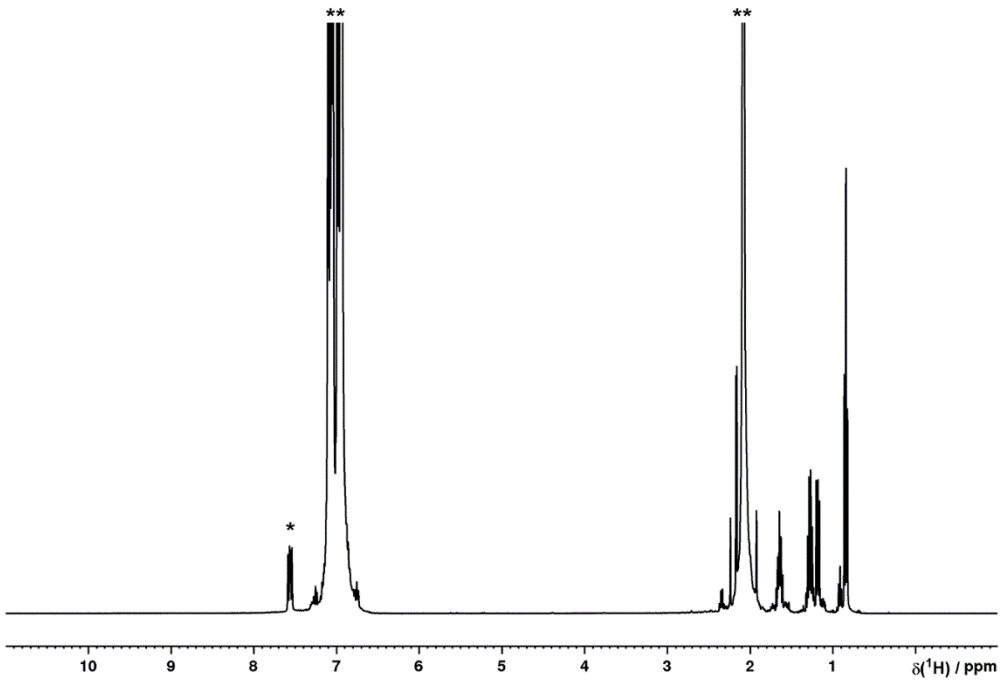

Figure S91. ^1H NMR spectrum of $P(C(O)Me)_3$ (**13**) generated *via* hydrostannylation of P_4 in PhMe followed by acylation, in the presence of Ph_3PO (*) as an internal standard. Solvent resonances (**) truncated for clarity.

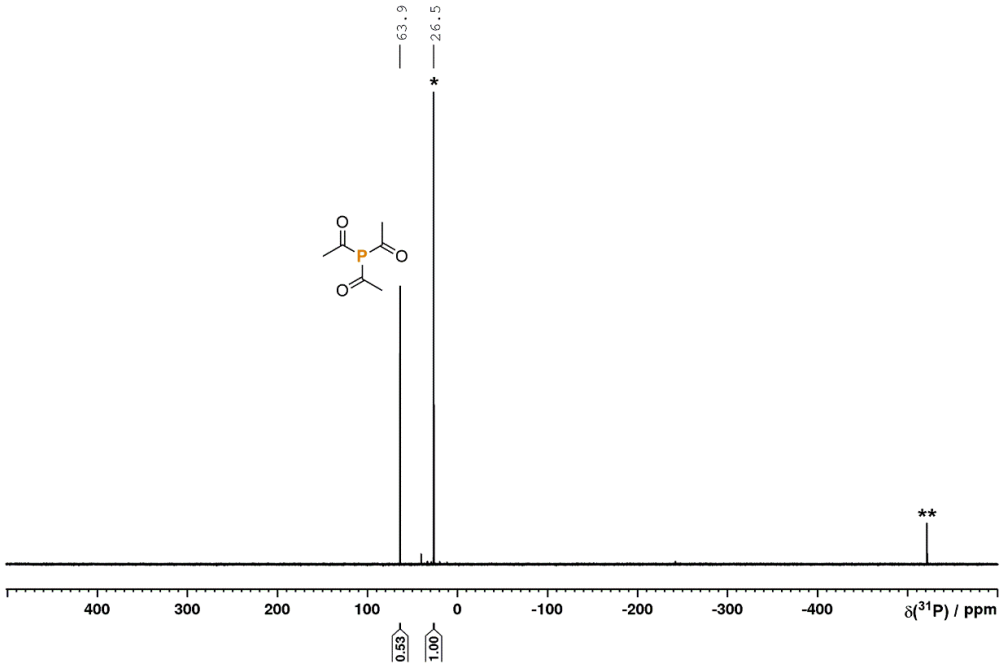

Figure S92. $^{31}P\{^{1}H\}$ NMR spectrum of $P(C(O)Me)_3$ (**13**) generated *via* hydrostannylation of P_4 in PhMe followed by acylation, in the presence of Ph_3PO (*) as internal standard (**minor residual P_4).

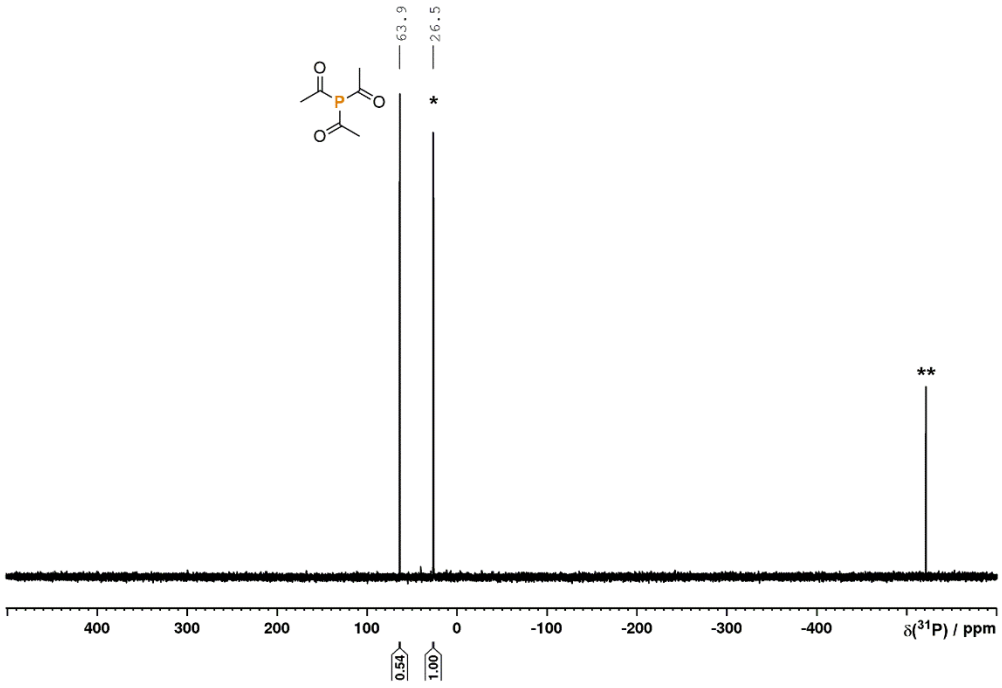

Figure S93. ^{31}P NMR spectrum of $P(C(O)Me)_3$ (**13**) generated *via* hydrostannylation of P_4 in PhMe followed by acylation, in the presence of Ph_3PO (*) as an internal standard (**minor residual P_4).

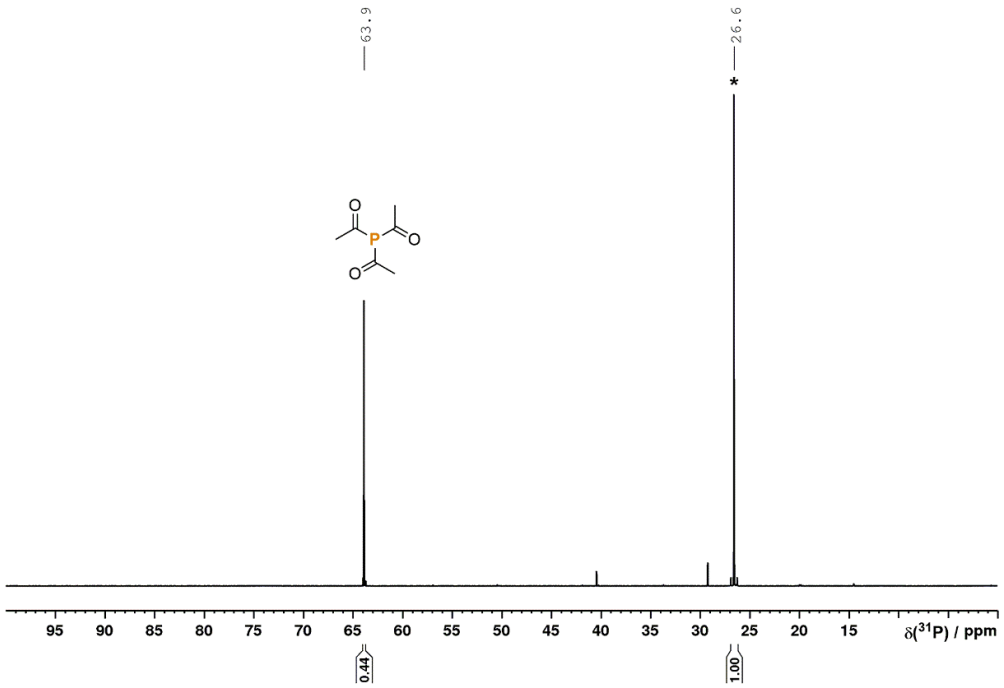

Figure S94. Quantitative $^{31}P\{^{1}H\}$ NMR spectrum (D1 = 22 s) of $P(C(O)Me)_3$ (**13**) generated *via* hydrostannylation of P_4 in PhMe followed by acylation, in the presence of Ph_3PO (*) as an internal standard.

2.4.2.11 Synthesis and isolation of [Bn$_4$P]Br (14) (without KHMDS)

To a 50 mL flat-bottomed Schlenk were added P_4 (62.0 mg, 0.5 mmol) and PhMe (25 mL). After stirring to obtain a homogeneous solution Bu_3SnH was added (847 µL, 3.15 mmol). The resulting colourless solution was stirred under irradiation with blue LED light (7X Osram OSLON SSL80, 455 nm (±15 nm), 20.3 V 1000mA) for 22 h, during which time the Schlenk tube was placed in a block cooled by circulating water to maintain near-ambient temperature. Benzyl bromide (2.4 mL, 20 mmol) was added and the reaction mixture heated to 60 °C with stirring for 3 days. After cooling to room temperature the pale yellow suspension was evaporated to dryness, and the resulting solid was washed with pentane (2 x 20 mL) and extracted with acetone (4 x 15 mL; undried, 'bench' acetone was used). Removal of volatiles under vacuum yielded the target product as a white solid (380 mg, 80%).

^{1}H NMR (400 MHz, 300 K, CD_3CN): δ = 7.36 ppm (3H, m), 7.15 ppm (2H, m), 3.73 ppm (d, $^{2}J(^{31}P\text{-}^{1}H)$ = 14.3 Hz). **$^{31}P\{^{1}H\}$ NMR** (121 MHz, 300 K, CD_3CN): δ = 25.8 ppm (s). **^{31}P NMR** (121 MHz, 300 K, CD_3CN): δ = 25.8 ppm (nonet, $^{2}J(^{31}P\text{-}^{1}H)$ = 14.3 Hz). **$^{13}C\{^{1}H\}$ NMR** (101 MHz, 300 K, C_6D_6): δ = 130.7 (d, $J(^{31}P\text{-}^{1}H)$ = 5.3 Hz), 129.3 (d, $J(^{31}P\text{-}^{1}H)$ = 2.9 Hz), 128.4 (d, $J(^{31}P\text{-}^{1}H)$ = 3.5 Hz), 127.8 (d, $J(^{31}P\text{-}^{1}H)$ = 8.1 Hz), 26.4 ppm (d, $J(^{31}P\text{-}^{1}H)$ = 43.2 Hz). **MS** (ESI, MeCN): *m*/*z* = 395.1940 (PBn_4^+). NMR data are consistent with previous reports of the chloride salt [Bn$_4$P]Cl.[4]

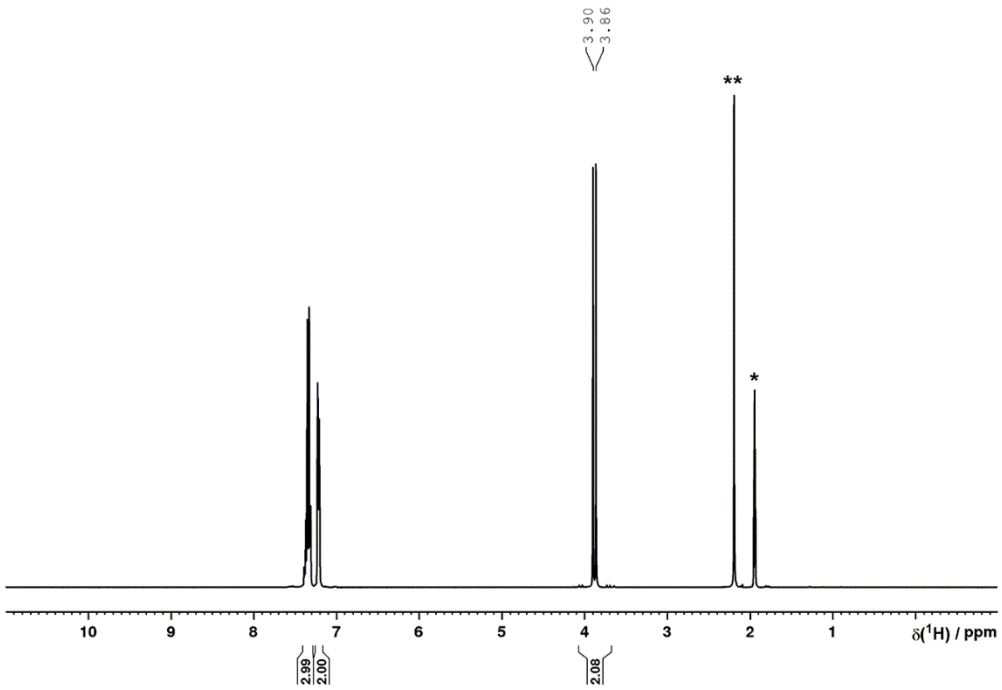

Figure S95. ^{1}H NMR spectrum of $[Bn_4P]Br$ (**14**) in CD_3CN (*solvent, **H_2O).

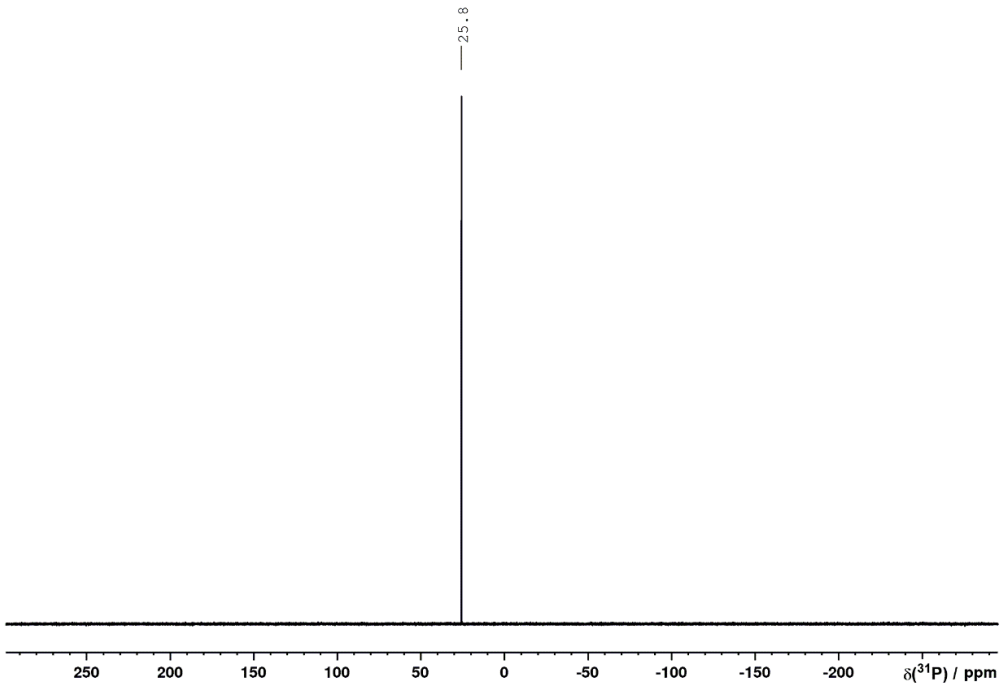

Figure S96. $^{31}P\{^{1}H\}$ NMR spectrum of $[Bn_4P]Br$ (**14**) in CD_3CN.

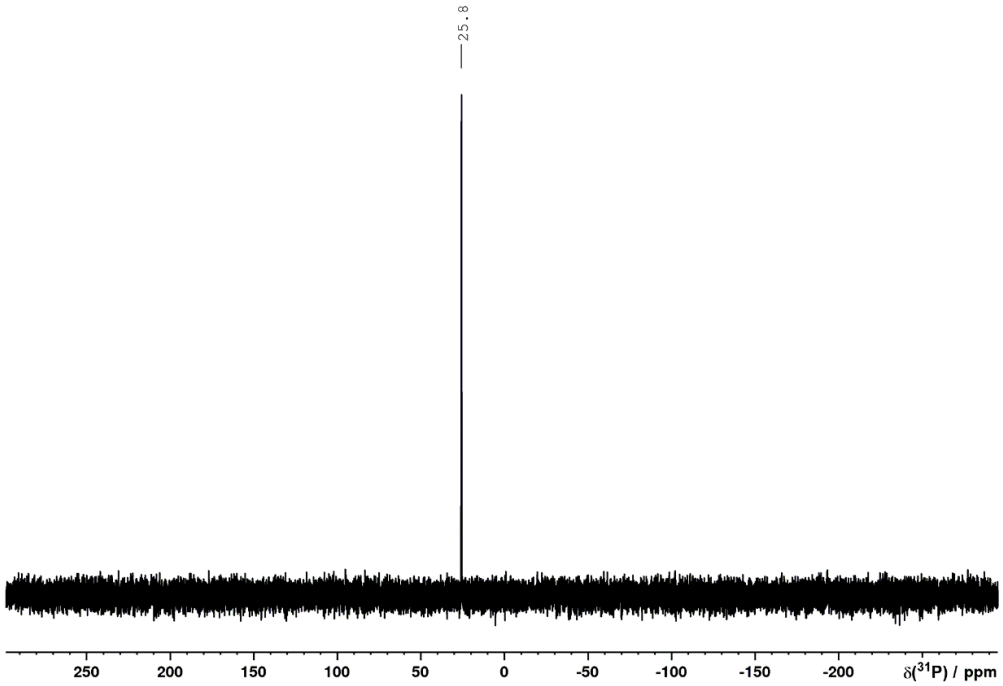

Figure S97. ^{31}P NMR spectrum of $[Bn_4P]Br$ (**14**) in CD_3CN.

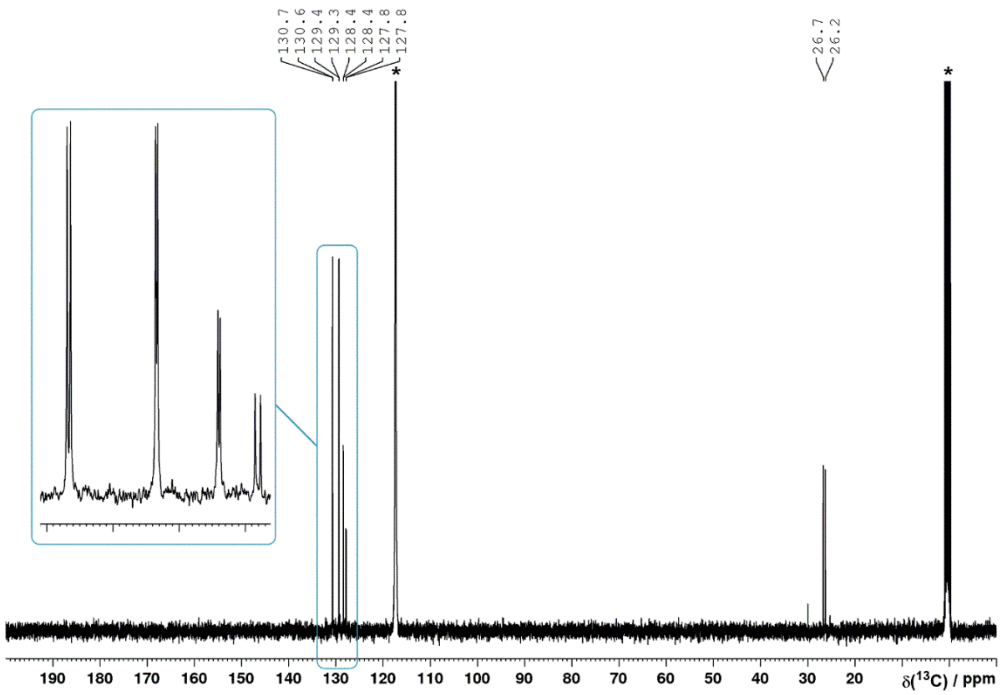

Figure S98. $^{13}C\{^1H\}$ NMR spectrum of $[Bn_4P]Br$ (**14**) in CD_3CN. Solvent resonances (*) truncated for clarity.

2.4.2.12 Synthesis and isolation of [Bn$_4$P]Br (14) (with KHMDS)

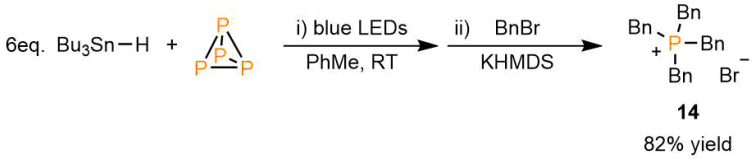

To a 50 mL flat-bottomed Schlenk were added P_4 (62.0 mg, 0.5 mmol), PhMe (25 mL), and Bu_3SnH (847 µL, 3.15 mmol). The resulting homogeneous, colourless solution was stirred under irradiation with blue LED light (7X Osram OSLON SSL80, 455 nm (±15 nm), 20.3 V 1000mA) for 22 h, during which time the Schlenk tube was placed in a block cooled by circulating water to maintain near-ambient temperature. Benzyl bromide (2.4 mL, 20 mmol) and KHMDS (399 mg, 2.0 mmol) were added and the reaction mixture heated to 60 °C with stirring for 3 days. After cooling to room temperature the pale yellow suspension was evaporated to dryness, and the resulting solid was washed with pentane (2 x 20 mL) and extracted with acetone (4 x 15 mL; undried, 'bench' acetone was used). Removal of volatiles under vacuum yielded the target product as a white solid (775 mg, 82%). For characterisation data, see Section 2.4.2.11.

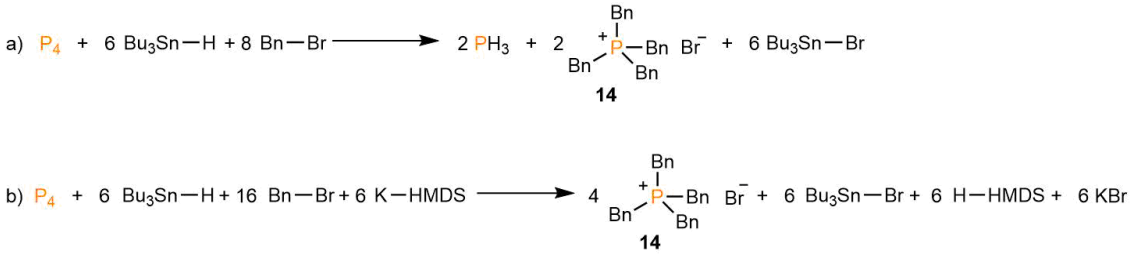

Scheme S2. Proposed balanced, overall equations for the formation of [Bn$_4$P]Br (**14**). a) In the absence of KHMDS, formation of PH_3 as a stoichiometric byproduct is proposed to occur. b) In the presence of KHMDS, **14** is proposed to be the only stoichiometric phosphorus-containing product.

2.4.2.13 Synthesis and isolation of [Et$_4$P]Br (15)

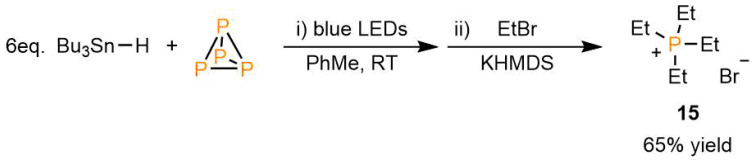

To a 50 mL flat-bottomed Schlenk were added P_4 (62.0 mg, 0.5 mmol) and PhMe (25 mL). After stirring to obtain a homogeneous solution Bu_3SnH was added (847 µL, 3.15 mmol). The resulting colourless solution was stirred under irradiation with blue LED light (7X Osram OSLON SSL80, 455 nm (±15 nm), 20.3 V 1000mA) for 22 h, during which time the Schlenk tube was placed in a block cooled by circulating water to maintain near-ambient temperature. Ethyl bromide (741 µL, 10 mmol) and KHMDS (798 mg, 4.0 mmol) were added and the reaction mixture heated to 100 °C with stirring for 3 days. After cooling to room temperature the pale yellow suspension was filtered, and the remaining solid was washed with PhMe (2 x 20 mL) and extracted into

acetonitrile (3 x 20 mL). Removal of volatiles under vacuum yielded the target product as a white solid (295 mg, 65%).

^{1}H NMR (400 MHz, 300 K, CD_3CN): δ = 2.21 ppm (2H, dq, $^{1}J(^{31}P\text{-}^{1}H)$ = 13.0 Hz, $^{3}J(^{1}H\text{-}^{1}H)$ = 7.7 Hz), 1.19 ppm (3H, dt, $^{2}J(^{31}P\text{-}^{1}H)$ = 18.0 Hz, $^{3}J(^{1}H\text{-}^{1}H)$ = 7.7 Hz). **^{31}P{^{1}H} NMR** (121 MHz, 300 K, CD_3CN): δ = 42.3 ppm (s). **^{31}P NMR** (121 MHz, 300 K, CD_3CN): δ = 42.3 ppm (m). **^{13}C{^{1}H} NMR** (101 MHz, 300 K, C_6D_6): δ = 11.7 (d, $^{1}J(^{31}P\text{-}^{1}H)$ = 49.6 Hz), 5.7 ppm (d, $^{2}J(^{31}P\text{-}^{1}H)$ = 5.3 Hz). **MS** (ESI, MeCN): *m*/*z* = 147.1295 (Et_4P^+). NMR data are consistent with previous reports of $[Et_4P][BAr^F{}_4]$ (Ar^F = 3,5-bis(trifluoromethyl)phenyl).[75]

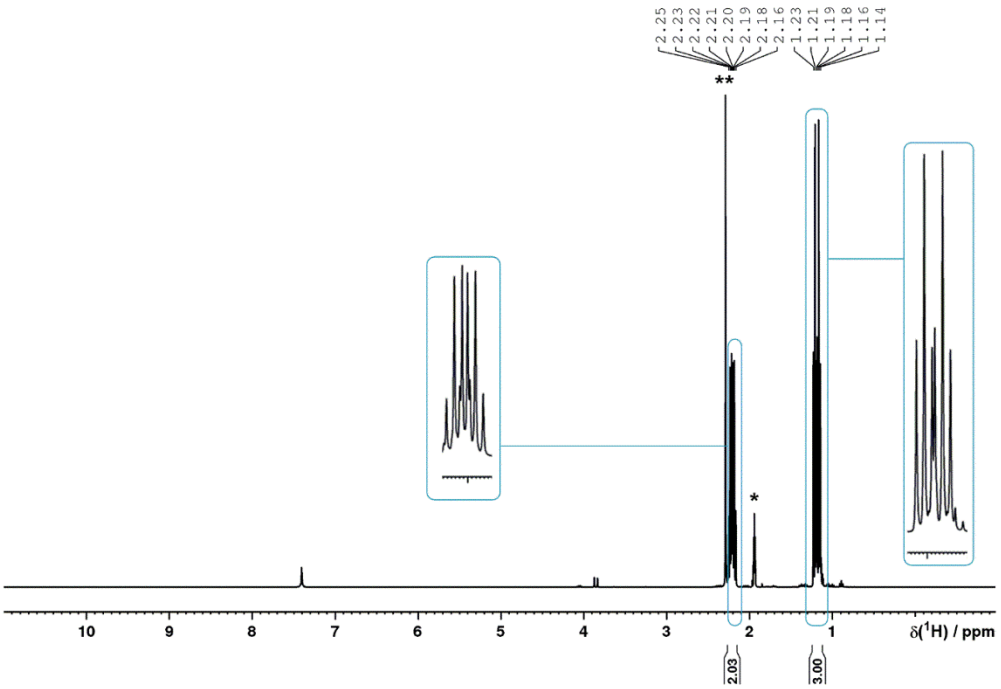

Figure S99. ^{1}H NMR spectrum of $[Et_4P]Br$ (**15**) in CD_3CN (*solvent, **H_2O).

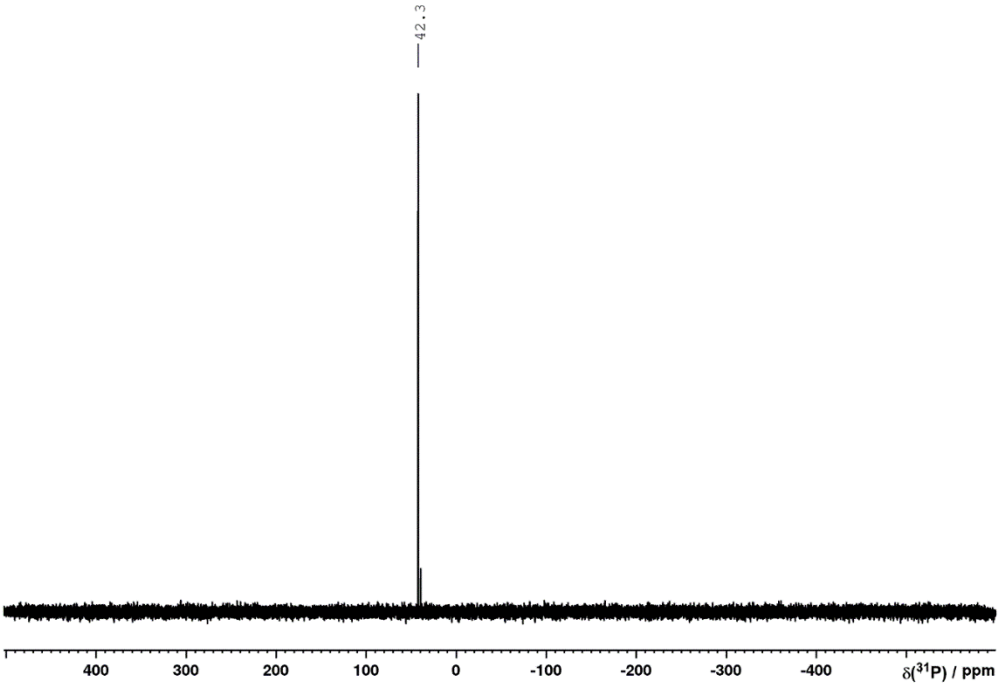

Figure S100. ^{31}P{^{1}H} NMR spectrum of $[Et_4P]Br$ (**15**) in CD_3CN.

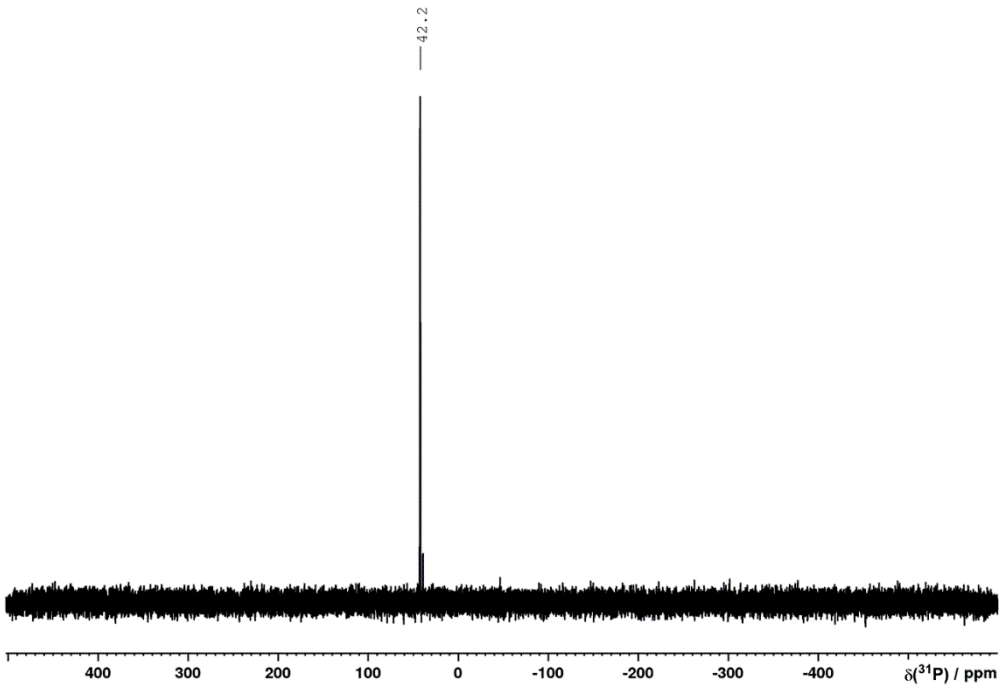

Figure S101. ^{31}P NMR spectrum of [Et_4P]Br (**15**) in CD_3CN.

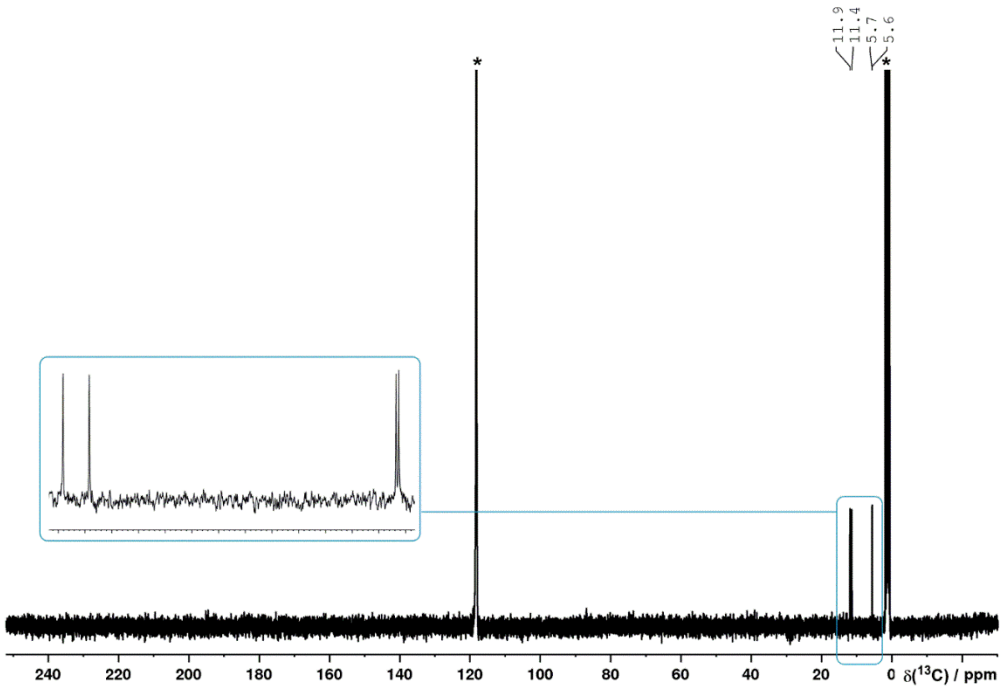

Figure S102. $^{13}C\{^1H\}$ NMR spectrum of [Et_4P]Br (**15**) in CD_3CN. Solvent resonances (*) truncated for clarity.

2.4.2.14 Alkylation of $(Bu_3Sn)_xPH_{3-x}$ using RBr (R = 2-ethylhexyl)

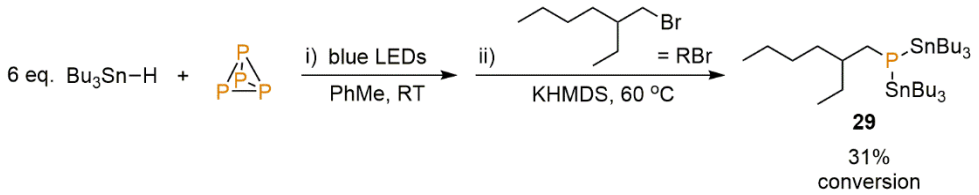

To a 10 mL, flat-bottomed, stoppered tube were added PhMe (500 µL), P_4 (0.01 mmol, as a stock solution in 77.4 µL PhH) and Bu_3SnH (16.1 µL, 0.06 mmol). The resulting colourless solution was stirred under irradiation with blue LED light (455 nm (±15 nm), 3.2 V, 700 mA, Osram OSLON SSL 80) for 18 h, during which time the tube was placed in a block cooled by circulating water to maintain near-ambient temperature. 3-(bromomethyl)heptane (35.1 µL, 0.20 mmol) and KHMDS (16.0 mg, 0.08 mmol) were added and the reaction mixture heated to 60 °C with stirring for 1 day. After cooling to room temperature, Ph_3PO (9.8 mg, 0.0352 mmol) was added as an internal standard, and the mixture analysed by ^{1}H, $^{31}P\{^{1}H\}$ and ^{31}P NMR spectroscopy as shown in Figures S103-105, below. The $^{31}P\{^{1}H\}$ and ^{31}P spectra indicated formation of one major P-containing species, characterised by a resonance at –208.4 ppm. Based on this upfield chemical shift, the presence of $^{117/119}Sn$ satellites ($^{1}J(^{31}P\text{-}^{117}Sn)$ = 796 Hz, $^{1}J(^{31}P\text{-}^{119}Sn)$ = 832 Hz), the intensity of these satellites, and the absence of $^{1}J(^{31}P\text{-}^{1}H)$ splitting in the proton-coupled spectrum, this species can reasonably be assigned as the mono-alkylated product $RP(SnBu_3)_2$ (**29**).[22] Using quantitative $^{31}P\{^{1}H\}$ NMR spectroscopy (D1 = 30 s; Figure S106), a total conversion of P_4 to this product of 31% was determined.

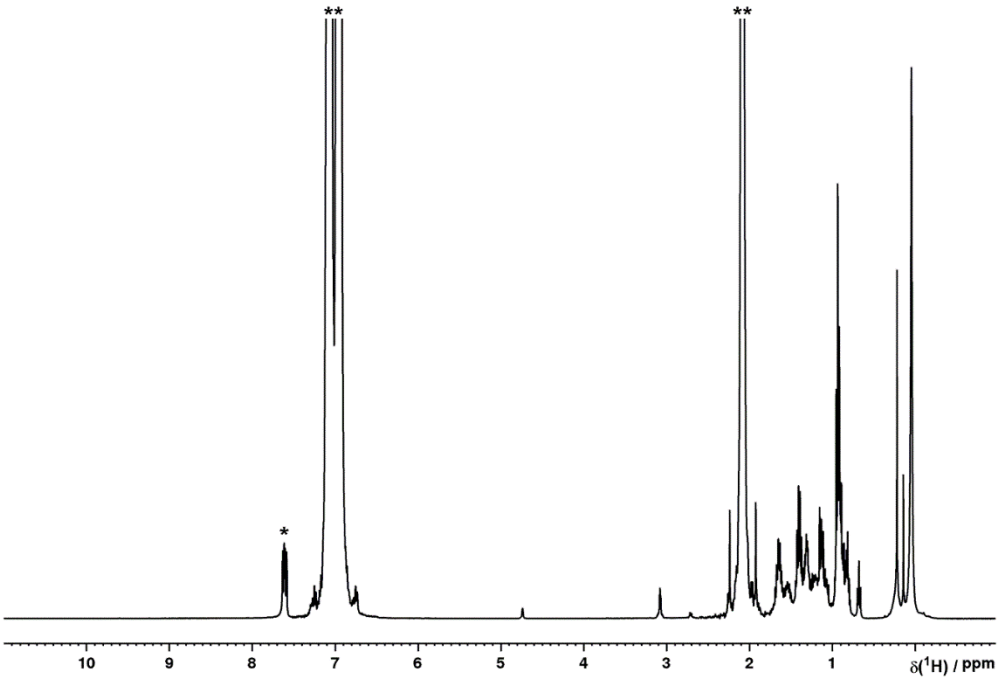

Figure S103. ^{1}H NMR spectrum for the hydrostannylation of P_4 in PhMe, followed by *in situ* alkylation with RBr and KHMDS and addition of Ph_3PO (*) as internal standard. Solvent resonances (**) truncated for clarity.

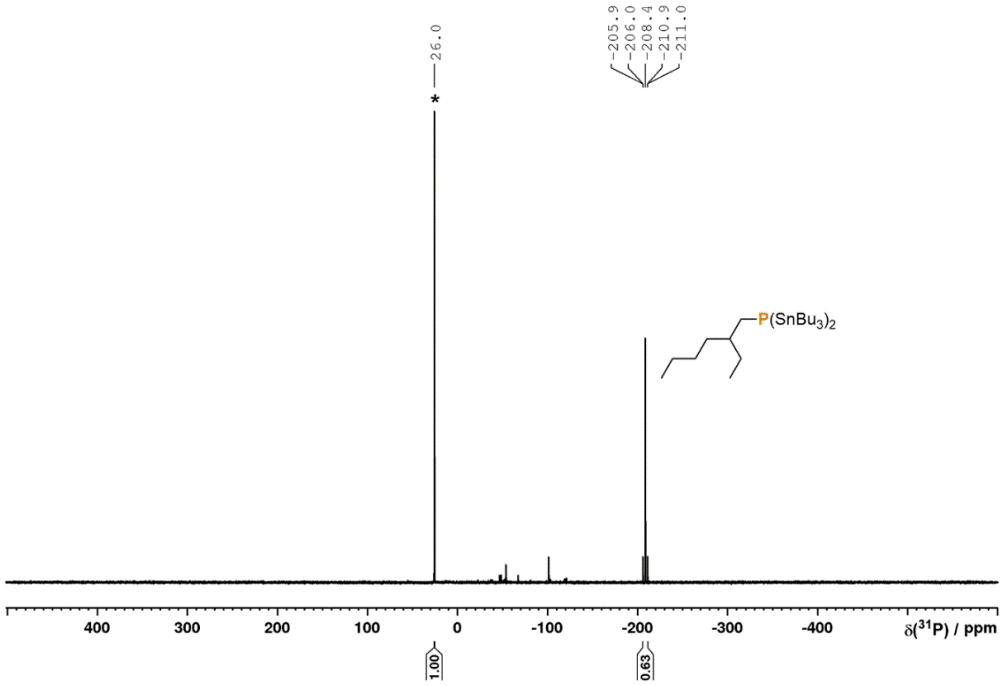

Figure S104. $^{31}P\{^{1}H\}$ NMR spectrum for the hydrostannylation of P_4 in PhMe, followed by *in situ* alkylation with RBr and KHMDS and addition of Ph_3PO (*) as internal standard.

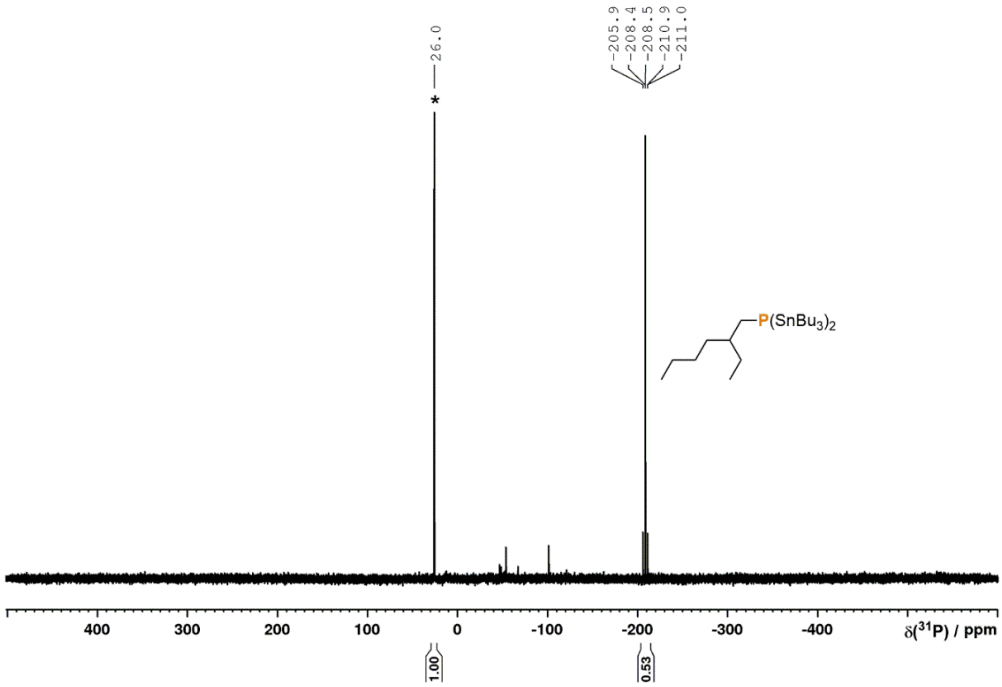

Figure S105. ^{31}P NMR spectrum for the hydrostannylation of P_4 in PhMe, followed by *in situ* alkylation with RBr and KHMDS and addition of Ph_3PO (*) as internal standard.

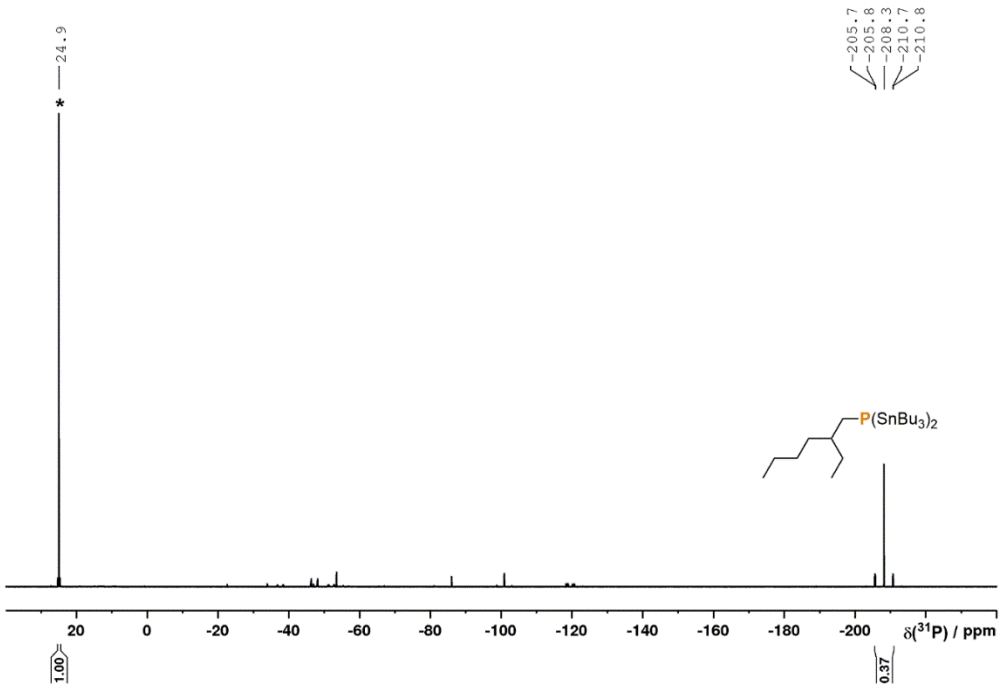

Figure S106. Quantitative $^{31}P\{^{1}H\}$ NMR spectrum (D1 = 30 s) for the hydrostannylation of P_4 in PhMe, followed by *in situ* alkylation with RBr and KHMDS and addition of Ph_3PO (*) as internal standard.

2.4.2.15 Alkylation of $(Bu_3Sn)_xPH_{3-x}$ using R'Br (R' = 2,4,4-trimethylpentyl)

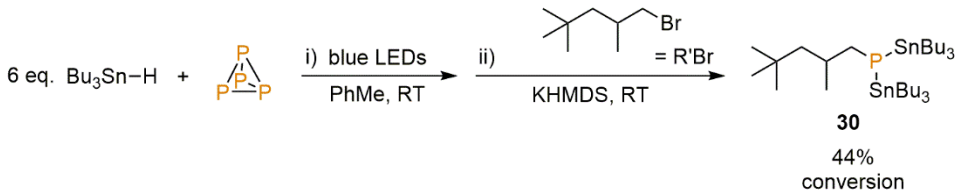

To a 10 mL, flat-bottomed, stoppered tube were added PhMe (500 µL), P_4 (0.01 mmol, as a stock solution in 77.4 µL PhH) and Bu_3SnH (16.1 µL, 0.06 mmol). The resulting colourless solution was stirred under irradiation with blue LED light (455 nm (±15 nm), 3.2 V, 700 mA, Osram OSLON SSL 80) for 18 h, during which time the tube was placed in a block cooled by circulating water to maintain near-ambient temperature. 1-bromo-2,4,4-trimethylpentane (27.9 µL, 0.16 mmol) and KHMDS (12.0 mg, 0.06 mmol) were added and the reaction mixture was stirred at room temperature for 3 days. Ph_3PO (9.3 mg, 0.0334 mmol) was then added as an internal standard, and the mixture analysed by ^{1}H, $^{31}P\{^{1}H\}$ and ^{31}P NMR spectroscopy as shown in Figures S107-109, below. The $^{31}P\{^{1}H\}$ and ^{31}P spectra indicated formation of one major P-containing species, characterised by a resonance at –209.3 ppm. Based on this upfield chemical shift, the presence of $^{117/119}Sn$ satellites ($^{1}J(^{31}P\text{-}^{117}Sn)$ = 794 Hz, $^{1}J(^{31}P\text{-}^{119}Sn)$ = 830 Hz), the intensity of these satellites, and the absence of $^{1}J(^{31}P\text{-}^{1}H)$ splitting in the proton-coupled spectrum, this species can reasonably be assigned as the mono-alkylated product $R'P(SnBu_3)_2$ (**30**).[37] Using quantitative $^{31}P\{^{1}H\}$ NMR spectroscopy (D1 = 30 s; Figure S110), a total conversion of P_4 to this product of 44% was determined.

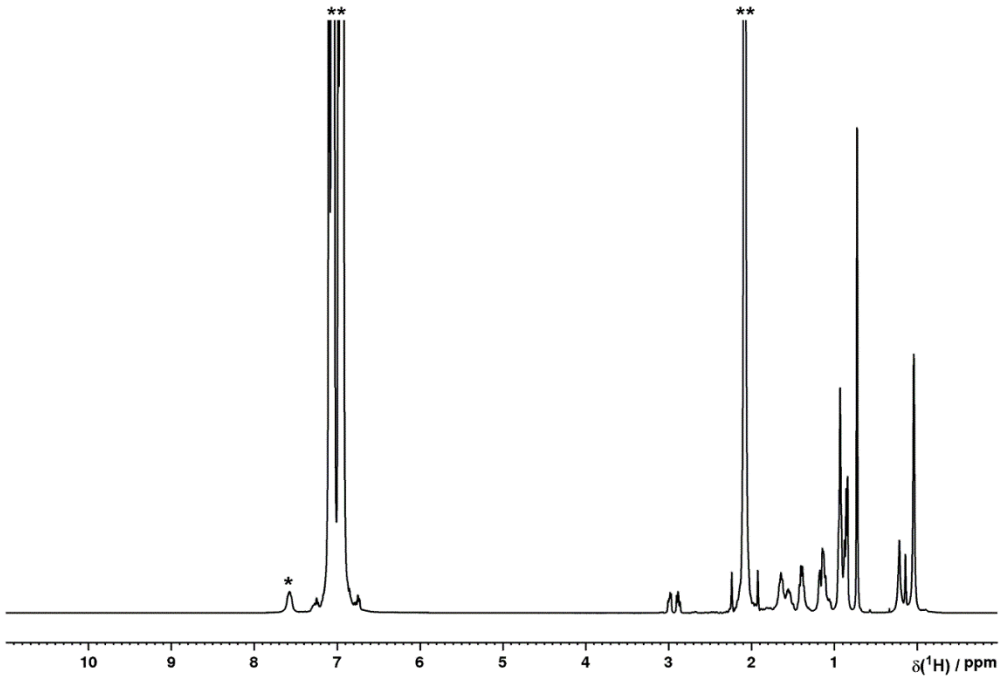

Figure S107. ^{1}H NMR spectrum for the hydrostannylation of P_4 in PhMe, followed by *in situ* alkylation with R'Br and KHMDS and addition of Ph_3PO (*) as internal standard. Solvent resonances (**) truncated for clarity.

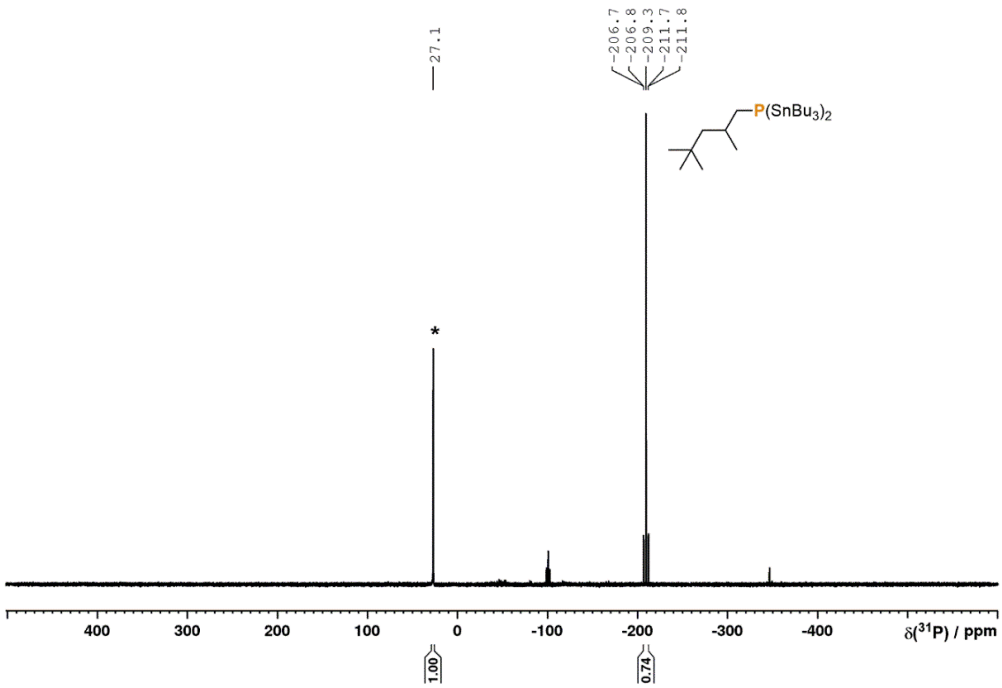

Figure S108. $^{31}P\{^{1}H\}$ NMR spectrum for the hydrostannylation of P_4 in PhMe, followed by *in situ* alkylation with R'Br and KHMDS and addition of Ph_3PO (*) as internal standard.

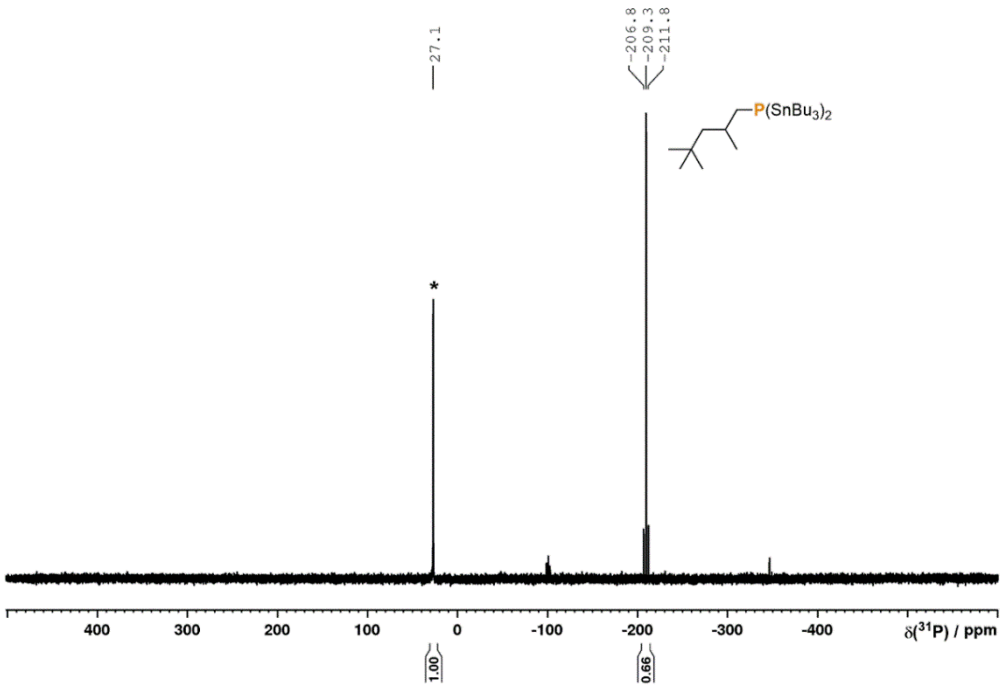

Figure S109. ^{31}P NMR spectrum for the hydrostannylation of P_4 in PhMe, followed by *in situ* alkylation with R'Br and KHMDS and addition of Ph_3PO (*) as internal standard.

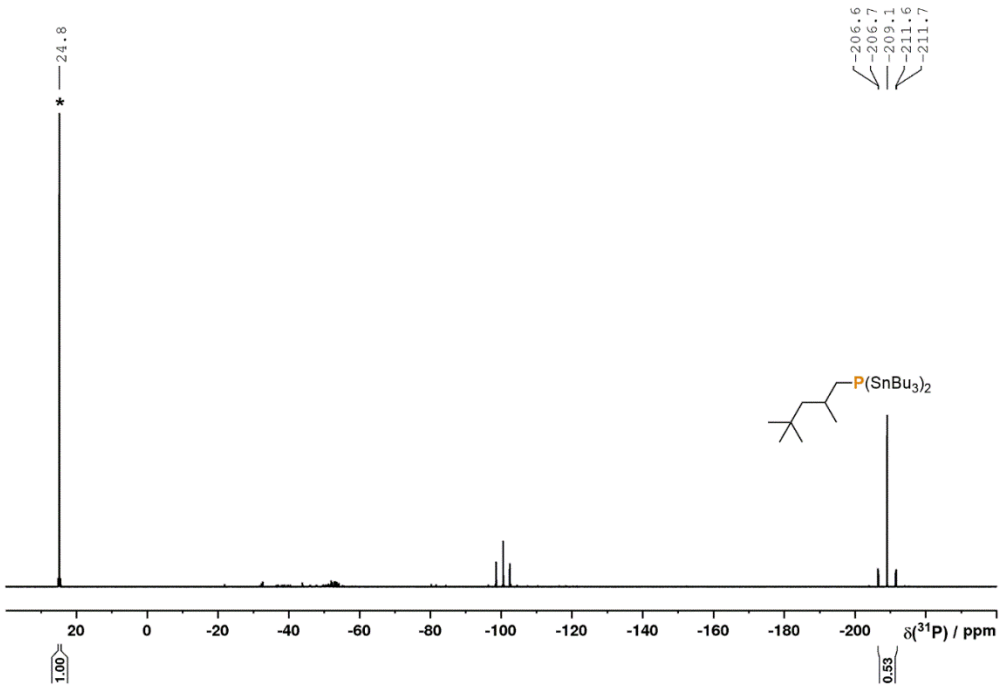

Figure S110. Quantitative $^{31}P\{^1H\}$ NMR spectrum (D1 = 30 s) for the hydrostannylation of P_4 in PhMe, followed by *in situ* alkylation with R'Br and KHMDS and addition of Ph_3PO (*) as internal standard.

2.4.2.16 Attempted arylation of $(Bu_3Sn)_xPH_{3-x}$ using PhBr

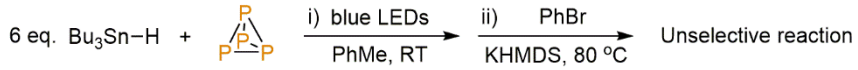

To a 10 mL, flat-bottomed, stoppered tube were added PhMe (500 µL), P_4 (0.01 mmol, as a stock solution in 77.4 µL PhH) and Bu_3SnH (16.1 µL, 0.06 mmol). The resulting colourless solution was stirred under irradiation with blue LED light (455 nm (±15 nm), 3.2 V, 700 mA, Osram OSLON SSL 80) for 18 h, during which time the tube was placed in a block cooled by circulating water to maintain near-ambient temperature. PhBr (8.4 µL, 0.8 mmol) and KHMDS (12.0 mg, 0.06 mmol) were added and the reaction mixture was heated to 80 °C with stirring for 3 days. After cooling to room temperature, Ph_3PO (10.0 mg, 0.0359 mmol) was added as an internal standard, and the mixture analysed by ^1H, $^{31}P\{^1H\}$ and ^{31}P NMR spectroscopy as shown in Figures S111-113, below. $^{31}P\{^1H\}$ and ^{31}P spectra, including a quantitative $^{31}P\{^1H\}$ spectrum (D1 = 30 s; Figure S114), did not reveal any major new products (no new peaks whose conversion from P_4 would exceed *ca*. 15%). Analogous experiments using PhI or PhCl in place of PhBr were similarly unsuccessful, as were reactions at other temperatures.

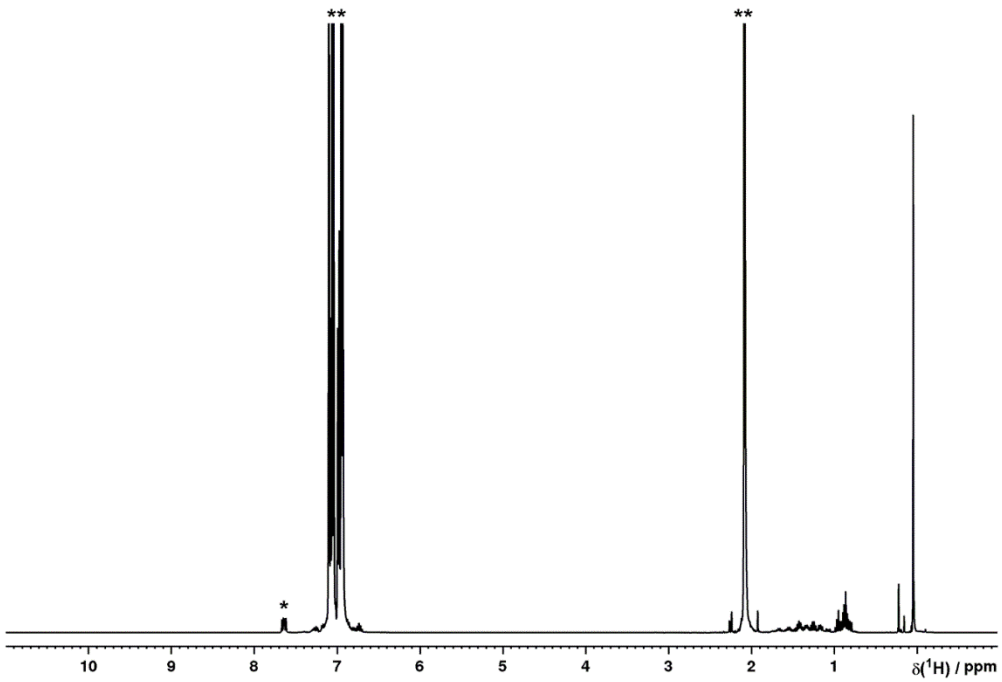

Figure S111. ^1H NMR spectrum for the hydrostannylation of P_4 in PhMe, followed by attempted *in situ* arylation with PhBr and KHMDS and addition of Ph_3PO (*) as internal standard. Solvent resonances (**) truncated for clarity.

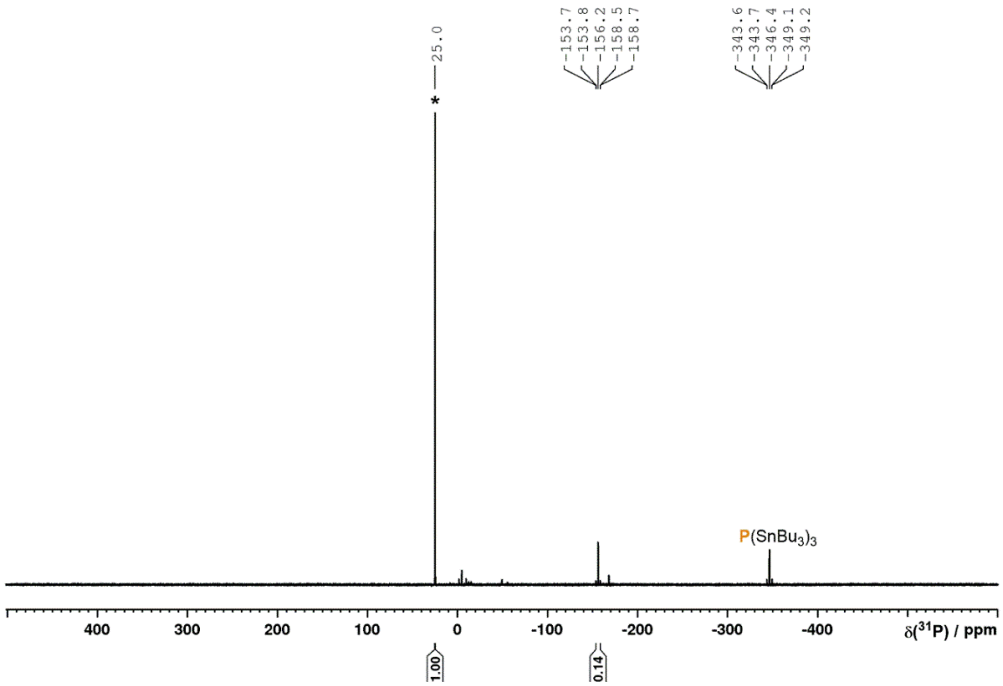

Figure S112. $^{31}P\{^{1}H\}$ NMR spectrum for the hydrostannylation of P_4 in PhMe, followed by attempted *in situ* arylation with PhBr and KHMDS and addition of Ph_3PO (*) as internal standard.

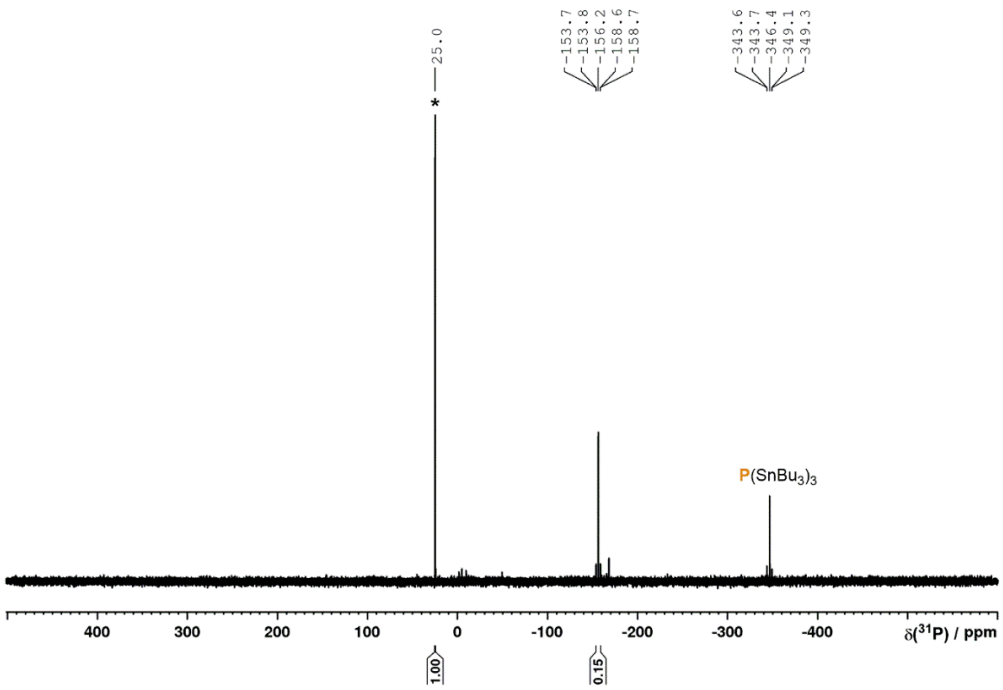

Figure S113. ^{31}P NMR spectrum for the hydrostannylation of P_4 in PhMe, followed by attempted *in situ* arylation with PhBr and KHMDS and addition of Ph_3PO (*) as internal standard.

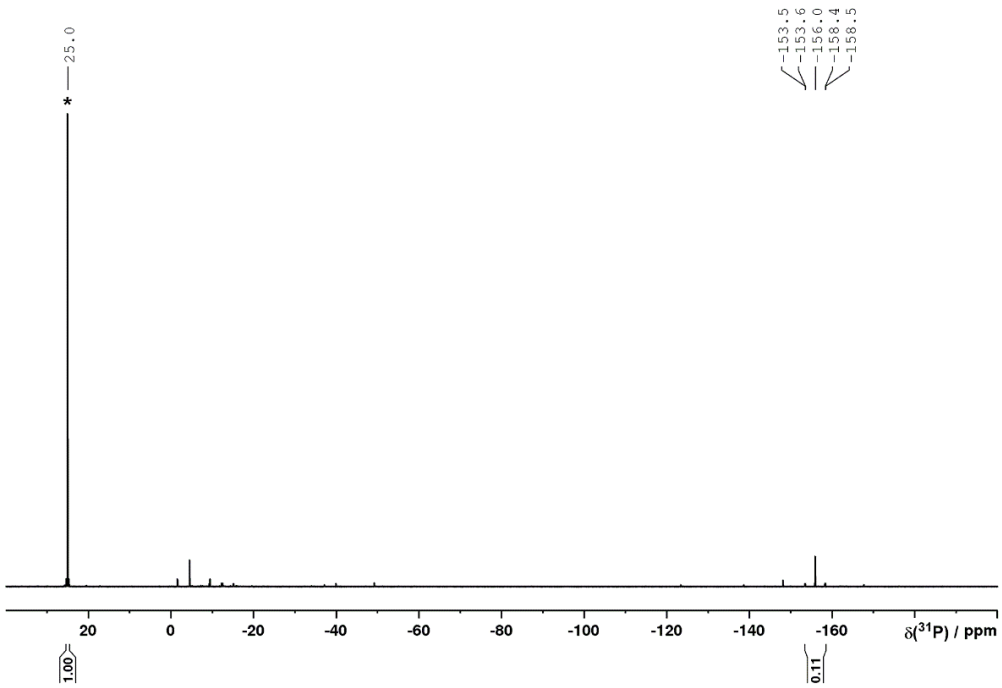

Figure S114. Quantitative $^{31}P\{^{1}H\}$ NMR spectrum (D1 = 30 s) for the hydrostannylation of P_4 in PhMe, followed by attempted *in situ* arylation with PhBr and KHMDS and addition of Ph_3PO (*) as internal standard.

2.4.2.17 Synthesis and isolation of THP (16)

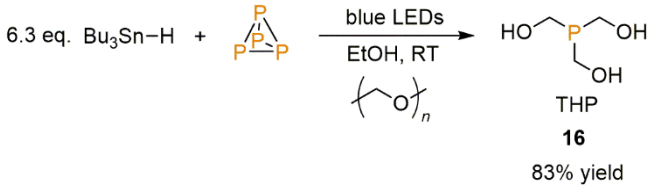

To a 50 mL flat-bottomed Schlenk were added P_4 (62.0 mg, 0.5 mmol) and PhH (5.0 mL). After stirring to obtain a homogeneous solution, EtOH (25 mL), Bu_3SnH (847 µL, 3.15 mmol) and paraformaldehyde (180 mg, 6.0 mmol) were added. The resulting suspension was stirred under irradiation with blue LED light (7X Osram OSLON SSL80, 455 nm (±15 nm), 20.3 V 1000mA) for 22 h, during which time the Schlenk tube was placed in a block cooled by circulating water to maintain near-ambient temperature. The resulting suspension was filtered and volatiles were removed under vacuum. To the oily residue thus obtained was added PhMe (20 mL) and degassed H_2O (20 mL). The biphasic mixture was thoroughly stirred for 30 min, the toluene phase was removed, and the aqueous phase was washed with further PhMe (2 x 20 mL). Following removal of volatiles from the aqueous phase under vacuum, THP was obtained as a colourless oil (206 mg, 83%).

^{1}H NMR (400 MHz, 300 K, D_2O): δ = 3.99 ppm (d, $^{2}J(^{31}P\text{-}^{1}H)$ = 5.2 Hz). **$^{31}P\{^{1}H\}$ NMR** (121 MHz, 300 K, D_2O): δ = –23.6 ppm (s). **^{31}P NMR** (121 MHz, 300 K, D_2O): δ = –23.6 ppm (s). **$^{13}C\{^{1}H\}$ NMR** (101 MHz, 300 K, D_2O): δ = 56.4 ppm (d, $^{1}J(^{31}P\text{-}^{13}C)$ = 8.5 Hz). **MS** (APCI, EtOH): *m*/*z* = 125.0364 ($[M+H]^+$). NMR data are consistent with previous reports.[76]

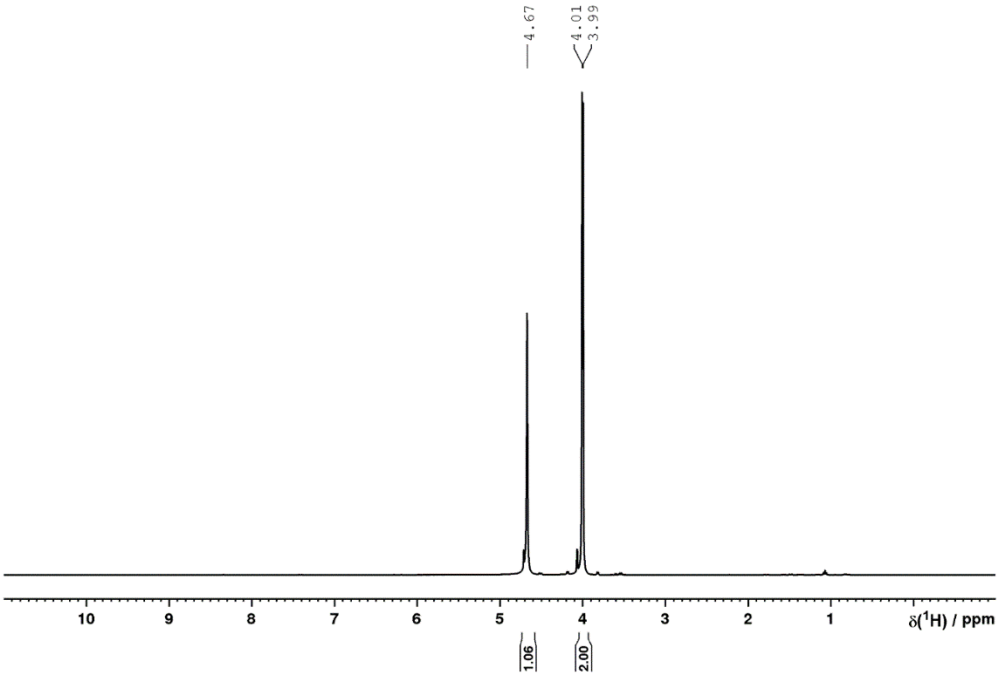

Figure S115. ^{1}H NMR spectrum of THP (**16**) in D_2O.

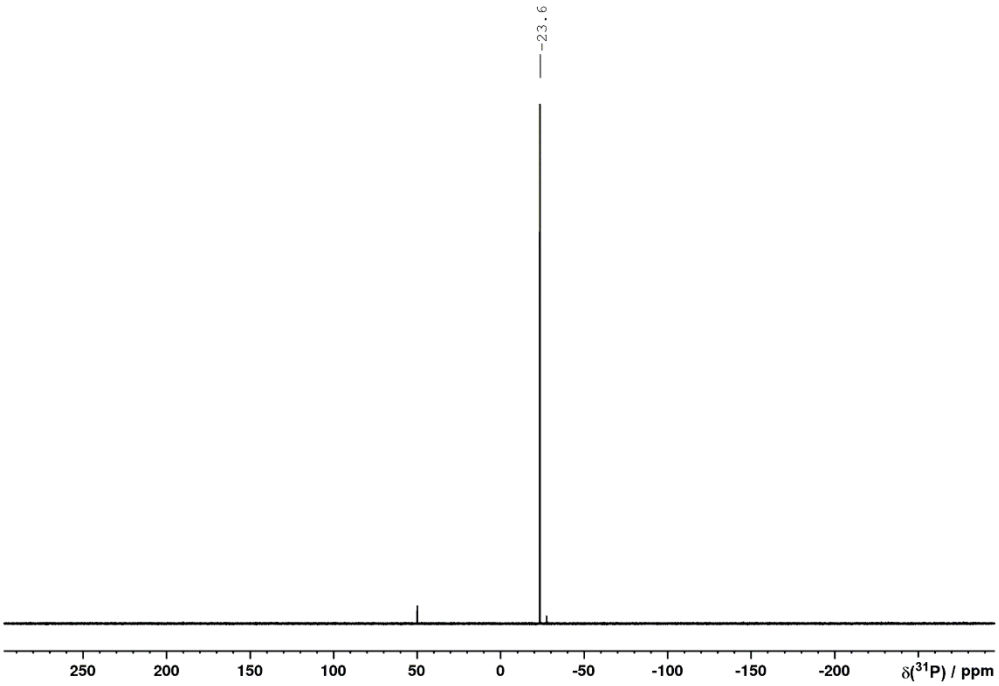

Figure S116. $^{31}P\{^{1}H\}$ NMR spectrum of THP (**16**) in D_2O.

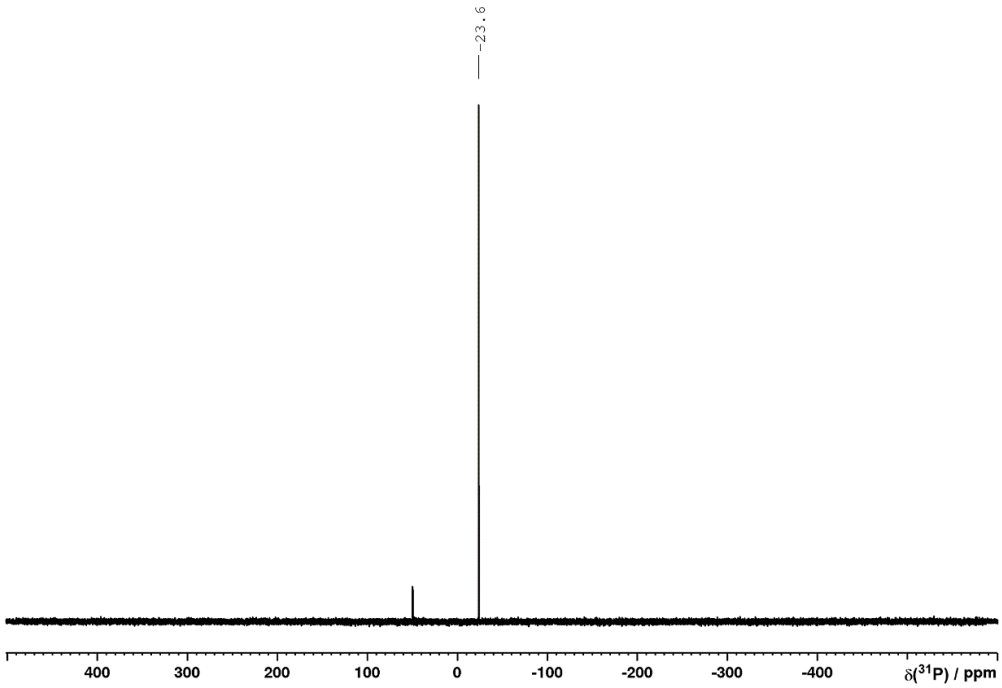

Figure S117. ^{31}P NMR spectrum of THP (**16**) in D_2O.

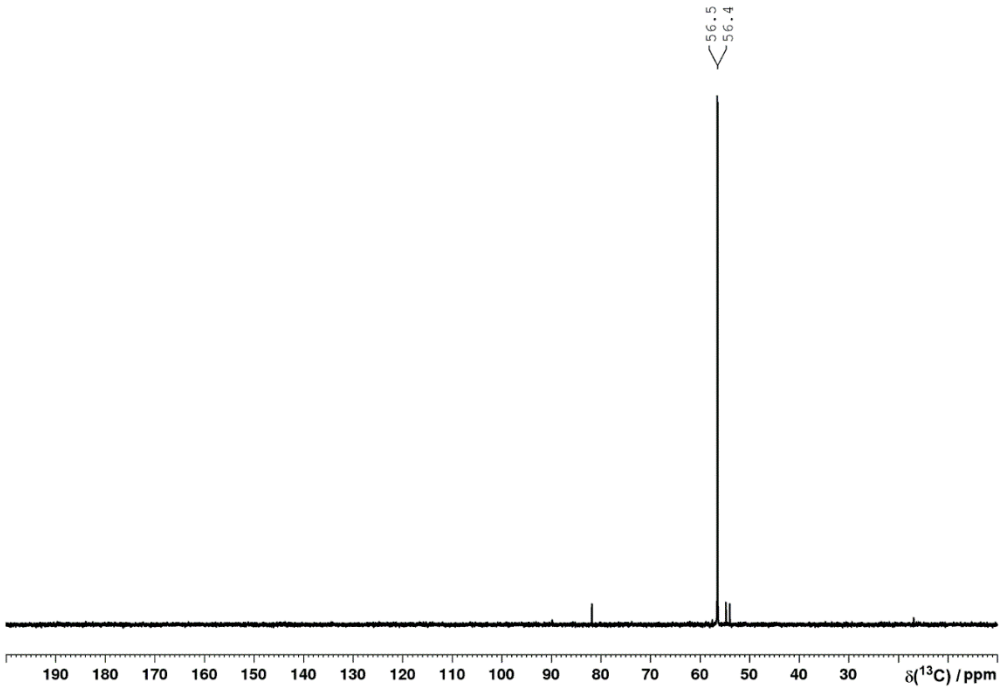

Figure S118. $^{13}C\{^1H\}$ NMR spectrum of THP (**16**) in D_2O.

2.4.2.18 Synthesis and isolation of THPC (17) *via* hydrostannylation under blue LEDs in PhMe, with recovery of Bu_3SnCl (20)

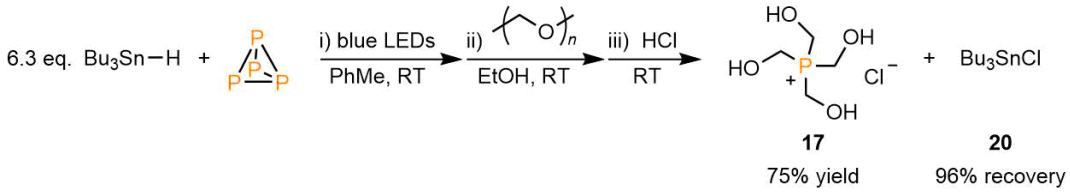

To a 50 mL flat-bottomed Schlenk tube were added P_4 (62.0 mg, 0.5 mmol) and PhMe (25 mL). After stirring to obtain a homogeneous solution, Bu_3SnH (847 µL, 3.15 mmol) was added. The resulting colourless, homogeneous mixture was stirred under irradiation with blue LED light (7X Osram OSLON SSL80, 455 nm (±15 nm), 20.3 V 1000mA) for 16 h, during which time the Schlenk tube was placed in a block cooled by circulating water to maintain near-ambient temperature. Following removal of volatiles under vacuum, EtOH (25 mL) and paraformaldehyde (750 mg, 25 mmol) were added, and the resulting suspension was stirred at room temperature for 16 h. The mixture was frozen in a liquid nitrogen bath and HCl (4.0 M in 1,4-dioxane, 5 mL, 20 mmol) was added. After thawing, the reaction mixture was stirred at room temperature for 2 h. The yellowish suspension was filtered, and volatiles were removed under vacuum. The remaining oily solid residue was triturated with Et_2O (20 mL) overnight, filtered and washed with further Et_2O (20 mL) to afford the desired product as a white solid (281 mg, 75%) after drying under vacuum.

The combined Et_2O washes from the above reaction were dried under vacuum to afford Bu_3SnCl (**20**) as a pale yellow oil (987 mg, 96%).

Spectroscopic data of THPC (**17**):

^{1}H NMR (400 MHz, 300 K, D_2O): δ = 4.67 ppm (d, $^2J(^{31}P\text{-}^1H)$ = 1.8 Hz). **$^{31}P\{^1H\}$ NMR** (121 MHz, 300 K, D_2O): δ = 27.0 ppm (s). **^{31}P NMR** (121 MHz, 300 K, D_2O): δ = 27.0 ppm (s). **$^{13}C\{^1H\}$ NMR** (101 MHz, 300 K, D_2O): δ = 49.1 ppm (d, $^1J(^{31}P\text{-}^{13}C)$ = 51.3 Hz). NMR data are consistent with previous reports.[77]

Spectroscopic data of recovered Bu_3SnCl (**20**):

^{1}H NMR (400 MHz, 300 K, $CDCl_3$): δ = 1.77-1.51 (2H, m), 1.41-1.21 (4H, m), 0.92 ppm (3H, t, $^3J(^1H\text{-}^1H)$ = 7.3 Hz). **$^{119}Sn\{^1H\}$ NMR** (149 MHz, 300 K, $CDCl_3$): δ = 157.5 ppm. **$^{13}C\{^1H\}$ NMR** (101 MHz, 300 K, $CDCl_3$): δ = 27.9 (s), 26.9 (s), 17.5 (s), 13.6 ppm (s). NMR data are consistent with previous reports.[78]

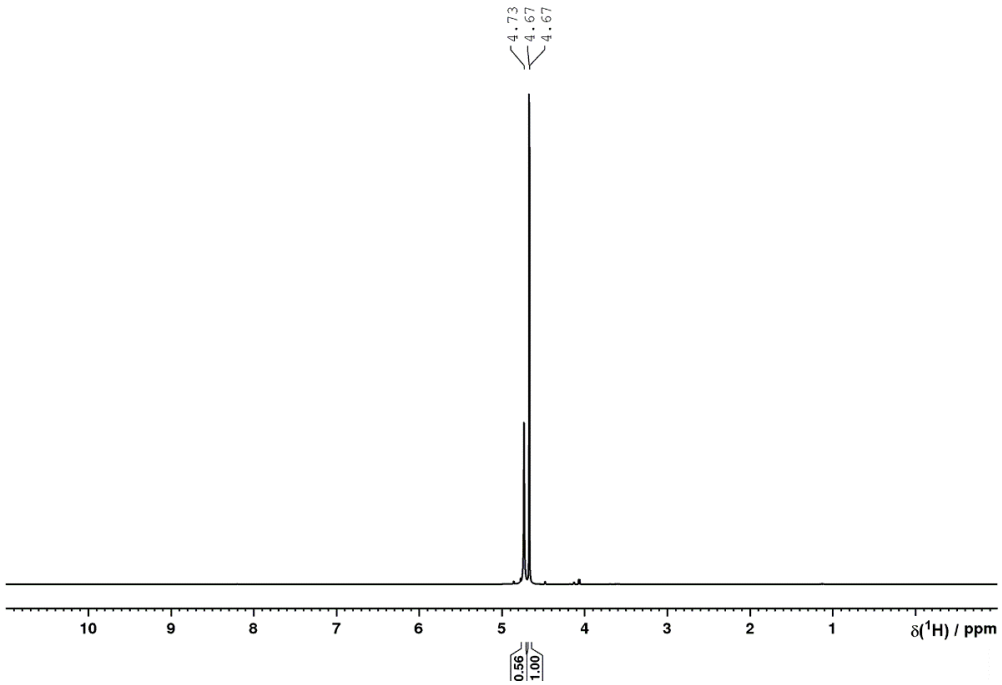

Figure S119. ^{1}H NMR spectrum of THPC (**17**) in D_2O.

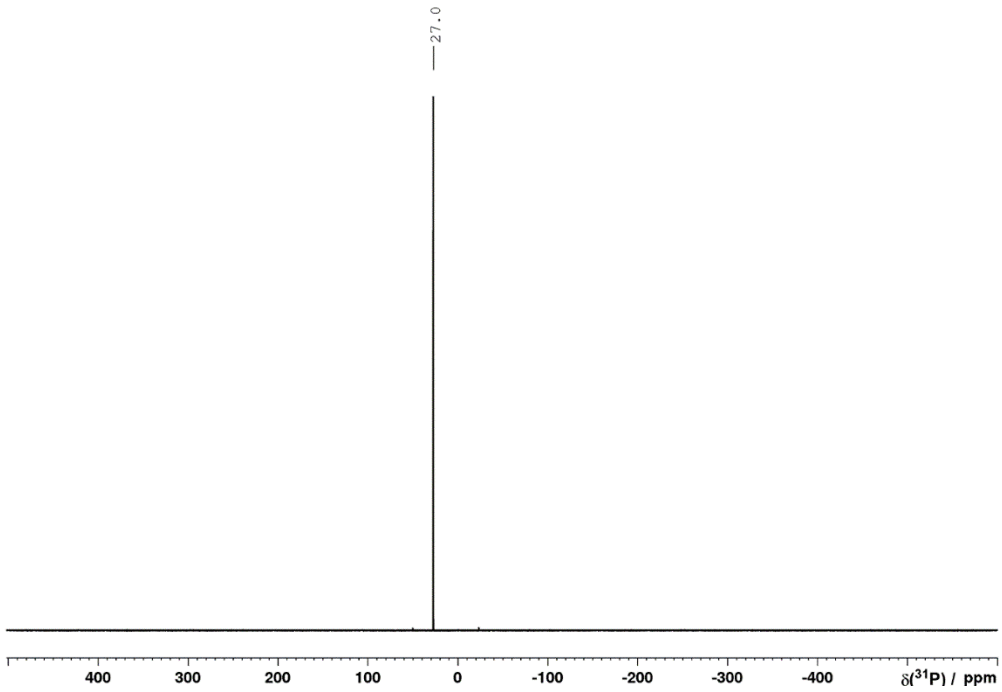

Figure S120. $^{31}P\{^{1}H\}$ NMR spectrum of THPC (**17**) in D_2O.

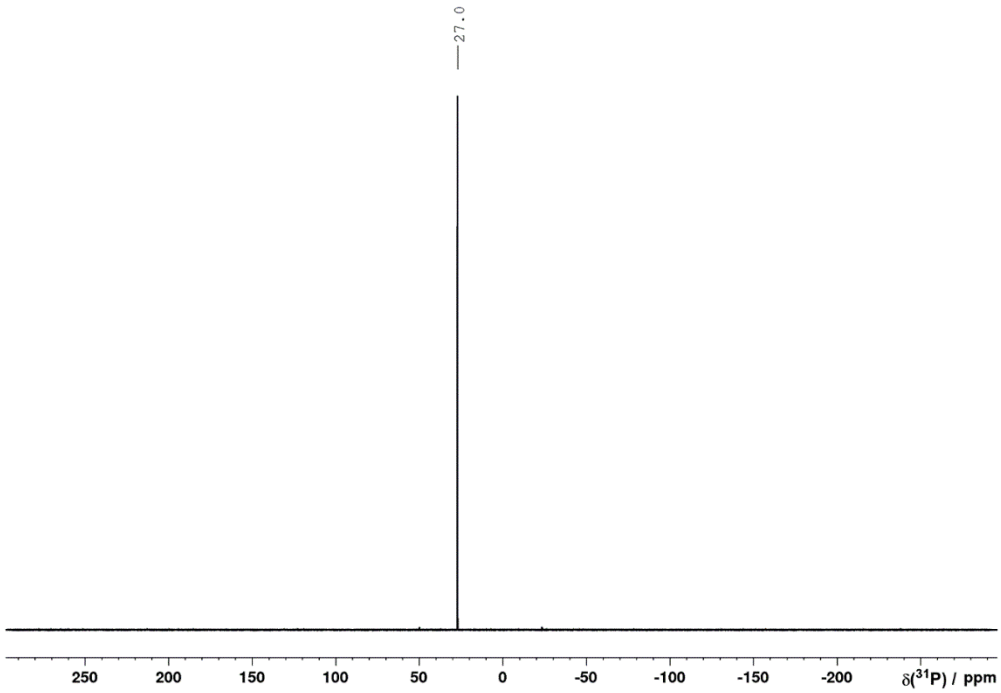

Figure S121. ^{31}P NMR spectrum of THPC (**17**) in D_2O.

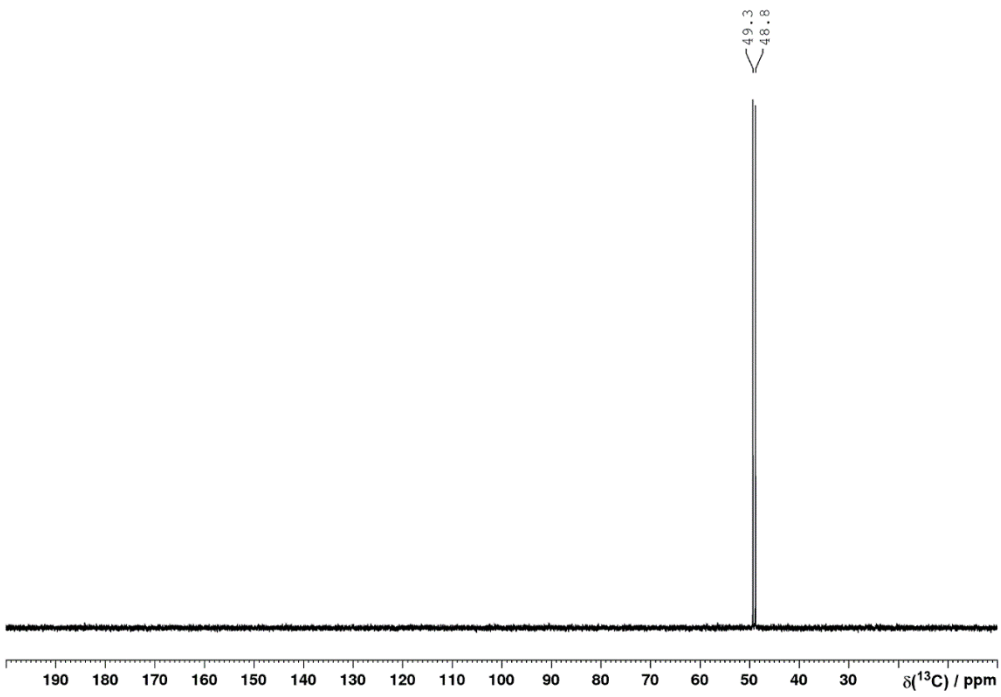

Figure S122. $^{13}C\{^{1}H\}$ NMR spectrum of THPC (**17**) in D_2O.

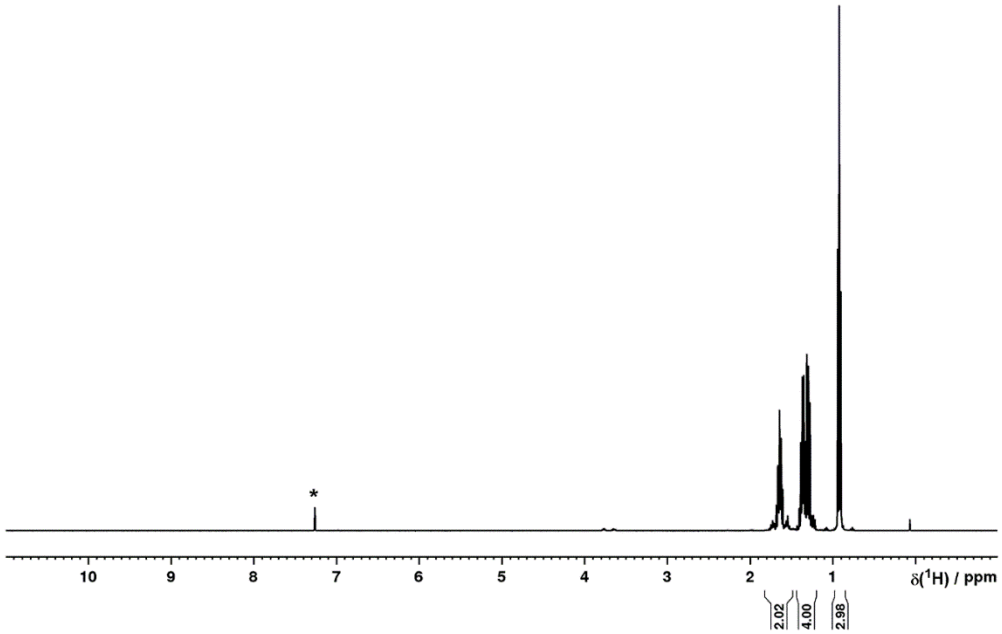

Figure S123. ^{1}H NMR spectrum of Bu_3SnCl (**20**) in $CDCl_3$ (*).

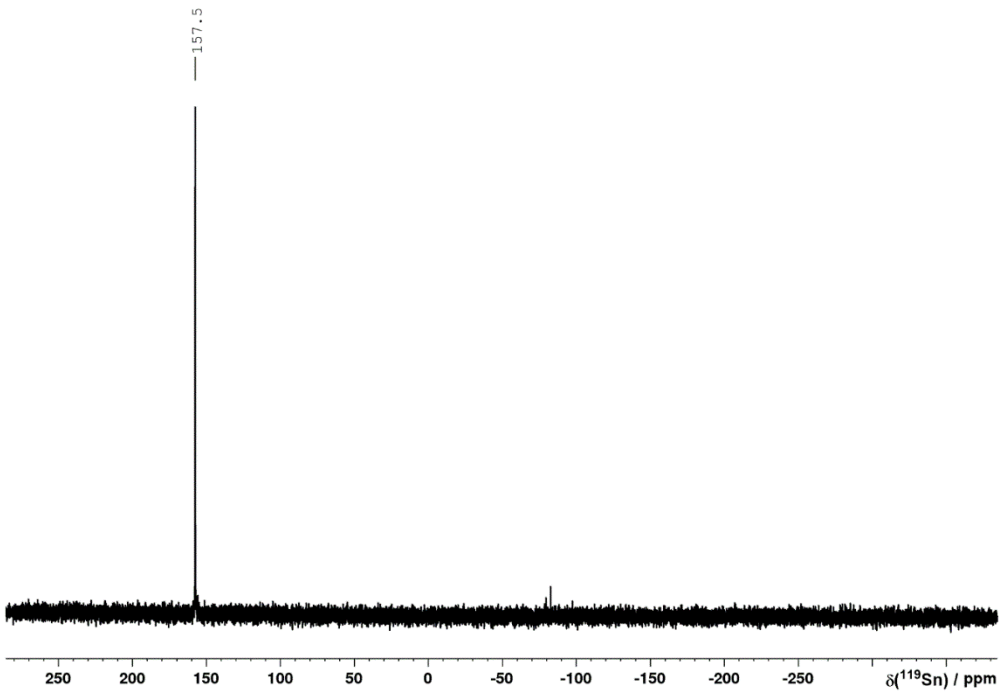

Figure S124. $^{119}Sn\{^{1}H\}$ NMR spectrum of Bu_3SnCl (**20**) in $CDCl_3$.

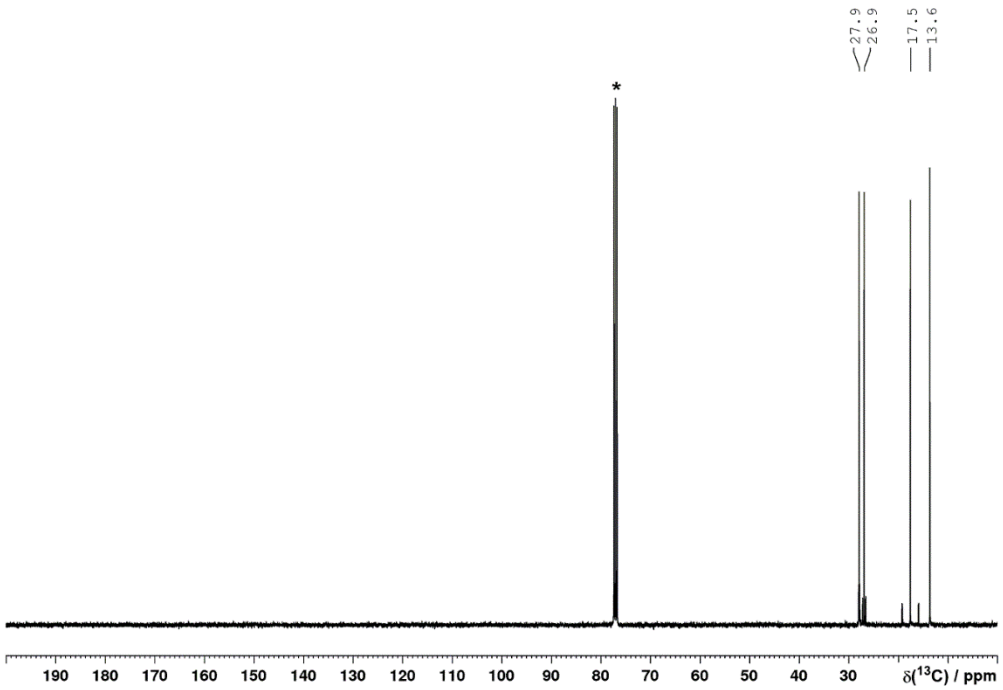

Figure S125. $^{13}C\{^{1}H\}$ NMR spectrum of Bu_3SnCl (**20**) in $CDCl_3$ (*).

2.4.2.19 Synthesis and isolation of THPC (17) *via* hydrostannylation under blue LEDs in EtOH, with recovery of Bu_3SnCl (20)

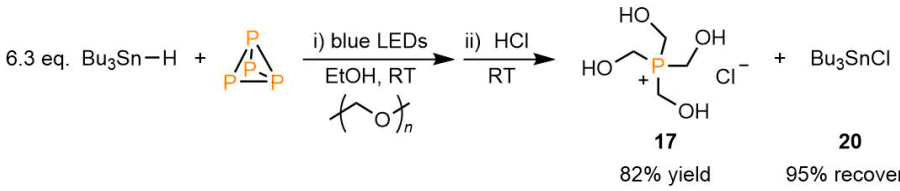

To a 50 mL flat-bottomed Schlenk were added P_4 (62.0 mg, 0.5 mmol) and PhH (5.0 mL). After stirring to obtain a homogeneous solution, EtOH (25 mL), Bu_3SnH (847 µL, 3.15 mmol) and paraformaldehyde (750 mg, 25 mmol) were added. The resulting suspension was stirred under irradiation with blue LED light (7X Osram OSLON SSL80, 455 nm (±15 nm), 20.3 V 1000mA) for 22 h, during which time the Schlenk tube was placed in a block cooled by circulating water to maintain near-ambient temperature. The resulting mixture was frozen and HCl (4.0 M in 1,4-dioxane, 5 mL, 20 mmol) was added. After thawing, the reaction mixture was stirred for 2 h. The resulting suspension was filtered to give a colourless solution. Removal of volatiles under vacuum yielded an oily solid residue that was triturated with Et_2O (20 mL) overnight to give THPC (**17**) as a white solid (312 mg, 82%) after filtration, washing with additional Et_2O (20 mL) and drying under vacuum.

The combined Et_2O washes from the above reaction were dried under vacuum to afford Bu_3SnCl (**20**) as a pale yellow oil (980 mg, 95%).

NMR data of product THPC and recovered Bu_3SnCl are identical to those given in Section 2.4.2.18.

2.4.2.20 Synthesis and isolation of THPC (17) *via* hydrostannylation using AIBN in PhMe (0.5 mmol scale)

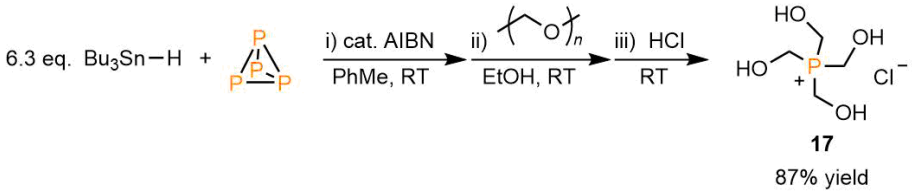

To a 50 mL Schlenk tube were added P_4 (62.0 mg, 0.5 mmol) and PhMe (25 mL). After stirring to obtain a homogeneous solution, Bu_3SnH (847 µL, 3.15 mmol) and AIBN (8.2 mg, 0.05 mmol) were added. The Schlenk tube was immediately and thoroughly wrapped in Al foil to exclude any ambient light, and the stirred reaction mixture was then heated to 30 °C for 16 h. Following removal of volatiles under vacuum, EtOH (25 mL) and paraformaldehyde (750 mg, 25 mmol) were added, and the resulting suspension was stirred at room temperature for 16 h. The mixture was frozen in a liquid nitrogen bath and HCl (4.0 M in 1,4-dioxane, 5 mL, 20 mmol) was added. After thawing, the reaction mixture was stirred at room temperature for 2 h. The resulting yellowish suspension was filtered, and volatiles were removed under vacuum. The remaining oily solid residue was triturated with Et_2O (20 mL) overnight, to give THPC (**17**) as a white solid (330 mg, 87%) after filtration, washing with additional Et_2O (20 mL) and drying under vacuum. NMR data are identical to those given in Section 2.4.2.18.

2.4.2.21 Synthesis and isolation of THPC (17) *via* hydrostannylation using AIBN in PhMe (5 mmol scale)

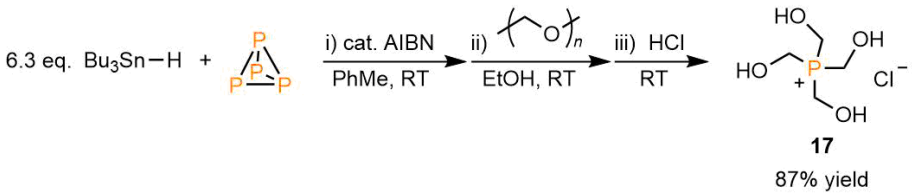

To a 500 mL round-bottomed Schlenk flask were added P_4 (620 mg, 5 mmol) and PhMe (250 mL). After stirring to obtain a homogeneous solution, Bu_3SnH (8.5 mL, 31.5 mmol) and AIBN (82.1 mg, 0.5 mmol) were added. The Schlenk flask was immediately and thoroughly wrapped in Al foil to exclude any ambient light, and the stirred reaction mixture was then heated to 30 °C for 16 h. Following removal of volatiles under vacuum, EtOH (250 mL) and paraformaldehyde (7.51 g, 250 mmol) were added, and the resulting suspension was stirred at room temperature for 16 h. The mixture was frozen in a liquid nitrogen bath and HCl (4.0 M in 1,4-dioxane, 50 mL, 200 mmol) was added. After thawing, the reaction mixture was stirred at room temperature for 4 h. The yellowish suspension was filtered through a bed of Celite in a glass frit (P4) column, and volatiles were removed under vacuum. The remaining oily solid residue was triturated with Et_2O (200 mL) overnight, filtered and washed with additional Et_2O (2 x 25 mL).

After drying thoroughly under vacuum, the desired product was obtained as an off-white solid (3.33 g, 87%). NMR data are identical to those given in Section 2.4.2.18.

2.4.2.22 Synthesis and isolation of THPO (18)

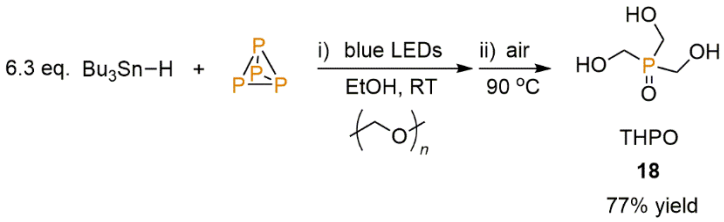

To a 50 mL flat-bottomed Schlenk were added P_4 (62.0 mg, 0.5 mmol) and PhH (5.0 mL). After stirring to obtain a homogeneous solution, EtOH (25 mL), Bu_3SnH (847 µL, 3.15 mmol) and paraformaldehyde (180 mg, 6.0 mmol) were added. The resulting suspension was stirred under irradiation with blue LED light (7X Osram OSLON SSL80, 455 nm (±15 nm), 20.3 V 1000mA) for 22 h, during which time the Schlenk tube was placed in a block cooled by circulating water to maintain near-ambient temperature. The resulting suspension was filtered and volatiles were removed under vacuum. Additional work-up was performed under air. To the oily residue thus obtained was added PhMe (20 mL) and H_2O (20 mL). The biphasic mixture was thoroughly stirred for 30 min and the aqueous phase was separated and washed with additional PhMe (3 x 15 mL), before being heated to 90 °C for 16 h while being kept open to air. Subsequent removal of volatiles yielded THPO (**18**) as a colourless oil (217 mg, 77%).

^{1}H NMR (400 MHz, 300 K, D_2O): δ = 4.04 ppm (d, $^2J(^{31}P\text{-}^1H)$ = 3.0 Hz). **^{31}P{^{1}H} NMR** (121 MHz, 300 K, D_2O): δ = 49.7 ppm (s). **^{31}P NMR** (121 MHz, 300 K, D_2O): δ = 49.7 ppm (s). **^{13}C{^{1}H} NMR** (101 MHz, 300 K, D_2O): δ = 54.3 ppm (d, $^1J(^{31}P\text{-}^{13}C)$ = 75.7 Hz). **MS** (ESI, EtOH): *m*/*z* = 141.0312 ($[M+H]^+$). NMR data are consistent with previous reports.[79]

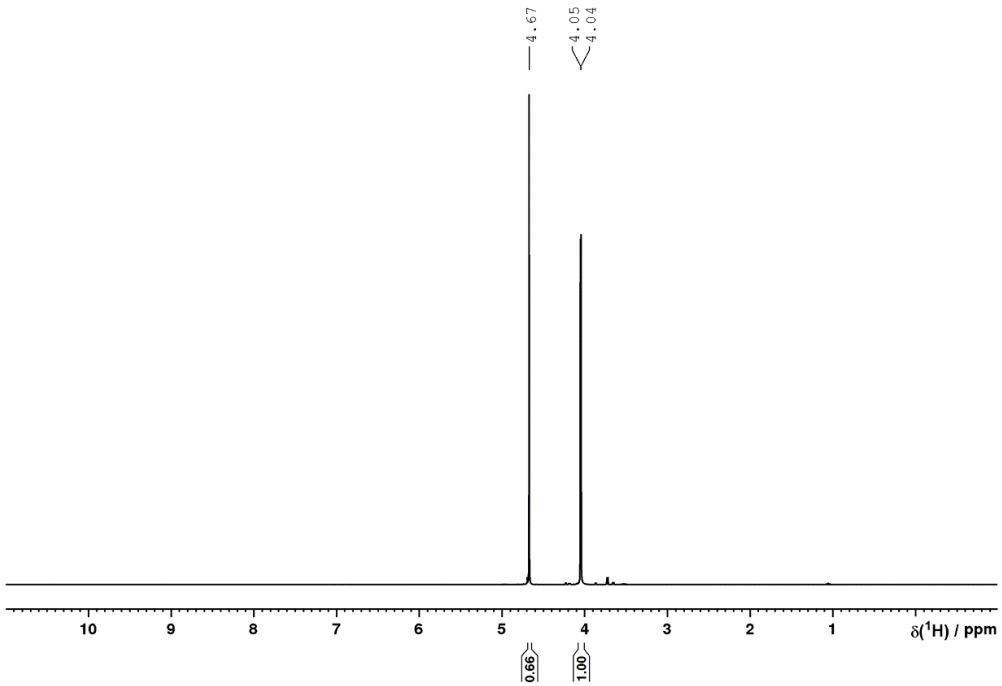

Figure S126. ^{1}H NMR spectrum of THPO (**18**) in D_2O.

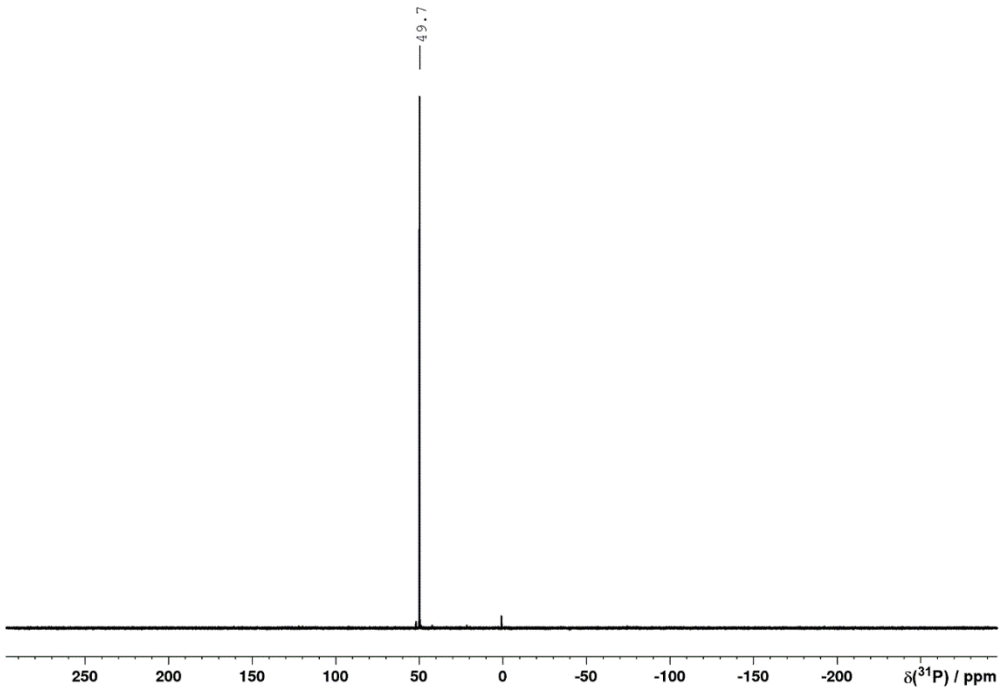

Figure S127. $^{31}P\{^{1}H\}$ NMR spectrum of THPO (**18**) in D_2O.

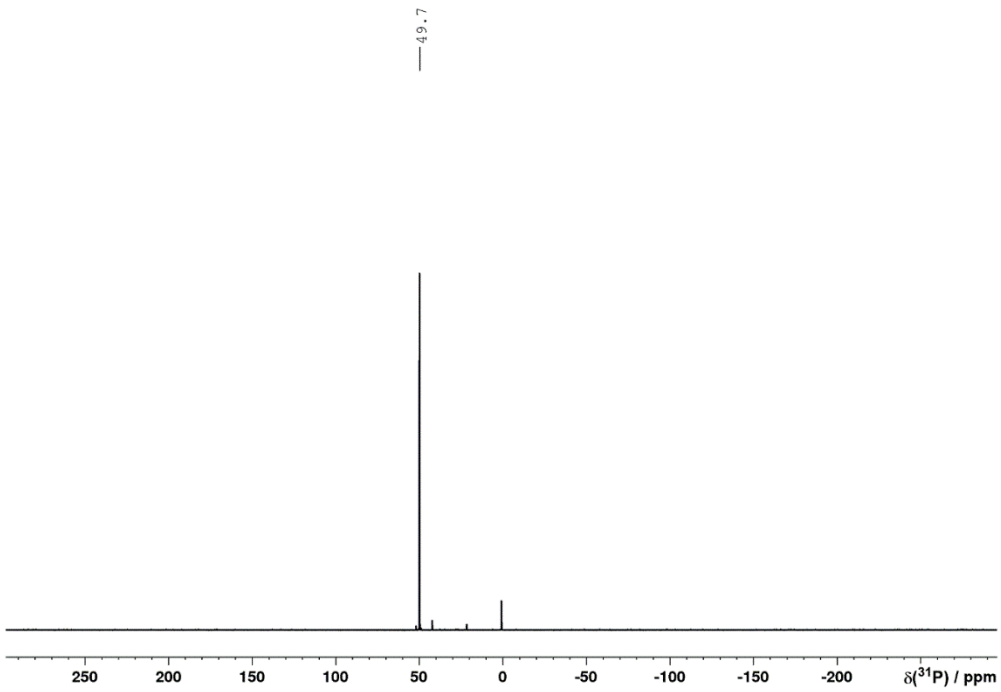

Figure S128. ^{31}P NMR spectrum of THPO (**18**) in D_2O.

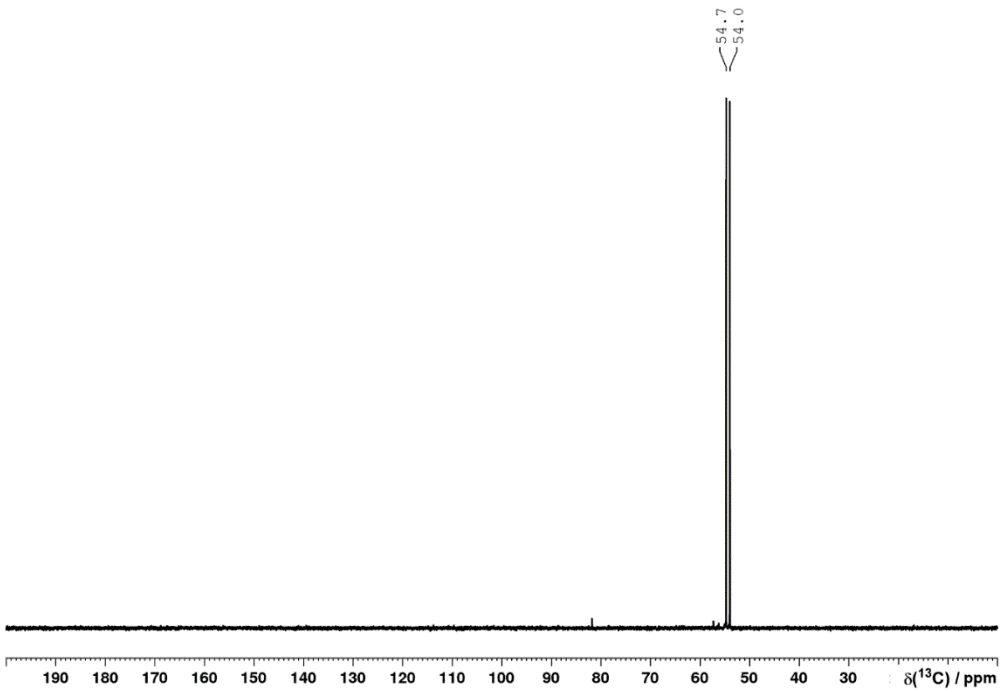

Figure S129. $^{13}C\{^{1}H\}$ NMR spectrum of THPO (**18**) in D_2O.

2.4.2.23 Synthesis and isolation of HPA (19), with recovery of Bu_3SnCl (20)

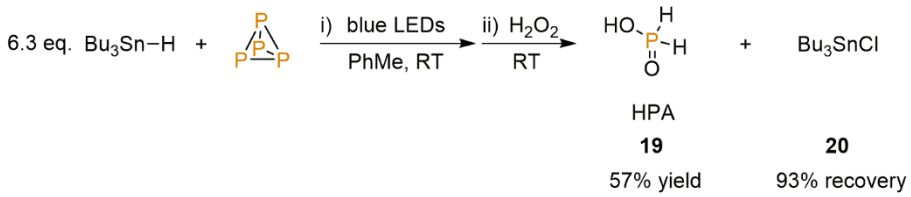

To a 50 mL flat-bottom Schlenk tube were added P_4 (62.0 mg, 0.5 mmol) and PhMe (25 mL). After stirring to obtain a homogeneous solution, Bu_3SnH (847 µL, 3.15 mmol) was added. The resulting colourless, homogeneous mixture was stirred under irradiation with blue LED light (7X Osram OSLON SSL80, 455 nm (±15 nm), 20.3 V 1000mA) for 16 h, during which time the Schlenk tube was placed in a block cooled by circulating water to maintain near-ambient temperature. The resulting solution was frozen in a liquid nitrogen bath and H_2O_2 (35% aq., 0.43 mL, 5.0 mmol) was added. After thawing, the reaction mixture was stirred at room temperature for 30 minutes. Subsequent work-up was performed under air. H_2O (20 mL) was added and, after mixing thoroughly, the organic phase was separated and washed with further H_2O (3 x 15 mL). Volatiles were removed under vacuum, and *n*-hexane (20 mL) and MeCN (20 mL) were added. HCl was added dropwise to the stirred biphasic mixture (4.0 M in 1,4-dioxane, 1.25 mL, 5 mmol), and after stirring for 1 h the MeCN layer was separated and volatiles were removed under vacuum. The resulting colourless oil was washed with further n-hexane (20 mL) and dried thoroughly under vacuum to yield the desired product as a colourless oil (127 mg, 57%). The material obtained in this manner typically contains *ca.* 10% $HP(O)(OH)_2$ (as judged by $^{31}P\{^1H\}$ NMR spectroscopy), which is a known oxidation product of $H_2P(O)OH$.[56] In order to ascertain the H_2O content, quantitative $^{31}P\{^1H\}$ NMR spectroscopic analysis (D1 = 14 s) was performed on a CD_3CN solution containing precisely known quantities of both this product (6.5 mg) and Ph_3PO (23.0 mg), with the latter acting as an internal standard for integration. In this manner the precise amount of HPA (and $HP(O)(OH)_2$) in the sample could be calculated, with the remaining mass being attributed to H_2O. The overall composition was thus determined to be $HPA\cdot(HP(O)(OH)_2)_{0.14}\cdot(H_2O)_{1.92}$, and this composition was used to calculate the isolated yield.

The combined *n*-hexane washes from the above reaction were dried under vacuum to afford Bu_3SnCl (**20**) as a pale yellow oil (953 mg, 93%).

<u>NMR data of HPA (**19**):</u>

^{1}H NMR (400 MHz, 300 K, CD_3CN): δ = 10.84 (s), 7.05 ppm (d, $^1J(^{31}P\text{-}^1H)$ = 575 Hz). **$^{31}P\{^1H\}$ NMR** (121 MHz, 300 K, CD_3CN): δ = 13.9 ppm (s). **^{31}P NMR** (121 MHz, 300 K, CD_3CN): δ = 13.9 ppm (d, $^1J(^{31}P\text{-}^1H)$ = 575 Hz). NMR data are consistent with previous reports.[80]

NMR data of Bu_3SnCl (**20**) were identical to those given in Section 2.4.2.18.

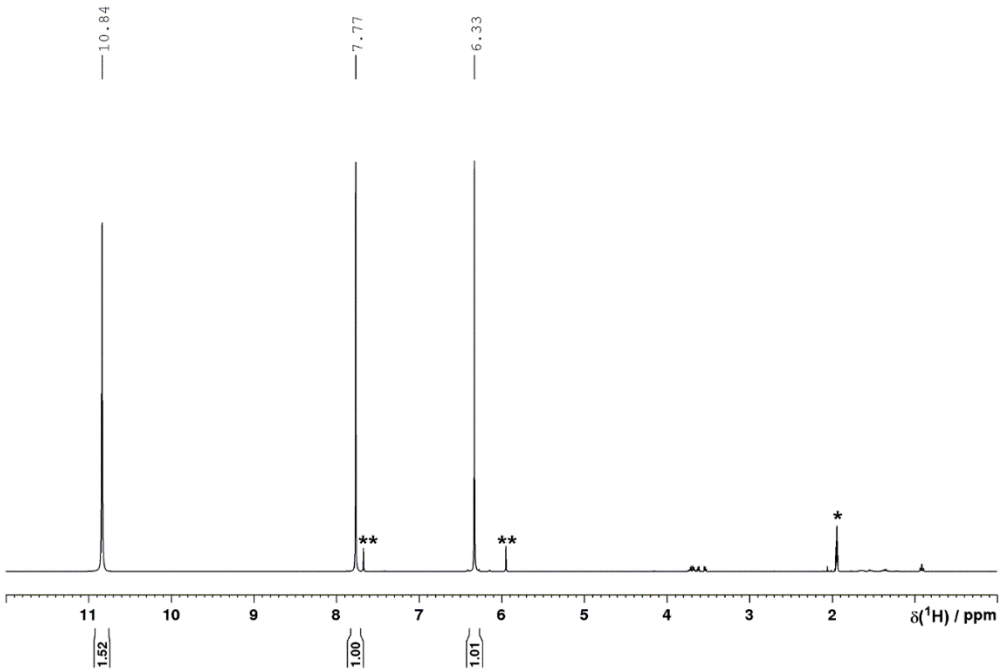

Figure S130. ^{1}H NMR spectrum of HPA (**19**) in CD_3CN (*solvent, **minor $HP(O)(OH)_2$).

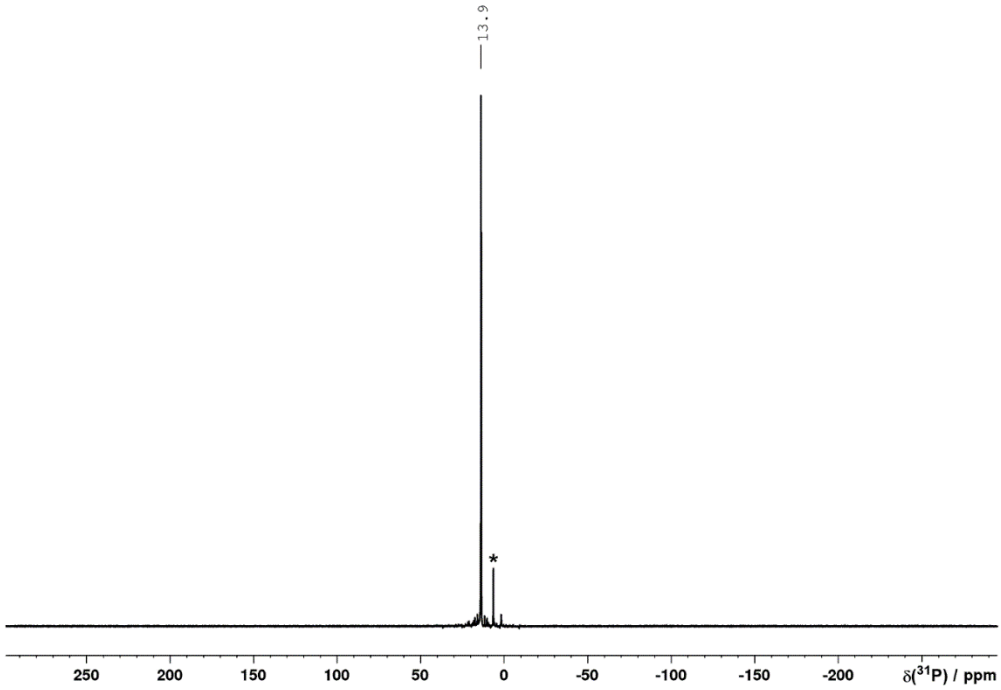

Figure S131. $^{31}P\{^{1}H\}$ NMR spectrum of HPA (**19**) in CD_3CN (*minor $HP(O)(OH)_2$).

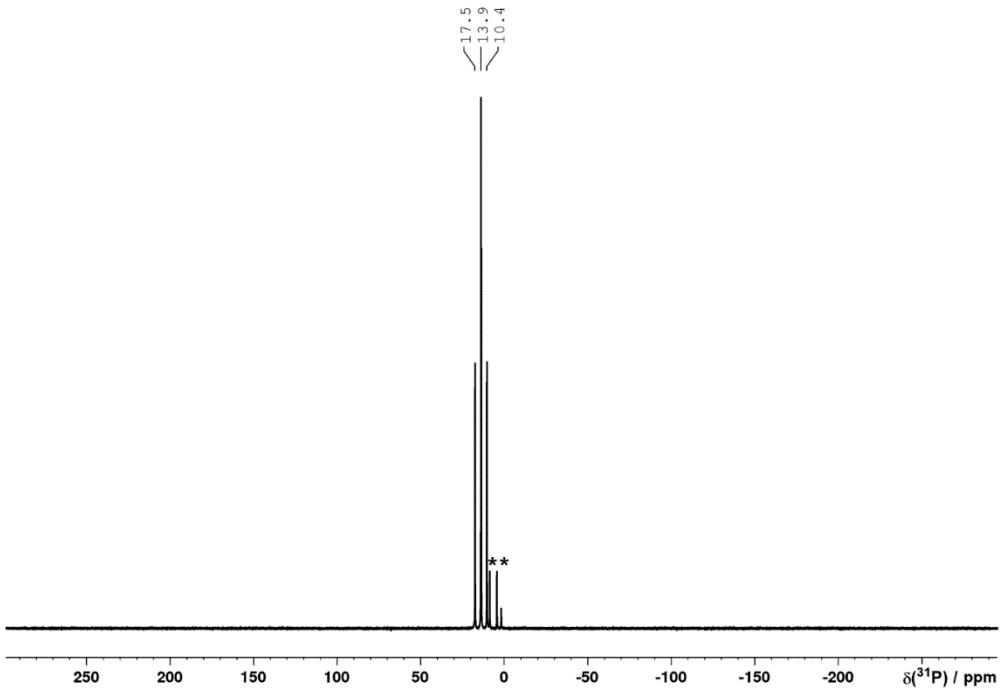

Figure S132. ^{31}P NMR spectrum of HPA (**19**) in CD_3CN (*minor $HP(O)(OH)_2$).

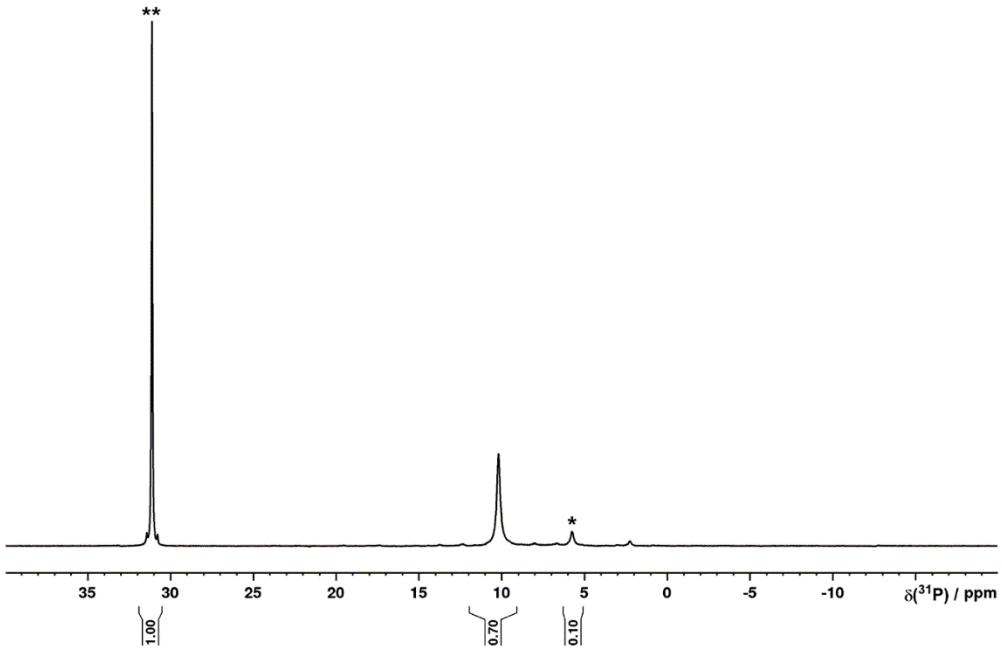

Figure S133. Quantitative $^{31}P\{^1H\}$ NMR spectrum (D1= 14 s) of HPA (**19**; 6.5 mg) in CD_3CN (*minor $HP(O)(OH)_2$, **23.0 mg Ph_3PO).

2.4.3 *In Situ* Generation and Recycling of Bu_3SnH

2.4.3.1 Hydrostannylation of P_4 using Bu_3SnOMe and PMHS under blue LED irradiation (0.01 mmol scale)

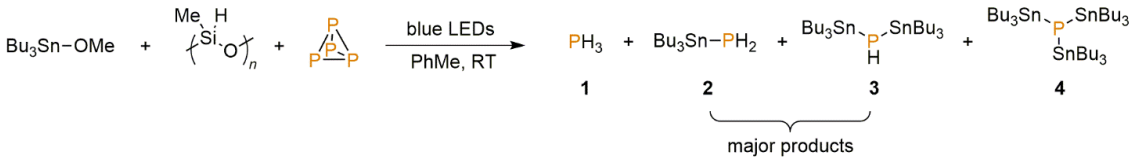

To a 10 mL, flat-bottomed, stoppered tube were added PhMe (500 µL), P_4 (0.01 mmol, as a stock solution in 77.4 µL PhH), Bu_3SnOMe (17.3 µL, 0.06 mmol), and PMHS (3.9 µL, 0.065 mmol). The tube was sealed, placed in a water-cooled block to maintain near-ambient temperature, and irradiated with blue light (455 nm (±15 nm), 3.2 V, 700 mA, Osram OSLON SSL 80) for 21 h. The resulting mixture was analysed by $^{31}P\{^1H\}$ NMR spectroscopy, as shown in Figure S134 below.

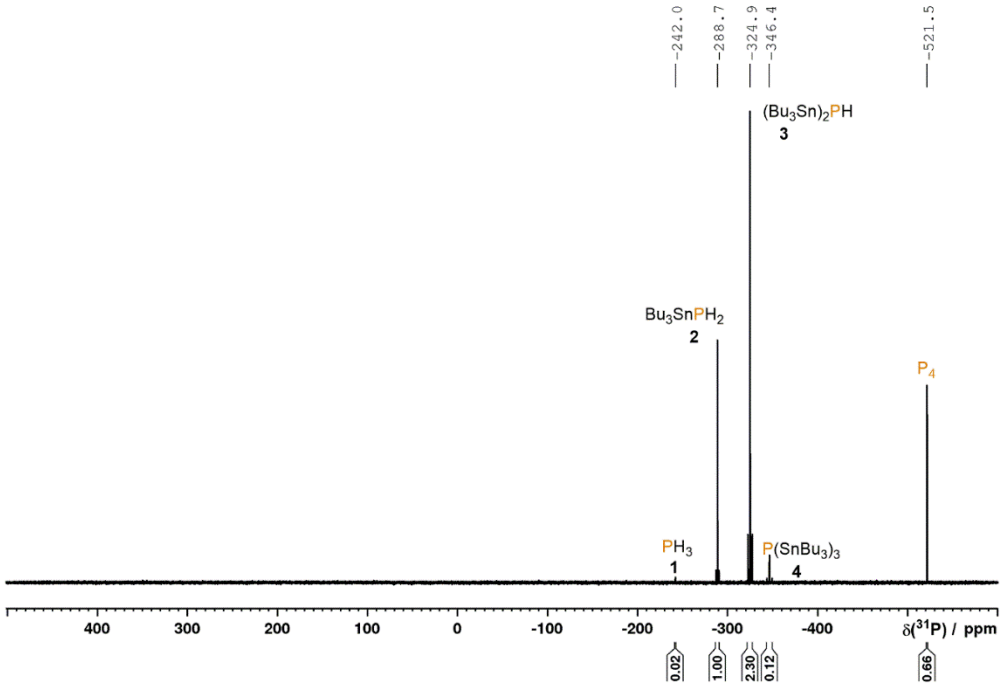

Figure S134. $^{31}P\{^1H\}$ NMR spectrum for the reaction of P_4, 6 eq. Bu_3SnOMe and 6.5 eq. PMHS in PhMe, driven by 455 nm LED irradiation for 21 h.

The $^{31}P\{^1H\}$ NMR spectrum of the reaction clearly shows consumption of P_4, and concomitant formation of the hydrostannylation products $(Bu_3Sn)_xPH_{3-x}$ (x = 0-3), as is also observed when Bu_3SnH is used as starting material (for example, see Figure S2). Close inspection, however, reveals a slightly increased fraction of $(Bu_3Sn)_2PH$ (**3**) relative to Bu_3SnPH_2 (**2**), as well as a significantly increased amount of residual, unreacted P_4. Both observations are attributed at least in part to a minor, competing side-reaction, in which the Bu_3SnOMe starting material reacts with Bu_3SnPH_2 to form $(Bu_3Sn)_2PH$ and MeOH, and is therefore unavailable for reduction by PMHS

and subsequent P_4 hydrostannylation (Scheme S3). Similar reactivity is observed during the selective synthesis of $P(SnBu_3)_3$ (**4**; Section 2.4.2.4). Furthermore, when the reaction was repeated using a two-fold excess of Bu_3SnOMe (12 eq.) under otherwise identical conditions, almost full P_4 consumption was observed, alongside formation of $(Bu_3Sn)_2PH$ as the clear major product (Figure S135). The feasibility of the reaction was further confirmed by independent addition of Bu_3SnOMe to an isolated sample of Bu_3SnPH_2 at RT in PhMe.

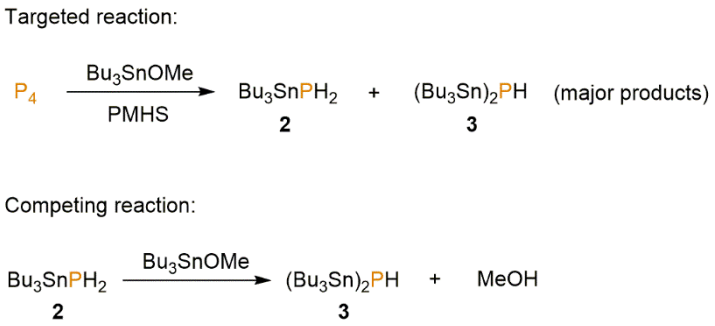

Scheme S3. Proposed side-reaction during the hydrostannylation of P_4 mediated by Bu_3SnOMe and PMHS.

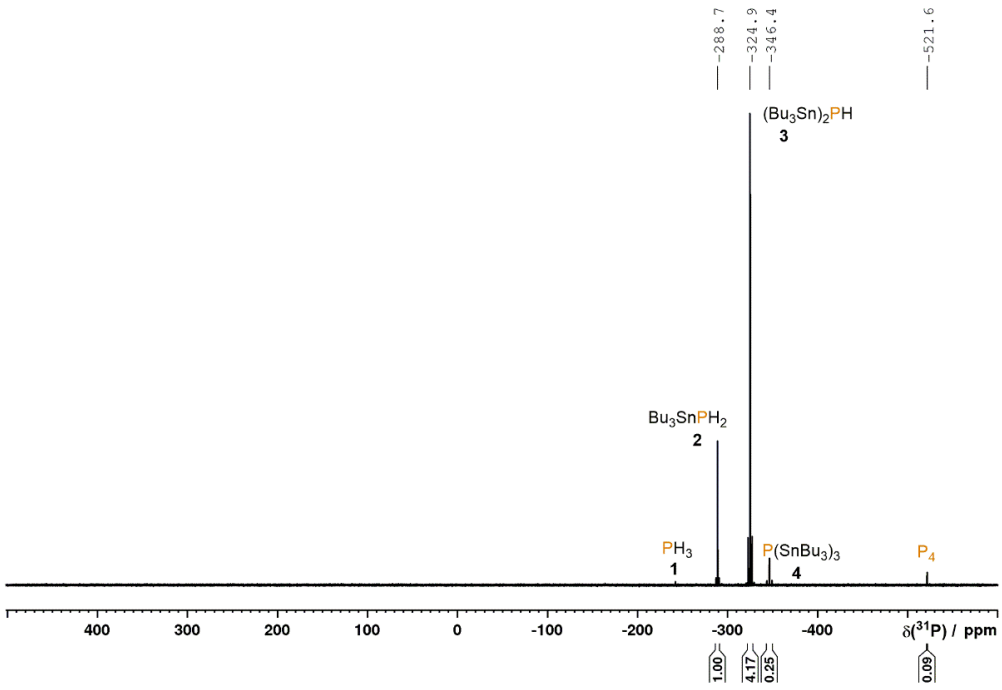

Figure S135. $^{31}P\{^1H\}$ NMR spectrum for the reaction of P_4, 12 eq. Bu_3SnOMe and 6.5 eq. PMHS in PhMe, driven by 455 nm LED irradiation for 21 h.

As a result of the above side-reaction a slight excess (8 eq.) of both Bu_3SnOMe and PMHS was used, in order to achieve improved reactivity, and near-complete P_4 conversion (Figure S136).

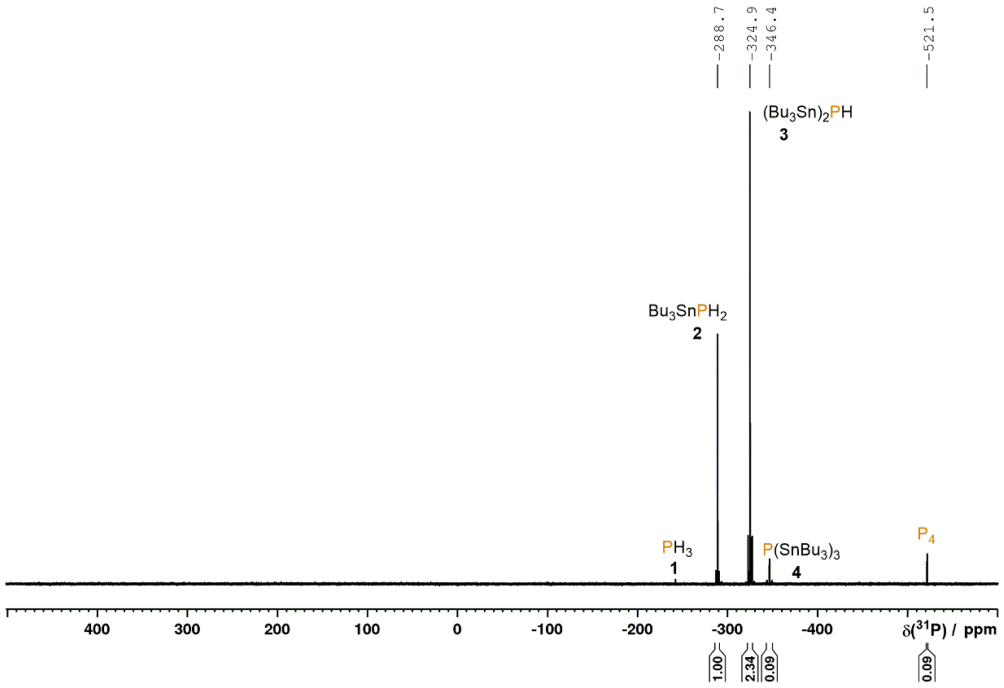

Figure S136. $^{31}P\{^{1}H\}$ NMR spectrum for the reaction of P_4, 8 eq. Bu_3SnOMe and 8 eq. PMHS in PhMe, driven by 455 nm LED irradiation for 21 h.

2.4.3.2 Hydrostannylation of P_4 using Bu_3SnOMe and PMHS initiated by AIBN (0.01 mmol scale)

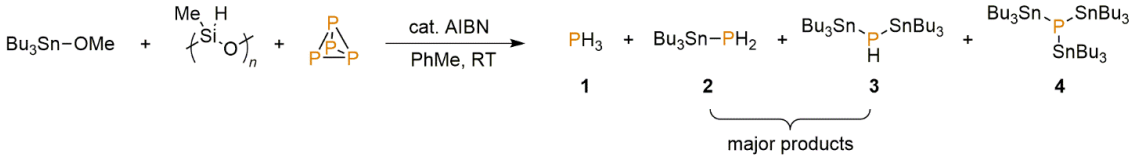

As for the blue LED-driven reactions, AIBN-initiated P_4 hydrostannylation was found to proceed in a very similar manner when Bu_3SnH was replaced with Bu_3OMe and PMHS. Again, however, slight modification of the initial reaction conditions was found to give improved performance.

To a 10 mL, flat-bottomed, stoppered tube were added PhMe (500 μL), P_4 (0.01 mmol, as a stock solution in 77.4 μL PhH), Bu_3SnOMe (23.0 μL, 0.08 mmol), PMHS (4.8 μL, 0.08 mmol) and AIBN (0.001 mmol, as a stock solution in 49.3 μL PhH). The tube was sealed, wrapped in Al foil to exclude light, and heated to 40 °C for 19 h. The resulting mixture was analysed by ^{1}H, $^{31}P\{^{1}H\}$ and ^{31}P NMR spectroscopy, as shown in Figure S137, below.

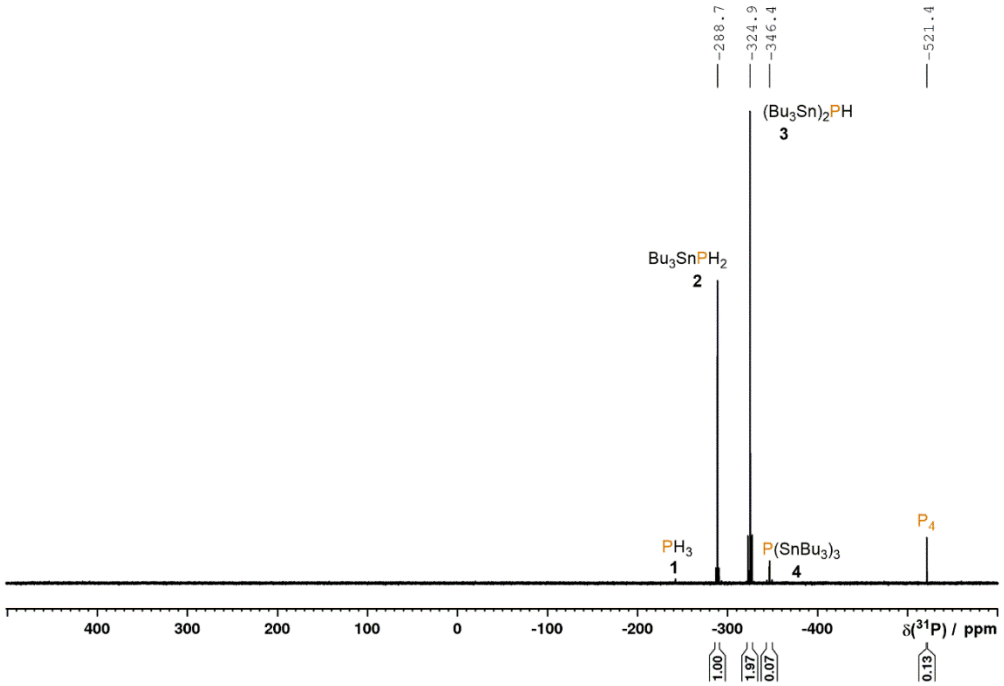

Figure S137. $^{31}P\{^{1}H\}$ NMR spectrum for the reaction of P_4, 8 eq. Bu_3SnOMe and 8 eq. PMHS in PhMe, driven by AIBN initiation at 40 °C for 19 h.

2.4.3.3 Hydrostannylation of P_4 using $(Bu_3Sn)_2O$ and PMHS

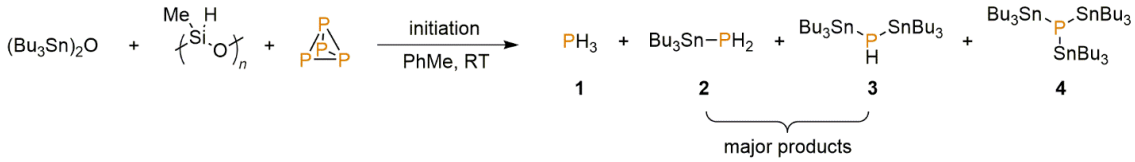

To a 10 mL, flat-bottomed, stoppered tube were added PhMe (500 µL), P_4 (0.01 mmol, as a stock solution in 86.0 µL PhH), $(Bu_3Sn)_2O$ (15.3 µL, 0.03 mmol) and PMHS (3.9 µL, 0.065 mmol). The tube was sealed, placed in a water-cooled block to maintain near-ambient temperature, and irradiated with blue light (455 nm (±15 nm), 3.2 V, 700 mA, Osram OSLON SSL 80) for 21 h. The resulting mixture was analysed by $^{31}P\{^{1}H\}$ NMR spectroscopy, as shown in Figure S138, below.

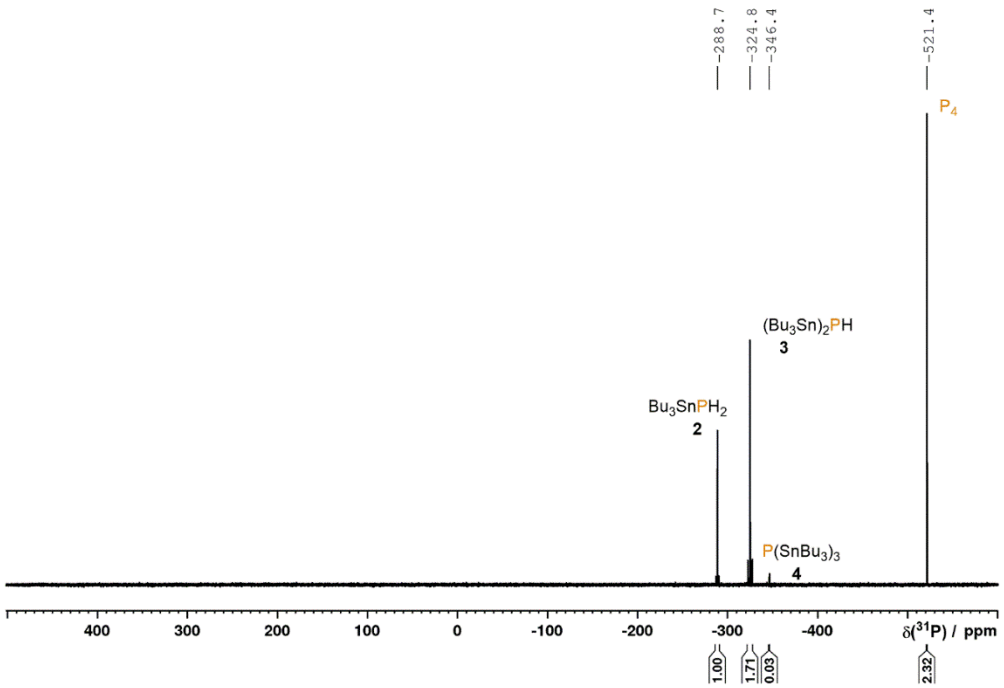

Figure S138. $^{31}P\{^{1}H\}$ NMR spectrum for the reaction of P_4, 3 eq. $(Bu_3Sn)_2O$ and 6.5 eq. PMHS in PhMe, driven by 455 nm LED irradiation for 21 h.

In contrast to reactions using Bu_3SnOMe (Sections 2.4.3.1 and 2.4.3.2), and despite the known ability of $(Bu_3Sn)_2O$ to act as a source of Bu_3SnH upon treatment with PMHS,[60] attempts to hydrostannylate P_4 *via* reaction with a mixture of $(Bu_3Sn)_2O$ and PMHS were initially found to give significantly inferior results, with very significant amounts of P_4 remaining (for example, see Figure S138, above). Nevertheless, satisfactory reactivity could be achieved by using ACN as an initiator under modified, and still relatively mild reaction conditions (Figure S139, below).

To a 10 mL, flat-bottomed, stoppered tube were added PhMe (500 µL), P_4 (0.01 mmol, as a stock solution in 77.4 µL PhH), $(Bu_3Sn)_2O$ (20.4 µL, 0.04 mmol), PMHS (4.8 µL, 0.08 mmol) and ACN (0.002 mmol, as a stock solution in 96.2 µL PhH). The tube was sealed, wrapped in Al foil to exclude light, and heated to 80 °C for 3 days. The resulting mixture was analysed by $^{31}P\{^{1}H\}$ NMR spectroscopy, as shown in Figure S139, below.

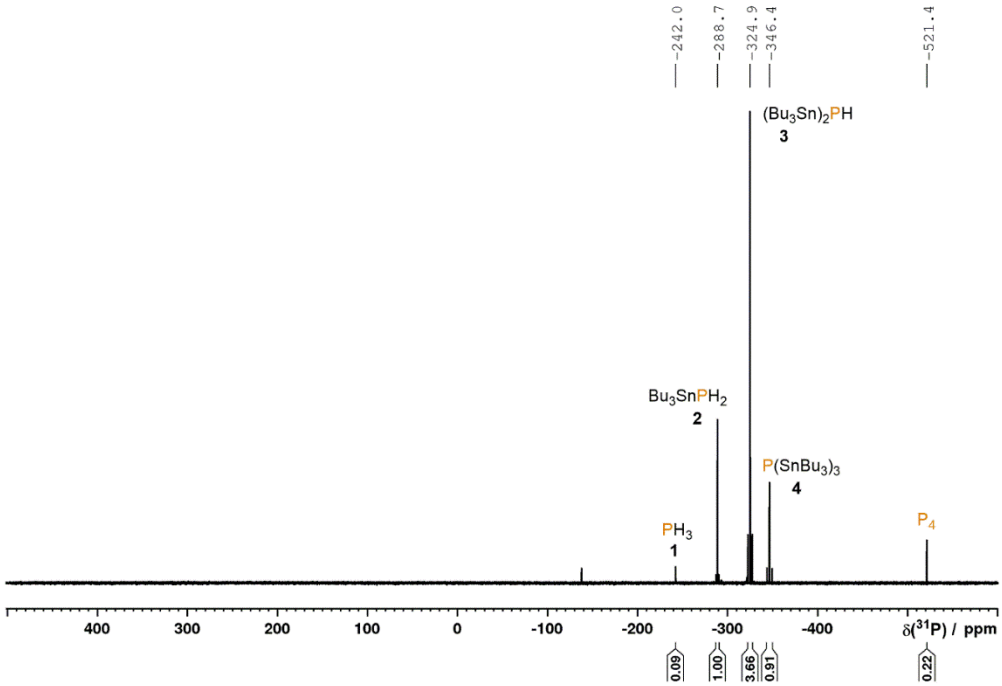

Figure S139. $^{31}P\{^{1}H\}$ NMR spectrum for the reaction of P_4, 4 eq. $(Bu_3Sn)_2O$ and 8 eq. PMHS in PhMe, driven by ACN initiation at 80 °C for 3 days.

2.4.3.4 Synthesis and isolation of THPC (17) *via* hydrostannylation starting from Bu_3SnOMe

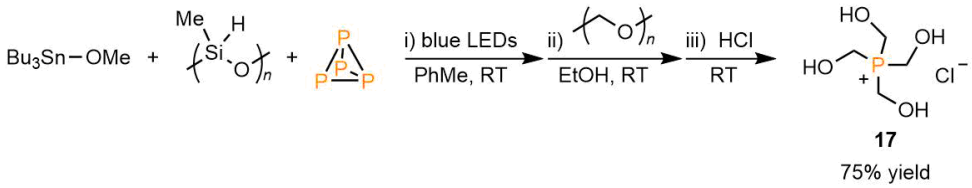

To a 50 mL flat-bottomed Schlenk tube were added P_4 (62.0 mg, 0.5 mmol) and PhMe (25 mL). After stirring to obtain a homogeneous solution, Bu_3SnOMe (1.15 mL, 4 mmol) and PMHS (239 µL, 4 mmol) were added. The resulting colourless, homogeneous mixture was stirred under irradiation with blue LED light (7X Osram OSLON SSL80, 455 nm (±15 nm), 20.3 V 1000mA) for 16 h, during which time the Schlenk tube was placed in a block cooled by circulating water to maintain near-ambient temperature. Following removal of volatiles under vacuum, EtOH (25 mL) and paraformaldehyde (750 mg, 25 mmol, 50 eq.) were added, and the resulting suspension was stirred at room temperature for 16 h. The mixture was frozen in a liquid nitrogen bath and HCl (4.0 M in 1,4-dioxane, 5 mL, 20 mmol) was added. After thawing, the reaction mixture was stirred at room temperature for 2 h. The pale yellow suspension was filtered, and volatiles were removed under vacuum. The oily solid residue was triturated with *n*-pentane (20 mL) overnight, filtered and washed with Et_2O (20 mL). The resulting white solid was then again dissolved in EtOH (2 x 20 mL). Following filtration, removal of volatiles under vacuum afforded the desired product as a white solid (330 mg, 87%). NMR data are identical to those reported in Section 2.4.2.18.

2.4.3.5 Synthesis and isolation of THPC (17) *via* hydrostannylation starting from $(Bu_3Sn)_2O$, with recycling of Bu_3SnCl (20) (0.5 mmol scale)

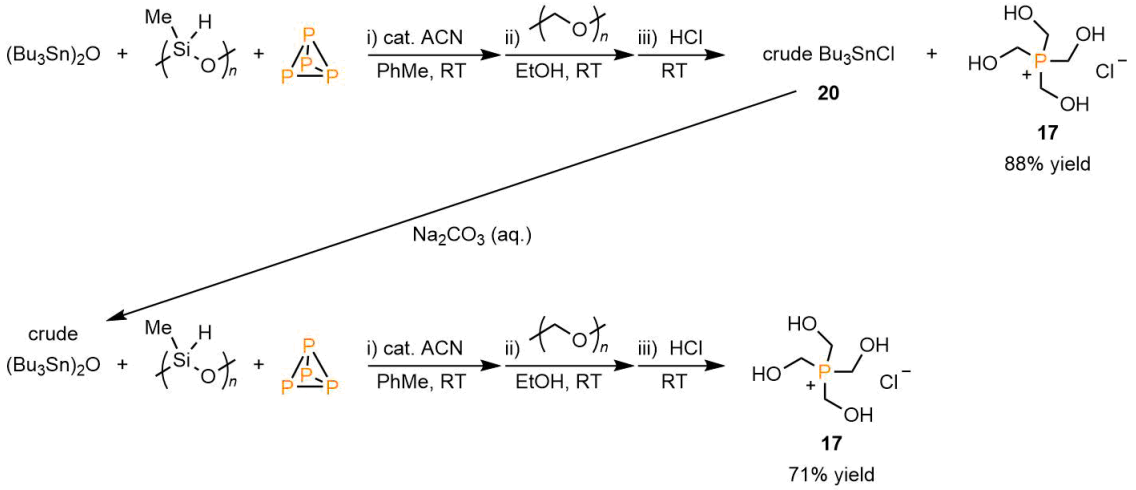

To a 50 mL Schlenk tube were added P_4 (62.0 mg, 0.5 mmol) and PhMe (25 mL). After stirring to obtain a homogeneous solution, $(Bu_3Sn)_2O$ (1.02 mL, 2 mmol), PMHS (239 µL, 4 mmol) and ACN (24.4 mg, 0.1 mmol) were added. The Schlenk tube was immediately and thoroughly wrapped in Al foil to exclude any ambient light, and the stirred reaction mixture was then heated to 80 °C for 3 days. Following removal of volatiles under vacuum, EtOH (25 mL) and paraformaldehyde (750 mg, 25 mmol) were added, and the resulting suspension was stirred at room temperature for 16 h. The mixture was frozen in a liquid nitrogen bath and HCl (4.0 M in 1,4-dioxane, 5 mL, 20 mmol) was added. After thawing, the reaction mixture was stirred at room temperature for 2 h. The pale yellow suspension was filtered, and volatiles were removed under vacuum. The remaining oily solid residue was triturated with Et_2O (20 mL) overnight, filtered and washed with further Et_2O (20 mL). The resulting white solid was then again dissolved in EtOH (2 x 20 mL). Following filtration and removal of volatiles under vacuum, the desired product was obtained as a white solid (335 mg, 88%). NMR data are identical to those reported in Section 2.4.2.18.

To the combined Et_2O washes from the above reaction was added a saturated aqueous solution of Na_2CO_3 (40 mL). The resulting biphasic mixture was stirred under open bench conditions for 16 h, and the organic phase was separated and washed with H_2O (4 x 15 mL). The organic phase was transferred into a 50 mL Schlenk tube and volatiles were removed under vacuum. The remaining procedure was performed under an inert atmosphere. A solution of P_4 (62.0 mg, 0.5 mmol) pre-dissolved in PhMe (25 mL) was added, followed by PMHS (239 µL, 4 mmol) and ACN (24.4 mg, 0.1 mmol). The Schlenk tube was immediately and thoroughly wrapped in Al foil to exclude any ambient light, and the stirred reaction mixture was then heated to 80 °C for 3 days. Following removal of volatiles under vacuum, EtOH (25 mL) and paraformaldehyde (750 mg, 25 mmol) were added, and the resulting suspension was stirred at room temperature for 16 h. The mixture was frozen in a liquid nitrogen bath and HCl (4.0 M in 1,4-dioxane, 5 mL, 20 mmol) was

added. After thawing, the reaction mixture was stirred at room temperature for 2 h. The pale yellow suspension was filtered, and volatiles were removed under vacuum. The remaining oily solid residue was triturated with Et_2O (20 mL) overnight, filtered and washed with further Et_2O (20 mL). The resulting white solid was then again dissolved in EtOH (2 x 20 mL). Following filtration and removal of volatiles under vacuum, the desired product was obtained as a white solid (270 mg, 71%). NMR data are identical to those reported in Section 2.4.2.18.

2.4.3.6 Synthesis and isolation of THPC (17) *via* hydrostannylation starting from $(Bu_3Sn)_2O$, with recycling of Bu_3SnCl (20) (5 mmol scale)

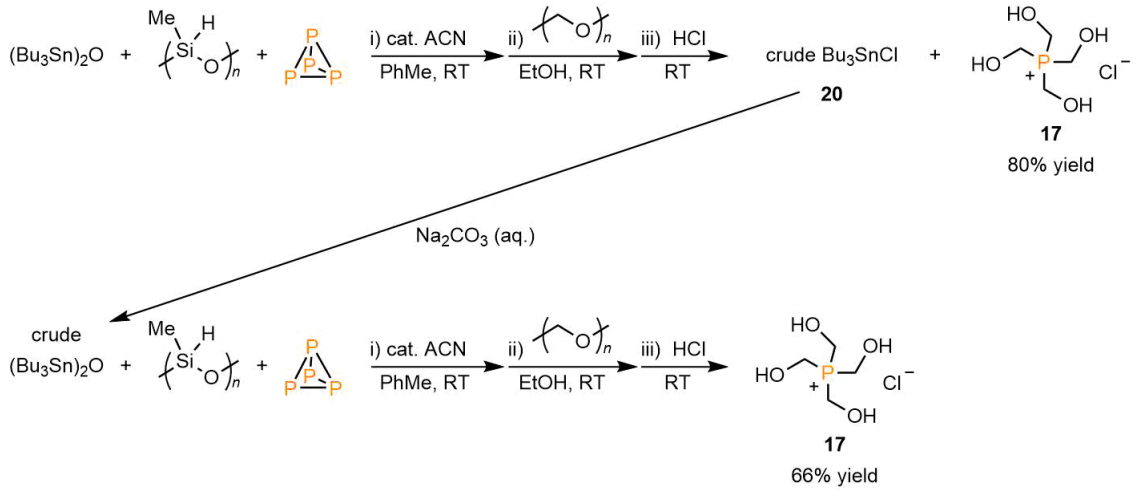

To a 500 mL round-bottomed Schlenk flask were added P_4 (620 mg, 5 mmol) and PhMe (250 mL). After stirring to obtain a homogeneous solution, $(Bu_3Sn)_2O$ (10.2 mL, 20 mmol), PMHS (2.3 mL, 40 mmol) and ACN (244 mg, 1 mmol) were added. The Schlenk flask was immediately and thoroughly wrapped in Al foil to exclude any ambient light, and the stirred reaction mixture was then heated to 80 °C for 3 days. Following removal of volatiles under vacuum, EtOH (250 mL) and paraformaldehyde (7.51 g, 250 mmol) were added, and the resulting suspension was stirred at room temperature for 16 h. The mixture was frozen in a liquid nitrogen bath and HCl (4.0 M in 1,4-dioxane, 50 mL, 200 mmol) was added. After thawing, the reaction mixture was stirred at room temperature for 4 h. The pale yellow suspension was filtered through a bed of Celite in a glass frit (P4) column, and volatiles were removed under vacuum. The remaining oily solid residue was triturated with Et_2O (200 mL) overnight, filtered and washed with further Et_2O (2 x 25 mL). The resulting white solid was then again extracted into EtOH (2 x 100 mL). Following filtration and removal of volatiles under vacuum, the desired product was obtained as a white solid (3.05 g, 80%). NMR data are identical to those reported in Section 2.4.2.18.

To the combined Et_2O washes from the above reaction was added a saturated aqueous solution of Na_2CO_3 (150 mL). The resulting biphasic mixture was stirred under open bench conditions for 24 h, and the organic phase was separated and washed with H_2O (4 x 100 mL). The organic phase

was transferred into a 500 mL Schlenk flask and volatiles were removed under vacuum. The remaining procedure was performed under an inert atmosphere. A solution of P_4 (620 mg, 5 mmol) pre-dissolved in PhMe (250 mL) was added, followed by PMHS (2.3 mL, 40 mmol) and ACN (244 mg, 1 mmol). The Schlenk tube was immediately and thoroughly wrapped in Al foil to exclude any ambient light, and the stirred reaction mixture was then heated to 80 °C for 3 days. Following removal of volatiles under vacuum, EtOH (250 mL) and paraformaldehyde (7.51 g, 250 mmol) were added, and the resulting suspension was stirred at room temperature for 16 h. The mixture was frozen in a liquid nitrogen bath and HCl (4.0 M in 1,4-dioxane, 50 mL, 200 mmol) was added. After thawing, the reaction mixture was stirred at room temperature for 4 h. The yellowish suspension was filtered through a bed of Celite in a glass frit (P4) column, and volatiles were removed under vacuum. The remaining oily solid residue was triturated with Et_2O (200 mL) overnight, filtered and washed with further Et2O (2 x 25 mL). The resulting white solid was then again extracted into EtOH (2 x 100 mL). Following filtration and removal of volatiles under vacuum, the desired product was obtained as a white solid (2.52 g, 66%). NMR data are identical to those reported in Section 2.4.2.18.

2.4.4 Catalytic functionalisation of P_4

2.4.4.1 Catalytic hydrostannylation of P_4 using Bu_3SnOMe and PMHS under near UV irradiation

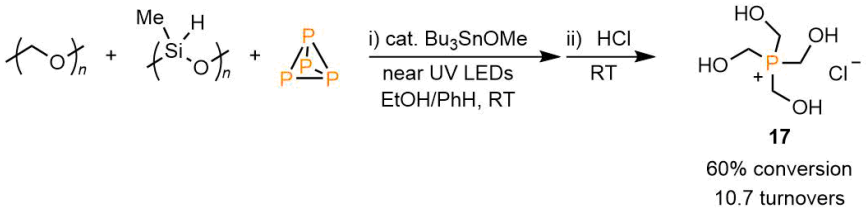

To a 10 mL, flat-bottomed, stoppered Schlenk tube were added EtOH (500 µL), P_4 (0.03 mmol, as a stock solution in 232 µL PhH), Bu_3SnOMe (2.9 µL, 0.01 mmol), PMHS (28.7 µL, 0.48 mmol) and paraformaldehyde (30 mg, 1.0 mmol). The tube was sealed, placed in a water-cooled block to maintain near-ambient temperature, and irradiated with near UV (365 nm) LEDs for 65 h. The mixture was then frozen in a liquid nitrogen bath and HCl (4.0 M in 1,4-dioxane, 0.1 mL, 0.4 mmol) was added. After thawing, the reaction mixture was stirred at room temperature for 1 h. Following addition of Ph_3PO (0.04 mmol, as a stock solution in 506 µL MeCN) as an internal standard, the resulting mixture was analysed by $^{31}P\{^1H\}$ NMR spectroscopy, as shown in Figure S140. The chemical shift observed for THPC (**17**) in these spectra is *ca.* 1 ppm downfield of that observed in spectra of isolated samples, which is attributed to solvent effects and the presence of excess HCl. That these peaks correspond to THPC was unambiguously confirmed by subsequent addition of an authentic sample to one representative reaction, which clearly increased the intensity of this peak.

Accurate conversion to THPC was measured by integration of a single-scan, inverse-gated $^{31}P\{^{1}H\}$ NMR spectrum (Figure S141), in line with our previously-described methodology.[21] For two independent runs, conversions of 57% and 62% were determined.

Turnover numbers (TONS; 10.2 and 11.2, respectively, for an average of 10.7) were calculated from these conversions by factoring in the 1:6 stoichiometry of the reaction between P_4 and Bu_3SnH. Because of this stoichiometry, full consumption of 1 eq. of P_4 relative to Bu_3SnOMe requires six turnovers of the catalyst (i.e. it must be used to regenerate Bu_3SnH six times). Equivalently, formation of 1 eq. of THPC (from 0.25 eq. P_4) requires 1.5 turnovers of the catalyst. The TON is therefore calculated as 1.5 times the molar ratio between the THPC formed and the Bu_3SnOMe catalyst employed. Relevant NMR data are provided below.

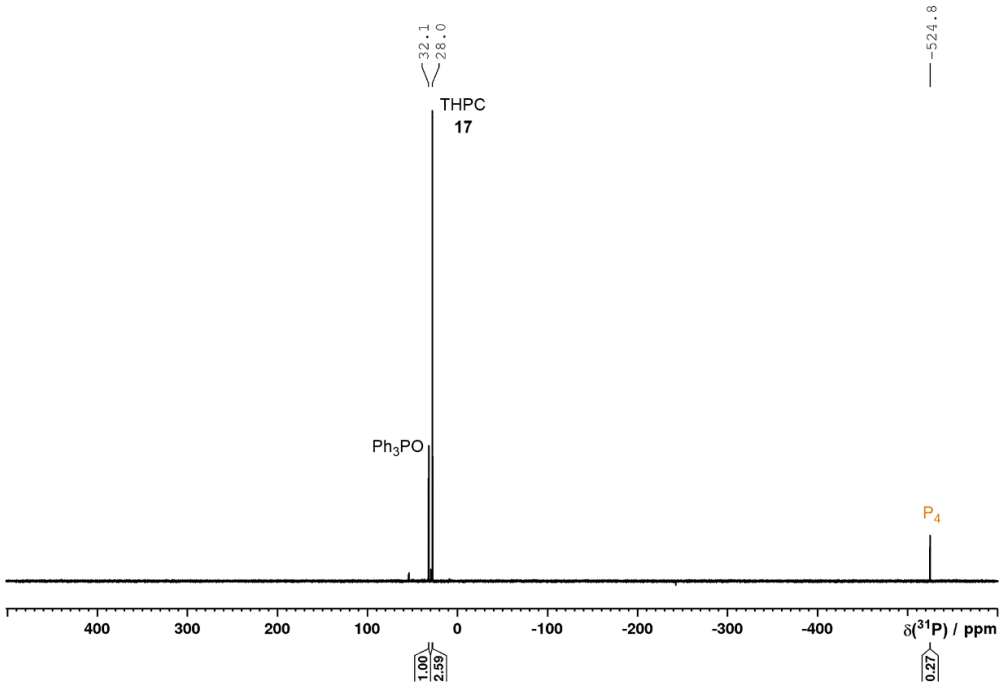

Figure S140. $^{31}P\{^{1}H\}$ NMR spectrum for the catalytic transformation of P_4 into THPC (**17**) *via* THP (**16**), driven by 455 nm LED irradiation.

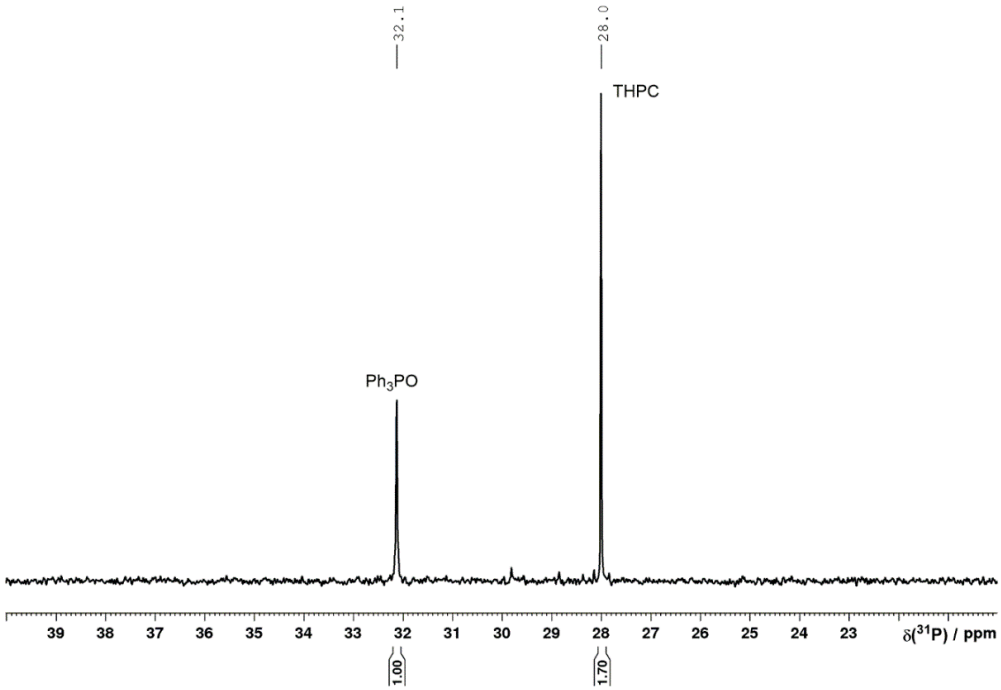

Figure S141. Quantitative single-scan, inverse-gated $^{31}P\{^{1}H\}$ NMR spectrum for the catalytic transformation of P_4 into THPC (**17**) *via* THP (**16**), driven by 455 nm LED irradiation.

A proposed mechanism for the catalytic reaction is outlined in Scheme S4. Complete hydrostannylation of P_4 is suggested to occur prior to H_2CO insertion and subsequent ethanolysis. This is supported by the lack of observable, partially-hydrostannylated intermediates in previous experiments (see Section 2.4.1.2, for example). Nevertheless, analogous insertion of H_2CO into these transient intermediates is also possible, and this option cannot be definitively excluded.

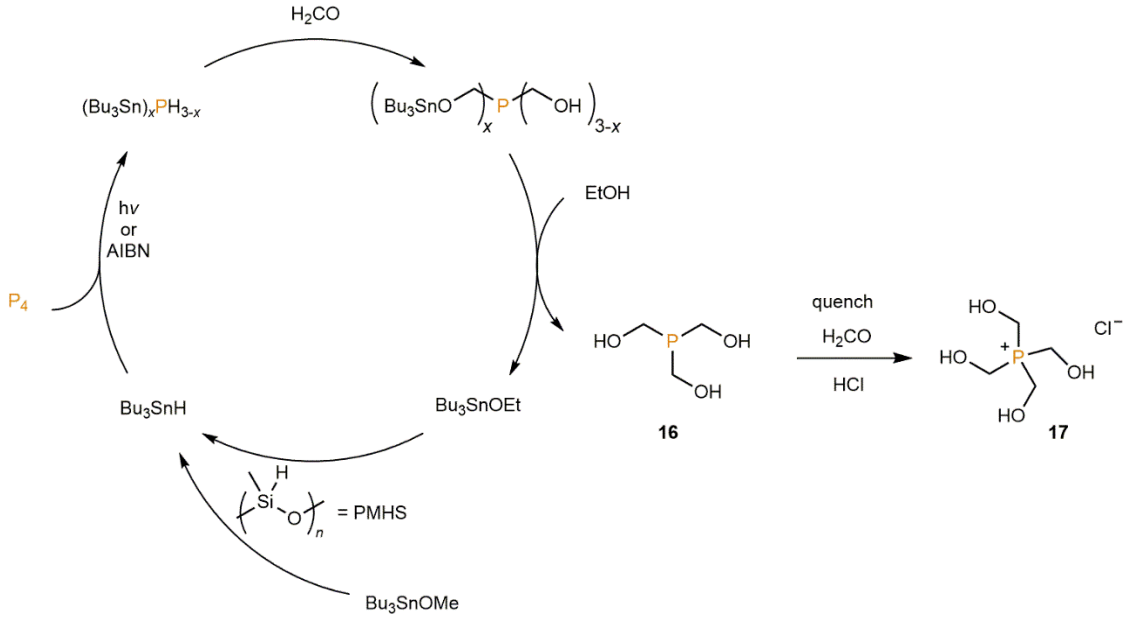

Scheme S4. A proposed, outline mechanism for the catalytic transformation of P_4 into THPC (**17**) *via* THP (**16**). Hydrostannylation of P_4 by Bu_3SnH is followed by insertion of formaldehyde into P–Sn and P–H bonds. Solvolysis of the resulting Sn–O bonds releases THP, which is transformed into THPC upon eventual quenching with HCl. This step also releases Bu_3SnOEt which can react with PMHS to regenerate Bu_3SnH and thereby close the catalytic cycle.

2.4.4.2 Catalytic hydrostannylation of P_4 using Bu_3SnOMe and PMHS initiated by AIBN

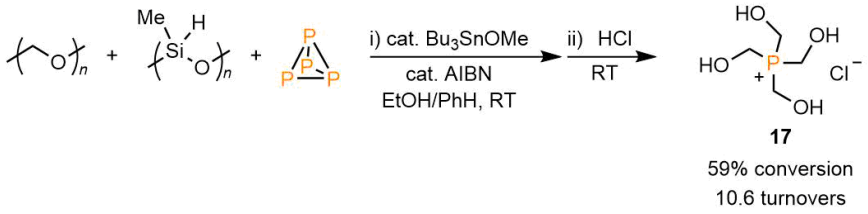

To a 10 mL, flat-bottomed, stoppered Schlenk tube were added EtOH (500 µL), P_4 (0.03 mmol, as a stock solution in 190 µL PhH), Bu_3SnOMe (2.9 µL, 0.01 mmol), PMHS (57.4 µL, 0.96 mmol), AIBN (0.01 mmol, as a stock solution in 37.0 µL PhH) and paraformaldehyde (30 mg, 1.0 mmol). The tube was sealed, wrapped in Al foil to exclude light, and heated to 60 °C for 65 h. The mixture was then frozen in a liquid nitrogen bath and HCl (4.0 M in 1,4-dioxane, 0.1 mL, 0.4 mmol) was added. After thawing, the reaction mixture was stirred at room temperature for 2 h. Following addition of Ph_3PO (0.04 mmol, as a stock solution in 497 µL MeCN) as an internal standard, the resulting mixture was analysed by $^{31}P\{^1H\}$ NMR spectroscopy, as shown in Figure S142, below. The chemical shift observed for THPC (**17**) in these spectra is *ca.* 1 ppm downfield of that observed in spectra of isolated samples, which is attributed to solvent effects and the presence of excess HCl. That these peaks correspond to THPC was unambiguously confirmed by subsequent addition of an authentic sample to one representative reaction, which clearly increased the intensity of this peak.

Accurate conversion to THPC was measured by integration of a single-scan, inverse-gated $^{31}P\{^1H\}$ NMR spectrum (Figure S143), in line with our previously-described methodology.[21] For two independent runs, conversions of 58% and 60% were determined.

Turnover numbers (TONS; 10.4 and 10.9, respectively, for an average of 10.6) were calculated from these conversions by factoring in the 1:6 stoichiometry of the reaction between P_4 and Bu_3SnH. Because of this stoichiometry, full consumption of 1 eq. of P_4 relative to Bu_3SnOMe requires six turnovers of the catalyst (i.e. it must be used to regenerate Bu_3SnH six times). Equivalently, formation of 1 eq. of THPC (from 0.25 eq. P_4) requires 1.5 turnovers of the catalyst. The TON is therefore calculated as 1.5 times the molar ratio between the THPC formed and the Bu_3SnOMe catalyst employed.

A proposed mechanism for the catalytic reaction is outlined in Scheme S4 (see above).

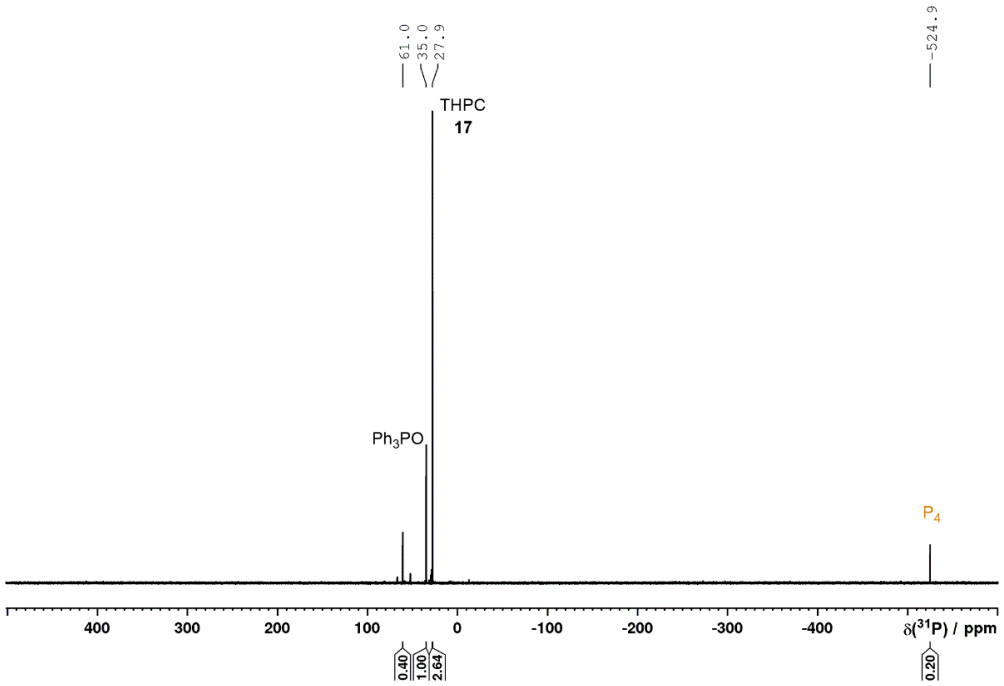

Figure S142. $^{31}P\{^{1}H\}$ NMR spectrum for the catalytic transformation of P_4 into THPC (**17**) *via* THP (**16**), driven by AIBN initiation.

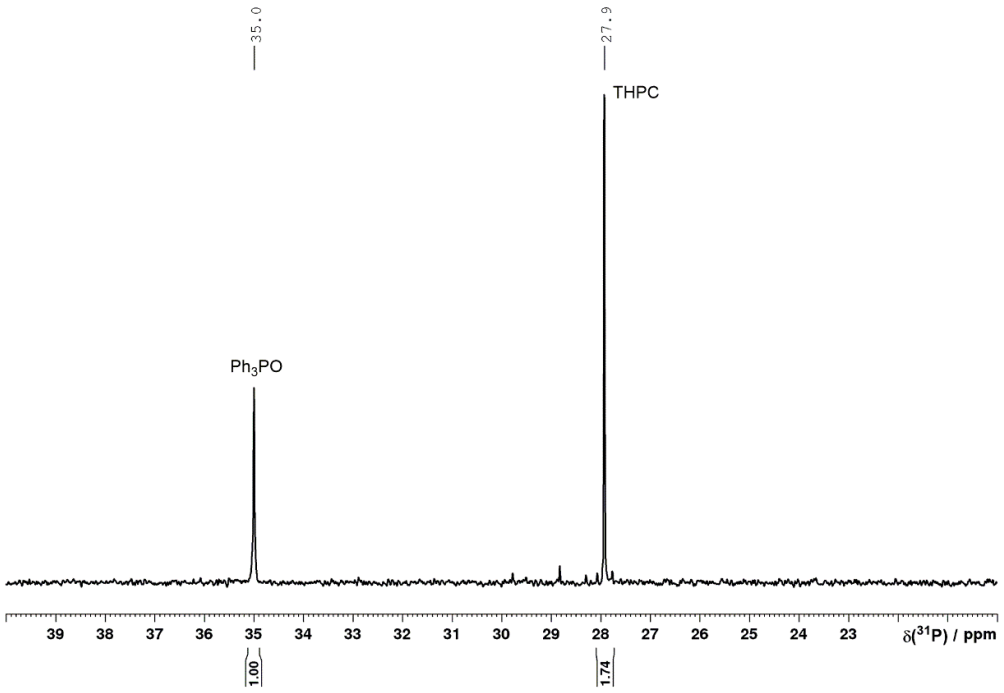

Figure S143. Quantitative single-scan, inverse-gated $^{31}P\{^{1}H\}$ NMR spectrum for the catalytic transformation of P_4 into THPC (**17**) *via* THP (**16**), driven by AIBN initiation.

2.5 References

[1] W. Gleason, *JOM* **2007**, *59*, 17–19.
[2] M. B. Geeson, C. C. Cummins, *ACS Cent. Sci.* **2020**, *6*, 848–860.
[3] M. B. Geeson, C. C. Cummins, *Science* **2018**, *359*, 1383–1385.
[4] M. B. Geeson, P. Ríos, W. J. Transue, C. C. Cummins, *J. Am. Chem. Soc.* **2019**, *141*, 6375–6384.
[5] R. W. Scholz, A. H. Roy, F. S. Brand, D. Hellums, A. E. Ulrich, *Sustainable Phosphorus Management*, Springer, **2014**.
[6] H. Ohtake, S. Tsuneda, *Phosphorus Recovery and Recycling*, Springer, **2019**.
[7] D. E. C. Corbridge, *Phosphorus. Chemistry, Biochemistry and Technology*, Elsevier, **2000**.
[8] H. Diskowski, T. Hofmann, *Ullmann's Encycl. Ind. Chem.* **2012**, *26*, 725–746.
[9] J. Svara, N. Weferling, T. Hofmann, *Ullmann's Encycl. Ind. Chem.* **2012**, *27*, 20–50.
[10] G. Bettermann, W. Krause, G. Riess, T. Hofmann, *Ullmann's Encycl. Ind. Chem.* **2012**, *27*, 1–18.
[11] B. M. Cossairt, N. A. Piro, C. C. Cummins, *Chem. Rev.* **2010**, *110*, 4164–4177.
[12] M. Caporali, L. Gonsalvi, A. Rossin, M. Peruzzini, *Chem. Rev.* **2010**, *110*, 4178–4235.
[13] M. Scheer, G. Balázs, A. Seitz, *Chem. Rev.* **2010**, *110*, 4236–4256.
[14] L. Xu, Y. Chi, S. Du, W. Zhang, Z. Xi, *Angew. Chem. Int. Ed.* **2016**, *128*, 9333–9336.
[15] G. Becker, H. Schmidt, G. Uhl, W. Uhl, *Inorg. Synth.* **1990**, 243–249.
[16] K. X. Bhattacharyya, S. Dreyfuss, N. Saffon-Merceron, N. Mézailles, *Chem. Commun.* **2016**, *52*, 5179–5182.
[17] D. H. R. Barton, J. Zhu, *J. Am. Chem. Soc.* **1993**, *115*, 2071–2072.
[18] D. H. R. Barton, R. A. V. Embse, *Tetrahedron* **1998**, *54*, 12475–12496.
[19] B. M. Cossairt, C. C. Cummins, *New J. Chem.* **2010**, *34*, 1533–1536.
[20] S. K. Ghosh, C. C. Cummins, J. A. Gladysz, *Org. Chem. Front.* **2018**, *5*, 3421–3429.
[21] U. Lennert, P. B. Arockiam, V. Streitferdt, D. J. Scott, C. Rödl, R. M. Gschwind, R. Wolf, *Nat. Catal.* **2019**, *2*, 1101–1106.
[22] P. B. Arockiam, U. Lennert, C. Graf, R. Rothfelder, D. J. Scott, T. G. Fischer, K. Zeitler, R. Wolf, *Chem. - A Eur. J.* **2020**, *26*, 16374–16382.
[23] G. Lu, J. Chen, X. Huangfu, X. Li, M. Fang, G. Tang, Y. Zhao, *Org. Chem. Front.* **2019**, *6*, 190–194.
[24] L. Riesel, M. Kant, R. Helbing, *ZAAC - J. Inorg. Gen. Chem.* **1990**, *580*, 217–223.
[25] B. Mathiasch, M. Dräger, *Angew. Chem. Int. Ed.* **1978**, *17*, 767–768.
[26] B. Mathiasch, *J. Organomet. Chem.* **1979**, *165*, 295–301.
[27] M. Dräger, B. Mathiasch, *Angew. Chem. Int. Ed.* **1981**, *20*, 1029–1030.
[28] A. Brenner, G. E. Riddell, *J. Res. Natl Bur.* **1946**, *37*, 31–34.
[29] H. Schmidbaur, U. Deschler, B. Milewski-mahrla, B. Zimmer-gasser, *Chem. Ber.* **1981**, *114*, 608–619.
[30] W. J. Vullo, *Ind. Eng. Chem. Prod. Res. Dev.* **1966**, *5*, 346–349.
[31] H. G. Kuivila, *Synthesis* **1970**, *10*, 499–509.
[32] W. P. Neumann, *Synthesis* **1987**, *8*, 665–683.
[33] M. Pereyre, J. P. Quintard, A. Rahm, *Tin in Organic Synthesis*, Butterworths, **1987**.
[34] T. V RajanBabu, P. C. Bulman Page, B. R. Buckley, *Encycl. Reagents Org. Synth.* **2004**.
[35] C. C. Cummins, C. Huang, T. J. Miller, M. W. Reintinger, J. M. Stauber, I. Tannou, D. Tofan, A. Toubaei, A. Velian, G. Wu, *Inorg. Chem.* **2014**, *53*, 3678–3687.
[36] A. D. Norman, *J. Organomet. Chem.* **1971**, *28*, 81–86.
[37] H. Schumann, *Angew. Chem. Int. Ed.* **1969**, *8*, 937–950.
[38] M. Peruzzini, I. De Los Rios, A. Romerosa, F. Vizza, *Eur. J. Inorg. Chem.* **2001**, 593–608.
[39] Z. N. Gafurov, A. A. Kagilev, A. O. Kantyukov, O. G. Sinyashin, D. G. Yakhvarov, *Pure Appl. Chem.* **2019**, *91*, 797–810.
[40] M. Chanon, M. L. Tobe, *Angew. Chem. Int. Ed.* **1982**, *21*, 1–23.
[41] K. Chanon, *Bull. Soc. Chim. Fr.* **1982**, 197-238.
[42] M. Julliard, M. Chanon, *Chem. Rev.* **1983**, *83*, 425–506.
[43] N. S. Simpkins, *Encycl. Reagents Org. Synth.* **2001**.
[44] S. A. Kates, F. Albericio, *Encycl. Reagents Org. Synth.* **2001**.

[45] F. Montanari, S. Quici, H. Henry-Riyad, T. Tidwell, A. Struder, T. Vogler, Y. Rao, C. Thang, Y. Zong, *Encycl. Reagents Org. Synth.* **2016**.
[46] A. Sato, H. Yorimitsu, K. Oshima, *J. Am. Chem. Soc.* **2006**, *128*, 4240–4241.
[47] A. Huber, A. Kuschel, T. Ott, G. Santiso-Quinones, D. Stein, J. Bräuer, R. Kissner, F. Krumeich, H. Schönberg, J. Levalois-Grützmacher, H. Grützmacher, *Angew. Chem. Int. Ed.* **2012**, *51*, 4648–4652.
[48] V. G. Becker, M. Rössler, W. Uhl, *Zeitschrift für Anorg. und Allg. Chemie* **1981**, *473*, 7–19.
[49] V. G. Becker, M. Rössler, G. Uhl, *Zeitschrift für Anorg. und Allg. Chemie* **1982**, *495*, 73–88.
[50] V. G. Becker, *Zeitschrift für Anorg. und Allg. Chemie* **1977**, *430*, 66–76.
[51] J. Verlhac, J. Quintard, L. De Chimie, D. Etain, U. A. Cnrs, *Tetrahedron Lett.* **1986**, *27*, 2361–2364.
[52] S. E. Vaillard, C. Mück-Lichtenfeld, S. Grimme, A. Studer, *Angew. Chem. Int. Ed.* **2007**, *46*, 6533–6536.
[53] J. E. Borger, A. W. Ehlers, J. C. Slootweg, K. Lammertsma, *Chem. Eur. J.* **2017**, *23*, 11738–11746.
[54] K. V. Katti, H. Gali, C. J. Smith, D. E. Berning, *Acc. Chem. Res.* **1999**, *32*, 9–17.
[55] M. Chen, C. Chen, Y. Tan, J. Huang, X. Wang, L. Chen, Y. Wang, *Ind. Eng. Chem. Res.* **2014**, *53*, 1160–1171.
[56] D. N. Akbayeva, F. K. Faisova, R. R. Abdreimova, M. Peruzzini, *J. Mol. Catal. A Chem.* **2007**, *267*, 181–193.
[57] E. Le Grognec, J. M. Chrétien, F. Zammattio, J. P. Quintard, *Chem. Rev.* **2015**, *115*, 10207–10260.
[58] J. M. Tsangaris, R. Willem, M. Gielen, in *Patai's Chem. Funct. Groups*, Wiley, **2009**.
[59] N. J. Lawrence, M. D. Drew, S. M. Bushell, *J. Chem. Soc. Perkin Trans.* **1999**, *1*, 3381–3391.
[60] K. Hayashi, J. Iyoda, I. Shiihara, *J. Organomet. Chem.* **1967**, *10*, 81–94.
[61] J. Lipowitz, S. A. Bowman, *J. Org. Chem.* **1973**, *38*, 162–165.
[62] J. H. Barnard, P. A. Brown, K. L. Shuford, C. D. Martin, *Angew. Chem. Int. Ed.* **2015**, *54*, 12083–12086.
[63] M. Nakajima, S. Nagasawa, K. Matsumoto, T. Kuribara, A. Muranaka, M. Uchiyama, T. Nemoto, *Angew. Chem. Int. Ed.* **2020**, *59*, 6847–6852.
[64] S. M. Thompson, U. Schubert, *Inorganica Chim. Acta* **2003**, *350*, 329–338.
[65] N. A. Bumagin, Y. V Gulevich, I. P. Beletskaya, *Izv. Akad. Nauk SSSR, Ser. Khim.* **1984**, *33*, 1044–1049.
[66] T. N. Mitchell, A. Amamria, H. Killing, D. Rutschow, *J. Organomet. Chem.* **1986**, *304*, 257–265.
[67] W. P. Neumann, B. Schneider, R. Sommer, *Justus Liebigs Ann. Chem.* **1966**, *692*, 1–11.
[68] Y. Kai, S. Oku, T. Tani, K. Sakurai, T. Tsuchimoto, *Adv. Synth. Catal.* **2019**, *361*, 4314–4323.
[69] C. M. Evans, M. E. Evans, T. D. Krauss, *J. Am. Chem. Soc.* **2010**, *132*, 10973–10975.
[70] Y. Li, S. Chakrabarty, C. Mück-Lichtenfeld, A. Studer, *Angew. Chem. Int. Ed.* **2016**, *55*, 802–806.
[71] P. G. Harrison, S. E. Ulrich, J. J. Zuckerman, *Inorg. Chem.* **1972**, *11*, 25–28.
[72] S. A. Laneman, F. R. Fronczek, G. G. Stanley, *Phosphorus Sulfur Silicon Relat. Elem.* **1989**, *42*, 97–102.
[73] E. A. V. Ebsworth, D. J. Hutchison, E. K. Macdonald, D. W. H. Rankin, *Inorg. Nucl. Chem. Lett.* **1981**, *17*, 19–21.
[74] G. D. Macdonell, A. Radhakrishna, K. D. Berlin, J. Barycki, R. Tyka, P. Mastalerz, *Tetrahedron Lett.* **1978**, *19*, 857.
[75] D. M. Kaphan, M. D. Levin, R. G. Bergman, K. N. Raymond, F. D. Toste, *Science* **2015**, *350*, 1235–1238.
[76] M. Caporali, L. Gonsalvi, F. Zanobini, M. Peruzzini, *Inorg. Synth.* **2010**, *35*, 96–102.
[77] W. J. Vullo, *J. Org. Chem.* **1968**, *33*, 3665–3667.
[78] A. G. Davies, A. Sella, R. Sivasubramaniam, *J. Organometalic Chem.* **2006**, *691*, 3556–3561.
[79] Z. Tan, C. Wu, M. Zhang, W. Lv, J. Qiu, C. Liu, *RSC Adv.* **2014**, *4*, 41705–41713.
[80] N. S. Golubev, R. E. Asfin, S. N. Smirnov, P. M. Tolstoi, *Russ. J. Gen. Chem.* **2006**, *76*, 915–924.

3 Hydrostannylation of Red Phosphorus: A Convenient Route to Monophosphines[a,b]

Abstract:

The preparation of valuable and industrially relevant organophosphorus compounds currently depends on indirect multi-step procedures involving difficult-to-handle white phosphorus as a common P atom source. Herein, we report a practical and versatile method for the synthesis of a variety of monophosphorus compounds directly from the bench-stable allotrope red phosphorus (P_{red}). The relatively inert P_{red} was productively functionalized by using the cheap and readily available radical reagent tri-*n*-butyltin hydride, and subsequent treatment with electrophiles yields useful P_1 compounds. Remarkably, these transformations require only modest inert atmosphere techniques and use only reagents that are inexpensive and commercially available, making this a convenient and practical methodology accessible in most laboratory settings.

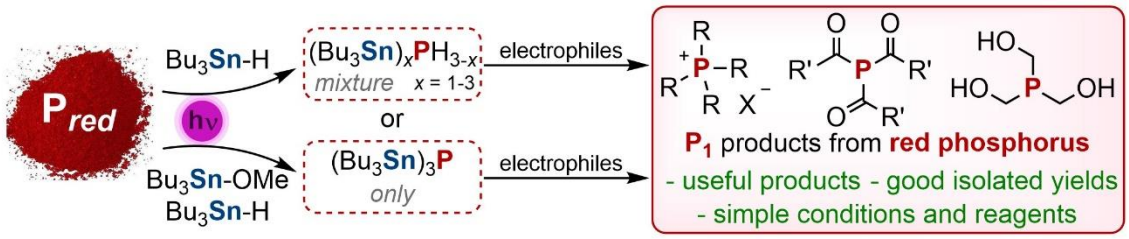

[a] Reproduced with permission from: J. Cammarata, D. J. Scott, and R. Wolf, *Chem. Eur. J.* **2022**, *28*, e202202456.

[b] Jose Cammarata performed all the experimental work, including the synthesis, isolation and characterisation of all products. Jose Cammarata and Daniel J. Scott wrote the manuscript, which was reviewed and edited by Robert Wolf. Daniel J. Scott and Robert Wolf supervised and directed the project.

3.1 Introduction

Organophosphorus products are ubiquitous throughout both industry and academia, with a wide range of applications in areas such as medicinal chemistry, materials science, catalysis and coordination chemistry, among many others. In essentially all cases these compounds are ultimately prepared using elemental phosphorus – particularly white phosphorus (P_4) – as their common P atom source.[1] However, the transformation of elemental phosphorus into these useful organophosphorus compounds currently relies on undesirable, multistep processes involving extremely hazardous, toxic and/or corrosive reactants and intermediates such as chlorine gas (Cl_2), phosphorus chlorides (PCl_3/PCl_5/$POCl_3$) and phosphine gas (PH_3).[1,2] Consequently, much effort has been invested over several decades into the development of alternative, *direct* transformations of elemental phosphorus into useful organophosphorus compounds, which would bypass these hazards while also improving step economy.[3] However, while the past few years have begun to see some progress in this area,[4] direct organofunctionalisation of elemental phosphorus remains in its infancy.[5]

The vast majority of studies in this area have focused on the chemistry of white phosphorus (P_4) due to its molecular nature and industrial relevance.[6] However, while P_4 may be the principal allotrope used for large-scale industrial applications, in most other contexts it is a highly undesirable starting material due to its notoriously pyrophoric character and significant toxicity. As a result, its safe handling and productive use typically require specific expertise and equipment (e.g. gloveboxes). These hazards also make P_4 very difficult to acquire commercially,[7] and collectively these factors render P_4 an impractical, unattractive or simply impossible precursor for many synthetic laboratories.

An alternative and much more attractive P atom source for academic and other laboratory-scale chemistry would be the allotrope *red* phosphorus (P_{red}). P_{red} is produced by thermolysis of P_4 at 200-300 °C,[1] and therefore less attractive from a strictly industrial standpoint. More relevant to most laboratory chemists, however, is that unlike P_4 (and, notably, other P atom sources relied on by synthetic laboratories such as PCl_3), P_{red} is both readily and inexpensively available, and bench-stable.[8] Unfortunately, this bench stability reflects much the lower reactivity of P_{red} in general when compared to P_4.

P_{red} therefore usually requires much harsher conditions and/or reagents for its activation, which can counteract is attractiveness for laboratory use, and which has contributed to the activation of P_{red} being far less studied than that of P_4.[1,8]

Those few systems that have been reported for the direct transformation of P_{red} typically depend on the use of harsh conditions and extremely strong reagents such as alkali metals. For example, significant contributions in this field have been provided by Trofimov and Gusarova, based on the activation of P_{red} by "superbasic" media (aqueous KOH/DMSO) and the direct phosphorylation of electrophilic alkenes, alkynes and (het)aryl halides to afford

organophosphorus compounds such as phosphines, phosphine oxides and phosphinic acids (Scheme 1b, top).[3b,9] A different approach, initially reported by Brandsma *et al.*[10] and later modified by the group of Grützmacher,[11] consists of the reduction of P_{red} with sodium metal and subsequent addition of *t*BuOH, to afford $NaPH_2$ as a sodium *tert*-butanolate aggregate which can also serve as a nucleophilic phosphorus synthon (Scheme 1b, bottom).[12]

Recently, we reported a breakthrough in the transformation of *white* phosphorus, by showing that P_4 can be transformed directly into useful P_1 products using only simple, readily available and easy-to-handle reagents.[13] Specifically, the stoichiometric hydrostannylation of P_4 was achieved using the cheap, classical radical reagent tri-*n*-butyltin hydride (Bu_3SnH) in the presence of a suitable radical initiator – either a chemical radical initiator such as azobis(isobutyronitrile) (AIBN) or irradiation with visible light – yielding the stannyl-substituted monophosphines $(Bu_3Sn)_xPH_{3-x}$ (x = 0–3) as a clean mixture. Significantly, each of these products can function as a chemically similar "P^{3-}" synthon, allowing the crude $(Bu_3Sn)_xPH_{3-x}$ mixture to be directly functionalized 'as is' with a variety of electrophiles to afford industrially relevant P_1 compounds in a 'one-pot' fashion (Scheme 1c).[13]

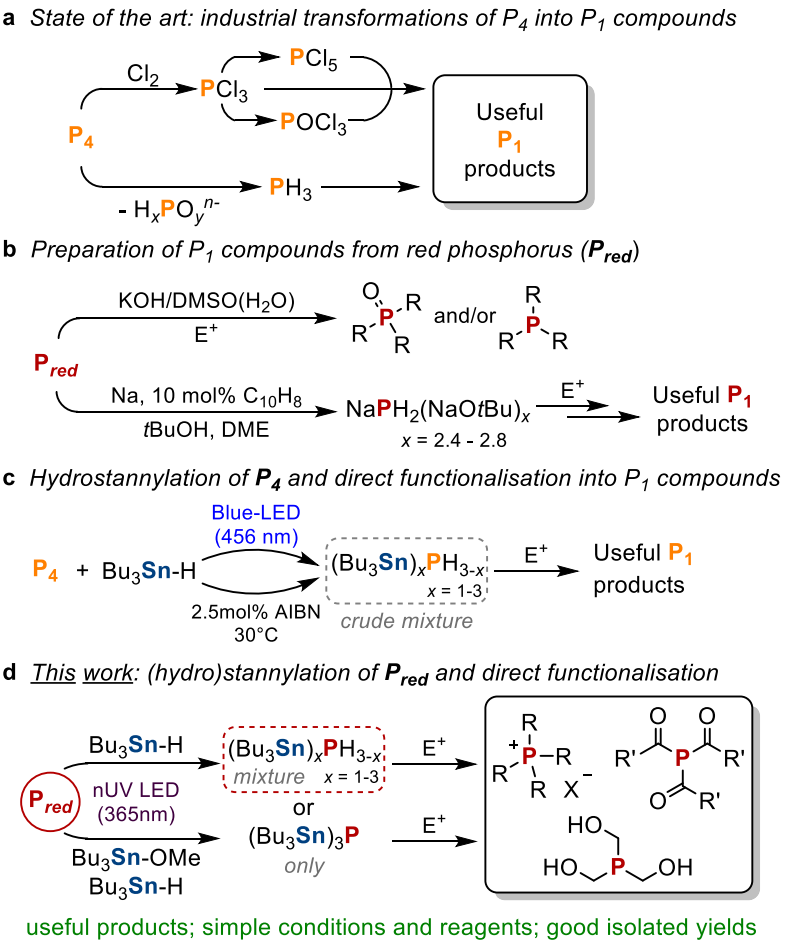

Scheme 1. a) Industrial routes for the transformation of P_4 into P_1 compounds. b) Previously reported methods for the transformation of P_{red} into P_1 compounds. c) Hydrostannylation of P_4 and direct preparation of P_1 compounds by reaction with electrophiles. d) (Hydro)Stannylation of P_{red} and direct transformation into useful P_1 products using electrophiles, as described herein. E^+ represents a generic electrophile.

Inspired by these results, we speculated that the same hydrostannylation strategy might also be applicable to the transformation of P_{red}, and allow the development of a procedure for its direct transformation into P_1 products that would avoid the very harsh, challenging reagents normally associated with the activation of P_{red}. This would also overcome the existing hydrostannylation procedure's current major drawback as a laboratory scale synthetic tool, which is that it requires pyrophoric P_4 as a substrate. Herein we describe the results of these studies, which have allowed for the simple and efficient preparation of a variety of valuable, industrially- and academically-relevant monophosphorus compounds directly from P_{red} using only commonly and cheaply available reagents (Scheme 1d). Importantly, this procedure requires only modest inert atmosphere techniques and can be performed without use of a glovebox, making it an unusually convenient and practical approach for the preparation of P_1 compounds from elemental phosphorus in a typical laboratory setting.

3.2 Results and Discussion

To begin, P_{red} functionalisation was tested using Bu_3SnH under similar conditions to those used previously for the hydrostannylation of P_4, as it was anticipated that an equivalent radical chain process should serve to cleave the P–P bonds of P_{red} and thus break its polymeric structure down to the same mixture of P_1 species.[13] Thus, P_{red} and Bu_3SnH were combined in PhMe in a 1:1.5 molar ratio to reflect the expected reaction stoichiometry, and irradiated with blue LED light (455 nm; chosen for consistency with our previous report) for three days.[14] Very gratifyingly, the formation of the anticipated hydrostannylated monophosphines $(Bu_3Sn)_xPH_{3-x}$ (x = 0–3) was observed by $^{31}P\{^1H\}$ NMR spectroscopy, clearly showing the viability of the desired transformation. Under these reaction conditions the conversion to $(Bu_3Sn)_xPH_{3-x}$ was relatively limited (<20%) and the corresponding ^1H NMR spectrum revealed that only a fraction of the Bu_3SnH was consumed, which is consistent with the more insoluble and inert nature of P_{red} in comparison to P_4. Nevertheless, using this reaction as a starting point, further investigations revealed that the use of near UV LED irradiation (365 nm), more concentrated reaction mixtures, slightly longer reaction times, and an excess of very cheap P_{red} each led to improved reaction outcomes (see Tables S1 and S2). Remarkably, following optimisation of the reaction conditions (365 nm LEDs, 1 equiv. Bu_3SnH, 6.7 equiv. P_{red}, 1.2 M PhMe, 4 d; Scheme 2a) the desired mixture of PH_3 (**1**), Bu_3SnPH_2 (**2**), $(Bu_3Sn)_2PH$ (**3**) and $(Bu_3Sn)_3P$ (**4**) could be obtained cleanly and near-quantitatively (for full details, see Section 3.4.1.1). Formally, the optimized reaction proceeds with relatively poor P atom economy, due to the use of an excess of P_{red}. While in an industrial context this could be problematic, in a laboratory setting it is mitigated by the extremely low cost of P_{red}, even in comparison with Bu_3SnH, which makes the latter the more sensible limiting reagent.

It is proposed that P_{red} hydrostannylation proceeds through a simple radical chain mechanism largely equivalent to that proposed for P_4 (Scheme 2b).[15] Interestingly, when the optimised

procedure was performed using less "driving", lower energy 455 nm LEDs, ^{31}P NMR analysis of the partially-converted reaction mixture showed a set of minor multiplets consistent with formation of $P_7(SnBu_3)_3$ (see Figure S5).[16] No analogous observation was ever made during our previous study of P_4 hydrostannylation.[13]

While far from conclusive, this suggests that P_{red} hydrostannylation may proceed through initial, rate-limiting excision of soluble, partially-reduced oligomeric P_n moieties from the solid surface, followed by rapid further reduction in solution (Scheme 2b). During reaction optimisation, $P_7(SnBu_3)_3$ was not observed for any reactions using the optimised wavelength of 365 nm, even when only partial conversions were achieved, which could indicate its faster hydrostannylation under these conditions (see Section 3.4.1.1).

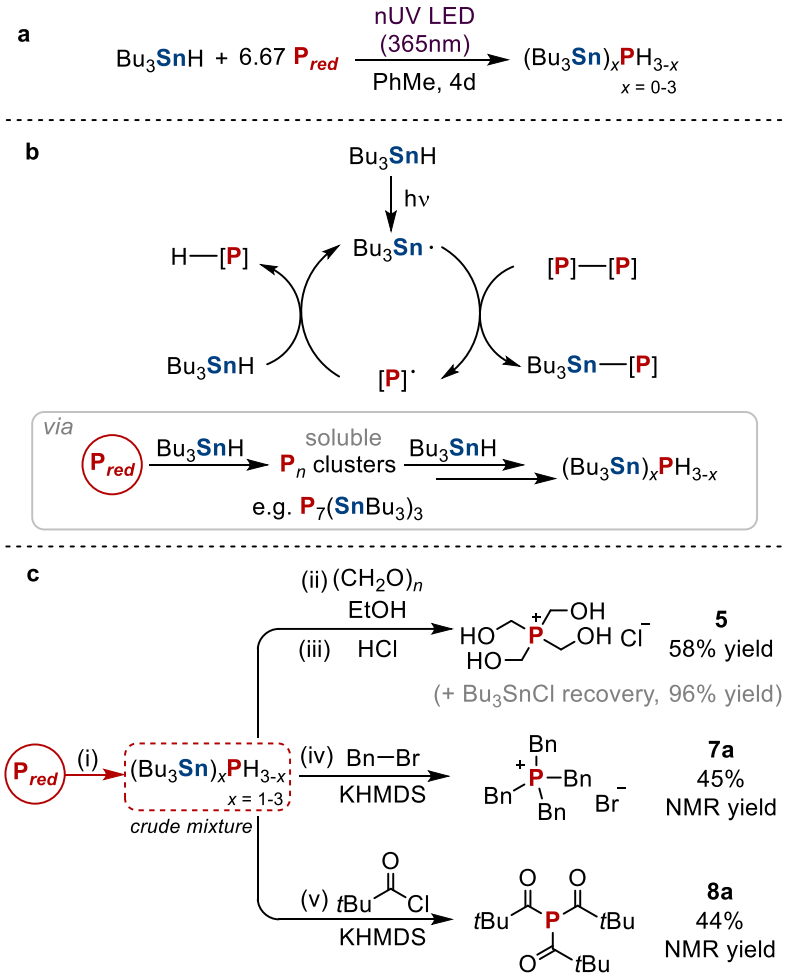

Scheme 2. a) Hydrostannylation of P_{red} with Bu_3SnH promoted by near-UV irradiation. b) Proposed radical chain mechanism for P_{red} hydrostannylation, proceeding by excision of P_n clusters such as $P_7(SnBu_3)_3$. c) Synthesis of P_1 products directly from P_{red} by hydrostannylation to $(Bu_3Sn)_xPH_{3-x}$ (x = 1–3). (i) Bu_3SnH (1 equiv.), P_{red} (6.67 equiv.), PhMe, 365 nm LEDs, room temperature (RT), 4 days; (ii) EtOH, 8.33 equiv. paraformaldehyde, RT, 16 h; (iii) 6.67 equiv. HCl (4.0 M in 1,4-dioxane), RT, 2 h; (iv) 6.67 equiv. BnBr, 1 equiv. KHMDS, 70°C, 3 days; (v) 2.67 equiv. *t*BuC(O)Cl, 0.67 equiv. KHMDS, RT, 1 day. Yields are defined relative to the limiting reagent (Bu_3SnH).

It is known from our previous work that the hydrostannylation products $(Bu_3Sn)_xPH_{3-x}$ (x = 1–3) possess reactive P–Sn and P–H bonds and can serve as a combined "P^{3-}" synthon to react with

suitable electrophiles and directly afford desirable organophosphorus compounds in a 'one-pot' fashion.[13] Thus, after performing the optimised hydrostannylation of P_{red}, addition of paraformaldehyde as a representative C-centred electrophile in ethanol followed by quenching with HCl allowed the product tetrakis(hydroxymethyl)phosphonium chloride (THPC) to be formed exclusively and with good conversion (70%, Section 3.4.1.2). Upon increasing the reaction to a preparative scale (0.6 mmol), THPC could be isolated in good yield (58%, see Scheme 2c and Sections 3.4.1.3 and 3.4.1.4) without having required isolation or purification of any intermediates. Notably, the by-product of this reaction, Bu_3SnCl (**6**), could also be recovered in excellent yield (96%) after a simple extraction procedure. This is significant because organotin derivatives can display appreciable toxicity and must be handled with commensurate care, and stoichiometric organotin waste is in principle one of the main limitations of this procedure. However, we have demonstrated previously that Bu_3SnCl recovery allows for easy recycling of the Bu_3Sn moiety, thus minimising organotin waste and potentially helping to mitigate against this issue.[13,17]

Further investigations showed that the selective alkylation and acylation of the hydrostannylated phosphine mixture could also be achieved in a similar fashion from P_{red}, by treating with benzyl bromide (BnBr; 45% conversion to $[Et_4P]Br$, **7a**) or pivaloyl chloride (*t*BuC(O)Cl; 44% conversion to $(t\text{BuC(O)})_3P$, **8a**), respectively, in the presence of base (see Scheme 2c and Section 3.4.1.2). Collectively, these initial results clearly demonstrate the principle of the desired, direct transformation of P_{red} into P_1 products. Nevertheless, it was noticed that the conversions achieved from P_{red} were consistently lower than those previously achieved when starting from P_4 (e.g., cf. 80% isolated yield for $[Bn_4P]Br$ from P_4).[13] It was speculated that this could arise from the previously-observed ability of the hydrostannylated monophosphine mixture $(Bu_3Sn)_xPH_{3-x}$ (x = 1–3) to scramble its H and Bu_3Sn ligands, which should be accelerated by the much higher concentrations used to reduce P_{red}.[13] This would increase the fraction of gaseous PH_3 in the mixture, which is liable to be unproductively lost during subsequent manipulations. Indeed, such PH_3 loss has been proposed to be a limiting factor even when P_4 is employed as the substrate.[4]

To attempt to mitigate this problem it was decided to investigate the selective conversion of P_{red} into the fully stannylated phosphine $(Bu_3Sn)_3P$ (**4**) as a single product, as an alternative to the more complex, PH_3-containing mixture $(Bu_3Sn)_xPH_{3-x}$ (x = 1–3).[5f] We previously found that addition of Bu_3SnOMe prior to the hydrostannylation of P_4 results in conversion of the initially-formed P–H bonds into P–Sn bonds, and that this can be used to selectively prepare **4** in excellent yield.[13] Satisfyingly, when the already-optimised hydrostannylation of P_{red} was repeated in the presence of Bu_3SnOMe the desired product **4** was formed seemingly quantitatively, without the need for any further reaction modifications (for further details see Section 3.4.2.1).

It was possible to isolate product **4** from this one-step reaction in excellent yield (86%, see Scheme 3a and Section 3.4.2.2). More significantly, it was confirmed that $(Bu_3Sn)_3P$ (**4**) could also serve as an intermediate "P^{3-}" synthon and be functionalised with suitable electrophiles in a similar fashion to the previous $(Bu_3Sn)_xPH_{3-x}$ mixture.[5f] For example, treatment of crude $(Bu_3Sn)_3P$ generated from P_{red} directly with paraformaldehyde in ethanol followed by quenching with HCl furnished THPC (**5**) in excellent isolated yield (85%, see Scheme 3b and Section 3.4.3.1). This yield is appreciably higher than that obtained from hydrostannylation in the absence of Bu_3SnOMe (Scheme 2c and see above), and is in excellent agreement with yields obtained previously using P_4.[13] Once again, Bu_3SnCl (**6**) could also be recovered from this reaction in excellent yield (98%) with minimal effort, for potential recycling.

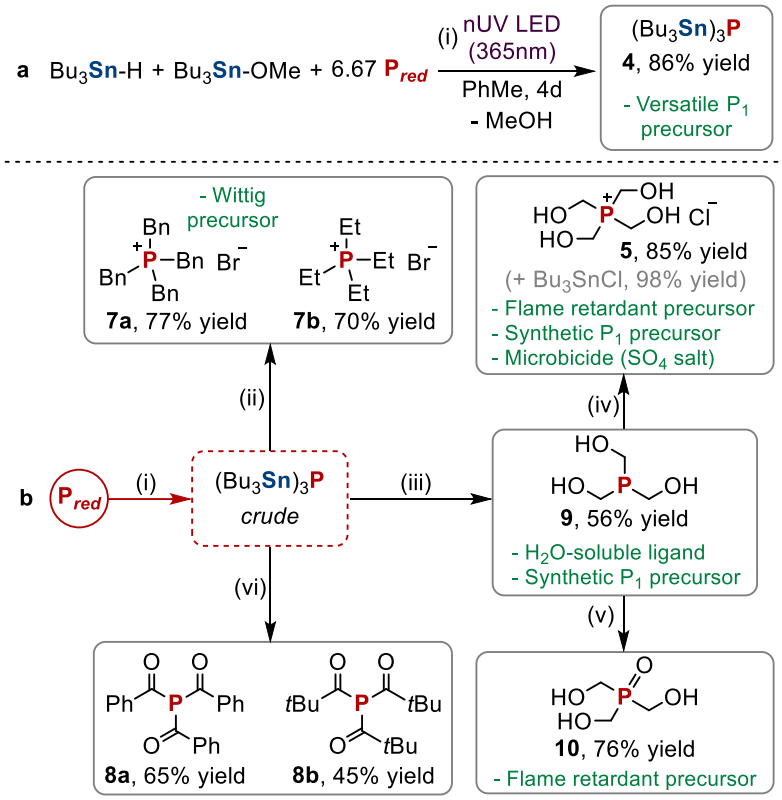

Scheme 3. a) One-pot synthesis of $(Bu_3Sn)_3P$ directly from P_{red} using Bu_3SnH and Bu_3SnOMe promoted by near-UV irradiation. b) Synthesis of P_1 products directly from P_{red} by stannylation to $(Bu_3Sn)_3P$. (i) Stannylation of P_{red} (6.67 equiv.) with Bu_3SnH (0.06 mmol, 1 equiv.), Bu_3SnOMe (0.06 mmol, 1 equiv.) and PhMe (50 µL), 365 nm LEDs, RT, 4 days; (ii) preparation of phosphonium salts $[R_4P]Br$ from crude $(Bu_3Sn)_3P$: 6.67 equiv. RBr (R=Bn or Et), 105 °C, 2 days; (iii) preparation of THP from crude $(Bu_3Sn)_3P$: EtOH, 12.5 equiv. paraformaldehyde, RT, 16 h; (iv) preparation of THPC from crude $(Bu_3Sn)_3P$: EtOH, 8.33 equiv. paraformaldehyde, RT, 16 h, then 6.67 equiv. HCl (4.0 M in 1,4-dioxane), RT, 2 h; (v) preparation of THPO from crude THP: PhMe/H_2O, air, 90 °C, 16 h; (vi) preparation of triacylphosphines $P(C(O)R)_3$ from crude $(Bu_3Sn)_3P$: 2.67 equiv. RC(O)Cl (R=Ph or *t*Bu), RT, 2 days. Yields are defined relative to the limiting reagent (Bu_3SnH/Bu_3SnOMe).

Similar reactions allowed the conversion of P_{red} directly into the corresponding phosphine $(HOCH_2)_3P$ (THP, **9**, by excluding the HCl quench) and phosphine oxide $(HOCH_2)_3PO$ (THPO, **10**, by quenching with air) as well as the phosphonium salts $[Bn_4P]Br$ and $[Et_4P]Br$ (**7a** and **7b** respectively, prepared using BnBr and EtBr) and the triacylphosphines (*t*BuC(O))$_3$P and

$(PhC(O))_3P$ (**8a** and **8b**, respectively, prepared using *t*BuC(O)Cl and PhC(O)Cl), in generally good to excellent isolated yields (Scheme 3b and Sections 3.4.3.2-3.4.3.7). The industrial and academic applications of these isolated products include flame retardants (**5** and **10**),[1b,18] Wittig reagents (**7**), and chemical precursors (**9**),[1b,19] among others. Significantly, the formation of **7** and **8** could be performed in the absence of base which contrasts with previous results where a base was necessary for functionalisation of the intermediate P–H bonds present in $(Bu_3Sn)_xPH_{3-x}$ (x = 1 or 2), thus highlighting an additional advantage of instead proceeding via $(Bu_3Sn)_3P$ only.[5f] From the results summarised in Scheme 3b, the scope of this new, direct P_{red} functionalisation reaction appears to closely match that of the corresponding P_4 functionalisation. In all cases the $(Bu_3Sn)_3P$ functionalisation step could be achieved using identical or near-identical conditions to those used previously for $(Bu_3Sn)_xPH_{3-x}$ functionalisation, and the isolated yields starting from P_{red} and P_4 are generally in excellent agreement (e.g. 77% vs. 80% for **7a,** 76% vs. 77% for **10**).[13] Finally, as a further demonstration of the utility of this method, the synthesis of the key intermediate $(Bu_3Sn)_3P$ (**4**) directly from P_{red} was investigated without the use of a glovebox. Although performing the reaction completely under air was detrimental (presumably due to sensitivity of the radical chain mechanism towards O_2), it was found that the use of 'bench' solvent, standard Schlenk techniques, and/or freeze-pump-thaw degassing instead of dried solvent in a glovebox led to only minor reductions in conversion (<10%, for full details see Section 3.4.4.1). As it is relatively air-stable,[20] $(Bu_3Sn)_3P$ can also subsequently be worked up under air. Thus, without a glovebox and using only simple, easily-reproducible air-exclusion techniques, this key species could be conveniently synthesised at preparative scale and in very good isolated yield (76%, see Section 3.4.4.2).

3.3 Conclusion

We have therefore described herein the development of a practical and highly versatile new method for the direct transformation of P_{red} into a variety of useful monophosphorus compounds. This system provides access to a wide variety of product structures, including examples with significant industrial and academic relevance. Despite the relative inertness of P_{red}, and unlike most other examples of productive P_{red} functionalisation, these transformations can be achieved without the need for especially powerful or elaborate reagents, or extremely rigorous inert atmosphere techniques. Instead, they require only simple, "familiar" reagents that can be handled in almost any standard synthetic laboratory. As a result, this method allows synthetic chemists to prepare useful P_1 compounds using P_{red} as a cheap and highly convenient P atom source, as an alternative to the more hazardous reagents that are currently standard (P_4, PCl_3, PH_3, *etc*.).

3.4 Supporting Information

General information

Unless stated otherwise, all reactions and manipulations were performed under an N_2 atmosphere (< 0.1 ppm O_2, H_2O) through use of MBraun Unilab and GS MEGA Line gloveboxes and standard Schlenk line techniques. All glassware was oven-dried (160 °C) overnight prior to use. PhH was distilled from Na/benzophenone and stored over molecular sieves (3 Å). MeCN was distilled from CaH_2 and stored over molecular sieves (3 Å). *n*-Hexane was purified using an MBraun SPS-800 system and stored over K. PhMe, Et_2O and THF were purified using an MBraun SPS-800 system and stored over molecular sieves (3 Å). EtOH was degassed and dried by standing over at least three sequential batches of molecular sieves (3 Å). C_6D_6 was distilled from K and stored over molecular sieves (3 Å). CD_3CN, CD_3OD and D_2O were used without purification. All reagents and starting materials were purchased from major suppliers. Liquids were degassed (if not supplied under inert atmosphere) but were otherwise used as supplied, unless stated otherwise. Bu_3SnH was supplied containing 0.05% BHT as stabilizer and was used as received. Bu_3SnOMe was degassed and stored over molecular sieves (3 Å). BnBr, EtBr, PhC(O)Cl and *t*BuC(O)Cl were distilled, degassed, and stored over molecular sieves (3 Å). Solids were dried under vacuum (with the exception of paraformaldehyde) but otherwise used as supplied, unless stated otherwise. Red phosphorus (≥97.0 %) was purchased from Sigma-Aldrich. NMR spectra were recorded at room temperature on Bruker Avance 400 (400 MHz) spectrometers and were processed using Topspin 3.2. Chemical shifts, δ, are reported in parts per million (ppm); ^{1}H NMR and ^{13}C NMR shifts are reported relative to $SiMe_4$ and were referenced internally to residual solvent peaks, while ^{31}P NMR and ^{119}Sn shifts were referenced externally to 85 % H_3PO_4 (aq.) and $SnMe_4$ (90% in C_6D_6), respectively. Except where stated otherwise, integrals for $^{31}P\{^{1}H\}$ and ^{31}P spectra are provided for the purposes of qualitative comparison only, and should not be considered quantitatively accurate. The abbreviations s, d, t, q, m are used to indicate singlets, doublets, triplets, quartets and multiplets, respectively.

Reactions driven by light were performed using apparatus that has been described in previous publications, in which reaction vessels are illuminated from beneath by LEDs while placed in a metal block through which cooling water is constantly circulated to maintain near-ambient temperature.[5b,e]

3.4.1 Hydrostannylation of Red Phosphorus (P_{red})

3.4.1.1 General procedure and optimisation for the hydrostannylation of P_{red} using Bu_3SnH and LED irradiation (0.06 mmol scale)

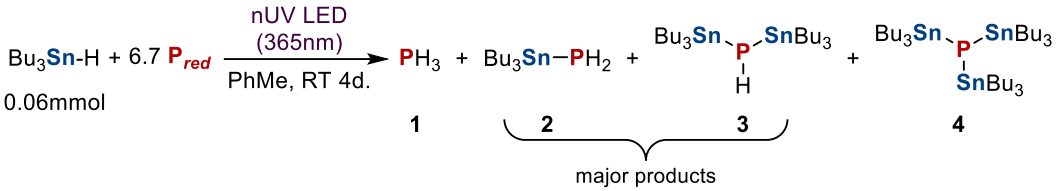

To a 10 mL, flat-bottomed, stoppered tube were added P_{red} (0.4 mmol, 12.4 mg), PhMe (50 µL) and Bu_3SnH (16.1 µL, 0.06 mmol). The tube was sealed, placed in a water-cooled block to maintain near-ambient temperature, and irradiated with UV light (365 nm, 4.3 V, 700 mA, Osram OSLON SSL 80) for 4 days (unless stated otherwise). Ph_3PO (0.02 mmol, stock solution in benzene) was subsequently added to act as an internal standard. The resulting mixture was analysed by ^{1}H, $^{31}P\{^{1}H\}$, ^{31}P, and $^{119}Sn\{^{1}H\}$ NMR spectroscopy, as shown in Figures S1-4, below.

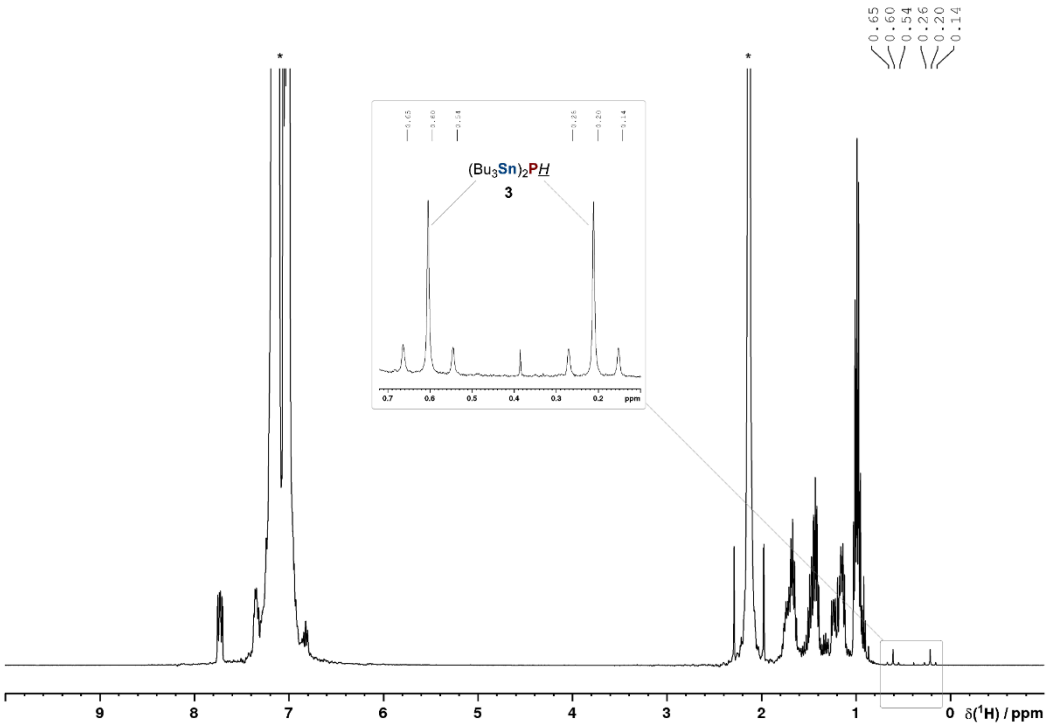

Figure S144. ^{1}H NMR spectrum for the reaction of P_{red} with Bu_3SnH (0.06 mmol) in PhMe and driven by 365 nm LED irradiation for 4 days. Solvent resonances are marked with an asterisk and are truncated for clarity. The inset shows an expansion of the doublet resonance with $^{117/119}Sn$ satellites attributed to the P*H* moiety of $(Bu_3Sn)_2PH$ (**3**).

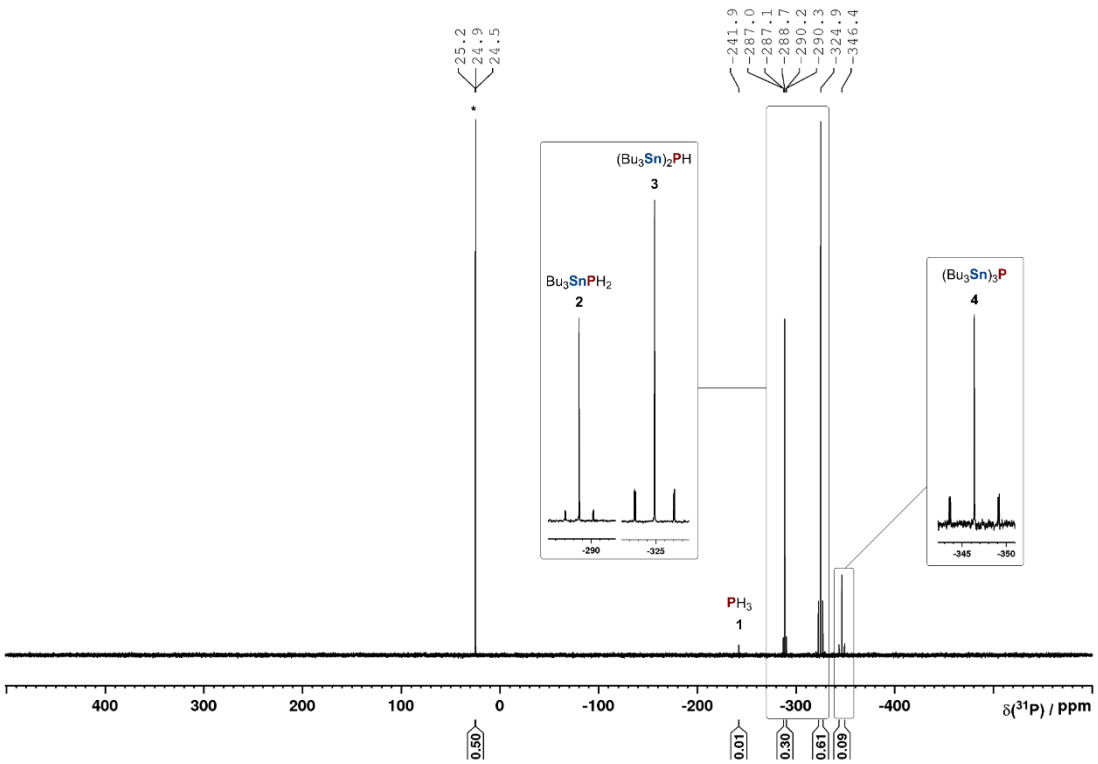

Figure S145. $^{31}P\{^{1}H\}$ NMR spectrum for the reaction of P_{red} with Bu_3SnH (0.06 mmol) in PhMe and driven by 365 nm LED irradiation for 4 days. The insets show expansions of the signals attributed to Bu_3SnPH_2 (**2**) and $(Bu_3Sn)_2PH$ (**3**), and to $(Bu_3Sn)_3P$ (**4**), highlighting the presence of $^{117/119}Sn$ satellites. * marks the internal standard Ph_3PO (0.02 mmol).

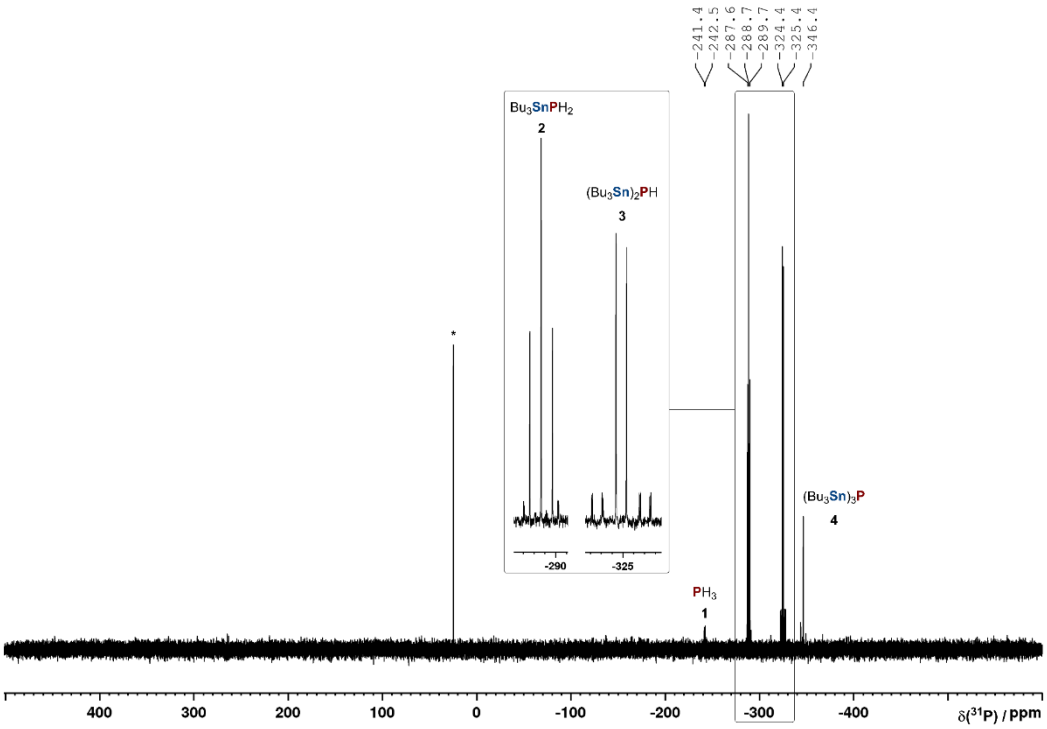

Figure S146. ^{31}P NMR spectrum for the reaction of P_{red} with Bu_3SnH (0.06 mmol) in PhMe and driven by 365 nm LED irradiation for 4 days. The insets show expansions of the signals attributed to Bu_3SnPH_2 (**2**) and $(Bu_3Sn)_2PH$ (**3**), highlighting their multiplicity due to $^{1}J(^{31}P\text{-}^{1}H)$ couplings. * marks the internal standard Ph_3PO (0.02 mmol).

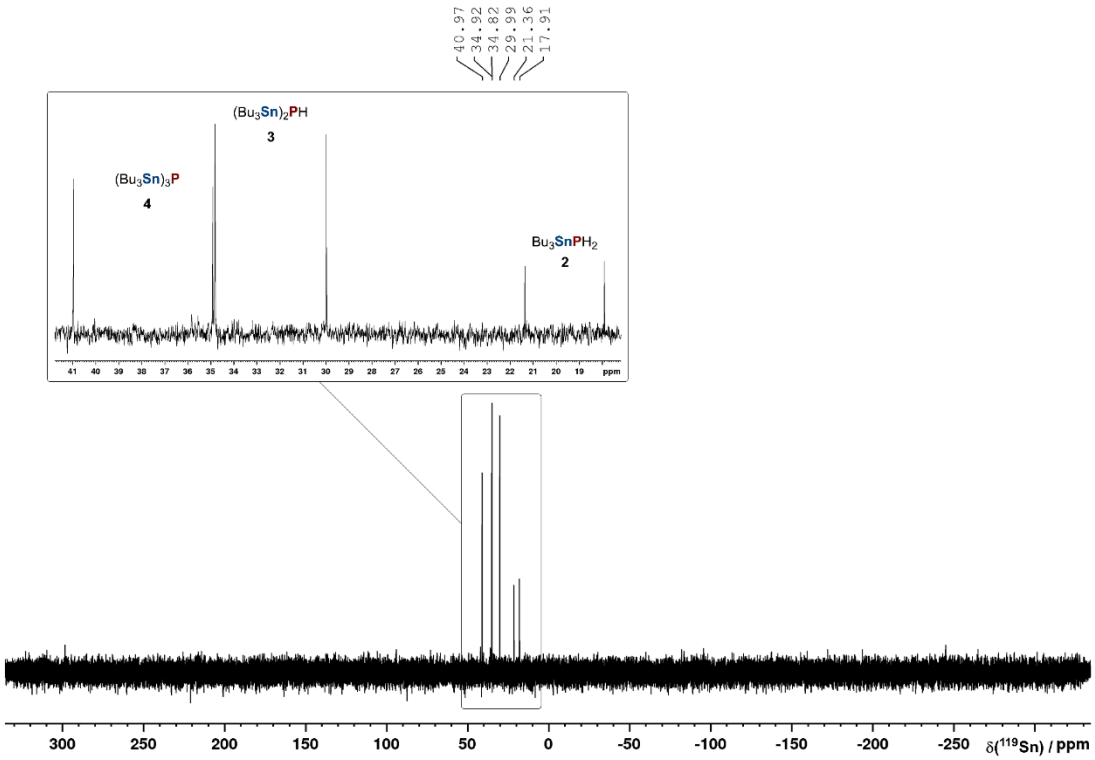

Figure S147. $^{119}Sn\{^{1}H\}$ NMR spectrum for the reaction of P_{red} with Bu_3SnH (0.06 mmol) in PhMe and driven by 365 nm LED irradiation for 4 days. The insets show expansions of the signals attributed to Bu_3SnPH_2 (**2**), $(Bu_3Sn)_2PH$ (**3**), and $(Bu_3Sn)_3P$ (**4**).

For reasons of experimental expediency, during the optimisation of the hydrostannylation of P_{red} acquisition of quick but non-quantitative $^{31}P\{^{1}H\}$ NMR spectra was used to analyse each experiment and to assess the relative total conversion to **1-4**. Although this did not directly provide precise, quantitative conversions it did allow for meaningful, qualitative comparisons between experiments. Under the optimized conditions highlighted in Table S1, entry 12 (and Table S2, entry 1) full consumption of the limiting reagent Bu_3SnH was observed (assessed by ^{1}H NMR spectroscopy), and the $^{31}P\{^{1}H\}$ and $^{119}Sn\{^{1}H\}$ spectra suggest clean conversion to the desired products **1-4** (Figures S1-4). It is therefore proposed that this procedure provides complete (or very nearly complete) conversion. Thus, for ease of interpretation, the integrals measured for **1-4** for all optimisation experiments have been normalized relative to the value for this experiment (defined as 99%) to provide the relative conversions indicated in Table S1.

Table S1. Optimisation of hydrostannylation of P_{red} using Bu_3SnH and near-UV LED irradiation (365 nm)[a]

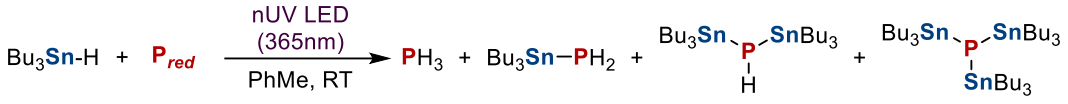

Entry	Bu_3SnH (mmol)	P_{red} (mmol)	PhMe (µL)	Time (days)	Full conv. of Bu_3SnH?[b]	Relative total conv. to **1-4** (%)[c]
1[d]	0.06	0.04	500	1	X	traces
2[d]	0.06	0.04	500	3	X	20
3	0.06	0.15	500	3	X	25
4	0.06	0.4	500	3	X	50
5	0.06	0.4	500 (THF)	3	X	49
6	0.06	0.4	500 (hexane)	3	X	48
7	0.06	0.4	500 (EtOH)	3	X	18
8	0.06	0.4	250	3	X	60
9	0.06	0.4	100	3	X	70
10	0.06	0.4	50	3	X	95
11	0.06	0.4	-	3	X	36
12	**0.06**	**0.4**	**50**	**4**	✓	**99**
13	0.12	0.4	100	4	X	60
14	0.12	0.8	100	4	X	27
15	0.12	0.8	50	4	X	75

[a] The general procedure described in this section was modified to use the indicated amount of reactants and solvent. [b] The full consumption of Bu_3SnH was assessed by ^1H NMR spectroscopy and the disappearance of the Sn*H* resonance that would otherwise be observed at *ca*. 5 ppm. [c] Conversions were calculated by integration of the ^{31}P resonances of **1-4** relative to an internal standard, which was then normalized relative to entry 12 (defined as 99%) as described in the text above. [d] Blue LED (455 nm).

Table S2. Hydrostannylation of P_{red} using Bu_3SnH and LED irradiation: screening of **LEDs**[a]

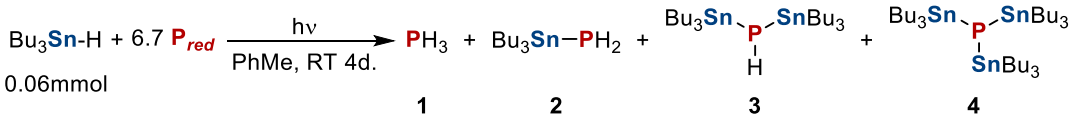

Entry	hν	Full conv. of Bu_3SnH?[b]	Relative total conv. to **1-4** (%)[c]
1	**365 nm**	✓	**99**
2	400 nm	X	33
3	420 nm	X	72[d]
4	455 nm	X	47[d]
5	520 nm	X	12
6	no hν, 100 °C[e]	X	7

[a] The general procedure described in this section was modified to use LEDs of the indicated wavelengths. [b] The full consumption of Bu_3SnH was assessed by ^1H NMR spectroscopy and the disappearance of the Sn*H* resonance that would otherwise be observed at *ca*. 5 ppm. [c] Conversions were calculated by integration of the ^{31}P resonances of **1-4** relative to an internal standard, which was then normalized relative to entry 1 (defined as 99%) as described in the text above. [d] Other signals were observed apart from those corresponding to **1-4**, attributed to $P_7(SnBu_3)_3$ (see Figure S5). [e] The reaction tube was wrapped in Al foil to exclude light, and heated to 100 °C for 4 days.

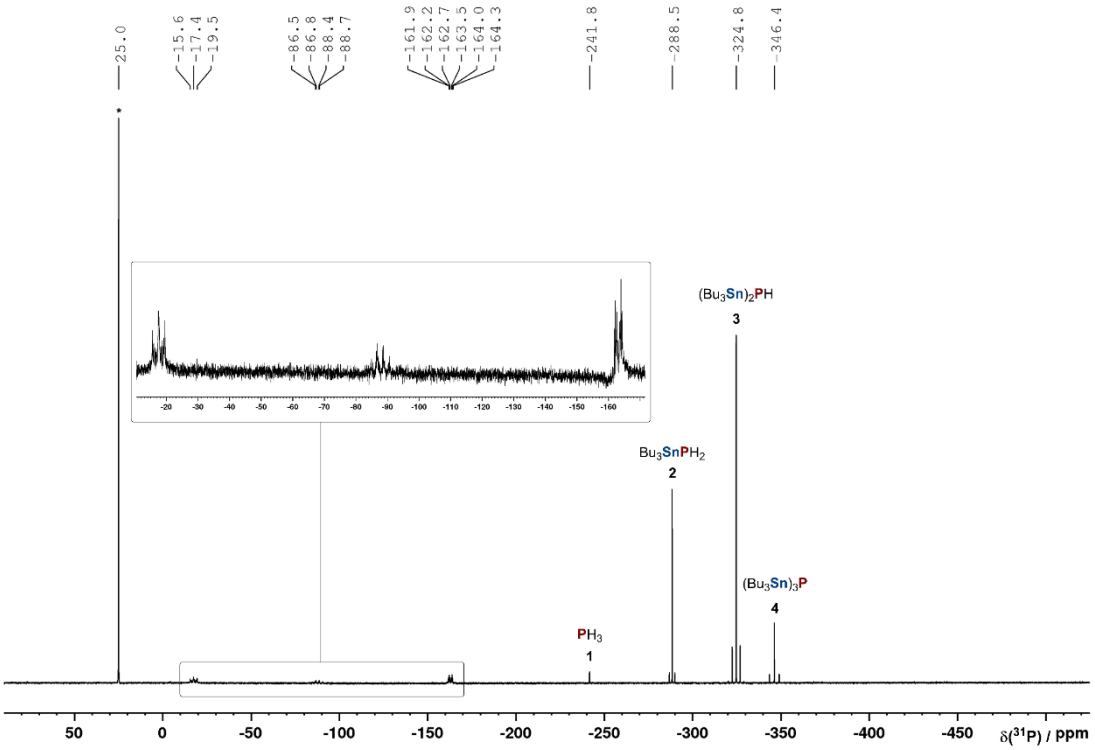

Figure S148. $^{31}P\{^{1}H\}$ NMR spectrum for the reaction of P_{red} with Bu_3SnH (0.06 mmol) in PhMe and driven by 455 nm LED irradiation for 4 days (Table S2, entry 4). The insets show expansion of minor signals attributed to $P_7(SnBu_3)_3$, which were assigned by comparison with those reported for $P_7(SnMe_3)_3$.[16] * marks the internal standard Ph_3PO.

3.4.1.2 General procedure for the functionalisation of the mixture $(Bu_3Sn)_xPH_{3-x}$ (x = 1–3)

The conversions of the products shown in this section were determined by a quantitative single-scan inverse-gated $^{31}P\{^{1}H\}$ NMR (DS = 0, D1 = 2 s) methodology that we have described previously, and whose use to quantify tertiary phosphines and quaternary phosphonium salts has previously been validated.[5e]

To a 10 mL, flat-bottomed, stoppered tube were added P_{red} (0.4 mmol, 12.4 mg), PhMe (50 µL) and Bu_3SnH (16.1 µL, 0.06 mmol). The tube was sealed, placed in a water-cooled block to maintain near-ambient temperature, and irradiated with UV light (365 nm, 4.3 V, 700 mA, Osram OSLON SSL 80) for 4 days. The resulting red suspension was filtered and extracted with PhMe (0.5 mL). The resulting clear yellowish solution was treated with the corresponding electrophiles as follows:

Reactivity toward paraformaldehyde: Volatiles were removed under vacuum. EtOH (0.5 mL) and paraformaldehyde (15.0 mg, 0.5 mmol) were added to the oily residue, and the resulting suspension was stirred at room temperature for 16 h. The mixture was frozen in a liquid-nitrogen bath, and HCl (4.0 M in 1,4-dioxane, 100 µL, 0.4 mmol) was added. After thawing, the reaction mixture was stirred at room temperature for 2 h. Ph_3PO (0.02 mmol, stock solution in benzene) was subsequently added to act as an internal standard. $^{31}P\{^{1}H\}$ NMR analysis of the resulting mixture showed the exclusive formation of THPC (**5**) with 70% conversion.

Reactivity toward benzyl bromide: Benzyl bromide (71.3 µL, 0.6 mmol) and KHMDS (12.0 mg, 0.06 mmol) were added to the yellowish solution, and heated to 70 °C with stirring for 3 days. After cooling to room temperature, Ph_3PO (0.02 mmol, stock solution in benzene) was subsequently added to act as an internal standard. $^{31}P\{^1H\}$ NMR analysis of the resulting mixture showed the formation of $[Bn_4P]Br$ (**7a**) as the main product with 45 % conversion.

Reactivity toward pivaloyl chloride: *t*BuC(O)Cl (19.6 µL, 0.16 mmol) and KHMDS (8.0 mg, 0.04 mmol) were added to the yellowish solution, and stirred at room temperature for 1 days. Ph_3PO (0.02 mmol, stock solution in benzene) was subsequently added to act as an internal standard. $^{31}P\{^1H\}$ NMR analysis of the resulting mixture showed the exclusive formation of $P(C(O)tBu)_3$ (**8a**) with 44 % conversion.

3.4.1.3 Synthesis and isolation of THPC (5) *via* hydrostannylation of P_{red} using Bu_3SnH (12 x 0.06 mmol scale) with recovery of Bu_3SnCl (6)

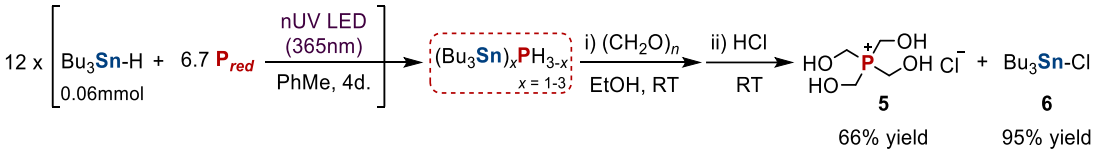

To provide sufficient material for reliable yield determination, a total of twelve reactions were performed in parallel using the following procedure: To a 10 mL, flat-bottomed, stoppered tube were added P_{red} (0.4 mmol, 12.4 mg), PhMe (50 µL) and Bu_3SnH (16.1 µL, 0.06 mmol). The tube was sealed, placed in a water-cooled block to maintain near-ambient temperature, and irradiated with UV light (365 nm, 4.3 V, 700 mA, Osram OSLON SSL 80) for 4 days. The twelve reactions were then combined in a 100 mL Schlenk using PhMe (3 x 0.5 mL) to transfer and wash each tube. The combined red suspension was filtered and the remaining solid extracted with additional PhMe (2 x 10 mL), followed by removal of volatiles under vacuum. EtOH (10 mL) and paraformaldehyde (180.2 mg, 6.0 mmol) were added to the oily residue, and the resulting suspension was stirred at room temperature for 16 h. The mixture was frozen in a liquid-nitrogen bath, and HCl (4.0 M in 1,4-dioxane, 1.2 mL, 4.8 mmol) was added. After thawing, the reaction mixture was stirred at room temperature for 2 h. Volatiles from the resulting yellowish suspension were removed under vacuum. The remaining oily solid residue was triturated with Et_2O (10 mL) overnight, filtered and washed with further Et_2O (2 x 5 mL). The resulting white solid was then again dissolved in EtOH (10 mL). Following filtration and removal of volatiles under vacuum, the desired product (**5**) was obtained as a white solid (60.0 mg, 66%).

The combined Et_2O washes from the above reaction were dried under vacuum to afford Bu_3SnCl (**6**) as a pale yellow oil (223 mg, 95%).

Spectroscopic data of THPC (**5**):

^{1}H NMR (400 MHz, 300 K, D_2O): δ = 4.67 ppm (d, $^{2}J(^{31}P\text{-}^{1}H)$ = 1.8 Hz). **^{31}P{^{1}H} NMR** (121 MHz, 300 K, D_2O): δ = 27.0 ppm (s). **^{31}P NMR** (121 MHz, 300 K, D_2O): δ = 27.0 ppm (s). **^{13}C{^{1}H} NMR** (101 MHz, 300 K, D_2O): δ = 49.1 ppm (d, $^{1}J(^{31}P\text{-}^{13}C)$ = 51.2 Hz). NMR data are consistent with our previous report.[13]

Spectroscopic data of recovered Bu_3SnCl (**6**):

^{1}H NMR (400 MHz, 300 K, $CDCl_3$): δ = 1.79-1.51 (2H, m), 1.41-1.9 (4H, m), 0.92 ppm (3H, t, $^{3}J(^{1}H\text{-}^{1}H)$ = 7.3 Hz). **^{119}Sn{^{1}H} NMR** (149 MHz, 300 K, $CDCl_3$): δ = 157.2 ppm. **^{13}C{^{1}H} NMR** (101 MHz, 300 K, $CDCl_3$): δ = 27.9 (s), 26.9 (s), 17.6 (s), 13.6 ppm (s). NMR data are consistent with our previous report.[13]

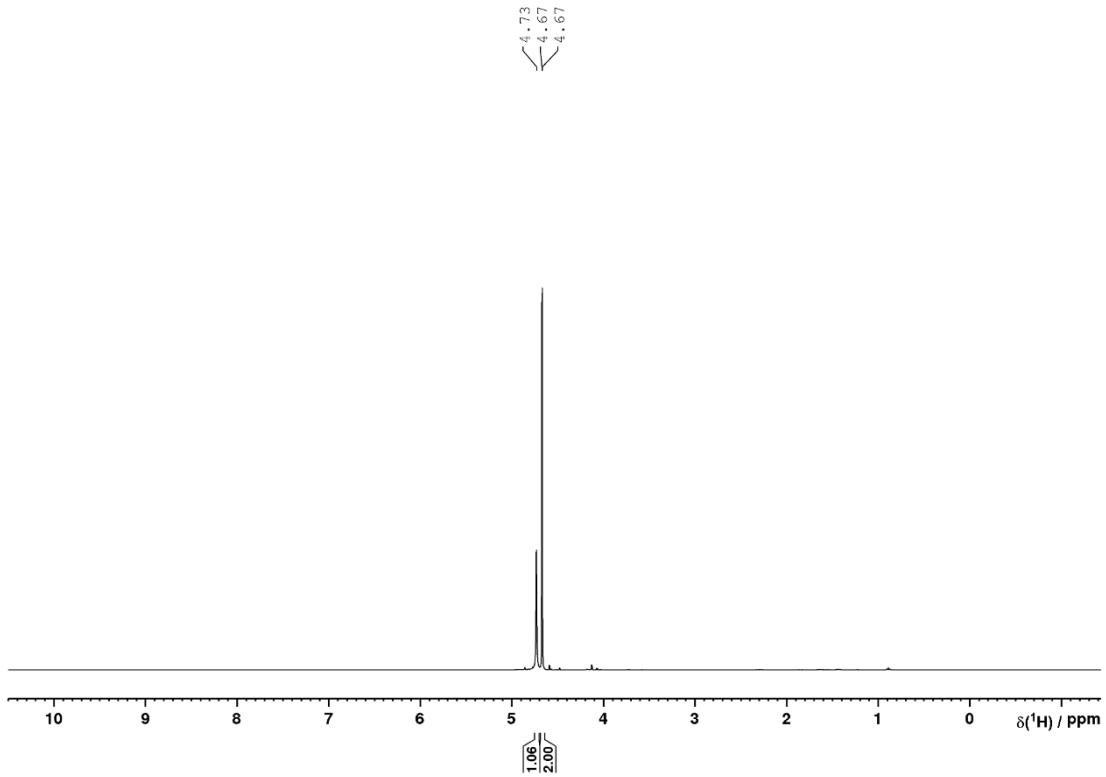

Figure S149. ^{1}H NMR spectrum of THPC (**5**) in D_2O.

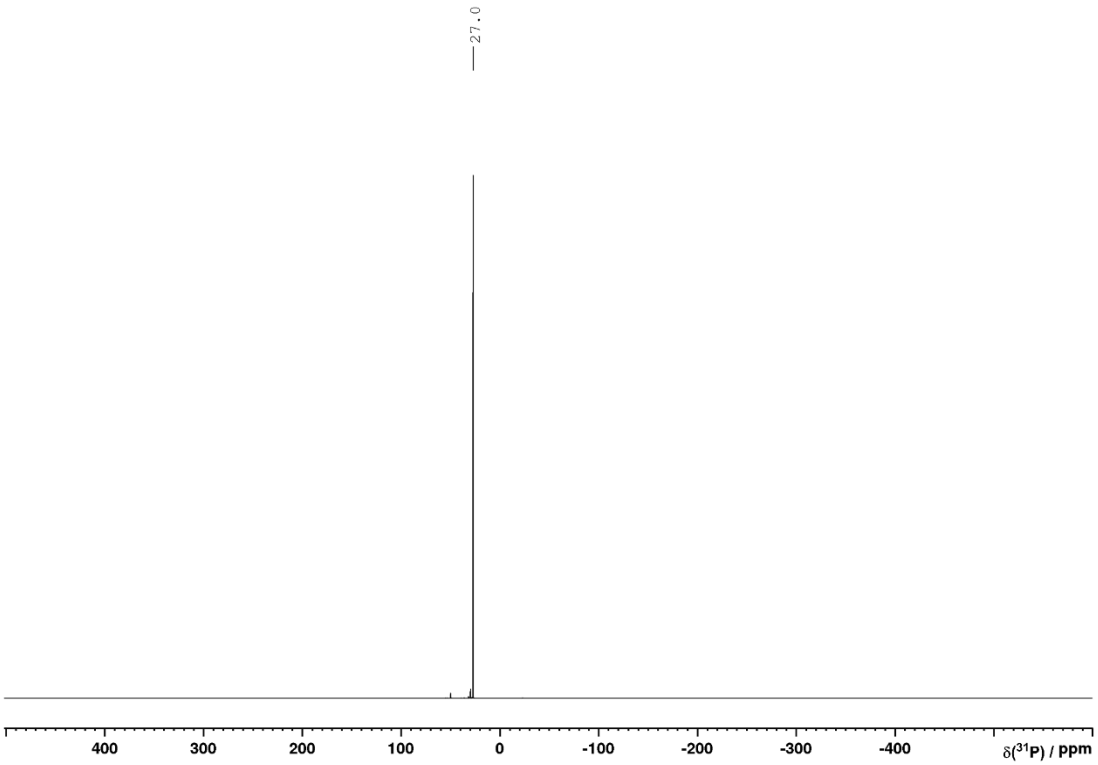

Figure S150. $^{31}P\{^{1}H\}$ NMR spectrum of THPC (**5**) in D_2O.

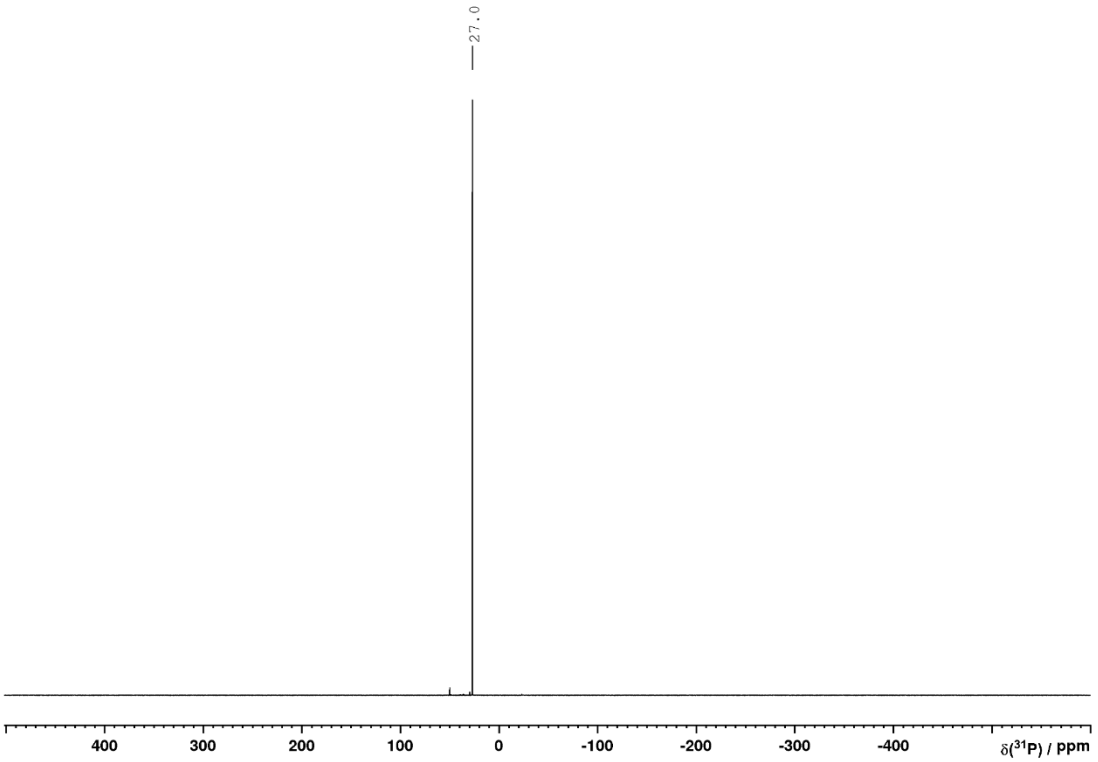

Figure S151. ^{31}P NMR spectrum of THPC (**5**) in D_2O.

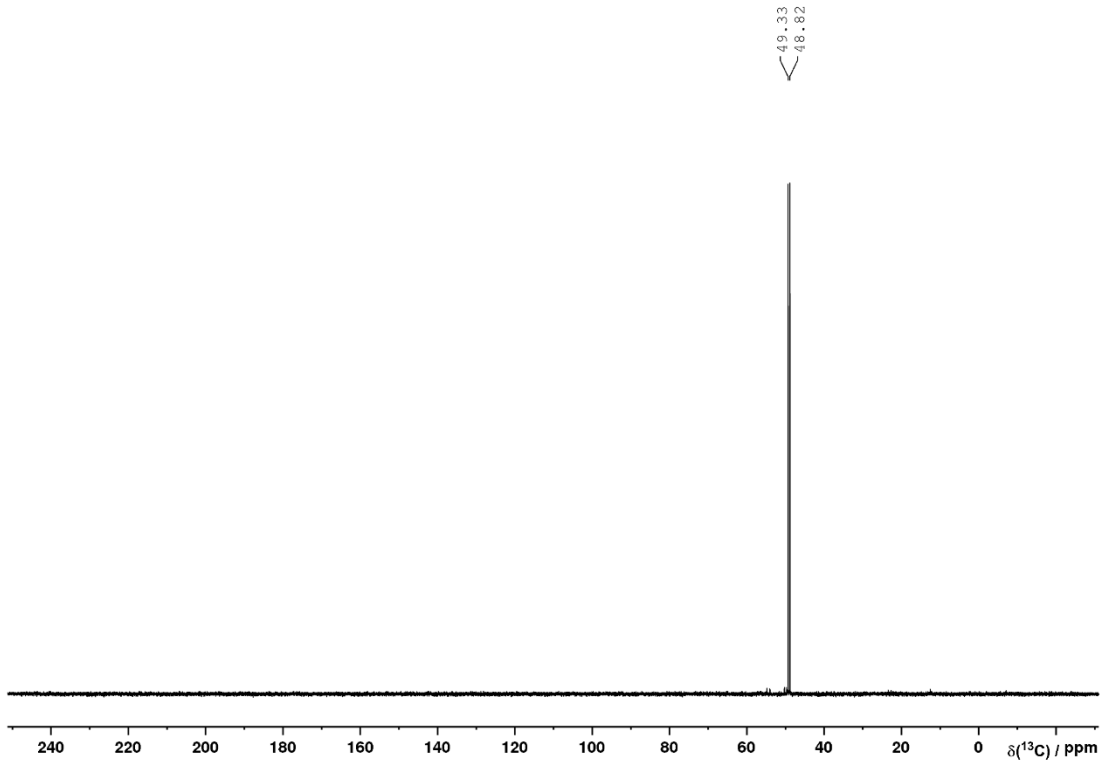

Figure S152. $^{13}C\{^{1}H\}$ NMR spectrum of THPC (**5**) in D_2O.

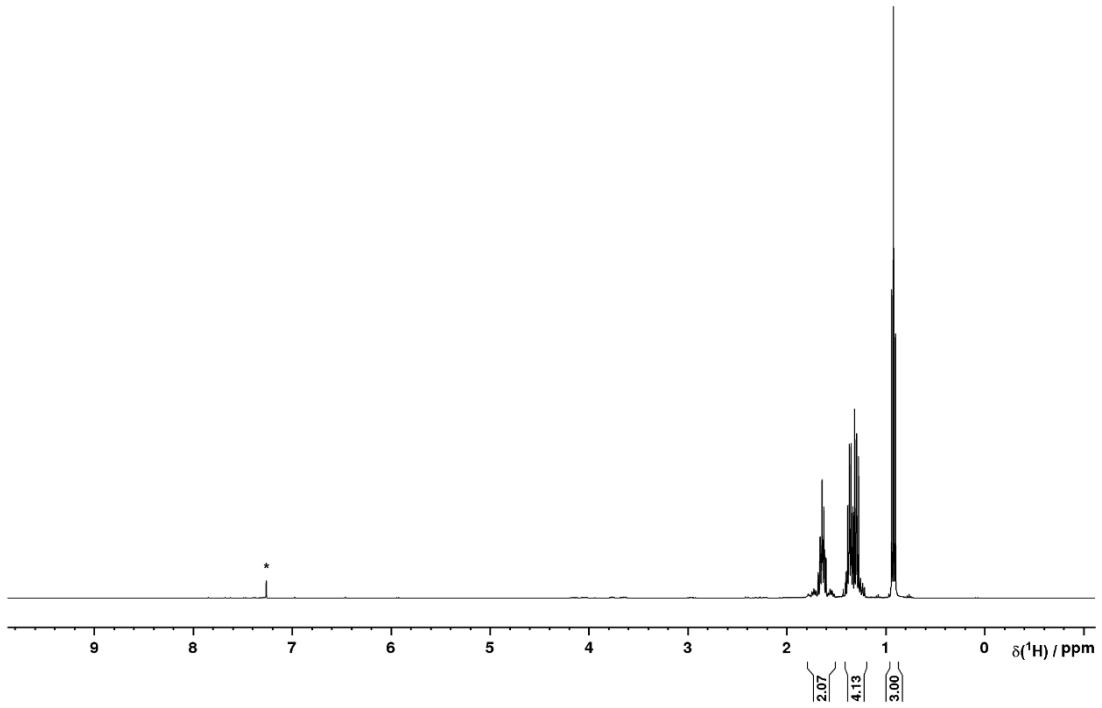

Figure S153. ^{1}H NMR spectrum of Bu_3SnCl (**6**) in $CDCl_3$ (*).

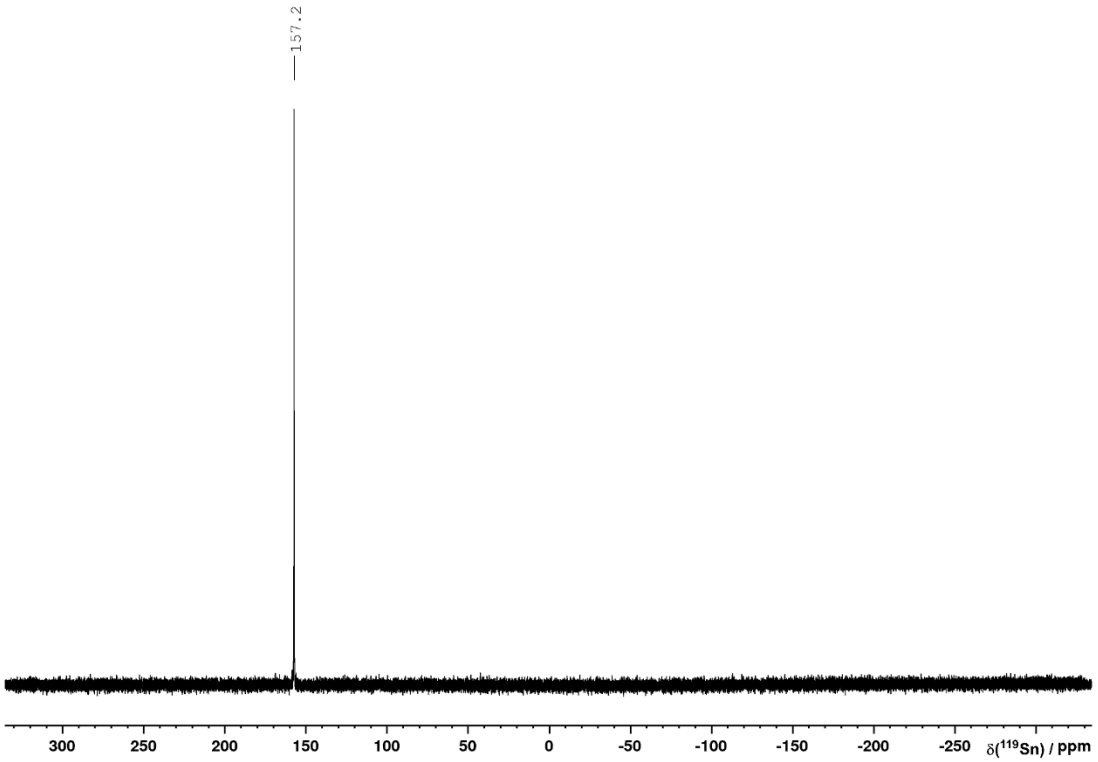

Figure S154. $^{119}Sn\{^{1}H\}$ NMR spectrum of Bu_3SnCl (**6**) in $CDCl_3$.

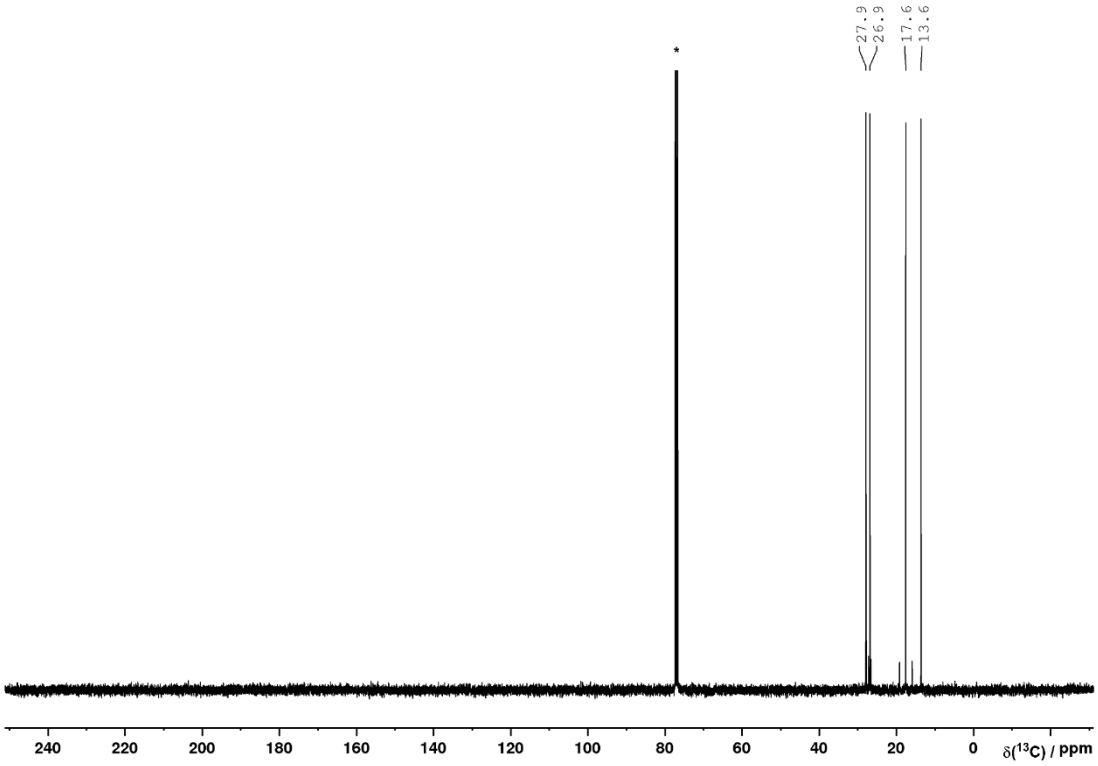

Figure S155. $^{13}C\{^{1}H\}$ NMR spectrum of Bu_3SnCl (**6**) in $CDCl_3$ (*).

3.4.1.4 Synthesis and isolation of THPC (5) *via* hydrostannylation of P_{red} using Bu_3SnH (0.6 mmol scale) with recovery of Bu_3SnCl (6)

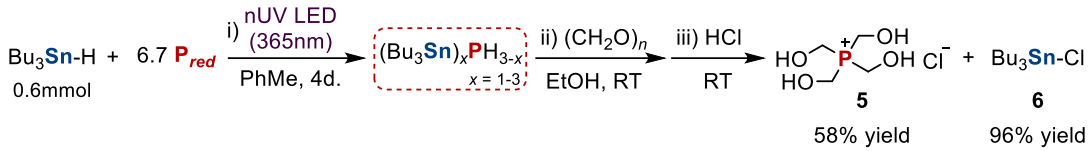

To a 50 mL, flat-bottomed, stoppered tube were added P_{red} (4.0 mmol, 124 mg), PhMe (250 µL) and Bu_3SnH (162 µL, 0.6 mmol). The tube was sealed, placed in a water-cooled block to maintain near-ambient temperature, and irradiated with UV light (365 nm, 14 V, 700 mA, Osram OSLON SSL 80) for 4 days. The red suspension was filtered and washed with additional PhMe (3 x 15 mL), followed by removal of volatiles under vacuum. EtOH (10 mL) and paraformaldehyde (150.1 mg, 5.0 mmol) were added to the oily residue, and the resulting suspension was stirred at room temperature for 18 h. The mixture was frozen in a liquid-nitrogen bath, and HCl (4.0 M in 1,4-dioxane, 1.0 mL, 4.0 mmol) was added. After thawing, the reaction mixture was stirred at room temperature for 2 h. Volatiles from the resulting yellowish suspension were removed under vacuum. The remaining oily solid residue was triturated with Et_2O (10 mL) overnight, filtered and washed with further Et_2O (2 x 10 mL). The resulting white solid was then again dissolved in EtOH (10 mL). Following filtration and removal of volatiles under vacuum, the desired product (**5**) was obtained as a white solid (44.0 mg, 58%).

The combined Et_2O washes from the above reaction were dried under vacuum to afford Bu_3SnCl (**6**) as a pale yellow oil (187 mg, 96%). NMR data are identical to those given in section 3.4.1.3.

3.4.2 Stannylation of Red Phosphorus (P_{red})

3.4.2.1 General procedure and optimisation for the stannylation of P_{red} using Bu_3SnH and Bu_3SnOMe under near-UV LED irradiation (0.06 mmol scale)

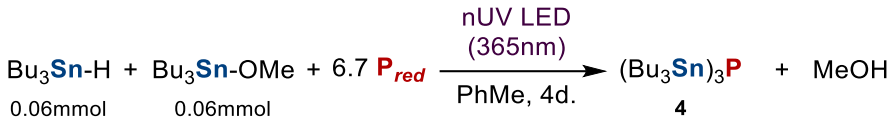

To a 10 mL, flat-bottomed, stoppered tube were added P_{red} (0.4 mmol, 12.4 mg), PhMe (50 µL), Bu_3SnH (16.1 µL, 0.06 mmol) and Bu_3SnOMe (17.3 µL, 0.06 mmol). The tube was sealed, placed in a water-cooled block to maintain near-ambient temperature, and irradiated with UV light (365 nm, 4.3 V, 700 mA, Osram OSLON SSL 80) for 4 days (unless stated otherwise). Ph_3PO (0.02 mmol, stock solution in benzene) was subsequently added to act as an internal standard. The resulting mixture was analysed by ^1H, $^{31}P\{^1H\}$, and ^{31}P NMR spectroscopy, as shown in Figures S13 and S14, below.

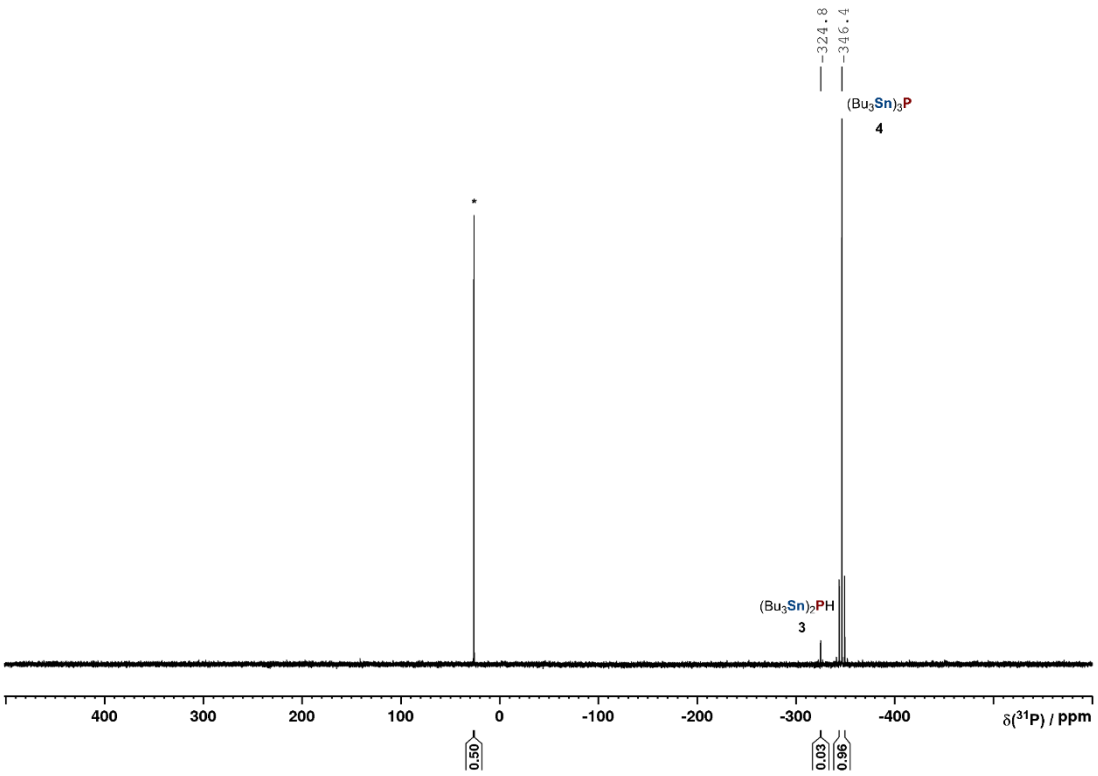

Figure S156. $^{31}P\{^1H\}$ NMR spectrum for the reaction of P_{red} with Bu_3SnH (0.06 mmol) and Bu_3SnOMe (0.06 mmol) in PhMe and driven by 365 nm LED irradiation for 4 days. * marks the internal standard Ph_3PO (0.02 mmol).

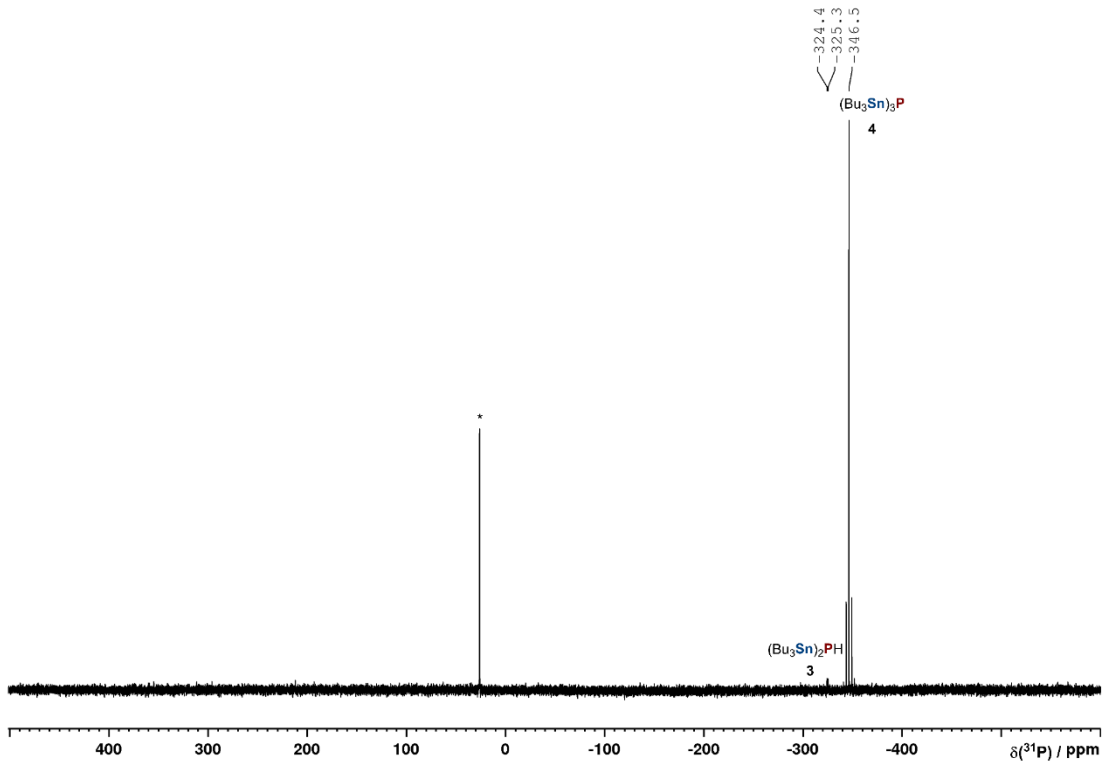

Figure S157. ^{31}P NMR spectrum for the reaction of P_{red} with Bu_3SnH (0.06 mmol) and Bu_3SnOMe (0.06 mmol) in PhMe and driven by 365 nm LED irradiation for 4 days. * marks the internal standard Ph_3PO (0.02 mmol).

Table S3. Stannylation of P_{red} using Bu_3SnH and Bu_3SnOMe under near UV LED irradiation: screening of **solvents**[a]

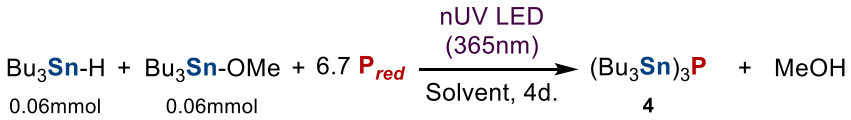

Entry	Solvent	Full conv. of Bu_3SnH?[b]	Conv. to **4** (%)[c]
1	PhMe	✓	96
2	THF	✓	91
3	Hexane	✓	90
4	EtOH	✓	75
5	Acetone	X	81
6	Acetonitrile	X	75

[a] The general procedure described in this section was modified to use the indicated solvents. [b] The full consumption of Bu_3SnH was assessed by ^{1}H NMR spectroscopy and the disappearance of the Sn*H* resonance that would otherwise be observed at *ca*. 5 ppm. [c] Conversions were calculated by integration of the ^{31}P resonance of **4** relative to an internal standard, which was then normalized relative to Table S1, entry 12 (defined as 99%) as described in section 3.4.1.1.

Table S4. Stannylation of P_{red} using Bu_3SnH and Bu_3SnOMe under LED irradiation: screening of **LEDs**[a]

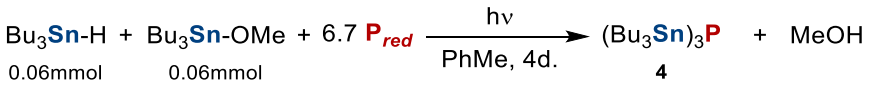

Entry	hν	Full conv. of Bu_3SnH?[b]	Conv. to **4** (%)[c]
1	365 nm	✓	96
2	400 nm	X	22
3	420 nm	X	50[d]
4	455 nm	X	28[d]
5	520 nm	X	7
6	no hν, 100 °C[e]	X	3

[a] The general procedure described in this section was modified to use LEDs of the indicated wavelengths. [b] The full consumption of Bu_3SnH was assessed by ^1H NMR spectroscopy and the disappearance of the Sn*H* resonance that would otherwise be observed at *ca*. 5 ppm. [c] Conversions were calculated by integration of the ^{31}P resonance of **4** relative to an internal standard, which was then normalized relative to Table S1, entry 12 (defined as 99%) as described in section 3.4.1.1. [d] Other signals were observed apart from the one corresponding to **4**, attributed to $P_7(SnBu_3)_3$ (see Figure S15). [e] The reaction tube was wrapped in Al foil to exclude light, and heated to 100 °C for 4 days.

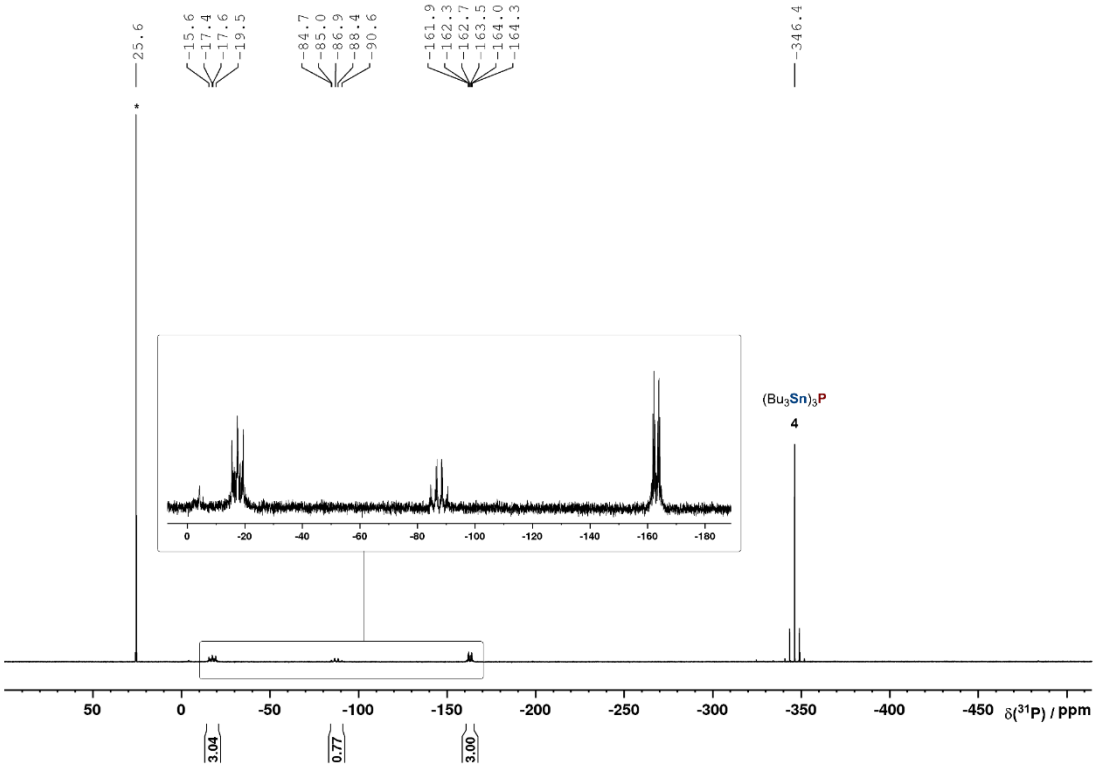

Figure S158. $^{31}P\{^1H\}$ NMR spectrum for the reaction of P_{red} with Bu_3SnH (0.06 mmol) and Bu_3SnOMe (0.06 mmol) in PhMe and driven by 455 nm LED irradiation for 4 days (Table S4, entry 4). The insets show expansion of minor signals attributed to $P_7(SnBu_3)_3$, which were assigned by comparison with those reported for $P_7(SnMe_3)_3$.[16] * marks the internal standard Ph_3PO.

3.4.2.2 Synthesis and isolation of $(Bu_3Sn)_3P$ (4)

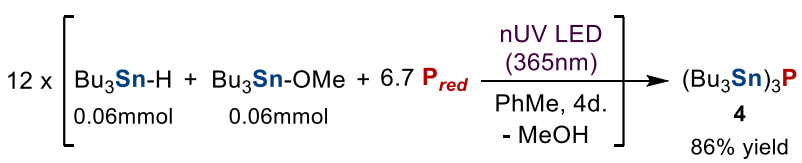

To provide sufficient material for reliable yield determination, a total of twelve reactions were performed in parallel using the following procedure: To a 10 mL, flat-bottomed, stoppered tube

were added P_{red} (0.4 mmol, 12.4 mg), PhMe (50 µL), Bu_3SnH (16.1 µL, 0.06 mmol) and Bu_3SnOMe (17.3 µL, 0.06 mmol). The tube was sealed, placed in a water-cooled block to maintain near-ambient temperature, and irradiated with UV light (365 nm, 4.3 V, 700 mA, Osram OSLON SSL 80) for 4 days. The twelve reactions were then combined in a 100 mL Schlenk using PhMe (3 x 0.5 mL) to transfer and wash each tube. The combined red suspension was filtered and the remaining solid extracted with additional PhMe (2 x 10 mL), followed by removal of volatiles under vacuum. After distillation of the resulting yellowish oil under vacuum (*ca.* 105 °C, 10^{-5} mbar), the product (**4**) was obtained as a colourless oil (371.8 mg, 86%).

^{1}H NMR (400 MHz, 300 K, C_6D_6): δ = 1.84-1.63 (2H, m), 1.53-1.40 (2H, m), 1.13-1.33 (2H, m), 0.99 ppm (3H, t, $^{3}J(^{1}H\text{-}^{1}H)$ = 7.3 Hz). **^{31}P{^{1}H} NMR** (121 MHz, 300 K, C_6D_6): δ = –346.5 ppm (s). **^{31}P NMR** (121 MHz, 300 K, C_6D_6): δ = –346.5 ppm (s). **^{119}Sn{^{1}H}** (149 MHz, 300 K, C_6D_6) δ = 37.5 ppm (d, $^{1}J(^{31}P\text{-}^{119}Sn)$ = 912 Hz, $^{2}J(^{119}Sn\text{-}^{117}Sn)$ = 280 Hz). **^{13}C{^{1}H} NMR** (101 MHz, 300 K, C_6D_6): δ = 30.0 (d, $J(^{31}P\text{-}^{1}H)$ = 1.4 Hz), 28.0 (s), 15.2 (d, $J(^{31}P\text{-}^{1}H)$ = 3.8 Hz), 13.9 ppm (s). NMR data are consistent with our previous report.[13]

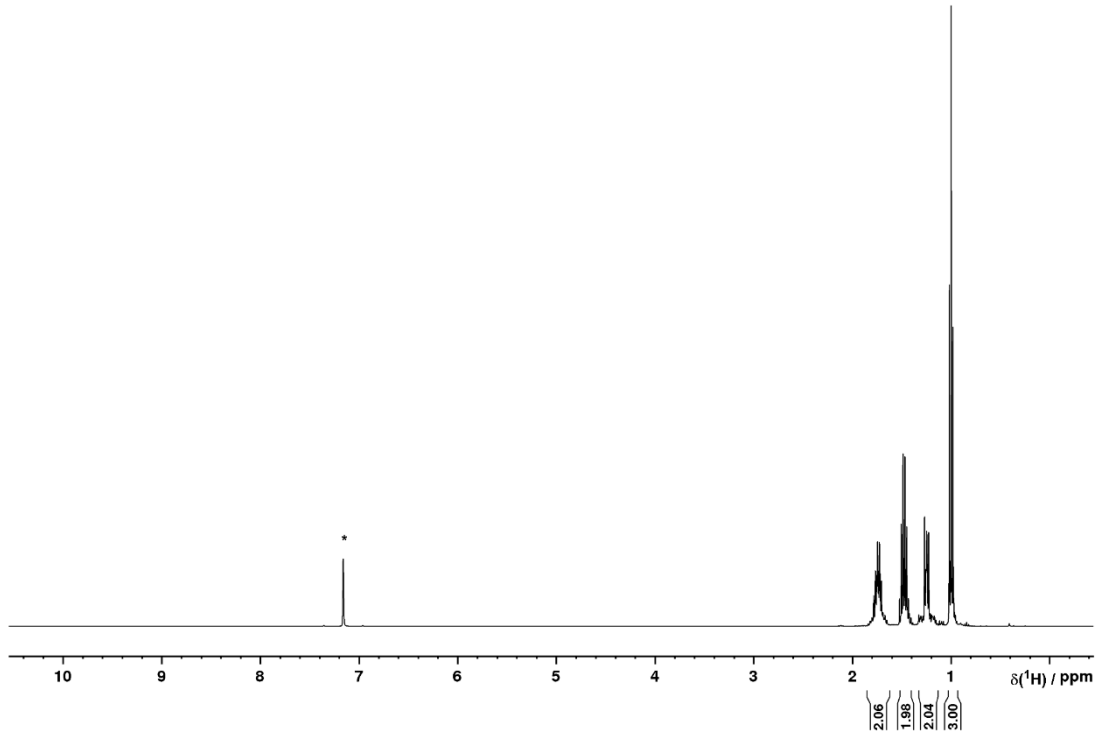

Figure S159. ^{1}H NMR spectrum of $(Bu_3Sn)_3P$ (**4**) in C_6D_6 (*).

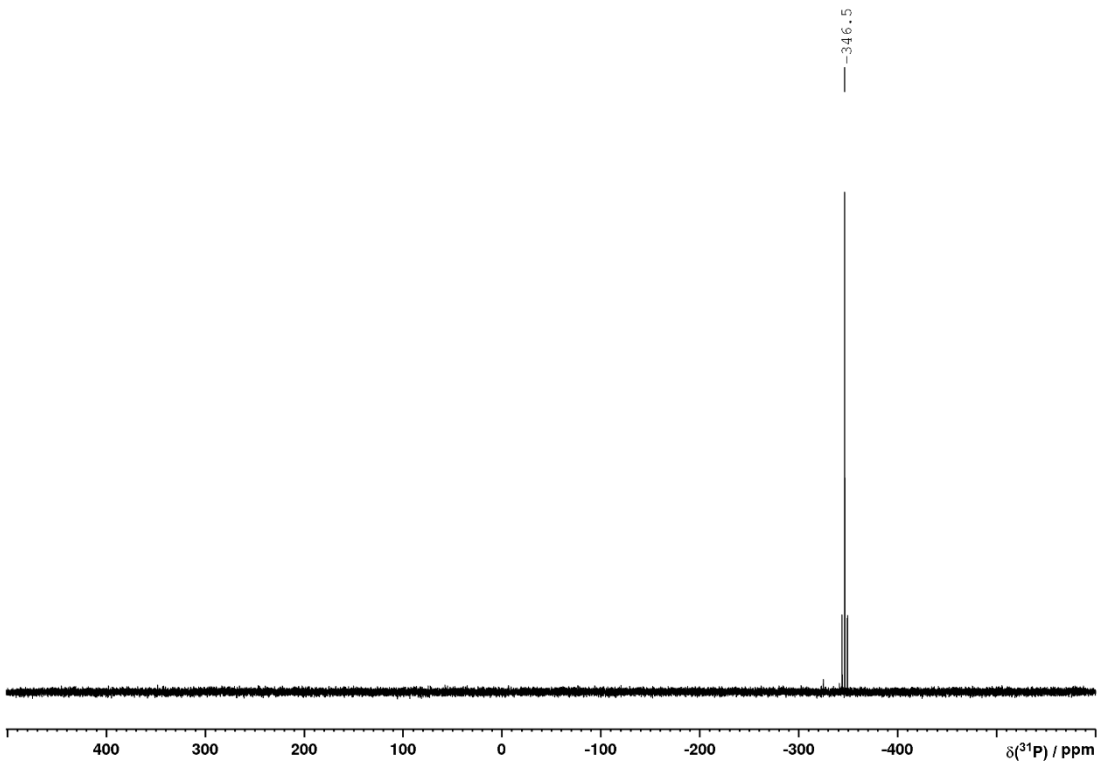

Figure S160. $^{31}P\{^{1}H\}$ NMR spectrum of $(Bu_3Sn)_3P$ (**4**) in C_6D_6.

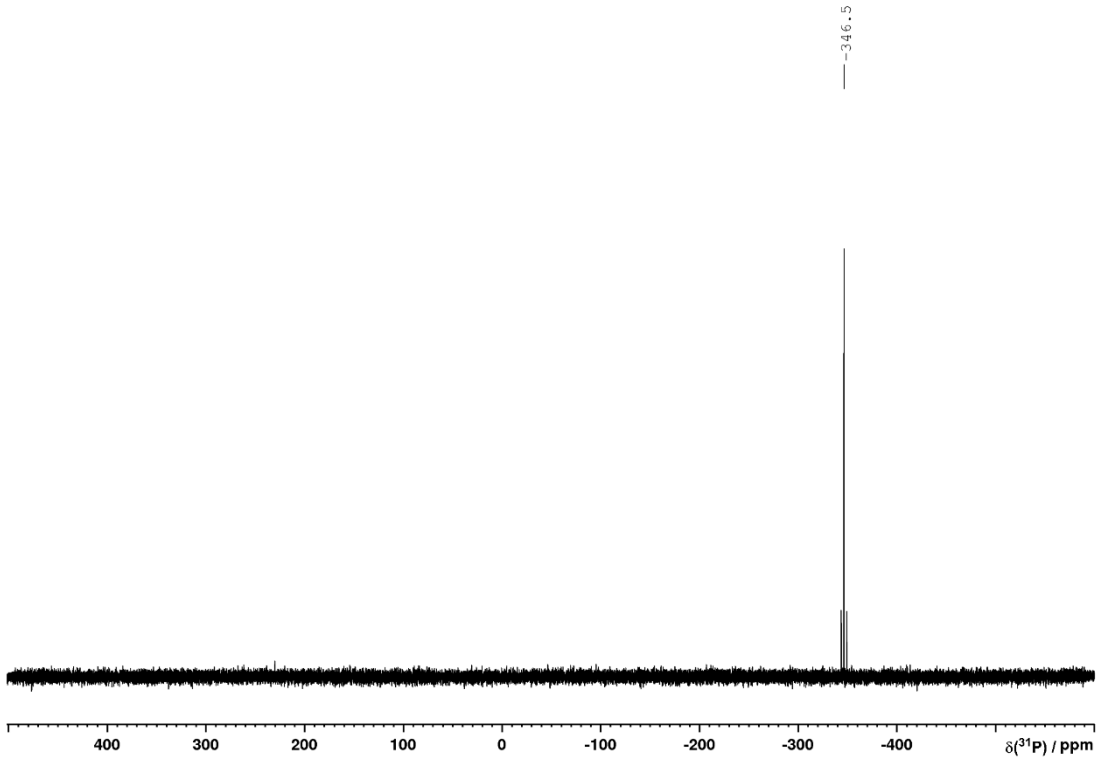

Figure S161. ^{31}P NMR spectrum of $(Bu_3Sn)_3P$ (**4**) in C_6D_6.

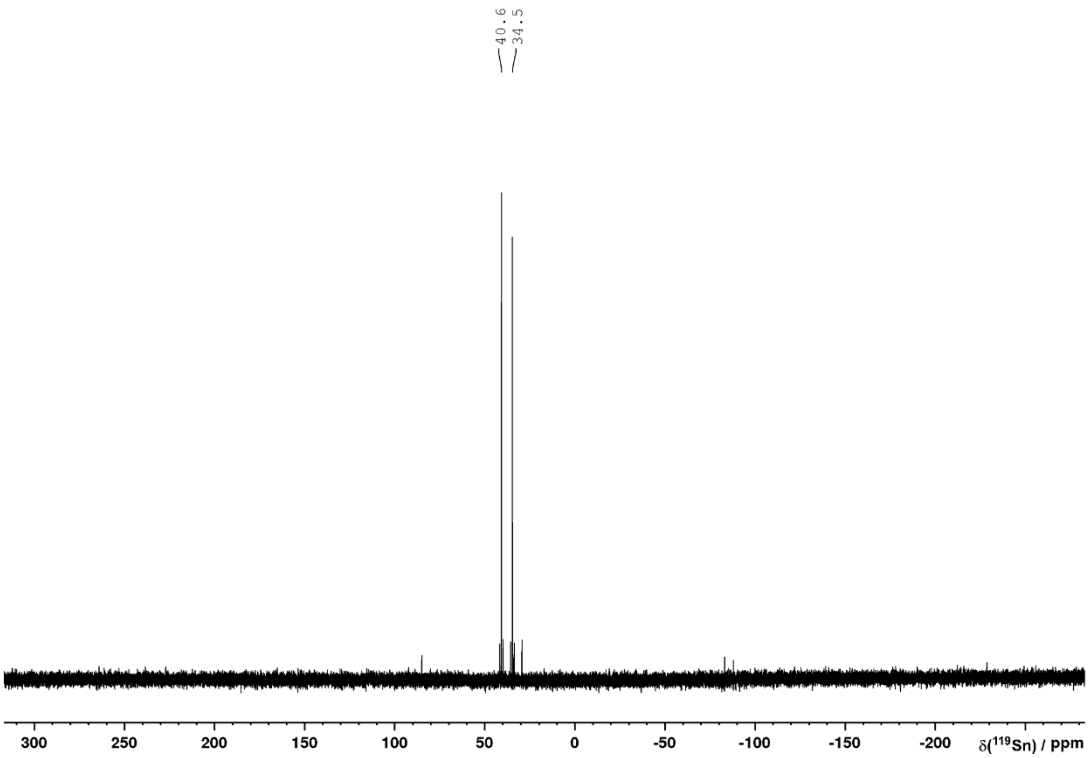

Figure S162. $^{119}Sn\{^{1}H\}$ NMR spectrum of $(Bu_3Sn)_3P$ (**4**) in C_6D_6.

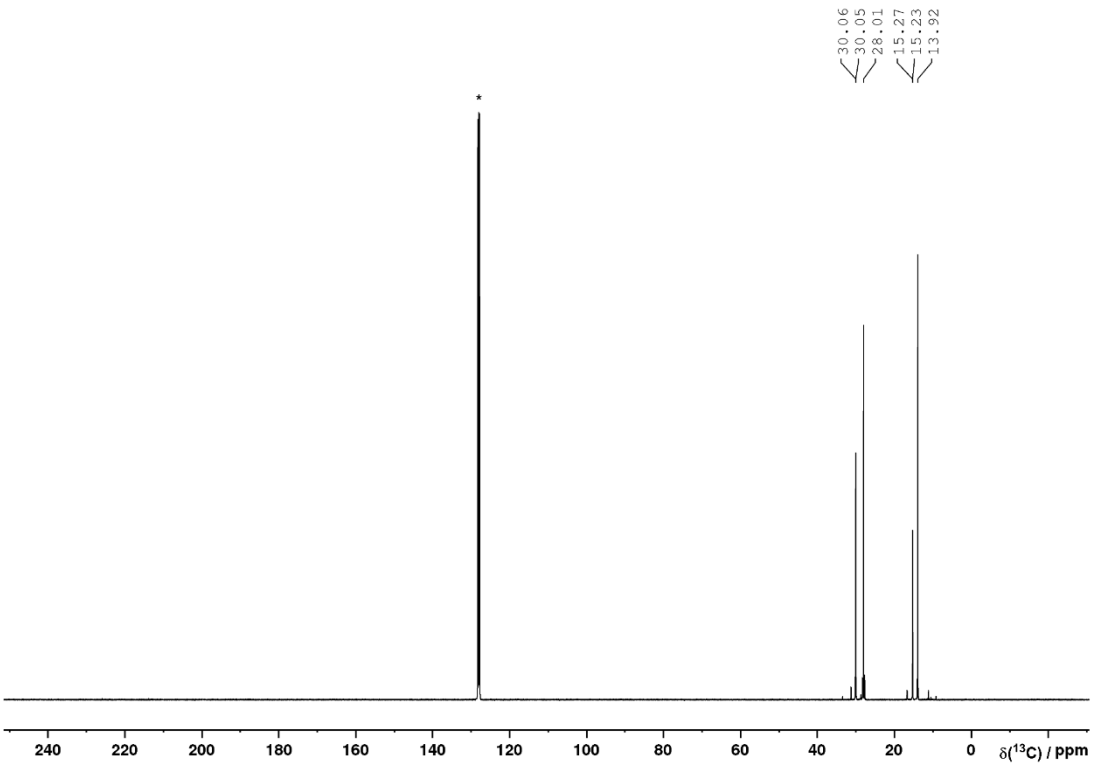

Figure S163. $^{13}C\{^{1}H\}$ NMR spectrum of $(Bu_3Sn)_3P$ (**4**) in C_6D_6 (*).

3.4.3 Synthesis and Isolation of Products Derived from $(Bu_3Sn)_3P$

3.4.3.1 Synthesis and isolation of THPC (5) *via* stannylation of P_{red} using Bu_3SnH and Bu_3SnOMe with recovery of Bu_3SnCl (6)

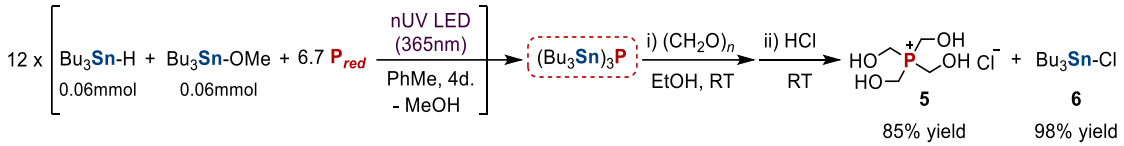

To provide sufficient material for reliable yield determination, a total of twelve reactions were performed in parallel using the following procedure: To a 10 mL, flat-bottomed, stoppered tube were added P_{red} (0.4 mmol, 12.4 mg), PhMe (50 µL), Bu_3SnH (16.1 µL, 0.06 mmol) and Bu_3SnOMe (17.3 µL, 0.06 mmol). The tube was sealed, placed in a water-cooled block to maintain near-ambient temperature, and irradiated with UV light (365 nm, 4.3 V, 700 mA, Osram OSLON SSL 80) for 4 days. The twelve reactions were then combined in a 100 mL Schlenk using PhMe (3 x 0.5 mL) to transfer and wash each tube. The combined red suspension was filtered and the remaining solid extracted with additional PhMe (2 x 10 mL), followed by removal of volatiles under vacuum. EtOH (10 mL) and paraformaldehyde (180.2 mg, 6.0 mmol) were added to the oily residue, and the resulting suspension was stirred at room temperature for 16 h. The mixture was frozen in a liquid-nitrogen bath, and HCl (4.0 M in 1,4-dioxane, 1.2 mL, 4.8 mmol) was added. After thawing, the reaction mixture was stirred at room temperature for 2 h. Volatiles from the resulting yellowish suspension were removed under vacuum. The remaining oily solid residue was triturated with Et_2O (10 mL) overnight, filtered and washed with further Et_2O (2 x 5 mL). The resulting white solid was then again dissolved in EtOH (10 mL). Following filtration and removal of volatiles under vacuum, the desired product (**5**) was obtained as a white solid (78.1 mg, 85%).

The combined Et_2O washes from the above reaction were dried under vacuum to afford Bu_3SnCl (**6**) as a pale yellow oil (461.4 mg, 98%). NMR data are identical to those given in section 3.4.1.3.

3.4.3.2 Synthesis and isolation of THP (9)

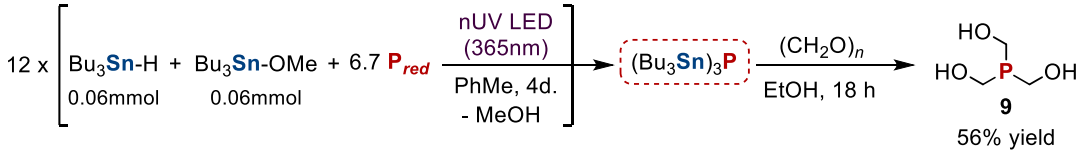

To provide sufficient material for reliable yield determination, a total of twelve reactions were performed in parallel using the following procedure: To a 10 mL, flat-bottomed, stoppered tube were added P_{red} (0.4 mmol, 12.4 mg), PhMe (50 µL), Bu_3SnH (16.1 µL, 0.06 mmol) and Bu_3SnOMe (17.3 µL, 0.06 mmol). The tube was sealed, placed in a water-cooled block to maintain near-ambient temperature, and irradiated with UV light (365 nm, 4.3 V, 700 mA, Osram OSLON SSL 80) for 4 days. The twelve reactions were then combined in a 100 mL Schlenk using PhMe (3 x 0.5 mL) to transfer and wash each tube. The combined red suspension was filtered and the remaining solid extracted with additional PhMe (2 x 10 mL), followed by removal of volatiles

under vacuum. EtOH (10 mL) and paraformaldehyde (180.2 mg, 6.0 mmol) were added to the oily residue, and the resulting suspension was stirred at room temperature for 16 h. Volatiles were removed under vacuum, and the oily residue was disolved in PhMe (10 mL). Following filtration, degassed H_2O (10 mL) was added to the solution. The biphasic mixture was thoroughly stirred for 30 min, the toluene phase was removed, and the aqueous phase was washed with further PhMe (2 x 10 mL). Following removal of volatiles from the aqueous phase under vacuum, THP (**9**) was obtained as a colourless oil (33.4 mg, 56%).

^{1}H NMR (400 MHz, 300 K, D_2O): δ = 3.99 ppm (d, $^{2}J(^{31}P\text{-}^{1}H)$ = 5.2 Hz). **^{31}P{^{1}H} NMR** (121 MHz, 300 K, D_2O): δ = –23.6 ppm (s). **^{31}P NMR** (121 MHz, 300 K, D_2O): δ = –23.6 ppm (s). **^{13}C{^{1}H} NMR** (101 MHz, 300 K, D_2O): δ = 56.4 ppm (d, $^{1}J(^{31}P\text{-}^{13}C)$ = 8.5 Hz). NMR data are consistent with our previous report.[13]

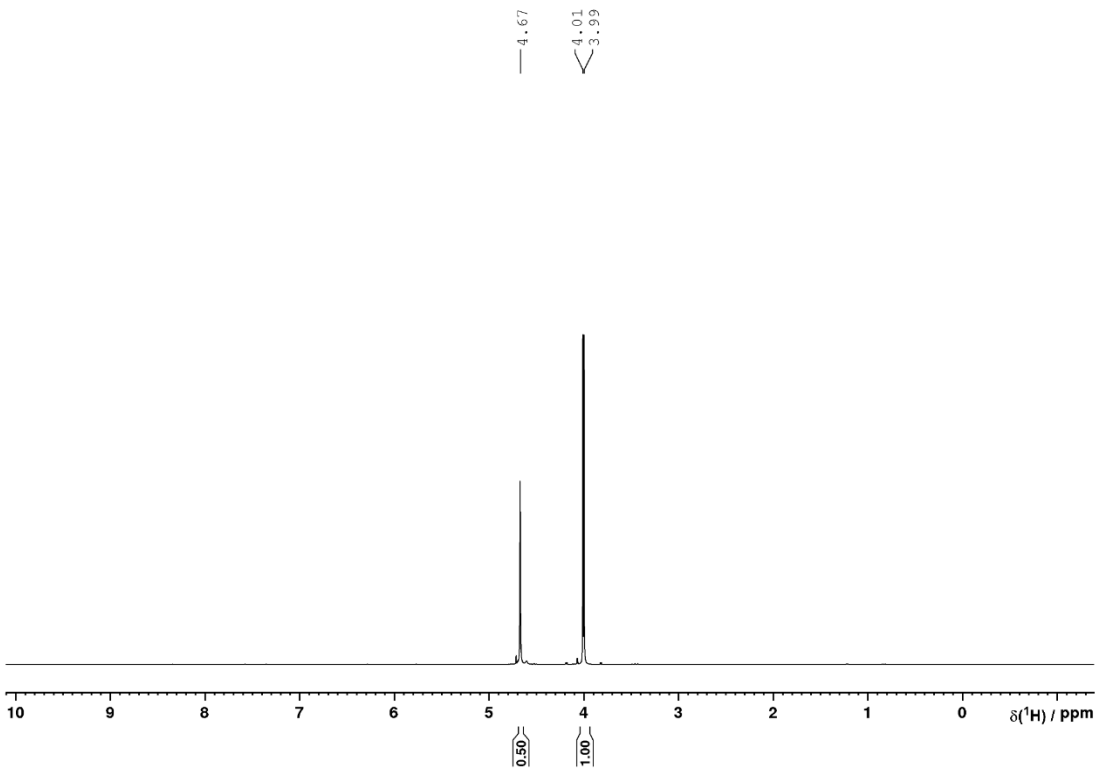

Figure S164. ^{1}H NMR spectrum of THP (**9**) in D_2O.

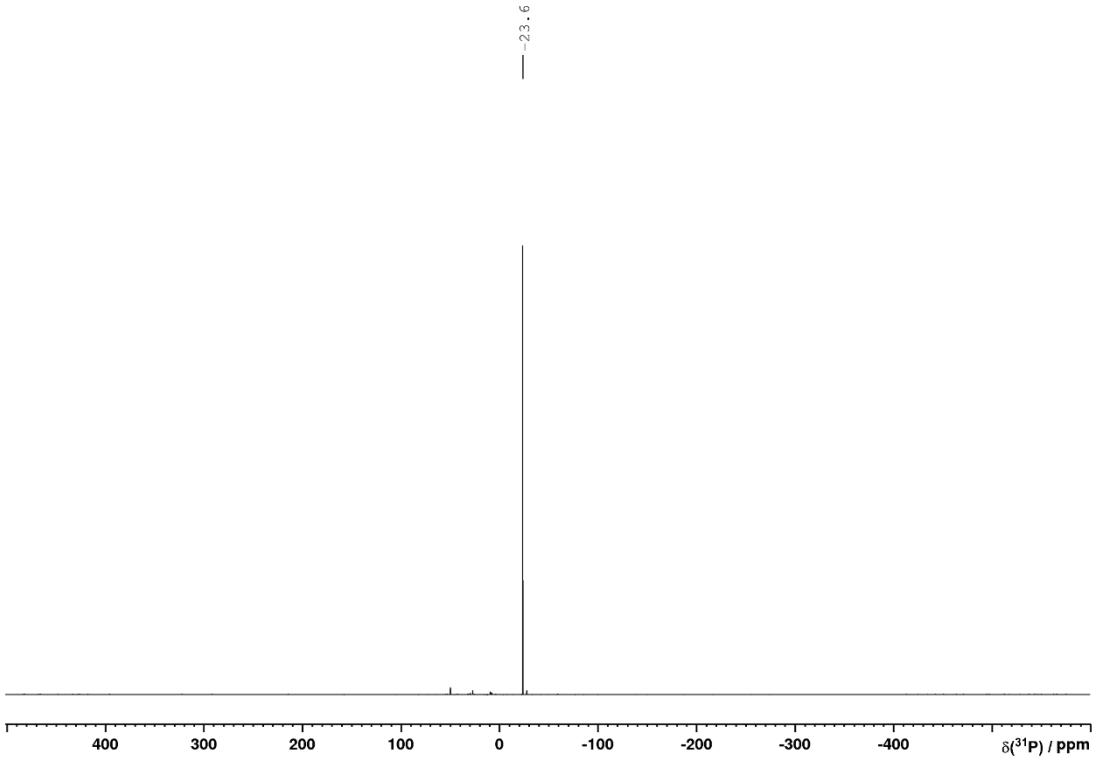

Figure S165. $^{31}P\{^{1}H\}$ NMR spectrum of THP (**9**) in D_2O.

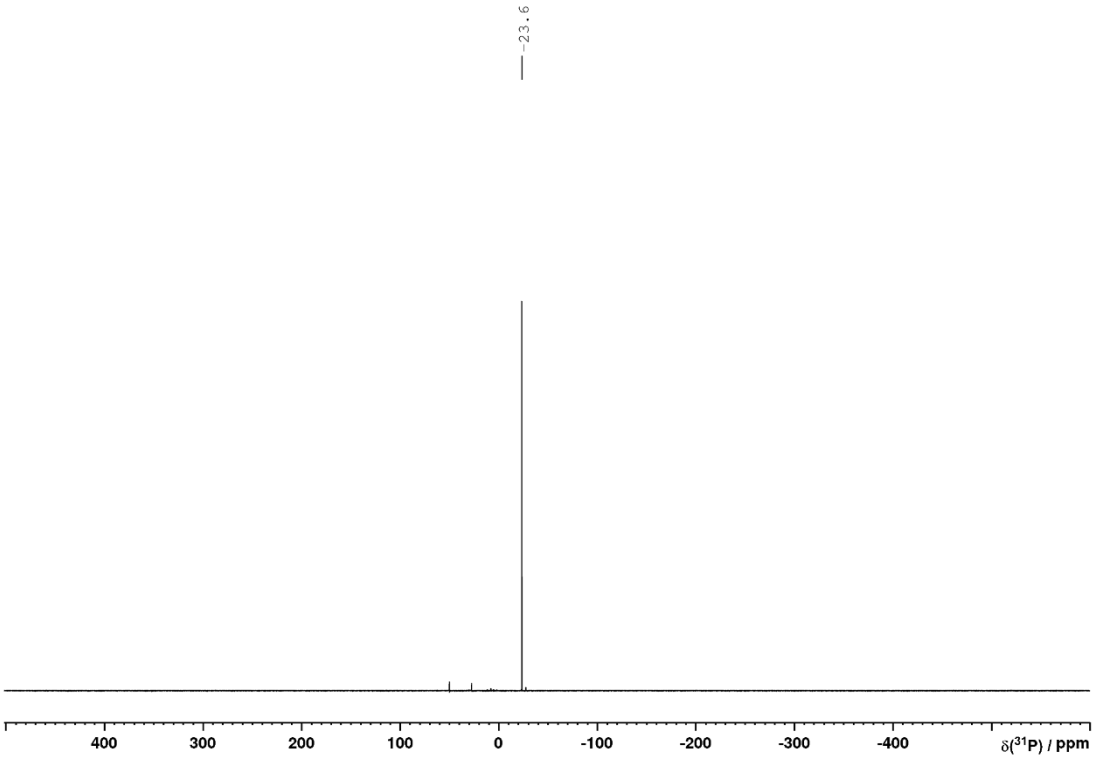

Figure S166. ^{31}P NMR spectrum of THP (**9**) in D_2O.

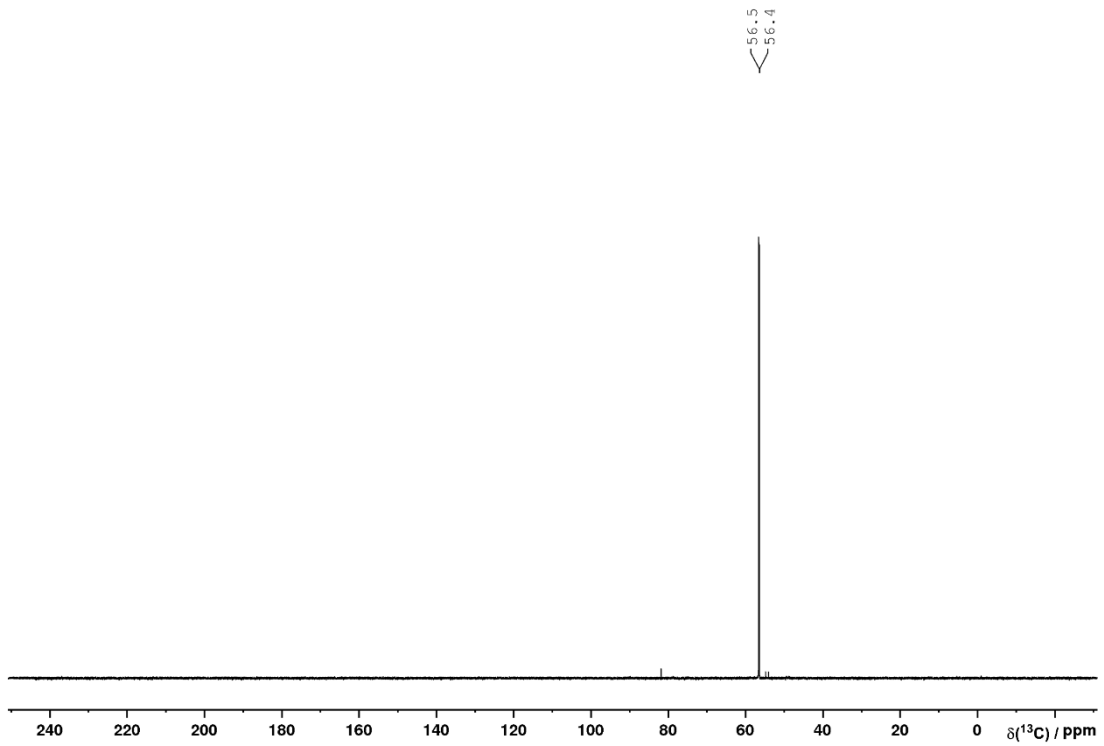

Figure S167. $^{13}C\{^{1}H\}$ NMR spectrum of THP (**9**) in D_2O.

3.4.3.3 Synthesis and isolation of $(HOCH_2)_3PO$ (10)

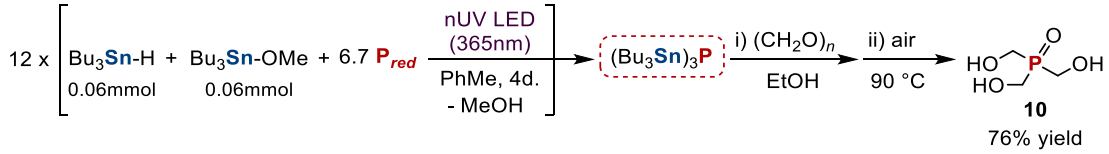

To provide sufficient material for reliable yield determination, a total of twelve reactions were performed in parallel using the following procedure: To a 10 mL, flat-bottomed, stoppered tube were added P_{red} (0.4 mmol, 12.4 mg), PhMe (50 µL), Bu_3SnH (16.1 µL, 0.06 mmol) and Bu_3SnOMe (17.3 µL, 0.06 mmol). The tube was sealed, placed in a water-cooled block to maintain near-ambient temperature, and irradiated with UV light (365 nm, 4.3 V, 700 mA, Osram OSLON SSL 80) for 4 days. The twelve reactions were then combined in a 100 mL Schlenk using PhMe (3 x 0.5 mL) to transfer and wash each tube. The combined red suspension was filtered and the remaining solid extracted with additional PhMe (2 x 10 mL), followed by removal of volatiles under vacuum. EtOH (10 mL) and paraformaldehyde (180.2 mg, 6.0 mmol) were added to the oily residue, and the resulting suspension was stirred at room temperature for 16 h. The resulting suspension was filtered and volatiles were removed under vacuum. Additional work-up was performed under air. To the oily residue thus obtained was added PhMe (10 mL) and H_2O (10 mL). The biphasic mixture was thoroughly stirred for 30 min and the aqueous phase was separated and washed with additional PhMe (3 x 10 mL), before being heated to 90 °C for 18 h while being kept open to air. Subsequent removal of volatiles yielded $(HOCH_2)_3PO$ (**10**) as a colourless oil (51.1 mg, 76%).

^{1}H NMR (400 MHz, 300 K, D_2O): δ = 4.04 ppm (d, $^{2}J(^{31}P\text{-}^{1}H)$ = 3.0 Hz). **$^{31}P\{^{1}H\}$ NMR** (121 MHz, 300 K, D_2O): δ = 49.7 ppm (s). **^{31}P NMR** (121 MHz, 300 K, D_2O): δ = 49.7 ppm (s). **$^{13}C\{^{1}H\}$ NMR** (101 MHz, 300 K, D_2O): δ = 54.3 ppm (d, $^{1}J(^{31}P\text{-}^{13}C)$ = 75.6 Hz). NMR data are consistent with our previous report.[13]

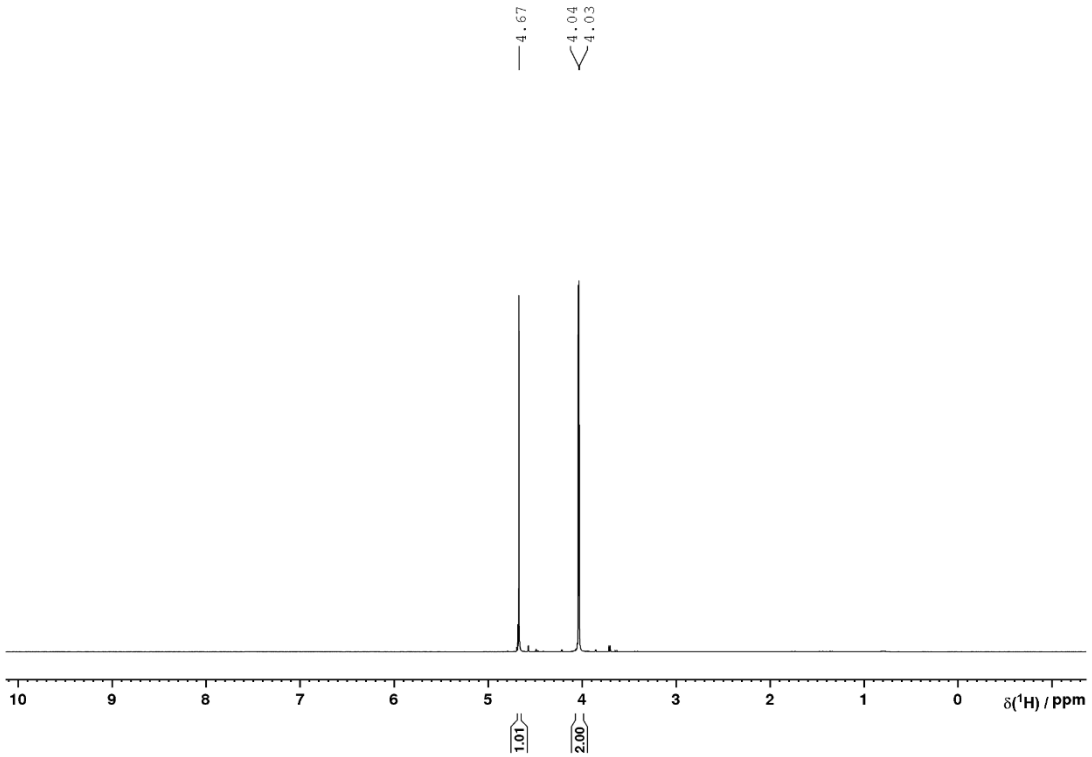

Figure S168. ^{1}H NMR spectrum of THPO (**10**) in D_2O.

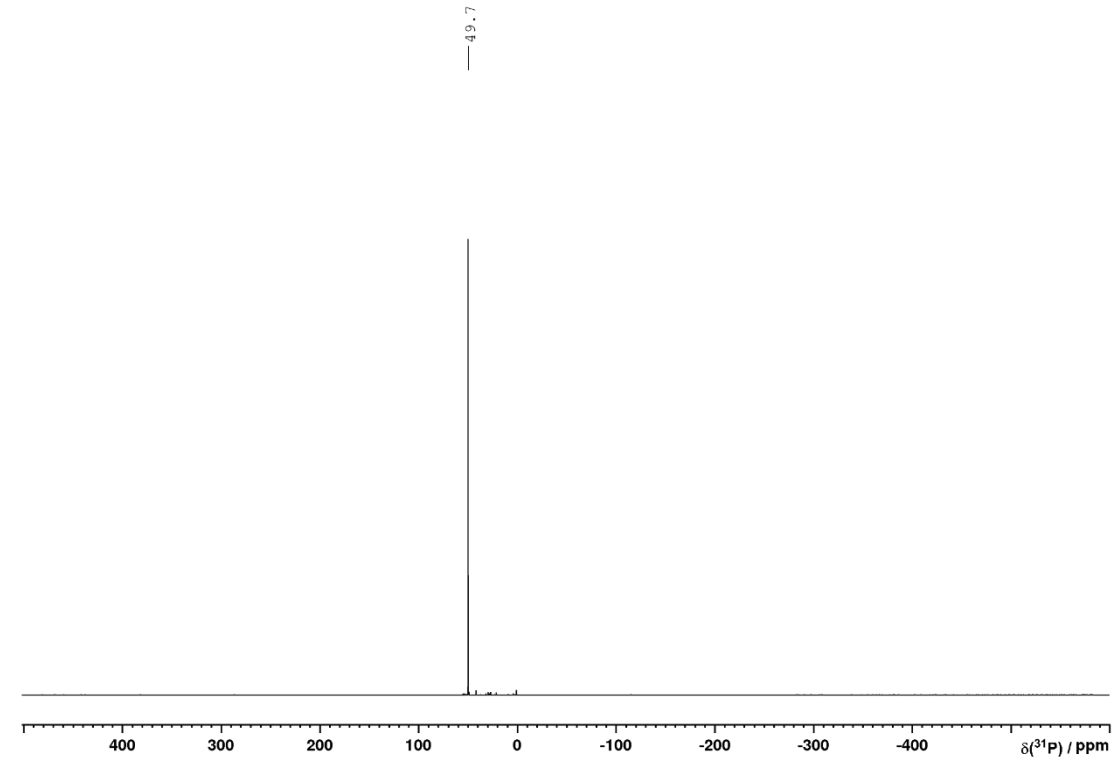

Figure S169. $^{31}P\{^{1}H\}$ NMR spectrum of THPO (**10**) in D_2O.

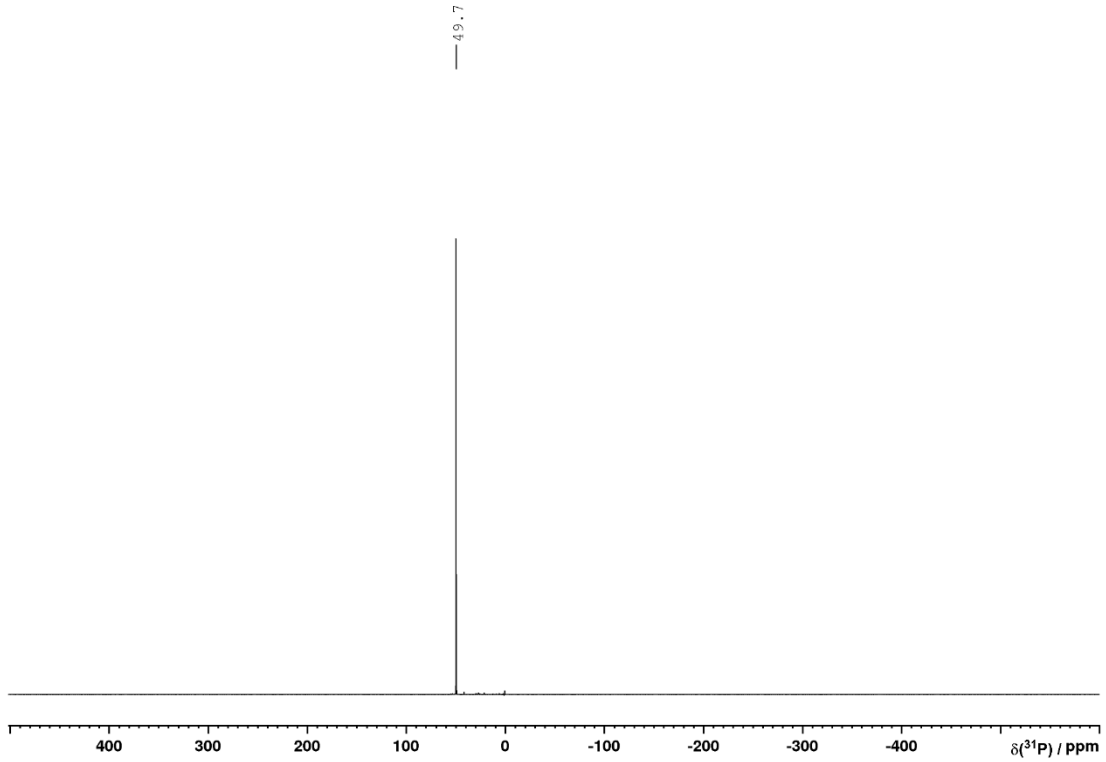

Figure S170. ^{31}P NMR spectrum of THPO (**10**) in D_2O.

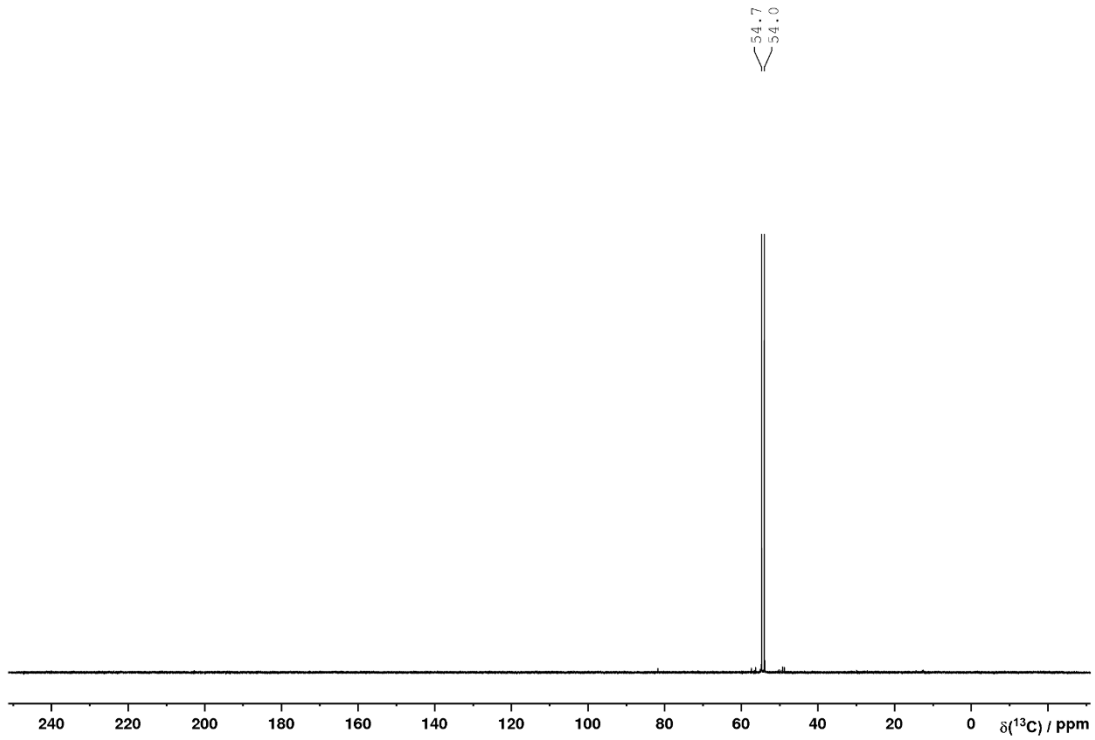

Figure S171. $^{13}C\{^1H\}$ NMR spectrum of THPO (**10**) in D_2O.

3.4.3.4 Synthesis and isolation of [Bn$_4$P]Br (7a)

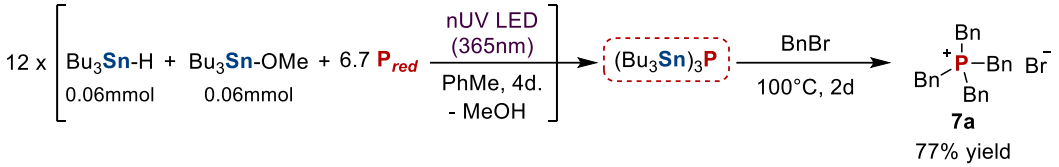

To provide sufficient material for reliable yield determination, a total of twelve reactions were performed in parallel using the following procedure: To a 10 mL, flat-bottomed, stoppered tube were added P_{red} (0.4 mmol, 12.4 mg), PhMe (50 µL), Bu_3SnH (16.1 µL, 0.06 mmol) and Bu_3SnOMe (17.3 µL, 0.06 mmol). The tube was sealed, placed in a water-cooled block to maintain near-ambient temperature, and irradiated with UV light (365 nm, 4.3 V, 700 mA, Osram OSLON SSL 80) for 4 days. The twelve reactions were then combined in a 100 mL Schlenk using PhMe (3 x 0.5 mL) to transfer and wash each tube. The combined red suspension was filtered and the remaining solid extracted with additional PhMe (2 x 10 mL), followed by removal of volatiles under vacuum. PhMe (10 mL) and benzyl bromide (571 µL, 4.8 mmol) were added to the oily residue, and heated to 100 °C with stirring for 2 days. After cooling to room temperature, volatiles from the reaction mixture were removed under vacuum. The remaining oily solid residue was triturated with hexane (10 mL) overnight, to give TBPB (**7a**) as a white solid (176.1 mg, 77%) after filtration, washing with additional hexane (2 x 10 mL) and drying under vacuum.

^{1}H NMR (400 MHz, 300 K, CD_3CN): δ = 7.36 ppm (3H, m), 7.15 ppm (2H, m), 3.73 ppm (2H, d, $^2J(^{31}P\text{-}^1H)$ = 14.3 Hz). **$^{31}P\{^1H\}$ NMR** (121 MHz, 300 K, CD_3CN): δ = 25.7 ppm (s). **^{31}P NMR** (121 MHz, 300 K, CD_3CN): δ = 25.7 ppm (m). **$^{13}C\{^1H\}$ NMR** (101 MHz, 300 K, C_6D_6): δ = 131.6 (d, $J(^{31}P\text{-}^1H)$ = 5.3 Hz), 130.2 (d, $J(^{31}P\text{-}^1H)$ = 2.9 Hz), 129.3 (d, $J(^{31}P\text{-}^1H)$ = 3.4 Hz), 128.8 (d, $J(^{31}P\text{-}^1H)$ = 8.1 Hz), 27.4 ppm (d, $J(^{31}P\text{-}^1H)$ = 43.2 Hz). NMR data are consistent with our previous report. [13]

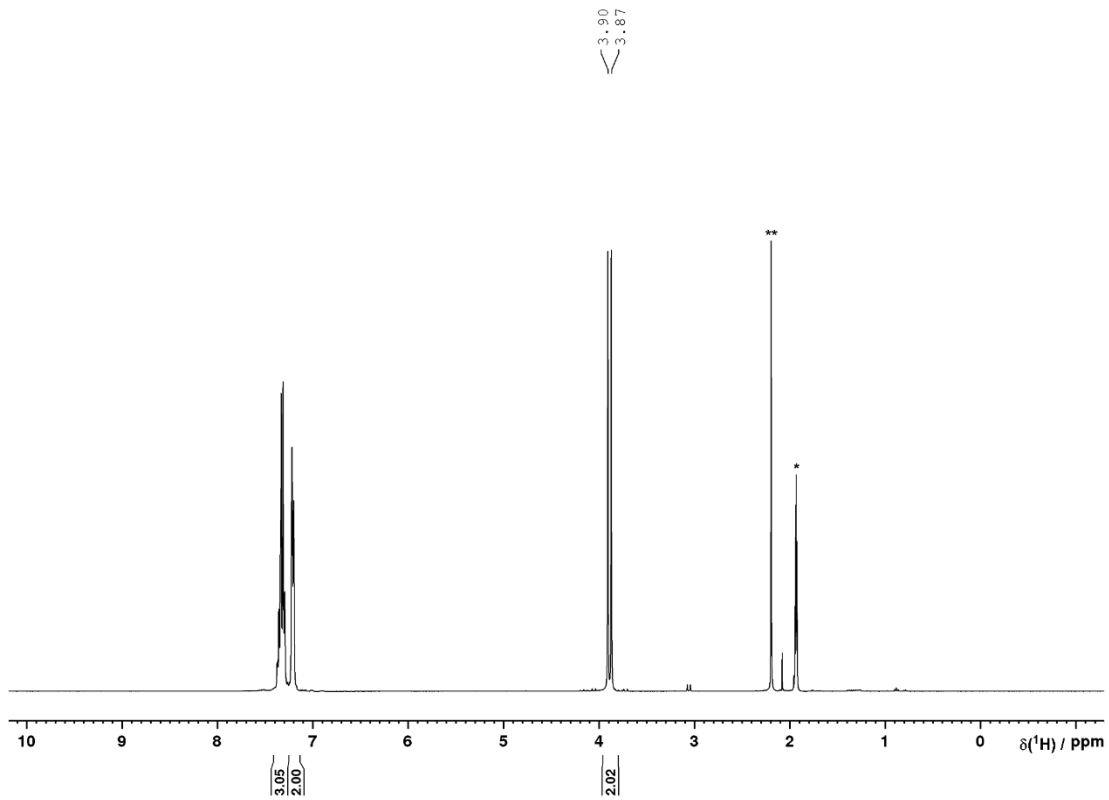

Figure S172. ^{1}H NMR spectrum of [Bn_4P]Br (**7a**) in CD_3CN (*solvent, **H_2O).

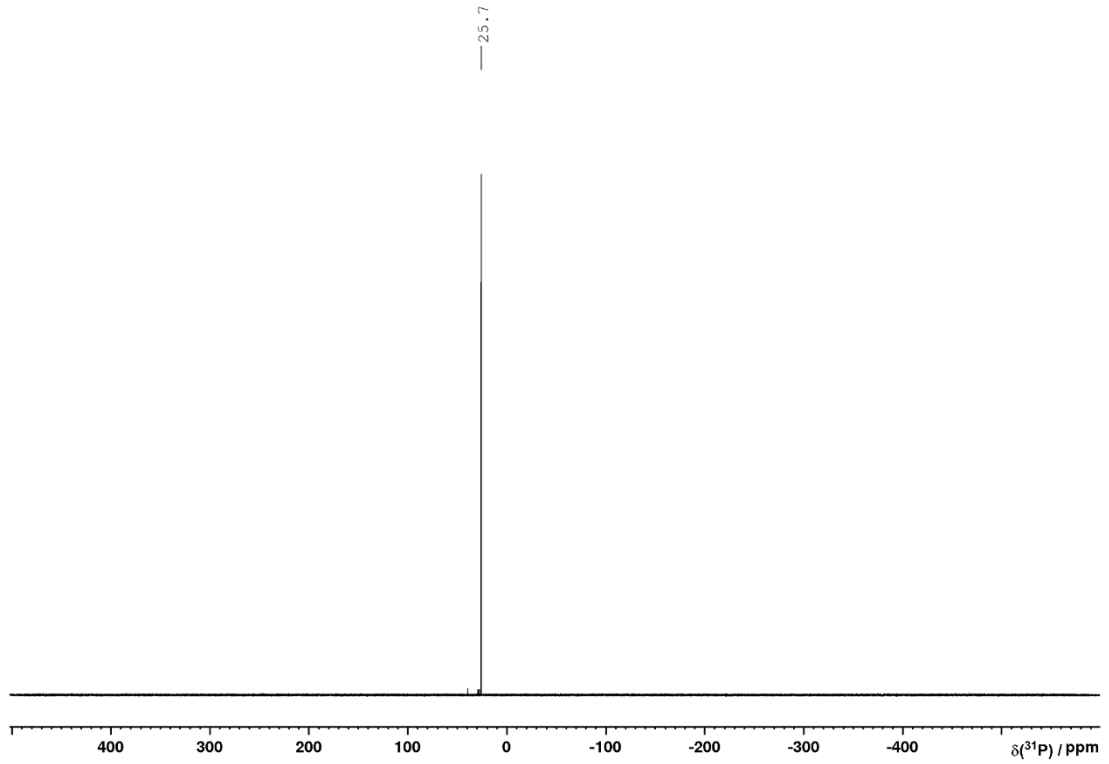

Figure S173. $^{31}P\{^{1}H\}$ NMR spectrum of [Bn_4P]Br (**7a**) in CD_3CN.

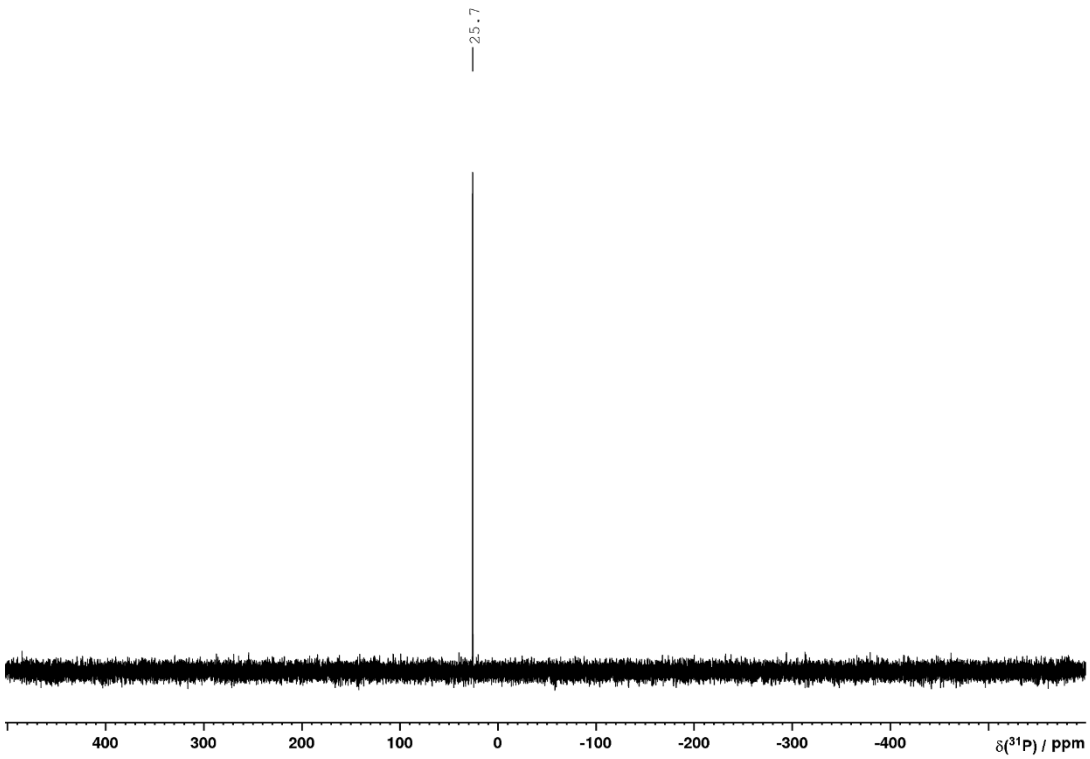

Figure S174. ^{31}P NMR spectrum of [Bn_4P]Br (**7a**) in CD_3CN.

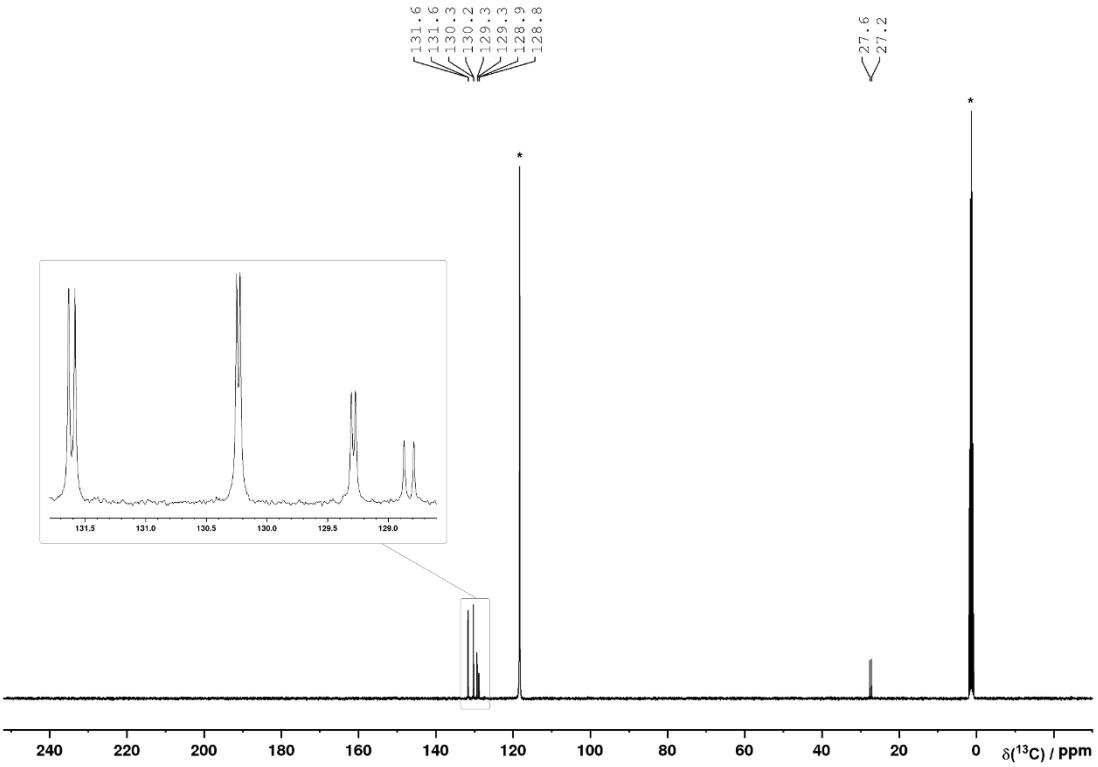

Figure S175. $^{13}C\{^1H\}$ NMR spectrum of [Bn_4P]Br (**7a**) in CD_3CN (*).

3.4.3.5 Synthesis and isolation of [Et$_4$P]Br (7b)

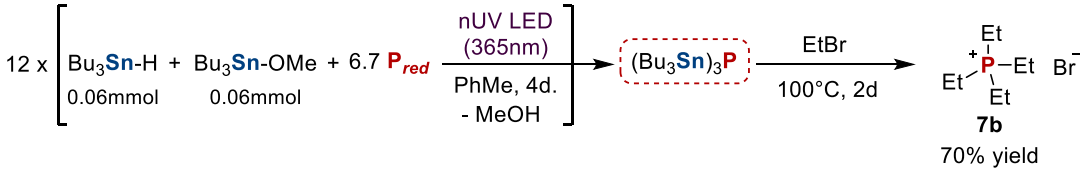

To provide sufficient material for reliable yield determination, a total of twelve reactions were performed in parallel using the following procedure: To a 10 mL, flat-bottomed, stoppered tube were added P_{red} (0.4 mmol, 12.4 mg), PhMe (50 µL), Bu_3SnH (16.1 µL, 0.06 mmol) and Bu_3SnOMe (17.3 µL, 0.06 mmol). The tube was sealed, placed in a water-cooled block to maintain near-ambient temperature, and irradiated with UV light (365 nm, 4.3 V, 700 mA, Osram OSLON SSL 80) for 4 days. The twelve reactions were then combined in a 100 mL Schlenk using PhMe (3 x 0.5 mL) to transfer and wash each tube. The combined red suspension was filtered and the remaining solid extracted with additional PhMe (2 x 10 mL), followed by removal of volatiles under vacuum. PhMe (10 mL) and ethyl bromide (358 µL, 4.8 mmol) were added to the oily residue, and heated to 100 °C with stirring for 2 days. After cooling to room temperature, volatiles from the reaction mixture were removed under vacuum. The remaining oily solid residue was triturated with hexane (10 mL) overnight, to give TEPB (**7b**) as a white solid (76.4 mg, 70%) after filtration, washing with additional hexane (2 x 10 mL) and drying under vacuum.

^{1}H NMR (400 MHz, 300 K, CD_3CN): δ = 2.19 ppm (2H, dq, $^2J(^{31}P\text{-}^1H)$ = 13.0 Hz, $^3J(^1H\text{-}^1H)$ = 7.7 Hz), 1.19 ppm (3H, dt, $^3J(^{31}P\text{-}^1H)$ = 18.0 Hz, $^3J(^1H\text{-}^1H)$ = 7.7 Hz). **^{31}P{^{1}H} NMR** (121 MHz, 300 K, CD_3CN): δ = 42.2 ppm (s). **^{31}P NMR** (121 MHz, 300 K, CD_3CN): δ = 42.2 ppm (m). **^{13}C{^{1}H} NMR** (101 MHz, 300 K, CD_3CN): δ = 11.7 (d, $^1J(^{31}P\text{-}^1H)$ = 49.5 Hz), 5.7 ppm (d, $^2J(^{31}P\text{-}^1H)$ = 5.4 Hz). NMR data are consistent with our previous report.[13]

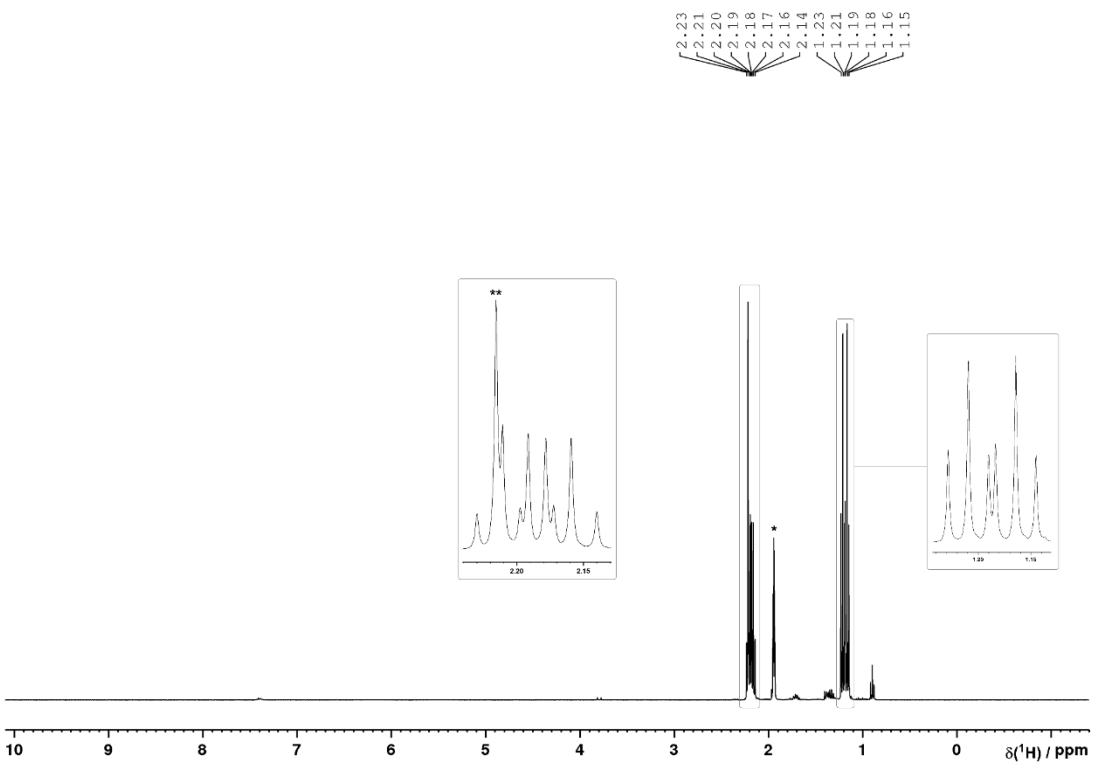

Figure S176. ^{1}H NMR spectrum of [Et_4P]Br (**7b**) in CD_3CN (* solvent, **H_2O).

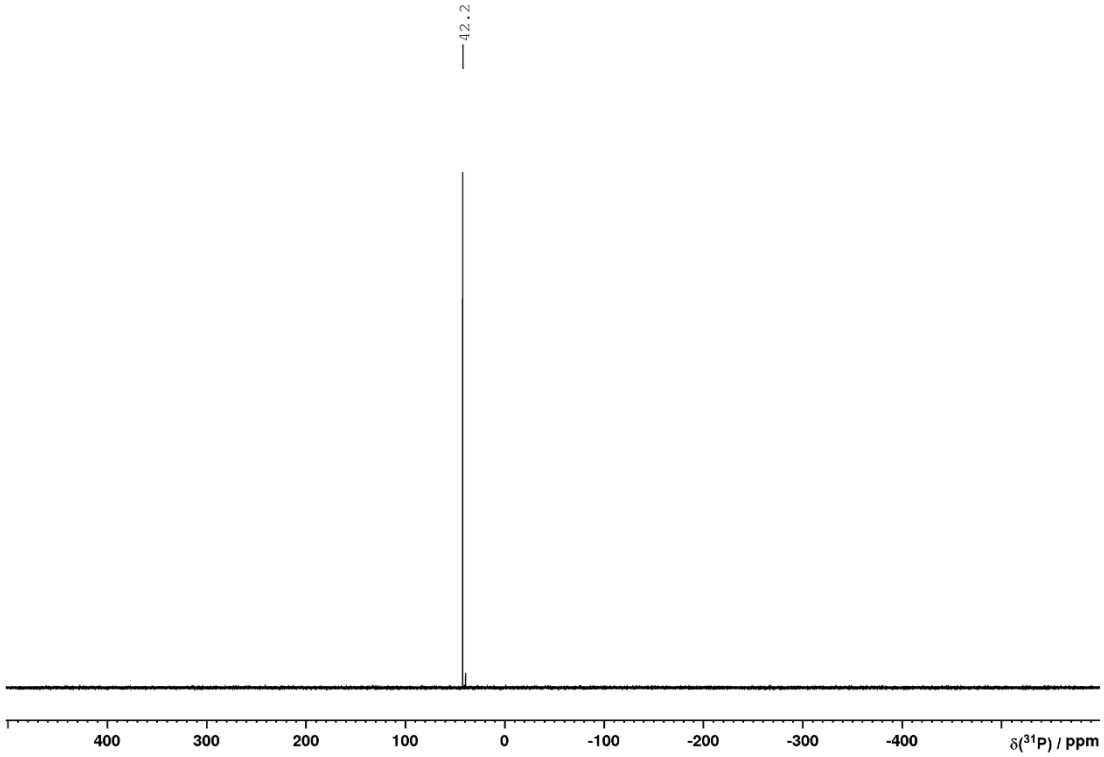

Figure S177. $^{31}P\{^{1}H\}$ NMR spectrum of [Et_4P]Br (**7b**) in CD_3CN.

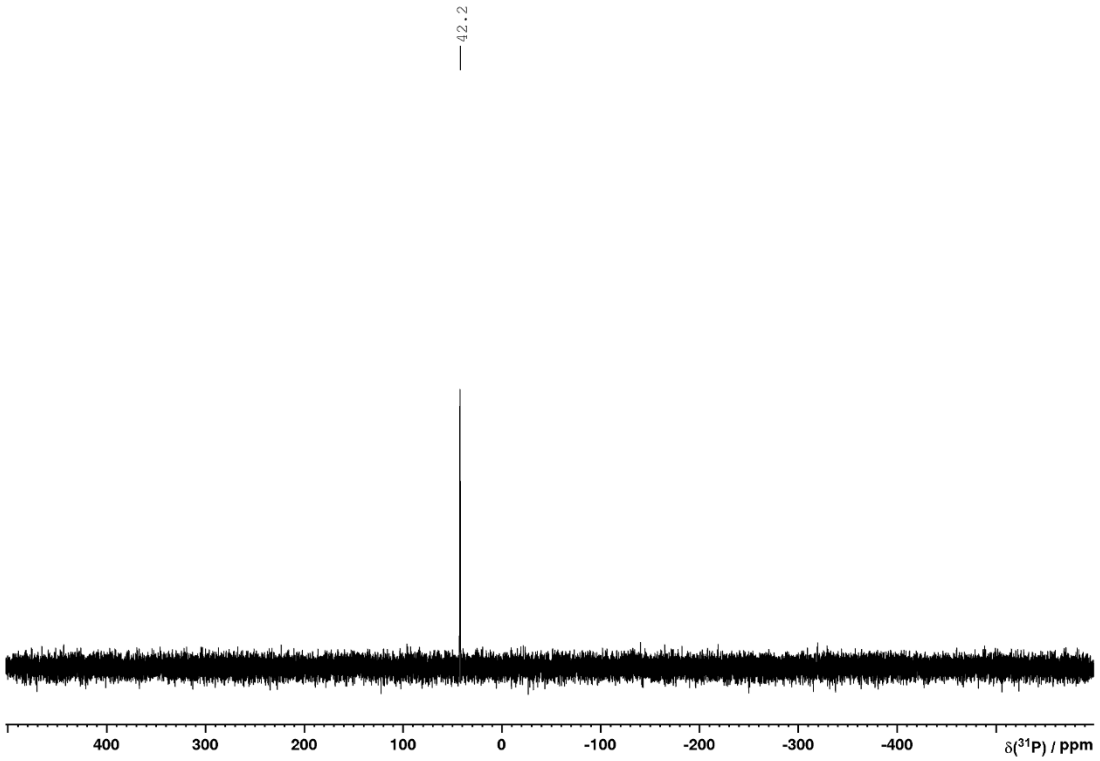

Figure S178. ^{31}P NMR spectrum of $[Et_4P]Br$ (**7b**) in CD_3CN.

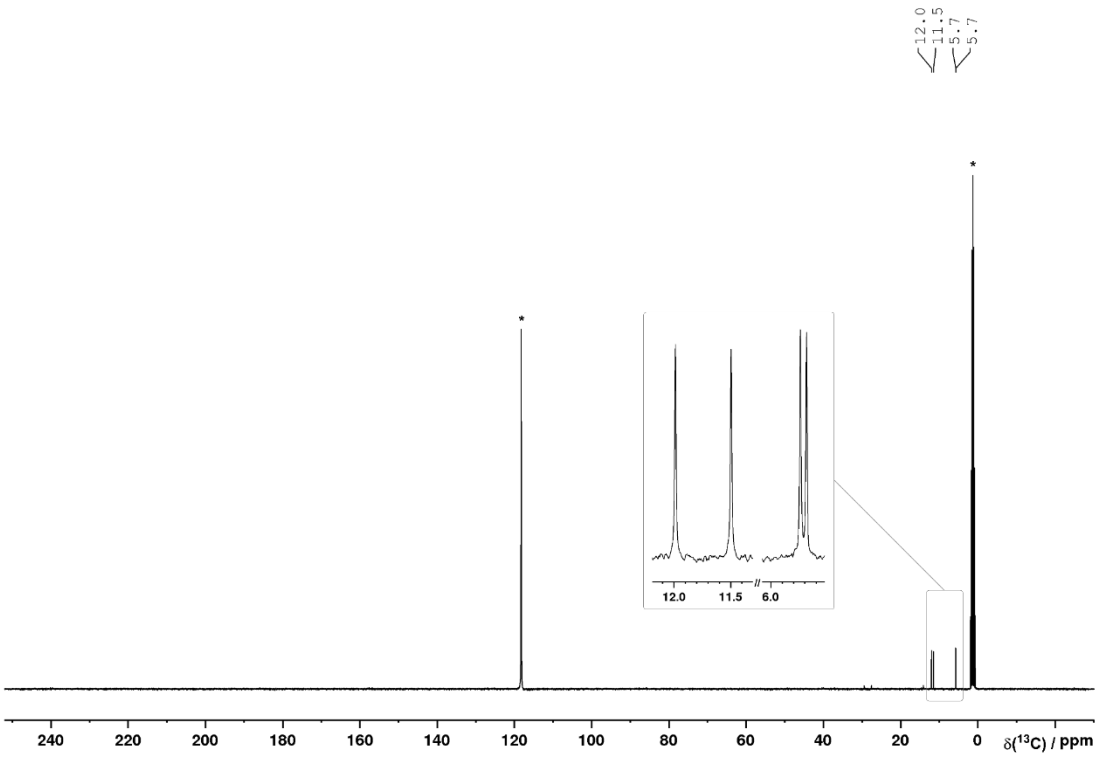

Figure S179. $^{13}C\{^1H\}$ NMR spectrum of $[Et_4P]Br$ (**7b**) in CD_3CN (*).

3.4.3.6 Synthesis and isolation of P(C(O)Ph)$_3$ (8a)

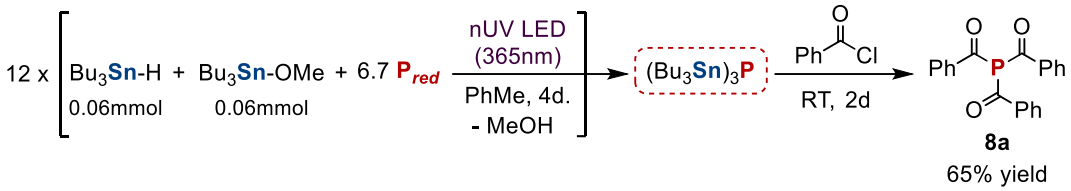

To provide sufficient material for reliable yield determination, a total of twelve reactions were performed in parallel using the following procedure: To a 10 mL, flat-bottomed, stoppered tube were added P_{red} (0.4 mmol, 12.4 mg), PhMe (50 µL), Bu_3SnH (16.1 µL, 0.06 mmol) and Bu_3SnOMe (17.3 µL, 0.06 mmol). The tube was sealed, placed in a water-cooled block to maintain near-ambient temperature, and irradiated with UV light (365 nm, 4.3 V, 700 mA, Osram OSLON SSL 80) for 4 days. The twelve reactions were then combined in a 100 mL Schlenk using PhMe (3 x 0.5 mL) to transfer and wash each tube. The combined red suspension was filtered and the remaining solid extracted with additional PhMe (2 x 10 mL), followed by removal of volatiles under vacuum. PhMe (10 mL) and PhC(O)Cl (223 µL, 1.92 mmol) were added to the oily residue, and the yellow mixture was stirred at room temperature for 2 days. Volatiles from the intense yellow mixture were removed under vacuum, and the remaining yellow solid was washed with *n*-hexane (3 x 10 mL). The remaining yellow residue was recrystallized from THF/*n*-hexane at –35 °C, to afford the desired product (**8a**) as yellow needles (108 mg, 65%).

^{1}H NMR (400 MHz, 300 K, C_6D_6): δ = 7.98 ppm (2H, m), 7.03 ppm (1H, tt, $^3J(^1H\text{-}^1H)$ =7.4 Hz, $^5J(^1H\text{-}^1H)$ =1.3 Hz), 6.96 ppm (2H, m). **^{31}P{^{1}H} NMR** (121 MHz, 300 K, C_6D_6): δ = 54.3 ppm (s). **^{31}P NMR** (121 MHz, 300 K, C_6D_6): δ = 54.3 ppm (s). **^{13}C{^{1}H} NMR** (101 MHz, 300 K, C_6D_6): δ = 205.8 (d, $J(^{31}P\text{-}^1H)$ = 32.8 Hz), 140.9 (d, $J(^{31}P\text{-}^1H)$ = 35.2 Hz), 133.9 (d, $J(^{31}P\text{-}^1H)$ = 1.1 Hz), 129.0 (d, $J(^{31}P\text{-}^1H)$ = 8.0 Hz), 128.9 ppm (d, $J(^{31}P\text{-}^1H)$ = 0.7 Hz). NMR data are consistent with our previous report.[13]

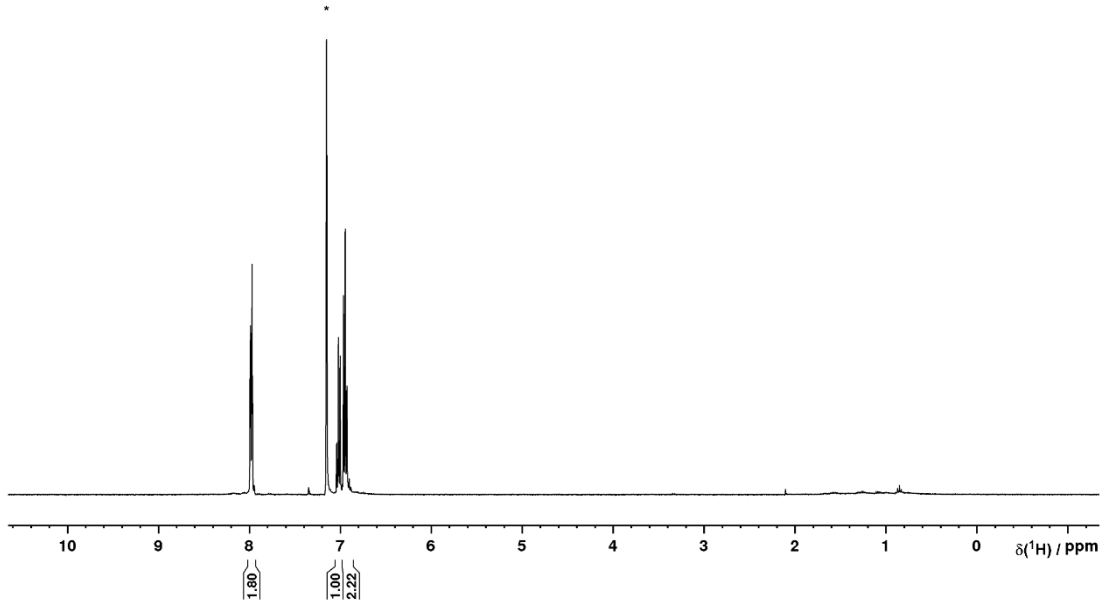

Figure S180. ^{1}H NMR spectrum of $P(C(O)Ph)_3$ (**8a**) in C_6D_6 (*).

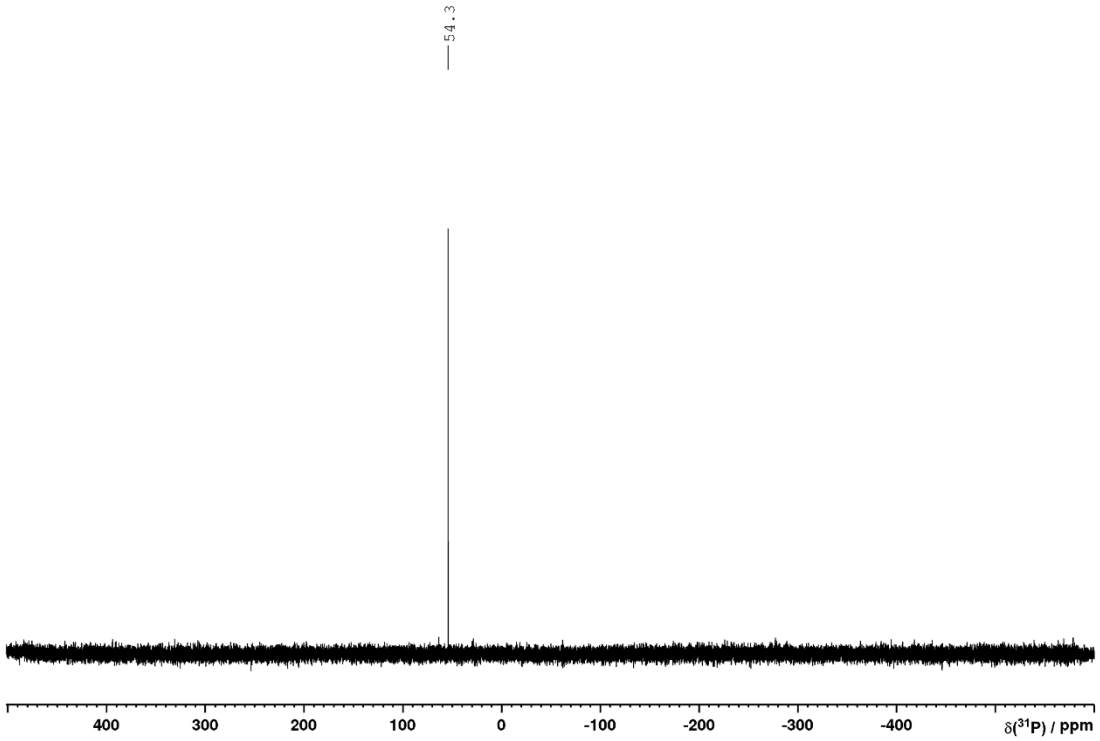

Figure S181. $^{31}P\{^{1}H\}$ NMR spectrum of $P(C(O)Ph)_3$ (**8a**) in C_6D_6.

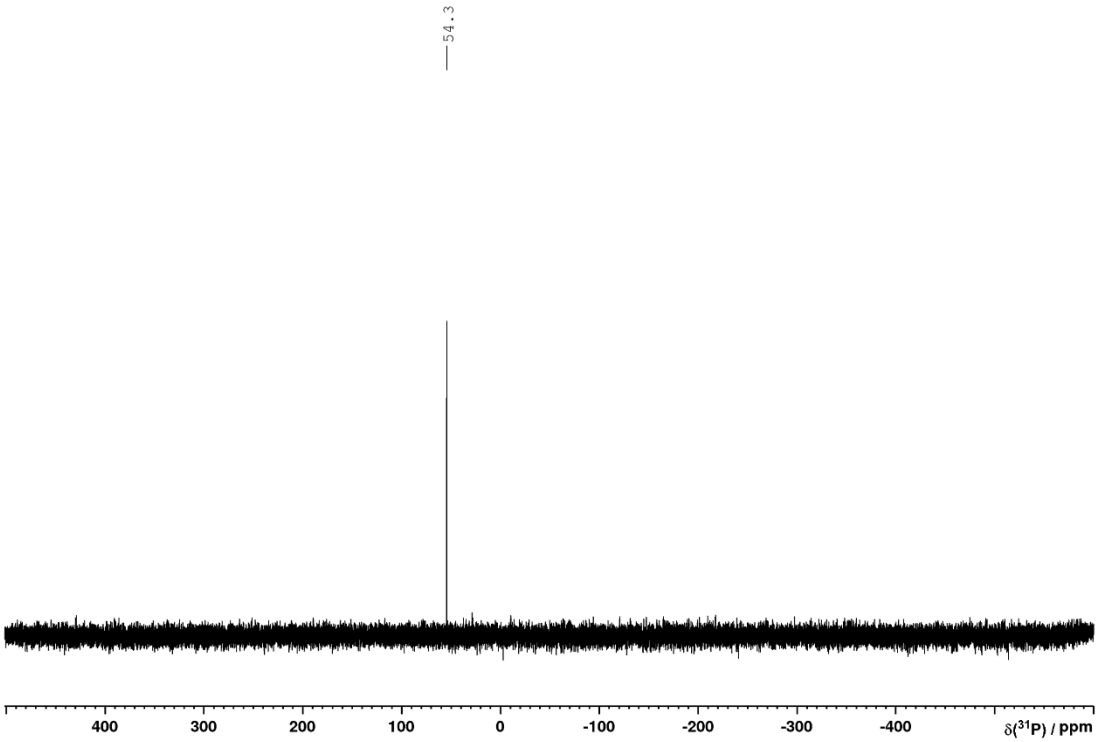

Figure S182. ^{31}P NMR spectrum of $P(C(O)Ph)_3$ (**8a**) in C_6D_6.

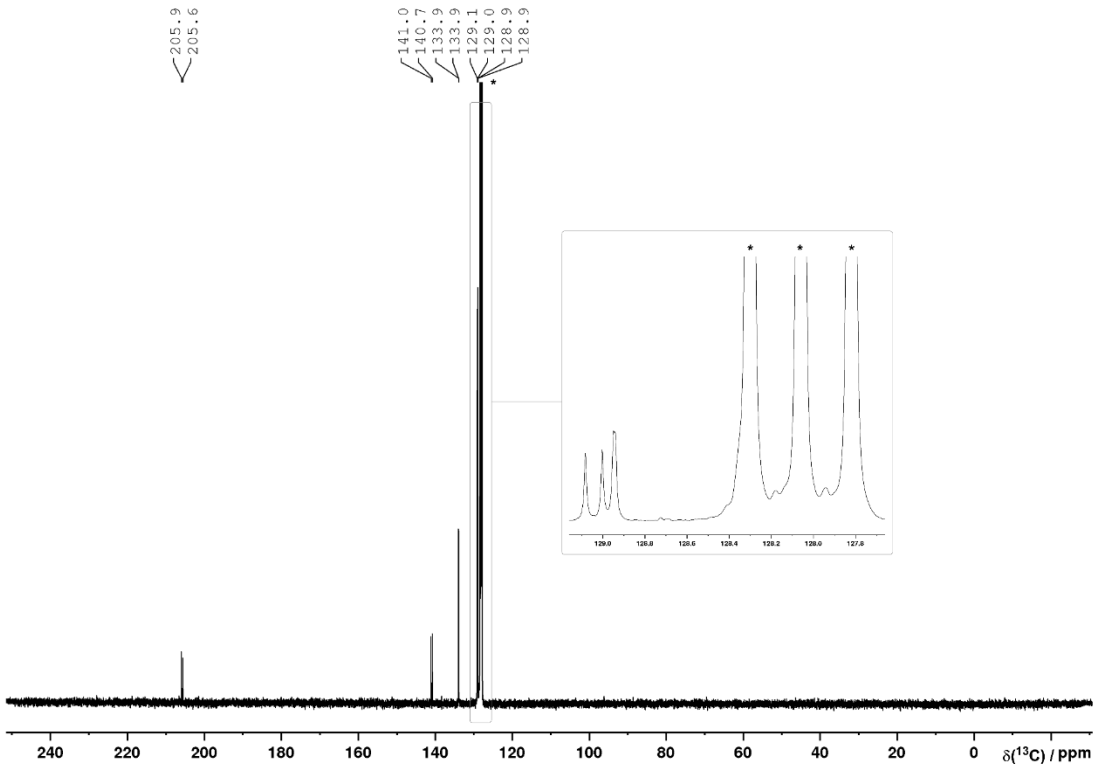

Figure S183. $^{13}C\{^1H\}$ NMR spectrum of $P(C(O)Ph)_3$ (**8a**) in C_6D_6. Solvent resonance (*) truncated for clarity.

3.4.3.7 Synthesis and isolation of P(C(O)*t*Bu)$_3$ (8b)

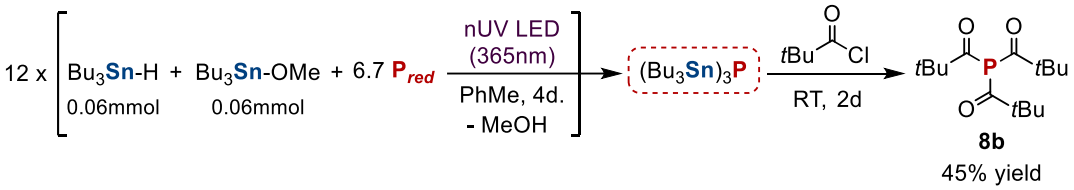

To provide sufficient material for reliable yield determination, a total of twelve reactions were performed in parallel using the following procedure: To a 10 mL, flat-bottomed, stoppered tube were added P_{red} (0.4 mmol, 12.4 mg), PhMe (50 µL), Bu_3SnH (16.1 µL, 0.06 mmol) and Bu_3SnOMe (17.3 µL, 0.06 mmol). The tube was sealed, placed in a water-cooled block to maintain near-ambient temperature, and irradiated with UV light (365 nm, 4.3 V, 700 mA, Osram OSLON SSL 80) for 4 days. The twelve reactions were then combined in a 100 mL Schlenk using PhMe (3 x 0.5 mL) to transfer and wash each tube. The combined red suspension was filtered and the remaining solid extracted with additional PhMe (2 x 10 mL), followed by removal of volatiles under vacuum. PhMe (10 mL) and *t*BuC(O)Cl (235 µL, 1.92 mmol) were added to the oily residue, and the yellowish mixture was stirred at room temperature for 1 day. Volatiles from the yellowish mixture were removed under vacuum, and the remaining yellow oily solid residue was recrystallized from *n*-hexane at −35 °C, to afford the desired product (**8b**) as colourless needles (62 mg, 45%).

^{1}H NMR (400 MHz, 300 K, C_6D_6): δ = 1.08 ppm (s). **^{31}P{^{1}H} NMR** (121 MHz, 300 K, C_6D_6): δ = 51.6 ppm (s). **^{31}P NMR** (121 MHz, 300 K, C_6D_6): δ = 51.6 ppm (s). **^{13}C{^{1}H} NMR** (101 MHz, 300 K, C_6D_6): δ = 221.3 (d, $^1J(^{31}P\text{-}^1H)$ = 47.9 Hz), 49.7 (d, $^2J(^{31}P\text{-}^1H)$ = 30.3 Hz), 25.4 ppm (d, $^3J(^{31}P\text{-}^1H)$ = 3.7 Hz). NMR data are consistent with our previous report.[13]

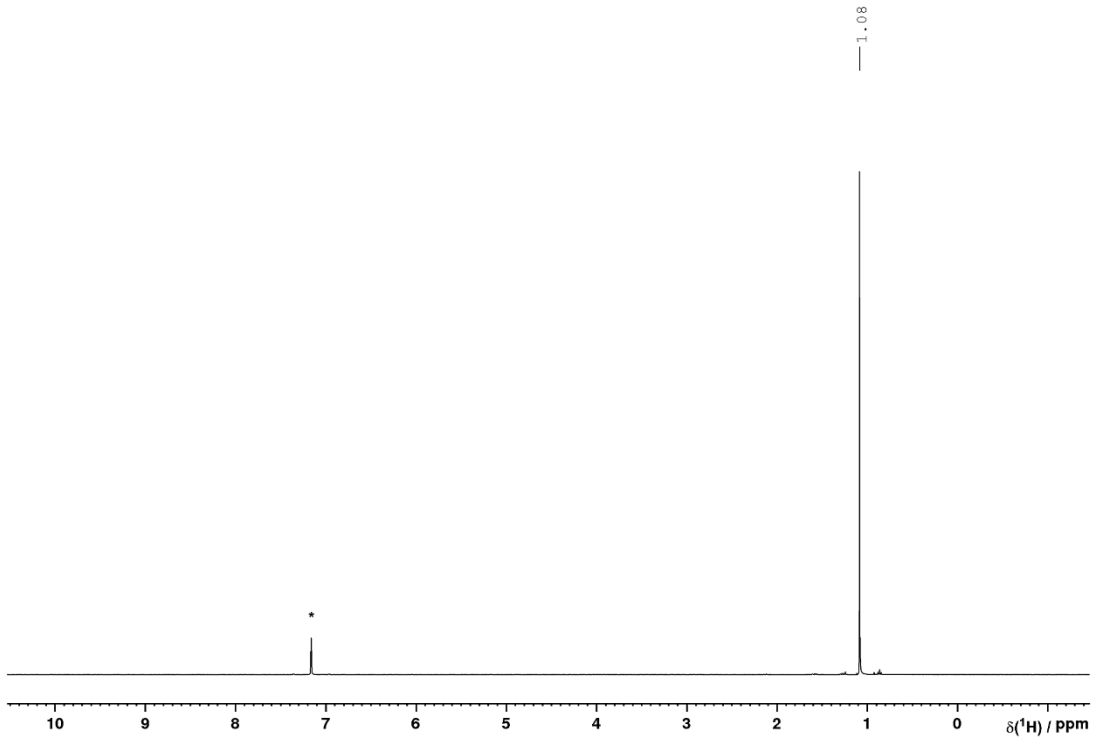

Figure S184. ^{1}H NMR spectrum of $P(C(O)tBu)_3$ (**8b**) in C_6D_6 (*).

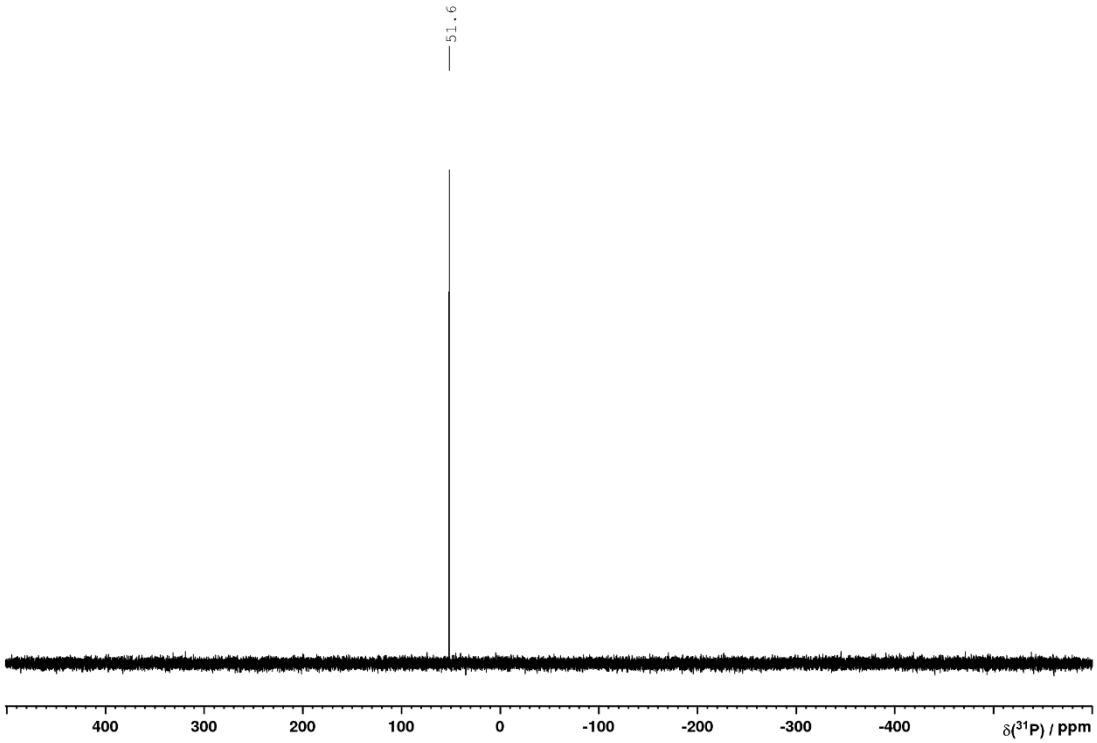

Figure S185. $^{31}P\{^{1}H\}$ NMR spectrum of $P(C(O)tBu)_3$ (**8b**) in C_6D_6.

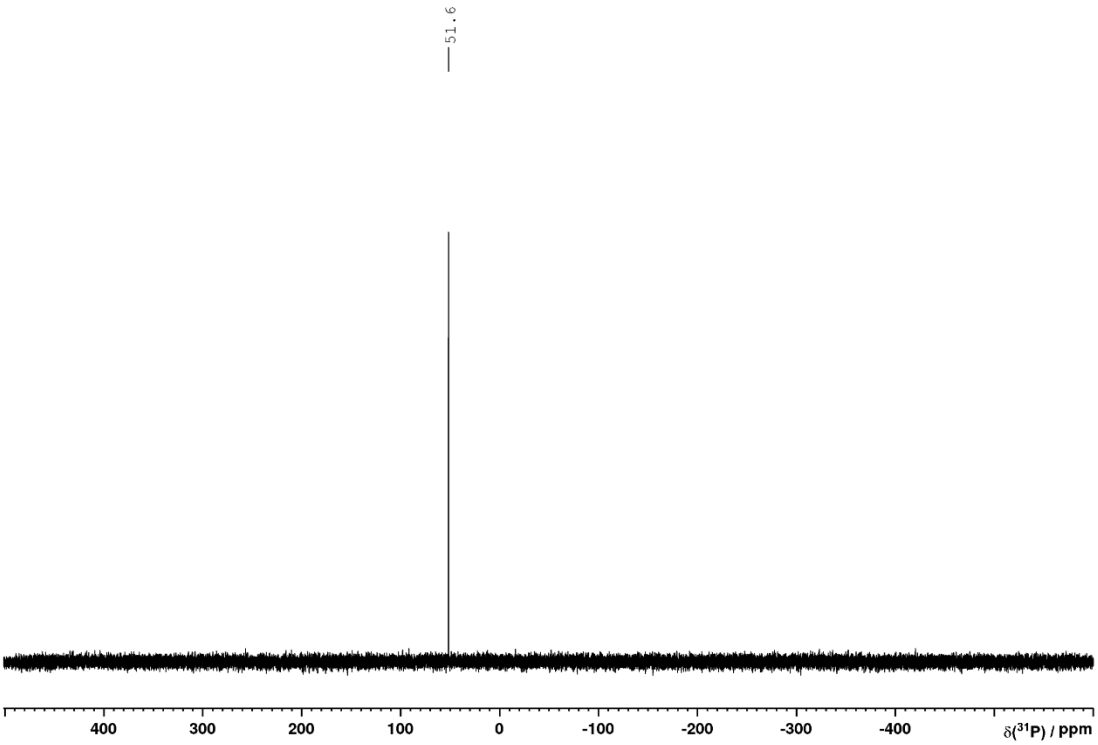

Figure S186. ^{31}P NMR spectrum of $P(C(O)tBu)_3$ (**8b**) in C_6D_6.

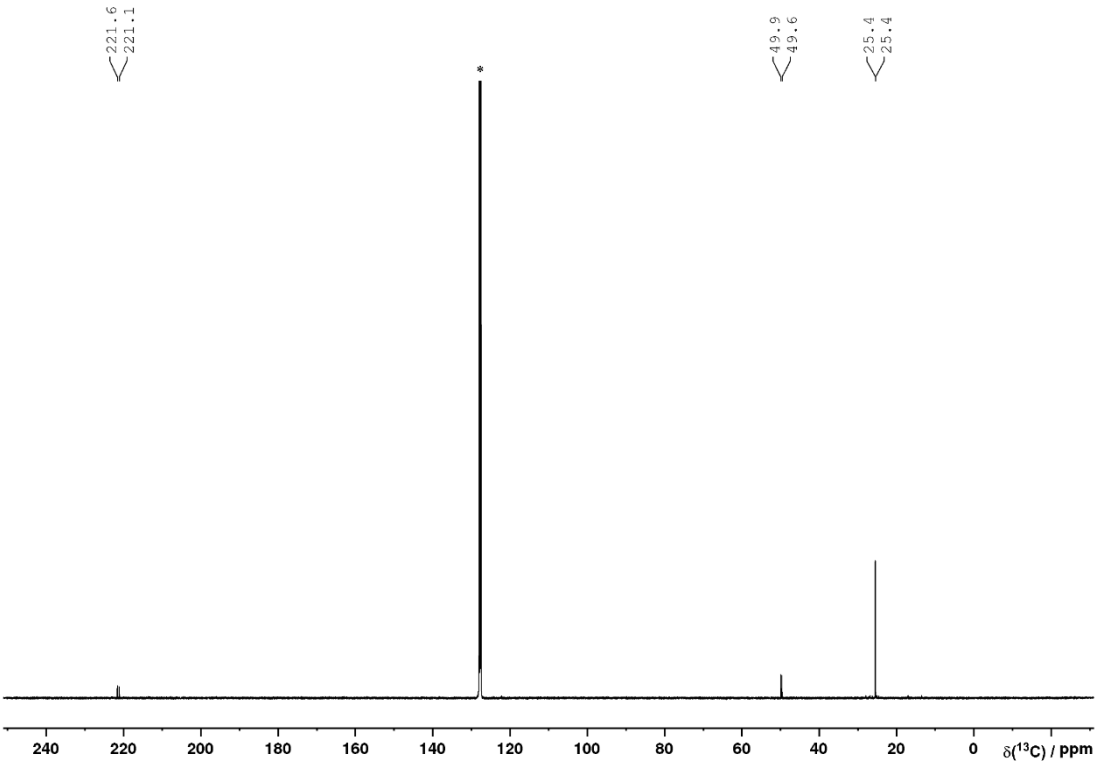

Figure S187. $^{13}C\{^1H\}$ NMR spectrum of $P(C(O)tBu)_3$ (**8b**) in C_6D_6 (*).

3.4.4 Stannylation of Red Phosphorus (P_{red}) without a glovebox

3.4.4.1 General procedures for the stannylation of P_{red} using Bu_3SnH and Bu_3SnOMe under near-UV LED irradiation without using a glovebox

The following procedures are initially prepared under open air conditions and without the use of a glovebox.

Standard Schlenk technique:

P_{red} (0.4 mmol, 12.4 mg) was weighed on the open bench and added to a 10 mL, flat-bottomed Schlenk tube. The atmosphere of the system was exchanged to N_2(g), with the help of a Schlenk line, by applying vacuum and then back-filling with N_2(g). This cycle was repeated three times. Under a flow of N_2(g), Bu_3SnOMe (17.3 μL, 0.06 mmol), undried 'bench' PhMe (50 μL) and Bu_3SnH (16.1 μL, 0.06 mmol) were added. The Schlenk tube was sealed, placed in a water-cooled block to maintain near-ambient temperature, and irradiated with UV light (365 nm, 4.3 V, 700 mA, Osram OSLON SSL 80) for 4 days. The reaction was opened to air, and Ph_3PO (12.6 mg, 0.0453 mmol) and 'bench' PhMe (500 μL) were added. The resulting mixture analysed by ^1H, $^{31}P\{^1H\}$, and ^{31}P NMR spectroscopy.

Freeze-pump-thaw:

To a 10 mL, flat-bottomed, stoppered Schlenk tube on the open bench were added P_{red} (0.4 mmol, 12.4 mg), undried 'bench' PhMe (50 μL), Bu_3SnH (16.1 μL, 0.06 mmol) and Bu_3SnOMe (17.3 μL, 0.06 mmol). The mixture was freeze-pump-thaw degassed three times using a Schlenk line in order to exchange the atmosphere of the system to N_2(g). The tube was sealed and placed in a water-cooled block to maintain near-ambient temperature, and irradiated with UV light (365 nm, 4.3 V, 700 mA, Osram OSLON SSL 80) for 4 days. The reaction was opened to air, and Ph_3PO (9.5 mg, 0.034 mmol) and 'bench' PhMe (500 μL) were added. The resulting mixture analysed by ^1H, $^{31}P\{^1H\}$, and ^{31}P NMR spectroscopy.

Open air:

To a 10 mL, flat-bottomed, stoppered tube on the open bench were added P_{red} (0.4 mmol, 12.4 mg), PhMe (50 μL), Bu_3SnH (16.1 μL, 0.06 mmol) and Bu_3SnOMe (17.3 μL, 0.06 mmol). The tube was sealed and placed in a water-cooled block to maintain near-ambient temperature, and irradiated with UV light (365 nm, 4.3 V, 700 mA, Osram OSLON SSL 80) for 4 days. The reaction was opened to air, and Ph_3PO (9.7 mg, 0.0349 mmol) and 'bench' PhMe (500 μL) were added. The resulting mixture analysed by ^1H, $^{31}P\{^1H\}$, and ^{31}P NMR spectroscopy.

Table S5. Stannylation of P_{red} using Bu_3SnH and Bu_3SnOMe under near UV LED irradiation, **without using a glove box**[a]

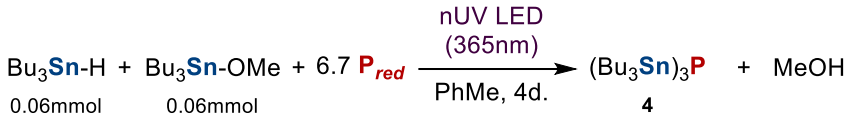

Entry	Procedure	Full conv. of Bu_3SnH?[b]	Conv. to **4** (%)[c]
1	Glovebox (dry PhMe)	✓	96
2	Glovebox ('bench' PhMe)	✓	95
3	Standard Schlenk technique	✓	92
4	Freeze-pump-thaw	✓	91
5	Open air (dry PhMe)	✓	33
6	Open air ('bench' PhMe)	✓	<5

[a] The general procedures for the stannylation of P_{red} described in this section or in section 3.4.2.1 ("glovebox") were used. [b] The full consumption of Bu_3SnH was assessed by ^1H NMR spectroscopy and the disappearance of the Sn*H* resonance that would otherwise be observed at *ca.* 5 ppm. [c] Conversions were calculated by integration of the ^{31}P resonance of **4** relative to an internal standard, which was then normalized relative to Table S1, entry 12 (defined as 99%) as described in section 3.4.1.1.

3.4.4.2 Synthesis and isolation of $(Bu_3Sn)_3P$ (4) without using a glovebox

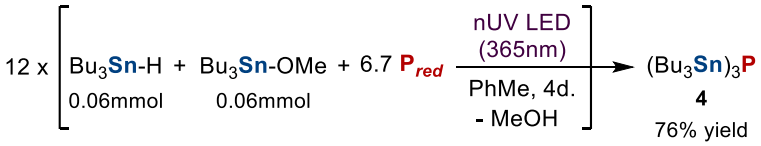

A total of twelve reactions were performed in parallel using the following procedure: P_{red} (0.4 mmol, 12.4 mg) was weighed and added on the open bench to a 10 mL, flat-bottomed, Schlenk tube. The atmosphere of the system was exchanged to N_2(g) using standard Schlenk line techniques (three cycles of vacuum and N_2(g)). Under a flow of N_2(g), Bu_3SnOMe (17.3 µL, 0.06 mmol), undried 'bench' PhMe (50 µL) and Bu_3SnH (16.1 µL, 0.06 mmol) were added. The Schlenk tube was sealed, placed in a water-cooled block to maintain near-ambient temperature, and irradiated with UV light (365 nm, 4.3 V, 700 mA, Osram OSLON SSL 80) for 4 days. The twelve reactions were opened to air and combined in a 100 mL Schlenk using 'bench' PhMe (3 x 0.5 mL) to transfer and wash each tube. The combined red suspension was filtered on the open bench and the remaining solid extracted with additional 'bench' PhMe (2 x 10 mL), followed by removal of volatiles under vacuum. After distillation of the resulting yellowish oil under vacuum (*ca.* 105 °C, 10^{-5} mbar), the product (**4**) was obtained as a colourless oil (329.1 mg, 76%).
NMR data are identical to those given in section 3.4.2.2.

3.4.5 (Hydro)Stannylation of Red Phosphorus (P_{red}) promoted by chemical radical initiators

3.4.5.1 General procedure and optimisation for the hydrostannylation of P_{red} using Bu_3SnH and AIBN (0.06 mmol scale)

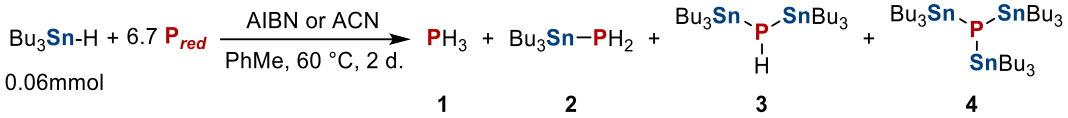

To a 10 mL, flat-bottomed, stoppered tube were added P_{red} (0.4 mmol, 12.4 mg), PhMe (50 µL), AIBN (azobis(isobutyronitrile), 0.006 mmol, as a stock solution in PhH) and Bu_3SnH (16.1 µL, 0.06 mmol). The tube was sealed, wrapped in Al foil to exclude light, and heated to 60 °C for 2 days. Ph_3PO (0.02 mmol, stock solution in benzene) was subsequently added to act as an internal standard. The resulting mixture was analysed by ^{1}H, $^{31}P\{^{1}H\}$, and ^{31}P NMR spectroscopy, as shown in Figures S45 and S46, below.

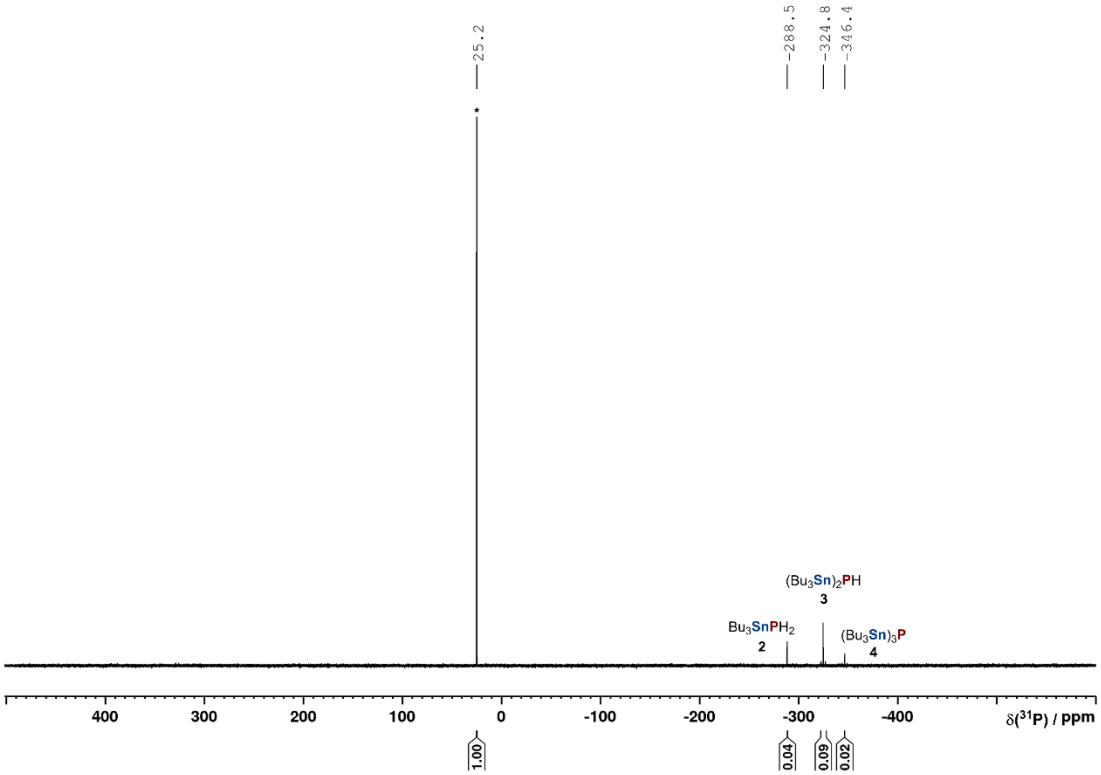

Figure S188. $^{31}P\{^{1}H\}$ NMR spectrum for the reaction of P_{red} with Bu_3SnH (0.06 mmol) and AIBN (0.006 mmol) in PhMe, heated to 60 °C for 2 days. * marks the internal standard Ph_3PO (0.04 mmol).

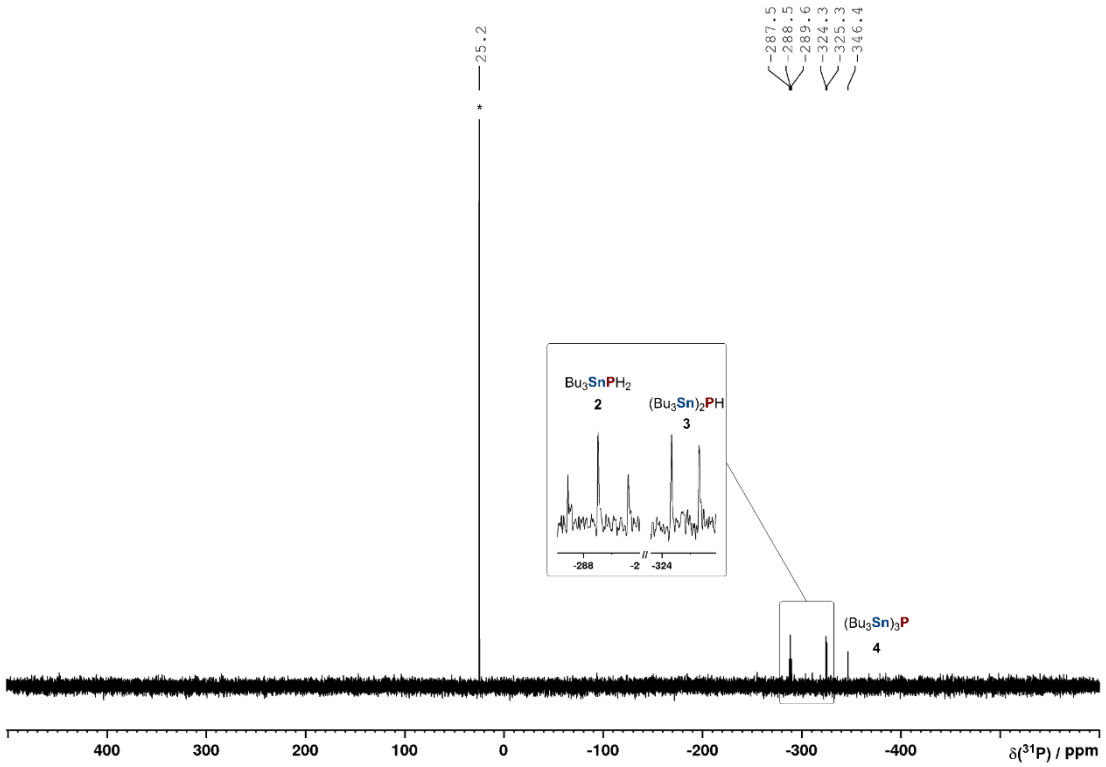

Figure S189. ^{31}P NMR spectrum for the reaction of P_{red} with Bu_3SnH (0.06 mmol) and AIBN (0.006 mmol) in PhMe, heated to 60 °C for 2 days. The insets show expansions of the signals attributed to Bu_3SnPH_2 (**2**) and $(Bu_3Sn)_2PH$ (**3**), highlighting their multiplicity due to $^1J(^{31}P\text{-}^1H)$ couplings. * marks the internal standard Ph_3PO (0.04 mmol).

Table S6. Optimisation of hydrostannylation of P_{red} using Bu_3SnH and AIBN or ACN[a]

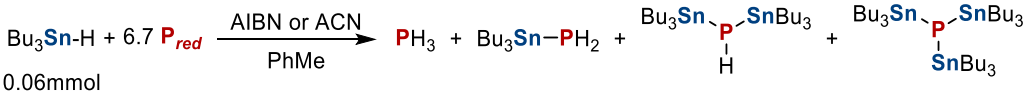

1 **2** **3** **4**

Entry	Radical initiator (mmol)	Temperature (°C)	Time (days)	Full conv. of Bu_3SnH?[b]	Relative total conv. to **1-4** (%)[c]
1	AIBN (0.006)	60	1	X	12
2	AIBN (0.006)	60	2	X	15
3	AIBN (0.012)	80	3	X	10
4	AIBN (0.012)	60	4	X	9[d]
5	AIBN (0.06)	80	4	X	5[d,e]
6	ACN (0.006)[f]	60	1	X	traces
7	ACN (0.006) [f]	60	2	X	traces
8	ACN (0.012) [f]	60	4	X	8
9	ACN (0.06) [f]	80	4	X	5[d]

[a] The general procedure described in this section was modified to use the indicated amount radical initiator, temperature and time. [b] The full consumption of Bu_3SnH was assessed by ^{1}H NMR spectroscopy and the disappearance of the Sn*H* resonance that would otherwise be observed at *ca.* 5 ppm. [c] Conversions were calculated by integration of the ^{31}P resonances of **1-4** relative to an internal standard, which was then normalized relative to Table S1, entry 12 (defined as 99%) as described in section 3.4.1.1.[d] Only product $(Bu_3Sn)_3P$ (**4**) was observed. [e] traces of P_4 were observed. [f] ACN (1,1'-azobis(cyclohexanecarbonitrile)) was used instead of AIBN.

3.4.5.2 General procedure and optimisation for the stannylation of P_{red} using Bu_3SnH, Bu_3SnOMe and AIBN (0.06 mmol scale)

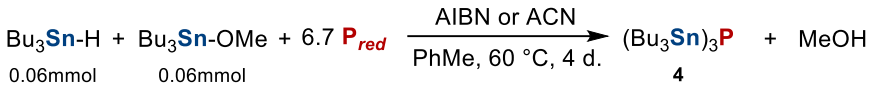

To a 10 mL, flat-bottomed, stoppered tube were added P_{red} (0.4 mmol, 12.4 mg), PhMe (50 µL), AIBN (azobis(isobutyronitrile), 0.012 mmol, as a stock solution in PhH), Bu_3SnH (16.1 µL, 0.06 mmol) and Bu_3SnOMe (17.3 µL, 0.06 mmol). The tube was sealed, wrapped in Al foil to exclude light, and heated to 60 °C for 4 days. Ph_3PO (0.02 mmol, stock solution in benzene) was subsequently added to act as an internal standard. The resulting mixture was analysed by ^{1}H, $^{31}P\{^{1}H\}$, and ^{31}P NMR spectroscopy, as shown in Figures S47 and S48, below.

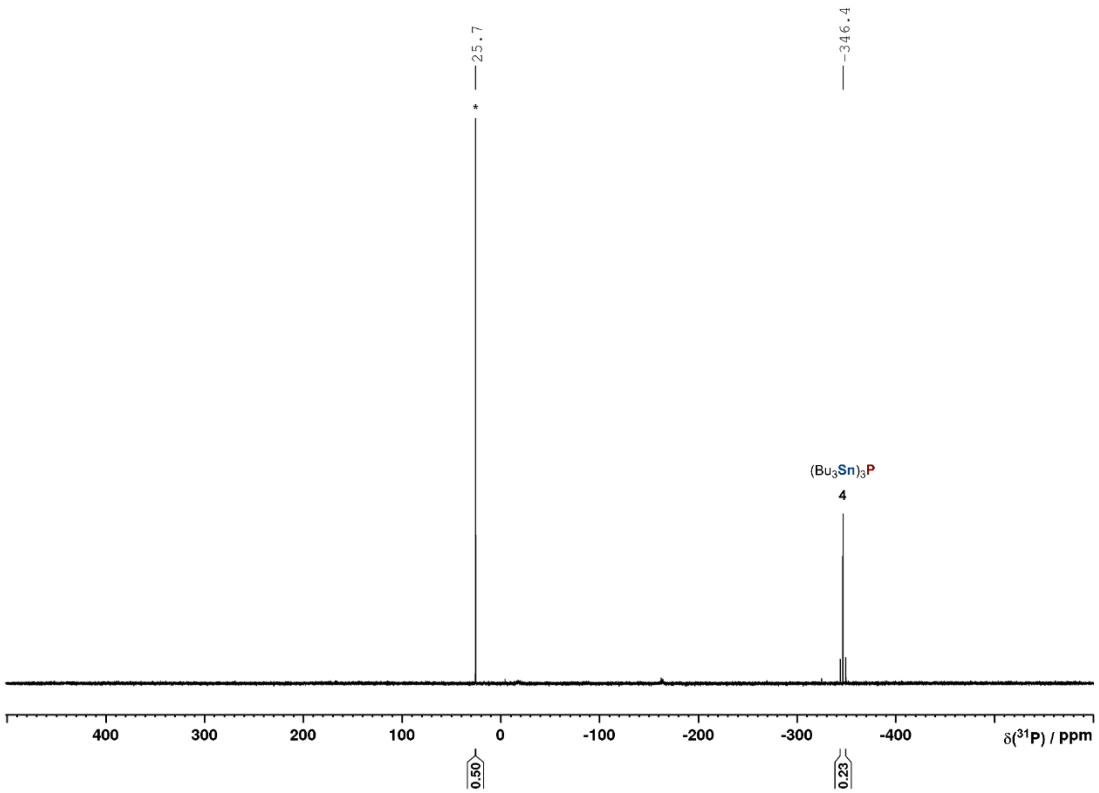

Figure S190. $^{31}P\{^{1}H\}$ NMR spectrum for the reaction of P_{red} with Bu_3SnH (0.06 mmol), Bu_3SnOMe (0.06 mmol) and AIBN (0.012 mmol) in PhMe, heated to 60 °C for 4 days. * marks the internal standard Ph_3PO (0.04 mmol).

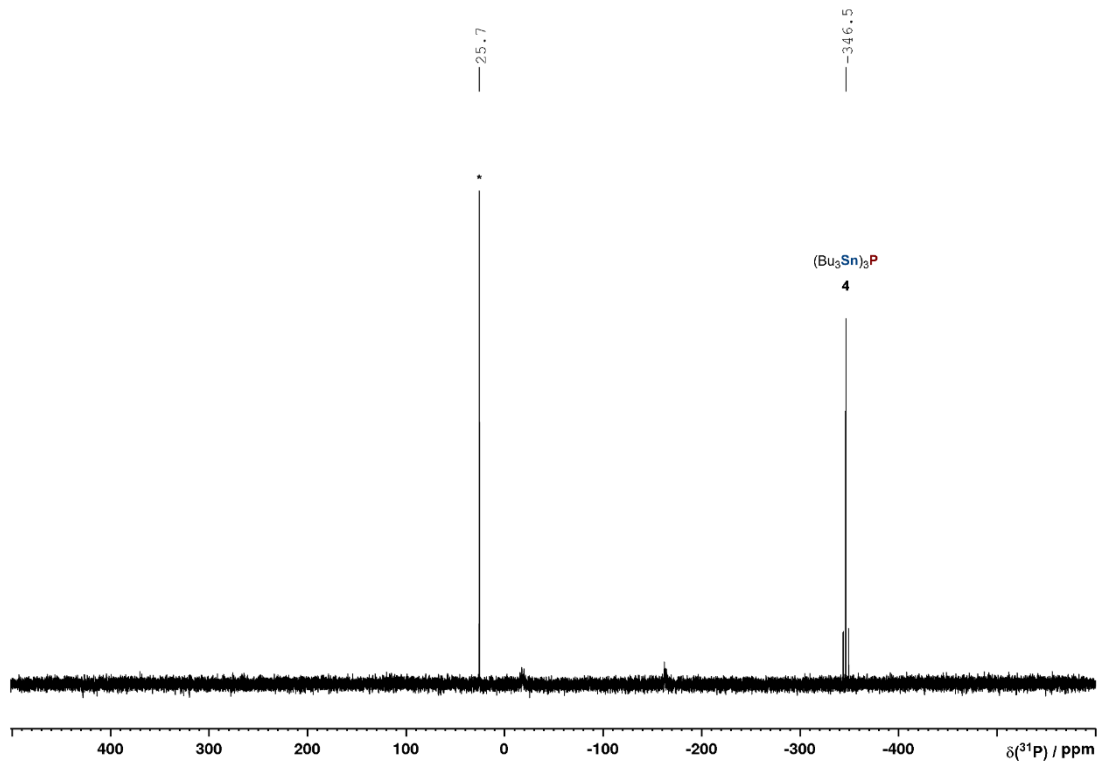

Figure S191. $^{31}P\{^{1}H\}$ NMR spectrum for the reaction of P_{red} with Bu_3SnH (0.06 mmol), Bu_3SnOMe (0.06 mmol) and AIBN (0.012 mmol) in PhMe, heated to 60 °C for 4 days. * marks the internal standard Ph_3PO (0.04 mmol).

Table S7. Optimisation of hydrostannylation of P_{red} using Bu_3SnH and AIBN or ACN[a]

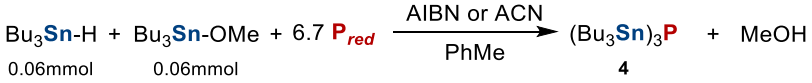

Entry	Radical initiator (mmol)	Temperature (°C)	Time (days)	Full conv. of Bu_3SnH?[b]	Conv. to **4** (%)[c]
1	AIBN (0.006)	60	2	X	20[d,e]
2	AIBN (0.006)	60	3	X	15[d]
3	AIBN (0.012)	40	2	X	8[d]
4	AIBN (0.012)	60	2	X	12[d]
5	AIBN (0.012)	60	3	X	17
6	AIBN (0.012)	60	4	X	23[d,e]
7	AIBN (0.012)	80	2	X	4
8	AIBN (0.12)	60	2	✓	traces
9	AIBN (012)	80	2	✓	traces
10	ACN (0.012)[f]	60	2	X	2[d]
11	ACN (0.12)[f]	60	2	✓	10

[a] The general procedure described in this section was modified to use the indicated amount radical initiator, temperature and time. [b] The full consumption of Bu_3SnH was assessed by ^{1}H NMR spectroscopy and the disappearance of the Sn*H* resonance that would otherwise be observed at *ca.* 5 ppm. [c] Conversions were calculated by integration of the ^{31}P resonance of **4** relative to an internal standard, which was then normalized relative to Table S1, entry 12 (defined as 99%) as described in section 3.4.1.1. [d] Product $(Bu_3Sn)_2PH$ (**3**) was observed in <5%. [e] Traces of signals attributed to $P_7(SnBu_3)_3$ were observed. [f] ACN (1,1'-azobis(cyclohexanecarbonitrile)) was used instead of AIBN.

3.5 References

[1] a) D. E. C. Corbridge, *Phosphorus. Chemistry, Biochemistry and Technology*, Elsevier, **2000**; b) J. Svara, N. Weferling, T. Hofmann, *Ullmann's Encycl. Ind. Chem.* **2012**, *27*, 20–50; c) H. Diskowski, T. Hofmann, *Ullmann's Encycl. Ind. Chem.* **2012**, *26*, 725–746; d) N. Weferling, S. M. Zhang, C. H. Chiang, *Procedia Eng.* **2016**, *138*, 291–301.

[2] a) G. Bettermann, W. Krause, G. Riess, T. Hofmann, *Ullmann's Encycl. Ind. Chem.* **2012**, *27*, 1–18; b) A. R. Jupp, S. Beijer, G. C. Narain, W. Schipper, J. C. Slootweg, *Chem. Soc. Rev.* **2021**, *50*, 87–101; c) M. Peruzzini, L. Gonsalvi, A. Romerosa, *Chem. Soc. Rev.* **2005**, *34*, 1038–1047.

[3] a) J. E. Borger, A. W. Ehlers, J. C. Slootweg, K. Lammertsma, *Chem. Eur. J.* **2017**, *23*, 11738–11746; b) N. K. Gusarova, B. A. Trofimov, *Russ. Chem. Rev.* **2020**, *89*, 225–249.

[4] For a very recent review of this area, see D. J. Scott, *Angew. Chem. Int. Ed.* **2022**, *61*, e202205019; *Angew. Chem.* **2022**, *134*, e202205019.

[5] a) M. Donath, K. Schwedtmann, T. Schneider, F. Hennersdorf, A. Bauzá, A. Frontera, J. J. Weigand, *Nat. Chem.* **2022**, *14*, 384–391; b) M. Till, V. Streitferdt, D. J. Scott, M. Mende, R. M. Gschwind, R. Wolf, *Chem. Commun.* **2022**, *58*, 1100–1103; c) S. Reichl, E. Mädl, F. Riedlberger, M. Piesch, G. Balázs, M. Seidl, M. Scheer, *Nat. Commun.* **2021**, *12*, 1–9; d) Y. Mei, Z. Yan, L. L. Liu, *J. Am. Chem. Soc.* **2022**, *144*, 1517–1522; e) U. Lennert, P. B. Arockiam, V. Streitferdt, D. J. Scott, C. Rödl, R. M. Gschwind, R. Wolf, *Nat. Catal.* **2019**, *2*, 1011–1106; f) M. Till, J. Cammarata, R. Wolf, D. J. Scott, *Chem. Commun.* **2022**, *58*, 8986–8989.

[6] a) B. M. Cossairt, N. A. Piro, C. C. Cummins, *Chem. Rev.* **2010**, *110*, 4164–4177; b) M. Caporali, L. Gonsalvi, A. Rossin, M. Peruzzini, *Chem. Rev.* **2010**, *110*, 4178–4235; c) M. Scheer, G. Balázs, A. Seitz, *Chem. Rev.* **2010**, *110*, 4236–4256; d) L. Giusti, V. R. Landaeta, M. Vanni, J. A. Kelly, R. Wolf, M. Caporali, *Coord. Chem. Rev.* **2021**, *441*, 213927; e) C. M. Hoidn, D. J. Scott, R. Wolf, *Chem. Eur. J.* **2021**, *27*, 1886–1902.

[7] C.-W. Hsu, Y.-C. Tsai, B. M. Cossairt, J. Arnold, C. C. Cummins, in *Inorg. Synth.* **2018**, pp. 123–134.

[8] M. Caporali, M. Serrano-Ruiz, M. Peruzzini, in *Chem. beyond Chlorine* (Eds.: P. Tundo, L.N. He, E. Lokteva, C. Mota), Springer International Publishing, **2016**, pp. 97–136.

[9] a) G. A. Abakumov, A. V. Piskunov, V. K. Cherkasov, I .L. Fedushkin, V. P. Ananikov, D. B. Eremin, E. G. Gordeev, I. P. Beletskaya, A. D. Averin, M. N. Bochkarev, et al., *Russ. Chem. Rev.* **2018**, *87*, 393–507; b) N. K. Gusarova, S. N. Arbuzova, B. A. Trofimov, *Pure Appl. Chem.* **2012**, *84*, 439–459; c) B. A. Trofimov, N. K. Gusarova, *Mendeleev Commun.* **2009**, *19*, 295–302; d) B. G. Sukhov, N. K. Gusarova, S. F. Malysheva, B. A. Trofimov, *Russ. Chem. Bull.* **2003**, *52*, 1239–1252.

[10] a) L. Brandsma, J. A. van Doom, R.-J. de Lang, N. K. Gusarova, B. A. Trofimov, *Mendeleev Commun.* **1995**, *5*, 14–15; b) S. N. Arbuzova, L. Brandsma, N. K. Gusarova, B. A. Ttofimov, *Recl. des Trav. Chim. des Pays-Bas* **1994**, *113*, 575–576.

[11] a) D. Stein, T. Ott, H. Grützmacher, *Z. Anorg. Allg. Chem.* **2009**, *635*, 682–686; b) M. Podewitz, J. D. Van Beek, M. Wörle, T. Ott, D. Stein, H. Rüegger, B. H. Meier, M. Reiher, H. Grützmacher, *Angew. Chem. Int. Ed.* **2010**, *49*, 7465–7469; *Angew. Chem.* **2010**, *122*, 7627-7631.

[12] a) A. Huber, A. Kuschel, T. Ott, G. Santiso-Quinones, D. Stein, J. Bräuer, R. Kissner, F. Krumeich, H. Schönberg, J. Levalois-Grützmacher, et al., *Angew. Chem. Int. Ed.* **2012**, *51*, 4648–4652; *Angew.*

Chem. **2012**, *124*, 4726-4730; b) G. Müller, M. Zalibera, G. Gescheidt, A. Rosenthal, G. Santiso-Quinones, K. Dietliker, H. Grützmacher, *Macromol. Rapid Commun.* **2015**, *36*, 553–557.

[13] D. J. Scott, J. Cammarata, M. Schimpf, R. Wolf, *Nat. Chem.* **2021**, *13*, 458-464.

[14] Proof-of-concept results have also been achieved using chemical radical initators such as AIBN instead of LED irradiation. However, for these systems we have thus far only been able to achieve low conversions (<20 % $(Bu_3Sn)_xPH_{3-x}$). See Section 3.4.5 for more details.

[15] As in the case using P_4, irradiation with LED light is proposed to induce the formation of an initial Bu_3Sn• radical which initiates the chain reaction. However, the precise details of this initiation are currently unclear and remain under investigation.

[16] This assignment is based on agreement with the reported chemical shifts and coupling patterns for analogous $P_7(SnMe_3)_3$, see: G. Fritz, K. D. Hoppe, W. Hönle, D. Weber, C. Mujica, V. Manriquez, H. G. v. Schnering, *J. Organomet. Chem.* **1983**, *249*, 63–80.

[17] The transformation of Bu_3SnCl into Bu_3SnH or Bu_3SnOMe, can be achieved in excellent yields by treatment with $NaBH_4$ or NaOMe respectively, see: a) L. V. Heumann, G. E. Keck, *Org. Lett.* **2007**, *9*, 10, 1951–1954; b) D. Ballivet-Tkatchenko, O. Douteau, S. Stutzmann, *Organometallics* **2000**, *19*, 4563-4567.

[18] M. Chen, C. Chen, Y. Tan, J. Huang, X. Wang, L. Chen, Y. Wang, *Ind. Eng. Chem. Res.* **2014**, *53*, 1160–1171.

[19] H. Schmidbaur, U. Deschler, B. Milewski-Mahrla, B. Zimmer-Gasser, *Chem. Ber.* **1981**, *114*, 608–619.

[20] We have previously demonstrated that the various components of the $(Bu_3Sn)_xPH_{3-x}$ mixture, including $(Bu_3Sn)_3P$, are sufficiently air-stable to allow them to be left under air overnight without appreciable change *versus* equivalent storage under N_2 (see ref. 13). However, longer term stability under air has yet to be established and so for safety reasons extended storage under air is currently not advised.

4 Unravelling White Phosphorus: Experimental and Computational Studies Reveal the Mechanisms of P_4 Hydrostannylation

Abstract:
The hydrostannylation of white phosphorus (P_4) allows this crucial industrial precursor to be easily transformed into useful P_1 products *via* direct, 'one-pot' (or even catalytic) procedures. However, a thorough mechanistic understanding of this transformation has remained elusive, hindering attempts to use this rare example of successful, direct P_4 functionalisation as a model for further reaction development. Here, we provide a deep and generalizable mechanistic picture for P_4 hydrostannylation by combining DFT calculations with *in situ* ^{31}P NMR reaction monitoring and kinetic trapping of previously unobservable reaction intermediates using bulky tin hydrides. The results offer important insights into both how this reaction proceeds and why it is successful and provide implicit guidelines for future research in the field of P_4 activation.

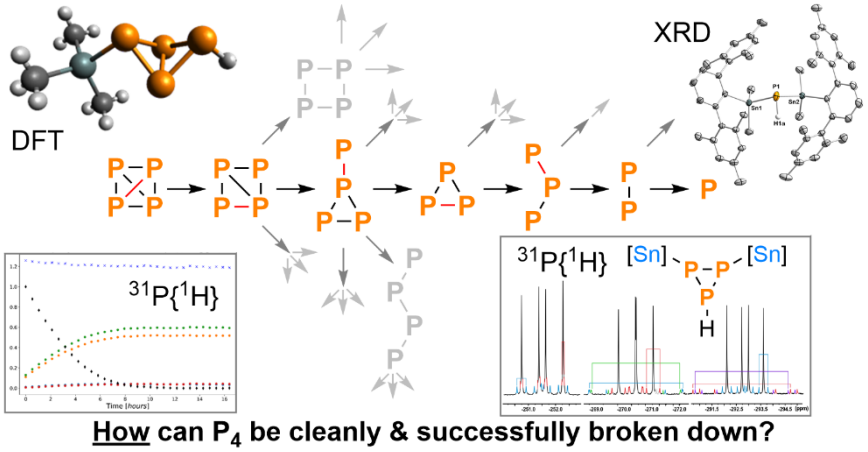

[a] Reproduced with permission from: J. Cammarata, F. F. Westermair, P. Coburger, D. Duvinage, M. Janssen, M. K. Uttendorfer, J. Beckmann, R. M. Gschwind, R. Wolf, and D. J. Scott, *Angew. Chem. Int. Ed.* **2024**, e202408423.

[b] Jose Cammarata performed the DFT calculations analysing the hydrostannylation mechanism described in sections 4.2.1 and 4.4.2. Preliminary DFT calculations were performed by Peter Coburger (Section 4.4.2.3). Daniel Duvinage and Marvin Janssen synthesised, and characterised the tin hydrides $ArSn(Me)_2H$ (Ar = Ter, Ter*, Fluind, Section 4.4.3); they were supervised by Jens Beckmann. Franz F. Westermair calculated NMR parameters (Section 4.4.4) and carried out all the *in situ* NMR monitoring experiments reported in sections 4.2.2, 4.4.1 and 4.4.3; he was supervised by Ruth M. Gschwind. Jose Cammarata performed *ex situ* experiments reported in section 4.4.4 and all other experimental work. Maria K. Uttendorfer solved and refined the single crystal X-ray structure of $[TerSn(Me)_2]_2PH$ (Section 4.4.4.5). Daniel J. Scott wrote the manuscript with contributions from Jose Cammarata and Franz F. Westermair, which was reviewed and edited by Ruth M. Gschwind and Robert Wolf. Robert Wolf and Daniel J. Scott supervised and directed the project.

4.1 Introduction

White phosphorus (P_4) provides a common starting point from which effectively all commercially relevant phosphorus compounds are currently prepared (with wet process H_3PO_4 and derived phosphate salts as the major exceptions).[1] This is achieved industrially through multistep procedures in which P_4 is first transformed into simple P_1 precursors such as PCl_3 (*via* reaction with Cl_2) or PH_3 (*via* disproportionation).[2] These can then be reacted in subsequent steps with suitable reagents (typically nucleophiles or unsaturated organic substrates, respectively) to eventually yield the target P_1 products of interest (Scheme 1a).[3]

The drawbacks of these industrial methods have long been recognized, with many critics emphasizing their use of extremely hazardous reagents and intermediates (e.g. Cl_2, PH_3), their poor step economy, and their production of undesirable stoichiometric waste. This has prompted extensive investigations over the last several decades into the fundamental reactivity of the P_4 molecule, in the hope that a better understanding of its basic chemistry might aid the development of new, improved methods for the transformation of P_4 that could eventually replace the current industrial state-of-the-art.[4] Particularly prominent has been the goal of achieving *direct* transformations in which P_4 would be converted into the target P_1 compounds in a single reaction, thus optimizing step economy while also bypassing the hazardous intermediates required currently.

Despite comprehensive and extended research in this area, it is only very recently that examples of direct P_4 conversion into genuinely useful P-containing products (and particularly organophosphorus products) have begun to appear in the literature.[5-7] As such, the number of successful systems reported remains very low, and those that have been disclosed continue to suffer from substantial drawbacks and limitations. Nevertheless, the independent emergence of several such reports has raised hopes for a new phase in P_4 chemistry research that will see an ongoing expansion in the number and variety of direct P_4 functionalisation methods, alongside steady improvements in reaction performance (practicality, atom economy, turnover, *etc*.). However, if this hope is to be realized, it is crucial for chemists to understand in detail *why* previous examples have been successful, in order to provide guidelines for future reaction development.[8]

As part of the recent advancement of this field, we have reported that the reduction of P_4 can be achieved very simply using the inexpensive, 'classical' radical reagent Bu_3SnH in combination with a source of radical initiation (light, or a chemical radical initiator).[9,10] This results in net hydrostannylation of P_4 to yield a clean mixture of the P_1 products $(Bu_3Sn)_xPH_{3-x}$ (x = 0 - 3), with Bu_3SnPH_2 and $(Bu_3Sn)_2PH$ as the major components. This mixture can then be treated directly with electrophiles to yield a wide variety of useful monophosphorus compounds in 'one-pot' fashion (Scheme 1b).

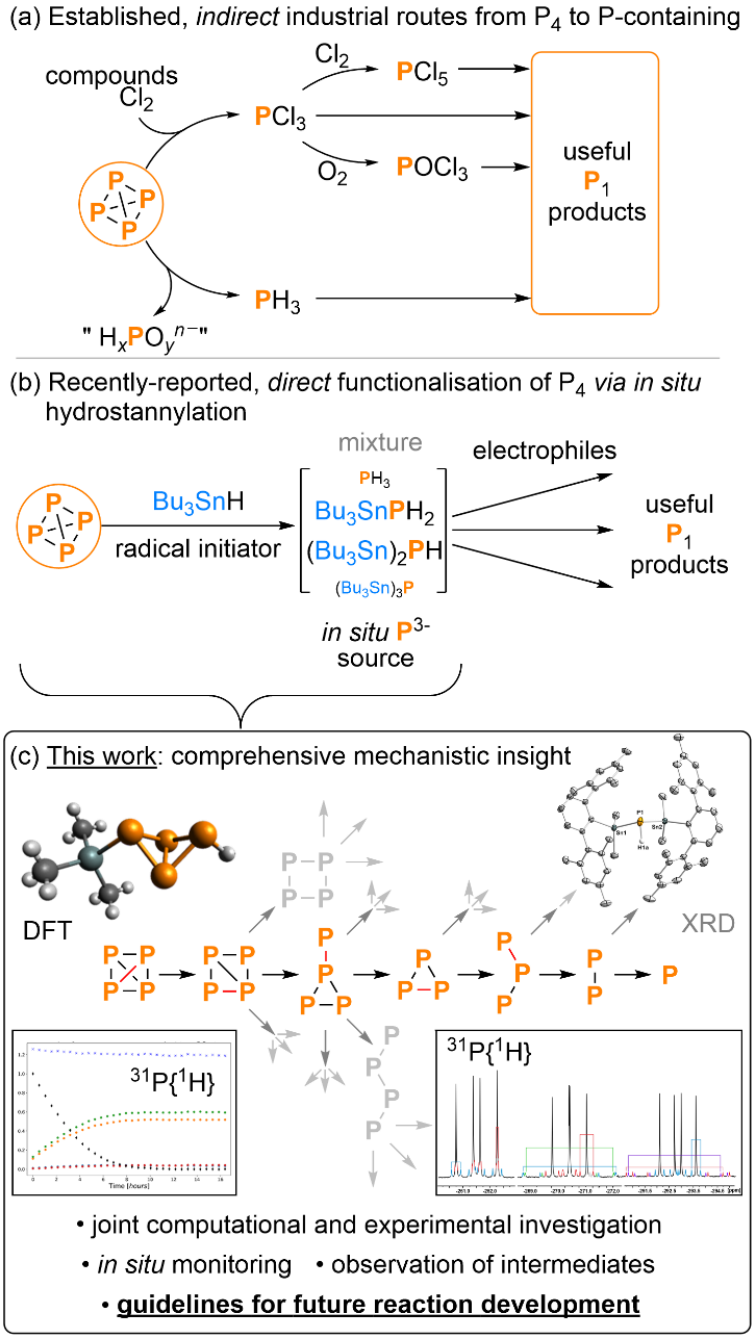

Scheme 1. Industrial routes for the utilisation of P_4 (a) and recently reported 'one-pot' transformation into useful products *via* hydrostannylation (b),[9] whose mechanism is investigated herein (c).

The hydrostannylation reaction was proposed to proceed *via* a relatively simple radical chain mechanism as shown in Scheme 2, in line with both initial experimental observations and the well-established, broader radical reactivity of Bu_3SnH.[11] Crucially, however, in that report we were able to suggest only a very rough outline of the overall mechanism, which did not offer any meaningful insight into the specific sequence of steps by which the P–P bonds of the P_4 tetrahedron are broken down. This is a critical omission, since P_4's tetrahedral structure means that its cleavage into P_1 species requires many distinct elementary reaction steps. In this case, hydrostannylation of a single P_4 molecule requires cleavage of six P–P bonds and formation of six P–H and six P–Sn bonds, with each step being in principle mechanistically different from

every other. Indeed, mechanistic complexity is a general feature of P_4 chemistry,[5] and one which is exacerbated by the known ability of P_n moieties to adopt an extremely wide range of stable structural motifs,[12] which can make it very difficult to target specific products in reactions involving P_4. In fact, even many of our own previous efforts in this area have been hampered by competing formation of undesired (and often insoluble) polyphosphorus products.[13]

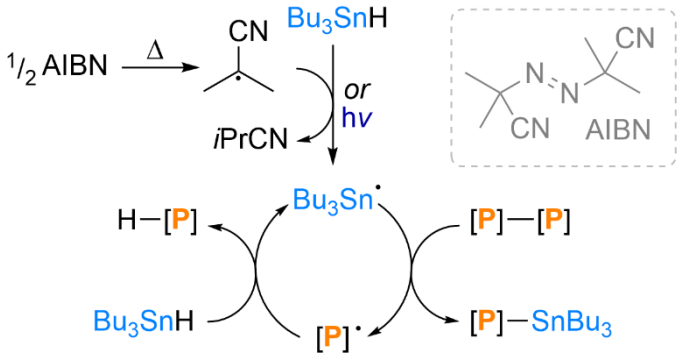

Scheme 2. Previously proposed outline for the mechanism of P_4 hydrostannylation.[9] [P]–[P] indicates a generic P–P bond derived from P_4.

It is thus very important to understand *why* the hydrostannylation of P_4 is able to proceed so cleanly and efficiently. As well as providing fundamental insight into the reactivity of P_4, such understanding would be a powerful tool as we and others seek both to generalize and optimize this P_4 hydrofunctionalisation reactivity, and to develop entirely new mechanistic strategies for P_4 functionalisation. With this goal in mind, we report herein a thorough study of the mechanism of P_4 hydrostannylation, which we have pursued both computationally and experimentally (Scheme 1c). From our results we are able to highlight several key factors that enable the success of this reaction, which will be valuable signposts for future studies targeting direct P_4 functionalisation.

4.2 Results and Discussion

To begin, the time course of the P_4 hydrostannylation reaction using Bu_3SnH was tracked by *in situ* $^{31}P\{^1H\}$ NMR spectroscopy. As shown in Figure 1, combination of P_4 with stoichiometric Bu_3SnH (6 eq., equating to 1 eq. per P–P bond) and 20 mol% azo*bis*(isobutyronitrile) (AIBN) as initiator at 298 K resulted in smooth consumption of the starting material over several hours, alongside concomitant, synchronous formation of the expected product mixture.[14] No significant loss in overall ^{31}P intensity was observed and, crucially, no signals corresponding to intermediates or side-products were observed in any of the individual spectra. This latter observation is consistent with previous $^{31}P\{^1H\}$ NMR analyses of reactions halted at partial conversion, which also showed only the final products and unreacted starting material.[9]

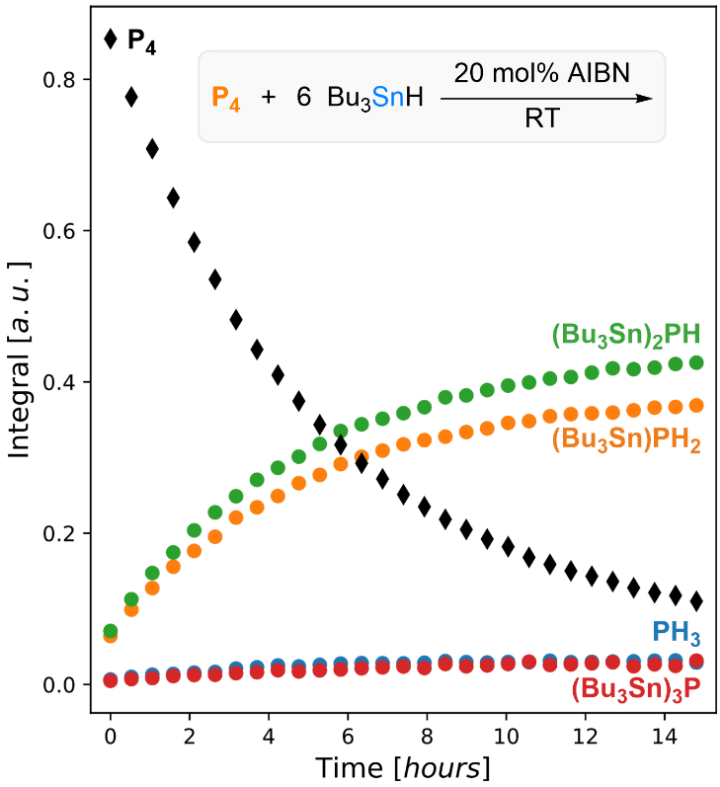

Figure 1. Evolution over time of P atom speciation in the reaction between P_4 and 6 eq. Bu_3SnH initiated by 20 mol% AIBN at 298 K in C_6D_6 as monitored by *in situ* $^{31}P\{^1H\}$ NMR spectroscopy.

A very similar evolution of the $^{31}P\{^1H\}$ NMR spectrum was observed using an *in situ* 455 nm light source instead of AIBN (see Figure S4), indicating a comparable mechanism. However, for reasons of both practical convenience and theoretical simplicity, AIBN initiation was chosen as the model system for further investigations.[15]

4.2.1 Computational investigation

In the absence of any spectroscopically observable intermediates, investigation of the hydrostannylation mechanism was continued through computational methods. DFT calculations were performed at the PBE-D3(BJ)/def2-TZVP level of theory on a model system in which the Bu_3Sn moiety was truncated to Me_3Sn for the sake of computational efficiency (for full details see Section 4.4.2).[16] Thermal fragmentation of AIBN is well known to result in formation of 2-cyanoisopropyl radicals, $^{\bullet}C(CN)Me_2$, that can then form $Me_3Sn^{\bullet}$ radicals through H atom abstraction (*cf.* Scheme 2).[14] And, indeed, these steps were both calculated to occur over moderate free energy barriers, consistent with previous experimental determinations (see Section 4.4.2.1).[14] An alternative initiation mechanism in which the AIBN-derived $^{\bullet}C(CN)Me_2$ radical instead adds to P was also calculated. However, this was found to be much less feasible and substantially uphill, which is consistent with experimental observations that AIBN does not react directly with P_4 alone even upon heating (see Sections 4.4.2.1 and 4.4.2.2).

First P–P cleavage: Following its formation, $Me_3Sn^{\bullet}$ is calculated to add to P_4 in a slightly uphill (2.2 kcal mol^{-1}) but otherwise essentially barrierless reaction to form the *exo* 'butterfly' radical $\mathbf{I}^{\bullet}$ (Figure 2). Alternate *endo* attack was calculated to be much less feasible (see Figure S9). $\mathbf{I}^{\bullet}$ can

then abstract a H atom from a further equivalent of Me_3SnH. This is again slightly uphill (by 1.6 kcal mol^{-1}), but this time proceeds over a modest activation barrier of 10.8 kcal mol^{-1}. This closes the initial stage of the radical chain by re-forming $Me_3Sn^{\bullet}$, while also generating the closed shell intermediate **II** (with *endo* attack again being less favourable than *exo*; Figure S9). The combined activation barrier for this stage is just 13.0 kcal mol^{-1}, which is consistent with the experimental observation of a radical chain process that occurs rapidly at around room temperature. However, comparison with later steps (*vide infra*) shows that this initial P–P cleavage in fact possesses both the highest individual activation barrier,[17] and the highest-lying transition state in the overall reaction mechanism. This is also the only P–P cleavage step that is endergonic overall. These calculations therefore suggest that cleavage of the first P–P bond in P_4 is the slowest step and hence rate-limiting for the radical chain part of the hydrostannylation mechanism in which P_4 is involved. This is fully in accord with the lack of P-containing intermediates observed experimentally during the reaction of P_4 with Bu_3SnH (*vide supra*) and, interestingly, also highlights a common misconception recently pointed out by Cummins and coworkers: that the P–P bonds in P_4 are unusually strained and therefore especially reactive due to P_4's small, 60° bond angles.[18] Clearly, in this case, it is the P–P bonds of the intact P_4 tetrahedron that are actually *least* reactive towards hydrostannylation (both kinetically and thermodynamically), out of any in the overall mechanism. This is presumably a consequence of P_4's noted spherical aromaticity.[19]

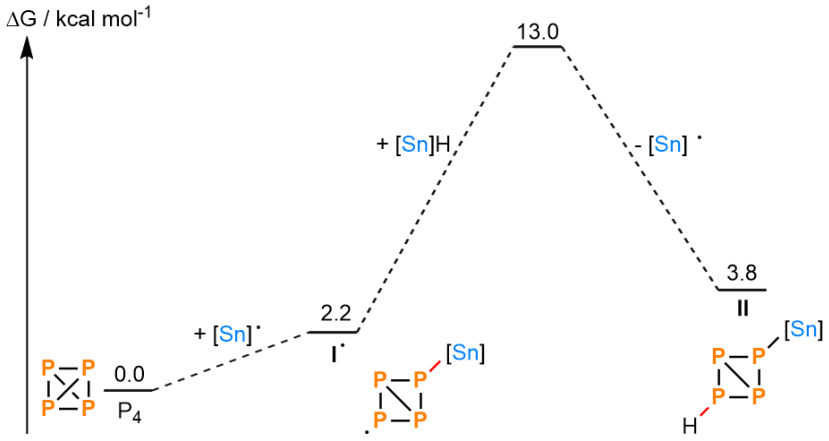

Figure 2. Calculated mechanism for hydrostannylation of the first P–P bond in P_4 by Me_3SnH, with relative free energies in kcal mol^{-1}. [Sn] = Me_3Sn. For simplicity, stereochemistry is not shown (see Figure S9).

<u>*Second P–P cleavage:*</u> While the first step offers only a single set of equivalent P–P bonds to cleave, the second step is significantly more complicated. Following the first hydrostannylation step and formation of **II**, the second $Me_3Sn^{\bullet}$ attack can in principle occur in at least five different ways, resulting in the five constitutional isomers **III**$^{\bullet}$ shown in Figure 3 (for further details see also Figure S10). Like attack on P_4, each option is calculated to be barrierless, but unlike for P_4 each option is exergonic, with the most favorable option found to be attack at the existing PH position leading to formation of intermediate **IIIa**$^{\bullet}$ containing a *cyclo*-P_3 ring (Figure 3). Notably,

though, the alternative *cyclo*-P_3 intermediate **IIIb•** is less than 2 kcal mol^{-1} higher in energy, suggesting only limited thermodynamic preference for one over the other. (Note that the lack of apparent activation barriers implies that formation of **IIIc•-IIIe•** should be no less kinetically feasible than formation of **IIIa•** or **IIIb•**. However, the former should preferentially equilibrate to the latter rather than react further; *vide infra*, and see Section 4.4.2.3.2 for more detailed discussion.) Once formed, H atom transfer to the lowest energy isomer **IIIa•** proceeds over an activation barrier slightly smaller than that for **I•** (10.7 kcal mol^{-1}), giving intermediate **IVa**. The corresponding transition state is lower lying than those for H atom transfer to any of the other isomers **III•**, but in the case of **IIIb•** the difference is very modest: only 0.2 kcal mol^{-1} (likely within these calculations' margin of error). While the H atom transfer step is slightly uphill the net P–P hydrostannylation that transforms **II** into **IVa** (or **IVb**) is exergonic, in contrast to the hydrostannylation of P_4 to **II** (*vide supra*). Notably, this general pattern of downhill, barrierless $Me_3Sn^•$ attack followed by slightly uphill H atom transfer from Me_3SnH resulting in net exergonic P–P cleavage is repeated in step 3 (*vide infra*).

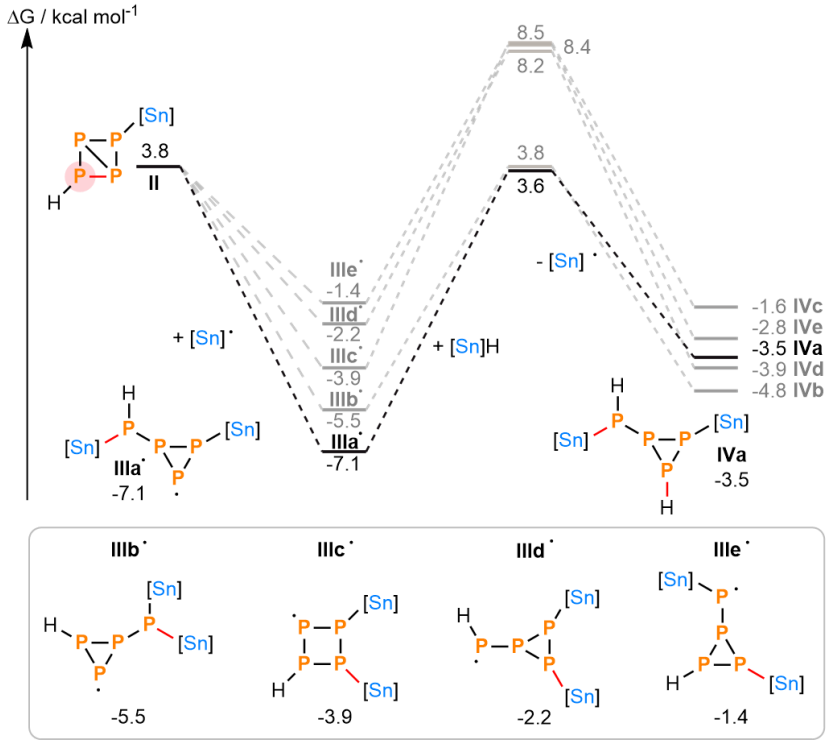

Figure 3. Calculated mechanisms for hydrostannylation of the second P–P bond in P_4 by Me_3SnH, with relative free energies in kcal mol^{-1}. For simplicity, stereochemistry is not shown (see Figure S10). [Sn] = Me_3Sn.

Third P–P cleavage: The complexity noted in the second P–P cleavage step is compounded in the third, with the five constitutional isomers **IV** each offering multiple options for the next $Me_3Sn^•$ addition. Of these isomers, formation of **IVa** and **IVb** appears to be kinetically preferred (for a more detailed discussion, see Section 4.4.2.3.2) but for the sake of practicality, calculations were limited to only isomer **IVa**, which was formally calculated to offer the lowest energy transition state.

Even after imposing this limitation, addition of $Me_3Sn^{\bullet}$ to **IVa** still leads to eight possible constitutional isomers **V**$^{\bullet}$, as shown in Figure 4 (see also Figure S11). As in the second step, these additions are all downhill and all essentially barrierless, with the *five* lowest energy isomers again being all rather similar in energy, separated by a span of just 2 kcal mol^{-1}, while the two lowest (**Va**$^{\bullet}$ and **Vb**$^{\bullet}$) are almost identical in energy. H atom transfer from Me_3SnH to **V**$^{\bullet}$ then gives the closed-shell intermediate isomers **VI**, which for the lowest-energy isomers of **V**$^{\bullet}$ is again slightly uphill. The relative conformational flexibility of many of these isomers makes calculation of the corresponding transition states more demanding and time consuming than in steps 1 and 2. Nevertheless, these were computed for the two lowest energy isomers, **Va**$^{\bullet}$ and **Vb**$^{\bullet}$. These again revealed only modest barriers of 10.3 kcal mol^{-1} and 12.9 kcal mol^{-1}, respectively. The former is thus kinetically preferred (see Section 4.4.2.3.3) and, notably, involves release of the first of the final P_1 products, $(Me_3Sn)_2PH$, alongside the *cyclo*-P_3 product $Me_3SnP_3H_2$, **VIa**.

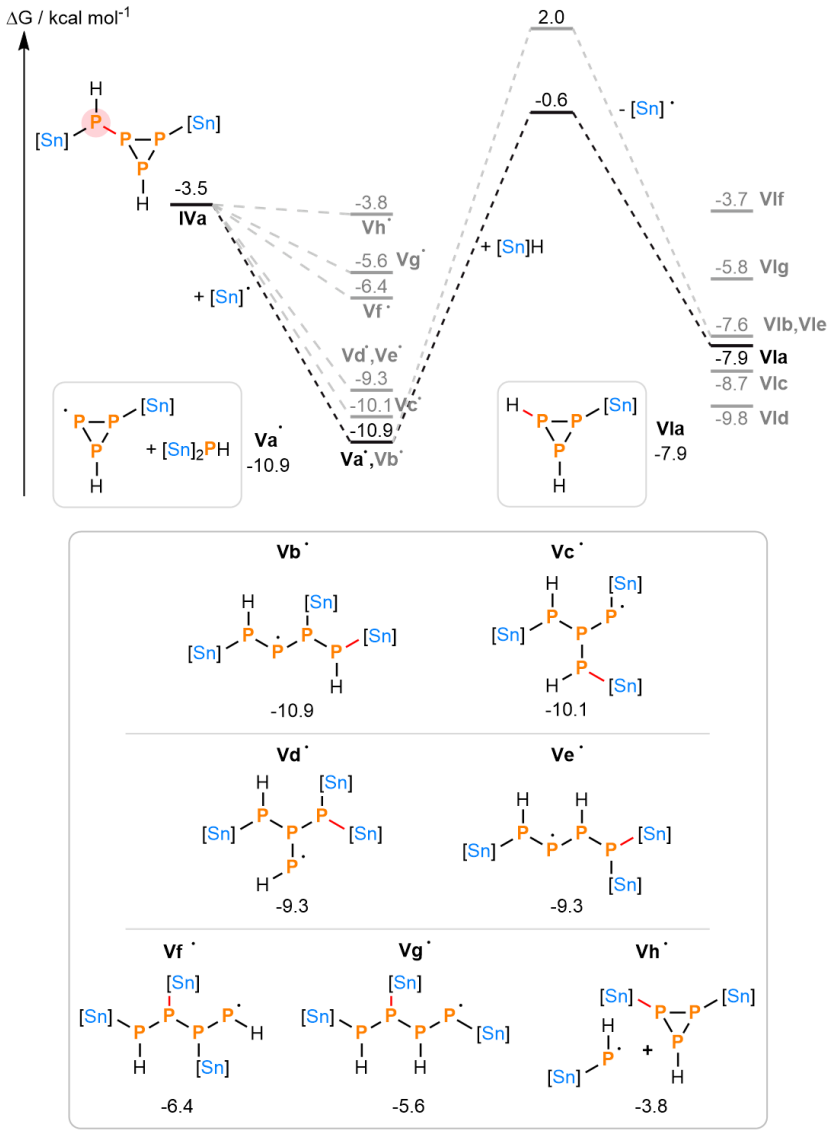

Figure 4. Calculated mechanisms for hydrostannylation of the third P–P bond in P_4 by Me_3SnH, with relative free energies in kcal mol^{-1}. For simplicity, stereochemistry is not shown (see Figure S11). [Sn] = Me_3Sn.

Fourth P–P cleavage: The fourth $Me_3Sn^{\bullet}$ attack step could again proceed from any of several different isomers **VI**, and for pragmatic reasons a single, representative example was again chosen as a focus for further calculations. In this case **VIa** was selected, as it is kinetically preferred out of the two products derived from the lowest energy isomers of **V**$^{\bullet}$, **Va**$^{\bullet}$ and **Vb**$^{\bullet}$, which are also the two isomers whose pathways were calculated in the most detail in the previous step (see also Figure S12). From **VIa** only three regiochemical options for $Me_3Sn^{\bullet}$ attack are available, leading to the intermediates **VII**$^{\bullet}$. H atom transfer from Me_3SnH then gives isomeric intermediates **VIII** (Figure 5). In this case all three regiochemical pathways were calculated in full. As for the previous steps, initial $Me_3Sn^{\bullet}$ attack is consistently downhill and effectively barrierless, and there is limited preference between the isomers **VII**$^{\bullet}$, which are all separated by a span of just 2 kcal mol^{-1}. However, there is a slightly more pronounced preference between the subsequent H atom transfer steps, with isomer **VIIc**$^{\bullet}$ providing an appreciably lower activation barrier than **VIIa**$^{\bullet}$ or **VIIb**$^{\bullet}$, leading to the ring opened P_3 chain **VIIIc**. Notably, this step is slightly exergonic, in contrast to the slightly endergonic H atom transfers calculated for steps 1-3.

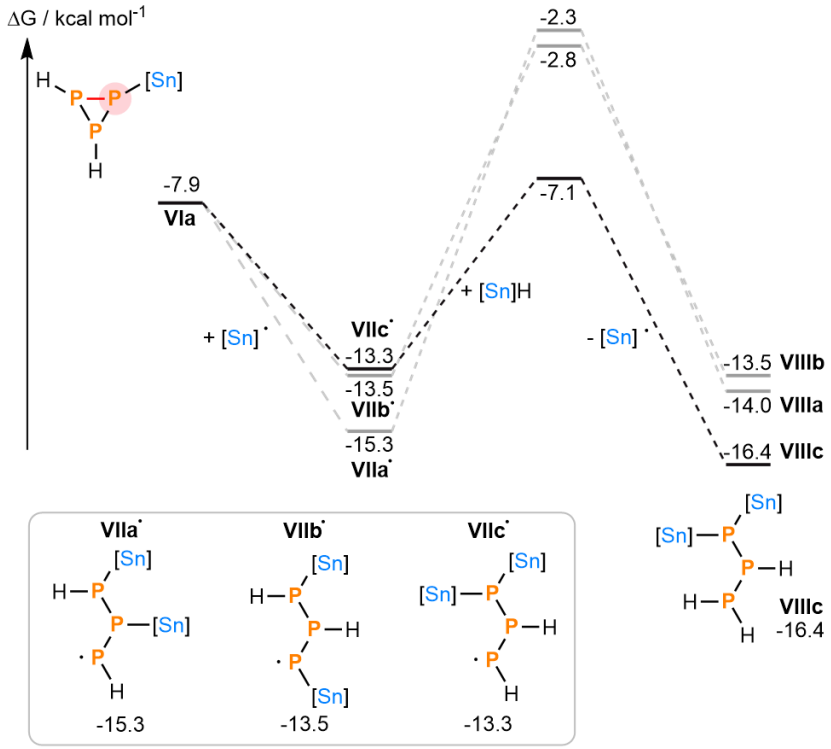

Figure 5. Calculated mechanisms for hydrostannylation of the fourth P–P bond in P_4 by Me_3SnH, with relative free energies in kcal mol^{-1}. For simplicity, stereochemistry is not shown (see Figure S12). [Sn] = Me_3Sn.

Fifth P–P cleavage: Proceeding from **VIIIc** (as the kinetically preferred product of the previous step; see Section 4.4.2.3.4) four options are available, leading initially to intermediates **IX**$^{\bullet}$ (Figure 6; see also Figure S13). Of these, two (**IXa**$^{\bullet}$ and **IXb**$^{\bullet}$) form exergonically, as in steps 2-4, but formation of the two higher energy isomers (**IXc**$^{\bullet}$ and **IXd**$^{\bullet}$) is slightly uphill (*cf.* step 1). Transition states for subsequent H atom transfer from Me_3SnH were calculated for the former pair, with **IXb**$^{\bullet}$ found to lead to a lower energy barrier, and formation of P_2H_4 (**Xb**) as the kinetically preferred product (see Section 4.4.2.3.5). As for the fourth, this fifth H atom transfer

is exergonic. This combined fifth step also yields the second P_1 product of the overall pathway, $(Me_3Sn)_3P$.

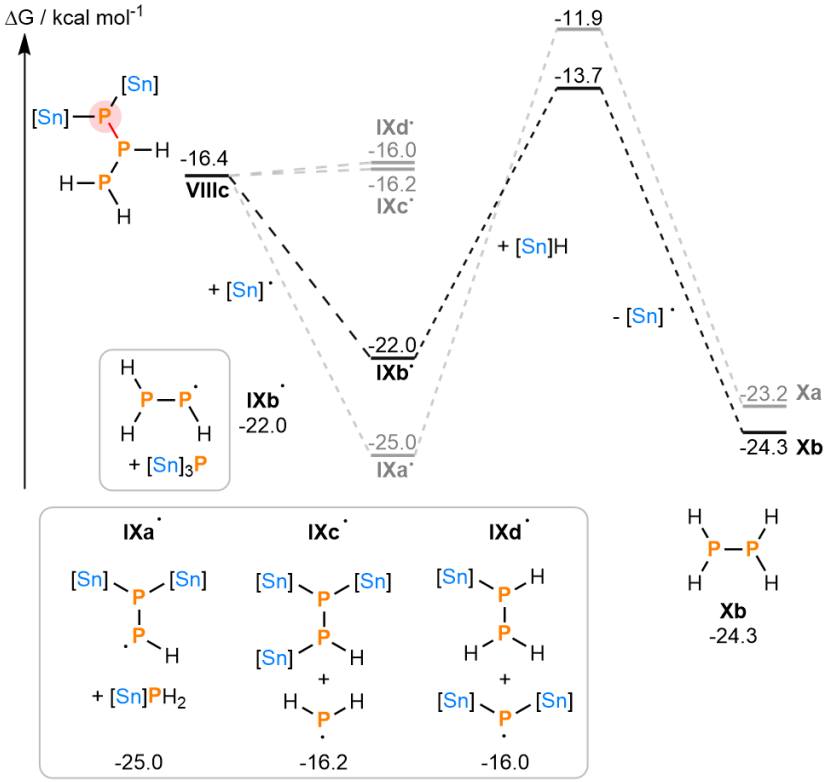

Figure 6. Calculated mechanisms for hydrostannylation of the fifth P–P bond in P_4 by Me_3SnH, with relative free energies in kcal mol^{-1}. For simplicity, stereochemistry is not shown (see Figure S13). [Sn] = Me_3Sn.

Final P–P cleavage: The symmetry and reduced size of **Xb** (P_2H_4) ensure that, gratifyingly, the final P–P bond cleavage calculation involves only a single regiochemical possibility (Figure 7). $Me_3Sn^{\bullet}$ attack yields the third P_1 product of this sequence, Me_3SnPH_2, and the simple P_1 radical $H_2P^{\bullet}$ (**XI**$^{\bullet}$). As in steps 2-5 this is downhill and effectively barrierless. A final H atom transfer from Me_3SnH then yields the final P_1 product, PH_3. As in steps 4 and 5 this transfer is also downhill and proceeds over a modest activation barrier (7.8 kcal mol^{-1}).

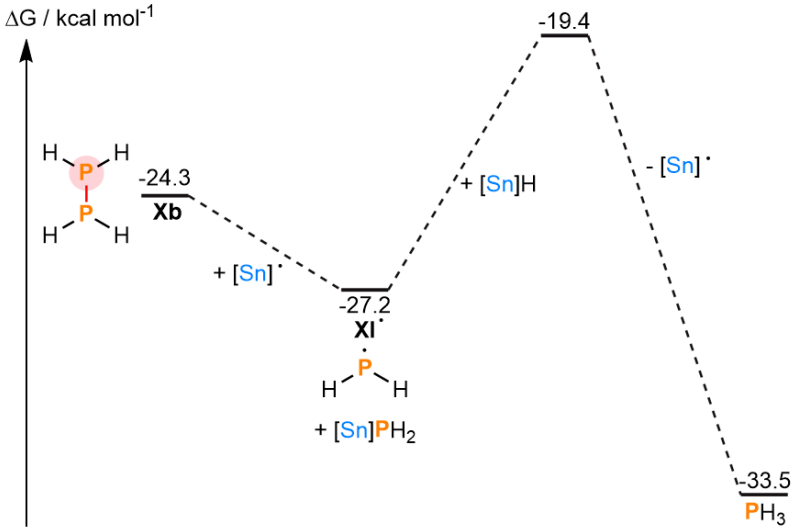

Figure 7. Calculated mechanisms for hydrostannylation of the final P–P bond in P_4 by Me_3SnH, with relative free energies in kcal mol^{-1}. [Sn] = Me_3Sn.

General observations: Comparing Figures 2-7, and the combined summary in Figure 8, it is possible to identify clear similarities between the multiple P–P cleavage steps. With the exception of the first, each is calculated to begin with exergonic, effectively barrierless attack of a $Me_3Sn^{\bullet}$ radical. The resulting P-centered radical intermediate then abstracts a H atom from Me_3SnH. This latter step becomes less endergonic as P_4 is broken down (e.g. for **I$^{\bullet}$→II**, **IIIa$^{\bullet}$→IVa**, and **Va$^{\bullet}$→VIa**) and is eventually exergonic during the final three P–P bond cleavages. Notably, each of the net hydrostannylation steps proceeds *via* a $Me_3Sn^{\bullet}$ addition that is exergonic to a similar extent (*ca.* 5-10 kcal mol^{-1}), and a H atom transfer that has a similar activation barrier (*ca.* 10 kcal mol^{-1}). Crucially, this ensures that there are no significant thermodynamic sinks at which the reaction would be expected to stall, or within which intermediates would be expected to accumulate. This can be attributed to the fact that *each step is in practice very chemically similar*, involving hydrostannylation of a comparable P–P single bond (*vide infra*).

The combined pathway shown in Figure 8 correctly predicts the formation of all four products observed experimentally: PH_3, Bu_3SnPH_2, $(Bu_3Sn)_2PH$, and $(Bu_3Sn)_3P$. However, it should be emphasized that *at every step there are clearly alternative, energetically accessible pathways*, often with only very small energetic differences between the competing options. For example, it has already been noted that in the second step, the two isomeric products **IVa** and **IVb** are both likely to be kinetically accessible, and while downstream pathways have so far been calculated exclusively from **IVa** it seems likely that similar investigation of **IVb** would reveal competing pathways with comparable activation barriers. Similarly, in the third step the *five* lowest energy isomers of intermediate **V$^{\bullet}$** span an energy range of well under 2 kcal mol^{-1}. Combined with the experimental observation that the four hydrostannylation products are not formed in equal amounts, these results strongly suggest that the product distribution observed experimentally is likely to be attributable less to the existence of a single, inherently preferred kinetic pathway, and more to simple statistical factors (*vide infra*). Indeed, a purely random distribution of H and R_3Sn moieties within the product mixture would be expected to result in 75% conversion to the two major products Bu_3SnPH_2 and $(Bu_3Sn)_2PH$, even in the complete absence of any kinetic or thermodynamic biases (which closely matches the combined yields obtained experimentally: *ca.* 76%).[9] This conclusion is further supported by calculations on selected other pathways, which also show similar activation barriers and other energetic changes for each P–P hydrostannylation step (Figures S15-19).

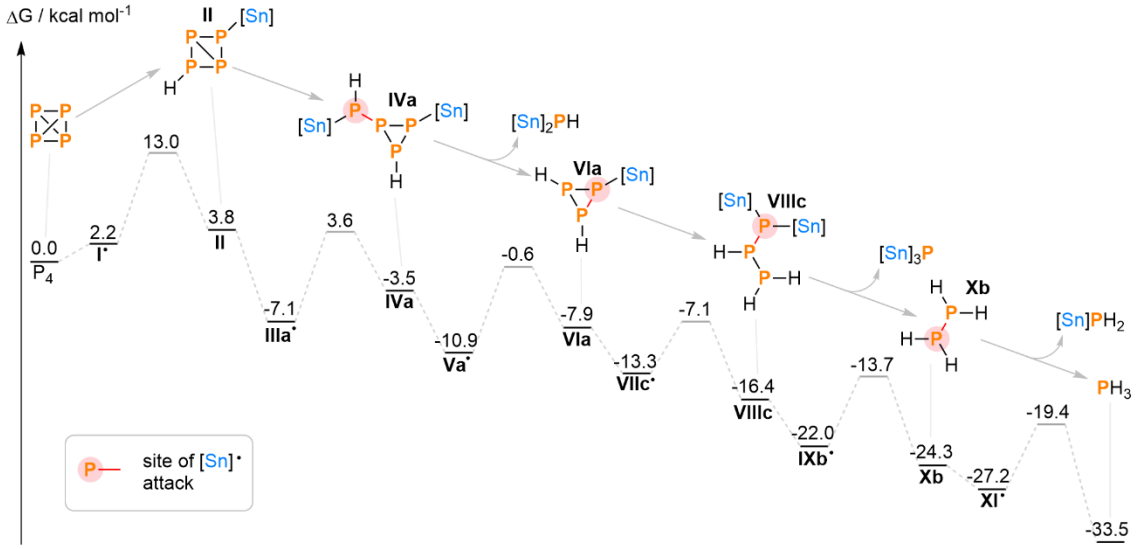

Figure 8. Combined calculated pathway for P_4 hydrostannylation, with relative free energies in kcal mol^{-1}. For simplicity, initiation, stereochemistry, addition of [Sn]•, loss of [Sn]H, and competing pathways are not shown (for these details, see Figures 2-7 and the SI). [Sn] = Me_3Sn.

4.2.2 Experimental study of bulkier hydrostannanes

As noted above, it was not possible to observe P_n reaction intermediates being formed and consumed while monitoring the reaction of P_4 with Bu_3SnH. Nor were intermediates observed during analogous experiments using Ph_3SnH (see Section 4.4.1.4), which our previous studies had been shown to also hydrostannylate P_4, albeit slightly less cleanly.[9] However, it was speculated that these species might become detectable if significantly bulkier hydrostannanes were employed. Increased steric hindrance should make each addition of an $R_3Sn^{\bullet}$ moiety progressively more difficult, so could potentially trap out partially reduced intermediates. Note that, by design, this will alter the kinetics and thermodynamics of individual steps and hence is likely to affect selectivity between specific intermediates. Nevertheless, observation of these intermediates should still provide experimental evidence to support the types of intermediate structures identified computationally. The hydrostannylation of P_4 was therefore investigated experimentally using the bulkier tin hydrides *i*Pr_3SnH, $TerSn(Me)_2H$, $Ter^*Sn(Me)_2H$ and $(Fluind)Sn(Me)_2H$, whose full structures are provided in Figure 9. While *i*Pr_3SnH was prepared in accordance with the literature,[20] $TerSn(Me)_2H$, $Ter^*Sn(Me)_2H$ and $(Fluind)Sn(Me)_2H$ are new compounds and were prepared *via* reaction of Me_2SnCl_2 with the corresponding aryllithium followed by $LiAlH_4$ reduction, as summarized in Scheme 3. These products were isolated in excellent yields (88-95%) and fully characterized by techniques including multinuclear NMR spectroscopy (^1H, ^{13}C, ^{119}Sn) and XRD (for full details, see Section 4.4.3).

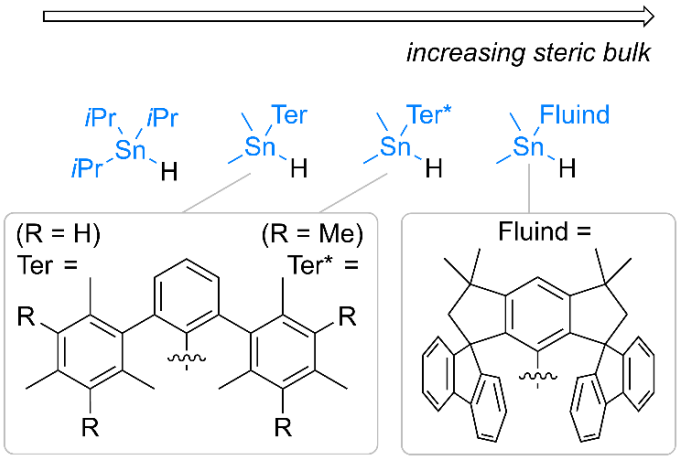

Figure 9. Full structures of bulkier hydrostannanes studied for hydrostannylation reactivity towards P_4.

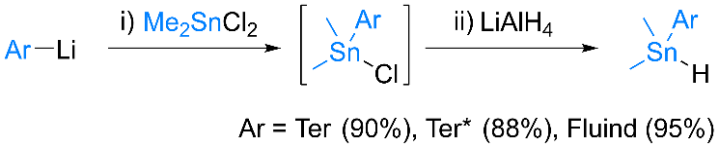

Scheme 3. Synthesis of bulky tin hydrides $ArSn(Me)_2H$.

Investigations with even the least bulky of these new hydrostannanes, iPr$_3$SnH, showed that increased steric profile has a marked impact on the P_4 hydrostannylation outcome, with both the light- and AIBN-initiated reactions resulting in exclusive formation of iPr$_3$SnPH$_2$ and (iPr$_3$Sn)$_2$PH without any appreciable PH_3 or (iPr$_3$Sn)$_3$P (Scheme 4a and Figures S31-34). This contrasts with results using Bu$_3$SnH but is consistent with the bulkier iPr$_3$Sn moieties needing to be distributed as evenly as possible across the available P atoms in order to minimize steric clash.[21] It also has significant synthetic implications, as a simpler P_1 mixture could streamline downstream functionalisation. Formation and loss of PH_3 has been identified as a possible yield-limiting factor in previous Bu$_3$SnH-based reactions,[5,10] which could be sidestepped using bulkier alternatives. Nevertheless, for iPr$_3$SnH it was still not possible to observe any intermediate P_n species (Figure S35).

Gratifyingly, when steric bulk was increased still further, clear observation of intermediate P_n species did become possible. Complete hydrostannylation of P_4 using $TerSn(Me)_2H$ or $Ter^*Sn(Me)_2H$ again resulted in clean, exclusive formation of R_3SnPH_2 and $(R_3Sn)_2PH$ as the final products (Scheme 4a and Sections 4.4.4.2 and 4.4.4.3), and for the $TerSn(Me)_2H$ case it was also possible to obtain an XRD structure of the latter (Scheme 4b), further confirming the identity of this product, since previous $(R_3Sn)_2PH$ had only been characterized spectroscopically.[9] However, $^{31}P\{^1H\}$ NMR spectroscopic monitoring of both reactions also allowed for clear observation of three new species characterized by singlet resonances at -220.0 and -226.5 ppm, and doublets of doublets centred at -251.5, -270.4 and -292.9 ppm (values for $TerSn(Me)_2H$; results for $Ter^*Sn(Me)_2H$ were very similar and are shown in Section 4.4.4.3).[22] These

resonances can be assigned based on a combination of $^{31}P\{^{1}H\}$, ^{31}P and $^{119}Sn\{^{1}H\}$ NMR spectroscopy (Figure 10; see also Section 4.4.4.2).

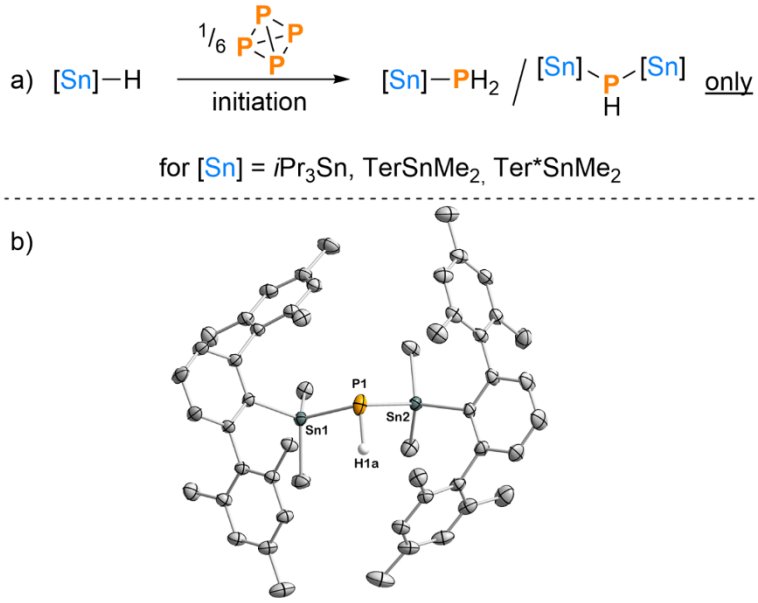

Scheme 4. (a) P_4 hydrostannylation using bulky tin hydrides, and (b) single-crystal XRD structure of $[Sn]_2PH$ for [Sn] = $TerSnMe_2$. Thermal ellipsoids are shown at 50%. For clarity, only one position of the disordered P-bound H atom is shown, and all other H atoms are omitted. C atoms are shown in grey, H is white, P in orange, and Sn in dark grey.

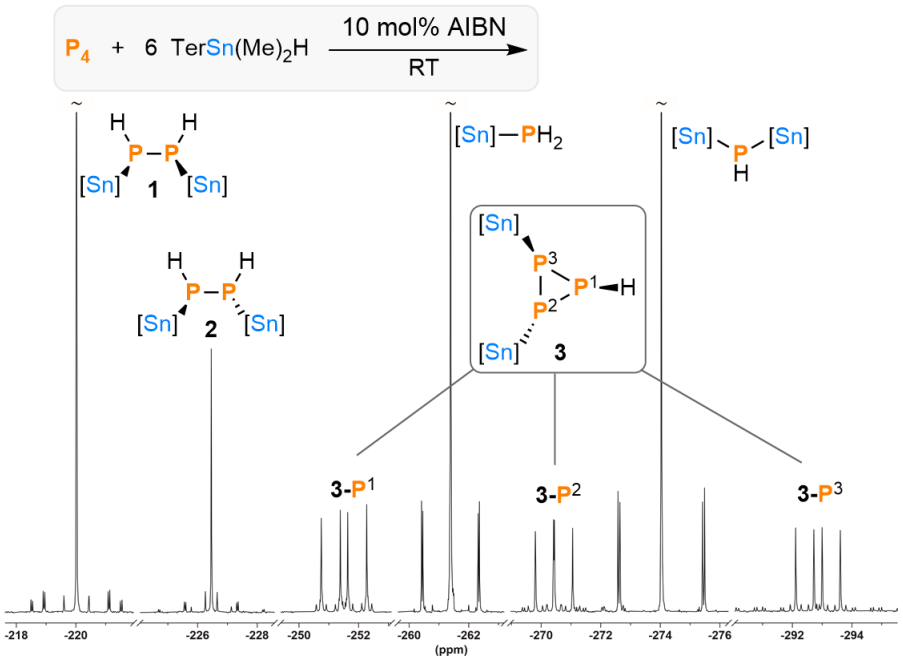

Figure 10. $^{31}P\{^{1}H\}$ NMR spectroscopic observation of reaction intermediates during the hydrostannylation of P_4 using $TerSn(Me)_2H$ (6 eq.) initiated by AIBN (10 mol%) in C_6D_6. [Sn] = $TerSnMe_2$. Peaks marked with ~ have been truncated for the sake of clarity. For expanded views of individual $^{31}P\{^{1}H\}$ and ^{31}P resonances, including isotopic satellites, see Figures S41-44.

The two singlets correspond to the meso and rac isomers of the symmetrical diphosphane $R_3SnP(H)–P(H)SnR_3$ (**1** and **2**, respectively). Both show AA'XX' splitting patterns in their ^{1}H-coupled ^{31}P spectra as well as satellites for both ^{1}J and ^{2}J coupling to ^{117}Sn and ^{119}Sn. Their relative assignment is based on comparison with related symmetrical diphosphanes in the

literature,[23] alongside DFT calculations (see Section 4.4.5). Meanwhile, the three other signals correspond to a single species (as confirmed by ^{31}P-^{31}P COSY): the *cyclo*-P_3 species $(R_3Sn)_2P_3H$ (**3**). Due to the relative orientations of the P–H and P–Sn bonds with respect to the P_3 plane this intermediate contains three distinct and mutually-coupled ^{31}P environments, resulting in three doublets of doublets in the $^{31}P\{^1H\}$ spectrum. For all three it is possible to identify their corresponding ^1J and/or ^2J couplings to both $^{117/119}$Sn and the ring ^{1}H (the latter being extracted from the proton-coupled ^{31}P spectrum), and thus to fully characterize the central Sn_2P_3H spin system.

The observation of the *cyclo*-P_3 species **3** as one of the only observable intermediates is highly interesting, as it is directly equivalent to the calculated structure **Vh$^\bullet$**. This was predicted to be kinetically accessible for less bulky Me_3SnH (Figure 4), confirming the ability of steric tuning to stabilize otherwise "invisible" reaction intermediates. Observation of **3** also supports the ability of steric factors to alter the reaction course. It seems clear that with the bulky R_3SnH hydrostannylation proceeds in such a way as to avoid installation of two R_3Sn moieties on a single P atom for as long as possible (leading to **3**), in contrast to the calculated pathways for less bulky Me_3SnH where **Vh$^\bullet$** was a relatively high energy isomer of **V$^\bullet$** (Figure 4).[24] Similarly, the Me_3Sn-substituted analogues of intermediates **1** and **2**, while not shown in Figure 8 (*cf.* P_2H_4 = **Xb**), were also calculated to be kinetically accessible intermediates (**IXi$^\bullet$**, **Xe**; Figures S15-S19). Formation of **1** and **2** can again be justified on steric grounds (for a fuller discussion, see Section 4.4.4.2).

The fact that only *specific* intermediates are observed when using $TerSn(Me)_2H$ or $Ter^*Sn(Me)_2H$ may imply much greater selectivity between the available pathways than with the less bulky Bu_3SnH (*vide supra*). To investigate this further, these reactions were monitored over time. Kinetic profiles were obtained for both the light- and AIBN-initiated reactions between P_4 and $TerSn(Me)_2H$, which are similar, except for a noticeable induction period for the former. This induction period may be caused by the light-induced initiation step,[15] or simply by low light intensity in the *in situ* NMR setup. However, following this induction period the light-driven reaction was found to be slightly faster than that driven by AIBN. It therefore gave a clearer picture of the total reaction course, and so is shown in Figure 11a (for the AIBN-driven profile see Figure S46 and for the similar profile using $Ter^*Sn(Me)_2H$ see Figure S52). Close inspection reveals that **3** is formed fairly rapidly after the induction period of the illuminated reaction before slowly decaying, in line with its role as a reaction intermediate. **1** and **2** follow a qualitatively similar profile, albeit slightly more slowly, indicating that they might be possible downstream products of **3** (although competing pathways cannot be fully excluded). Interestingly, the formation of $(R_3Sn)_2PH$ lags noticeably behind that of the other final product R_3SnPH_2. While an equimolar mixture is observed experimentally after complete hydrostannylation, early on, formation of R_3SnPH_2 significantly outpaces that of $(R_3Sn)_2PH$. This is fully consistent with the

fact that initial formation of intermediate **3** from P_4 + 3 R_3SnH must be balanced by concomitant formation of R_3SnPH_2 (see Figure 11b) and so synchronous formation of these two species is immediately observed. Only upon subsequent breakdown of **3** does more hindered $(R_3Sn)_2PH$ begin to form (for more detailed mechanistic discussion, see Scheme S1 and Section 4.4.4.2).[25] Increasing steric bulk of the tin hydride yet further, beyond $TerSn(Me)_2H$ and $Ter^*Sn(Me)_2H$, was found to completely shut down reactivity. No reaction with P_4 could be observed using $(Fluind)Sn(Me)_2H$, revealing an upper limit on the steric bulk range that is tolerated for P_4 hydrostannylation (see Section 4.4.4.4).

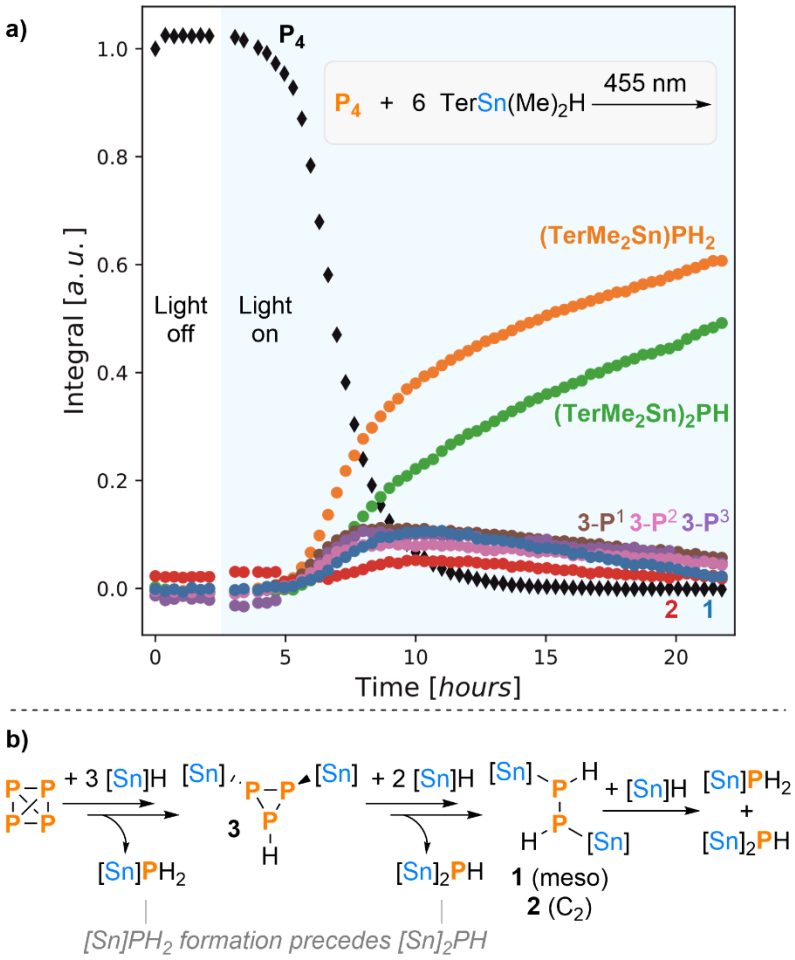

Figure 11. (a) Evolution over time of P atom speciation in the reaction between P_4 and 6 eq. $TerSn(Me)_2H$ initiated under 455 nm LED irradiaton at 298 K in C_6D_6 as monitored by *in situ* $^{31}P\{^1H\}$ NMR spectroscopy (irradiation period shaded in light blue); and (b) outline reaction pathway.

4.2.3 Discussion and analysis of results

From the computational and experimental results described above it is possible to draw several important conclusions:

1) P_4 hydrostannylation is able to proceed efficiently as a result of activation barriers that are consistently low for each P–P cleavage step.

These low barriers allow an efficient radical chain reaction to occur even at room temperature and prevent the formation of major thermodynamic sinks that might otherwise hinder reaction progress.

2) It is possible to identify preferred pathways for P_4 degradation by hydrostannylation using bulky tin hydrides.

This steric control can also be used to conveniently influence the final product distribution, which should in turn allow for improved onward reactivity. However:

3) For less bulky tin hydrides multiple P_4 hydrostannylation pathways are energetically accessible and are likely to operate in parallel.

Fortunately, each of these pathways is expected to lead to the same eventual set of products, $(R_3Sn)_xPH_{3-x}$. Thus, the reaction with Bu_3SnH in particular succeeds not by ensuring a single, specific mechanistic *pathway* but rather by ensuring a specific reaction *outcome*, even if this is achieved *via* multiple pathways in parallel. This mechanistic flexibility is facilitated by the next conclusion:

4) Each P–P cleavage step is mechanistically and energetically similar, especially for less bulky tin hydrides.

While in principle each P–P bond cleavage represents a distinct mechanistic step, in practice each such step is very similar, involving hydrostannylation of a closely comparable P–P single bond *via* a common sequence of $R_3Sn^{\bullet}$ radical attack and H atom transfer, all with similar activation barriers. This near equivalence prevents the formation of intermediate thermodynamic sinks and ensures that each P–P cleavage step can be achieved using the same tin hydride reagent. Crucial to facilitating this is the fact that *each P–P cleavage step has only a small impact on the reactivity of the remaining P–P bonds*.

This is a powerful guideline for the development of future P_4 functionalisation chemistry and suggests the targeting of other mechanisms that would break P_4 down "bond by bond", rather than *via* fundamental changes to the electronic structure of the overall P_n motif. Indeed, this conclusion may also help to explain the success of the "oxidative onioation" recently reported by the Weigand group, which is another particularly prominent example of recent successful P_4 activation and transformation, and also appears to satisfy this criterion.[6d,26] Conversely, this conclusion highlights a potentially significant challenge for the development of "inner sphere" transition metal (TM) mediated processes for P_4 functionalisation. These are approaches that have traditionally been heavily emphasized in the field of P_4 chemistry, and reactions of P_4 with TM complexes are by now well known to result in a wide variety of remarkable and academically fascinating TM-bound P_n moieties. However, it is also well known that these different P_n moieties can display markedly different electronic structures (single *vs.* multiple bonds, π-delocalisation, *etc*.) and reactivities, even when bound to the same TM fragment, and can therefore require very different reagents and/or conditions for functionalisation. This presents a significant limiting factor that any system seeking to functionalise P_4 *via* a sequence of TM-bound P_n moieties must overcome (for further discussion see Section 4.4.6).[6a,6g]

4.3 Conclusion

We have described herein the mechanism of our recently reported hydrostannylation of P_4. This complex reaction can be used to facilitate the convenient transformation of P_4 directly into myriad useful P_1 products, but many aspects of its mechanism had previously remained unclear. Through a combination of computational and experimental study we have been able to identify a preferred sequence of elementary bond cleavage steps through which breakdown of the P_4 tetrahedron can occur, but also demonstrated that many competing pathways are available, all eventually leading to the same set of products $(R_3Sn)_xPH_{3-x}$. These conclusions are supported by DFT calculations and observation of intermediates that have been stabilized by increasing their steric bulk.

From these results it has been possible to identify key, underpinning mechanistic factors that allow the hydrostannylation reaction to proceed so efficiently, and which can act as useful guidelines to aid in the development of future P_4 functionalisation reactions. In particular, these studies suggest that it is beneficial for P_4 functionalisation reactions to transform their substrate "one P–P bond at a time", while ensuring that the remaining P–P bonds remain electronically similar (*cf.* the simplified mechanism in Scheme 2). We believe that these insights will help to guide future research towards the goal of practical, direct P_4 functionalisation, and we ourselves are currently using them as we continue our efforts to improve and diversify our already-reported strategies.

4.4 Supporting Information

General Experimental Methods

Unless stated otherwise, all reactions and manipulations were performed under an N_2 or Ar atmosphere (< 0.1 ppm O_2, H_2O) through use of MBraun Unilab and GS MEGA Line gloveboxes, and standard Schlenk line techniques. All glassware was oven-dried (160 °C) overnight prior to use. Anhydrous *n*-hexane and PhMe were purified using an MBraun SPS-800 system and stored over molecular sieves (3 Å). Et_2O was dried by distillation from sodium/benzophenone and stored over molecular sieves (3 Å). C_6D_6 was distilled from K and stored over molecular sieves (3 Å). *i*Pr_3SnH, 2,6-$Mes_2C_6H_3I$, 2,6-$PmpC_6H_3Li$ and $FluindLi(THF)_2$ (Fluind = dispiro[fluorene-9,3'-(1',1',7',7'-tetramethyl-s-hydrindacen-4'-yl)]) were prepared in accordance with the literature. [21,27-30] All other reagents and starting materials were purchased from major suppliers and used as received, including Me_2SnCl_2, $LiAlH_4$, Ph_3SnH and AIBN. Bu_3SnH was supplied containing 0.05% BHT as stabilizer and was also used as received.

Except where noted otherwise below, NMR spectra were recorded at room temperature on Bruker Avance 400 (400 MHz) or Bruker Avance Neo 600 MHz spectrometers. Chemical shifts, δ, are reported in parts per million (ppm); ^1H NMR and ^{13}C NMR shifts are reported relative to $SiMe_4$ and were referenced internally to residual solvent peaks (C_6HD_5: 7.16 ppm for C_6D_6) in the ^1H NMR spectra, and to the peak of the deuterated solvent (C_6D_6: 128.06 ppm) in the $^{13}C\{^1H\}$ NMR spectra.[31], while ^{31}P NMR and ^{119}Sn shifts were referenced externally to 85 % H_3PO_4 (aq.) and $SnMe_4$ (90% in C_6D_6), respectively. Except where stated otherwise, integrals for $^{31}P\{^1H\}$ and ^{31}P spectra are provided for the purposes of qualitative comparison only, and should not be considered quantitatively accurate. Assignment of the ^1H and $^{13}C\{^1H\}$ resonance signals was made in accordance with the COSY, HSQC and HMBC spectra. The abbreviations s, d, t, q, m are used to indicate singlets, doublets, triplets, quartets and multiplets, respectively.

ESI HRMS spectra were measured on a Bruker Impact II spectrometer. Dichloromethane/acetonitrile or dichlormethane/methanol solutions ($c = 1 \cdot 10^{-5}$ mol·L^{-1}) were injected directly into the spectrometer at a flow rate of 3 µL·min^{-1}. Nitrogen was used both as a drying gas and for nebulisation with flow rates of approximately 5 L·min^{-1} and a pressure of 5 psi. Pressure in the mass analyzer region was usually about $1 \cdot 10^{-5}$ mbar. Spectra were collected for 1 min and averaged. The nozzle-skimmer voltage was adjusted individually for each measurement. IR spectra were recorded on a Nicolet Thermo iS10 scientific spectrometer with a diamond ATR unit. The absorption bands are reported in cm^{-1} with indicated relative intensities: s (strong, 0 – 33 % T); m (medium, 34 – 66 % T), w (weak, 67 – 100 % T), and br (broad).

4.4.1 Initial $^{31}P\{^1H\}$ NMR spectroscopic monitoring experiments

4.4.1.1 General methods for *in situ* measurements

NMR spectroscopic measurements for *in-situ* reaction monitoring were recorded on a Bruker Avance III 600 MHz spectrometer equipped with a 5 mm TBI-P probe (^1H, ^{31}P, X) with z-gradient or a 5 mm TBI-F probe (^1H, ^{19}F, X) with z-gradient or on a Bruker Avance Neo 600 MHz spectrometer equipped with a 5 mm BBO-Prodigy probe (X, ^1H) with z-gradient.

^1H-NMR measurements were performed using a standard Bruker pulse program with 90° (zg) or 30° (zg30) excitation pulse.

Quantitative ^{31}P-NMR measurements were typically carried out with a standard Bruker pulse program with inverse-gated ^1H-decoupling and a 30° excitation pulse (zgig30), with a relaxation delay of usually 25 seconds to obtain quantitative spectra, if not stated otherwise.

Two ^{31}P-NMR kinetic experiments were recorded with ^1H-power gated decoupling, using a 90° excitation pulse (zgpg) to enhance sensitivity. These spectra cannot be used for quantitative analysis due to NOE-effects.

Two ^{31}P-NMR kinetic experiments were recorded with inverse-gated ^1H-decoupling, using an unpublished broadband-excitation pulse kindly provided by Prof. Dr. Burkhard Luy, Karlsruhe Institute of Technology, which allows uniform excitation over the whole spectral width of ^{31}P, for the sake of introducing phase- and integration errors from the long duration of the pulse (0.5 milliseconds) (bulu-zgig). These spectra should also not be treated as quantitative.

^{119}Sn-NMR measurements were performed using a standard Bruker pulse program with power-gated ^1H-decoupling and 90° excitation pulse (zgpg).

Data were processed with the Bruker software TopSpin 4.2.0. Integration was done using the 'intser' command and the output analysed and visualised using self-written Python scripts. ^1H NMR chemical shifts are reported relative to the residual proton signal of C_6D_6 at 7.16 ppm. ^{31}P NMR chemical shifts were externally referenced to 85 % H_3PO_4 (aq.). ^{119}Sn NMR chemical shifts were externally referenced to Me_3SnCl in D_2O at 39.3 ppm.

For in-situ illumination with 455 nm light, an Osram Oslon SSL80 royal-blue LED was used in combination with a 1000 µm high NA glass fiber in a previously described setup.[32] 365 nm illumination was carried out with a Laser Components LEUVA66X00RV00 UV-LED.

4.4.1.2 AIBN-initiated hydrostannylation using Bu_3SnH

A reaction solution was prepared by combining P_4 (0.01 mmol, as a stock solution in 124.6 µL C_6D_6) and Bu_3SnH (16.2 µL, 0.06 mmol) and AIBN (0.002 mmol, as a stock solution in 25.8 µL C_6D_6) in C_6D_6 (0.5 mL) inside a glovebox and transferred into an NMR tube with a screw cap. The tube was immediately transferred into a 600 MHz NMR spectrometer and subjected to $^{31}P\{^1H\}$ NMR analysis every 15 minutes. The P_4 starting material and products $(Bu_3Sn)_xPH_{3-x}$ (x = 0–3) could be identified based on their known chemical shifts.[9] The resulting reaction profile is shown in Figure 1 (Section 4.2), and below in Figure S1.

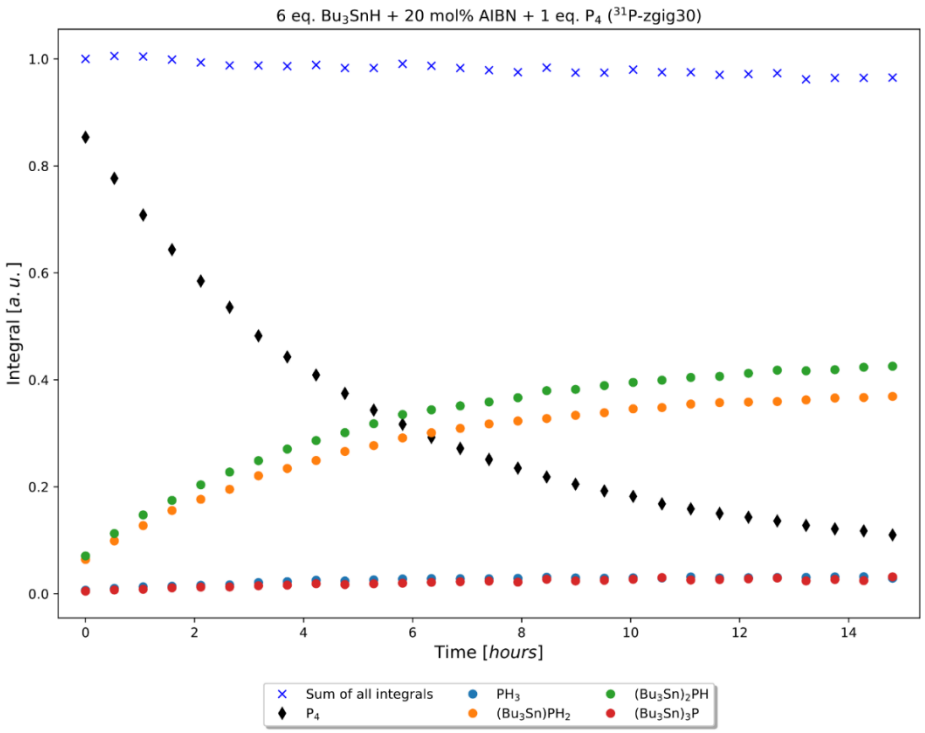

Figure S192. Evolution over time of P atom speciation in the reaction between P_4 and 6 eq. Bu_3SnH initiated by 20 mol% AIBN in C_6D_6 at room temperature.

No other transient ^{31}P-containing species could be observed during this experiment. In addition, no overall loss of ^{31}P integral intensity was observed, which could have indicated formation of polymeric side-products that are either insoluble, or give signals too broad to be observed by NMR spectroscopy.

A detailed kinetic analysis of this reaction is beyond the scope of this manuscript and – given the multitude of available pathways and the similarity of many of the activation barriers involved (e.g. initial $Bu_3Sn^{\bullet}$ formation from Bu_3SnH and $^{\bullet}C(CN)Me_2$, initial $Bu_3Sn^{\bullet}$ attack on P_4, *etc.*) – potentially rather complex. Nevertheless, during the course of this study several different iterations of the above reaction were monitored using different initial [Bu_3SnH] and/or [AIBN], as part of the unsuccessful effort to observe well-defined intermediates. And from the analysis of these experiments several relevant observations can be made.

Plots of the integral of $Bu_3Sn\underline{H}$ against reaction time, *t*, reveal a clear, consistent exponential decay, indicating net first-order (or pseudo-first order) kinetics (Figure S2). Likewise, plots of the integral of P_4 against reaction time, *t*, show equivalent exponential decay, within error, consistent with 6 equivalents of tin hydride reacting overall with one equivalent of P_4 (Figure S3). Since no internal standard was employed, the reaction rates given in Table S1 were normalized relative to the reaction where 6 equivalents Bu_3SnH and 10 mol% AIBN were employed.

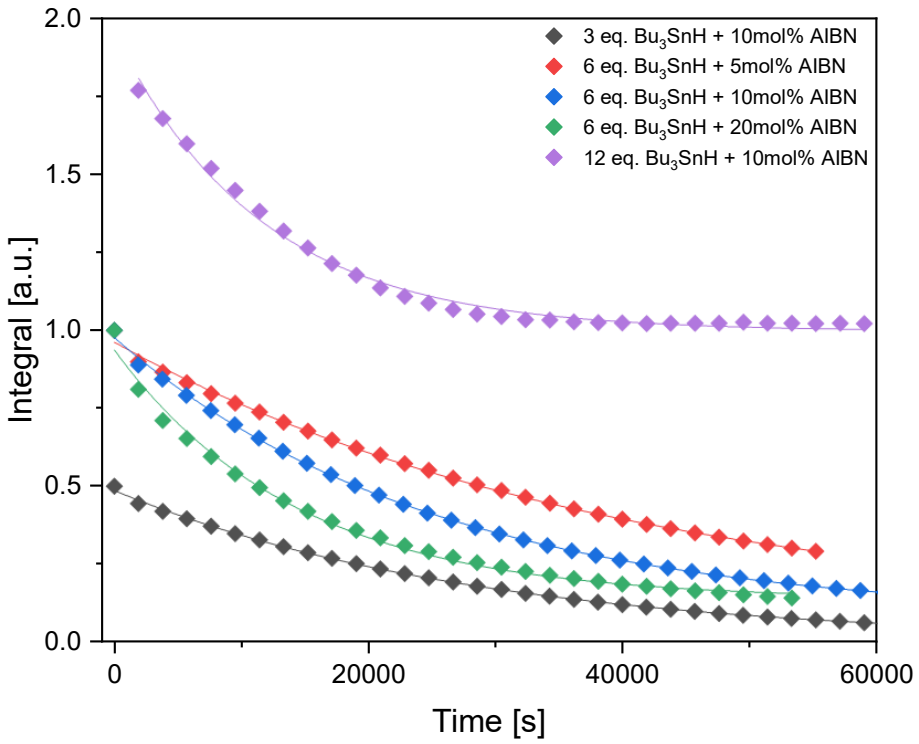

Figure S193. Plots of [Bu_3SnH] (measured by integration of the Sn*H* ^{1}H NMR resonance) against *t* for reactions of P_4 with various concentrations of Bu_3SnH and AIBN at room temperature in C_6D_6. Aside from scaling the amounts of Bu_3SnH and AIBN, experimental procedures are as outlined above.

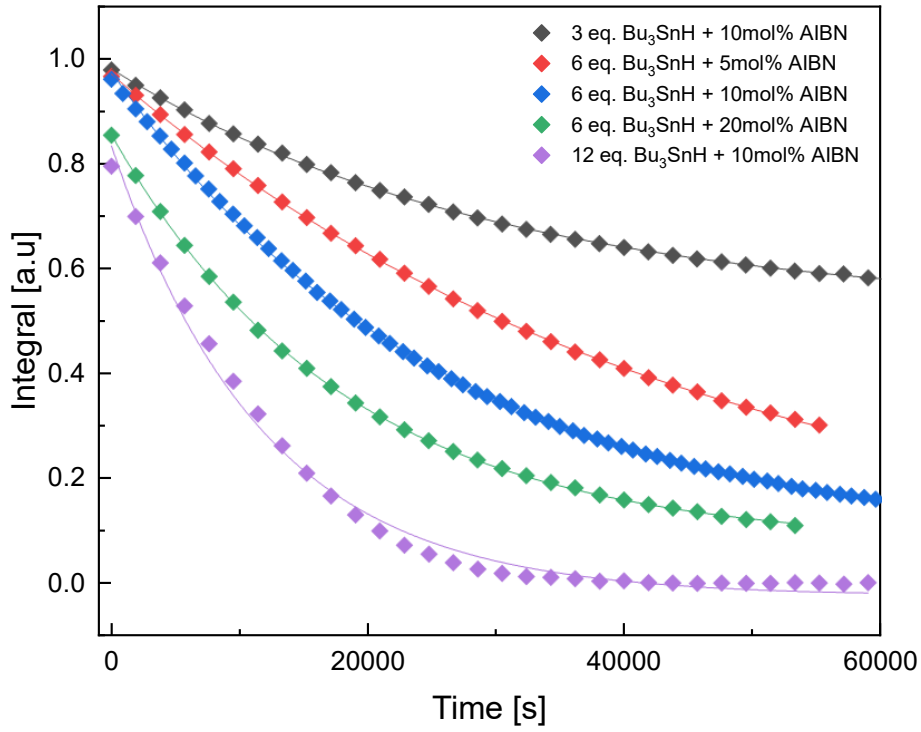

Figure S194. Plots of [P_4] (measured by integration of the ^{31}P NMR resonance) against *t* for reactions of P_4 with various concentrations of Bu_3SnH and AIBN at room temperature in C_6D_6. Aside from scaling the amounts of Bu_3SnH and AIBN, experimental procedures are as outlined above.

Table S1. Relative pseudo-first order rates constants, *k*, obtained *via* least-squares fitting of the data in Figure S2 and S3. Relative rates are given, since no internal standard was used.

Bu_3SnH loading / eq.	AIBN loading / mol%	P_4: *relative k* / s^{-1}	Bu_3Sn-H: *relative k* / s^{-1}
6	10	1.0	1.0
6	20	1.4	1.9
6	5	0.7	0.6
12	10	2.2	2.2
3	10	0.9	0.9

4.4.1.3 Light-initiated hydrostannylation using Bu_3SnH

A reaction solution was prepared by combining P_4 (0.01 mmol, as a stock solution in 124.6 μL C_6D_6) and Bu_3SnH (16.2 μL, 0.06 mmol) in C_6D_6 (0.3 mL) inside a glovebox and transferred into an NMR tube incorporating apparatus for *in situ* illumination that has been described previously.[32] The tube was immediately transferred into a 600 MHz NMR spectrometer and subjected to $^{31}P\{^1H\}$ NMR analysis every 15-30 minutes. The P_4 starting material and products $(Bu_3Sn)_xPH_{3-x}$ (x = 0-3) could be identified based on their known chemical shifts,[9] and the resulting reaction profile is shown in Figure S4, below.

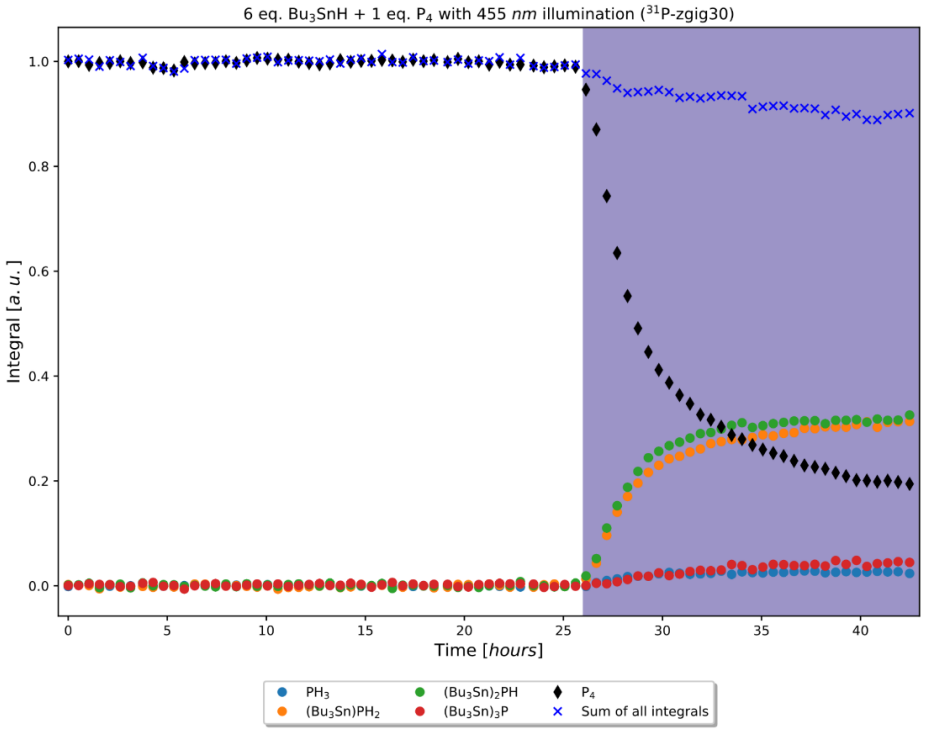

Figure S195. Evolution over time of P atom speciation in the reaction between P_4 and 6 eq. Bu_3SnH initiated by *in situ* 455 nm LED irradiation (starting after 26 h, illumination period indicated by blue shading) in C_6D_6 at room temperature.

The results confirmed that there is negligible reactivity in the dark. However, upon irradiation consumption of P_4 and formation of the expected products immediately began to be observed. This light-dependence was further illustrated through an "on/off" experiment in which the reaction was cycled between 2 h periods of darkness and irradiation, with reaction progress only being observed during the latter (Figure S5).

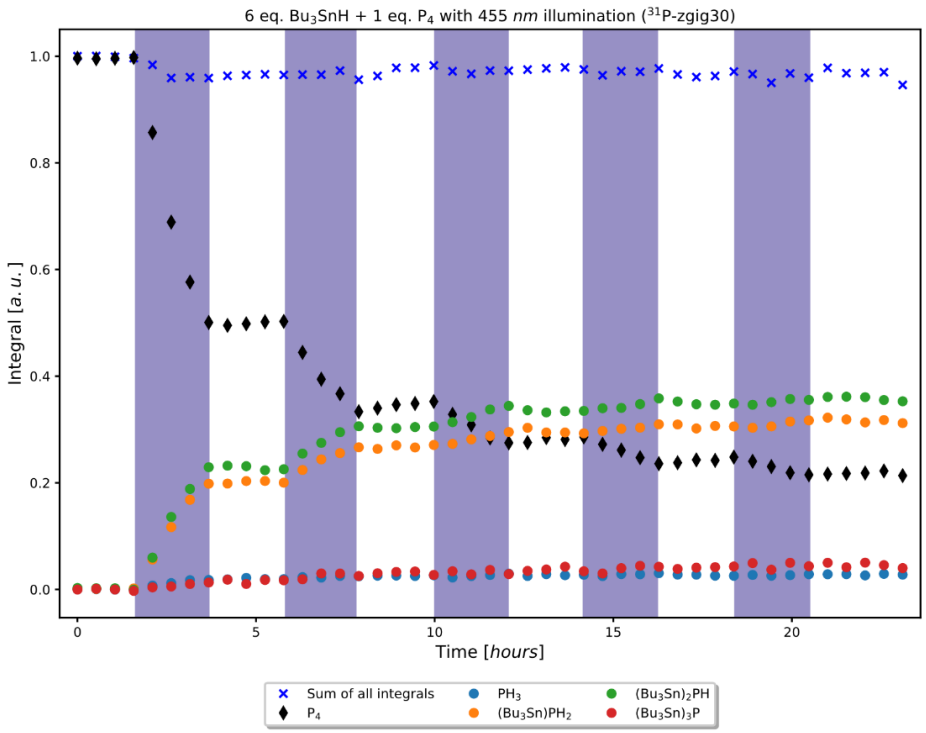

Figure S196. Evolution over time of P atom speciation in the reaction between P_4 and 6 eq. Bu_3SnH initiated by *in situ* 455 nm LED irradiation in C_6D_6 at room temperature. The reaction was cycled between light and darkness over time, with periods of illumination indicated by blue shading.

4.4.1.4 Hydrostannylation using Ph_3SnH

In our initial report we noted that as well as Bu_3SnH, Ph_3SnH can also be used for the hydrostannylation of P_4, achieving very similar net results (albeit with some competing formation of the distannane $Ph_3SnSnPh_3$).[9] As such, efforts were made to monitor this reaction over time, as well. Unfortunately, initial attempts using AIBN initiation led to reactions that had reached completion during the time needed for sample preparation, transfer from glovebox to spectrometer, and shimming (*ca.* 20 min). As such it was not possible to obtain a reaction profile for these experiments (although the results do indicate significantly faster kinetics for Ph_3SnH than Bu_3SnH). Instead, a light-initiated reaction was monitored, following a procedure equivalent to that described in Section 2.3, but using Ph_3SnH in place of Bu_3SnH (Figure S6). A very similar outcome was observed, with P_4 consumption and final product formation beginning immediately upon the start of 455 nm irradiation (traces of product observed prior to illumination are attributed to minor light exposure during sample preparation, *etc.*). As with Bu_3SnH, no intermediate resonances attributable to reaction intermediates were detected.

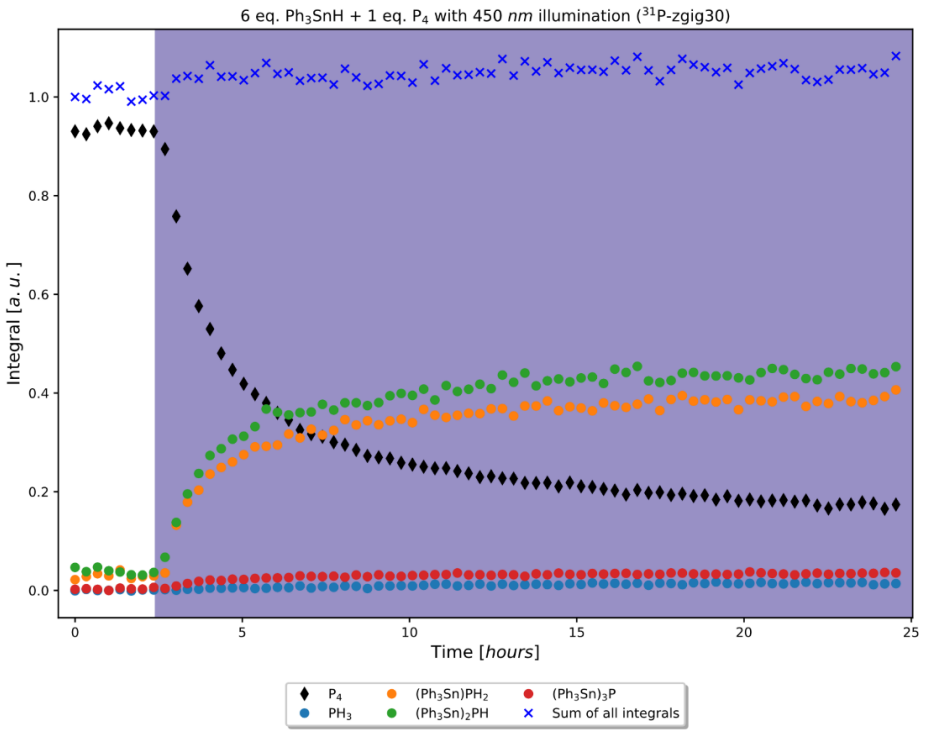

Figure S197. Evolution over time of P atom speciation in the reaction between P_4 and 6 eq. Ph_3SnH initiated by *in situ* 455 nm LED irradiation (starting after 3 h, illumination period indicated by blue shading) in C_6D_6 at room temperature.

4.4.2 Computational investigations into the radical hydrostannylation of P_4

General methods

All calculations were carried out with the ORCA program package.[33,34] Unless stated otherwise, all calculations were carried out on isolated molecules (in the gas phase) at 298 K. Density fitting techniques, also called resolution-of-identity approximation (RI)[35], were used for GGA calculations and the RIJCOSX[36] approximation was used for hybrid-GGA DFT calculations. Atom-pairwise dispersion corrections with the Becke-Johnson damping (D3BJ)[37,38] were used for all DFT calculations. Pictures were rendered with the software Avogadro.[39] All geometries were obtained at the PBE-D3BJ/def2-TZVP level of theory.

4.4.2.1 Mechanisms of initiation

In our initial report,[9] initiation was proposed to proceed *via* fragmentation of AIBN followed by H atom abstraction from Me_3SnH. The former step has not been calculated as it is well established experimentally, [14] but the latter step was calculated, to allow for direct comparison with an alternative mechanism for initiation *via* attack of the initally-formed radical $^{\bullet}C(CN)Me_2$ on P_4 rather than Me_3SnH. As expected, H atom transfer from Me_3SnH to $^{\bullet}C(CN)Me_2$ is calculated to proceed over only a modest activation barrier of 15.1 kcal mol^{-1} (Figure S7a), which is only slightly higher than the largest activation barrier identified during the subsequent P–P cleavage steps (13.7 kcal mol^{-1}, *en route* to **II**; Figure 2). This elementary step is also exergonic by 8.4 kcal mol^{-1}. In contrast, $^{\bullet}C(CN)Me_2$ attack on P_4 is calculated to be significantly uphill (by

13.3 kcal mol^{-1}), with an activation barrier of 15.9 kcal mol^{-1} (Figure S7b). Not only is this larger than the activation barrier for H atom transfer from Me_3SnH to $^{\bullet}C(CN)Me_2$, it is also much higher than the low barrier to P_4 attack by $Me_3Sn^{\bullet}$, clearly supporting initiation occurring *via* the latter mechanism. These calculations are consistent with experimental investigations that show no appreciable reaction between AIBN and P_4 even under considerably more forcing conditions (Section 3.2.2), which further supports this conclusion.

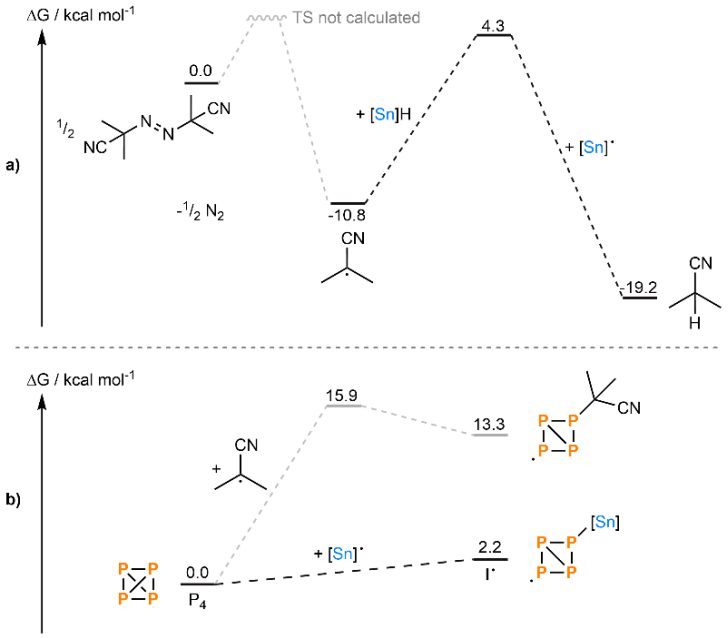

Figure S198. Calculated mechanisms for initiation *via* AIBN fragmentation and subsequent (a) H atom abstraction from Me_3SnH or (b) addition to P_4 (also shown for ease of comparison is $Me_3Sn^{\bullet}$ addition to P_4). [Sn] = Me_3Sn.

4.4.2.2 Experimental investigation of AIBN reactivity towards P_4

To a 10 mL, flat-bottomed, stoppered tube were added PhMe (500 µL), P_4 (0.01 mmol, as a stock solution in 97.6 µL PhH) and AIBN (10.7 mg, 0.065 mmol). The tube was sealed and heated to 80 °C for 18 h. The resulting mixture was analysed by $^{31}P\{^1H\}$ NMR spectroscopy, as shown in Figure S8, below.

The resulting $^{31}P\{^1H\}$ spectrum indicates retention of the P_4 starting material and no significant reaction with AIBN, despite the use of stoichiometric quantities and elevated temperatures sufficient to ensure (near)-complete AIBN fragmentation within the reaction timeframe.[14] An equivalent lack of reaction is also observed in reactions at lower temperatures (60 °C, room temperature) or with higher AIBN loadings (13.5 eq.). This observation is interesting not only due to its mechanistic relevance (effectively excluding AIBN activation of P_4 as a means of initiation) but also because of the apparent contrast with previous reports in which addition of organic radicals to P_4 is proposed to be a key step.[6b,6c,6f,6h,6i,8,40] One possible explanation for this seeming discrepancy could be the relatively electrophilic character of the AIBN-derived radical, which may discourage reaction with P_4 (which also generally shows electrophilic rather than nucleophilic behaviour).

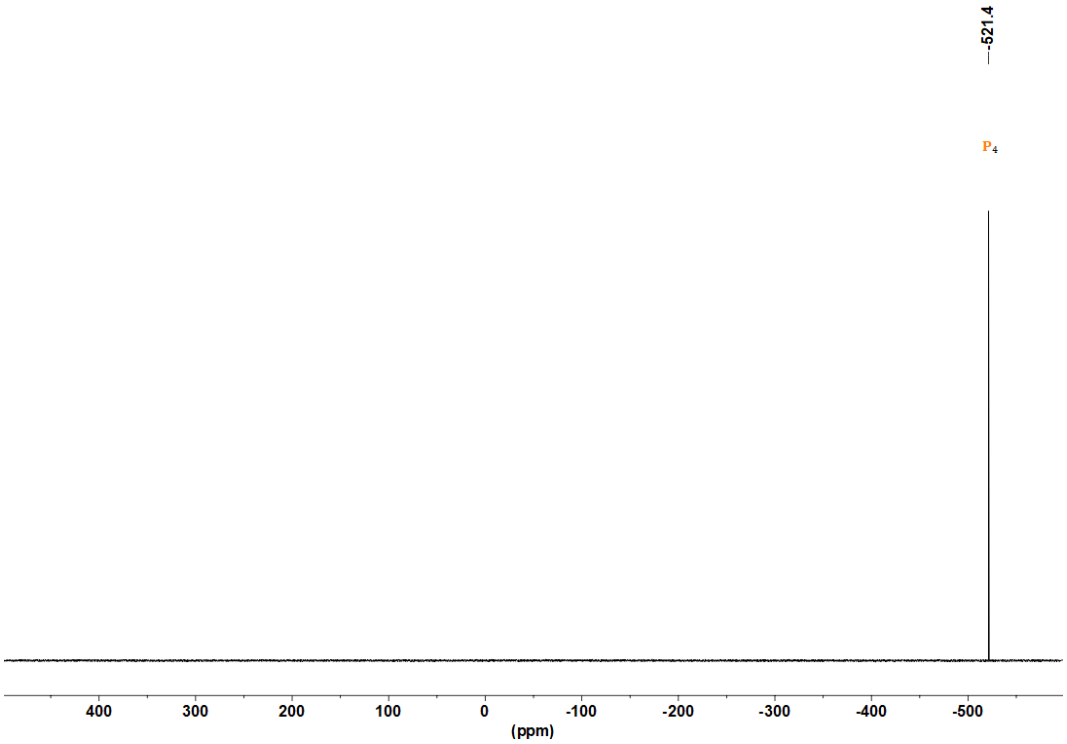

Figure S199. $^{31}P\{^{1}H\}$ NMR spectrum for the reaction of P_4 (0.01mmol) with AIBN (0.065 mmol in PhMe, heated to 80 °C for 18 h.

4.4.2.3 Mechanisms of P_4 hydrostannylation by Me_3SnH

Given the sheer number of pathways that are available, an exhaustive calculation of every possible sequence of P–P cleavage steps during the hydrostannylation of P_4 is impractical. Attention was therefore focused on a more specific, representative subset. To achieve this, the sequence decribed below was carried out. In order to limit this study to a manageable number of calculations the possibility of intermediates isomerising between steps was not considered, and nor was *aggregation* of P_4 to larger P_n moieties (for example by addition of P_4 to intermediates such as **I˙**). However, based on the consistent similarities between P–P cleavage steps noted in Section 4.2, it seems very unlikely that such processes would impact the overall conclusion: that multiple pathways are able to compete in parallel to generate the same set of final products. Indeed, intuitively, the possibility of yet further pathways being available would only seem to reinforce the likelihood of this conclusion.

4.4.2.3.1. 1st P–P cleavage:

Addition of $Me_3Sn^{\bullet}$ to P_4 was calculated to occur most favourably *via* an *exo* attack to generate the *exo*-butterfly radical intermediate **I˙**, as shown in Figure S9 (and Figure 2, Section 4.2.1). This was found to be slightly uphill, with relaxed surface scans revealing no identifiable transition state.

Due to P_4's symmetrical structure, only one regiochemical possibility exists for this first step. However, an alternative stereochemical option does exist. *Endo* attack of $Me_3Sn^{\bullet}$ would give the

alternative *endo* isomer ^{endo}**I**$^{\bullet}$, and this option was also calculated. ^{endo}**I**$^{\bullet}$ was actually found to be slightly lower in energy than **I**$^{\bullet}$; however its barrier for formation was much higher (and higher than any of the downstream steps calculated), and so this pathway was not considered further.

H atom abstraction from Me_3SnH by the radical **I**$^{\bullet}$ was then calculated, and found to be slightly endergonic with a modest activation barrier, as discussed in Section 4.2.1. *Exo* addition of the H atom was found to be slightly preferable to the *endo* alternative on both thermodynamic and kinetic grounds, and so this option was carried forward for calculation of the second P–P cleavage step.

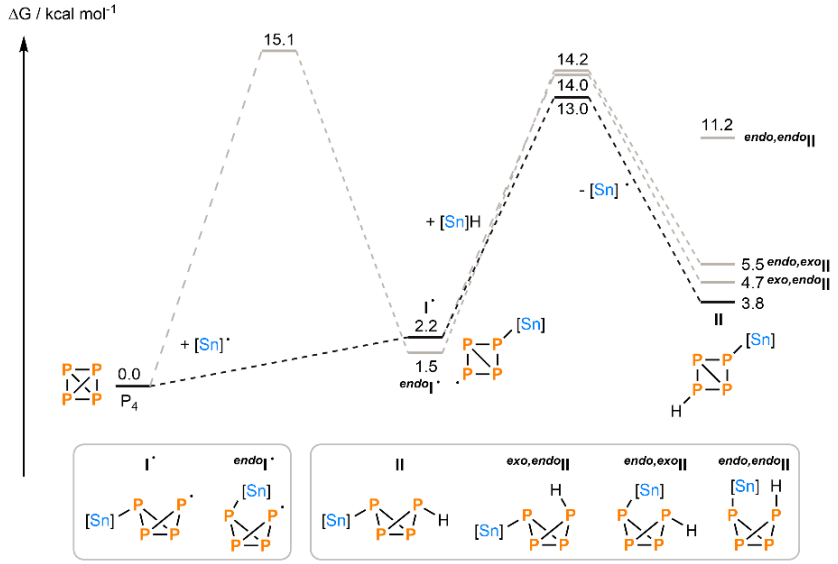

Figure S200. Calculated mechanism for hydrostannylation of the first P–P bond in P_4 by Me_3SnH, including stereochemistry, with relative free energies in kcal mol^{-1}. [Sn] = Me_3Sn.

4.4.2.3.2. 2nd P–P cleavage:

For the resulting intermediate **II**, $Me_3Sn^{\bullet}$ attack could occur on any of the three chemically distinct P–P bonds, two of which are unsymmetrical and so can each be attacked with two possible regiochemical outcomes, resulting in five possible intermediate constitutional isomers **III**, as shown in Figure S10 (and Figure 3, Section 4.2.1).

All five options were calculated and found to be exergonic and essentially barrierless, with no transition states identified by relaxed surface scans. In principle, more than one diastereochemical option is available for each of these steps (*cf.* the 1st step, above). However, to limit the number of calculations required to a reasonable level, only one specific option was calculated in each case. This was done by initially locating the $Me_3Sn^{\bullet}$ at a chemically reasonable position (based on sterics, expected reaction geometry, *etc.*) and optimising without restriction, in line with standard practice. (This treatment was repeated for steps 3-6.)

The apparent lack of kinetic barriers suggests formation of all five isomers, **III**$^{\bullet}$**,** should be kinetically feasible.

For each of the isomers of **III**$^{\bullet}$ H atom abstraction from Me_3SnH was then calculated. The process with the lowest *overall* barrier was found to be reaction *via* the lowest-energy isomer **IIIa**$^{\bullet}$, to

give the closed-shell intermediate **IVa**. However, it should be emphasised that if there is any kinetic preference for **IVa** over **IVb** it is extremely modest (likely within the margin of error), and both pathways are likely to be kinetically competitive. Assigning a formal kinetic product is also complicated by the lack of apparent kinetic barriers for the formation of **III**$^{\bullet}$. A possible kinetic argument in favour of **IVa** over **IVb** can be made if an equilibrium between **IIIa**$^{\bullet}$ and **IIIb**$^{\bullet}$ is assumed (i.e. if formation of **IIIa**$^{\bullet}$ or **IIIb**$^{\bullet}$ is reversible), since in this case **IIIa**$^{\bullet}$ provides the lowest energy onward transition state (albeit only by a very small margin as already noted). However, starting from **IIIb**$^{\bullet}$, the barrier for this equilibrium (*via* reversion of **IIIb**$^{\bullet}$ to **II**) is essentially identical to that of the forward reaction (**IIIb**$^{\bullet}$ → **IVb**), suggesting only partial reversibility at most, and in the absence of reversibility the barrier for **IIIb**$^{\bullet}$ → **IVb** is in fact slightly lower than for **IIIa**$^{\bullet}$ → **IVa**. Again, this implies that formation of **IVb** is likely to be kinetically competitive with formation of **IVa**.

In contrast, H atom abstraction by any of the other isomers (**IIIc**$^{\bullet}$-**IIIe**$^{\bullet}$) involves transition state energies that are appreciably higher than for reversion to **II**, suggesting that they should react preferentially *via* reversion to **II** and equilibration to the thermodynamically preferred isomers **IVa** or **IVb**, which provide lower energy onward transition states.

Based on these arguments, both **IVa** and **IVb** could reasonably be taken forward for further calculations. However, for the sake of practicality, and to minimise the number of possible downstream steps requiring investigation, it was decided to investigate only a single isomer, with **IVa** being arbitrarily chosen (*vide infra*).

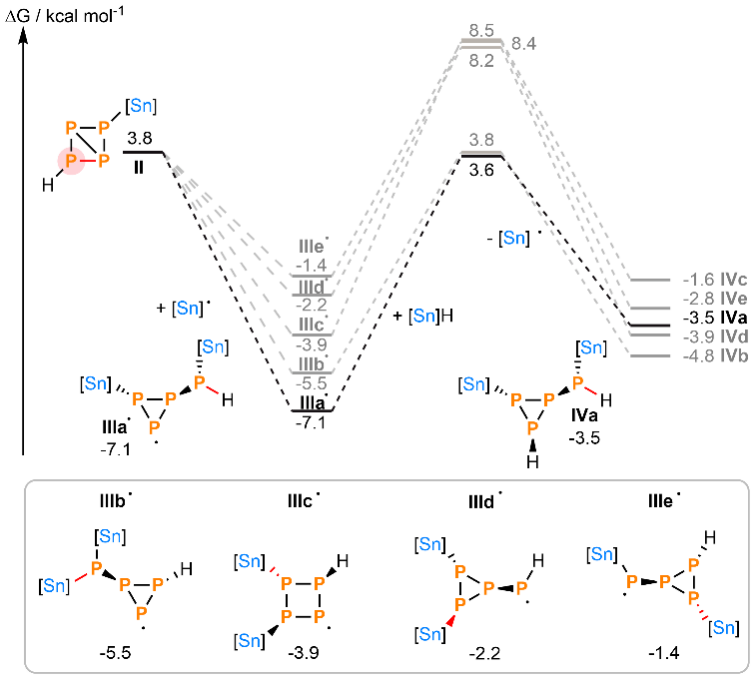

Figure S201. Calculated mechanism for hydrostannylation of the second P–P bond in P_4 by Me_3SnH, including relative stereochemistry, with relative free energies in kcal mol^{-1}. [Sn] = Me_3Sn.

4.4.2.3.3. 3rd P–P cleavage:

The addition of $Me_3Sn^{\bullet}$ to **IVa** was calculated using the same strategy as for addition to **II** discussed above. In this case, eight constitutional isomers of the intermediate **V$^{\bullet}$** are available, and formation of each was calculated to be essentially barrierless (Figure S11 and Figure 4). The energies of the subsequent product isomers **VI**, derived upon H atom transfer to **V$^{\bullet}$**, were also calculated. However, for the sake of computational efficiency (particularly because the conformational flexibility of most of the isomers of **V$^{\bullet}$** complicates the calculation of transition states), activation barriers were only calculated for the two lowest energy isomers, i.e. for **Va$^{\bullet}$ → VIa** and **Vb$^{\bullet}$ → VIb**. Of these, **Va$^{\bullet}$ → VIa** was found to be kinetically preferred (note that equilibration of **Va$^{\bullet}$** and **Vb$^{\bullet}$** *via* reversion to **IVa** is more accessible than either forward reaction, making the argument for kinetic preference more clear cut than in step 2), and so this option was taken forward to provide the starting point for the fourth P–P cleavage step (*vide infra*). However, it should be emphasised that the possibility of other pathways (i.e. H atom transfer to **Vc$^{\bullet}$-Vh$^{\bullet}$**) being kinetically competitive cannot be excluded, especially given that reversion of any of the isomers of **V$^{\bullet}$** to **IVa** is calculated to have a lower barrier than **Va$^{\bullet}$ → VIa** (i.e. interconversion between the isomers of **V$^{\bullet}$** should be more facile than onward reactivity). However, the existence of any extra pathways would reinforce the overall conclusion of this study (i.e. that the observed reaction outcome is likely due to an ensemble of pathways operating in parallel).

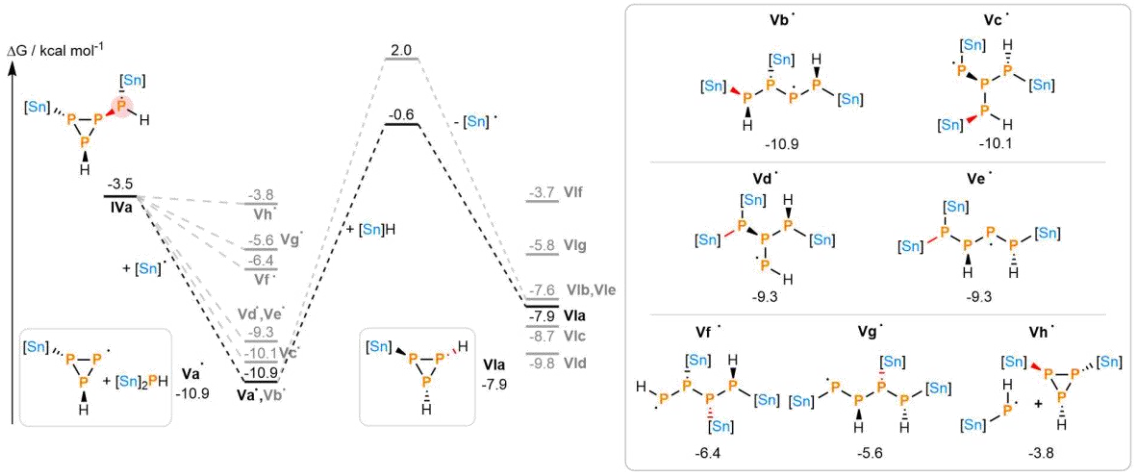

Figure S202. Calculated mechanism for hydrostannylation of the third P–P bond in P_4 by Me_3SnH, including relative stereochemistry, with relative free energies in kcal mol^{-1}. [Sn] = Me_3Sn.

4.4.2.3.4. 4th P–P cleavage:

Three regiochemical options for $Me_3Sn^{\bullet}$ attack on **VIa** are available, all of which were calculated using the same strategy as in the second and third steps, and found to be effectively barrierless (Figure S12 and Figure 5). The reduced size of this system relative to the previous step (P_3 *vs.* P_4 fragments, fewer isomers) allowed transition states for all three onward H atom transfer steps (**VII$^{\bullet}$ → VIII**) to be calculated. Of these options, **VIIc$^{\bullet}$ → VIIIc** was found to be both kinetically and thermodynamically preferred, so **VIIIc** was taken forward for calculation of the fifth P–P

cleavage step (*vide infra*). Notably, for both **VIIa•** and **VIIb•** reversion to **VI** followed by conversion to **VIIIc** *via* **VIIc•** should be lower in energy than direct H atom transfer.

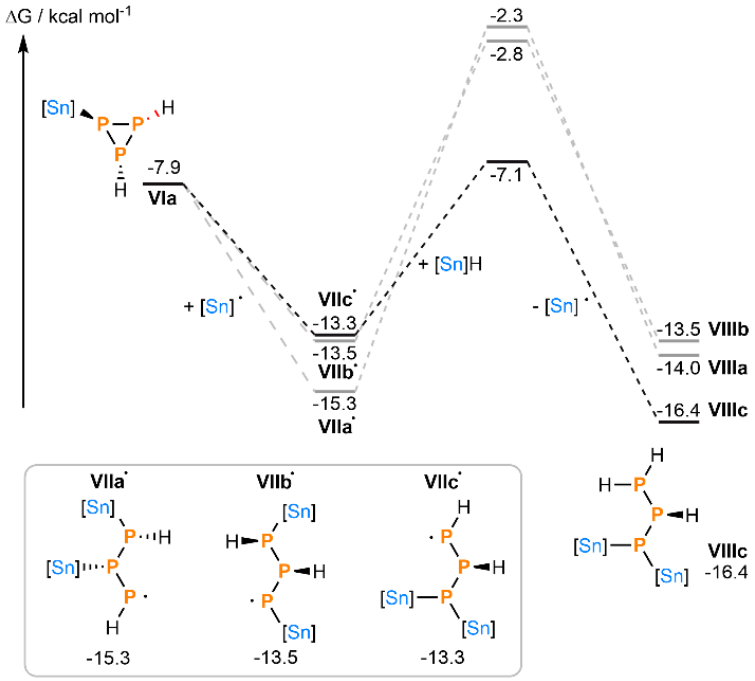

Figure S203. Calculated mechanism for hydrostannylation of the fourth P–P bond in P_4 by Me_3SnH, including relative stereochemistry, with relative free energies in kcal mol^{-1}. [Sn] = Me_3Sn.

4.4.2.3.5. 5th P–P cleavage:

Starting from **VIIIc**, the fifth step offers four options for $Me_3Sn^•$ attack, which were again calculated using the same strategy as for the second-fourth steps, and again found to be effectively barrierless (Figure S13 and Figure 6). Two of these options were calculated to be downhill (leading to **IXa•** and **IXb•**), but two were calculated to be slightly uphill (leading to **IXc•** and **IXd•**). For simplicity, onward H atom transfer reactivity was calculated only for the former pair, with **IXb•** found to lead to the lower activation barrier, *en route* to product **Xb**, which was then taken forward for the final P–P cleavage step. Again, it can be noted that H atom transfer to **IXa•** to form **Xa** has a higher activation barrier than transformation to **Xb** *via* reversion to **VIIIc** and formation of **IXb•**, making **Xb** the kinetically preferred product.

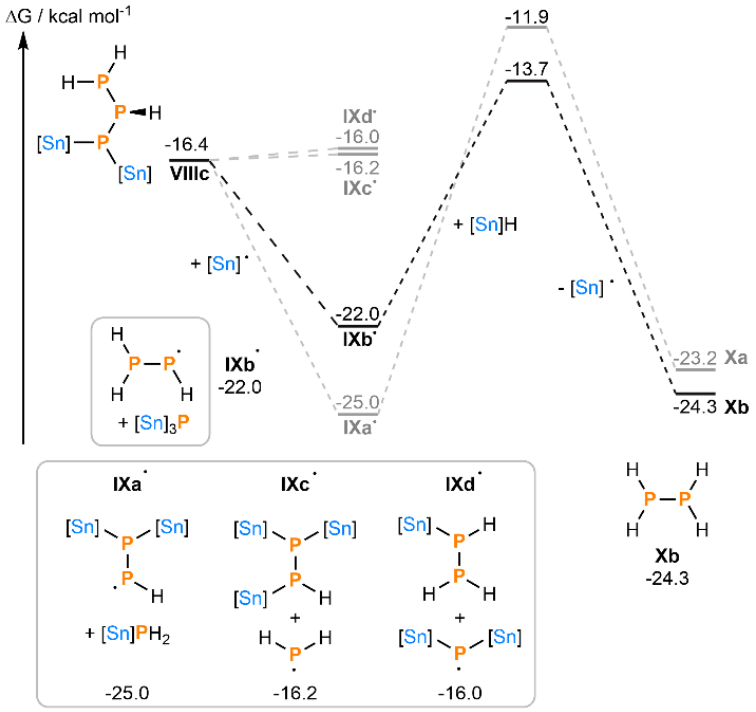

Figure S204. Calculated mechanism for hydrostannylation of the fifth P–P bond in P_4 by Me_3SnH, including relative stereochemistry, with relative free energies in kcal mol^{-1}. [Sn] = Me_3Sn.

4.4.2.3.6. 6th P–P cleavage:

Starting from **Xb**, only one option is available for the final $Me_3Sn^{\bullet}$ attack, which was again calculated using the same strategy as for the second-fifth steps (Figure 7, and repeated for convenience in Figure S14). This was again calculated to be essentially barrierless, generating intermediate **XI•** that can engage in a final H atom transfer step to generate the final product PH_3.

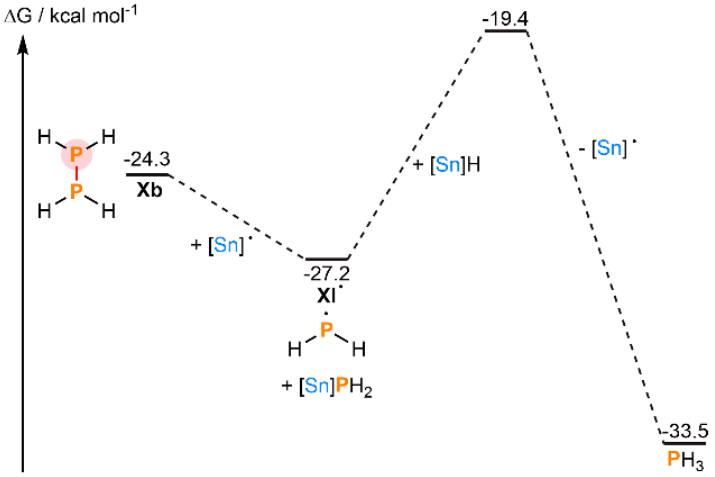

Figure S205. Calculated mechanism for hydrostannylation of the final P–P bond in P_4 by Me_3SnH, with relative free energies in kcal mol^{-1}. [Sn] = Me_3Sn.

4.4.2.3.7. Alternative P–P cleavage steps:

During the course of this study, a handful of other possible P–P bond cleavage steps were also calculated, in addition to the primary sequence summarised above. For completeness, these are summarised in Figures S15-19. Notably, all show similar patterns of reactivity (i.e. similar

activation barriers, *etc*.) to the steps that make up the main pathway, further supporting the conclusion that multiple competing pathways are likely to be energetically accessible.

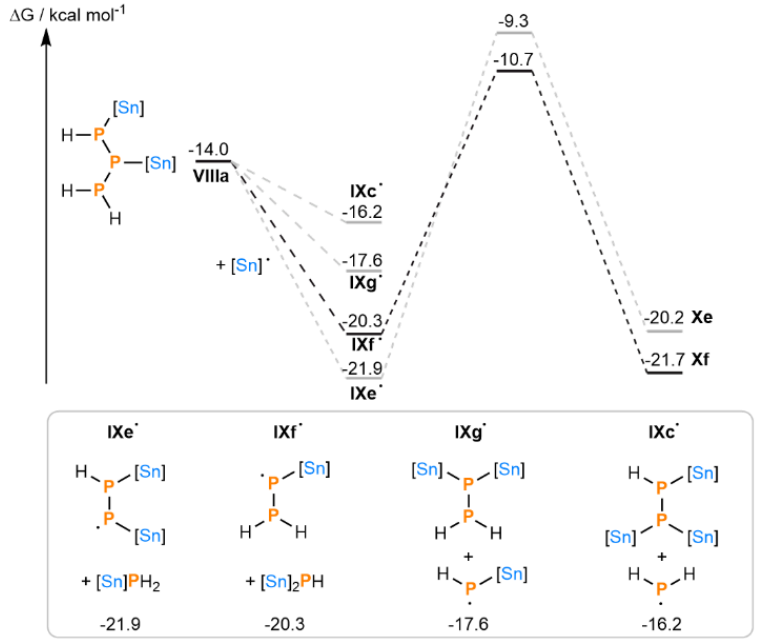

Figure S206. Calculated mechanism for an alternative hydrostannylation of the fifth P–P bond in P_4 by Me_3SnH, starting from **VIIIa** instead of **VIIIc**, with relative free energies in kcal mol^{-1}. [Sn] = Me_3Sn.

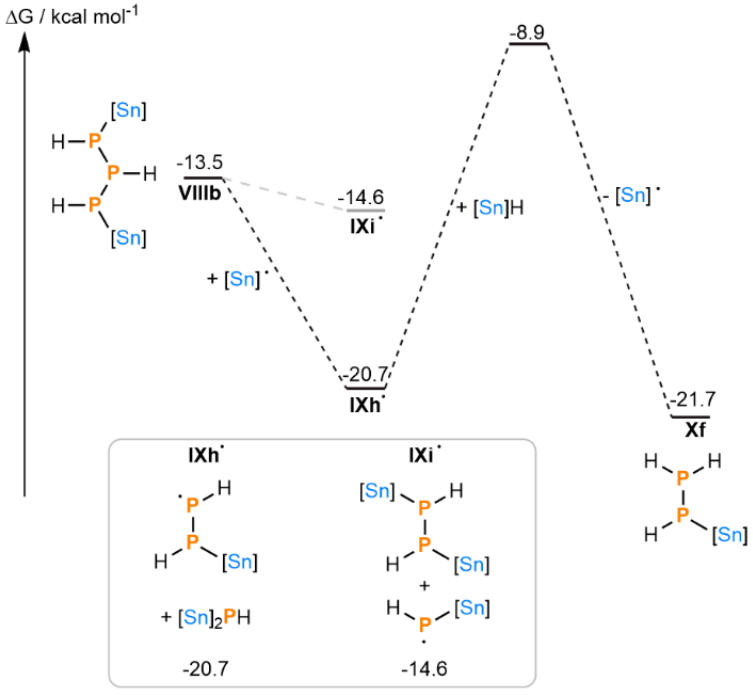

Figure S207. Calculated mechanism for an alternative hydrostannylation of the fifth P–P bond in P_4 by Me_3SnH, starting from **VIIIb** instead of **VIIIc**, with relative free energies in kcal mol^{-1}. [Sn] = Me_3Sn.

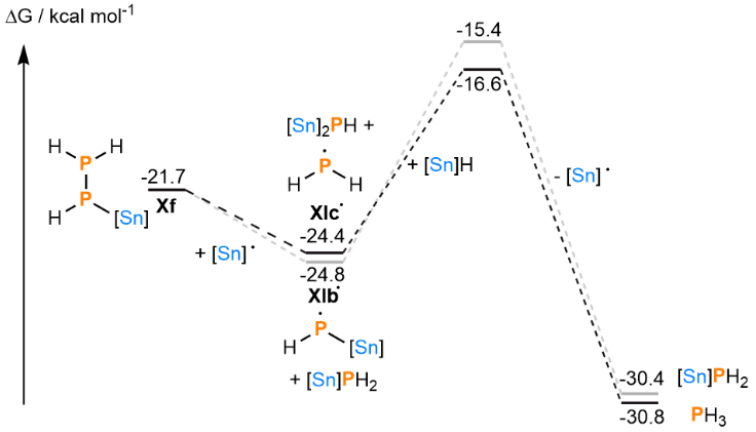

Figure S208. Calculated mechanism for an alternative hydrostannylation of the final P–P bond in P_4 by Me_3SnH, starting from **Xf** (which would be derived from H atom transfer to **IXf•** or **IXh•**) instead of **Xb**, with relative free energies in kcal mol^{-1}. [Sn] = Me_3Sn.

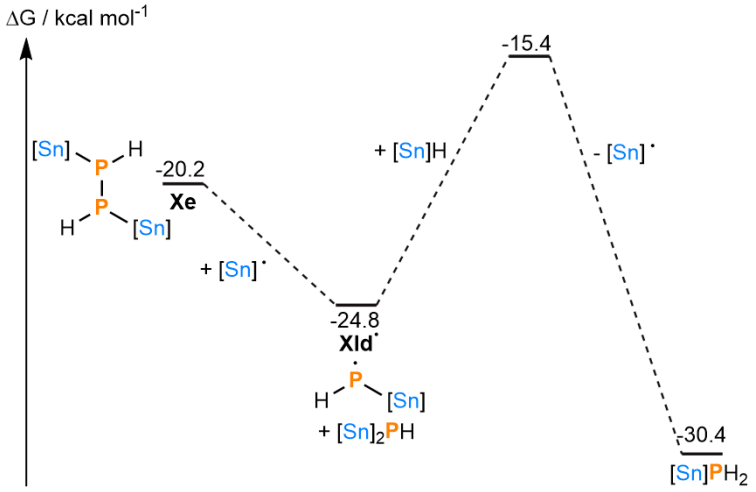

Figure S209. Calculated mechanism for an alternative hydrostannylation of the final P–P bond in P_4 by Me_3SnH, starting from **Xe** (which would be derived from H atom transfer to **IXe•**) instead of **Xb**, with relative free energies in kcal mol^{-1}. [Sn] = Me_3Sn.

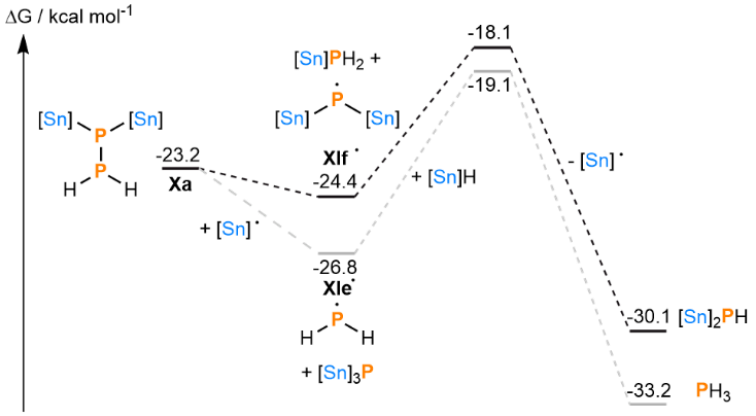

Figure S210. Calculated mechanism for an alternative hydrostannylation of the final P–P bond in P_4 by Me_3SnH, starting from **Xa** (which would be derived from H atom transfer to **IXa•**) instead of **Xb**, with relative free energies in kcal mol^{-1}. [Sn] = Me_3Sn.

4.4.3 Synthesis and characterisation of new bulkier hydrostannanes

4.4.3.1 TerSn(Me)$_2$H (2,6-Mes$_2$C$_6$H$_3$Sn(CH$_3$)$_2$H)

2,6-Mes$_2$C$_6$H$_3$I (5.00 g, 11.3 mmol, 1.00 eq.) was suspended in a Schlenk tube in Et$_2$O (80 mL) and cooled to 0 °C, to which *n*-butyllithium (2.5 M in *n*-hexane, 5.00 mL, 12.5 mmol, 1.10 eq.) was added dropwise over the course of 5 minutes. After stirring for 1 hour the solution was transferred dropwise to a cooled suspension of dimethyltin dichloride (2.50 g, 11.3 mmol, 1.00 eq.) in Et$_2$O. The reaction mixture was stirred for an additional hour at 0 °C and then for 2 hours at room temperature. The solvent was removed under reduced pressure to remove butyl iodide. Afterwards it was suspended in Et$_2$O (50 mL) and cooled to -20 °C. To this LiAlH$_4$ (0.429 g, 11.3 mmol, 1.00 eq.) was added as a solid. The reaction mixture was stirred for 2 hours at -20 °C and then the solvent was removed under reduced pressure. The residual solid was extracted with toluene (50 mL) and filtered through a pad of celite to remove any insoluble material. The solvent was removed in vacuum to afford the target compound as a crystalline solid (4.70 g, 10.1 mmol, 90%).

Crystals suitable for X-ray structure determination were grown from a hot toluene solution.

^{1}H NMR (600 MHz, C$_6$D$_6$): δ = 7.25 (t, ^{3}J(^{1}H-^{1}H) = 7.54 Hz, 1H, H4), 6.96 (d, ^{3}J(^{1}H-^{1}H) = 7.57 Hz, 2H, H3 and H5), 6.84 (s, 4H, H9 and H11), 4.81 (hept, 1H, ^{3}J(^{1}H-^{1}H) = 2.57 Hz, ^{1}J(^{1}H-^{119}Sn) = 1796.74 Hz, SnH), 2.18 (s, 6H, H14), 2.08 (s, 12H, H13 and H15), -0.24 (d, ^{3}J(^{1}H-^{1}H) = 2.57 Hz, 6H, SnCH$_3$) ppm.**^{13}C{^{1}H} NMR (151 MHz, C$_6$D$_6$)**: δ = 150.01 (s, C2 and C6), 141.13 (s, C8), 140.19 (s, C1), 136.59 (s, C10), 135.84 (s, C8 and C12), 129.44 (s, C3), 128.26 (s, C9 and C11), 127.25 (s, C3 and C5), 20.85 (s, C14) 20.77 (s, C13 and C15), -10.16 (s, SnCH$_3$) ppm. **^{119}Sn NMR (C$_6$D$_6$, 224 MHz)**: δ = -145.60 (dp, ^{2}J(^{119}Sn-^{1}H) = 57.07 Hz, ^{1}J(^{119}Sn-^{1}H) = 1793.76 Hz) ppm. **HRMS ESI (m/z):** [M-H]$^+$ calculated. for C$_{26}$H$_{31}$Sn, 463.14470; found, 463.14441. **IR** (ATR, neat): $\tilde{\nu}$ = 1833 cm^{-1} (s, Sn-H). Melting Point: 104 °C.

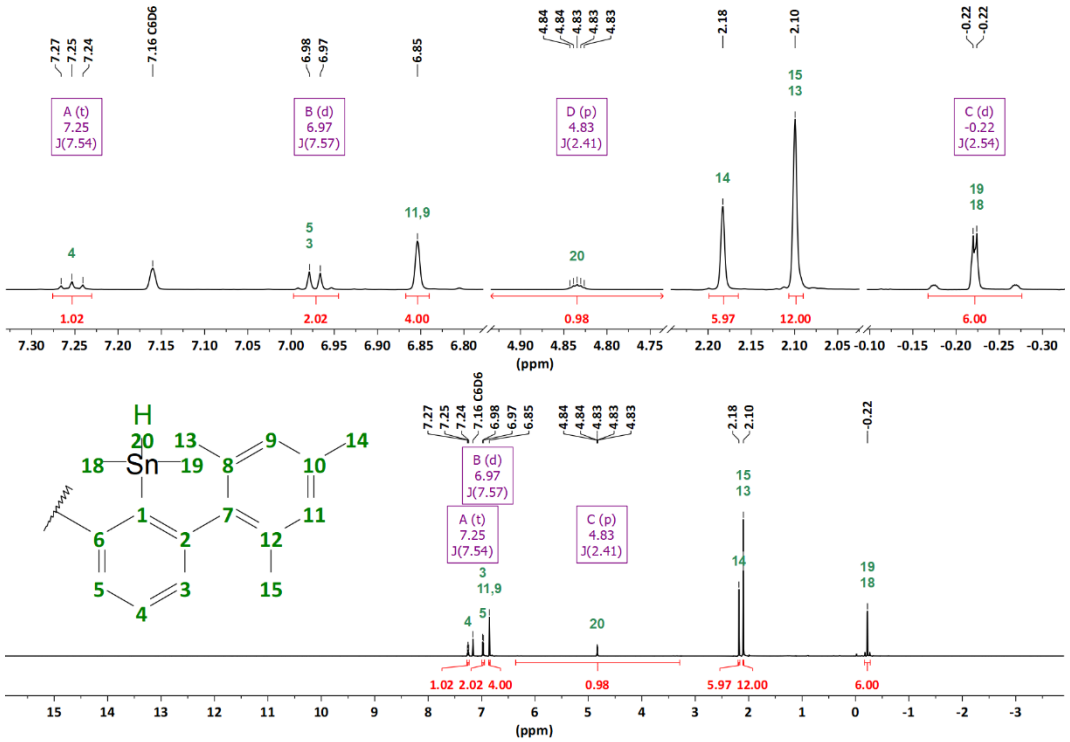

Figure S211. ^{1}H NMR (C_6D_6, 600 MHz) spectrum of $TerSn(Me)_2H$.

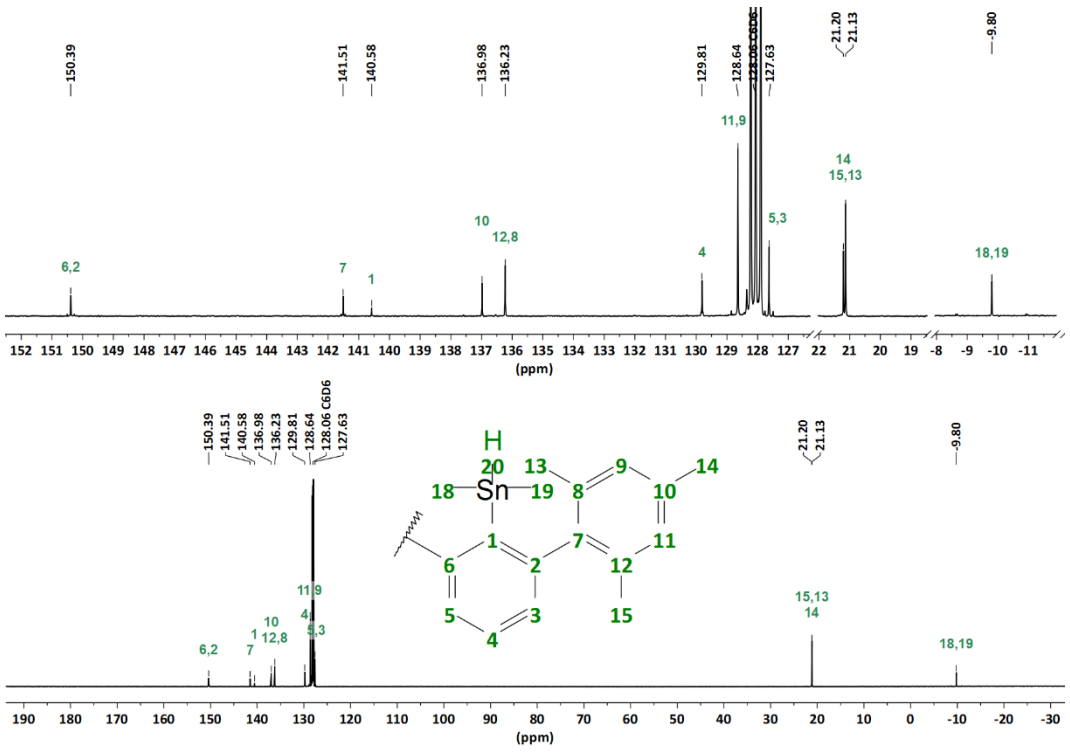

Figure S212. $^{13}C\{^{1}H\}$ NMR (C_6D_6, 151 MHz) spectrum of $TerSn(Me)_2H$.

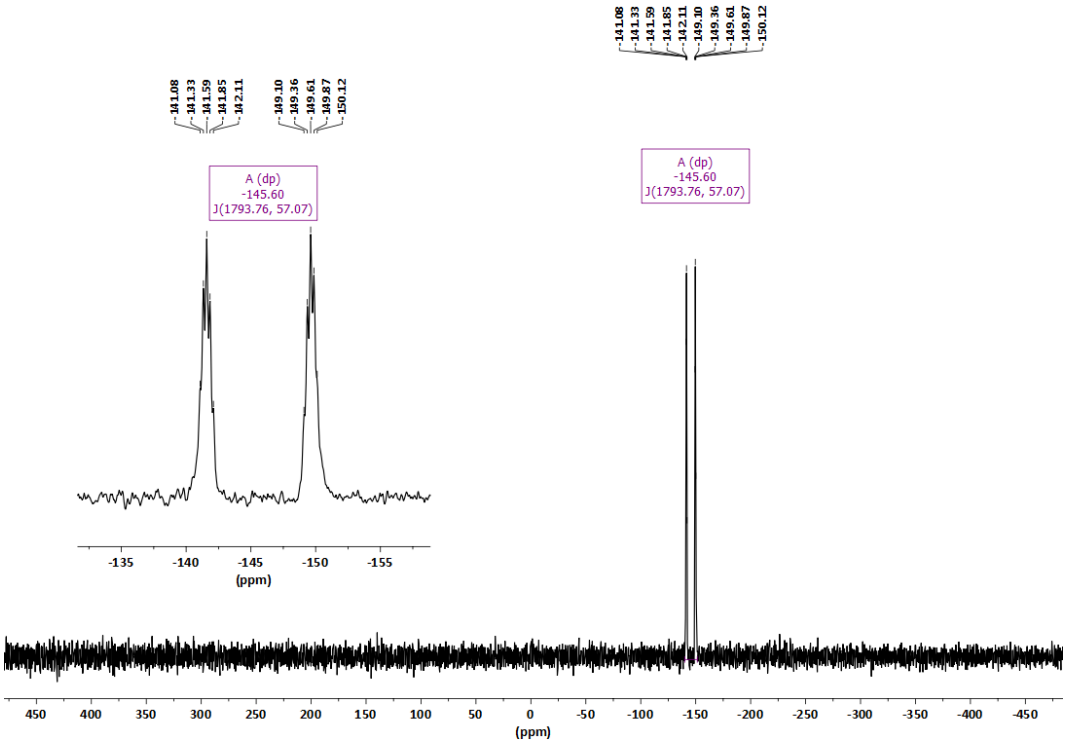

Figure S213. ^{119}Sn NMR (C_6D_6, 224 MHz) spectrum of $TerSn(Me)_2H$.

4.4.3.2 Ter*Sn(Me)$_2$H (2,6-Pmp$_2$C$_6$H$_3$Sn(CH$_3$)$_2$H)

Me_2SnCl_2 (0.219 g, 1.00 mmol, 1.00 eq.) was placed in a Schlenk tube and dissolved in Et_2O (5 mL) and cooled to 0 °C. Separately 2,6-$Pmp_2C_6H_3Li$ (0.376 g, 1.00 mmol, 1.00 eq.) was dissolved in Et_2O (5 mL) and added dropwise to the Me_2SnCl_2 solution over the course of 10 minutes. After 2 hours the solvent was removed under vacuum and the residual solid was dissolved in fresh Et_2O. This solution was cooled to -60 °C and $LiAlH_4$ (0.107 g, 2.8 mmol, 2.8 eq.) was added as a solid. The reaction mixture was stirred for an additional 4 hours at -20 °C. After this, the solvent was removed under reduced pressure and the product was dried at 60 °C for 18 hours. The residual solid was suspended in toluene (16 mL) and filtered through a PTFE syringe filter. The solvent of the filtrate was removed under reduced pressure and the solid was dissolved in hot *n*-hexane (2 mL) and cooled to 0 °C, during which the product crystallized. The residual solution was decanted off and the solid was dried under reduced pressure to obtain the title compound as a colourless solid (457 mg, 0.879 mmol, 88%).

Crystals suitable for X-ray structure determination were grown from a hot *n*-hexane solution.

^{1}H NMR (600 MHz, C_6D_6): δ = 7.33 (t, $^3J(^1H\text{-}^1H)$ = 7.52 Hz, 1H, H4), 7.09 (d, $^3J(^1H\text{-}^1H)$ = 7.55 Hz, 2H, H3 and H5), 4.78 (hept, 1H, $^3J(^1H\text{-}^1H)$ = 2.43 Hz, H20), 2.14 (s, 12H, H13 and H17), 2.13 (s, 6H, H15), 2.13 (s, 12H, H14 and H16), -0.31 (d, $^3J(^1H\text{-}^1H)$ = 2.52 Hz, 6H, H18 and H19) ppm.**^{13}C{^{1}H} NMR (151 MHz, C_6D_6)**: δ = 152.32 (s, C2 and C6), 142.14 (s, C7), 141.85 (s, C1), 134.00 (s, C10), 132.45 (s, C8 and C12), 131.79 (s, C9 and C11), 129.55 (s, C4), 127.62 (s, C3 and C5), 18.86 (s, C13 and C17), 16.83 (s, C15), 16.69 (s, C14 and C16), -9.90 (s, C18 and C19)

ppm. **^{119}Sn NMR (C_6D_6, 224 MHz)**: δ = -147.88 (dp, $^2J(^{119}Sn\text{-}^1H)$ = 57.65 Hz, $^1J(^{119}Sn\text{-}^1H)$ = 1791.78 Hz) ppm. **HRMS ESI (m/z):** $[M\text{-}H]^+$ calculated. for $C_{26}H_{31}Sn$, 519.20740; found, 519.20696. **IR** (ATR, neat): $\tilde{\nu}$ = 1827 cm^{-1} (s, Sn-H). Melting Point: 167 °C.

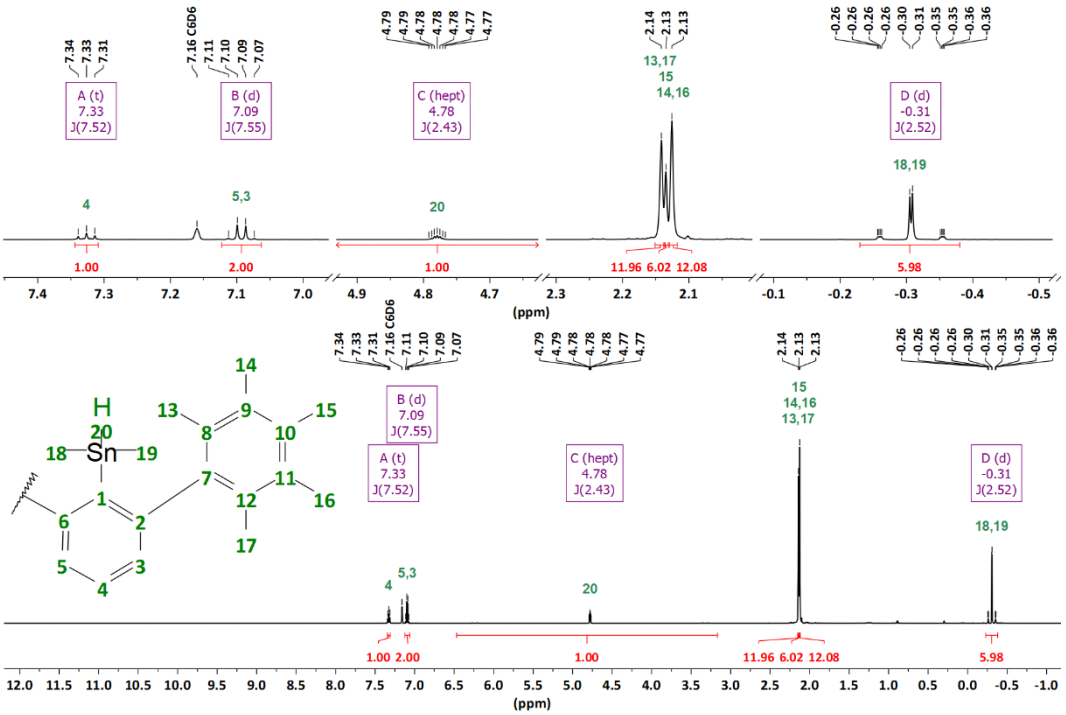

Figure S214. ^1H NMR (C_6D_6, 600 MHz) spectrum of Ter*Sn(Me)$_2$H.

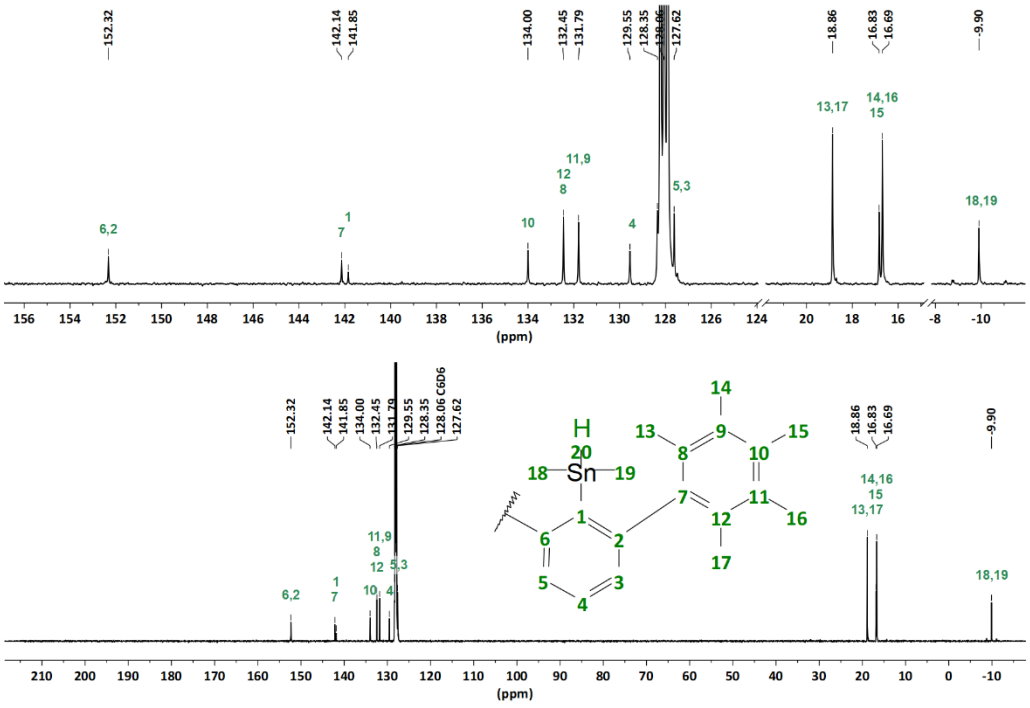

Figure S215. $^{13}C\{^1H\}$ NMR (CD_2Cl_2, 151 MHz) spectrum of Ter*Sn(Me)$_2$H.

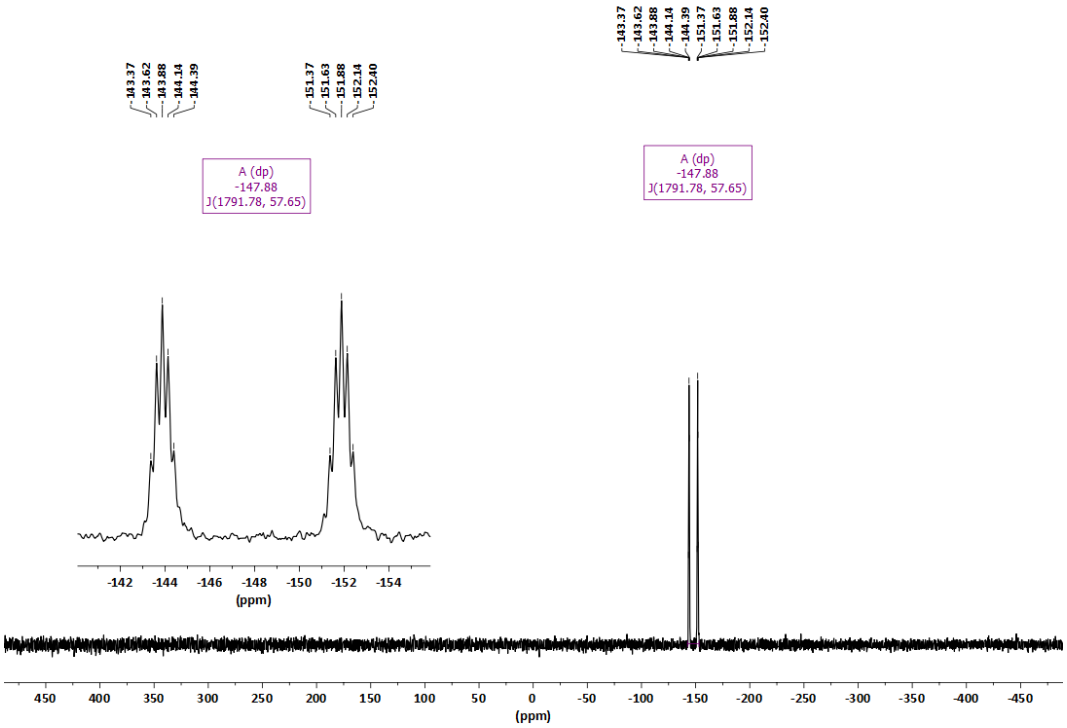

Figure S216. ^{119}Sn NMR (C_6D_6, 224 MHz) spectrum of Ter*Sn(Me)$_2$H.

4.4.3.3 (Fluind)Sn(Me)$_2$H

This synthesis is modified from a known literature procedure for the synthesis of FluindSn(CH$_3$)$_2$Cl.[41]

Me_2SnCl_2 (0.219 g, 1.00 mmol, 1.00 eq.) was placed in a Schlenk tube and dissolved in toluene (5 mL) and cooled to 0 °C. Separately FluindLi(THF)$_2$ (0.665 g, 1.00 mmol, 1.00 eq.) was suspended in toluene (5 mL) and added dropwise to the Me_2SnCl_2 solution over the course of 10 minutes. After 2 hours the solvent was removed under vacuum and the residual solid was suspended in Et_2O (10 mL). This suspension was cooled to -60 °C and $LiAlH_4$ (0.114 g, 3.00 mmol, 3.00 eq.) was added as a solid. The reaction mixture was stirred for an additional 4 hours at -20 °C. After this, the solvent was removed under reduced pressure and the product was dried at 60 °C. The residual solid was dissolved in toluene (10 mL) and filtered through a PTFE syringe filter. The solvent was removed under vacuum to obtain the target compound as a colourless solid (629 mg, 0.948 mmol, 95%).

Crystals suitable for X-ray structure determination were grown from a hot toluene/*n*-hexane (1:4) solution.

^{1}H NMR (600 MHz, C_6D_6): δ = 7.49 (d, ^{3}J(^{1}H-^{1}H) = 7.17 Hz, 4H, H14 and H21), 7.40 (s, H4), 7.19 (d, ^{3}J(^{1}H-^{1}H) = 7.52 Hz, 4H, H11 and H18), 7.10 (td, ^{3}J(^{1}H-^{1}H) = 7.45 Hz, ^{4}J(^{1}H-^{1}H) = 1.15 Hz, 4H, H13 and H20), 7.03 (td, ^{3}J(^{1}H-^{1}H) = 7.47 Hz, ^{4}J(^{1}H-^{1}H) = 1.17 Hz, 4H, H12 and H19), 3.91 (hept, ^{3}J(^{1}H-^{1}H) = 2.80 Hz, 1H, H24), 2.32 (s, 4H, H6), 1.46 (s, 12H, H8 and H9), -1.04 (d, ^{3}J(^{1}H-^{1}H) = 2.81 Hz, 6H, H22 and H23) ppm.**^{13}C{^{1}H} NMR (151 MHz, C_6D_6)**: δ = 156.45 (s, C10 and C17), 155.58 (s, C3), 151.67 (s, C2), 141.02 (s, C15 and C16), 137.50 (s, C1), 128.35

(s, C12 and C19), 127.35 (s, C13 and C20), 124.76 (s, C11 and C18), 120.67 (s, C14 and C21), 118.12 (s, C4), 66.57 (s, C5), 59.95 (s, C6), 42.49 (s, C7), 32.62 (s, C8 and C9), -9.95 (s, C22 and C23) ppm. **^{119}Sn NMR (C_6D_6, 224 MHz)**: δ = -161.41 (dp, $^2J(^{119}Sn\text{-}^1H)$ = 57.68 Hz, $^1J(^{119}Sn\text{-}^1H)$ = 1806.85 Hz) ppm. **HRMS ESI (m/z):** $[M\text{-}H]^+$ calculated. for $C_{42}H_{39}Sn$, 663.20771; found, 663.20749. **IR** (ATR, neat): $\tilde{\nu}$ = 1927 cm^{-1} (m, br, Sn-H). Melting Point: 248 (decomp.) °C.

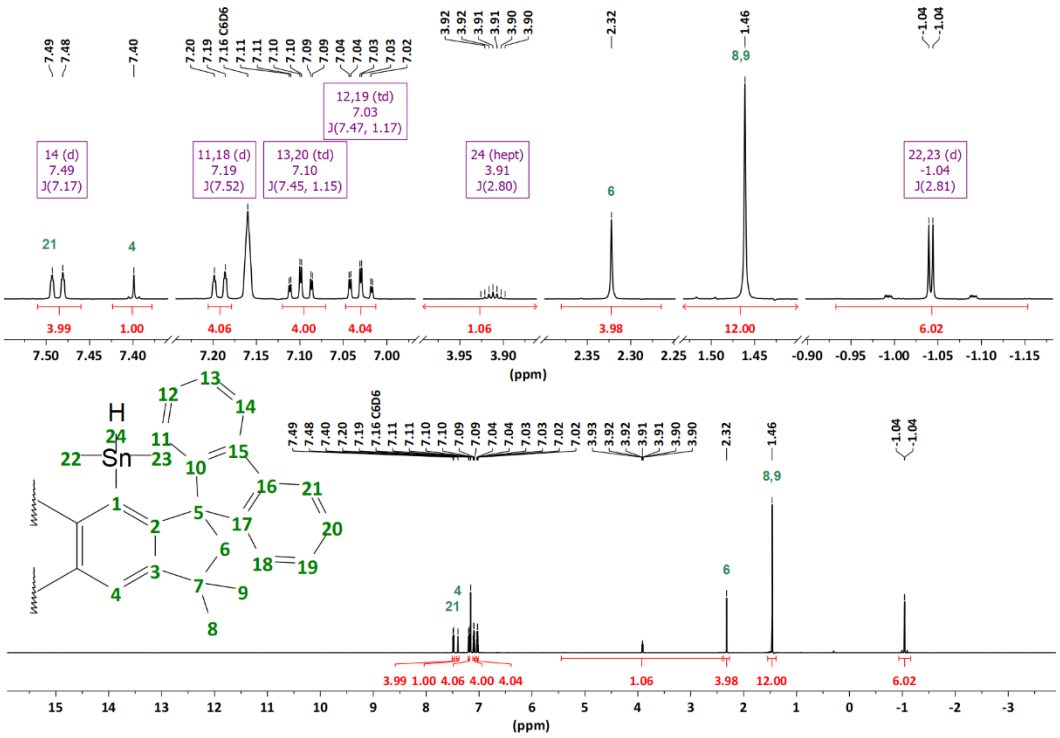

Figure S217. ^{1}H NMR (C_6D_6, 600 MHz) spectrum of FluindSn(Me)$_2$H.

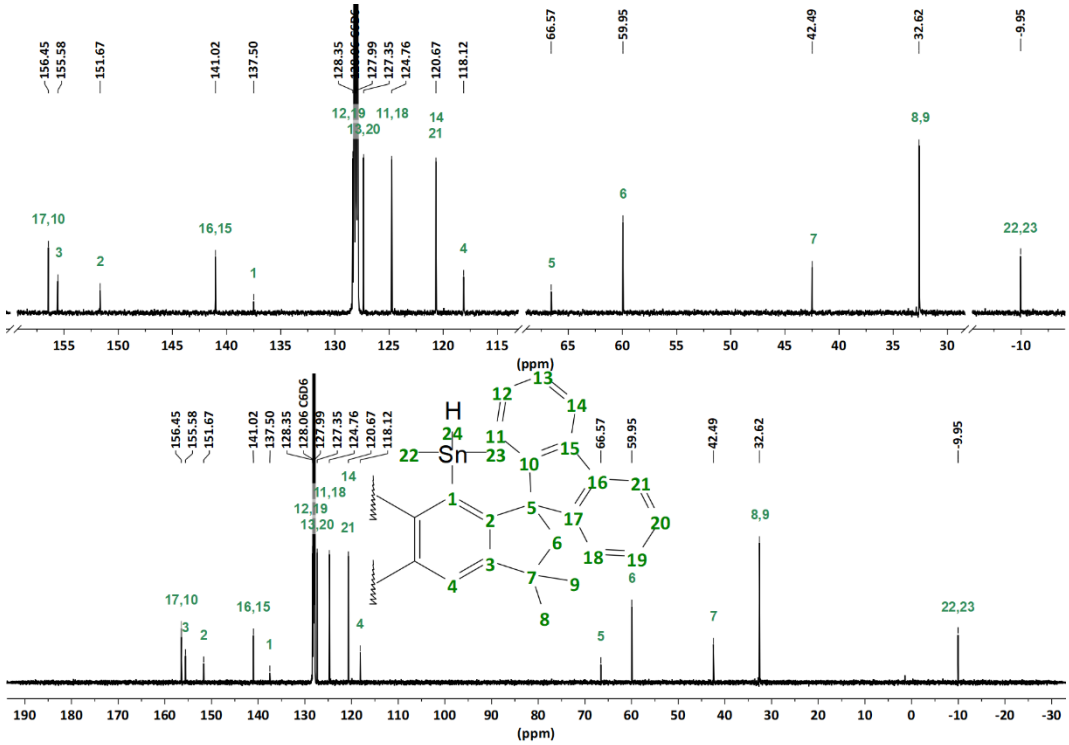

Figure S218. $^{13}C\{^1H\}$ NMR (CD_2Cl_2, 151 MHz) spectrum of FluindSn(Me)$_2$H.

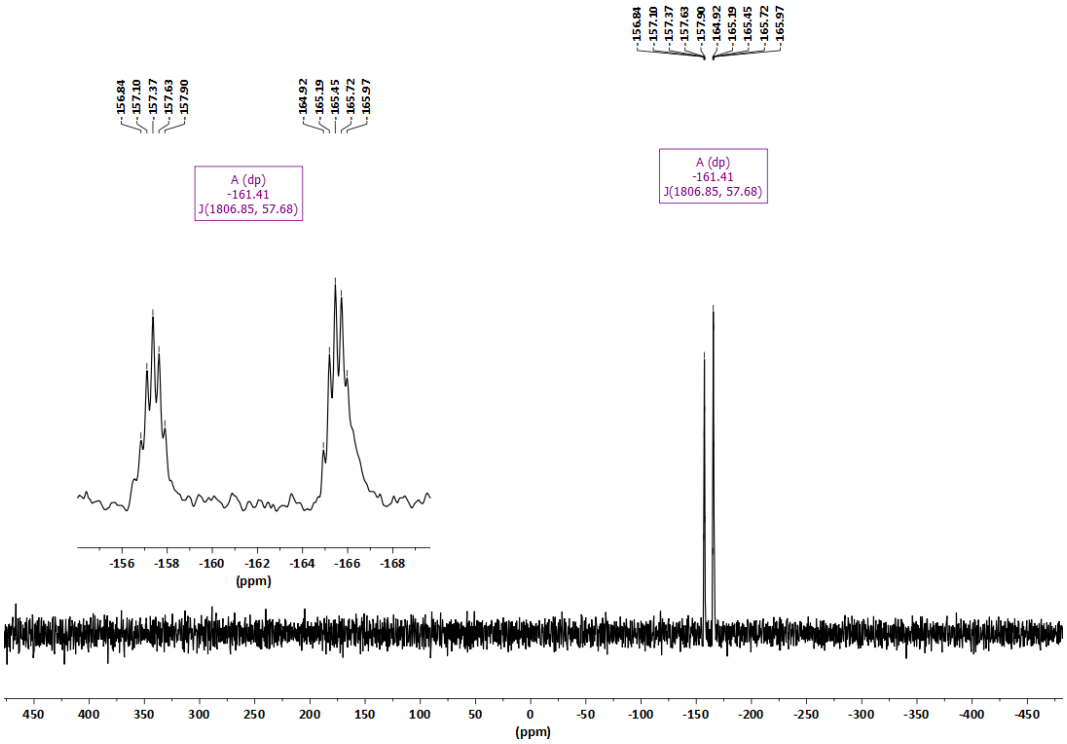

Figure S219. ^{119}Sn NMR (C_6D_6, 224 MHz) spectrum of FluindSn(Me)$_2$H.

4.4.3.4 Crystallographic characterisation of new hydrostannanes

Single crystal X-ray diffraction data for TerSn(Me)$_2$H was collected at 150 K due to a phase transition at 140 K and for Ter*Sn(Me)$_2$H and FluindSn(Me)$_2$H at 100 K using an open flow nitrogen stream on a Bruker Venture D8 diffractometer with a Photon 100 detector in shutterless mode using a microfocus source (Moκα = 0.71073 Å). All structures were solved by the SHELXT structure solution program using Intrinsic phasing and refined with the SHELX program package using Least Squares minimisation as implemented in Olex2.[42,43] All non-hydrogen atoms were refined using anisotropic displacement parameters. Hydrogen atoms at the Sn atoms were located from the Fourier difference map and had their positions and isotropic displacement parameter refined freely. Hydrogen atoms attached to carbon atoms were included in geometrically calculated positions using a riding model. Crystal and refinement data are collected in Table S2, and the structures themselves are illustrated in Figure S29. Crystallographic data for these structures has been deposited with the Cambridge Crystallographic Data Centre, CCDC, 12 Union Road, Cambridge CB21EZ, UK. Copies of this data can be obtained free of charge on quoting the depository numbers: 2315115, 2315154, 2315177; E-mail: deposit@ccdc.cam.ac.uk, http://www.ccdc.cam.ac.uk.

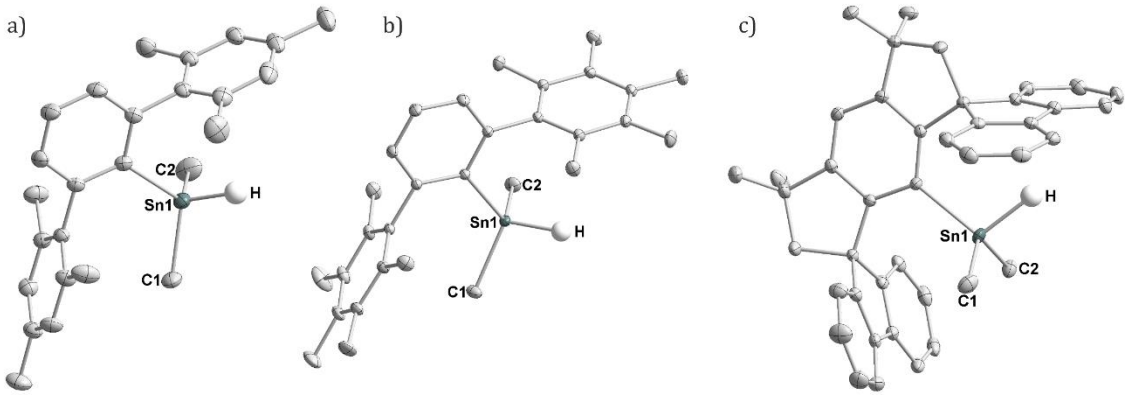

Figure S220. Single-crystal XRD structures of (a) TerSn(Me)$_2$H, (b) Ter*Sn(Me)$_2$H, (c) FluindSn(Me)$_2$H. Thermal ellipsoids are shown at 50%. H atoms, except for those bound directly to Sn, are omitted for clarity. For (c) FluindSn(Me)$_2$H the less occupied position of the disorder is omitted for clarity. C atoms are shown in grey, H in white, and Sn in dark grey.

Table S2. Crystal data and structure refinement of TerSn(Me)$_2$H, Ter*Sn(Me)$_2$H and FluindSn(Me)$_2$H.

	TerSn(Me)$_2$H	**Ter*Sn(Me)$_2$H**	**FluindSn(Me)$_2$H**
Formula	$C_{26}H_{32}Sn$	$C_{30}H_{40}Sn$	$C_{42}H_{40}Sn$
Formula weight, g mol^{-1}	463.20	519.31	663.43
Crystal system	Monoclinic	Triclinic	Triclinic
Crystal size, mm	0.18 × 0.18 × 0.14	0.32 × 0.14 × 0.10	0.26 × 0.26 × 0.10
Space group	$P2_1/c$	P-1	P-1
a, Å	17.9790(8)	8.9780(7)	9.6930(5)
b, Å	8.5727(4)	9.0895(7)	11.5749(7)
c, Å	15.9417(7)	18.2993(15)	15.9229(9)
α, º	90	78.754(3)	70.426(3)
β, º	106.5900(10)	89.042(3)	82.300(3)
γ, º	90	60.517(3)	73.912(3)
V, Å^3	2354.79(18)	1269.47(18)	1615.65(16)
Z	4	2	2
ρ_{calcd}, Mg m^{-3}	1.307	1.359	1.364
μ (Mo $K\alpha$), mm^{-1}	1.092	1.021	0.819
F(000)	952.0	540.0	684.0
2θ range, deg	4.728 to 56.556	5.272 to 73.206	5.368 to 54.206
Index ranges	–23 ≤ h ≤ 23	–14 ≤ h ≤ 14	–12 ≤ h ≤ 12
	–11 ≤ k ≤ 11	–15 ≤ k ≤ 15	–14 ≤ k ≤ 14
	–20 ≤ l ≤ 21	–30 ≤ l ≤ 30	–20 ≤ l ≤ 20
No. of reflns collected	100484	94845	44401
No. indep. Reflns	14937	12450	7116
No. refined params	256	296	422
GooF (F^2)	1.141	1.063	1.049
R_1 (F) ($I > 2\sigma(I)$)	0.0264	0.0217	0.0302
wR_2 (F^2) (all data)	0.0551	0.0534	0.0726
Largest diff peak/hole, e Å^{-3}	0.40 / –0.64	0.63 / –0.38	0.74 / –0.77
CCDC number	2315115	2315154	2315177

4.4.4 $^{31}P\{^1H\}$ NMR spectroscopic monitoring experiments with bulkier hydrostannanes

4.4.4.1 *i*Pr_3SnH

Ex situ, under LED irradiation (455 nm)

To a 10 mL, flat-bottomed, stoppered tube were added C_6D_6 (500 µL), P_4 (0.01 mmol, as a stock solution in 124.6 µL C_6D_6) and *i*Pr_3SnH (15.0 mg, 0.06 mmol). The tube was sealed, placed in a water-cooled block to maintain near-ambient temperature, and irradiated with blue light (455 nm (±15 nm), 3.2 V, 700 mA, Osram OSLON SSL 80) for 24 h. The resulting mixture was analysed by ^1H, $^{31}P\{^1H\}$, and ^{31}P NMR spectroscopy, as shown in Figures S30-S32, below.

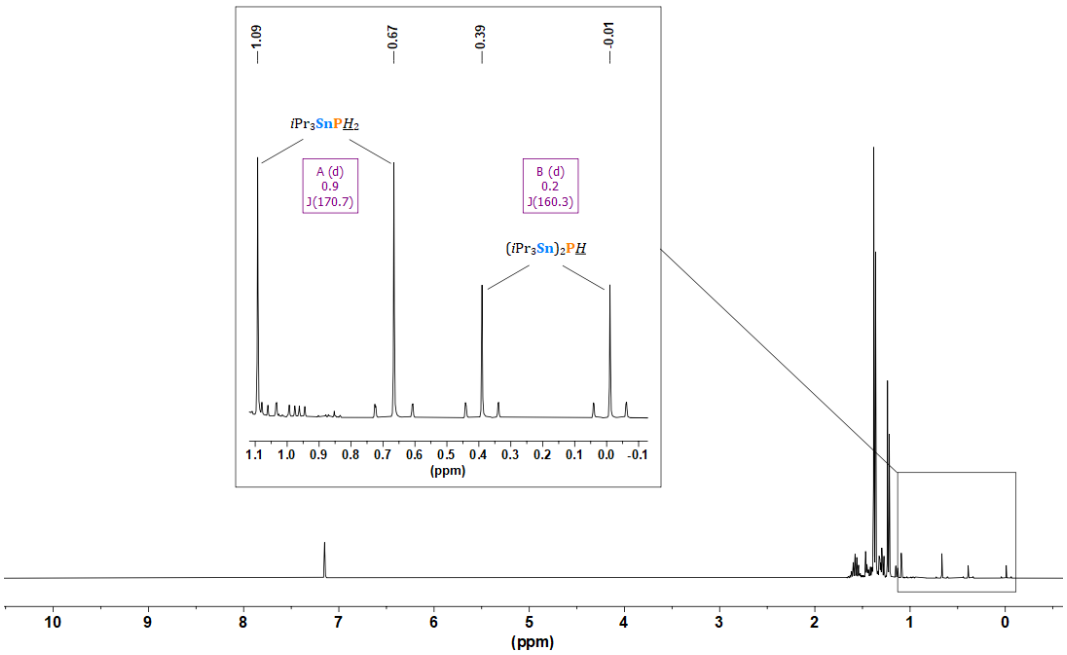

Figure S221. ^1H NMR spectrum for the *ex situ* reaction of P_4 (0.01 mmol) with *i*Pr_3SnH (0.06 mmol) in C_6D_6 and driven by 455 nm LED irradiation for 24 h. The inset shows expansions of the doublet resonance with $^{117/119}Sn$ satellites attributed to the P*H*$_2$ and P*H* moieties of ^{i}Pr_3SnPH_2 and (^{i}$Pr_3Sn)_2PH$, respectively.

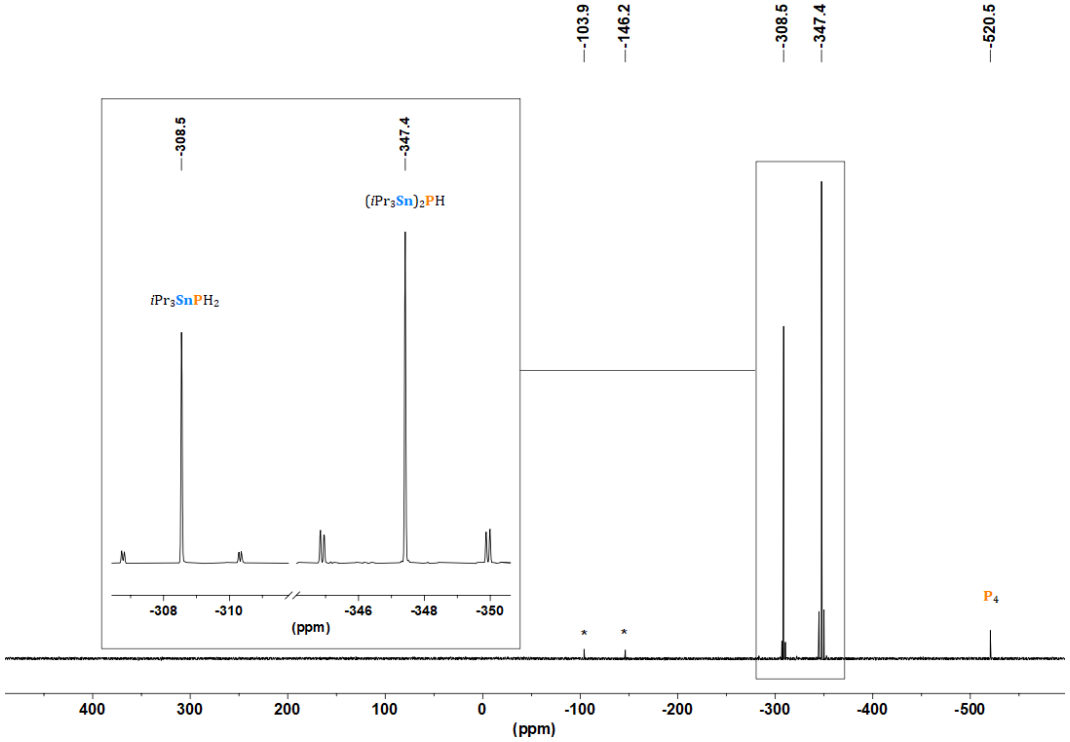

Figure S222. $^{31}P\{^{1}H\}$ NMR spectrum for the *ex situ* reaction of P_4 (0.01 mmol) with *i*Pr_3SnH (0.06 mmol) in C_6D_6 and driven by 455 nm LED irradiation for 24 h. The inset shows expansions of the signals attributed to *i*Pr_3SnPH_2 and (*i*$Pr_3Sn)_2PH$, highlighting the presence of $^{117/119}Sn$ satellites. * marks minor, unknown side products.

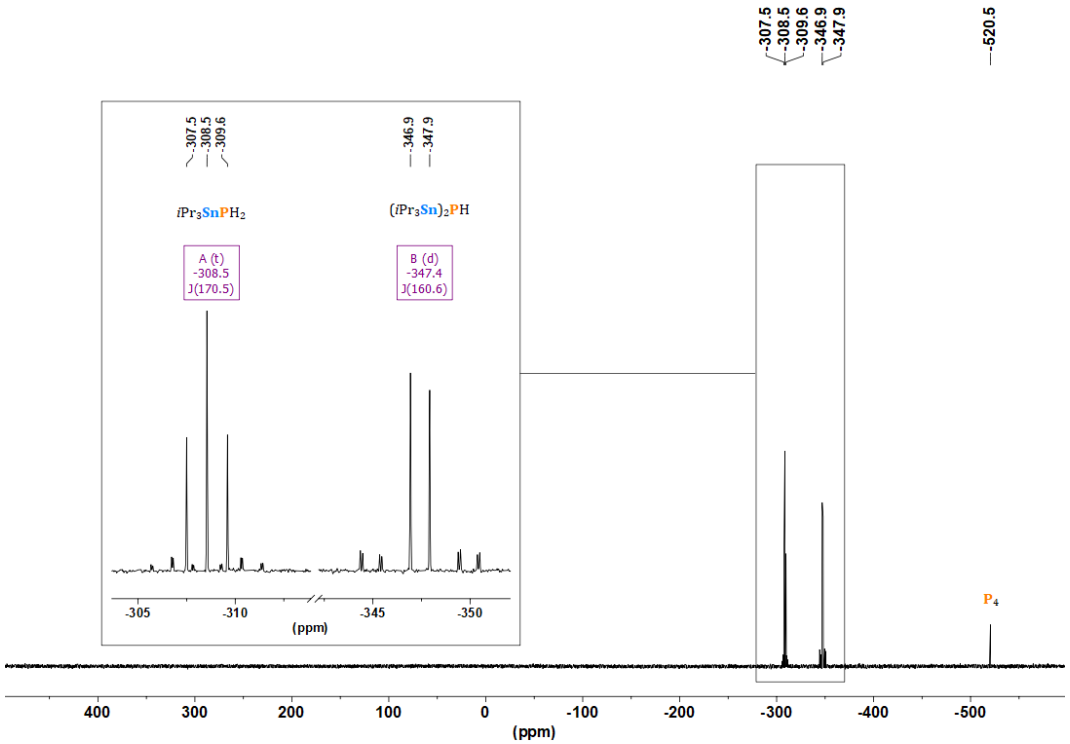

Figure S223. ^{31}P spectrum for the *ex situ* reaction of P_4 (0.01 mmol) with *i*Pr_3SnH (0.06 mmol) in C_6D_6 and driven by 455 nm LED irradiation for 24 h. The inset shows expansions of the signals attributed to *i*Pr_3SnPH_2 and (*i*$Pr_3Sn)_2PH$, highlighting their multiplicity due to $^{1}J(^{31}P\text{-}^{1}H)$ couplings.

Ex situ, with AIBN

To a 10 mL, flat-bottomed, stoppered tube were added C_6D_6 (500 µL), P_4 (0.01 mmol, as a stock solution in 124.6 µL C_6D_6), *i*Pr_3SnH (15.0 mg, 0.06 mmol) and AIBN (0.001 mmol, as a stock solution in 12.9 µL C_6D_6). The tube was sealed, wrapped in Al foil to exclude light, and heated to 60 °C for 24 h. The resulting mixture was analysed by $^{31}P\{^1H\}$, and ^{31}P NMR spectroscopy, as shown in Figures S33 and S34, below.

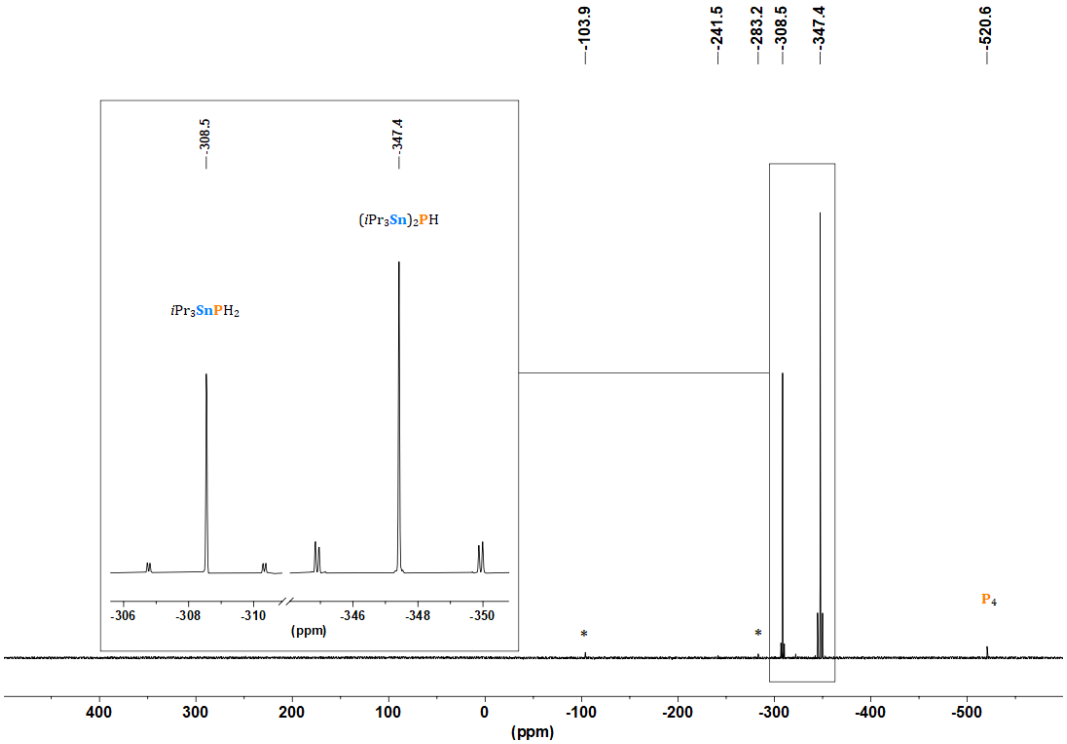

Figure S224. $^{31}P\{^1H\}$ NMR spectrum for the *ex situ* reaction of P_4 (0.01 mmol) with *i*Pr_3SnH (0.06 mmol) and AIBN (0.001 mmol) in C_6D_6, heated to 60 °C for 24 h in the dark. The inset shows expansions of the signals attributed to *i*Pr_3SnPH_2 and (*i*$Pr_3Sn)_2PH$, highlighting the presence of $^{117/119}Sn$ satellites. *marks minor, unknown side products.

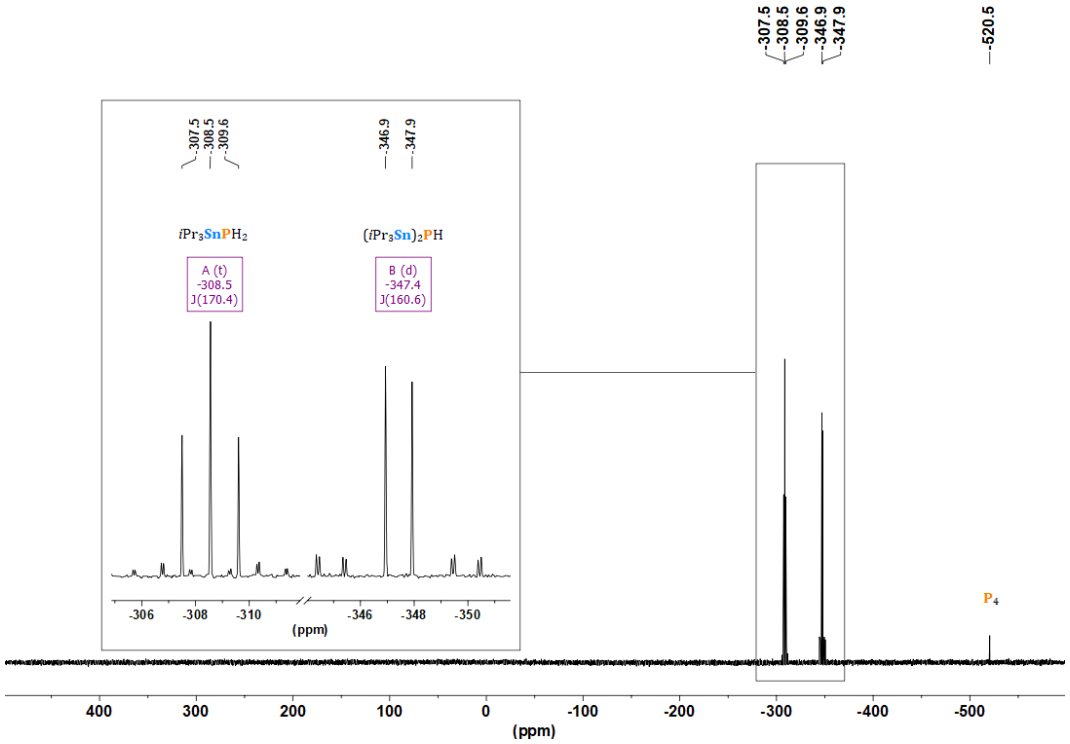

Figure S225. ^{31}P NMR spectrum for the *ex situ* reaction of P_4 (0.01 mmol) with *i*Pr_3SnH (0.06 mmol) and AIBN (0.001 mmol) in C_6D_6, heated to 60 °C for 24 h in the dark. The inset shows expansions of the signals attributed to *i*Pr_3SnPH_2 and (*i*$Pr_3Sn)_2PH$, highlighting their multiplicity due to $^1J(^{31}P\text{-}^1H)$ couplings.

In situ, with AIBN

This reaction was prepared in the same manner as the *ex situ* experiment described immediately above, but was transferred to a screw-cap NMR tube and monitored by *in situ* $^{31}P\{^1H\}$ NMR spectroscopy (for general details, see Section 4.4.1.1) at room temperature. As in the equivalent reaction with Bu_3SnH steady consumption of P_4 and concomitant product formation were observed, with no intermediates being detected. However, unlike for Bu_3SnH, only two products were observed to form: *i*Pr_3SnPH_2 and (*i*$Pr_3Sn)_2PH$, in an approximately 1:1 ratio (Figure S35).

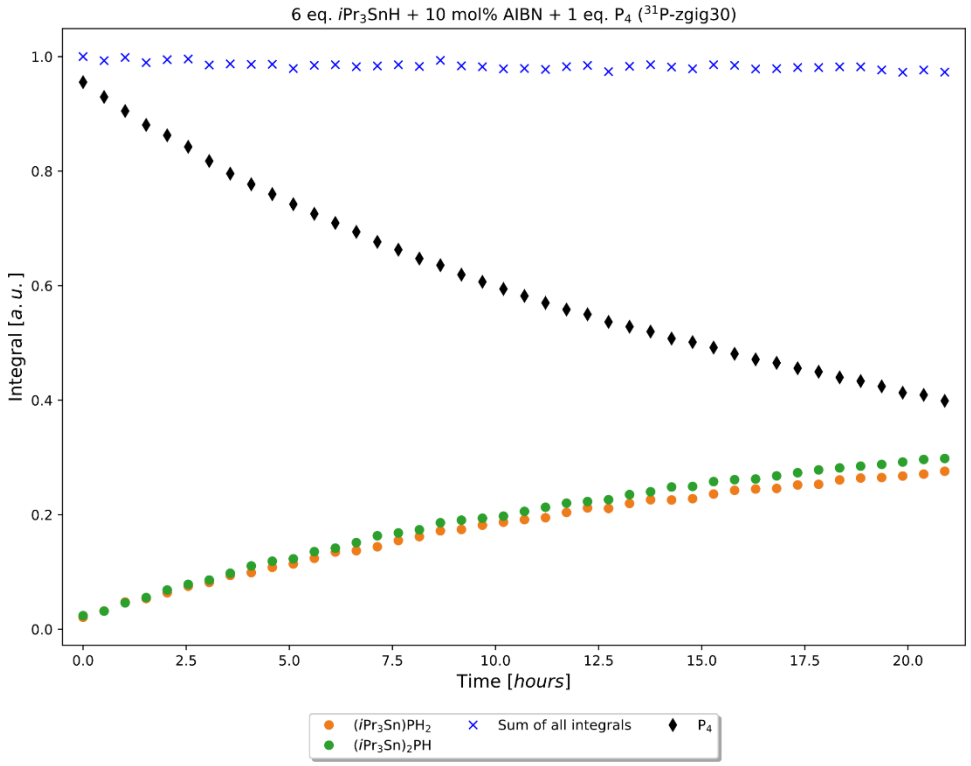

Figure S226. Evolution over time of P atom speciation in the reaction between P_4 and 6 eq. *i*Pr_3SnH initiated by 10 mol% AIBN in C_6D_6 at room temperature.

4.4.4.2 TerSn(Me)$_2$H

Ex situ, under LED irradiation (455 nm)

To a 10 mL, flat-bottomed, stoppered tube were added PhMe (500 µL), P_4 (0.01 mmol, as a stock solution in 88.6 µL PhH) and TerSn(Me)$_2$H (27.8 mg, 0.06 mmol). The tube was sealed, placed in a water-cooled block to maintain near-ambient temperature, and irradiated with blue light (455 nm (±15 nm), 3.2 V, 700 mA, Osram OSLON SSL 80) for 18 h. The resulting mixture was analysed by $^{31}P\{^1H\}$ and ^{31}P NMR spectroscopy, as shown in Figures S36 and S37, below.

Crystals of [TerSn(Me)$_2$]$_2$PH suitable for X-ray structure determination were grown by removing volatiles from the product mixture under vacuum, re-dissolving in *n*-hexane, and cooling to −35 °C (see section 4.4.4.5).

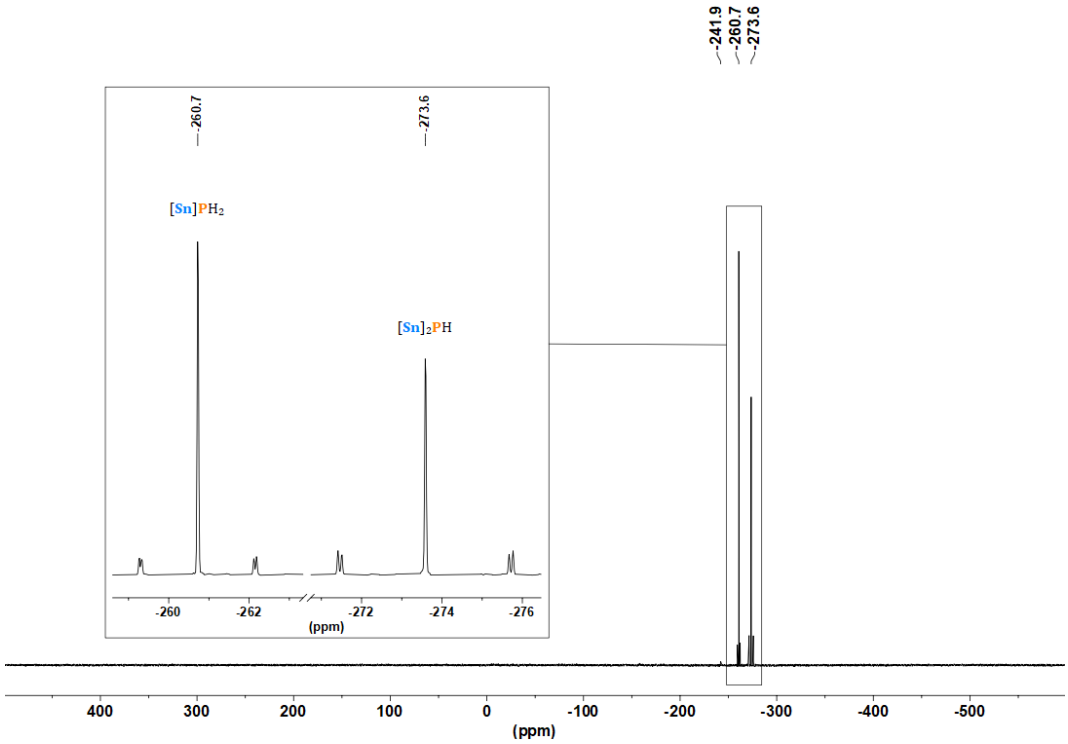

Figure S227. $^{31}P\{^{1}H\}$ NMR spectrum for the *ex situ* reaction of P_4 (0.01 mmol) with $TerSn(Me)_2H$ (0.06 mmol) in PhMe and driven by 455 nm LED irradiation for 18 h. The inset shows expansions of the signals attributed to $[Sn]PH_2$ and $[Sn]_2PH$ ([Sn] = $TerSn(Me)_2$), highlighting the presence of $^{117/119}Sn$ satellites.

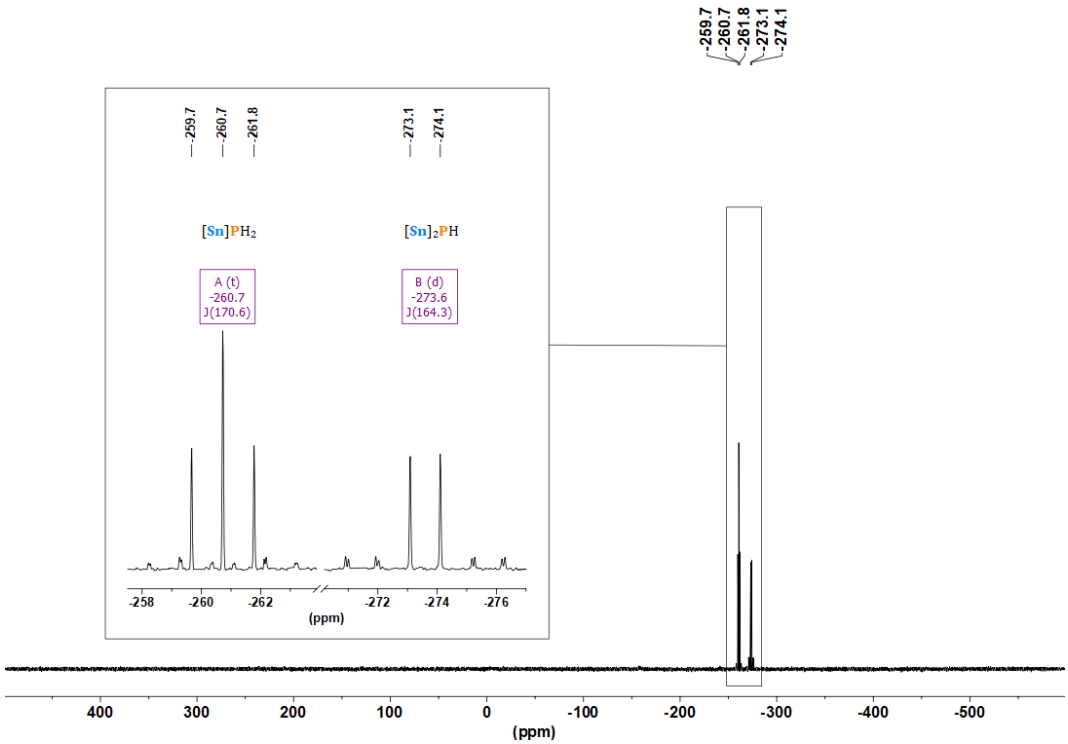

Figure S228. ^{31}P NMR spectrum for the *ex situ* reaction of P_4 (0.01 mmol) with $TerSn(Me)_2H$ (0.06 mmol) in PhMe and driven by 455 nm LED irradiation for 18 h. The inset shows expansions of the signals attributed to $[Sn]PH_2$ and $[Sn]_2PH$ ([Sn] = $TerSn(Me)_2$), highlighting their multiplicity due to $^{1}J(^{31}P\text{-}^{1}H)$ couplings.

Ex situ, with AIBN

To a 10 mL, flat-bottomed, stoppered tube were added C_6D_6 (500 µL), P_4 (0.01 mmol, as a stock solution in 124.6 µL C_6D_6), $TerSn(Me)_2H$ (27.8 mg, 0.06 mmol) and AIBN (0.001 mmol, as a stock solution in 12.9 µL C_6D_6). The tube was sealed, wrapped in Al foil to exclude light, and heated to 60 °C for 24 h. The resulting mixture was analysed by $^{31}P\{^1H\}$, and ^{31}P NMR spectroscopy, as shown in Figures S38 and S39, below.

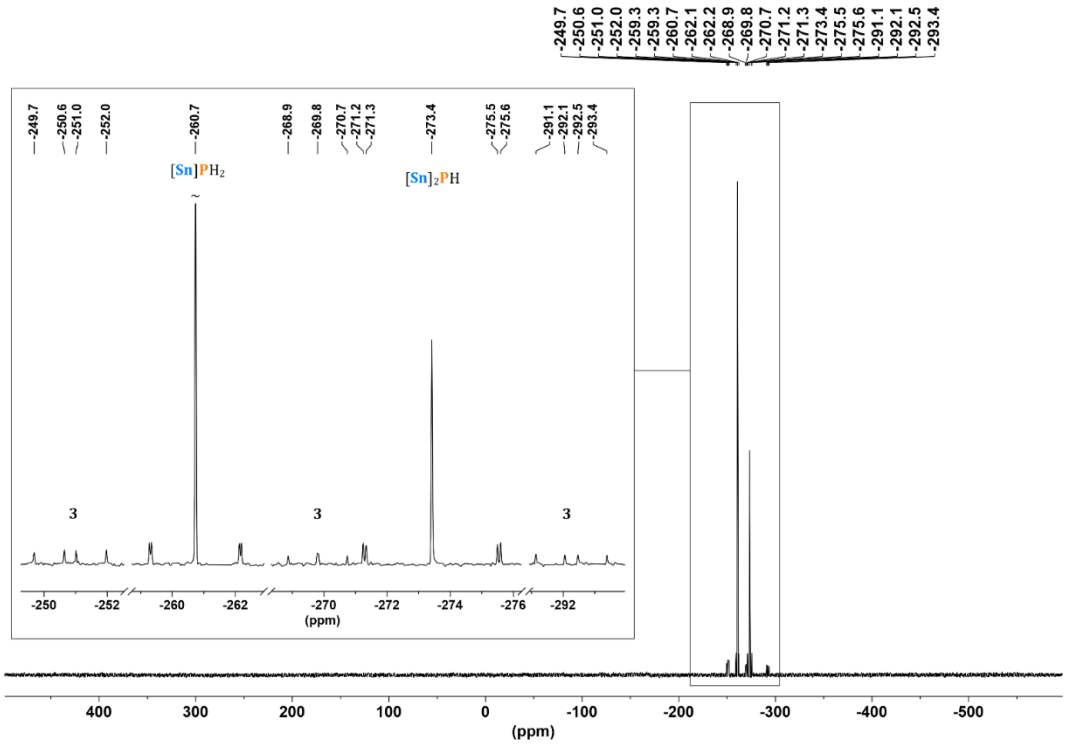

Figure S229. $^{31}P\{^1H\}$ NMR spectrum for the *ex situ* reaction of P_4 (0.01 mmol) with $TerSn(Me)_2H$ (0.06 mmol) in C_6D_6 and AIBN (0.001 mmol) in C_6D_6, heated to 60 °C for 24 h in the dark. The inset shows expansions of the signals attributed to $[Sn]PH_2$ and $[Sn]_2PH$ ([Sn] = $TerSn(Me)_2$), highlighting the presence of $^{117/119}Sn$ satellites. Peak marked with ~ has been truncated for the sake of clarity.

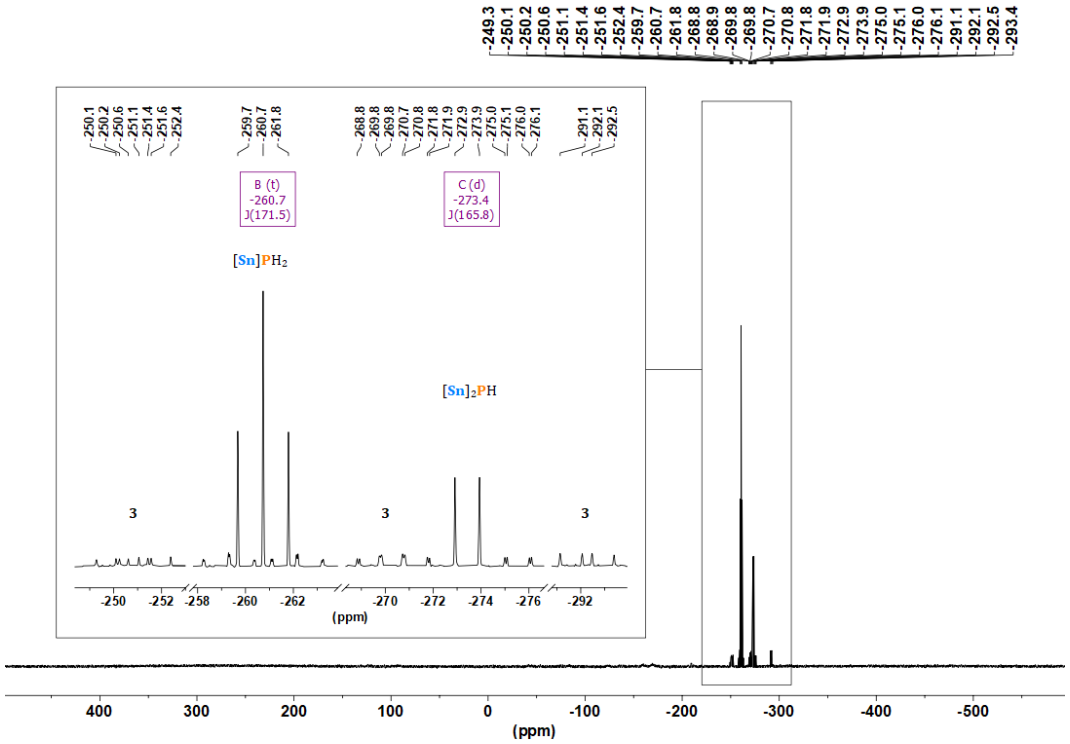

Figure S230. ^{31}P NMR spectrum for the *ex situ* reaction of P_4 (0.01 mmol) with $TerSn(Me)_2H$ (0.06 mmol) in C_6D_6 and AIBN (0.001 mmol) in C_6D_6, heated to 60 °C for 24 h in the dark. The inset shows expansions of the signals attributed to $[Sn]PH_2$ and $[Sn]_2PH$ ([Sn] = $TerSn(Me)_2$), highlighting the presence of $^{117/119}Sn$ satellites.

In situ, with AIBN

To a screw-capped NMR tube were added C_6D_6 (500 μL), P_4 (0.01 mmol, as a stock solution in 124.6 μL C_6D_6), $TerSn(Me)_2H$ (27.8 mg, 0.06 mmol), and AIBN (0.001 mmol, as a stock solution in 12.9 μL C_6D_6). The resulting solution was monitored by *in situ* $^{31}P\{^1H\}$ NMR spectroscopy (for general details, see Section 4.4.1.1) at room temperature.

In addition to resonances for the P_4 starting material and the final products $[Sn]PH_2$ and $[Sn]_2PH$ (where [Sn] = $TerSnMe_2$), five further resonances were observed as the reaction progressed, which can be assigned to reaction intermediates. A representative spectrum showing all detected resonances is shown in Figure 10 (Section 4.2.2), and in Figure S40, below.

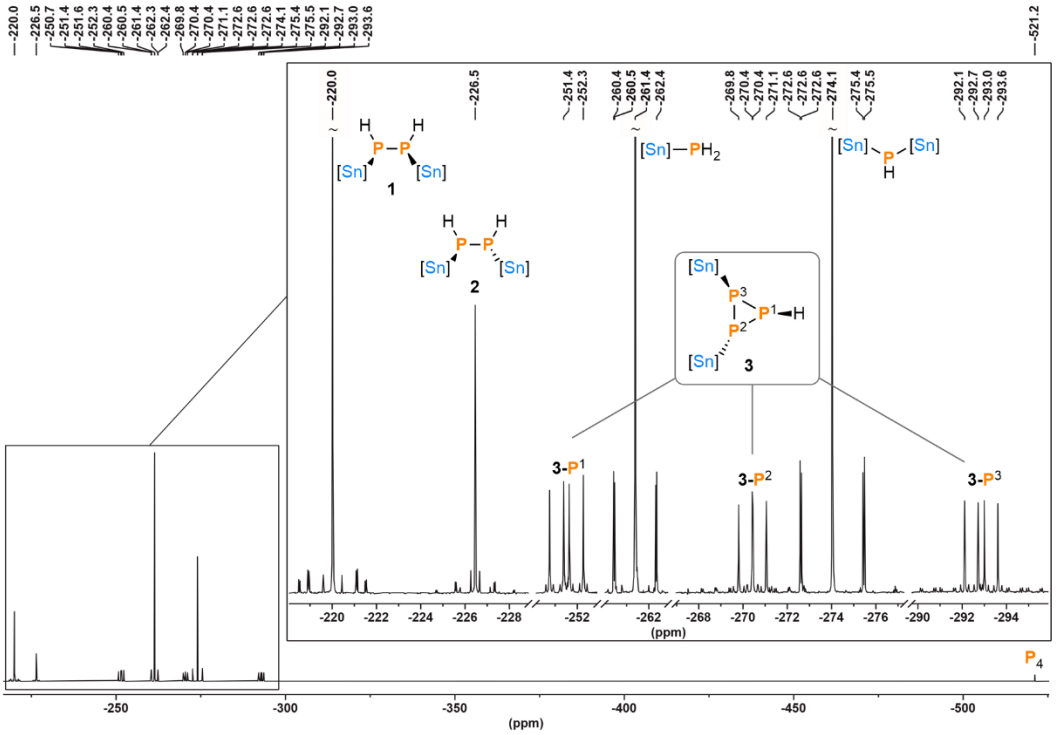

Figure S231. $^{31}P\{^{1}H\}$ NMR spectroscopic observation of reaction intermediates during the hydrostannylation of P_4 using $TerSn(Me)_2H$ (6 eq.) initiated by AIBN (10 mol%) in C_6D_6 at room temperature. [Sn] = $TerSnMe_2$. Peaks marked with ~ have been truncated for the sake of clarity.

Of the five signals assigned to intermediates, the two singlets -220.0 ppm and -226.5 ppm can be attributed to the meso and C_2 isomers of the symmetrical diphosphane [Sn]P(H)–P(H)[Sn] (**1** and **2**, respectively). The presence of a higher-order spin system is evident both from the pattern of the $^{117/119}$Sn satellites and the corresponding ^{1}H-coupled ^{31}P spectra (Figures S41 and S42), with very similar patterns having been reported for silylated diphosphanes, HypP(H)–P(H)Hyp (Hyp = $Si(SiMe_3)_3$).[44] Note that ^{119}Sn and ^{1}H(P*H*) resonances for these intermediates could not be resolved.

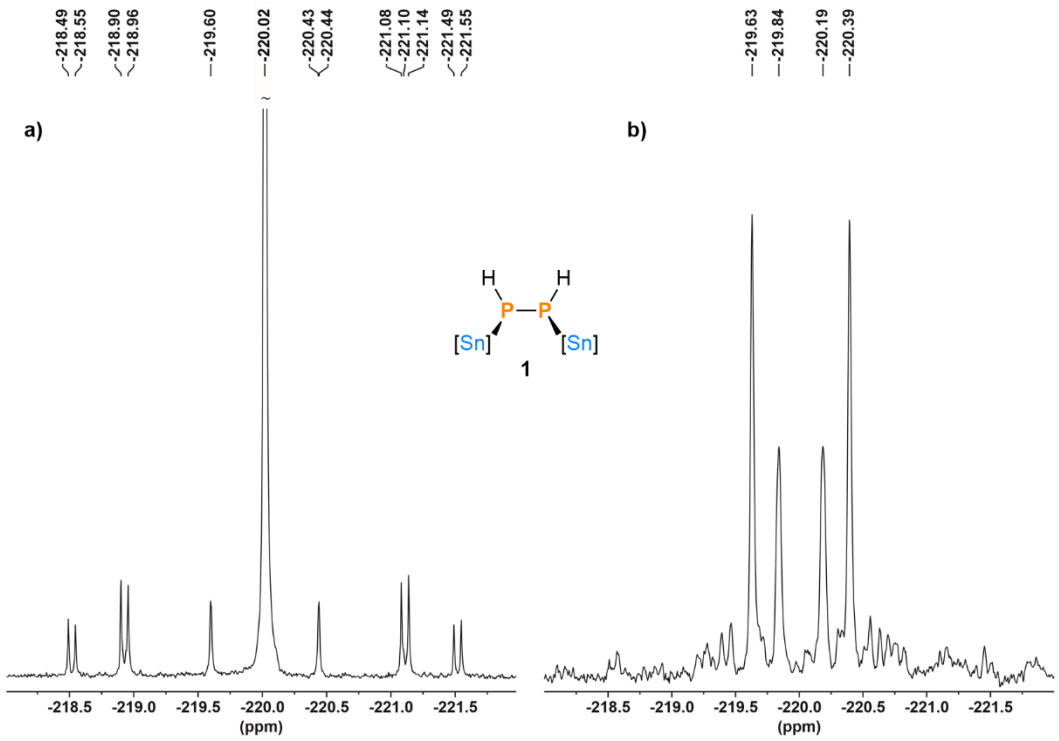

Figure S232. (a) $^{31}P\{^{1}H\}$ and (b) ^{31}P NMR resonances of **1** (meso-[Sn]P(H)–P(H)[Sn]), as observed during *in situ* experiments. [Sn] = $TerSnMe_2$. Peak marked with ~ has been truncated for the sake of clarity.

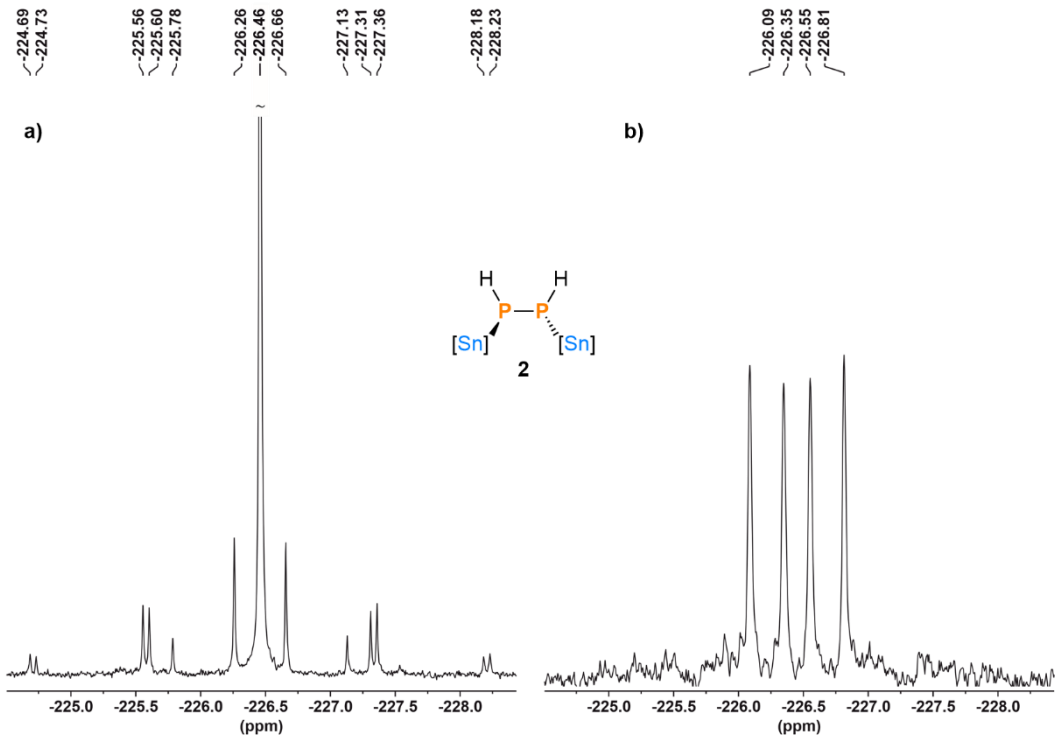

Figure S233. (a) $^{31}P\{^{1}H\}$ and (b) ^{31}P NMR resonances of **2** (C_2-[Sn]P(H)–P(H)[Sn]), as observed during *in situ* experiments. [Sn] = $TerSnMe_2$. Peak marked with ~ has been truncated for the sake of clarity.

The remaining three doublet of doublet signals show mutual coupling constants, suggesting they can be assigned to a single species. This was confirmed by ^{31}P-COSY (Figure S43), and based on the observation of ^{31}P–^{31}P, ^{31}P–^{1}H and ^{31}P–$^{117/119}$Sn coupling constants (Figure S44) as well as ^{119}Sn NMR spectra (Figure S45) this species is assigned as the *cyclo*-P_3 structure $[Sn]_2P_3H$, **3**, whose P_3 ring is substituted by two [Sn] moieties in a trans arrangement, and one H atom. The H atom is trans to one [Sn] group and cis to the other, resulting in three distinct ^{31}P environments and hence the three observed signals.

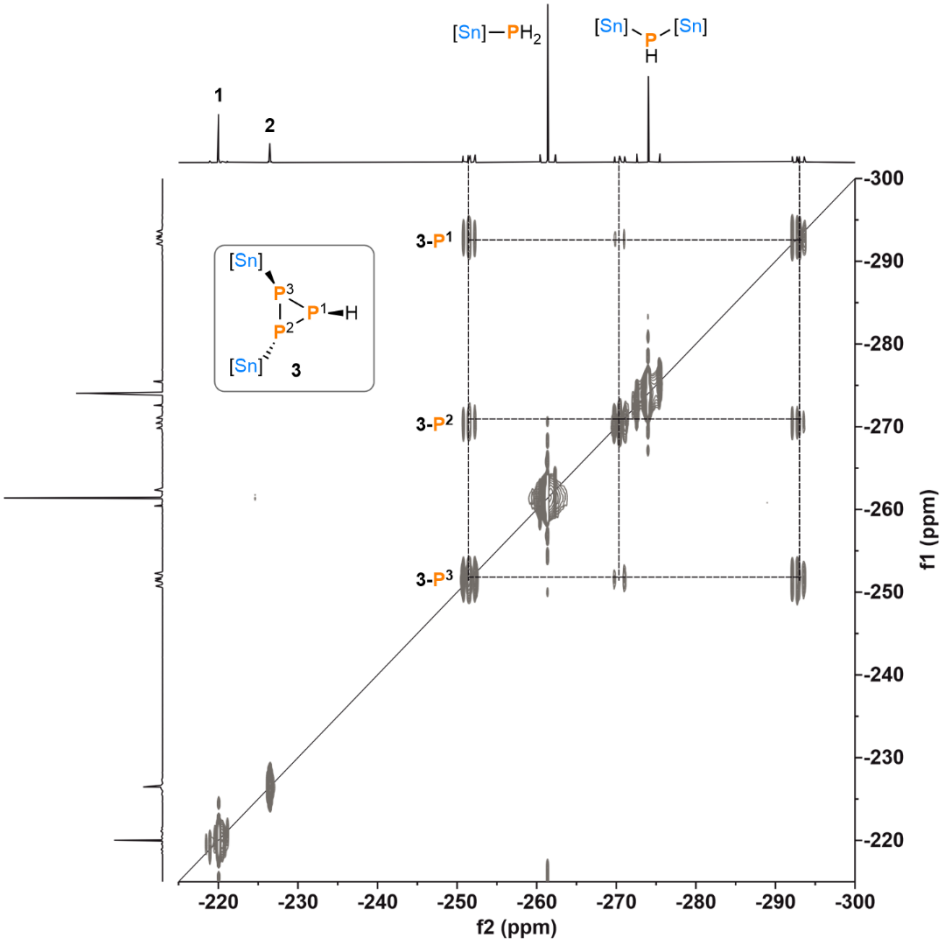

Figure S234. ^{31}P COSY spectrum showing coupling between the three resonances attributed to intermediate **3** ($[Sn]_2P_3H$), as observed during *in situ* experiments. [Sn] = $TerSnMe_2$.

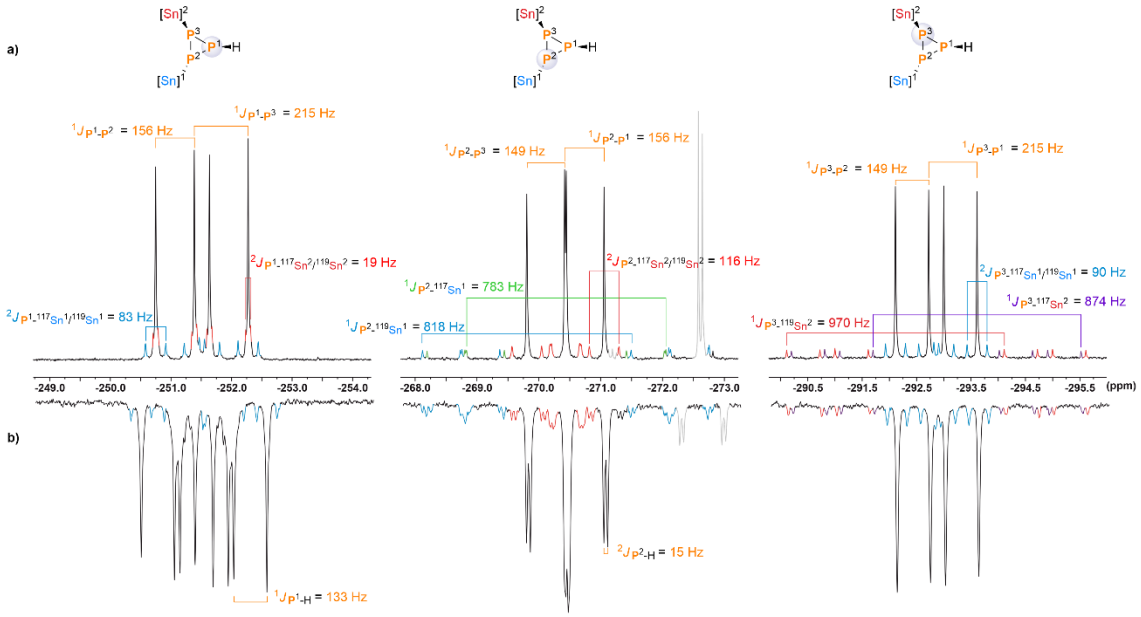

Figure S235. (a) $^{31}P\{^{1}H\}$ and (b) ^{31}P NMR resonances of **3** ($[Sn]_2P_3H$), as observed during *in situ* experiments. [Sn] = $TerSnMe_2$.

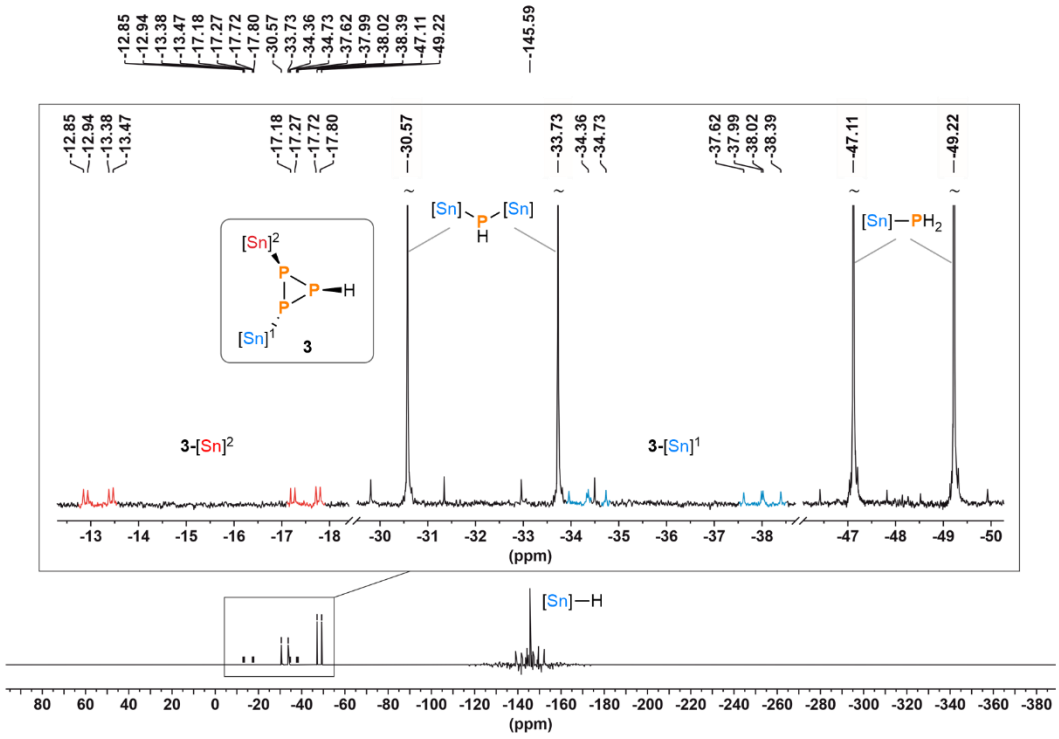

Figure S236. $^{119}Sn\{^{1}H\}$ NMR resonances of **3** ($[Sn]_2P_3H$), as observed during *in situ* experiments. [Sn] = $TerSnMe_2$. The ^{119}Sn-NMR signal of [Sn]H is strongly distorted due to artifacts from proton decoupling. Peaks marked with ~ have been truncated for the sake of clarity.

These structural assignments were further confirmed by DFT calculations (see Section 4.4.5), which were also used as the basis for distinguishing between **1** and **2** (although this should be viewed as a tentative assignment only).

The evolution of ^{31}P speciation in the *in situ* experiment is shown in Figure S46, below. P_4 has an unusually long T_1 relaxation time (*ca*. 40 s). However, to avoid undesirably long acquisition times, this experiment used a D_1 delay of just 2.0 s between scans. As a result, the P_4 concentration is underestimated by these measurements, leading to an apparent increase in overall integral intensity as P_4 is converted into other species.

It can be seen qualitatively that formation of [Sn]PH_2 begins immediately. Similarly, **3** appears to form immediately before plateauing, as expected for an intermediate. In contrast, formation of [Sn]$_2$PH seems to lag behind formation of [Sn]PH_2 by an amount that appears fixed once **3** reaches its plateau (notably, a fixed difference rather than a fixed *ratio*). Formation of **1** and **2** also appears to plateau, albeit more slowly than for **3**, which would be consistent with **1** and **2** being downstream intermediates from **3**.

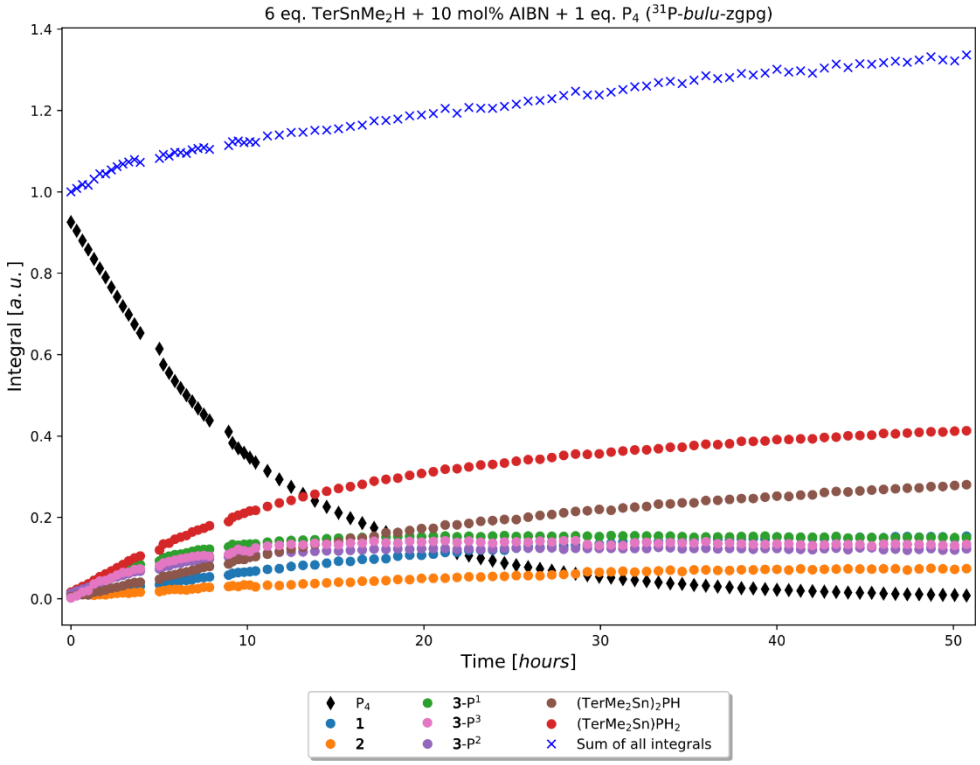

Figure S237. Evolution over time of P atom speciation in the reaction between P_4 and 6 eq. TerSn(Me)$_2$H initiated by 10 mol% AIBN at 298 K in C_6D_6 as monitored by *in situ* $^{31}P\{^1H\}$ NMR spectroscopy.

Based on these observations, hydrostannylation of P_4 using TerSn(Me)$_2$H appears to follow the same general mechanism as using smaller Bu_3SnH/Me_3SnH (Scheme 2). However, it is proposed that the increased steric bulk of the more hindered "TerSnMe_2" moiety significantly affects the preferred sequence of P–P cleavage steps, and biases the overall mechanism towards a single sterically-preferred pathway, in contrast to the "ensemble mechanism" suggested for Bu_3SnH/Me_3SnH. (Note, however, that the continued existence of other, competing pathways whose intermediates remain "invisible" cannot be fully excluded.)

This pathway is summarized in Scheme S1. The first P–P addition must still furnish the butterfly-type structre ^{Ter}**II**, and the second is expected to occur without any change in regioselectivity since the (modest) preference for **IIIa•/IVa** calculated for Me_3SnH already keeps the two R_3Sn moieties as separated as possible (and, notably, much further apart than in **IIIb•/IVb**, the closest kinetic competitor). This would give ^{Ter}**IVa**. Based on the experimental observation of **3** (= ^{Ter}**VIh**) as an intermediate, the third addition is proposed to occur at the *exo* P–P bond of ^{Ter}**IV•**. This is a divergence with the mechanism calculated for Me_3SnH, but attack on the unstannylated P atom (trans to the existing ring-bound [Sn] group) would plausibly help to minimize steric clash. The fourth addition is then presumed to occur at the least hindered position on the *cyclo*-P_3 ring (PH). Similarly, the fifth addition is proposed to occur at one of the less hindered, terminal positions of the P_3 chain (generating the observed symmetrical isomers **1** and **2**). The final addition then has only one possible regiochemical outcome. Notably, this pathway readily accounts for immediate formation of $[Sn]PH_2$ and an initial observable intermediate **3**, followed by further transformation of **3** into $[Sn]PH_2$ + 2 $[Sn]_2PH$, *via* downstream intermediate **1** or **2**.

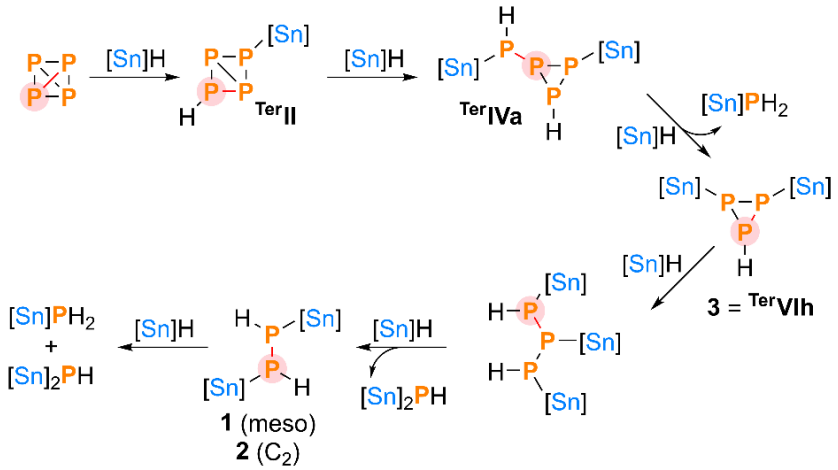

Scheme S1. Sequence of P–P cleavage steps proposed to occur preferentially during hydrostannylation of P_4 using $TerSn(Me)_2H$. [Sn] = $TerSnMe_2$. Bonds cleaved are highlighted in red.

In situ, under LED irradiation (455 nm)

A reaction solution was prepared by combining P_4 (0.01 mmol, as a stock solution in 124.6 µL C_6D_6) and $TerSn(Me)_2H$ (27.8 mg, 0.06 mmol) in C_6D_6 (0.3 mL) inside a glovebox and transferred into an NMR tube incorporating apparatus for *in situ* illumination.[32] The tube was immediately transferred into a 600 MHz NMR spectrometer and subjected to $^{31}P\{^1H\}$ NMR analysis every 15-30 minutes. The resulting reaction profile is shown in Figure 11 (Section 4.2.2), and below in Figure S47.

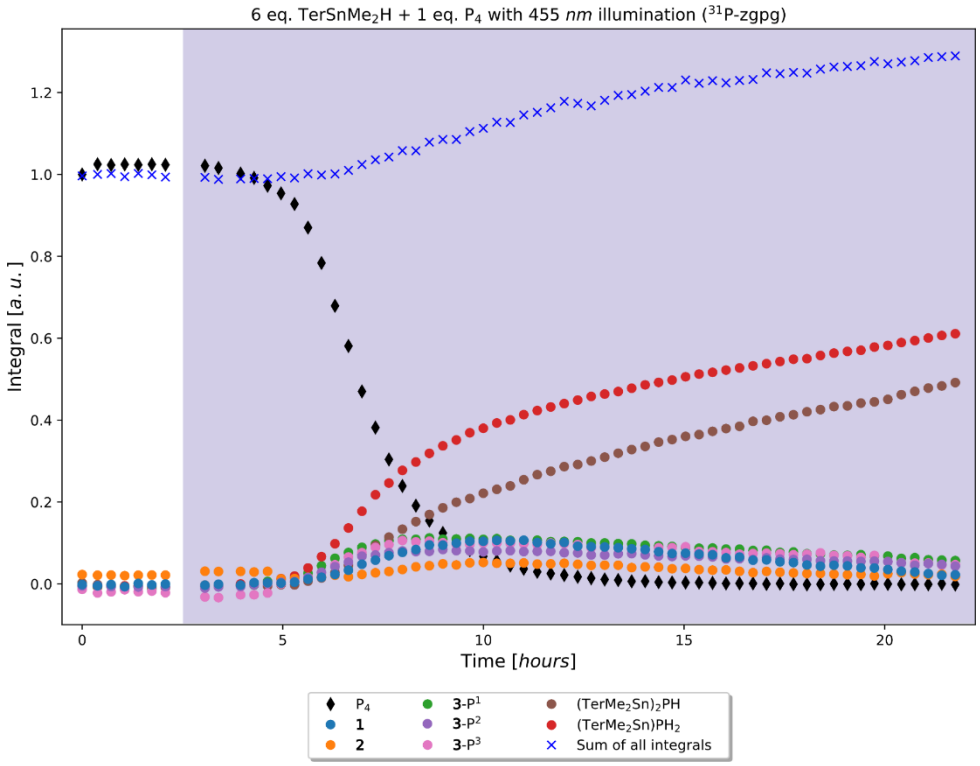

Figure S238. Evolution over time of P atom speciation in the reaction between P_4 and 6 eq. TerSn(Me)$_2$H initiated by *in situ* 455 nm LED irradiation (starting after 3 h, illumination period indicated by blue shading) in C_6D_6 at room temperature.

4.4.4.3 Ter*Sn(Me)$_2$H

Ex situ, under LED irradiation (455 nm)

To a 10 mL, flat-bottomed, stoppered tube were added C_6D_6 (500 µL), P_4 (0.005 mmol, as a stock solution in 62.3 µL C_6D_6), Ter*Sn(Me)$_2$H (15.6 mg, 0.03 mmol). The tube was sealed, placed in a water-cooled block to maintain near-ambient temperature, and irradiated with blue light (455 nm (±15 nm), 3.2 V, 700 mA, Osram OSLON SSL 80) for 24 h. The resulting mixture was analysed by $^{31}P\{^1H\}$ and ^{31}P NMR spectroscopy, as shown in Figures S48, and S49, below.

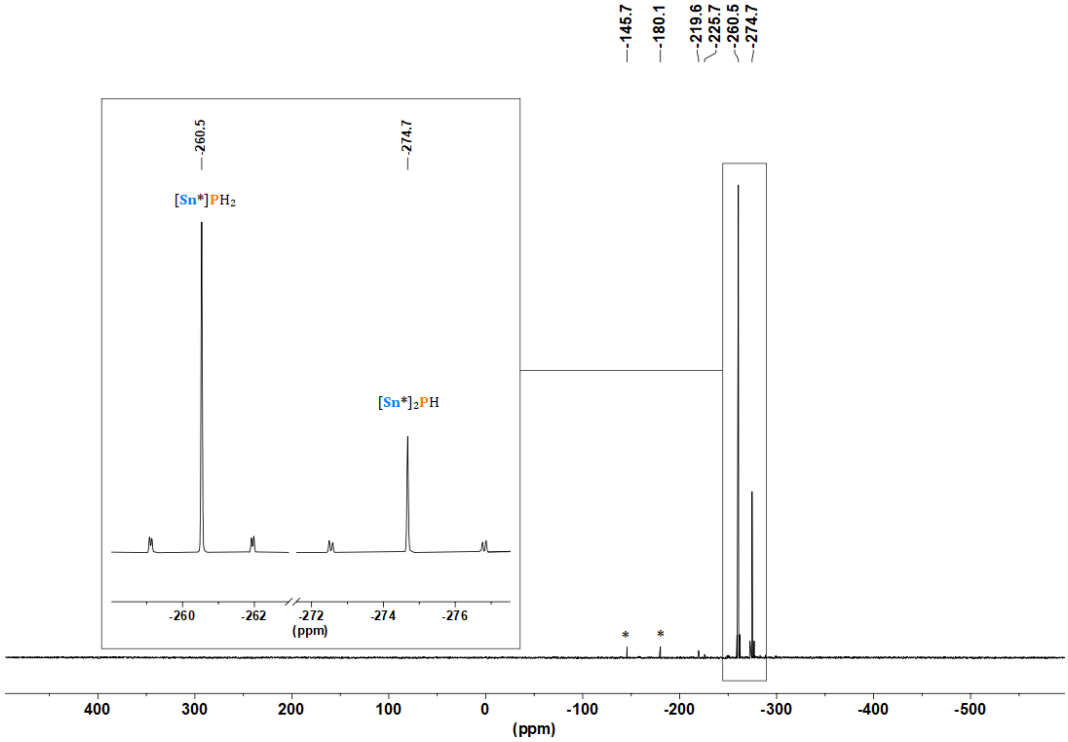

Figure S239. $^{31}P\{^{1}H\}$ NMR spectrum for the *ex situ* reaction of P_4 (0.005 mmol) with Ter*Sn(Me)$_2$H (0.03 mmol) and AIBN (0.0005 mmol) in C_6D_6, and driven by 455 nm LED irradiation for 24 h. The [Sn*] = Ter*Sn(Me)$_2$. *marks minor, unknown side products.

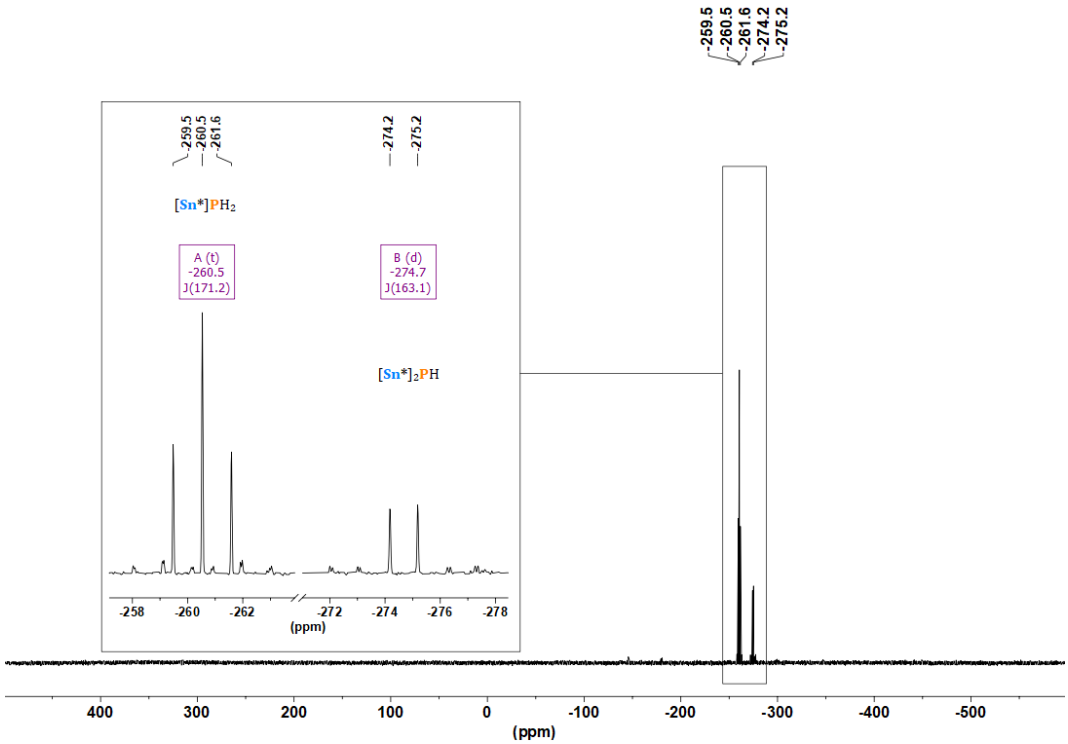

Figure S240. ^{31}P NMR spectrum for the *ex situ* reaction of P_4 (0.005 mmol) with Ter*Sn(Me)$_2$H (0.03 mmol) and AIBN (0.0005 mmol) in C_6D_6, and driven by 455 nm LED irradiation for 24 h. The [Sn*] = Ter*Sn(Me)$_2$.

Ex situ, with AIBN

To a 10 mL, flat-bottomed, stoppered tube were added C_6D_6 (500 μL), P_4 (0.005 mmol, as a stock solution in 62.3 μL C_6D_6), Ter*Sn(Me)$_2$H (15.6 mg, 0.03 mmol) and AIBN (0.0005 mmol, as a stock solution in 6.5 μL C_6D_6). The tube was sealed, wrapped in Al foil to exclude light, and heated to 60 °C for 24 h. The resulting mixture was analysed by $^{31}P\{^1H\}$, and ^{31}P NMR spectroscopy, as shown in Figures S50 and S51, below.

In addition to the expected products [Sn*]PH$_2$ and [Sn*]$_2$PH ([Sn*] = Ter*SnMe$_2$) a major set of three coupled doublets of doublets was observed, as were two more minor singlets. Based on the similar observations made using TerSn(Me)$_2$ these species were assigned as **1***, **2*** and **3***.

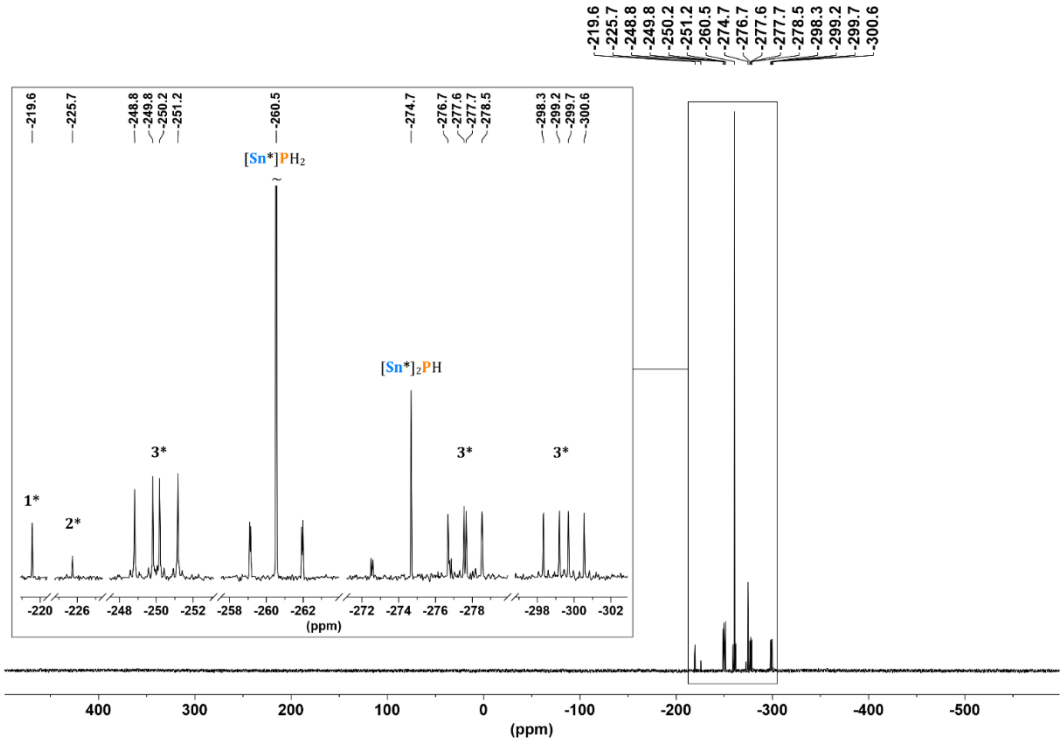

Figure S241. $^{31}P\{^1H\}$ NMR spectrum for the *ex situ* reaction of P_4 (0.005 mmol) with Ter*Sn(Me)$_2$H (0.03 mmol) and AIBN (0.0005 mmol) in C_6D_6, heated to 60 °C for 24 h in the dark. [Sn*] = Ter*Sn(Me)$_2$. Peak marked with ~ has been truncated for the sake of clarity.

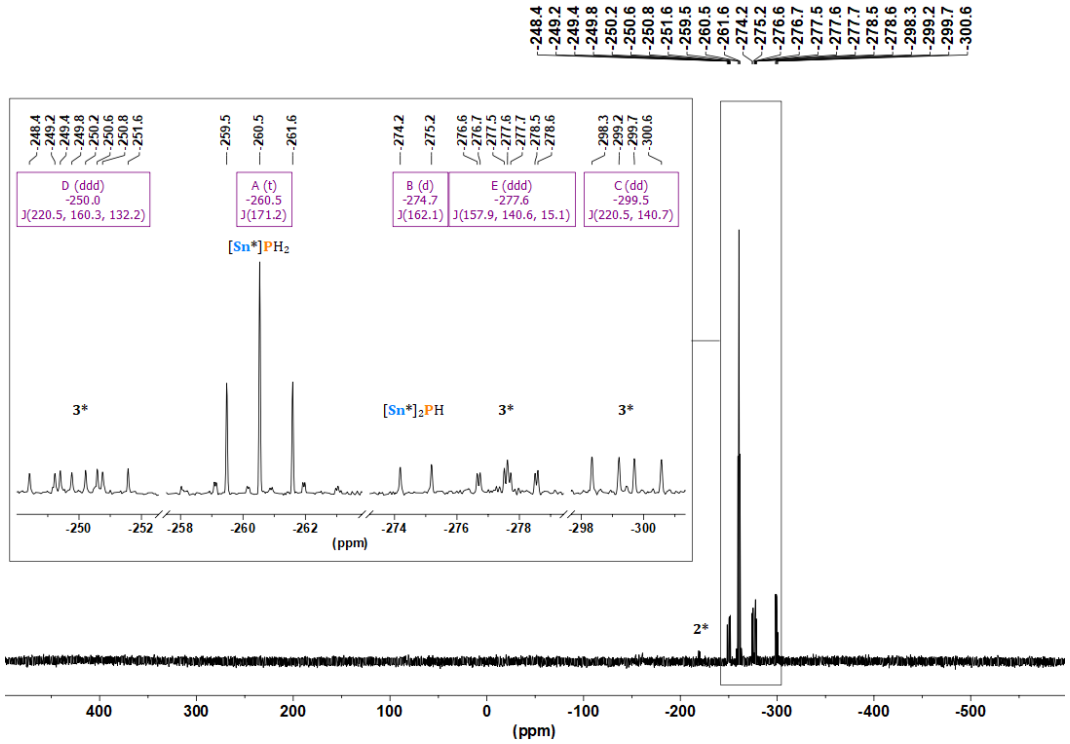

Figure S242. ^{31}P NMR spectrum for the *ex situ* reaction of P_4 (0.005 mmol) with Ter*Sn(Me)$_2$H (0.03 mmol) and AIBN (0.0005 mmol) in C_6D_6, heated to 60 °C for 24 h in the dark. [Sn*] = Ter*Sn(Me)$_2$.

In situ, with AIBN

This reaction was prepared in the same manner as the *ex situ* experiment described immediately above, but was transferred to a screw-cap NMR tube and monitored by *in situ* $^{31}P\{^1H\}$ NMR spectroscopy (for general details, see Section 4.4.1.1) at room temperature (Figure S52).

Under these lower temperature conditions only formation of [Sn*]PH_2 and **3*** was observed during the timeframe of the experiment, with neither [Sn*]$_2$PH nor **1***/**2*** being detected. This can be contrasted with the results using TerSn(Me)$_2$H where the equivalent species *were* observed at room temperature, highlighting the enhanced steric impact of the slightly larger Ter* group, which further hinders reactivity.

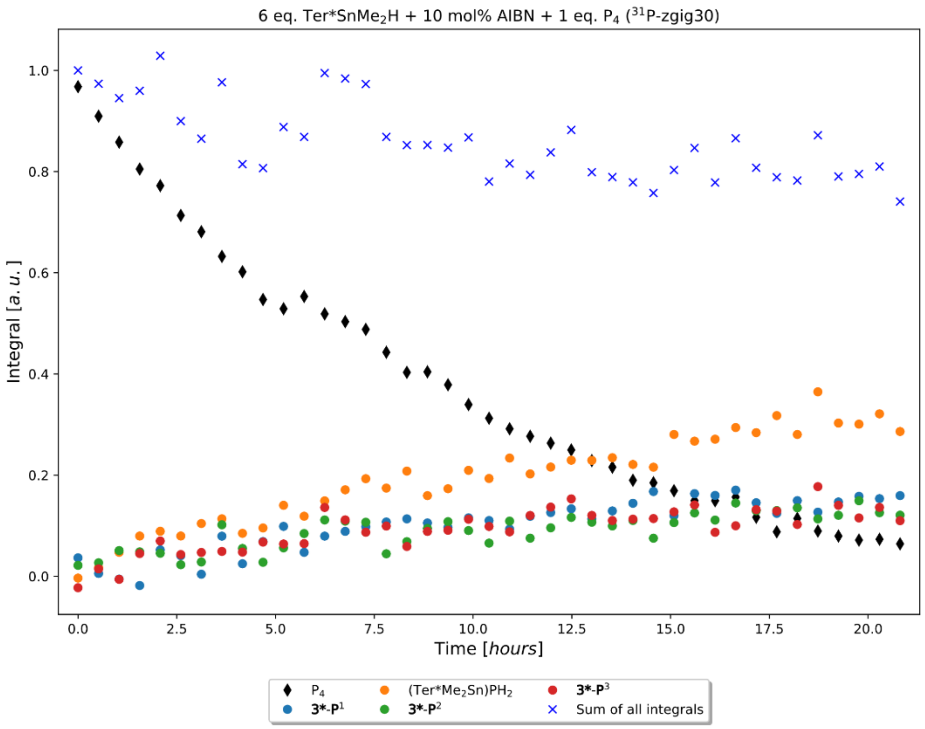

Figure S243. Evolution over time of P atom speciation in the reaction between P_4 and 6 eq. Ter*Sn(Me)$_2$H initiated by 10 mol% AIBN at 298 K in C_6D_6 as monitored by *in situ* $^{31}P\{^1H\}$ NMR spectroscopy.

4.4.4.4 (Fluind)Sn(Me)$_2$H

To a 10 mL, flat-bottomed, stoppered tube were added C_6D_6 (600 µL), P_4 (0.005 mmol, as a stock solution in 62.3 µL C_6D_6), (Fluind)Sn(Me)$_2$H (19.9 mg, 0.03 mmol) and AIBN (0.0025 mmol, as a stock solution in 32.2 µL C_6D_6). The tube was sealed, wrapped in Al foil to exclude light, and heated to 60 °C for 4 d. The resulting mixture was analysed by $^{31}P\{^1H\}$NMR spectroscopy, as shown in Figure S53 below.

No appreciable consumption of P_4 was observed. Similar experiments using 455 nm irradiation also led to only minor P_4 consumption.

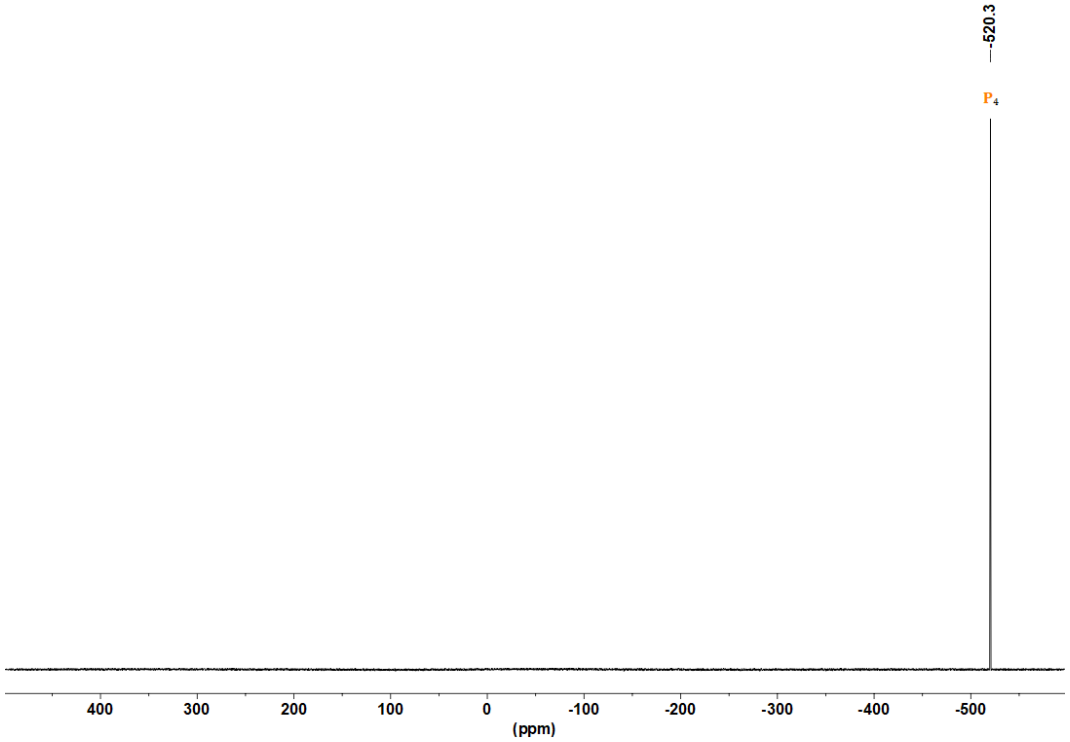

Figure S244. $^{31}P\{^{1}H\}$ NMR spectrum for the *ex situ* reaction of P_4 (0.005 mmol) with (Fluind)Sn(Me)$_2$H (0.03 mmol) and AIBN (0.0025 mmol) in C_6D_6, heated to 60 °C for 4 d in the dark.

4.4.4.5 Crystallographic characterisation of [TerSn(Me)$_2$]$_2$PH

Single crystal X-ray diffraction data for [TerSn(Me)$_2$]$_2$PH was recorded on a Rigaku XtaLAB Synergy DW R (DW system, HyPix-Arc 150) diffractometer with microfocus Cu-Kα radiation (λ = 1.54184 Å). The crystal was selected under mineral oil, mounted on a micromount loop and quench-cooled using an Oxford Cryosystems open flow N_2 cooling device. Data processing, reduction and multi-scan absorption correction[45,46] was performed with the program CrysAlisPro (Rigaku Oxford Diffraction, 2021). Using Olex2,[43] the structure was solved with the SHELXT[42a] structure solution program using Intrinsic Phasing and refined using olex2.refine.[47] All non-hydrogen atoms were refined using anisotropic displacement parameters. All hydrogen atoms but the P bound hydrogen atom were located in idealized positions and refined isotropically with a riding model. The P bound hydrogen atom was located from the electron density map and had its position and isotropic displacement parameter refined freely. The disorder of the P bound hydrogen atom was treated with a geometrical restraint. To compute the non-spherical atomic form factors, the programNoSpherA2[48] was used and the wavefunction calculations were performed with ORCA 5.0[34,49-51] (on the R2SCAN/x2c-TZVP level of theory).[52,53] Crystallographic data for this structure has been deposited with the Cambridge Crystallographic Data Centre, CCDC, 12 Union Road, Cambridge CB21EZ, UK. Copies of this data can be obtained free of charge on quoting the depository number: 2315067; E-mail: deposit@ccdc.cam.ac.uk, http://www.ccdc.cam.ac.uk.

Crystal and refinement data are collected in Table S3, and the structure itself is illustrated in Figure S54.

Table S3. Crystal data and structure refinement of $[TerSn(Me)_2]_2PH$.

	$[TerSn(Me)_2]_2PH$
Formula	$C_{52}H_{63}PSn_2$
Formula weight, g mol^{-1}	956.474
Crystal system	123.00(10)
Crystal size, mm	monoclinic
Space group	$P2_1/n$
a, Å	8.36845(3)
b, Å	21.44921(9)
c, Å	26.28771(12)
α, º	90
β, º	90.5395(4)
γ, º	90
V, $Å^3$	4718.35(3)
Z	4
ρ_{calcd}, Mg m^{-3}	1.346
μ (Mo *K*α), mm^{-1}	8.971
F(000)	1968.4
2θ range, deg	0.462 × 0.13 × 0.091
Index ranges	Cu Kα (λ = 1.54184)
	5.32 to 150.36
	$-8 \leq h \leq 10$, $-26 \leq k \leq 26$, $-32 \leq l \leq 32$
No. of reflns collected	131932
No. indep. Reflns	9583 [R_{int} = 0.0258, R_{sigma} = 0.0091]
No. refined params	9583/2/692
GooF (F^2)	1.055
R_1 (*F*) ($I > 2\sigma(I)$)	R_1 = 0.0167, wR_2 = 0.0414
wR_2 (F^2) (all data)	R_1 = 0.0170, wR_2 = 0.0416
Largest diff peak/hole, e $Å^{-3}$	0.49/-0.49
CCDC number	2315067

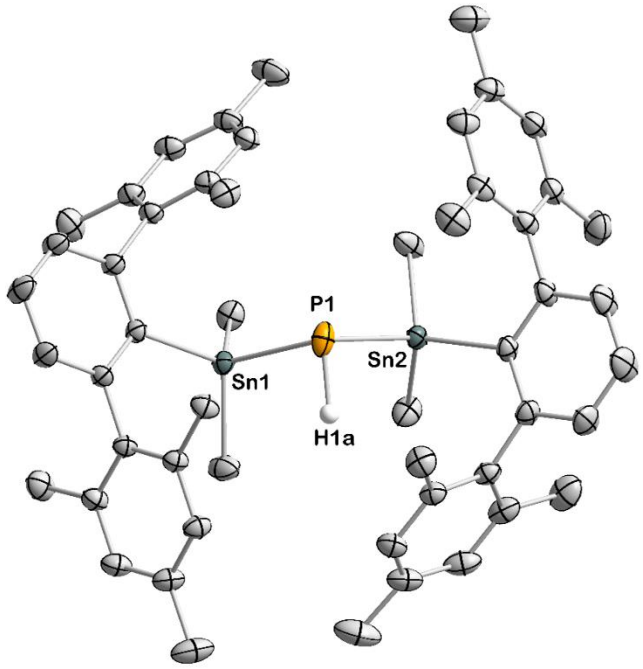

Figure S245. Single-crystal XRD structure of [TerSn(Me)$_2$]$_2$PH. Thermal ellipsoids are shown at 50%. H atoms, except for the one bound directly to P, are omitted and only one position of the disordered P-bound H atom is shown for clarity. C atoms are shown in grey, H in white, P in orange, and Sn in dark grey.

4.4.5 Computational studies on NMR parameters of H/Sn substituted phosphines

The molecules were modeled in Avogadro 4.2.1, geometry optimisation carried out with the ORCA 5.0.4 software package[33] using the composite method B97-3c,[54] which includes dispersion correction. NMR parameters of the optimized structures were calculated using the TPSSH functional[55] and ZORA-DEF2-TZVPP basis set[56] for all nuclei except Sn, where the SARC-ZORA-TZVPP basis[57] set was used. Chemical shifts and J-coupling constants were only calculated for the Sn, P and P-*H* nuclei of interest.

The conversion of ^{31}P absolute chemical shieldings σ_i to chemical shifts δ_i was done using linear regression referencing according to

$$\delta_i = A \cdot \sigma_i + B, \qquad A = -0.7351, \qquad B = 179.62\ ppm$$

with A and B being empirical values to account for systematic errors of the geometry optimisation and NMR calculation method.

Using these methods, NMR parameters were calculated both for compounds **1**-**3** and for a selection of related H/Sn-substituted phosphines whose NMR parameters are known from experiment, with the latter being used to validate the computational methodology. The results of these calculations are summarized in Table S4. After simple linear regression, a good correlation of calculated and experimental ^{31}P chemical shifts δ_{31P} for the set of compounds can be obtained. Deviations from the experimental values are intrinsically present, since no solvent effects were included into the calculations, thus chemical shifts are not scaling 1:1 linearly with the observed shift values. To the best of our knowledge, a calculation scheme like this has not been used

previously to obtain $^{1}J(^{31}P\text{-}^{119}Sn)$ coupling constants. Scaling according to the equation above eliminates this systematic error and allows for a quick evaluation of whether a measured ^{31}P chemical shift will fit to a proposed PSn-Cluster under similar conditions.

The calculated values for $^{1}J(^{31}P\text{-}^{119}Sn)$ accord reasonably well with the experimentally observed scalar couplings. This again corroborates the structural assignments and may be useful to further evaluate Sn-P cluster structures with fast computational methods.

Table S4. Summary of observed and calculated ^{31}P-chemical-shifts and $^{1}J(^{31P}\text{-}^{119}Sn)$ coupling constants.

Compound	^{31}P NMR shifts (ppm)		$^{1}J(^{31}P\text{-}^{119}Sn)$ coupling (Hz)	
	Observed δ_{31P}	Calculated δ_{31P}	Observed *J*	Calculated *J*
Bu_3SnPH_2	−289	−295	522	587
$(Bu_3Sn)_2PH$	−325	−321	730	774
$(Bu_3Sn)_3P$	−347	−343	911	943
$(Ph_3Sn)PH_2$	−288	−282	545	581
$(Ph_3Sn)_2PH$	−315	−331	741	705
$(Ph_3Sn)_3P$	−326	−329	884	885
$i Pr_3SnPH_2$	−309	−290	589	614
$(iPr_3Sn)_2PH$	−348	−326	834	817
$Ter(Me)_2SnPH_2$	−261	−262	470	548
$(Ter(Me)_2Sn)_2PH$	−274	−288	705	730
1 $(Ter(Me)_2Sn)_2P_2H_2$-meso	−220	−218	higher order	/
2 $(Ter(Me)_2Sn)_2P_2H_2$-C2	−226	−231	higher order	/
3-P^1-H	−251	−241	No P–Sn bond	/
3-P^2-$[Sn]^1$	−270	−286	818	901
3-P^3–$[Sn]^2$	−293	−298	970	1049

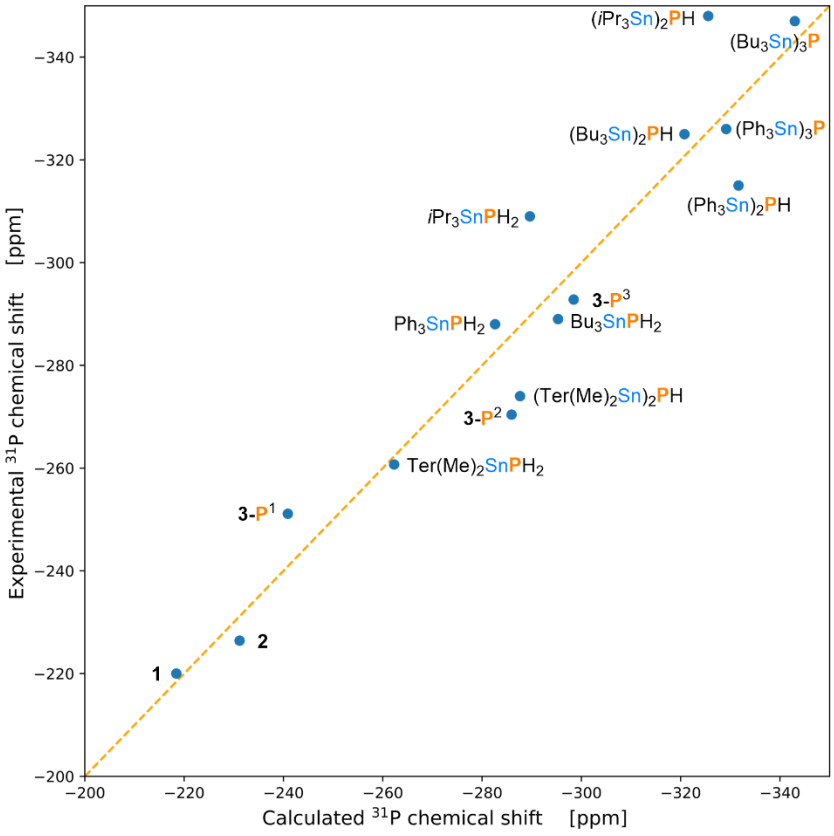

Figure S246. Plotted correlation between calculated and experimentally determined ^{31}P NMR chemical shifts.

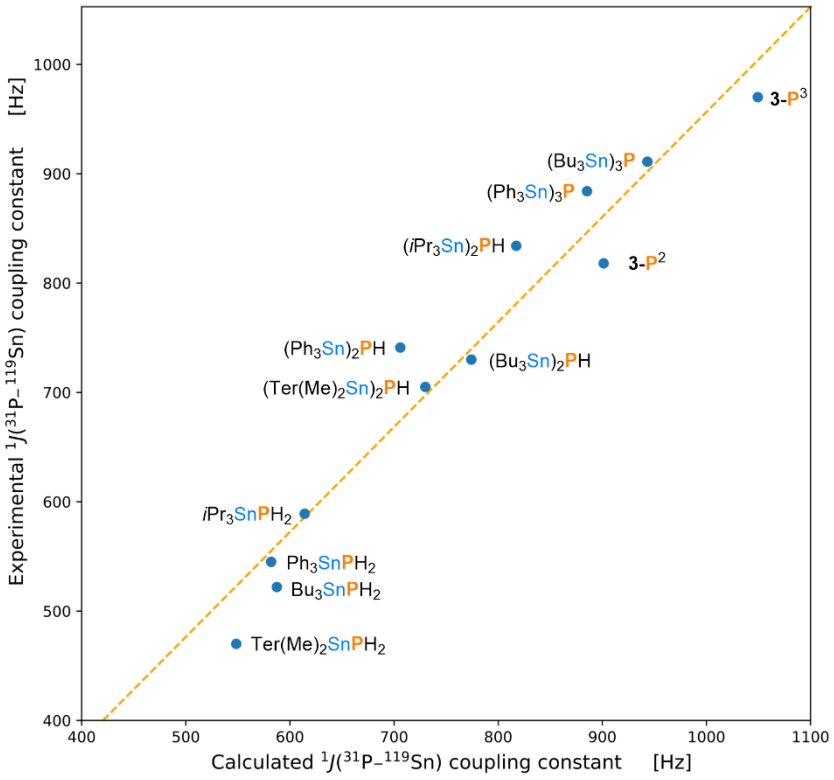

Figure S247. Plotted correlation between calculated and experimentally determined $^{1}J(^{31}P\text{-}^{119}Sn)$ coupling constants.

4.4.6 Discussion of transition metal mediated P_4 functionalisation

The divergent reactivity of different transition metal (TM)-bound P_n moieties means that during TM-mediated breakdown of P_4 each of the P atoms and P–P bonds originating from P_4 can end up manifesting very different reactivity, suggesting that it should be difficult to functionalize them with a common set of simple, mutually-compatible reagents. This presents a potentially significant problem for attempts at inner-sphere TM-mediated breakdown of P_4 into P_1 products since, for example, functionalisation of a P_4 intermediate may lead to formation of a P_3 intermediate with very dissimilar reactivity.

As such, it is interesting to note that Scheer *et al.* have recently reported the direct transformation of P_4 into phosphines RR'R''P *via* formation of the TM complex Cp*FeP_5 (Scheme S2).[6g] This shows that the above problem does not fully preclude the development of effective procedures for TM-mediated P_4 conversion, and it is therefore interesting to consider *how* this system manages to succeed, despite this apparent obstacle.

In this case, success can likely be attributed to RR'R''P formation occurring entirely at a single P atom located on a single P_5 moiety. Once the product has been excised from the P_5 ring the remaining *cyclo*-P_4 moiety is not functionalized further, but rather converted back to the original P_5 ring by reaction with fresh P_4. Thus the diversity of TM·P_n moieties involved is helpfully kept to a minimum. It may also help that functionalisation of the P_5 moiety is achieved sequentially using otherwise likely-incompatible reagents, rather than having all P–P cleavage steps happen 'in one go'.

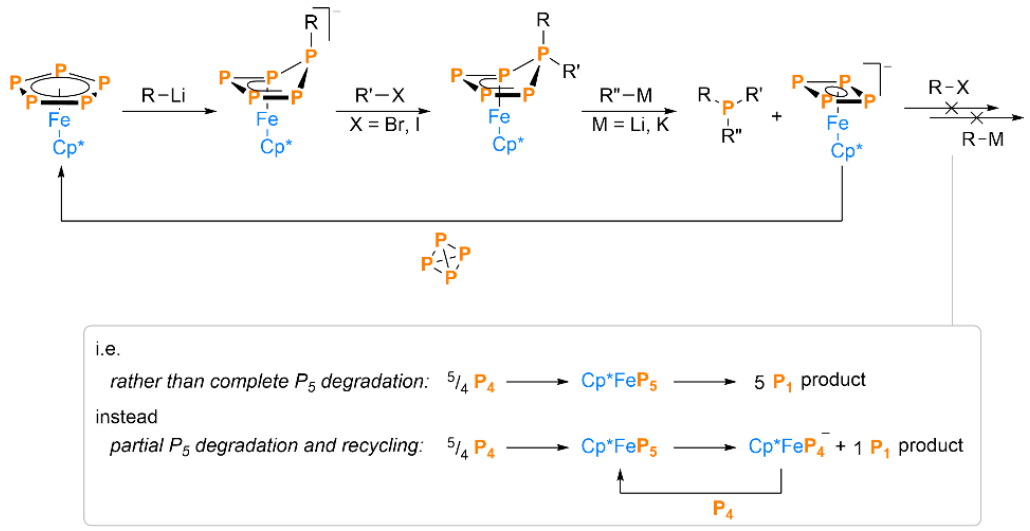

Scheme S2. Functionalisation of Cp*FeP_5 recently reported by Scheer *et al.*[6g]

4.4.7 Cartesian coordinates of optimized structures

Note that while some structures are relevant to more than one step, for brevity their coordinates are only listed once in this section.

4.4.7.1 Initiation

AIBN
E= -530.43110266 Eh
0 1

C	-6.73358357114728	1.90000704495178	1.63297789624721
C	-6.14526887832600	0.57527590626278	2.09305293769457
H	-6.68958467789029	1.95504696351539	0.54496338030616
H	-6.16628399267082	2.72646512121529	2.05883191995213
H	-7.77149208598595	1.99747153479384	1.95061507057777
C	-4.66474396163330	0.44618697147950	1.72605910288852
H	-4.54509179425014	0.49249854939705	0.64367102157362
H	-4.25848095469666	-0.49838844051664	2.08743482903047
H	-4.11479094448360	1.27163513880411	2.18115738575326
C	-6.88659350185766	-0.53680152519881	1.48583225788907
N	-7.46449053697556	-1.38872146364098	0.97571010924807
N	-8.53484905517407	2.34383218310642	6.64488647365408
C	-7.62128292031758	1.80972157790932	6.19772423968283
H	-5.17199539213139	2.87152576517874	5.82405896974038
C	-6.43776980808615	1.11480310669302	5.67729273027721
C	-5.18148584054262	1.83773532871347	6.16921230834698
H	-4.30197306780097	1.32077154950678	5.78174828132487
H	-5.14961192208079	1.82789992838706	7.25863321786287
C	-6.46297008697325	-0.34303903458334	6.10989749060113
H	-7.33471182009729	-0.85618985117478	5.70426691388549
H	-5.56918735182448	-0.85240528554835	5.75248727588525
H	-6.49596836078477	-0.39399628077941	7.19850807690325
N	-6.21255178671691	0.33330874151304	3.56133818490430
N	-6.47011768755229	1.33520647001471	4.20460992577043

N_2
E= -109.45946664 Eh
0 1

N	-5.24852135223168	-1.87993607150872	0.70313804588179
N	-4.93317864776832	-2.91375392849128	0.84002195411821

$^{\bullet}$C(CN)Me$_2$
E= -210.50298904 Eh
0 2

C	-7.16243138854857	1.06559324867526	0.07449569382908
C	-5.75555966606522	0.58286185830772	0.05074217055648
H	-7.35395047960832	1.72925610121400	-0.77642839525333
H	-7.34940794083417	1.65567232996323	0.97922931984843
H	-7.87841114969421	0.24589109230958	0.04322899501803
C	-4.63959117561663	1.56669575730585	0.06249393628400
H	-4.69905473991686	2.22365719275432	-0.81300038479448
H	-3.66493352667547	1.08141727752095	0.06409192279180
H	-4.70847890827036	2.21356613651884	0.94447382619041
C	-5.48597070315845	-0.77519817431721	0.01664384432620
N	-5.25759032161170	-1.91680282025255	-0.01799092879663

Me$_3$SnH
E= -334.45306553 Eh
0 1

Sn	-6.04471667208550	0.33284160579064	0.38585898860526
C	-7.71073127776283	-0.82831122829153	1.07102915111342
H	-7.40809971322585	-1.43674482176383	1.92467936063237
H	-8.06703535137819	-1.48923307853153	0.28038348036314
H	-8.52919079948289	-0.17654228763201	1.37822361613702
C	-4.49479454034692	-0.98497549741784	-0.28862299278680
H	-3.61978984365241	-0.41541993363825	-0.60385958039123
H	-4.84474622633764	-1.58366861053805	-1.13017019072076
H	-4.20148444456054	-1.65639892611004	0.51961102706190
C	-5.30862551989089	1.54303464840539	1.99503785789955
H	-6.07816567053497	2.23852704188395	2.33151435304507
H	-4.43742575389723	2.11525142695790	1.67425342800372
H	-5.02041604962666	0.90799357813743	2.83410633460966
H	-6.54115813721747	1.34597608274776	-0.91038483357233

TS($^{\bullet}$C(CN)Me$_2$→HC(CN)Me$_2$)
E= -544.93208170 Eh
im. freq.= 719.72 *i*
0 2

C	-7.02259941555450	0.58272437556449	0.48690908870365
C	-5.54400331592240	0.63263788793260	0.72833978320201
H	-7.24906758443347	0.73921608054211	-0.57418380913086
H	-7.52238922113426	1.37284744743811	1.05269327911369
H	-7.44572725463089	-0.37822920743029	0.78114599533671
C	-4.84835226604250	1.94960606004738	0.56098213663636
H	-4.85046191274758	2.26109114503518	-0.49004478718730
H	-3.81098373719960	1.89897884989052	0.89357095309334
H	-5.36288673403643	2.72239987294627	1.13741162690191
C	-4.80315101747374	-0.52648503654576	0.42062354703670
N	-4.18789793206751	-1.48859710799128	0.22631810685753
H	-5.53034348400700	0.54516577236568	2.35980991264618
Sn	-5.62877328961959	0.56364390022379	4.18122583747022
H	-8.35009893516860	0.63322040152826	4.32344236372562
H	-4.26618556480406	-1.76614305220791	4.50954604150198
H	-6.03064635931650	3.24288243553296	4.51117090400724
H	-4.28805380837913	2.91323532833016	4.54782734003896
H	-3.17071000098147	-0.41150048269370	4.83260286453668
H	-7.81120312812581	-1.05517083691664	4.39236572309927
C	-7.60949373067832	-0.04480992944714	4.74902351812438
C	-4.17881865037122	-0.79347047410538	4.99348747928699
C	-5.26416446006701	2.56327853140329	4.88506619985277
H	-7.70459294899112	-0.03029029212084	5.83614008653508
H	-4.34711179671462	-0.91253636892314	6.06510544797065
H	-5.28418345153084	2.57800469960111	5.97619036063939

HC(CN)Me$_2$
E= -211.13175702 Eh
0 1

C	-7.14359627165181	1.05970702855674	-0.04532441047755
C	-5.75205906106006	0.55802443843765	-0.42644296128321
H	-7.33852210619739	2.01127227039293	-0.54337220113809
H	-7.21347853315789	1.21413609844946	1.03294727001623
H	-7.91646858250299	0.34880388920177	-0.33927478054455
C	-4.65552081782110	1.55347002596461	-0.05229711729354
H	-4.83385449793600	2.50239486530725	-0.56134532662867
H	-3.67011519883375	1.18526376492804	-0.33943324022100
H	-4.65267077773814	1.73538684168632	1.02402323378706
C	-5.49345770807070	-0.73909943664365	0.19253968522003
N	-5.28562521479336	-1.75674242342320	0.68595310174594
H	-5.72191123023679	0.39212263714207	-1.50930325318265

Me$_3$Sn$^{\bullet}$
E= -333.83773926 Eh
0 2

Sn	-0.04181811914409	-0.11771975225806	2.18561965993890
C	0.01624841845516	-0.03766963620385	0.02408622563928
C	1.95707088074064	-0.56728058815974	2.88224279632402
C	-0.55523065397075	1.85612096675477	2.90912231806715
H	0.34106820462594	-0.99425367785191	-0.38489706900594
H	0.72681657543460	0.73715997838795	-0.27485231550035
H	-0.96671998773747	0.20757913395128	-0.37752448186928
H	-1.54006851800091	2.15245397070418	2.54845420629491
H	0.18832079417249	2.56651605051999	2.53892030643005
H	-0.55323100757316	1.87485945633416	3.99882489447740
H	2.27918565815780	-1.54435600176422	2.52254509139057
H	1.99099649044407	-0.55860348753939	3.97155273552864
H	2.63847126439568	0.19588358712484	2.49769563228466

P_4
E= -1365.03900477 Eh
0 1

P	-8.63724066817835	1.73405756013613	0.95356065420993
P	-7.30344057381550	1.81815961948766	-0.77432824026063
P	-6.96619533814420	0.33677370507047	0.79516442354124
P	-8.68358341986195	0.14155911530574	-0.53970683749054

TS($^{\bullet}$C(CN)Me$_2$→$^{\bullet}$P$_4$C(CN)Me$_2$)
E= -1575.51660155 Eh
im. freq.= 282.91 *i*
0 2

P	-9.18339464947762	3.26921534550439	0.39885091559647
P	-7.89665556026854	1.39907387994771	0.09926708701424
P	-7.47683203644588	2.85712317029539	1.68360163984355
P	-9.25993916443638	1.61111959666613	1.80511390061052
N	-9.79884369142118	4.43464597297972	3.92737967181232
C	-10.03885756473454	4.69168837132315	2.82489250889223
H	-8.57702758581726	6.24263320612897	1.21816469246345
C	-10.30312718651071	4.96800585615511	1.46037255112464
C	-9.61994783829653	6.18844881602649	0.90591818957018
H	-10.12784776108779	7.09499071380136	1.25423062019150
H	-12.11294445417595	3.79042306853096	1.39740028081834
C	-11.72079596462249	4.73262217256001	1.01454114102353
H	-9.66058257520279	6.18052088290283	-0.18547228768262
H	-12.36725630384738	5.54151296678704	1.37340525256139
H	-11.77487766365258	4.71938598038982	-0.07619616384001

$^{\bullet}$P$_4$C(CN)Me$_2$
E= -1575.52083035 Eh
0 2

C	-7.08735576209223	1.16879404201634	0.65087741087312
C	-5.67297603039902	0.64300391834781	0.86258124596311

H	-7.27002189685421	1.31641646435180	-0.41641475512892
H	-7.21150757785303	2.12905852619275	1.15462129406168
H	-7.84001914041938	0.47685784580870	1.03003678327340
C	-4.62659314218273	1.62413666980242	0.32359985246687
H	-4.77147961891649	1.77917079394561	-0.74789107219492
H	-3.61170854679090	1.25610511017752	0.48217471730177
H	-4.73219050809867	2.58459020287984	0.83175476107557
C	-5.52354245165176	-0.64849110212585	0.20955274959073
N	-5.40365712907633	-1.67750727643042	-0.29271855801529
P	-7.06778861321436	-0.17722569833279	3.68664400561671
P	-5.90869842830933	0.44472436510758	5.42709481506997
P	-6.23871874774672	1.86107173782412	3.80136660142719
P	-5.15694240639482	0.28716440043456	2.68413014861900

4.4.7.2 First P–P cleavage

I˙

E= -1698.87329909 Eh

0 2

P	-1.95523966599795	-1.67253689686902	2.74605314937196
P	-4.46913481145529	-1.75104588972784	3.78802426030406
P	-3.64964678899596	-0.29707612212079	2.37015468200861
P	-2.81542757308502	-0.43707801362512	4.36931651554389
Sn	-0.07502888407850	-0.06570514227185	2.04485724530151
C	0.00879311068946	-0.06560143856404	-0.09861950975743
C	1.74654435191822	-0.82572726558248	2.88612211424798
C	-0.48175123769149	1.90665066206422	2.77896956639695
H	0.83447392423197	0.56515094414195	-0.43235579842360
H	-0.92378221563992	0.32562000100411	-0.50521193561982
H	0.16242055058868	-1.07789405977524	-0.47240897596584
H	-1.46724553645603	2.23853193473814	2.45265525883124
H	0.27268975288791	2.59356365941020	2.39124909644244
H	-0.44879161676758	1.91659140180575	3.86818390953441
H	2.58342993775571	-0.19270279932788	2.58655002116582
H	1.92775103073342	-1.84183155510255	2.53547485654537
H	1.67954567136235	-0.83277942019756	3.97409554407247

TS(I˙→II)

E= -2033.30911684 Eh

im. freq.= 771.71 *i*

0 2

H	0.06423181035575	-1.73612866467063	3.30241068825383
Sn	-0.20889869110693	-0.00204390311150	2.34204877368218
P	2.14953408882840	-2.62985782909297	6.79502752708436
P	0.57377560193294	-2.87782050273250	4.42838091071761
P	2.36010497775788	-1.65044831208672	4.81973330963943
P	0.56817678001534	-1.31073628529748	5.97583112593764
Sn	3.39345664481709	-0.82075258000473	8.10313762842307
C	2.67156601350831	1.12652783338235	7.55877446665433
C	5.47989741859054	-0.98037588984864	7.62234351453257
C	3.07403098652855	-1.16847994766599	10.19684985254107
H	2.73970662199042	1.27021447539667	6.48028876189557
H	3.27835294742562	1.88380077580779	8.05849278734947
H	1.63207068845080	1.24445352049963	7.86452605220644
H	3.62390732459128	-0.42954613041045	10.78181568131370
H	3.41987858782449	-2.16513919731435	10.47169273413654
H	2.01253664912419	-1.08633604478284	10.43152999218820
H	5.61866341980464	-0.85782730354501	6.54786373461452
H	5.86631657617706	-1.95540985461302	7.91942018339593
H	6.04039977564852	-0.20266808123123	8.14353225675101
C	0.77437304305083	1.62247735157282	3.36050967235314
H	1.84839295782703	1.44193547604309	3.39601127026933
H	0.39741716102985	1.70688404163896	4.37938120924122
H	0.58276377781308	2.55543478466263	2.82571809278882
C	0.59614159731586	-0.18734197178691	0.35166637906147
H	0.09581557022091	-0.99121866101514	-0.18838513477562
H	1.66415204387254	-0.40067182221209	0.39719213293675
H	0.44509818382991	0.74959369382293	-0.18854866801024
C	-2.32330748212930	0.39805420668573	2.22762646999092
H	-2.74646706000616	0.47819953260103	3.22890791137537
H	-2.83160982266577	-0.40301422413359	1.69076304260614
H	-2.48625819242375	1.33865151344217	1.69739764084497

II

E= -1699.48597461 Eh

0 1

P	2.60825079651189	-0.27852527900993	2.25044672203470
P	4.83618138677669	0.90114854014262	3.61294963869152
P	2.72930937079770	0.66783647939390	4.25216617051788
P	3.17430640760397	1.85064563304859	2.50069754164659
Sn	0.11767835233257	0.08158718528474	1.89492329543462
C	-0.47884956851307	2.02029042606585	2.58867641859464
C	-0.90658708668548	-1.44399803208477	3.00011104950728
C	-0.26247665066296	-0.12429133016896	-0.20608062449968
H	-0.15551634111142	2.16966592351333	3.61877548901145
H	-1.56665037597744	2.09482322070214	2.54211007348659
H	-0.04123314402378	2.79952592334858	1.96503170424256
H	0.24993368701561	0.66368396790055	-0.75828784086817
H	-1.33420845352469	-0.05088767232442	-0.39675450940367
H	0.09295656157647	-1.09217111849208	-0.56034463311294
H	-0.70608613549304	-1.32503104317873	4.06516545889515
H	-0.57060112492773	-2.43215906141740	2.68557342335666
H	-1.98166070287450	-1.36523508574272	2.83138429056076
H	5.11858302117921	2.03432132301868	4.44554633190407

TS(P_4→^{endo}I˙)

E= -1698.85266583 Eh

im. freq.= 426.07 *i*

0 2

P	-1.57480120697798	-1.77046254310728	3.32773860787774
P	-0.43583404017023	-3.38658668505784	1.86555816494630
P	-2.56382806563936	-2.92728581609856	1.76031466196820
P	-1.75996055451919	-3.99998056932073	3.50278421792178
Sn	0.11979233480492	-0.12307434317281	2.15348788415684
C	0.04019206741265	-0.31625045167003	0.01733273193828
C	2.09080134191980	-0.51574669675289	2.89977819731121
C	-0.52138035353784	1.84283819825781	2.76775683764214
H	0.56407874269684	0.52838244205018	-0.43428065483292
H	-0.99473964236641	-0.31546560261065	-0.32393880443456
H	0.51892423153487	-1.24399119474817	-0.29377853101321
H	-1.52082114141880	2.05029290786230	2.38554220771636
H	0.17214337778540	2.58911275753851	2.37514875719156
H	-0.53508473672533	1.90997480662649	3.85575450367283
H	2.79305029133586	0.21046373590877	2.48684170429270
H	2.39933908117814	-1.51957659563192	2.60876560103477
H	2.10108827268671	-0.44046435007314	3.98722391260984

^{endo}I˙

E= -1698.87441458 Eh

0 2

P	-1.95593742446611	-1.41141655072623	3.20357813874249
P	-0.25436499289183	-3.30228643246608	1.87971584717959
P	-2.42830487280259	-3.17331076716201	1.96766050559187
P	-1.27144144701074	-3.41674062009697	3.80445514207427
Sn	0.06288032839554	-0.22791118385495	2.08064891870088
C	0.02787875750900	-0.24151812029489	-0.06235322410595
C	1.97883476734465	-0.68453964044533	2.92560817791604
C	-0.49102228723822	1.75432301507173	2.72293391525905
H	0.46648894959237	0.68256471212208	-0.44234071816186
H	-1.00121217431683	-0.31450315066555	-0.41504199461839
H	0.59190043855142	-1.09506458462984	-0.43708563018021
H	-1.47828896020575	2.01418997547220	2.33918051479031
H	0.23570408133839	2.47558070151534	2.34414196324213
H	-0.51038256827896	1.81060303805192	3.81176690574504
H	2.57841432074204	0.22367291825386	3.00162643000221
H	2.49167923596744	-1.41164308949813	2.29639795290389
H	1.85013384777019	-1.10982022064716	3.92113715491859

TS(I˙→^{exo,endo}II)

E= -2033.30746346 Eh

im. freq.= 489.11 *i*

0 2

P	2.40841218277469	-0.51377098509146	2.46539602352361
P	4.46221203944362	0.25538174212727	4.66604627349224
P	2.27644801996696	0.08399548148143	4.60054100856517
P	3.29421045099721	1.39245769918736	3.19626804919228
Sn	0.14610569874089	0.36002218464731	1.71120353226947
C	-0.16960179577729	2.35735566714214	2.42283749071271
C	-1.32873935747759	-0.96929539205896	2.52443160331601
C	0.12429731327998	0.30442455920749	-0.43411844096584
H	-0.05179146054949	2.38972391487390	3.50598537196713
H	-1.17984642635458	2.67780938805844	2.16340712853869
H	0.54935979804334	0.03890690437426	1.96889109148410
H	0.87098127716742	0.99218815069318	-0.83149279518070
H	-0.85916151719989	0.59789179431750	-0.80430236531698
H	0.34799389275413	-0.70246557906304	-0.78751825080701
H	-1.27019845364115	-0.95787481506598	3.61308191821001
H	-1.15552766021558	-1.98639439567358	2.17225361238654
H	-2.32756913134244	-0.65380242456771	2.21953253916452
H	4.80178503433358	-1.06972537376691	3.62325505487172
H	4.16432491667123	-1.60519853708919	-0.08351084707276
C	5.17807889211717	-1.63286811544824	0.31539974424641
H	5.80360841153457	-2.25316754716414	-0.32917481569583
H	5.57990938034438	-0.61950066585933	0.32896091730172
H	2.78528493368369	-3.77315949576921	2.10881609483546
C	3.77452892084830	-4.09248583080111	2.43554331559321
Sn	5.14991370888322	-2.44555553888970	2.30591203280633
H	4.12024430254008	-4.90618698730733	1.79500255624777
H	3.71137213159531	-4.45403607640496	3.46200483588292
C	7.13482775642812	-3.15843322457825	2.77888623394869
H	7.41726622912131	-3.93465968739836	2.06449830052230
H	7.85522278789415	-2.34246127566453	2.71630125972729
H	7.16228772339453	-3.57783553844834	3.78480152623277

^{exo,endo}II

E= -1699.48458835 Eh

0 1

P	2.62125967782586	-0.36029845841697	2.25968102547963
P	4.88882259832934	0.95826392726916	3.78921359629020
P	2.76198786296987	0.57140952574505	4.25955846717542

P	3.26692482773391	1.74114036844592	2.50203013961839
Sn	0.13208463575774	0.04990729475995	1.88564911201067
C	-0.40815976567377	2.00217014699475	2.58881373585586
C	-0.93158816954655	-1.44570508195562	2.99639585709671
C	-0.27518159753755	-0.14165591839895	-0.21279057855617
H	-0.07838161051440	2.13408994621128	3.61940732580650
H	-1.49291457548149	2.11211273277034	2.54534740166258
H	0.05318957338114	2.77158755907560	1.97011860009444
H	0.23551123931026	0.64609381366751	-0.76681216558340
H	-1.34876440882590	-0.05966553028723	-0.38902079562392
H	0.06844876228225	-1.10997483224051	-0.57726537551261
H	-0.70233054061976	-1.34935762779056	4.05792483721808
H	-0.64485811127045	-2.44305532041003	2.66239231144376
H	-2.00598776394417	-1.32042121743424	2.85374183676092
H	5.12170736582369	-0.24405132800545	3.05879466876293

TS(^{endo}I'→^{endo,exo}II)
E= -2033.30715223 Eh
im. freq.= 796.30 *i*
0 2

P	-1.50744335387707	-2.16046268013774	2.90373188945154
P	0.86703799471121	-3.47992656789805	1.62614712637516
P	-1.29457218743605	-3.86146625453138	1.51185192766667
P	-0.28930354238907	-3.92118666101954	3.43924812409003
Sn	0.09611745906437	-0.34725630737063	2.06072245210472
C	0.26196934112421	-0.31033670660618	-0.07768011655972
C	2.00049149003384	-0.31663658504431	3.04692775285168
C	-1.02147615009396	1.38591758538926	2.68459846318839
H	0.27012830235277	0.71994927225761	-0.43665647084309
H	-0.58446765774211	-0.83501804908328	-0.52106416486448
H	1.18234398984432	-0.81022559571654	-0.37883447336939
H	-1.99079685417147	1.40886736459913	2.18548623571293
H	-0.46946733413583	2.29155714757912	2.42670957937312
H	-1.18225616443522	1.36600134422948	3.76299508666836
H	2.34410405236867	0.71266623149685	3.16130673870521
H	2.72253496138603	-0.88141737375889	2.45786648197745
H	1.91439867513319	-0.77431264244945	4.03257963949208
H	1.24608368952988	-5.07219916013889	1.35571695840342
Sn	0.97173879846469	-7.07774202776328	1.10178220456022
H	0.39637355430883	-7.79367402821949	3.67493640695230
H	-1.16622039699153	-6.77081472809494	-0.55967627811655
H	3.33232368891299	-8.25324892521196	1.82406205828088
H	3.43903758314825	-7.75836639785690	0.12252908995591
H	0.31903885377029	-6.72484916615855	-1.53019651667127
H	-1.10696461029262	-7.35710843533156	2.83976231721594
C	-0.16119989728256	-7.89000653709358	2.74348273363216
C	-0.18872617231781	-7.22998871888471	-0.70834167157889
C	2.79487894122192	-8.21004980278669	0.87680716930203
H	-0.36070966207952	-8.94709891648911	2.55481635583791
H	-0.32468527374429	-8.28145182617562	-0.96967472971561
H	2.54424788161360	-9.22626485172969	0.56443762992072

^{endo,exo}II
E= -1699.48332552 Eh
0 1

P	2.54867929375395	0.54245788634840	1.63084945500577
P	4.40048185616795	-0.01637584043454	3.94248763380066
P	2.52481809416700	1.12914048101186	3.75652361623590
P	4.23331232927102	1.65450197243258	2.51586651036697
Sn	3.20207735574868	-1.92763645566756	1.49438908361721
C	2.63485566986263	-3.08539396996764	3.20693749860416
C	5.26302260254735	-2.18055947607333	0.96123545201095
C	1.96800772529522	-2.51632981686055	-0.16529956188088
H	3.50703182074268	-3.24737572724783	3.83962686075701
H	2.22721486699614	-4.04593586480394	2.88826080725933
H	1.87913169305292	-2.54927439027477	3.78094242180284
H	0.91395690305382	-2.43088974703364	0.10078186756896
H	2.18197867404395	-3.55318850953608	-0.43072565975719
H	2.16339369952680	-1.88284805767744	-1.03091396000499
H	5.87792360737133	-2.16295731539994	1.86039453199856
H	5.57605521884978	-1.37163097812765	0.30079146961035
H	5.39815513940043	-3.13192544198257	0.44436608912237
H	4.98300345014828	0.69972125129469	5.04355588388196

^{endo,endo}II
E= -1699.47423495 Eh
0 1

P	2.64714428780813	0.47793127601730	1.85206147849550
P	4.56770781256127	0.01951271474481	4.44745678029267
P	2.60646385462928	0.95370109340001	4.00609076286542
P	4.34980887011499	1.49829355704657	2.81277810390365
Sn	3.16988229881781	-1.98370782231126	1.51826297874107
C	2.62943013712007	-3.20783157420907	3.19787950718374
C	5.21960693230470	-2.25801850142841	0.94843334991538
C	1.88275127969966	-2.45162564455583	-0.13463644697668
H	3.52218444429190	-3.51958701260286	3.74054607150119
H	2.09632857740802	-4.09239658108527	2.84690109672583
H	1.98415223372553	-2.64620007481772	3.87328858009875
H	0.83933215097190	-2.34870398368394	0.16431395492772
H	2.05947894802496	-3.47904519220023	-0.45676245671812
H	2.07662738997684	-1.77914566646728	-0.97023889622775
H	5.88164802062482	-1.86309645374691	1.71860906827210
H	5.41364268766229	-1.73311200565937	0.01280380271745
H	5.42505475210134	-3.32045857007553	0.80895109031441
H	4.40930532215643	-1.16242955836496	3.67839117396763

4.4.7.3 Second P–P cleavage

IIIa$^{\bullet}$
E= -2033.34115394 Eh
0 2

P	-9.08028111769771	0.34638027548036	-0.66664245883960
P	-8.05620389213606	-1.07969065272234	-3.57892396587231
P	-7.78818857636186	-1.28989785521173	-1.41693107413077
P	-6.44622218108342	-0.01846163022721	-2.61938697431283
Sn	-4.60366756586053	-1.75673956781420	-2.71041422434098
C	-3.65303477605742	-1.60712334997732	-0.79284059949519
C	-3.26625219265219	-1.18864774177483	-4.28527806289004
C	-5.41071203317204	-3.71145975721413	-3.03551678143100
H	-2.88723180477389	-0.18223077819098	-4.10737861782102
H	-3.78935435949390	-1.20667376082153	-5.24161612980036
H	-2.42592954069039	-1.88311810751663	-4.32824157121649
H	-3.20233373391821	-0.62154718729493	-0.67410653541932
H	-2.87563143363659	-2.36690707870140	-0.69919590491024
H	-4.39420390629795	-1.75809692871135	-0.00764619196763
H	-6.18417881480807	-3.91917684109964	-2.29615484895822
H	-4.61662860515773	-4.45408425426509	-2.94407265940540
H	-5.84670051185671	-3.77220622676130	-4.03242566779182
H	-9.94986971639446	-0.52036955823915	0.05959881159957
Sn	-7.61799358504153	0.77569209839460	1.34782773173139
C	-5.82392294133414	1.74068355588324	0.68016794039856
C	-7.13423635155041	-1.07118063446978	2.32866287257763
C	-8.70611833160366	2.06170197627720	2.67831931428437
H	-8.84101541170071	3.04319081982156	2.22346112935393
H	-8.15463942198545	2.17538495701292	3.61292635766376
H	-9.68590513418560	1.63611558847479	2.89629799103272
H	-6.74166954929771	-1.78447455213722	1.60360447686574
H	-8.02740555875155	-1.49423861288451	2.78908914102171
H	-6.38349992341029	-0.89670425113922	3.10111310131308
H	-5.17894613323436	1.01932999126723	0.17901525460767
H	-5.29263035353260	2.15958360581710	1.53629873839823
H	-6.06561254232277	2.54075645874545	-0.01921059224515

TS(IIIa$^{\bullet}$→IVa)
E= -2367.77708488 Eh
im. freq.= 342.20 *i*
0 2

P	-9.69470719208407	-0.56606552779112	-1.38602323977716
P	-7.84131348578280	-1.91283311313409	-4.07095616734076
P	-7.98249030934994	-1.90043442715303	-1.89162064639787
P	-6.71670111276337	-0.42578162281354	-2.91527819954473
Sn	-4.55841892522453	-1.73456402340950	-2.79884873281430
C	-3.32359289704677	-0.80791430736344	-1.30459240736732
C	-3.65685674558960	-1.56175015322985	-4.73733401092703
C	-4.89389978049894	-3.79092853926497	-2.30508074407577
H	-3.46951190521329	-0.51486744849536	-4.97692003781979
H	-4.32601896277525	-1.98310463210115	-5.48795749901731
H	-2.71121266352529	-2.10552816664010	-4.75901696481380
H	-3.18789148656437	0.25011110038510	-1.52985254121163
H	-2.34620342068759	-1.29285785987726	-1.28300183592891
H	-3.78470481776790	-0.90492962582327	-0.32131619985456
H	-5.37847624974015	-3.87103880234461	-1.33246891772346
H	-3.93555956890989	-4.31223823650405	-2.27575290212094
H	-5.53274176207408	-4.25383069711787	-3.05688068830450
H	-10.34744049955757	-1.55466770412284	-0.59582761187736
Sn	-8.55582433576860	0.53074666748528	0.57928929246562
C	-7.76811910907368	2.41048060320262	-0.08060370785230
C	-6.94513579358345	-0.67588861365320	1.32399683316461
C	-10.03203207254962	0.83369521250672	2.10893831753166
H	-10.86491782242675	1.41721603256710	1.71597232559964
H	-9.58795296950132	1.37294301866433	2.94714245992898
H	-10.40878272634168	-0.12531561944658	2.46540246667136
H	-6.22358774567581	-0.85736263650845	0.52740813572867
H	-7.31720719942471	-1.63422770879757	1.68623185776006
H	-6.44856729479090	-0.15100221833955	2.14191492762394
H	-7.16352293940258	2.25828128434817	-0.97479316859270
H	-7.14382121325414	2.84020921695365	0.70442967978532
H	-8.57504346208864	3.10484780692275	-0.31366871260250
Sn	-10.06914243373182	0.86789436916331	-4.62141876613835
C	-12.17669399130883	0.52844688169903	-4.37171969503774
H	-12.40789284029772	0.44898735893299	-3.30986216007901
H	-12.47806669191173	-0.39115580903562	-4.87328609696396
H	-12.73233205147043	1.36442194638032	-4.80117362392103
C	-9.63560275363317	1.21656250584186	-6.70710705257631
H	-10.09716455881446	2.15158626425488	-7.03078280078322
H	-10.02526299313225	0.40071766115341	-7.31664992899226
H	-8.55781841624701	1.28545388305495	-6.85782694686027
C	-9.45622000930333	2.58746352290365	-3.49024986847333
H	-8.36883071856503	2.63767742100038	-3.44440542196151
H	-9.85115622588119	2.51375233920551	-2.47790571582356
H	-9.84063348899390	3.49188507308975	-3.96645287049225

H	-9.06865632767145	-0.73812267674867	-4.30310041219223

IVa

E= -2033.95073883 Eh

0 1

P	-9.15829812152495	-0.04658349318398	-0.34134036485821
P	-8.32866963586198	-2.08853017086258	-3.02007565583009
P	-7.74607701340921	-1.64081344097112	-0.92687147454413
P	-6.84363763493486	-0.52266796845364	-2.59303264321663
Sn	-4.77616211837829	-1.97445444793403	-2.67067724328382
C	-3.60588170762208	-1.39785816413424	-0.96776624613497
C	-3.72472447549894	-1.53594403007675	-4.48857490435933
C	-5.27244905899667	-4.05533614654667	-2.55766634527766
H	-3.51126819219536	-0.46870208800499	-4.55106468310517
H	-4.32698058487812	-1.82720479048264	-5.34939600908141
H	-2.78363053697819	-2.08753948815355	-4.51286528087899
H	-3.36274351651586	-0.33586412312619	-1.01217348960024
H	-2.67775219189294	-1.97088076952068	-0.94230100896409
H	-4.16816984972350	-1.59616420074955	-0.05486955830888
H	-5.85551899614469	-4.25135525848614	-1.65772379531423
H	-4.35207454148588	-4.64050005276180	-2.52115441561754
H	-5.85400083593732	-4.35462962516553	-3.42910101634310
H	-9.79226097801449	-0.80747650875842	0.68498207777639
Sn	-7.52415852607916	1.03751914153623	1.25213424365695
C	-6.11829630730531	2.13233683573842	0.06134421534289
C	-6.48814241322872	-0.43447863516629	2.42175600384970
C	-8.62600629298322	2.35098840888740	2.54487354744064
H	-9.21580209361147	3.05440958094837	1.95730302442448
H	-7.93318890540993	2.90978764423861	3.17601038338227
H	-9.29557947811184	1.77364372051967	3.18286159709009
H	-5.95504440473270	-1.12310860590851	1.76630824214829
H	-7.19566644500504	-1.00292637609844	3.02581007309320
H	-5.77091558787162	0.05640094834529	3.08152524234234
H	-5.45780683387492	1.43810496754161	-0.45801432308086
H	-5.51892957363263	2.78243143528380	0.70070036684386
H	-6.63980469376187	2.73843445007967	-0.67883466305958
H	-9.42144845439805	-1.17691874857328	-3.06295589653214

IIIb˙

E= -2033.33859296 Eh

0 2

P	-10.19235451895602	-1.65495731027914	-0.82528652910282
P	-9.27042702962039	-2.77437943090522	-2.46225223999009
P	-8.08210570525794	-2.28885031496718	-0.70672100848547
P	-7.24461901763920	-0.39886638487215	-1.51644650058000
Sn	-5.01391993264667	-1.39374465626325	-2.11558681600712
C	-3.93479166094911	-2.11297879859567	-0.40295718333588
C	-3.90154128773698	0.14625316602155	-3.11055079752724
C	-5.40619044254359	-3.03529720539443	-3.43789184127006
H	-3.71438010493812	0.97515465646303	-2.42745498385229
H	-4.46619415990949	0.51416022261806	-3.96740097661447
H	-2.94566885383263	-0.24877739060773	-3.45811558894178
H	-3.65292179583545	-1.28952165358245	0.25329590556894
H	-3.02908319104047	-2.62484391259227	-0.73255176453891
H	-4.55406628130063	-2.81706742199767	0.15351252398874
H	-5.94411242759870	-3.82022005148616	-2.90583292663820
H	-4.46642022857217	-3.44148905766624	-3.81543018297190
H	-6.01381978650911	-2.69911343083167	-4.27809404797209
H	-10.70753480270867	-2.80412100533844	-0.15401439918406
Sn	-6.70540139274784	0.63776594177584	0.71780843810537
C	-4.91966320831022	1.81738986516366	0.52159058470600
C	-6.46710245428939	-0.83509955149022	2.25903860259675
C	-8.37676984445785	1.89881827881057	1.17621160588201
H	-8.44612439627610	2.70213279431875	0.44238288938967
H	-8.26619398716646	2.33206321998962	2.17135684043129
H	-9.29519977271575	1.31221958893809	1.14022968786810
H	-5.62484554531778	-1.48916521638024	2.03714896283414
H	-7.37097598141787	-1.43854731402485	2.34221498835720
H	-6.28818196332444	-0.33089683089233	3.21026460921652
H	-4.04822421921692	1.17535201474646	0.39034200160855
H	-4.77902093159033	2.42001075552510	1.42021240548305
H	-5.00236507557372	2.48237643379656	-0.33861225902389

TS(IIIb˙→IVb)

E= -2367.77684859 Eh

im. freq.= 593.78 *i*

0 2

P	-10.62264920138737	0.24867790283560	-2.63779245471501
P	-9.74085883200065	0.35016012725744	-4.64199020174226
P	-8.80702560664887	-0.89577348877002	-3.09984086601178
P	-7.29696456650678	0.52349903311962	-2.34627308987078
Sn	-5.41846090225295	-0.73982630286085	-3.44605799042150
C	-5.37004361849156	-2.80891006526098	-2.86994244986054
C	-3.55719058160692	0.19709176509211	-2.93795636561546
C	-5.78917590117154	-0.61878664318513	-5.55610407789141
H	-3.33999660483502	0.05523896664717	-1.87921116514336
H	-3.60639636715098	1.26536574281007	-3.14937645078513
H	-2.75151620593069	-0.24398419680982	-3.52694784641206
H	-5.07951120745146	-2.91158588513800	-1.82407721345225
H	-4.64833646916752	-3.34364394719866	-3.48973346302087
H	-6.35483148757276	-3.25517892469490	-3.01099361470757
H	-6.73251445496957	-1.11293815572018	-5.79011597928063
H	-4.98465103815204	-1.10961708164488	-6.10602103010588
H	-5.85222284027709	0.42413418257828	-5.86661460307536
H	-11.49331410630165	-0.85903896430523	-2.88886820223079
Sn	-7.23103796996738	-0.44952309152801	-0.02437786412689
C	-5.20693103042690	-0.45250839425626	0.69384957107762
C	-8.02980115249236	-2.44072326401569	0.01765922438036
C	-8.44778085877725	0.83639140569989	1.18703829510159
H	-8.03491019122783	1.84528503921326	1.18888223969221
H	-8.48863899701371	0.46430711863439	2.21183586576273
H	-9.45763868394177	0.87120638163198	0.77752805069501
H	-7.45660495839936	-3.09561487876347	-0.63799234447396
H	-9.06845299384048	-2.43135219320362	-0.31304008192144
H	-7.98410912442477	-2.82649618813467	1.03757893506694
H	-4.61574833587232	-1.19998776909995	0.16368965547693
H	-5.19509058027394	-0.68708345077019	1.75933071083537
H	-4.75243550589708	0.52737280390621	0.54461746343865
H	-10.45045194093991	-1.13226418451257	-5.15296126896700
Sn	-10.65741784550636	-3.05193705773618	-5.25184274859766
H	-13.11625817492066	-3.13052726814041	-6.44016561625995
H	-8.38137396023387	-3.24804410556392	-6.74983368692104
H	-12.17336384565310	-3.56398879670095	-3.03524927846850
H	-10.45097694839773	-3.73815102610526	-2.63299921058023
H	-8.02141190110238	-3.68163640236859	-5.06674973837657
H	-11.86989607154878	-3.03724252233693	-7.69958431409522
C	-12.13940817380690	-3.50127429538573	-6.75075364742217
C	-8.73879874109529	-3.79837133978379	-5.87907200867945
C	-11.21547181725438	-3.95375204337994	-3.37907090450275
H	-12.19891009239112	-4.58269825130168	-6.88984760378001
H	-8.81638215428480	-4.85597934835301	-6.13832897687515
H	-11.29843795843000	-5.03502094239553	-3.50936365313509

IVb

E= -2033.95274518 Eh

0 1

P	-9.79882702093618	-2.81581014190555	0.00662682580978
P	-8.51629213895895	-4.01941427982513	-1.35140848738969
P	-7.60899998488411	-2.60375702913816	0.07057206990412
P	-7.55993803463892	-0.90922119151513	-1.35048099367537
Sn	-5.21455810791248	-1.28935897324994	-2.17659591299599
C	-4.02077564202547	-2.40844615836662	-0.78834626046002
C	-4.33112461097442	0.63385924609235	-2.54582158607952
C	-5.39163950909641	-2.39868370268303	-4.00280740490153
H	-4.17566563458618	1.16842221237009	-1.60828081297030
H	-4.98218471798262	1.22828921205924	-3.18752001953015
H	-3.36708498851081	0.51042392422040	-3.04164269994299
H	-4.00488581950623	-1.92257286216895	0.18643501167384
H	-3.00075375313532	-2.47806930806643	-1.17010262483212
H	-4.42617454204037	-3.41384260890066	-0.67490516251689
H	-5.94936146465073	-3.31696292044370	-3.81686705848582
H	-4.40323057275869	-2.65205434620669	-4.38913344869270
H	-5.92713658549085	-1.80957032986933	-4.74749454613000
H	-9.84392883784690	-3.77197969959879	1.06173598032691
Sn	-7.15035900837946	0.82574933618451	0.42294671763511
C	-5.34891236407704	0.43931618337228	1.52797731326339
C	-8.82408219663010	0.73702023826343	1.76062869888654
C	-7.05699872152967	2.74243834688963	-0.53669502416483
H	-6.22297503431846	2.77674571658391	-1.23763066460765
H	-6.92320776465019	3.52526342757156	0.21145159395291
H	-7.98354719190900	2.92712056440517	-1.08064936837864
H	-8.83597849925660	-0.22266204510830	2.27744509962899
H	-9.75334722257507	0.84638376065219	1.20157658654801
H	-8.75296735903283	1.53866186621776	2.49749029903880
H	-5.37162058238281	-0.57709134701320	1.92181988190648
H	-5.27442232528636	1.13965261673811	2.36159585007433
H	-4.47081964838194	0.55505771091009	0.89225205610610
H	-8.37896011565469	-5.14115741847109	-0.48539200900108

IIIc˙

E= -2033.33604055 Eh

0 2

P	-7.80589631990372	-2.84812355223838	-4.11178314652015
P	-9.27989939664299	-3.45828127336592	-2.62350351471447
P	-7.15643162099923	-1.16641757726711	-2.79928972033101
Sn	-4.76142562783724	-1.91625817621927	-2.52921839589823
C	-3.82793590877287	-0.73392053788750	-1.00097705983920
C	-3.84979656084080	-1.57294957889718	-4.43981093296469
C	-4.71440268330287	-3.99741940662227	-2.02941588435473
H	-3.88339788142473	-0.51254719682016	-4.69111294432452
H	-4.38282050346191	-2.13719614518015	-5.20595368449792
H	-2.80898502953666	-1.89935274098043	-4.42157349007131
H	-3.84509161507772	0.32012528239715	-1.27868682689237
H	-2.79157480464852	-1.04937053855547	-0.87161811909438
H	-4.35502636664573	-0.86042669996905	-0.05509564211519
H	-5.16378186705033	-4.15491203753656	-1.04915348927439
H	-3.68255930719588	-4.35153484823797	-2.01342410656401
H	-5.27545553884774	-4.56363014750076	-2.77310474532756

Sn	-9.35664777038725	-1.50349717951093	-5.59689401751326
C	-10.58080889206575	-2.88311924881382	-6.69039379911981
C	-8.05156282831292	-0.38757335661091	-6.88624236357460
C	-10.53655432781988	-0.21033385100846	-4.36383448402709
H	-11.21841902854761	-0.80662171838425	-3.75828217051733
H	-11.11121564466220	0.47854463310269	-4.98465906320537
H	-9.87877931944070	0.35966509282572	-3.70751598664001
H	-7.45504189362341	-1.06837294034119	-7.49354178059076
H	-7.38536932131076	0.22996111217090	-6.28308883002472
H	-8.63481318843375	0.25886456304646	-7.54356542171900
H	-9.95768201302441	-3.53318477477011	-7.30443245519426
H	-11.26838373926734	-2.33532113559848	-7.33641352467466
H	-11.15826255337365	-3.49455769159434	-5.99689344589644
P	-8.07204430857239	-2.35490187244796	-1.16320334073143
H	-9.05189413915777	-1.43420645718428	-0.69144761378695

TS(IIIc'→IVc)
E= -2367.76935064 Eh
im. freq.= 819.09 *i*
0 2

P	-8.01211792566107	-3.20231204258458	-4.58325611825265
P	-9.48746761367828	-3.91053168672615	-3.09926878149257
P	-7.14769389505215	-1.81431529416607	-3.06436438168849
Sn	-4.99430895862991	-3.05769928165645	-2.63668957809848
C	-4.54295130543541	-2.91896099374980	-0.54522292086967
C	-3.49618829905938	-2.06967861937957	-3.81446449362070
C	-5.16660088374777	-5.09710711001357	-3.27837474809902
H	-3.38424877876806	-1.03555094803315	-3.48812616808372
H	-3.78711638104754	-2.07772335617774	-4.86547603285414
H	-2.53778265630989	-2.58079174980465	-3.71195719768664
H	-4.42216204895168	-1.87448462342667	-0.25717395403923
H	-3.61798867293939	-3.45589049837577	-0.32981611983270
H	-5.35297291747678	-3.35768306221835	0.03665355812205
H	-4.30897548122319	-5.67463477433820	-2.92947110648313
H	-5.20959809100883	-5.13227327789732	-4.36660472329686
H	-6.08151924329689	-5.53740871662331	-2.88314989637393
Sn	-9.60320957412788	-1.52528538236740	-5.59790331319280
C	-11.04245377248740	-2.64235495331257	-6.72925771086278
C	-8.43610268116332	-0.22929290854433	-6.85069943629627
C	-10.56309909749962	-0.39278942395332	-4.05088471923362
H	-11.19220871107799	-1.04840951819366	-3.44931726150993
H	-11.18031827633934	0.38968123967992	-4.49521905461098
H	-9.80845907815489	0.06812079259392	-3.41317206923858
H	-7.96450036614415	-0.80089917612918	-7.64991837710162
H	-7.66320564860364	0.25584217356481	-6.25398476390035
H	-9.07621089050179	0.53702047332000	-7.29050636306696
H	-10.54586147386207	-3.21551563339648	-7.51207278836571
H	-11.76401042987487	-1.96475309965352	-7.18788112804761
H	-11.57294651778577	-3.32750116931624	-6.06738516325620
P	-8.41377951146396	-2.79364230361358	-1.51744986805383
H	-9.36158581822105	-1.74207898498616	-1.37395897877822
H	-8.78484285502628	-5.35273286445199	-2.51980285604573
Sn	-8.27845049767571	-6.81354837364068	-1.31170024211088
H	-10.34298099536817	-6.41502296892142	0.42344348378429
H	-8.44451868629239	-8.82871845498058	-3.14722191986067
H	-7.00255715368788	-5.33985648009525	0.58243582348150
H	-5.77801983258157	-6.17359747038098	-0.39780735039485
H	-6.74798122706114	-8.33761244883675	-2.97683314879300
H	-10.89313660524657	-7.49165958156042	-0.87544204623309
C	-10.06740456913198	-7.26531592846662	-0.20082072857131
C	-7.66929035929712	-8.54944916642866	-2.43368114378077
C	-6.74117593516912	-6.28189666435405	0.10046991828158
H	-9.88632595820866	-8.12988304090327	0.44107484108905
H	-7.49685556221528	-9.38408187676596	-1.75105062577461
H	-6.66358476343857	-7.06365077073156	0.85902965309600

IVc
E= -2033.94770323 Eh
0 1

P	-7.51626981783322	-2.69080043303453	-4.46241987445809
P	-8.70798618913605	-3.53282646215517	-2.78162725622411
P	-6.87584789170816	-0.99681072252808	-3.15265174346555
Sn	-4.63041713253193	-1.93885410488269	-2.50853421733894
C	-3.98282183894218	-0.89018777495348	-0.75243266272931
C	-3.37293899972281	-1.57474132598431	-4.20686997227473
C	-4.74495858634630	-4.04548540639277	-2.11931871413559
H	-3.31310273353691	-0.50525584423459	-4.40917384400826
H	-3.79208342865548	-2.07828047768600	-5.07875446425025
H	-2.36863738180388	-1.95993334465558	-4.02569258266375
H	-3.84068335788542	0.16780675337652	-0.97268581503702
H	-3.04238559516591	-1.30875669371640	-0.39120763756766
H	-4.73799452039115	-0.99276785477451	0.02752819255663
H	-5.33394194973273	-4.23201652690302	-1.22130851552678
H	-3.73985112404572	-4.44496801332546	-1.97489068705595
H	-5.20862903617093	-4.55020768268792	-2.96726631363839
Sn	-9.40847712936318	-1.49161868832642	-5.61536329609765
C	-10.71436200435472	-2.98193227202048	-6.43576045455822
C	-8.49211815150471	-0.32356815403958	-7.16226310097718
C	-10.46750956786227	-0.21059357598666	-4.25796044957810
H	-11.03238153352456	-0.80421439748049	-3.53937433349116
H	-11.15912220565315	0.42098743093391	-4.81794768306352
H	-9.75999765294513	0.42480187620088	-3.72474242758191
H	-7.98359611211805	-0.97558153684103	-7.87244560933213
H	-7.76532059370636	0.36174158961921	-6.72501459008553
H	-9.24903063650373	0.25676119570410	-7.69184290760169
H	-10.17106838675896	-3.60892374104071	-7.14286284532157
H	-11.54697464226394	-2.50233156070037	-6.95258881298835
H	-11.10793571927305	-3.60827639309945	-5.63487791575285
P	-8.03101535514206	-1.87538710162936	-1.46593683835879
H	-9.20452925069081	-1.09466242696778	-1.65782651654070
H	-7.71572147472638	-4.44699632978772	-2.33157611085281

IIId'
E= -2033.33324449 Eh
0 2

P	-9.56406310542356	0.07612454823220	-2.43058850417062
P	-7.88903477229072	-2.40027732711273	-3.98353412338323
P	-8.00998496279682	-1.37691184520528	-2.02071481331223
P	-6.57961431556113	-0.68623283924631	-3.54728217271117
Sn	-4.64788872074239	-2.12480345294262	-2.75706779910276
C	-3.21676239354215	-0.84400111643952	-1.80037845508218
C	-3.80622702595286	-2.99577236233947	-4.52560677198774
C	-5.32780851407737	-3.65609854640761	-1.42350290311723
H	-3.43389939420359	-2.21654935454200	-5.19103945624271
H	-4.57075646459381	-3.57258625536020	-5.04669356310373
H	-2.98125699606353	-3.65825016434960	-4.25918996387175
H	-2.92596525730453	-0.03897448465900	-2.47561675756427
H	-2.32869052877168	-1.41885312016406	-1.53266711309875
H	-3.64329507973756	-0.41047064657782	-0.89566677799505
H	-5.63674479165146	-3.22324938877045	-0.47291237933945
H	-4.51422857324937	-4.36311260481854	-1.25191925032879
H	-6.17224294160913	-4.18555035920959	-1.86489186737286
H	-10.50673051069955	-0.57482412506913	-1.57781493295535
Sn	-9.51865900925200	-1.31218933394175	-5.61808301270105
C	-8.98626996031578	-2.38588015982371	-7.40578754931152
C	-9.21888635919494	0.78191162649890	-5.94428724252144
C	-11.53708098307863	-1.81003515717001	-5.08972226692087
H	-11.57406597958434	-2.81047554779464	-4.65804952274619
H	-12.16764160546463	-1.78613920223156	-5.97992611555757
H	-11.91682737371717	-1.09551611180805	-4.35972180216655
H	-8.24668984848062	1.07664890046360	-5.54876694703605
H	-9.99377883983737	1.34552413641653	-5.42575040517121
H	-9.25449208619921	0.99476236030126	-7.01379430133626
H	-7.96036706052703	-2.15230421332096	-7.69234300520140
H	-9.65386334341267	-2.09655548974296	-8.21930753734781
H	-9.07190320266425	-3.46067836286489	-7.24361268724211

TS(IIId'→IVd)
E= -2367.76982152 Eh
im. freq.= 503.97 *i*
0 2

P	-9.72403829890887	0.56166317890701	-2.55827496550129
P	-7.89333941502282	-2.13654309875620	-3.86323311846819
P	-8.16934752405251	-0.90615749058037	-2.05607766102871
P	-6.73563761614048	-0.28085313258187	-3.61295618791842
Sn	-4.68956005871626	-1.34903854638735	-2.58347665573186
C	-3.50116264382756	0.21047478567681	-1.70425847434918
C	-3.62640733849818	-2.30232882849689	-4.18454122528122
C	-5.24423160878484	-2.78959968721883	-1.09970522812330
H	-3.28138906083382	-1.56086148142328	-4.90533317191963
H	-4.28648852364060	-3.00880616155635	-4.68826476258773
H	-2.76388933826724	-2.84170784820307	-3.79006144201553
H	-3.20824224649011	0.93848046060277	-2.46101134368575
H	-2.60166346659361	-0.21881924520915	-1.25978897203485
H	-4.07047580694303	0.71821681969915	-0.92604659854523
H	-5.65852631525889	-2.29126511611201	-0.22375457193713
H	-4.36126108013469	-3.35987306699323	-0.80640184912266
H	-5.99139295053774	-3.47099122777329	-1.50696041648894
H	-10.38146821847472	0.44830953215201	-1.29986905697407
Sn	-9.60033660403810	-1.36911203094656	-5.57564180148065
C	-9.08508981279648	-2.60802761487037	-7.25774357603472
C	-9.41744942189816	0.69279211926757	-6.12937276037708
C	-11.56949401897472	-1.89224979363345	-4.90660157953954
H	-11.56266193471328	-2.89283854666603	-4.47374558799856
H	-12.26146920965138	-1.87619518556519	-5.75026461027358
H	-11.90014893098219	-1.17913319978854	-4.15225351141717
H	-8.47927682947017	1.09315715718901	-5.74436081742611
H	-10.24379102434704	1.25959035168749	-5.70184411407956
H	-9.42776430200422	0.77813496265031	-7.21702732300457
H	-8.08268922823313	-2.36337398454565	-7.61079904485373
H	-9.79464035551133	-2.44534068988902	-8.07087030873039
H	-9.11108373117725	-3.66017976950932	-6.97273708150825
H	-6.47851931484059	0.41884155590019	0.13564886391752
C	-6.58573344311077	1.42647074405234	0.53698300120275
H	-5.62016359055765	1.77298537406918	0.91021131407715
H	-7.29537467703384	1.39825978327221	1.36446105487767
H	-5.51853883135344	2.40395926194028	-3.00759223317052
C	-5.75469424664319	3.26530625141563	-2.38437610097331
H	-4.85931675992187	3.57397999971526	-1.84127274504523
Sn	-7.30634774551479	2.76257792029954	-0.98624861965652

H	-8.70893656387390	1.84614971615457	-1.87576289810476
H	-6.08490253235892	4.08416004290453	-3.02385585955067
C	-8.03256153994924	4.56400812110898	-0.06072767288516
H	-7.21063319889330	5.05631135609166	0.46296952566332
H	-8.82001174236367	4.33301764141304	0.65676218953632
H	-8.42728889865806	5.24462861053650	-0.81510200144957

IVd

E= -2033.95134584 Eh

0 1

P	-9.61503881812363	0.01573960612941	-2.35681109360889
P	-7.89596914383565	-2.47613787811272	-4.01414158563310
P	-8.06669088169778	-1.53057964866608	-2.03280981869464
P	-6.63170916459926	-0.74669095793157	-3.50303659497291
Sn	-4.66039228599965	-2.14892033262863	-2.76079530922449
C	-3.24157012091860	-0.86710657434358	-1.78467969289830
C	-3.81762858333514	-2.95436445334013	-4.55973261797379
C	-5.28729278226082	-3.72907283869308	-1.45938547971622
H	-3.46751885222272	-2.15015972657788	-5.20730017707382
H	-4.57632409921934	-3.53183926891140	-5.08854793403241
H	-2.97703597657689	-3.60719764067884	-4.31951061447116
H	-2.98669258463365	-0.02863245952578	-2.43326486255487
H	-2.33302258051013	-1.42839649386191	-1.55973499808014
H	-3.65781865173251	-0.48131514570449	-0.85390300408396
H	-5.64465002926239	-3.32423883658155	-0.51331131299365
H	-4.44227903777692	-4.39398480475728	-1.27221156258333
H	-6.09040797772923	-4.29718313189489	-1.92910461030486
H	-10.64305320573334	-0.68072679747824	-1.66193099106209
Sn	-9.51908055371186	-1.36582792641017	-5.62227227232967
C	-9.05950956830980	-2.44825969244713	-7.42380869237309
C	-9.17255484311590	0.72192334431366	-5.94190186675904
C	-11.54388583098023	-1.79402225126386	-5.05006883355065
H	-11.61072499610540	-2.79608840286982	-4.62586733762994
H	-12.18922468397521	-1.73973147854368	-5.92830477100031
H	-11.88517734182266	-1.07001072263268	-4.31064760153796
H	-8.19107488707477	0.99098592487600	-5.55117033424013
H	-9.93023459233268	1.29862403414999	-5.41280447485373
H	-9.21152391733254	0.94184543599216	-7.00982939711706
H	-8.03370190702864	-2.24213707140995	-7.73133503905431
H	-9.73525668893292	-2.14040871008337	-8.22364773771176
H	-9.16936406885794	-3.52075650491884	-7.26100998393641
H	-9.26576134425159	0.78688140480638	-1.21395939794318

IIIe˙

E= -2033.33203870Eh

0 2

H	6.26784110007609	1.36802730565232	4.99939727876020
Sn	5.51551279845439	3.92529732308090	3.37644894007894
P	2.55375767133331	-0.54455913688927	3.56461646344662
P	5.65487417565164	0.35011921989058	4.20659230671653
P	3.61450761925720	1.13082721810327	4.46414525546583
P	4.75207947256385	1.62982583836634	2.63755881972141
Sn	0.53439620983431	0.85583224892714	3.00975418668481
C	-0.65039299415836	1.08523555724908	4.78773618729085
C	-0.59065149705298	-0.19924516926425	1.51941696534571
C	1.11258894647736	2.79195906521542	2.27693686418163
H	-0.98281562884705	0.11009998474376	5.14382930237773
H	-1.52387895269597	1.70213149551318	4.57061999903209
H	-0.06061563069765	1.56575994057819	5.56858159415084
H	0.22984886793524	3.32712158729610	1.92314915186468
H	1.82150282855455	2.68498019833140	1.45586094034103
H	1.57996709231111	3.36493207508998	3.07819136703175
H	-1.54966936134083	0.29554618164656	1.35879860576934
H	-0.77128215845904	-1.22377820270180	1.84546290273051
H	-0.03982317626872	-0.22049314970773	0.57887531211697
C	4.99685853255597	4.28237656130441	5.42507476920446
H	5.36268626995062	3.47872460887047	6.06387652306371
H	3.91440132482379	4.34734819883946	5.52895283650054
H	5.44711001030422	5.22305981689768	5.74690463347165
C	7.64478017778960	3.98973350401137	3.11108585156947
H	7.89805882990587	3.80862389667992	2.06637972948157
H	8.11856343361356	3.22546334896202	3.72744187513651
H	8.02776234455150	4.96856519536896	3.40406450905138
C	4.54648330410929	5.34348908795902	2.09143690557306
H	4.86902465058572	5.19437287732059	1.06062997482918
H	4.79828447336248	6.36009834443328	2.39703799448137
H	3.46494926551885	5.21541497823160	2.14325195452951

TS(IIIe˙→IVe)

E= -2367.76952229 Eh

im. freq.= 602.91 *i*

0 2

H	6.65319079021021	0.82387097583222	5.37231109089544
Sn	5.71963985236453	3.62286769362795	4.36645990584604
P	3.22906324180146	-1.04177269969991	3.25361797523802
P	6.19998517149835	-0.00942451821534	4.30401140769577
P	4.07723006151406	0.51392982990084	4.55928317538085
P	5.26482267153826	1.53267920982491	3.01886253638473
Sn	1.11852603896820	0.26231190427900	2.83943718227616
C	1.61416881175148	2.31647136542468	2.45040209660232
C	-0.19851255472197	0.18904304442698	4.53571825919951
C	0.14390120045444	-0.62030086158288	1.14404396915423
H	2.02238920871967	2.76972524461317	3.35443605512049
H	0.71813132904631	2.86266092260340	2.15081614941738
H	2.35812208665487	2.38161745578155	1.65661617040451
H	-0.79660287323620	-0.10441023076031	0.94468415902887
H	-0.06386310343614	-1.67250992477968	1.33992877688021
H	0.78409434782077	-0.54597470572803	0.26483476295528
H	-1.11507793354201	0.73756900219838	4.31209144736323
H	0.28380193829465	0.64518344068075	5.40011282855944
H	-0.45491504630921	-0.84365323196595	4.77513810140085
C	5.06603061664114	3.39075080237048	6.39668938322525
H	5.41344219098607	2.44350144022369	6.80930134049501
H	3.97765841758734	3.41203982377972	6.44068663339706
H	5.46925034054889	4.20813967564112	6.99700557312940
C	7.83343687203423	3.99435279163013	4.31101652087863
H	8.17581193938244	4.07443633808597	3.27918901492201
H	8.36568998742699	3.17593863666164	4.79654830482092
H	8.06194628117237	4.92431935484569	4.83399723733420
C	4.64804253864747	5.21435339983805	3.40262108208983
H	4.99795588296312	5.32906442153563	2.37640800620715
H	4.80543516628581	6.15204052973489	3.93765556558742
H	3.58134483454987	4.98966113543303	3.38648001435951
H	2.59656213945735	-1.78114855736070	4.72953449275656
Sn	2.51629249935176	-2.22350467081244	6.58237730307902
H	0.26251460146206	-3.75850592795781	6.72232841200632
H	1.64472466788643	-4.79729920455702	6.32044741610318
C	1.30872637939283	-3.96936153328527	6.94462144064918
H	0.69449462643286	-0.46796972206751	7.60295042585018
H	2.25456843300278	0.35766869626257	7.38448885199032
H	4.98386197142818	-3.37813665486314	6.46825119643182
H	5.14654534747689	-1.69595713083410	7.00188425088835
C	1.77363594269067	-0.55993841160007	7.72413111283391
C	4.56251475020184	-2.60935712798581	7.11606583538957
H	1.39614146104781	-4.25856962234803	7.99370953800346
H	2.00175685538936	-0.71182469271722	8.78079926500058
H	4.62181001715884	-2.94499770611599	8.15302573276344

IVe

E= -2033.94962365 Eh

0 1

H	6.51777116293063	0.78971513827211	5.88686040558748
Sn	5.64258536049816	3.44475824576299	4.25961922761656
P	2.90402405501562	-1.11653164365191	4.10143759278500
P	5.99986876776855	-0.20089070442742	5.00232096662905
P	3.93501082987697	0.55928381682354	5.11047788041153
P	5.21661249220065	1.10825407193696	3.40530570850448
Sn	1.11433362366020	0.36919799265656	3.12045722735769
C	1.98320130867312	1.48780398917243	1.51243734816968
C	0.32579389121562	1.70202009639628	4.60747882639165
C	-0.44129681048576	-0.90737524038013	2.37867448626689
H	2.59090865910359	2.29984276519253	1.91108962838554
H	1.19167201645826	1.90772981160468	0.88966996942257
H	2.61542676120040	0.84250749266100	0.90333225818367
H	-1.21446679006548	-0.30523362872183	1.89893537564673
H	-0.89091871371033	-1.47031355701874	3.19693996638446
H	-0.03419588810712	-1.60833290113873	1.64978803392830
H	-0.36799132533600	2.40526526236399	4.14400745358805
H	1.13621928923823	2.25912428831991	5.07796002564488
H	-0.20153955259995	1.13473575581744	5.37481267485514
C	5.90515685994455	3.49306725024773	6.38706435429589
H	6.91269816572516	3.18195719123194	6.66200211820422
H	5.17967759534478	2.83832552934506	6.87038536061694
H	5.74458374526039	4.51523048008345	6.73443321067880
C	7.37718963106151	4.21257741260546	3.25766040478765
H	7.23361970135506	4.17062671931604	2.17774505730022
H	8.25463505646533	3.62128348875702	3.52020641841511
H	7.54826522725914	5.24937348674381	3.55126187486038
C	3.89950493699563	4.56750054438192	3.70289064048514
H	3.78194008073296	4.56816314849598	2.61882958664426
H	3.99228026036518	5.59865513803211	4.04728243560254
H	3.01373892549521	4.12146432663103	4.15632197116625
H	2.11168067645970	-1.46504576751323	5.23514151118314

4.4.7.4 Third P–P cleavage

$(Me_3Sn)_2PH$

E= -1009.59731951 Eh

0 1

P	-9.27028367417931	-0.27825866161086	-0.45852185088210
Sn	-7.99866152623144	0.90334426153167	1.35203122189747
C	-6.27451572951600	1.78776432054004	0.43258349098289
C	-7.39890501317862	-0.56801993971132	2.79518573876655
C	-9.11117221548755	2.43002493017660	2.38087617574503
H	-9.30568540302671	3.27853759024108	1.72431542471772
H	-8.53294910337380	2.77793500511970	3.23891984581536
H	-10.06167160343542	2.03115182951292	2.73635956618313
H	-6.82793570799174	-1.36032876867133	2.31094009983478
H	-8.27818120228378	-1.00643670858989	3.26826941919463
H	-6.78055636332638	-0.10190863651860	3.56419982043193
H	-5.68606381650810	1.02018882865271	-0.07076720076038

H	-5.65321063528421	2.27020095967191	1.18862009005852
H	-6.58122682803032	2.53400171737037	-0.30043642314775
Sn	-10.55418257436917	1.68595038198542	-1.35304247272027
C	-9.21149747914344	3.32281687924329	-1.71967570410864
C	-12.09793273560910	2.30310929421300	0.00457275894728
C	-11.43672184346904	1.07885323388346	-3.21300318578121
H	-10.32527633063919	-0.66875925916808	0.41452437025927
H	-11.65926797597802	2.72481481256466	0.90833208196105
H	-12.71549247832236	1.44706049962165	0.27834155187673
H	-12.73061942030705	3.05576387383009	-0.46908546211247
H	-8.84681570269723	3.73974113050884	-0.78032847464240
H	-9.73206539269401	4.10729445143867	-2.27117412018670
H	-8.35875543999293	2.98652189291908	-2.31030685482269
H	-10.65843526282239	0.74651067830294	-3.90030004254595
H	-11.97845106368644	1.91191546174235	-3.66385535454965
H	-12.13126567841605	0.25504994119959	-3.04515451041212

Va˙

E= -1358.20292528 Eh

0 2

P	-7.90093545122749	-2.17351115561838	-2.31653765459743
P	-6.88065688965715	-0.80471721052803	-0.94179876742880
P	-6.50735631026189	-0.62980932388143	-3.05506082453023
Sn	-4.43136073745763	-2.09533454558035	-3.11177421849515
C	-2.84127355107693	-0.90726513293072	-2.30775130725035
C	-4.07653462569238	-2.56927115427814	-5.17365838056814
C	-4.72000111965624	-3.86809669008214	-1.94641495306201
H	-3.94147240150416	-1.65294099081828	-5.74838923798841
H	-4.92406595081831	-3.12156280785474	-5.57939873974097
H	-3.17766878284355	-3.18137290330935	-5.26347048704212
H	-2.73283203955828	0.01456465218174	-2.87936301950818
H	-1.90405859188674	-1.46417611667101	-2.35207739016532
H	-3.05874459218751	-0.65796639028663	-1.26917277698399
H	-5.03932896664175	-3.60512136872767	-0.93810156089627
H	-3.77503380987963	-4.41117713750265	-1.89125727624862
H	-5.47460624160984	-4.50725347484549	-2.40335317180891
H	-9.07492993804054	-1.38306824926672	-2.48602023368512

TS(Va˙→VIa)

E= -1692.63957486 Eh

im. freq.= 552.56 *i*

0 2

P	-7.30586985130880	-2.71414201566318	-0.42116604725080
P	-5.77037670164689	-1.37612298322640	0.38752196475429
P	-6.71765225327363	-0.90830937230881	-1.53120951099386
Sn	-4.86348089316136	-1.97427259741396	-2.88703591862330
C	-3.09968179530866	-0.83007942531472	-2.46883875505267
C	-5.40026048754864	-1.79836130003171	-4.95879222113214
C	-4.58702949535629	-4.03297778162698	-2.36010663080330
H	-5.46822094086893	-0.74735932849931	-5.24055067569553
H	-6.36361198677266	-2.27588525595525	-5.13908654748644
H	-4.64426664786203	-2.28312959437472	-5.57856006888141
H	-3.28067677647110	0.22586528369833	-2.67089895634814
H	-2.27194008709082	-1.17344371769101	-3.09110033753146
H	-2.83214916639422	-0.94905365504118	-1.41892059470307
H	-4.36276546922628	-4.12017708616952	-1.29715777531255
H	-3.75491850221153	-4.44073234873017	-2.93662847763870
H	-5.48920449799267	-4.60344965661389	-2.57868571459159
H	-8.41415126014469	-2.07859255138593	0.22430615840090
Sn	-8.35156165994351	0.92057420066602	1.30350917654463
H	-6.89628993194782	-0.38292290888024	1.13640009253030
C	-8.64724117826520	1.33443544372766	3.39789318513567
C	-10.21433800324997	0.27968178384530	0.43432586410566
C	-7.64266429621185	2.69819585981243	0.32283911463398
H	-10.63972599921021	-0.53971728413178	1.01384343727957
H	-10.04985691600234	-0.05240806877208	-0.59048456892782
H	-10.91592959247436	1.11688057717410	0.43169510855079
H	-6.78647660666518	3.10804825692868	0.85929969230847
H	-8.43687875993246	3.44689211050685	0.29651703567727
H	-7.34357465769485	2.45793538060937	-0.69719615748827
H	-8.99957513181961	0.44251554972657	3.91628923644624
H	-9.39186779447587	2.12537236712515	3.50964496276901
H	-7.71274265946720	1.66351011801044	3.85284392932430

VIa

E= -1358.81350048 Eh

0 1

P	-7.90415524455461	-2.19189677178274	-2.49331322104441
P	-6.92746270086229	-0.95820515597042	-0.93151703960346
P	-6.50810865399932	-0.58686084180171	-3.06023182666939
Sn	-4.45141983510416	-2.06319339380828	-3.11309769604112
C	-2.83460619495955	-0.89494980586637	-2.32974917992692
C	-4.10123014934526	-2.57767638827932	-5.16479123497512
C	-4.73722863491022	-3.82186162231797	-1.91987314179033
H	-3.92510337704351	-1.67565346898829	-5.75127684349417
H	-4.96704068266917	-3.10069326244036	-5.57121812470835
H	-3.22760535431528	-3.22656981865285	-5.24247656531170
H	-2.69137485031020	0.00379962491828	-2.92988621942461
H	-1.91335970514479	-1.47946259953205	-2.34172561355698
H	-3.05665222761502	-0.60412284827113	-1.30274140466292
H	-5.14491693846533	-3.55703933206570	-0.94396388844507
H	-3.77214039353599	-4.31090826369086	-1.77754506363292
H	-5.41972355568881	-4.51148304454897	-2.41526343542571
H	-9.06850014431271	-1.38477418955026	-2.62849654687140
H	-7.94978135716375	0.02605118264900	-0.83189295441542

Vb˙

E= -2367.80023082 Eh

0 2

P	-5.71209579438605	-3.84144578891704	1.56201609264030
P	-7.67723498153504	-4.55114698451300	-3.17083123851949
P	-6.42391456269313	-4.97264520348187	-0.16700244892630
P	-6.78102635986773	-3.33466560249838	-1.54507588917249
Sn	-4.42649891301782	-3.16198515307520	-2.47371539294716
C	-3.01732288177195	-3.15408771932245	-0.86317792154839
C	-4.26947650475719	-1.27981941705203	-3.50319705756916
C	-4.06182195163694	-4.82362214472022	-3.77596016231345
H	-4.52532562388950	-0.47163049705636	-2.81701856446022
H	-4.93328511503755	-1.23393479834264	-4.36520584632714
H	-3.24167920418605	-1.13973511082936	-3.84273608409784
H	-3.17944429446094	-2.29154350845304	-0.21719055652893
H	-2.00956912619665	-3.10106494629046	-1.27883345161794
H	-3.11262966907273	-4.06244894337978	-0.26914347686065
H	-4.20840077258681	-5.75000719516083	-3.22091191780205
H	-3.03590974306870	-4.78074485562274	-4.14499467294736
H	-4.74753114654072	-4.81022728571185	-4.62253264634329
H	-5.69611853621101	-2.53575086740559	0.99000347248316
Sn	-8.02397915700126	-3.55521873446478	2.55182439466415
C	-8.67967400362937	-5.49853108488758	3.17006121496385
C	-9.36962147232030	-2.72989926759857	1.10172351370682
C	-7.83899955093049	-2.23595721961532	4.23791834059465
H	-7.16129484719730	-2.66585074879534	4.97563144846961
H	-8.81751287529694	-2.08684792243061	4.69758282046739
H	-7.44870115635907	-1.26945516314528	3.91845842371945
H	-9.57154939374129	-3.46866801336762	0.32613826076951
H	-8.92701767883223	-1.84932406393440	0.63681919648867
H	-10.30656460210468	-2.45192797783859	1.58783839660241
H	-8.74447025873924	-6.15370462693434	2.30116120308026
H	-9.66271522916806	-5.42935270380774	3.63817264718840
H	-7.97624766171799	-5.92541685865808	3.88514691829826
H	-10.73674892299074	-2.97217594307648	-5.01865702676782
H	-10.11787420012988	-2.41598684114547	-6.58634966538913
H	-8.15483086498783	-0.00926873012334	-4.75938007447725
H	-8.89532652723246	-0.68969405343474	-3.29323544219594
C	-9.94765511757789	-3.10681687470093	-5.75902575689358
C	-8.05162410395802	-0.76566991024124	-3.97955958745158
H	-9.98991733388480	-4.12814475227884	-6.13808583168272
H	-7.13326916834989	-0.58342407512996	-3.42377763483441
Sn	-8.03490649035606	-2.71885795657928	-4.86771472889202
H	-6.66514465756639	-2.10506151393630	-7.13511408856683
C	-6.51985617723942	-2.88243604763684	-6.38315945555975
H	-5.51948356708013	-2.78008598206241	-5.96410595201143
H	-6.59843689836340	-3.85736448531691	-6.86548662745408
H	-9.00711290232781	-4.39077242702593	-2.68477714397834

TS(Vb˙→VIb)

E= -2702.23280023 Eh

im. freq.= 760.83 *i*

0 2

P	-6.38684135851999	-4.77669078719590	1.72189741770226
P	-8.65780823336199	-5.30904517271833	-2.92385730153652
P	-7.85467692201216	-5.49299817168387	0.26888061063396
P	-7.62727921850583	-4.09375800297926	-1.37165159360409
Sn	-5.24680313018424	-4.35765674717705	-2.21808425944878
C	-4.04575149254596	-5.76780416647068	-1.12768830118092
C	-4.34037845646950	-2.42284823009974	-2.00357900103274
C	-5.26835500106664	-4.86073140507021	-4.30914806076478
H	-4.32041258749037	-2.12920460665447	-0.95410246836908
H	-4.89960687017406	-1.67425787365576	-2.56571341142759
H	-3.31720225911354	-2.45509802262567	-2.38242000402909
H	-3.23718368143724	-5.23258017266748	-0.62798023142431
H	-3.61854377919577	-6.49062502977802	-1.82340319108654
H	-4.63357523223798	-6.29575961416057	-0.37815072865334
H	-4.48981901418821	-5.59712639845441	-4.51044293272487
H	-5.07329541136178	-3.96452873177092	-4.89809012166139
H	-6.22920928854723	-5.28368918399065	-4.60131357646057
H	-5.40755080885521	-4.22368759865104	0.84713834486522
Sn	-7.46647999262726	-2.52994566369012	2.18032574534139
C	-9.56836576548836	-2.59073310127295	1.77437586560621
C	-6.50819801746243	-1.02733081132008	0.98639107522299
C	-7.13343479720841	-2.11325618260970	4.26184439545381
H	-7.61890542430519	-2.87162700852770	4.87656693763399
H	-7.54145960215841	-1.13404202144909	4.51803965641103
H	-6.06466147580738	-2.11787436219800	4.47808790956128
H	-6.68783542692519	-1.23561631115213	-0.06823518146088
H	-5.43408695539394	-1.02203137339795	1.17432319084966
H	-6.91307756221704	-0.04418213204806	1.23278534992142
H	-9.72743738441495	-2.65883037549892	0.69848810615737
H	-10.03476572948396	-1.67984893664471	2.15378340327467
H	-10.02531718419939	-3.45524696806710	2.25505452816070

H	-11.05491239357583	-4.52656375091572	-5.95831841555907
H	-10.52223521867201	-2.99513455012306	-6.67896192422115
H	-10.94972804217286	-1.19838336652610	-3.47801439642008
H	-11.72291294339739	-2.72985098055381	-3.01585192846147
C	-10.19671873395176	-3.87402165500840	-6.12020629549134
C	-10.77699450578070	-2.18932900187754	-3.05553828953978
H	-9.45111932420986	-4.41073420775614	-6.70728869058644
H	-10.38437809051693	-2.08180632164073	-2.04385545939242
Sn	-9.35389039209507	-3.26759087935731	-4.24092242468033
H	-7.97030680330453	-1.08931249376408	-5.04877624127670
C	-7.64220563573522	-2.02113570380083	-4.58517274414520
H	-7.15686581063822	-1.78569269668308	-3.63756354023601
H	-6.92888562134879	-2.51230641672861	-5.24570877176812
H	-9.90317854618216	-5.30870219715430	-2.23184557766401
H	-4.81879662514021	-7.98775068553314	-3.36684590780727
H	-5.80656369224494	-9.39652497044101	-3.79989167829231
C	-5.83244101215060	-8.38650357092304	-3.38521789267559
H	-6.45828442530339	-7.75692393618684	-4.01650371300106
H	-4.33986428879814	-9.20771209805662	-0.15400982137173
H	-5.28067368993320	-10.66539494673348	-0.53394890148079
C	-5.33892393134983	-9.64443332047043	-0.15135133420537
Sn	-6.65969158202707	-8.47973837168835	-1.39848361462194
H	-7.05146927337194	-6.81802620846770	-0.46948933265204
H	-5.71017748717568	-9.67058696959352	0.87314658991273
C	-8.58546453932532	-9.43233593777527	-1.50064674671998
H	-8.48561616849087	-10.43111024230311	-1.92989504158698
H	-9.25115349994769	-8.83964672967520	-2.12857917014329
H	-9.01954966019193	-9.51591262627710	-0.50409090784097

VIb

E= -2368.41024256 Eh

0 1

P	-6.07356684676659	-4.41723656073568	2.00027115026505
P	-8.07487689921712	-5.50930823237393	-2.74190311669527
P	-7.29872991270211	-5.48346844992108	0.52030887785442
P	-7.24098167629910	-4.12528631233740	-1.20550514302036
Sn	-4.84207311871073	-4.26717469997291	-1.98188530027342
C	-3.88420404797401	-6.02655027839918	-1.22058839438914
C	-3.77691919429200	-2.51453596953394	-1.34524656872189
C	-4.86012240996373	-4.33604587913448	-4.12765812433656
H	-3.60400394035789	-2.54442893095014	-0.26925669866999
H	-4.34858708952307	-1.61780147518588	-1.58481938914087
H	-2.81374452474086	-2.46868428283059	-1.85608956874701
H	-2.86685309575962	-6.07049304674158	-1.61317345738501
H	-4.42503945603228	-6.91809851471150	-1.53827162570449
H	-3.84197309201971	-6.00283344716806	-0.13162808710328
H	-3.85163720058310	-4.54386210820462	-4.48893674093097
H	-5.19059374536003	-3.38003796296851	-4.53225458033825
H	-5.52880499370804	-5.12487894971754	-4.47290198886199
H	-5.06756775527711	-3.88293130103895	1.14477153843393
Sn	-7.42538493879148	-2.27833864575711	2.06290040435959
C	-9.47830511957606	-2.68574215592831	1.60473379726243
C	-6.59952038134543	-0.81017973422337	0.73528603119598
C	-7.26762923790434	-1.57373078511745	4.08513772765091
H	-7.72628084236628	-2.29227893000470	4.76530705642236
H	-7.77726694865424	-0.61428908099864	4.18781982928220
H	-6.22050521803068	-1.44872058013748	4.36218208073643
H	-6.76728067833919	-1.12539541935688	-0.29411294319750
H	-5.52871117496534	-0.70239861644251	0.90906891865346
H	-7.08431769259681	0.15288036393560	0.90383300999204
H	-9.58791075547061	-2.84709899673507	0.53324095634225
H	-10.09249059765536	-1.83598038090802	1.90783778800303
H	-9.81755986536072	-3.57629978334902	2.13354336339469
H	-10.69851616785393	-5.18154360038252	-5.68913973872550
H	-10.46395509903566	-3.57406991249594	-6.40416732783002
H	-11.37494579086296	-2.11442424305829	-3.22886476594799
H	-11.56128378686751	-3.73959110744757	-2.53636300654332
C	-9.97817946473895	-4.37932539187539	-5.85081339027352
C	-10.85228662965757	-2.93600861488524	-2.73631666582929
H	-9.14792445884578	-4.76496502264980	-6.44319102760191
H	-10.44429746477638	-2.58052192697828	-1.78970903954602
Sn	-9.24825289019481	-3.64022511419744	-3.97157064064180
H	-8.44037506795487	-1.13386711372408	-4.59708606426663
C	-7.87828002405749	-2.02265405958610	-4.30595004908643
H	-7.32898340151957	-1.80215525977837	-3.38981573198688
H	-7.17344064026215	-2.26972736752797	-5.09937177244018
H	-9.25612380856439	-5.78524811404701	-1.99465138443253
H	-6.31880285446391	-6.44871400423690	0.16330980281928

Vc˙

E= -2367.79889709 Eh

0 2

P	-8.18357052848750	1.37456437505542	-0.67140097848750
P	-6.39431128132932	0.48893297330802	-3.57444839209109
P	-7.31624946905327	-0.33865591111978	-1.76715507505735
P	-5.75978670985105	-0.99227163075292	-0.48235799974702
Sn	-4.40357060531706	-2.28739462965945	-2.16287126633852
C	-3.31159796536687	-3.69957823607334	-0.96514765235852
C	-2.97726343840135	-1.02326804910501	-3.15738899983891
C	-5.64178936758486	-3.32879075353360	-3.56986912033409
H	-2.45268459814321	-0.40351909280853	-2.42968952223513
H	-3.48667312375825	-0.38512476253672	-3.87843749727463
H	-2.24822213050296	-1.64552598507425	-3.67959951793544
H	-2.68032788229769	-3.17344178224329	-0.24844644714872
H	-2.67924391246024	-4.31865293882235	-1.60387798250529
H	-4.00128331982889	-4.34368370473470	-0.41937517650367
H	-6.38588023100535	-3.92193214131724	-3.03863990261520
H	-5.02402030857416	-3.99068595292199	-4.17916975287816
H	-6.14652777766359	-2.61083610752975	-4.21493359247182
Sn	-5.40679100855550	2.70416342066770	-2.86287320769521
C	-3.99497028585515	3.18078191120749	-4.41130496175031
C	-4.36015226098546	2.43359802181506	-1.02027221586887
C	-6.87140686345925	4.26802516711667	-2.74413084622821
H	-7.43898377172798	4.32159613100213	-3.67362443656814
H	-6.36827434049763	5.22336388753483	-2.58456810391181
H	-7.54807918977876	4.07353038406870	-1.91308066226891
H	-3.60686410768973	1.65400603828871	-1.13191033088445
H	-5.05627005681253	2.14584098091420	-0.23321319880730
H	-3.86945563476496	3.36914364177325	-0.74609153856592
H	-3.28684004884345	2.36040989864656	-4.53289079232692
H	-3.44531379811010	4.08468637751700	-4.14299018940336
H	-4.50661424466377	3.34949747173709	-5.35941976730987
H	-7.59541617639168	0.99753995219123	-4.13761633929466
Sn	-10.43643132575774	1.37622736670729	-1.81358268020068
C	-10.23575786166224	2.23405223935386	-3.77022592298135
C	-11.71076914593579	2.61135205848901	-0.60372614999553
C	-11.21197218647135	-0.61639295935594	-1.95509996944110
H	-8.66078178865854	0.56827314935695	0.40090955731065
H	-11.31288143656990	3.62510153851210	-0.55449863629718
H	-11.77584645540913	2.20785891596277	0.40702414150741
H	-12.71224692171557	2.64425492551300	-1.03538084348363
H	-9.56838349939506	3.09499012413924	-3.74026527983208
H	-11.21491421164963	2.55829108948356	-4.12639524724711
H	-9.83609641243266	1.49745969277251	-4.46745679744793
H	-10.47981576866566	-1.25812674879168	-2.44546681255083
H	-12.13775411461650	-0.61868332850335	-2.53234999878379
H	-11.41192445329808	-1.00957701825055	-0.95811989385162

VIc

E= -2368.41206492 Eh

0 1

P	-8.17426158306336	1.25346678369404	-0.71793363237860
P	-6.38044753015863	0.45561507202691	-3.54248999497178
P	-7.43861101593770	-0.49428305012562	-1.87022578532112
P	-5.64592242205722	-0.91412914409895	-0.64408337433819
Sn	-4.33869391787121	-2.31391888531893	-2.29507187380191
C	-3.25227460999053	-3.69570468894254	-1.05668973062598
C	-2.93236243102963	-1.04340948340318	-3.29801329470293
C	-5.59372419244663	-3.37276262897455	-3.67098421151396
H	-2.45573945457847	-0.37665757419747	-2.57830684855119
H	-3.44603551773813	-0.45017014610101	-4.05360608526787
H	-2.16247281463203	-1.64992917928048	-3.77770670698676
H	-2.62426892894379	-3.15106456108665	-0.35109164260113
H	-2.61580538908515	-4.32734433162106	-1.67871707874370
H	-3.94093146335465	-4.33079218558734	-0.49908901747216
H	-6.32386476746464	-3.97024243086718	-3.12540217145402
H	-4.98277725181452	-4.03113782356545	-4.29078783849090
H	-6.11648605937653	-2.66015274986033	-4.30759037652161
Sn	-5.42044571367190	2.67066946704953	-2.77838946216421
C	-3.88983813535331	3.04793520778566	-4.24192390862999
C	-4.51182569415007	2.59159208692863	-0.84321547713348
C	-6.89953621584514	4.22287183902547	-2.89380685296731
H	-7.39204564463208	4.19837321181569	-3.86628864733953
H	-6.42345120111442	5.19632835892642	-2.76381681630397
H	-7.63991105539222	4.07807580564402	-2.10738076774757
H	-3.74780931129224	1.81540250123399	-0.81435328336395
H	-5.26459561592535	2.37588495141845	-0.08736023017745
H	-4.04962879337090	3.55929677840532	-0.63840650269547
H	-3.12284678903559	2.27491909147875	-4.18024401509060
H	-3.42794190721514	4.01955652207136	-4.05814128840337
H	-4.31185500365604	3.04320220211845	-5.24745181703125
H	-7.53865095011728	1.01312560510967	-4.14579627782881
Sn	-10.46182185898436	1.36738587337622	-1.77590274662108
C	-10.29527875320927	2.19070454301301	-3.75016195730848
C	-11.63586223471584	2.67167038472998	-0.53643778443361
C	-11.34603867521173	-0.58451738121186	-1.85786091986034
H	-8.67561037755862	0.47464953627724	0.36624624880663
H	-11.19512075470371	3.66866715287784	-0.51729248532851
H	-11.67584439550866	2.28454262828806	0.48207283338782
H	-12.65210389895885	2.74099917094872	-0.92732110586659
H	-9.67756613244197	3.08830985817924	-3.73457810640963
H	-11.28801510423695	2.45056239055669	-4.12117358977518
H	-9.84800864447906	1.46266130882612	-4.42721378239189
H	-10.67624017249600	-1.26708212099934	-2.38088003225227
H	-12.30155099588729	-0.54275509986430	-2.38284067738612
H	-11.51128083830794	-0.95854625892346	-0.84707389083713
H	-6.21342578298487	-2.06585860777580	-0.02921699310273

Vd˙

E= -2367.79768708 Eh

0 2

P	-6.96971301380930	1.22443511868551	-0.44062759699621
P	-9.95175498894854	-0.42581008697312	-1.37136687992433
P	-7.86577526605962	-0.71315331683594	-1.04395455915814
P	-7.19256487570145	-1.30584586660507	-3.03590007691408
Sn	-4.85171426228893	-1.96346761639822	-2.42653494053899
C	-3.86515757321584	-0.60390350524998	-1.08972641062029
C	-3.75260534001931	-2.07808203380575	-4.26979621104919
C	-4.98211834484980	-3.89063433657825	-1.49546228343936
H	-3.60324638012109	-1.08214382468166	-4.68811393925075
H	-4.29486456881368	-2.68728499484613	-4.99349312372299
H	-2.77615644606671	-2.53071886252595	-4.09033998028064
H	-3.90147109202189	0.41324665768967	-1.47542249390496
H	-2.82361951283383	-0.91366410587718	-0.98318226765253
H	-4.34074936088896	-0.62879114834795	-0.11026344901225
H	-5.69886547298072	-3.85018212655136	-0.67456554946006
H	-4.00841249687106	-4.18735794455488	-1.10270762443799
H	-5.31809721047941	-4.63305212454126	-2.21942134098607
H	-8.15785104018355	2.00327416872602	-0.44319037725339
Sn	-6.99330741075820	0.71112030192306	2.03101356375336
C	-6.09219411708063	2.36111823899656	3.06725184703986
C	-5.82235498238158	-1.06269072764098	2.30935715241630
C	-8.99667023627605	0.38333116794212	2.72275441543829
H	-9.61537203711786	1.25801162847024	2.52163150880460
H	-8.98522525991508	0.19696622272034	3.79796438037859
H	-9.42669050666823	-0.48139260354770	2.21723402363053
H	-4.75931567134616	-0.84173090489654	2.21265224661061
H	-6.10590560119000	-1.81000289059222	1.56775221093494
H	-6.00885468142028	-1.46693229327832	3.30543867619479
H	-5.07888912664628	2.51916588949823	2.69734922059260
H	-6.04928881421825	2.14424578187748	4.13571591350303
H	-6.67088786156637	3.27241918549653	2.91583282168902
H	-10.12187188109106	0.21278466825886	-0.10831915569341
Sn	-6.81113275868750	0.83366126106416	-4.29865648787652
C	-6.62155792672589	0.21667734340214	-6.34863429038820
C	-5.02512975891906	1.89967310915798	-3.76136642475170
C	-8.54499402521952	2.06509642123549	-4.04145280621700
H	-5.09311244260116	2.24302086525693	-2.72991500709778
H	-4.91593477064130	2.75991203786412	-4.42455894398068
H	-4.14882666692526	1.26034283217346	-3.87200165761094
H	-9.44380902634789	1.48443262629070	-4.24694923140284
H	-8.49678994818715	2.91137831752401	-4.72884657327980
H	-8.59325871928718	2.43750006827928	-3.01855208567358
H	-5.77289633851270	-0.45995252549200	-6.45644587597588
H	-6.46134627831393	1.08681096242585	-6.98743341585504
H	-7.52603590580083	-0.30000103513827	-6.66993692058070

VId

E= -2368.41379442 Eh

0 1

P	-6.98602456448655	1.15710119473200	-0.43250265646090
P	-9.85049103448352	-0.38166715572935	-1.25259788428189
P	-7.72259614086507	-0.87657274175636	-0.91083359605148
P	-7.23418544828059	-1.28486729051146	-3.01483366786596
Sn	-4.92121397326666	-2.13320643662565	-2.56313814202538
C	-3.84543774877168	-0.91260457156783	-1.16182537880442
C	-3.88435267123831	-2.19874012994784	-4.44469586750940
C	-5.15933465788367	-4.10627282212928	-1.75789320173184
H	-3.70719578230704	-1.19034424562574	-4.81986794381279
H	-4.47614729621482	-2.74910439992011	-5.17670613923261
H	-2.92274786560364	-2.69913848983941	-4.32083126083964
H	-3.83542262771200	0.12621691064291	-1.48726203780474
H	-2.81922703011692	-1.27520601941988	-1.07912967726163
H	-4.31900477155113	-0.97118234301117	-0.18211158458698
H	-5.81823422515041	-4.06321971588856	-0.89006716502740
H	-4.19402763236934	-4.51304731462339	-1.45304738421552
H	-5.60445866552157	-4.76158675527574	-2.50682422306249
H	-8.22204623178279	1.85571651632093	-0.54065007902162
Sn	-7.04226547601645	0.84117338570016	2.06513421205249
C	-6.63673809121462	2.73632362904703	2.98675607051036
C	-5.48241462086308	-0.55994410808241	2.50815874941542
C	-8.92245994162769	0.06763487443766	2.75230704391284
H	-9.73552429617533	0.73920699272786	2.47607538280093
H	-8.89903709498327	-0.03099959550830	3.83894219340799
H	-9.10173084140339	-0.91326875843130	2.31172470036480
H	-4.51407047484012	-0.15723148668825	2.21055160101845
H	-5.66369480716929	-1.49049496023192	1.97017296246401
H	-5.46515762606759	-0.76903309504330	3.57884179554447
H	-5.70754769343541	3.15115725936228	2.59562759772948
H	-6.54063539975979	2.60807319431696	4.06605887397419
H	-7.44799715032291	3.43664021676590	2.78645368684911
H	-10.19266759128462	-0.30715058197273	0.12561245163930
Sn	-6.73588662327505	0.89919518770050	-4.15738806318253
C	-6.63328110431428	0.35486477439386	-6.23421624405282
C	-4.85641857022200	1.79907898166403	-3.63173747716473
C	-8.34582092988868	2.27799289746050	-3.83217714875025
H	-4.88386010713779	2.13232957328353	-2.59513057636926
H	-4.68580037703691	2.65691254824647	-4.28524241898593
H	-4.03718049835834	1.09196665989576	-3.76318751367016
H	-9.25260230921879	1.73949514347502	-3.55933973627481
H	-8.52473146176082	2.84677143854661	-4.74602261415668
H	-8.08527484236452	2.96496416458067	-3.02693625624601
H	-5.86277653047197	-0.40212947643765	-6.38503762243987
H	-6.38730869693035	1.23153008273439	-6.83615892184889
H	-7.59087809901040	-0.04777687667900	-6.56504550662746
H	-10.28004037724019	-1.73211175508846	-1.36808933231761

Ve˙

E= -2367.79762744 Eh

0 2

P	-12.07709314655056	1.89988931978236	-2.28948934611034
P	-9.32929007631832	0.63647606011013	-3.61959091986448
P	-9.94676004173605	2.32405483712002	-2.40342035990851
P	-7.34480344977807	1.29354587943684	-4.34441522056762
Sn	-6.22608412941248	1.37832186369907	-2.08611464129064
C	-6.21835155154536	3.43277941285919	-1.48131036196856
C	-4.20175613490517	0.69700827939187	-2.33305029694159
C	-7.22102397776285	0.19841995838840	-0.59443963089928
H	-3.73752257030645	1.19523803894738	-3.18457045423776
H	-4.17390720341776	-0.38095117919527	-2.49418205162102
H	-3.62880136016916	0.93164992418205	-1.43450022185226
H	-5.71648800392487	4.04163505438238	-2.23361280996777
H	-5.69921228807516	3.54233715219703	-0.52769636151390
H	-7.24636636242607	3.77891953653164	-1.37358744311893
H	-8.20168283253024	0.62459507318625	-0.38432747041477
H	-6.62454799842531	0.21057275319888	0.31965621673369
H	-7.34400420236846	-0.83067650243932	-0.92859515063298
H	-12.13860702716998	0.75755432993539	-3.13892324221297
Sn	-11.94287657731921	0.54956339837505	-0.14835933012130
C	-13.95977309444809	0.06476344605412	0.40569033685972
C	-11.05901812387928	1.83232660081844	1.31986662156708
C	-10.78920974663139	-1.23128049640661	-0.45485214346490
H	-11.45477893546582	-2.06328201008418	-0.68659290887080
H	-10.21981168532299	-1.46601904800794	0.44536333912278
H	-10.10062583815732	-1.08251655263027	-1.28682733023951
H	-11.62040120597247	2.76465349505583	1.38498513610310
H	-10.02892835103000	2.05822723571608	1.04490114577963
H	-11.07162432485785	1.34173372129232	2.29423198487800
H	-14.54063018206154	0.97866783748066	0.53026975433372
H	-13.96221802500754	-0.48984775500911	1.34553941752726
H	-14.42547452827402	-0.54823023003938	-0.36640234352448
Sn	-6.66820033709219	-1.04443861270625	-4.99360678421858
C	-4.70167835708630	-0.97037853006215	-5.84989178510007
C	-8.10393097847985	-1.66776839257493	-6.46220309913584
C	-6.72647301646356	-2.43617823947807	-3.35808503162207
H	-9.10067609533716	-1.67995087825756	-6.01964762821782
H	-7.86406489995861	-2.67111911081265	-6.81779120313496
H	-8.10009233919921	-0.97947547671505	-7.30756668485123
H	-6.55606369715999	-3.44595099425813	-3.73516625200144
H	-7.70740650366595	-2.39681296843484	-2.88354135637093
H	-5.96099945100820	-2.20558306356296	-2.61704253890930
H	-4.67634513954416	-0.23701350555533	-6.65611369413410
H	-4.43709820607340	-1.94932698440246	-6.25262012607999
H	-3.96961786579692	-0.68952632909890	-5.09295672865998
H	-10.08009013788342	0.94045365158992	-4.79006100112395

VIe

E= -2368.41025831 Eh

0 1

P	-12.18911210637975	1.97388797730941	-2.25578856946168
P	-9.36971532717710	0.46647427546521	-3.50077943820782
P	-10.05108990189036	2.35325200656623	-2.59519893868450
P	-7.43503102422810	1.22208850607423	-4.27691027642859
Sn	-6.28766135832286	1.34705256792498	-2.03698074571137
C	-6.38788229033347	3.38488144766827	-1.38344580696705
C	-4.22873605982855	0.78689417487431	-2.30512556118956
C	-7.21773138503168	0.08313412167827	-0.57271734103689
H	-3.80013630324758	1.32734534602719	-3.14966607721134
H	-4.13927326840463	-0.28427324056736	-2.48803632888628
H	-3.66344596258204	1.03708056332632	-1.40595620967719
H	-5.91757924248413	4.03808715785022	-2.11887339130280
H	-5.87521791041596	3.49742584144756	-0.42663322690148
H	-7.43329758900671	3.67152638368771	-1.26941875158045
H	-8.24300295098126	0.40843296063574	-0.39883709572637
H	-6.66270015273692	0.15411019808851	0.36428709588788
H	-7.22732537526310	-0.95371813929532	-0.90589498423542
H	-12.39034725631559	0.89482092296846	-3.16139976288337
Sn	-11.94658011360439	0.59132909890448	-0.16299006498891
C	-13.93670349177409	0.32747952513782	0.59694054644698
C	-10.78784469476797	1.79784997821574	1.17788951531751
C	-11.03751694641606	-1.32404543751927	-0.47514125309439
H	-11.69927362769744	-1.95171196848089	-1.07257041142604
H	-10.86522202887331	-1.80487597947216	0.48924337643110
H	-10.09127871078431	-1.21202256875647	-1.00228203262446
H	-11.25856496246828	2.77461550977154	1.29250942614076
H	-9.78102272604563	1.93892809416694	0.78551549977089
H	-10.72711428574433	1.31523391460766	2.15431085325988
H	-14.40311086766138	1.29845557096119	0.76426049589656
H	-13.90907656086798	-0.22108190558645	1.53964417466344
H	-14.53991966124056	-0.23397865785094	-0.11737665249340

Sn	-6.63377164927568	-1.04822942724243	-5.00687108177186
C	-4.68853795664701	-0.82581867460398	-5.88388815624669
C	-8.04793565194745	-1.69669117669346	-6.48578298584289
C	-6.58298462462112	-2.48685075120301	-3.41262075984581
H	-9.03678641138301	-1.79362323220331	-6.03637384191578
H	-7.74931000367038	-2.66372062973892	-6.89358272379443
H	-8.09815082518588	-0.96886140174323	-7.29603039054984
H	-6.36605836062091	-3.47523679030851	-3.82099206537925
H	-7.55317013728814	-2.51353655633282	-2.91582167096830
H	-5.81439105769513	-2.23248278795522	-2.68258842013894
H	-4.71447669119016	-0.05049175351004	-6.64990888876765
H	-4.37959995462438	-1.76647364476022	-6.34222833809045
H	-3.95998345444711	-0.54680258128183	-5.12278990460420
H	-10.08404763718506	0.57498443234560	-4.72586302368704
H	-10.18215144164261	3.12675672940225	-3.77721581149235

Vf'

E= -2367.79308968 Eh

0 2

P	-8.34569017549641	-3.86328091736091	-3.43477751721724
P	-10.02381811372612	-4.49949756413301	-2.18226839968700
P	-7.13826913353828	-2.93999659224586	-1.82110612708351
Sn	-4.99594979002231	-2.68955556800755	-3.14954399014280
C	-4.19403053612454	-0.73111326652483	-2.80016352378095
C	-5.33805201025450	-2.96969869263667	-5.24869115441016
C	-3.62832683002017	-4.17816627222026	-2.43253284948509
H	-5.78284656872337	-2.07718375848609	-5.68846893071624
H	-6.00070556942281	-3.81944856761853	-5.41381178541149
H	-4.38306995008799	-3.16257971741148	-5.74021072230973
H	-4.85869430918384	0.02798261968447	-3.21277087186127
H	-3.21705694980545	-0.64500123586367	-3.27850771034846
H	-4.07938015256498	-0.55604645060705	-1.73021454994680
H	-3.43122183170019	-4.02781411350135	-1.37086473037669
H	-2.68660803125135	-4.11445519319372	-2.98008359297639
H	-4.05609891532563	-5.17050812124574	-2.57684810717840
Sn	-9.14834242916315	-1.77867160592331	-4.63774221763386
C	-8.99896132900344	-2.25914378650898	-6.72370853247815
C	-7.87563474986813	-0.10289983951612	-4.18143566848865
C	-11.18928823801074	-1.27759823008460	-4.21754469111900
H	-11.75744082709975	-2.18464917269454	-4.00839544209082
H	-11.61099716876580	-0.79318996565409	-5.09989384267891
H	-11.25783570022942	-0.59665949193507	-3.37047587723646
H	-6.99664015036403	-0.11021982936086	-4.82616108066600
H	-7.55333385806084	-0.12758926875110	-3.13999962793905
H	-8.42986136207936	0.82105219710850	-4.35364288160742
H	-7.97008344932654	-2.50242555860634	-6.98825067661527
H	-9.33210680017207	-1.41156163187892	-7.32499050762335
H	-9.63253063381043	-3.11887296937679	-6.94428114639578
H	-6.69744422654868	-4.18891371883530	-1.29724396621130
P	-11.63583352189988	-5.02041771401969	-3.46561559422982
Sn	-10.93977632215030	-2.72580198362611	-0.62841910436725
H	-10.76077479530348	-5.50199427071631	-4.48449766761190
C	-13.05848002445189	-2.63857435265947	-0.94922455023472
C	-10.53229967407434	-3.47914905621670	1.33667156956079
C	-10.03395704454413	-0.79130597788799	-0.83532466495972
H	-10.90470186612627	-4.49935595517024	1.43031824991314
H	-11.01552892181912	-2.85219178734271	2.08784708811242
H	-9.45579740268801	-3.47876074930737	1.51077070722568
H	-13.48792089777311	-3.63805021805916	-0.88225517380551
H	-13.27408831868874	-2.22753413080782	-1.93480768975566
H	-13.51219393860791	-2.00324819316879	-0.18654136813377
H	-9.39045423036760	-0.74430799697429	-1.71086199629044
H	-9.42324954062992	-0.60063466164546	0.04715478949346
H	-10.81075371112434	-0.02948302894795	-0.91387387320024

VIf

E= -2368.40412701 Eh

0 1

P	-8.24613127498912	-3.41617993444891	-3.52266751172572
P	-9.58374314890292	-4.48951522984253	-2.15204370242743
P	-7.00169050097489	-2.40910228570359	-1.98478183934464
Sn	-4.91207038199609	-2.54311811307356	-3.39696659742017
C	-3.35200488399598	-1.42977786427407	-2.42853036176941
C	-5.34350274143370	-1.70027776113714	-5.32217098445965
C	-4.37687505950817	-4.60634316295812	-3.61273856865094
H	-5.70086921900086	-0.67531813200738	-5.22498032110791
H	-6.10431000070742	-2.30203591036410	-5.81986372101149
H	-4.43982750240759	-1.70218242134384	-5.93355666449359
H	-3.64364498639236	-0.38329271684231	-2.33665822810354
H	-2.43238487848506	-1.49134679918354	-3.01247691436917
H	-3.16498050033782	-1.83206837428076	-1.43261274617310
H	-4.03123150336290	-5.00664117019816	-2.65945883286789
H	-3.58508781644274	-4.71908193131633	-4.35482781515548
H	-5.25520013346408	-5.16438285067825	-3.93829812198766
Sn	-9.39792912347243	-1.42099892250861	-4.58658443921802
C	-9.22750947572349	-1.77957748116259	-6.69629259991557
C	-8.36705714429881	0.39888902365466	-4.07189202505605
C	-11.48876497283678	-1.19706535557017	-4.15572982839771
H	-12.00256318539320	-2.14710764938538	-4.29607218815576
H	-11.89269588243537	-0.46765267749370	-4.86068202983284
H	-11.65287449842224	-0.83348244353393	-3.14289728169851
H	-7.75843417055314	0.72696546760624	-4.91495522309911
H	-7.72439323685526	0.24947651348374	-3.20360796548780
H	-9.09697048461559	1.17470783648820	-3.83699803678321
H	-8.18154290434029	-1.77775989144993	-7.00338011109029
H	-9.75880074521944	-1.00226506693939	-7.24818059499638
H	-9.66555917686610	-2.74822956094783	-6.93871162082047
H	-6.66368149512147	-3.63510754431872	-1.34047205842879
P	-11.13754482226873	-4.98903279321219	-3.65083201868712
Sn	-10.86515001179892	-2.84882191978305	-0.70308045821229
H	-12.08221486010142	-5.46433646296313	-2.70235965859097
H	-10.65427678984030	-6.29427354755477	-3.93867148622183
C	-12.97098833152247	-2.93436160765707	-1.13242092025044
C	-10.55792227360829	-3.58778009030832	1.28944431981534
C	-10.14031473758512	-0.83183468116757	-0.78774284195085
H	-10.84160488870237	-4.63886861257022	1.34871945291814
H	-11.15860329634211	-3.01650624839215	1.99916172058924
H	-9.50519992338515	-3.49291438934837	1.55777676039859
H	-13.37528663227477	-3.89553620321493	-0.81366402981877
H	-13.16488466882608	-2.80064105405047	-2.19583923794584
H	-13.47600075436533	-2.14046767313643	-0.57920553130568
H	-9.57135735471109	-0.64583343846582	-1.69594670062441
H	-9.48149124001825	-0.66265019840618	0.06379830673514
H	-10.98113838609320	-0.13801867003902	-0.74017874279959

Vg'

E= -2367.79176700 Eh

0 2

P	-10.39657961968390	-1.83934835657270	-2.31118751930774
P	-7.93725349790133	-1.60570089117841	-4.42632495058182
P	-8.78984275799899	-0.37199850837719	-2.81102280311937
P	-5.96411794677413	-0.84310823647695	-4.71553012107948
Sn	-7.17247523714521	-1.20056978726531	-1.03928592536721
C	-8.28774163916248	-1.18698829718509	0.79533761737496
C	-5.52872372216703	0.16606949507566	-0.89794880976098
C	-6.52963042752549	-3.19305964385551	-1.49314610638590
H	-5.88800198929300	1.15621491401034	-0.61709243866882
H	-5.02189122479387	0.22711979276429	-1.86046773513772
H	-4.82525004401122	-0.18575774598704	-0.14144351470266
H	-8.77842094709551	-0.22364521518790	0.93679664216375
H	-7.60855137028161	-1.36262986513683	1.63123371594063
H	-9.04257770609080	-1.97321918935255	0.78155968429396
H	-7.39009823026420	-3.78962544367036	-1.79681198816240
H	-6.07641342613376	-3.63796884230382	-0.60582614938835
H	-5.80106277581175	-3.17865850128343	-2.30306042804989
H	-10.78620077142442	-1.15756208411412	-1.12200067486336
Sn	-12.17033452509962	-0.62469708985099	-3.63564318954315
C	-14.00938913336346	-1.73083887956107	-3.55434580048134
C	-11.51679062346874	-0.45413440192957	-5.67314823939399
C	-12.41563391198233	1.33426269644004	-2.79953184407351
H	-12.85034222124420	1.26481977389256	-1.80196327565847
H	-13.06790806059782	1.94015555235089	-3.43015521961821
H	-11.43915705445559	1.81451347700160	-2.73031609202890
H	-11.22959374885490	-1.42838627159805	-6.06930521953946
H	-10.66430245744443	0.22338076955789	-5.73163354933372
H	-12.32857738586868	-0.05108039713956	-6.28104720669733
H	-13.85841119701981	-2.73633988183875	-3.94785872964099
H	-14.77047362783358	-1.22701055103634	-4.15233538222398
H	-14.36228843403091	-1.80455157159440	-2.52532166829830
Sn	-5.98323886070073	-1.30758869617922	-7.18618022276234
C	-3.98967921621590	-1.01983394889487	-7.92258534609272
C	-7.34145644991667	0.05276017308722	-8.14497834525916
C	-6.61811215812045	-3.33000941426185	-7.52638021678651
H	-8.34107202945251	-0.05193019997212	-7.72224930320757
H	-7.38700365043710	-0.16532132033337	-9.21327464773068
H	-7.00455830135198	1.07985261084340	-8.00545257733665
H	-6.59561502333549	-3.55171808275112	-8.59460587587660
H	-7.63318485013096	-3.46852360756522	-7.15356212006017
H	-5.95525553328582	-4.01924734546705	-7.00344925370478
H	-3.32052066109532	-1.76174141221288	-7.48644039344175
H	-3.63044981325501	-0.02398518496167	-7.66258783360990
H	-3.98022420787244	-1.12726964890648	-9.00836185385501
H	-8.66076353000644	-1.07209074102202	-5.52782508894217

VIg

E= -2368.40748487 Eh

0 1

P	-10.39676576634171	-2.14394562245180	-2.46947965966359
P	-8.12219372149459	-1.46802565840163	-4.67826003638848
P	-9.00737524882566	-0.45927830442998	-2.90901188177539
P	-7.50697657583164	0.35743396070586	-5.78882586773318
Sn	-7.11961244657364	-1.21437554014023	-1.40821907329403
C	-7.48858936682900	-0.45982265764583	0.56686684862109
C	-5.31638170426879	-0.37122457416087	-2.21410047068918
C	-6.99016949048510	-3.35241266374261	-1.38623395744613
H	-5.42896217363016	0.70368209454927	-2.35653252976006
H	-5.09060537919648	-0.83704037123817	-3.17392781238384
H	-4.48539594038687	-0.55323983013070	-1.53069486184100
H	-7.50342334278587	0.63012570963457	0.55657711930334
H	-6.70246761343346	-0.79843946197691	1.24353451558005

H	-8.44843676046295	-0.82330166802764	0.93528325624528
H	-7.87620728110726	-3.78000686896753	-0.91786438639178
H	-6.10399613414626	-3.65935770560982	-0.82841768701069
H	-6.92013291659247	-3.72110634678915	-2.40949153903392
H	-10.61711949363434	-1.77569610745840	-1.11051288254974
Sn	-12.39905497376290	-0.83012695371782	-3.27547050368888
C	-14.16661554616082	-2.04709030816915	-3.16157082844015
C	-12.01074538611207	-0.27152198465810	-5.30884610220309
C	-12.60094356001750	0.92187727500531	-2.05600923720783
H	-12.93120807509126	0.64849876161202	-1.05345747183835
H	-13.32693346505462	1.60804332050819	-2.49478025051408
H	-11.63340281996460	1.42035429471556	-1.99151425259698
H	-11.92953803475133	-1.15698409726680	-5.93975646198981
H	-11.08211432516618	0.29791117198079	-5.36623060099439
H	-12.82799258706564	0.35017350392448	-5.67800505578526
H	-14.06262945461908	-2.92093559853200	-3.80521821630462
H	-15.03335363750200	-1.46929802369276	-3.48647692294248
H	-14.33175250412986	-2.38148713757731	-2.13695831001616
Sn	-6.03109254085369	-0.99975862663036	-7.32674578049295
C	-4.55966642832195	-2.03467971289123	-6.15778605159329
C	-5.08861652220001	0.30337658797630	-8.74791584692270
C	-7.29928154469010	-2.41344556925291	-8.32398526484708
H	-5.84284050738218	0.84120862727690	-9.32241196756238
H	-4.47126434184174	-0.28059736291257	-9.43230453435006
H	-4.45583079432673	1.02634804699848	-8.23241616841362
H	-8.06798155953032	-1.89603861498347	-8.89851798622618
H	-7.77937998170890	-3.06016431229997	-7.58887419205475
H	-6.70766721804381	-3.03142547830275	-9.00102916593810
H	-3.90501394248861	-1.32035622778167	-5.65754977885084
H	-3.95494055341600	-2.68161376732594	-6.79520636799546
H	-5.06394689232994	-2.64415821003837	-5.40739967942151
H	-9.34775244048687	-1.58457208230044	-5.39113447477476
H	-6.40717900695353	0.60685409461731	-4.91971761982217

Vh

E= -1692.10683267 Eh

P	-7.71612665207127	-2.44840118716531	-4.69941932758126
P	-8.52260325153740	-2.27422295311125	-2.65071680699681
P	-7.05497569896513	-0.80289203112856	-3.40206495126797
Sn	-6.94842174321703	-3.91601733680203	-1.54787340127736
C	-6.02219498849969	-2.91710568093506	0.11187813294250
C	-5.46596336122825	-4.60902869938543	-2.93187633677570
C	-8.13175846643720	-5.56694196377306	-0.85406297355236
H	-5.03287587260365	-3.77884269489670	-3.48959166630049
H	-5.91645888755963	-5.30598565694900	-3.63757567176524
H	-4.67486934831865	-5.11608689135992	-2.37678253644247
H	-5.41909550152932	-2.08318051920890	-0.24799620112231
H	-5.37918071325700	-3.61086175381110	0.65568909206281
H	-6.78401033494735	-2.53426836410627	0.79121248864311
H	-8.90157217382089	-5.21591101391594	-0.16638990066072
H	-7.49683802741291	-6.28746784369112	-0.33606559636875
H	-8.61143857488295	-6.06280272482455	-1.69819964982998
Sn	-9.54437131641580	-1.13019492357225	-5.84717379228794
C	-10.98441674316828	-2.55769452156875	-6.55175292590988
C	-8.65195581207507	-0.09933482022916	-7.50500732581518
C	-10.45924695031928	0.26314740942388	-4.50043633634797
H	-10.99223964557288	-0.27031928473214	-3.71424583553825
H	-11.16250097005027	0.88551069011284	-5.05628966582454
H	-9.70234870750874	0.90153972709070	-4.04489616285366
H	-8.18046230138932	-0.81220226192028	-8.18173273260952
H	-7.89755730158231	0.59967781568621	-7.14361695997025
H	-9.41635467804922	0.45471522524192	-8.05204803270257
H	-10.50984227897641	-3.26589520157003	-7.23147270938441
H	-11.78978321553044	-2.04514121189011	-7.08007079327382
H	-11.40744324578192	-3.10546686021507	-5.70938587828382
H	-5.84884323729148	-1.44347446679349	-2.98693554290511

$(Me_3Sn)HP^{\bullet}$ = XIb$^{\bullet}$

E= -675.68135662 Eh

0 2

P	-2.04379445914334	1.02420699181242	-1.05586605321901
Sn	0.02017449621090	0.01765076694463	-0.03142632070508
C	-0.08876049093769	0.22964690246720	2.10049820108619
C	1.75847419366742	1.04342106938557	-0.76720497365601
C	0.14482498475284	-2.06337830198265	-0.55190878133248
H	1.69221949965412	2.10724944172850	-0.53887130700074
H	1.83934679582860	0.91810492725541	-1.84718939506377
H	2.65290946468595	0.63421241446371	-0.29458225208024
H	-0.13497387268385	1.28405898955917	2.37428145407432
H	0.79472345895238	-0.21488084591420	2.56133805643013
H	-0.97653803160648	-0.27259483290225	2.48577145474191
H	-0.70940304268924	-2.60532501799211	-0.14601920849694
H	1.06243568811034	-2.48942916993056	-0.14284539821437
H	0.15347177518984	-2.17770709554591	-1.63604382776817
H	-1.59464045999178	0.67751376025108	-2.36530164879572

4.4.7.5 Fourth P–P cleavage

VIIa$^{\bullet}$

E= -1692.66305762 Eh

0 2

P	-7.44517683831796	-2.10486246962328	-5.11252275106819
P	-7.47113111476989	-4.09723968192506	-4.35036926208966
P	-6.32977788345552	-0.64420108576472	-3.90301479189258
Sn	-4.77549116509255	-2.03943510533161	-2.48840666704193
C	-3.51288317279726	-0.63209655150895	-1.46730668705589
C	-3.59629185822836	-3.30341204350238	-3.75749676559434
C	-5.81901298731289	-3.21999687326140	-1.02962477020353
H	-2.90320167272722	-2.71422162757810	-4.35709936504908
H	-4.25021900170069	-3.87882783646793	-4.41253235928643
H	-3.02471343708541	-3.99576375160541	-3.13745307481234
H	-2.97323036064480	-0.01568653470548	-2.18639010467637
H	-2.79267018941833	-1.16417661723735	-0.84360573406293
H	-4.11531178875449	0.01693425514928	-0.83066918267536
H	-6.79757885629030	-2.78872613126670	-0.81943625431063
H	-5.23844293117685	-3.24785345429349	-0.10592939245014
H	-5.95325280705261	-4.23580466651786	-1.40116558696642
Sn	-5.99569841597315	-2.29482555094054	-7.16312923755323
C	-5.50728505589244	-4.35597744789624	-7.48207977960910
C	-4.24660496877530	-1.07853995023064	-6.92911260882379
C	-7.18529286826720	-1.55023521564288	-8.78061396423139
H	-8.08559493297192	-2.15598049259582	-8.88607751677237
H	-6.62084392506128	-1.58525389832345	-9.71361845183336
H	-7.47698937795010	-0.51914124970252	-8.57961441797091
H	-3.52914595525441	-1.56859464101321	-6.27225885197887
H	-4.52142102087260	-0.11471955854574	-6.50091042833581
H	-3.78552872032838	-0.91862044499469	-7.90491649880007
H	-4.88119822217294	-4.72737267534083	-6.67121849343512
H	-4.96862077223122	-4.45910985068953	-8.42528911626300
H	-6.41791594253139	-4.95329438402998	-7.52471667736660
H	-7.31865502623081	-0.49659935300420	-2.89197940586041
H	-7.90540873066154	-3.69250511160918	-3.05586180192992

TS(VIIa$^{\bullet}$→VIIIa)

E= -2027.09529536 Eh

im. freq.= 532.20 *i*

0 2

P	-8.12438432130121	-2.48887521390727	-4.17984625345853
P	-7.46194022030602	-4.45058610257637	-3.44592342007379
P	-6.66203174162530	-1.05545806812200	-3.37121625367350
Sn	-4.70806326942698	-2.36231052718693	-2.44319028725576
C	-3.31846913362418	-0.83810035170524	-1.83015331303736
C	-3.76422321352489	-3.53068873779222	-3.97295138057819
C	-5.20793693365307	-3.54715597114237	-0.72304027563340
H	-3.76219715094080	-2.99356856576296	-4.92189954656250
H	-4.29422809783532	-4.47484893181935	-4.09288946836417
H	-2.73103783282042	-3.72982202271177	-3.68373504709125
H	-3.00299009367329	-0.24942233867478	-2.69207372486078
H	-2.44047658675695	-1.30442675685951	-1.37927956141870
H	-3.77646342968860	-0.17098809570608	-1.09910812536937
H	-6.10723573639667	-3.15187195803602	-0.25044901550916
H	-4.38710012454015	-3.52140404932157	-0.00406596249473
H	-5.39457111126258	-4.57593052034292	-1.03023725186580
Sn	-7.20929903403341	-2.65593449699869	-6.52622941264666
C	-6.24562256295098	-4.53989321380539	-6.88206343665411
C	-5.85469163321960	-1.03936414089032	-6.90562526622342
C	-8.89794239027317	-2.47983990104607	-7.84217333355369
H	-9.67148143263283	-3.19897755814061	-7.57391557073251
H	-8.58885429994625	-2.66241260144472	-8.87277196934085
H	-9.31869252828668	-1.47646280982968	-7.77080292897263
H	-4.97666543002152	-1.11635986963832	-6.26437882347323
H	-6.34556577332608	-0.08716406557589	-6.70687945616517
H	-5.53814015744058	-1.07169112367360	-7.94951494634178
H	-5.30283898626498	-4.59278752028482	-6.33930312157458
H	-6.04827651921634	-4.64071112996421	-7.95075986835153
H	-6.88285148553220	-5.36421001548604	-6.56170446434948
H	-7.28391059759830	-0.92192065663781	-2.09883047386441
H	-8.35817562332067	-4.48238220276616	-2.33867510729858
H	-8.71701599050021	-5.24679051362432	-4.42408353212650
Sn	-10.28452419145472	-5.77536540610326	-5.36235651493691
H	-10.58734799536526	-8.24834008871358	-4.24660070218792
H	-12.37975288393840	-4.16847293159113	-4.71926789837198
H	-9.06501620805097	-7.30624603179177	-7.26590251696861
H	-9.27225902581390	-5.66266346226494	-7.90053303476831
H	-11.04163562050283	-3.15924671963875	-5.29738199195764
H	-11.47016460876215	-7.05756679653473	-3.27022148591572
C	-11.23857316695040	-7.37516172736802	-4.28708984186894
C	-11.60044240805998	-4.07787348684298	-5.47671484886199
C	-9.75001640781800	-6.46077253483186	-7.33260416216459
H	-12.16710955630495	-7.64814471787040	-4.79194557164910
H	-12.06442901112101	-4.02900775880699	-6.46304889834308
H	-10.65246547390998	-6.77781830616387	-7.85897193308418

VIIIa

E= -1693.27621558 Eh

0 1

P	-8.14865842766517	-2.45219186762496	-4.19375373820297
P	-7.52066908627272	-4.44324875935020	-3.45586244871734
P	-6.65840765788958	-1.05428652934832	-3.38349610497698
Sn	-4.69415651464597	-2.34890114489330	-2.46488301745109
C	-3.34249423952388	-0.82137302336307	-1.78735735161034

C	-3.73071375471220	-3.49163552155435	-4.00081487023251
C	-5.21402094737378	-3.58593351049681	-0.78806312114593
H	-3.72831729259594	-2.94997532224002	-4.94689674851977
H	-4.25373884142247	-4.43888719664883	-4.12781251910179
H	-2.69793834785937	-3.68692091699165	-3.70799019141166
H	-3.00737172629552	-0.21511733828473	-2.62928690133471
H	-2.47406585712937	-1.28477921773088	-1.31575295045168
H	-3.83261767662885	-0.17211153925840	-1.06121309888233
H	-6.06792470059352	-3.16018329693439	-0.26040880787082
H	-4.36862152448617	-3.64643357677593	-0.10053242642582
H	-5.47351546013161	-4.58554512305791	-1.13530275876190
Sn	-7.20824178450891	-2.65195598244046	-6.53114920760265
C	-6.28520869636342	-4.56155321936686	-6.85626275079059
C	-5.81714827397589	-1.06506896736914	-6.90092343695055
C	-8.89427261667552	-2.47496649669600	-7.84461984655267
H	-9.62972583908914	-3.24575967473603	-7.61241497096570
H	-8.57625820086342	-2.59165459849790	-8.88187519430166
H	-9.36128926771350	-1.49740808769954	-7.72363471399626
H	-4.94715652086280	-1.15723262841754	-6.25100709024171
H	-6.28986979720862	-0.10191150229459	-6.71173879818182
H	-5.49118277145049	-1.10927687132157	-7.94148194770572
H	-5.39572484636008	-4.67133689616738	-6.23755712313145
H	-5.99982217836132	-4.63892533213646	-7.90686173643297
H	-6.98050991206509	-5.36850395765331	-6.62387896246118
H	-7.26880859991412	-0.91286664983687	-2.10665990552812
H	-8.35955157817937	-4.44748631656579	-2.30770117213790
H	-8.45655706118207	-5.17982893424675	-4.23497608792134

VIIb˙

E= -1692.66005077 Eh

0 2

P	-3.37082032476186	-0.00029262466348	-1.14894790576726
P	-3.23909381607283	-1.03916851340757	0.79089089231803
P	-2.10132445615479	1.71900807651929	-0.98209704591428
Sn	0.01271226836396	0.43528424971969	-0.48267362195416
C	0.38220719170968	0.35922836977434	1.62977556506525
C	1.58456831988722	1.55174365984090	-1.43136239374124
C	-0.06585072375740	-1.54317227990816	-1.31267900118697
H	1.61907757740406	2.56503921906497	-1.03002518435586
H	1.41260076406088	1.60499963583804	-2.50645551656659
H	2.54507575231006	1.06701327684334	-1.24868296151177
H	0.31862016773385	1.35819751286840	2.06129725568608
H	1.38012529445788	-0.04355901202718	1.81124953833149
H	-0.36020956866397	-0.28416641820324	2.10100630814236
H	-0.69477102536465	-2.18251181528064	-0.69352523185940
H	0.94270970041352	-1.95873377993301	-1.34661833069353
H	-0.47375359499651	-1.51099263496587	-2.32281843934977
H	-4.63809261255488	0.62965383423604	-1.04884848353262
Sn	-5.05496780607016	-2.72804300612559	0.34079848697916
C	-4.12619119977079	-4.26595114733744	-0.82533258288995
C	-5.72362843644392	-3.50001642992378	2.22795542583513
C	-6.69606933389212	-1.86251740007265	-0.73649637462035
H	-7.13197414959818	-1.04004588552002	-0.16902121261740
H	-7.46141715079925	-2.62181020845494	-0.90570913748094
H	-6.35397755330902	-1.48679357019089	-1.70104556331270
H	-3.68616678474402	-3.83162091783872	-1.72363763943504
H	-4.86463054553345	-5.01301079631356	-1.11960870955313
H	-3.34062229517664	-4.75236329636299	-0.24663389234500
H	-4.88376106777779	-3.92522856597963	2.77768521354591
H	-6.46850453026430	-4.27974287913388	2.06114041093173
H	-6.17238239011297	-2.70550493424754	2.82439791367842
H	-4.01923766692152	-0.14540171881418	1.57219221817435

TS(VIIb˙→VIIIb)

E= -2027.09620347 Eh

im. freq.= 750.49 *i*

0 2

P	-4.20531842128533	-0.76573660837834	-1.28491910723393
P	-3.76376457894695	-1.28380338393054	0.80950681582185
P	-2.71986161841542	0.76807149707787	-1.77325488175349
Sn	-0.64712854911790	-0.48812462150463	-1.09370256120004
C	-0.09902792006659	-0.08279124878290	0.93699378743791
C	0.86900418583347	0.31254859806662	-2.39208905504991
C	-0.81980484079099	-2.60528001184047	-1.42583788585170
H	1.04678552276933	1.36116691246766	-2.15167618279543
H	0.55455122487424	0.23862336236765	-3.43328403879788
H	1.80093175318892	-0.24115919076863	-2.26629932299859
H	-0.15037697634133	0.98861087481959	1.13144147307488
H	0.92164598080691	-0.42734370413126	1.11326826770009
H	-0.78160270732888	-0.60265086278700	1.60783223527615
H	-1.80740848614315	-2.96215320732767	-1.13413841185457
H	-0.06797532853297	-3.12400438708786	-0.82893664743614
H	-0.65385906861914	-2.83422440412703	-2.47889325169170
H	-5.30580906341696	0.10390370260538	-1.07338267815699
Sn	-5.59389682399777	-3.00303042756205	0.94958228081558
C	-4.89425166639935	-4.59631722744661	-0.30037914290301
C	-5.79900663153244	-3.64432354113197	2.98733701855746
C	-7.45331268076530	-2.21991478202082	0.21887051844495
H	-7.77759471689868	-1.38383878757743	0.83893441923053
H	-8.21833677174882	-2.99754476973076	0.24325396725323
H	-7.33354700405847	-1.87439036398142	-0.80812550822835
H	-4.67038041154316	-4.20412489183619	-1.29314257973215
H	-5.65298286985550	-5.37505163784878	-0.38891657075988
H	-3.98773149120707	-5.03143742119878	0.12161750047594
H	-4.84442162746807	-4.01882411313400	3.35752602975446
H	-6.54109024514737	-4.44151643617574	3.05256131391750
H	-6.12029706487899	-2.81236225868246	3.61448688238936
H	-4.42686568866542	-0.21858728865610	1.47350431042905
Sn	-2.55434783934016	-1.16495794678515	-4.86066215053144
C	-3.36448414855817	-3.09787001662164	-4.37096526605705
H	-3.51482331457669	-3.66946150940575	-5.28924153917207
H	-4.31931929053975	-2.97255419370363	-3.86125750210366
H	-2.68532505013142	-3.64334925998534	-3.71638437682605
C	-0.58187562372758	-1.41231641511743	-5.69902611211778
H	0.08214284770364	-1.89741092702060	-4.98313052101280
H	-0.16034879703486	-0.44520919243018	-5.97400417118082
H	-0.64888456901636	-2.03454485194320	-6.59386085455626
C	-3.82824294317790	-0.23505221908783	-6.32523360440483
H	-3.47150358981867	0.76772635867183	-6.56026173085997
H	-4.84744734739188	-0.16751083918647	-5.94410624033742
H	-3.83080007519597	-0.83443171594888	-7.23779490024084
H	-2.50603567349435	0.00430335880938	-3.31490002473385

VIIIb

E= -1693.27546294 Eh

0 1

P	-3.72357276694773	-0.51204995308379	-1.69473463703433
P	-3.30405774038144	-1.43785026321918	0.26354878038801
P	-2.15958888114760	1.05271948114302	-1.62790366449882
Sn	-0.18802769019653	-0.53237816432819	-1.62270285953976
C	0.60234822607941	-0.66961970051922	0.36329019113336
C	1.26342738010122	0.38574581600189	-2.91316116119217
C	-0.69881735605051	-2.47285632978066	-2.38468425408097
H	1.46096015329871	1.40874086956027	-2.59147859001560
H	0.89437562496942	0.40384484018720	-3.93905464802102
H	2.19657428331636	-0.17901122952058	-2.88321925027104
H	0.75452989032787	0.32904290753745	0.77349463556001
H	1.55766311427234	-1.19660811368004	0.34843028206148
H	-0.10010257967382	-1.21223246737953	0.99541753751642
H	-1.25397359200779	-3.03465966423220	-1.63390623652488
H	0.21791805274286	-3.01189290994295	-2.62971213195860
H	-1.30936072691040	-2.37886347253792	-3.28264981475826
H	-4.80953785033532	0.31695497560322	-1.30328818265049
Sn	-5.39426449749970	-2.83865972049013	0.30601850595995
C	-5.06017637653748	-4.44194226720782	-1.07420901596483
C	-5.65561522215878	-3.58008433654642	2.30202408696064
C	-7.09809991442706	-1.68089622027585	-0.29216557487916
H	-7.20796312578748	-0.81162568510119	0.35649406224328
H	-8.00027065939429	-2.29113019050553	-0.22390292752891
H	-6.97778202777688	-1.34276935587309	-1.32156102354722
H	-4.78965799597071	-4.03316647466003	-2.04826458981668
H	-5.96464926719377	-5.04230426860881	-1.18095508285723
H	-4.24990631211049	-5.08006906648144	-0.72087215973911
H	-4.75814341246388	-4.10728515617268	2.62585317410186
H	-6.50069430981112	-4.26967070546743	2.33131106069793
H	-5.84949733537889	-2.75538523522894	2.98816968030459
H	-3.77970269327382	-0.41174471578332	1.12452611022247
H	-2.08241439167257	1.20477677659395	-3.04312230227089

VIIc˙

E= -1692.65980546 Eh

0 2

P	-7.60734091067801	-1.93328882635743	-1.61359951604232
P	-9.28707217484440	-0.65420778923897	-1.15929234831754
P	-6.06878050231432	-0.47427751002966	-2.23378476312481
Sn	-4.46408415644539	-2.17689147531703	-3.17137655737800
C	-2.45048194635629	-1.57420990874089	-2.72729001801224
C	-4.75103205722364	-2.14525617756730	-5.29784842239911
C	-4.82239572229840	-4.15761162037926	-2.42649011515229
H	-4.48549244340059	-1.16416156003191	-5.69229771529670
H	-5.79460368926578	-2.34876879409811	-5.53912805713240
H	-4.12326192428351	-2.90166853627601	-5.77151558771524
H	-2.30914148009509	-0.52061455285332	-2.96904114786184
H	-1.75712286133040	-2.16793332380315	-3.32516126809314
H	-2.22373218737515	-1.72990433357928	-1.67227649731913
H	-4.81855631315185	-4.16047255804953	-1.33751840654609
H	-4.03555439162553	-4.82024228830763	-2.79127790311407
H	-5.78611290478108	-4.52726835734252	-2.77639428478462
H	-8.00396958023215	-2.41974971623979	-2.89038759039914
Sn	-5.04672489178877	-0.26432108571376	0.06296927818327
C	-4.38387197890949	-2.15022826686829	0.85248569760579
C	-3.41444640766466	1.12100824191363	-0.09027843110598
C	-6.56506106371995	0.53440450572175	1.34867830387903
H	-6.95282369082325	1.46523358774297	0.93480427706294
H	-6.14389479950530	0.72783321076163	2.33668104254575
H	-7.38811636244715	-0.17389579570428	1.44496886763739
H	-5.20993186155241	-2.86157524891860	0.83136169157572
H	-4.05820393928088	-2.01756193057888	1.88554727955525
H	-3.55289370782237	-2.54903081040433	0.27084675496452
H	-2.59582813707069	0.68756869153941	-0.66402689508157

H	-3.05288194376679	1.37098687629134	0.90850383127141
H	-3.74967543324059	2.03387930443205	-0.58275841023776
H	-10.2072305367060	-1.72636395200281	-1.35588308916703

TS(VIIc˙→VIIIc)

E= -2027.10293611 Eh

im. freq.= 364.90 *i*

0 2

P	-8.12786234750712	-1.99129265467725	-2.06733773974088
P	-9.45642727866301	-1.18168377244938	-0.52513934978893
P	-6.78040515569119	-0.24031480199487	-2.24096066766846
Sn	-5.00213053464472	-1.45245435419785	-3.53288061727811
C	-3.50393313935219	-0.02208673655399	-4.09211233684222
C	-6.00016204448006	-2.21585868665037	-5.27170750213545
C	-4.14373045036533	-3.08153307830947	-2.42926533100694
H	-6.49271007330077	-1.40411084509058	-5.80775940875601
H	-6.74978054023257	-2.94891680519128	-4.97166300496363
H	-5.28188584895324	-2.69743012213157	-5.93686343821585
H	-3.96317068650472	0.79220446740452	-4.65309313410031
H	-2.74712501962628	-0.49974940682428	-4.71625863791839
H	-3.02249038708976	0.38763972299368	-3.20429537404105
H	-3.51735179586089	-2.71126363821166	-1.61751567381673
H	-3.53376685498627	-3.69622155352766	-3.09299819814839
H	-4.94399149587000	-3.69425474935917	-2.01370876497295
H	-8.90805649836262	-1.65703942139155	-3.21166673199286
Sn	-5.76706181603934	-0.28235888788213	0.06190329796430
C	-5.88486665296674	-2.21707746123071	0.97487024832876
C	-3.71830913146281	0.33557388640567	-0.14584163825504
C	-6.82314825012452	1.17288200391140	1.22969797038569
H	-6.76362521092779	2.14833070655301	0.74610357066182
H	-6.38575479189263	1.24194520172636	2.22698284925615
H	-7.86939809766031	0.87983532288375	1.31574644005040
H	-6.92126773301246	-2.55393702239123	0.99606705231770
H	-5.51081651432438	-2.15222283287214	1.99806746494033
H	-5.28533841408603	-2.93601870999704	0.41777990100416
H	-3.13395435782151	-0.42669773883001	-0.66170777614791
H	-3.28484398694855	0.49899589625242	0.84205498358301
H	-3.66294405720187	1.26696402637662	-0.71039712940722
H	-10.64018522000856	-1.72729907146500	-1.09371421789926
H	-9.67391165622313	0.34268421852703	-1.46475717694834
Sn	-9.67227765512590	1.80464569843439	-2.64447642659076
H	-8.27260019598518	0.84663616123380	-4.76657151226982
H	-12.39268054562780	1.89925199000920	-2.89715147887994
H	-7.26190699581059	2.91278660902968	-2.09346531463480
H	-8.45708347140618	3.54479650698431	-0.93869764200798
H	-11.91081012940266	2.90257824138892	-1.51626348705687
H	-9.98709848462256	0.42499743948591	-4.97692700533319
C	-9.29505535383564	1.21237736348833	-4.67715818656868
C	-11.66383986562009	2.62876655556053	-2.54229710235579
C	-8.27491674372379	3.29818304017973	-1.98506592958295
H	-9.43152566559239	2.07045286541695	-5.33838449244221
H	-11.72495244465297	3.52023276803106	-3.16977050086124
H	-8.38653640640238	4.20252165895190	-2.58622084986301

VIIIc

E= -1693.28014147 Eh

0 1

P	-7.62390568593204	-1.93794232240602	-1.60939004994098
P	-9.24316460080350	-0.43675466628822	-1.51637474784490
P	-6.04914324192591	-0.49847594045915	-2.21756361785286
Sn	-4.46367737536077	-2.20386593163401	-3.16673845693797
C	-2.44660653964377	-1.58543959018523	-2.76148858962685
C	-4.79900626797673	-2.19832909373451	-5.28661385300861
C	-4.80615044696290	-4.17642828416570	-2.39316415358328
H	-4.52471970338844	-1.22808826051837	-5.70133236917940
H	-5.85237533472598	-2.38427601511073	-5.49806274844430
H	-4.19900711644386	-2.97376291327689	-5.76535858859594
H	-2.31654846694471	-0.53494395962815	-3.02268102032396
H	-1.75605397934235	-2.18416621890723	-3.35749006985688
H	-2.20612378857285	-1.72064540516049	-1.70664780671977
H	-4.75688667658213	-4.17197400661235	-1.30520290087478
H	-4.04166784239342	-4.85000013273073	-2.78453755475656
H	-5.78685446691416	-4.54010573952457	-2.70000279258452
H	-7.87909542230658	-2.45770593814382	-2.90875683542420
Sn	-5.04481332489369	-0.27064036864749	0.07966353042184
C	-4.31405111878326	-2.13495013096854	0.86205931133701
C	-3.45624016506105	1.16720658113671	-0.05340257708172
C	-6.59274792058567	0.44762338137012	1.37727322852738
H	-7.05046766037218	1.34463756455444	0.96093448997727
H	-6.17228594723179	0.67844036510271	2.35759655465190
H	-7.36330715087705	-0.31512628090303	1.49351428324672
H	-5.11893120748482	-2.87059587604089	0.85735032998852
H	-3.97689474497050	-1.98893827981188	1.88979491441950
H	-3.48004144521086	-2.51251142418004	0.27059419860572
H	-2.65564475955913	0.79125158013086	-0.69046620898891
H	-3.05232554363372	1.36537159441424	0.94078545531900
H	-3.83457304412773	2.09951438140197	-0.47294073879436
H	-10.31008834842143	-1.37463237095783	-1.45272019634240
H	-9.39723066256690	-0.19539629811508	-2.90541041973162

4.4.7.6 Fifth P–P cleavage

IXa˙

E= -1350.82584959 Eh

0 2

P	-7.70714827732524	-1.75424300896723	-1.68473458805887
P	-5.99161979426918	-0.55446673743604	-2.17994980524589
Sn	-4.43289315592785	-2.23930773267835	-3.20592585303524
C	-2.41593151358006	-1.59983089100164	-2.82692905321708
C	-4.83858296113213	-2.23847888997844	-5.31098661686967
C	-4.76474793166534	-4.19130363590783	-2.38633221508907
H	-4.52915637985537	-1.28924612571426	-5.74833120688864
H	-5.90689950388264	-2.37314834502629	-5.48165676023524
H	-4.29648147080194	-3.05086153811280	-5.79734277562319
H	-2.29201986618865	-0.55507584771022	-3.11244128190727
H	-1.72314120384088	-2.20982407262302	-3.40887652222033
H	-2.17458580978275	-1.70987124616142	-1.76917697934434
H	-4.63249111013522	-4.16716270850371	-1.30519066994535
H	-4.05797508755721	-4.90085434004678	-2.81984358271414
H	-5.78073535170435	-4.51725029812008	-2.60891250306582
H	-7.82560685541776	-2.34105922693156	-2.98043326654238
Sn	-5.04698163023931	-0.26960707778882	0.12968933770810
C	-4.28424397365974	-2.12019725566526	0.91015419495774
C	-3.47454763517893	1.18479411740105	-0.00124689332164
C	-6.63703404296018	0.42619441329620	1.38430931764940
H	-6.98711482568639	1.39995873318819	1.04194361560102
H	-6.28386723525623	0.51387141903312	2.41288290141495
H	-7.46759290425983	-0.27929436983640	1.35233618527055
H	-5.07678102454569	-2.86903470206763	0.90988454904981
H	-3.93799870455744	-1.97194173886002	1.93450452737970
H	-3.45042096515021	-2.48241858503673	0.30855918399382
H	-2.67806276347336	0.82143967141068	-0.65103037587274
H	-3.06101004814505	1.37528995180519	0.99044786887409
H	-3.86448797382101	2.11803006804016	-0.40765073270225

TS(IXa˙→Xa)

E= -1685.25813666 Eh

im. freq.= 759.05 *i*

0 2

P	-8.03351353295921	-2.50816286537844	-0.94605572817798
P	-6.90798555025886	-0.81607962437746	-1.80108066836768
Sn	-5.30120100453810	-2.11060961435134	-3.22292366852706
C	-3.44775411896934	-1.02681471228819	-3.30300852091406
C	-6.20573072730226	-2.17496101399002	-5.16856956747306
C	-4.96900153087316	-4.10902213501581	-2.51828762331885
H	-6.28664147501584	-1.16464213544238	-5.57042986279449
H	-7.20577527462303	-2.60443139949779	-5.09800823301521
H	-5.60730061077702	-2.78280350356939	-5.84881636731394
H	-3.63199724951984	0.00662357118850	-3.59830072427719
H	-2.77897083405859	-1.48737656657526	-4.03174699597082
H	-2.96032760704249	-1.03478945807440	-2.32777261156127
H	-4.48894599182058	-4.09139569252202	-1.54048737401681
H	-4.32660746724410	-4.63925778075960	-3.22360189137829
H	-5.91832218063001	-4.63764360923725	-2.43521789468308
H	-8.29330330840278	-3.16003782491633	-2.18585939692748
Sn	-5.50249653445669	-0.37363791708275	0.22639242511971
C	-4.18947292298734	-2.00236658530617	0.70828852576752
C	-4.35281173210219	1.39839913415691	-0.15452805438364
C	-6.87659781249697	-0.05896580775830	1.84288068054107
H	-7.54092458160798	0.77345357733681	1.60869652694890
H	-6.33361044314382	0.16517423353372	2.76217576404667
H	-7.47572577198873	-0.95733055991243	1.99533958365585
H	-4.76206497575067	-2.92824170361829	0.76836853024772
H	-3.71294340816637	-1.81613146519378	1.67223094458182
H	-3.41394539606274	-2.10946135147415	-0.05075682704198
H	-3.68747918403917	1.23926688398613	-1.00351899873510
H	-3.75299482641204	1.64933102854232	0.72158306080855
H	-5.01793012443017	2.23266591226927	-0.37891009934608
H	-9.51864394693289	-1.69421452467563	-1.18501548511418
Sn	-10.68182230897095	-0.43316667948449	-2.10076048836612
H	-10.34978044860692	1.58356207259618	-0.29109537188514
H	-9.11657796189226	-0.46539335762671	-4.31899635091459
H	-13.06478895380894	-0.73050928219891	-0.78667961629756
H	-13.03534600713703	-1.82809206089364	-2.18038415283116
H	-10.50984025783878	-1.53494632184402	-4.59451224479151
H	-9.18337042901477	1.77533427769350	-1.61709144193696
C	-10.21884179950036	1.53868071872275	-1.37257207436469
C	-10.19426847727469	-0.57156355240731	-4.19272383087801
C	-12.78876512636884	-0.82314189950014	-1.83721784602076
H	-10.87898201134367	2.27131926251572	-1.84131271739702
H	-10.69861933547188	0.22397750678922	-4.74466090692882
H	-13.36422675815388	-0.10019717435807	-2.41936240576613

Xa

E= -1351.43838986 Eh

0 1

P	-7.98896822879304	-2.55326868868729	-0.96812279206646
P	-6.95411171987155	-0.79045566816835	-1.84651252409435
Sn	-5.30342155387854	-2.09493374612712	-3.22484778592189
C	-3.43504171193725	-1.03664920252858	-3.25985122819502
C	-6.12863844971784	-2.15721962275329	-5.20554767168320

C	-5.02047213565489	-4.10334526539358	-2.52113904135849
H	-6.24260382464137	-1.14367537683524	-5.59071268982302
H	-7.10808604472171	-2.63619386423142	-5.18580992962043
H	-5.47348493002871	-2.72033884250954	-5.87219418273137
H	-3.60102670782636	0.00262728386373	-3.54550923952970
H	-2.76362147056728	-1.49731683120033	-3.98601733833956
H	-2.96014674283324	-1.06260970507808	-2.27898805347890
H	-4.58681248159118	-4.10242819755690	-1.52198879562888
H	-4.34787147232093	-4.62651874281175	-3.20307571088670
H	-5.97277291623221	-4.63275599498125	-2.49109136102065
H	-8.54298331885454	-3.03318510179252	-2.18768048745005
Sn	-5.52197345866410	-0.36549054521497	0.17500050203753
C	-4.22422391768812	-2.00449661220036	0.66482431958950
C	-4.37192582138125	1.40814075695549	-0.19284503429343
C	-6.88378546589606	-0.06174818369825	1.80643165301303
H	-7.57295905433693	0.75057833879187	1.57416123078152
H	-6.33358001159618	0.18634240836480	2.71523866137011
H	-7.45781324893716	-0.97254855139777	1.98210713029122
H	-4.80441224115768	-2.92584765217473	0.72270042227516
H	-3.75723482305723	-1.81963318088083	1.63364885205342
H	-3.44168350254017	-2.11971721279669	-0.08536529016524
H	-3.69078162478255	1.24863390411546	-1.02896953995823
H	-3.78980020823929	1.66474489345263	0.69341443026314
H	-5.03690917139092	2.23832759580570	-0.43208763846065
H	-9.18386374086162	-1.86249839233083	-0.62612086696837

$(Me_3Sn)_3P$
E= -1692.65980546 Eh
0 1

P	-7.16483580322155	-0.24953981262701	-1.37957884552407
Sn	-5.77334884650269	-1.61425403133997	-2.94598212935988
C	-4.18666325204371	-0.35714874331798	-3.65625830566778
C	-7.01625384219960	-2.19482543707897	-4.59971678133137
C	-4.90161772271171	-3.37740743275558	-2.07581259151523
H	-7.50539112984490	-1.31600099501526	-5.02093192946593
H	-7.78049678178102	-2.90336621727924	-4.27905039140233
H	-6.40697156970681	-2.66432256335182	-5.37382769874185
H	-4.60079058676460	0.53283141462774	-4.13044802245265
H	-3.57667954704546	-0.89754090127056	-4.38219038334499
H	-3.55363160382503	-0.04927165024436	-2.82349785275166
H	-4.19913056000557	-3.10889445095116	-1.28657595248275
H	-4.36319405982044	-3.92977435643197	-2.84831882586753
H	-5.67664429179881	-4.01984017480288	-1.65920996137968
Sn	-5.95137147146134	-0.72304651891160	0.75821092636294
C	-6.14907409319686	-2.73174953958016	1.50572641776556
C	-3.86456117842791	-0.30704952517973	0.44862078440982
C	-6.73733264440987	0.61997619547283	2.23694589741940
H	-6.63642183531099	1.65000896013083	1.89482672111747
H	-6.19423960704724	0.50159104318885	3.17611173798708
H	-7.79287069576612	0.40765500163383	2.40919232538387
H	-7.19523840187796	-2.97334229521245	1.69434767303859
H	-5.59794828983913	-2.81612235918444	2.44429562309136
H	-5.74157910413573	-3.44758873515708	0.79246032088947
H	-3.41884380819025	-1.05060047420162	-0.21298669163023
H	-3.33739030117701	-0.32977234983040	1.40380369083200
H	-3.74273838999097	0.67976262288686	0.00124800879836
H	-9.99364527433053	-1.54132889204320	-3.66625784326965
C	-10.47039325426024	-1.36650088475670	-2.70134039507018
H	-10.77193829011657	-0.32036638952462	-2.64360490577261
H	-11.35654953350967	-1.99880507576585	-2.62524634732823
H	-8.19274875052720	-4.16597278258826	-2.18955170282665
Sn	-9.09572437458895	-1.81721591928120	-1.11671134860632
C	-8.61730203275292	-3.91235116214823	-1.21793496859253
H	-9.53248585325553	-4.49069411694073	-1.07697021653983
H	-7.90616399751557	-4.18217918609305	-0.43780118281824
C	-10.01318111142630	-1.41367829683423	0.78358416716150
H	-10.18521599133986	-0.34265853240995	0.89413571764040
H	-10.96940014750429	-1.93479608458379	0.85217323909976
H	-9.37134197076884	-1.75348935124682	1.59732202274461

IXb˙
E= -684.23321649 Eh
0 2

P	-8.08070897978483	-2.41594694703541	-1.75845799183545
P	-9.12972612284881	-0.51521405570690	-1.70815347710883
H	-7.25628883624939	-1.98444831225429	-2.83702497734667
H	-10.30687896162906	-0.98207557091480	-1.07206452861174
H	-9.67988709948788	-0.50474511408860	-3.01694902509730

TS(IXb˙→Xb)
E= -1018.67319634 Eh
im. freq.= 658.17 *i*
0 2

P	-7.55669373354324	-2.38024889392964	-1.76784827839680
P	-8.60620170839089	-1.09351302955284	-0.30653061053770
H	-6.72960506054019	-1.30592293788681	-2.20137455224875
H	-9.73939504680262	-1.93825500293024	-0.17490006309830
H	-9.23690225197792	-0.25822796833117	-1.26517094094339
H	-6.31019930295628	-2.67648785902825	-0.56143342343626
Sn	-5.14648919711443	-2.33419752870168	0.92049452457681
H	-7.12153223673983	-2.17575991872907	2.78118514990518
H	-3.58336860270264	-4.57420671265969	0.91132987969657
H	-5.55254186627696	0.35242859748004	0.93494462326748
H	-4.14389838951919	-0.00578591299433	-0.08620296144804
H	-2.82194308060136	-3.33585921270406	-0.10723137730394
H	-6.47642358614332	-3.83199131054931	2.77643526910059
C	-6.21235252597221	-2.77530016423144	2.73452698338465
C	-3.34714457648246	-3.51313519174956	0.83137789129847
C	-4.64503466899665	-0.24570587022646	0.85190638744573
H	-5.58242440827803	-2.53399961667354	3.59308005082519
H	-2.69358684691823	-3.23189297732318	1.65958275818208
H	-3.97790291004280	0.00017151072151	1.68035868973033

Xb = P_2H_4
E= -684.85224864 Eh
0 1

P	-7.51911228213633	-2.02536444677048	-1.90169679498231
P	-9.01885616154680	-0.39577233431868	-1.65773638061868
H	-6.48239498997444	-1.13582960158210	-2.29585810187715
H	-10.05539961538252	-1.28511677698287	-1.26270817447232
H	-9.42738882415334	-0.44536792755009	-3.01884078563307
H	-7.11149812680657	-1.97590891279578	-0.54030976241647

IXc˙
E= -1684.72851274 Eh
0 1

H	-5.49324605080325	-3.70805633121696	-0.12255337144181
H	-6.21199522531579	-2.08394267971464	-0.12983631978459
C	-6.01248222440868	-2.96916558751830	-0.73460708204889
H	-6.95981455218653	-3.38767575548696	-1.07580427065705
H	-3.29764190091326	-0.49947516813012	-1.29570152430005
H	-2.42518409311816	-2.04275543914942	-1.23363981068782
C	-3.04523560148512	-1.39840351709441	-1.85880786625080
Sn	-4.83309122921962	-2.43774789699471	-2.44549280468605
H	-6.81706461899430	-0.30805100163990	-2.79354841817196
H	-2.47623115472173	-1.11090644987246	-2.74336119352243
P	-6.22434223392770	-0.94571265750080	-3.92169922443241
C	-4.33019468831090	-4.18926504973517	-3.57595782280424
P	-7.82044943673144	-2.48007907651720	-4.22196667295358
H	-3.81969234736679	-4.90858463000447	-2.93394751259294
H	-5.24121424418706	-4.64585912657287	-3.96392027695698
H	-3.67694254973968	-3.92977681967944	-4.40885664413920
H	-4.79388474104450	-2.37136614512045	-6.51330808365623
Sn	-7.48738460827051	-2.64304422396929	-6.70473380798979
H	-5.18329190696375	-4.09975505194155	-6.63621260690681
C	-5.41585824527848	-3.10791764594563	-7.02337589726221
H	-7.43110475318802	0.01750882461526	-7.25433633058243
C	-7.94336025752644	-0.81555556513604	-7.73564098477644
H	-9.01726343692134	-0.62772989465310	-7.72966331457392
H	-8.54255003372578	-5.14420462886005	-6.90576694137974
C	-8.73909719649388	-4.22028828837078	-7.45009025493816
H	-5.19107822248080	-3.07968763346633	-8.09070157789109
H	-9.79010630423714	-3.95740371660148	-7.32599380138208
H	-7.60545423429197	-0.89104195315381	-8.77069396201397
H	-8.53972466676805	-4.38417324183523	-8.51020374081996
H	-12.29828586480531	-1.21273504948459	-5.14495747034964
H	-11.13787657320437	-1.79436350541193	-6.35212709148113
C	-11.38229194412385	-1.78751051387098	-5.28913745988658
H	-11.55092685763578	-2.81281045625063	-4.95933870231458
H	-9.50116186464163	1.10688590266492	-5.98883181115117
H	-9.95473285937101	1.78617281984170	-4.40980210155321
C	-9.32106747148602	1.05613504802613	-4.91577219179367
Sn	-9.77308799791250	-0.90651759894213	-4.17058349740457
H	-8.27587932059688	1.29881920477724	-4.72163572575306
C	-10.28463939253832	-0.74025652333670	-2.09230976358372
H	-11.12863637163268	-0.06087704077366	-1.96262660881277
H	-10.54640393983396	-1.71881818277628	-1.69010591219804
H	-9.43097878359632	-0.34969775319653	-1.53677954411371

$(Me_3Sn)_2P$˙
E= -1008.97300199 Eh
0 2

P	-6.11927452751413	-0.54124390233318	-2.24540718349896
Sn	-4.47094821877905	-2.17709989575890	-3.18479068388549
C	-2.43478248195917	-1.64637574826993	-2.73311552657728
C	-4.71565695656083	-2.18940229477586	-5.31785416453407
C	-4.87340366875789	-4.14643861055150	-2.42146389551929
H	-4.43220067860556	-1.22215526462501	-5.73351477802251
H	-5.75690987727036	-2.38867432882914	-5.57230728447338
H	-4.08690277960130	-2.96358115201707	-5.76071995452287
H	-2.23157343833554	-0.62507341027685	-3.05589546231507
H	-1.76226418810730	-2.32339397669125	-3.26283045124359
H	-2.23874036528932	-1.72439193279946	-1.66356049020939
H	-4.78692944623348	-4.15650082311490	-1.33541659778756
H	-4.15476824054467	-4.85114613432616	-2.84334113961820
H	-5.88031320260703	-4.45724787149411	-2.70056744580846
Sn	-5.07627171559043	-0.26890727196880	0.01831178855857
C	-4.28405677364182	-2.09295953231670	0.84199956963888
C	-3.50028656720419	1.18727233043957	-0.12351009347230
C	-6.58662272572133	0.44915992287272	1.36495996310405

H	-6.99454125918929	1.39457796731438	1.00683460788128
H	-6.15617689660798	0.59963790145096	2.35654809794616
H	-7.39657031044719	-0.27725831100339	1.43855645440425
H	-5.07815627828485	-2.83268378899073	0.94861596760247
H	-3.86587029585319	-1.88424358965520	1.82853978638542
H	-3.49810727529856	-2.50605881632510	0.21021550189859
H	-2.70494820946041	0.82007795822853	-0.77175622544640
H	-3.09107867537690	1.37721885490467	0.87030320406798
H	-3.88958494715782	2.11999172091252	-0.53132356455274

IXd˙

E= -1018.14422327 Eh

0 1

P	-3.43463847967205	-0.15343780506294	-1.02074129058541
P	-3.54214025806395	-1.02455827053313	1.01934048549740
H	-2.08926280742128	0.29787792374672	-0.93329459604381
Sn	-5.32372961317677	-2.71619203376870	0.45254580104227
C	-4.40502693337542	-4.21392197447280	-0.77660274537512
C	-5.98177570080498	-3.57432185896688	2.30379458430424
C	-6.95723376130158	-1.79233413609981	-0.58669729909492
H	-7.46758379871778	-1.09106202876602	0.07382289403840
H	-7.66723953676933	-2.55201925464683	-0.91696885818551
H	-6.58591751980534	-1.24896819565024	-1.45584003548500
H	-4.09789175653097	-3.78638330493576	-1.73163320502978
H	-5.11416018536446	-5.02071737619289	-0.96800994716184
H	-3.52816102749875	-4.62537529989146	-0.27612769206653
H	-5.13720700022887	-4.02740417091672	2.82335746436299
H	-6.73253566135577	-4.34200381074029	2.11046781103907
H	-6.41852198921617	-2.80594244550202	2.94195551052434
H	-4.51221088560296	-0.09166777464475	1.48277097549671
H	-3.04273308509343	-1.36531818295541	-1.65104985727752

4.4.7.7 Sixth P–P cleavage

Me_3SnPH_2

E= -676.30558319 Eh

0 1

P	-2.81201260480117	1.67930210027558	3.17773689923815
Sn	-1.13876431612028	0.59297526653051	1.64326865756235
H	-3.24842334098322	0.42962817949309	3.69715220021181
H	-3.82799527544379	1.69824249112229	2.18285409017271
C	-0.44180547249197	2.06386715359104	0.24583658035546
H	0.00153694927950	2.90640585433468	0.77729386252111
H	-1.26722697034154	2.42896608431106	-0.36586583827567
H	0.31153427263498	1.62353091741855	-0.40927279113668
C	0.49344738417860	-0.07605411940201	2.86174601683436
H	1.26089336304546	-0.53837231342180	2.23923844082573
H	0.14576705804850	-0.80654928203007	3.59279508989829
H	0.93258361375999	0.76963637573117	3.39180088812534
C	-2.01145458278921	-1.06214197808275	0.59241822438377
H	-1.26357872253243	-1.54492376067852	-0.03864815194125
H	-2.83166471182548	-0.71260249300328	-0.03533729684345
H	-2.39867664361787	-1.79168047618959	1.30406312806792

XI˙ = H_2P˙

E= -342.38901676 Eh

0 2

P	-5.48770299446212	-0.51334426298580	0.00997450380146
H	-5.80484252137937	-1.49807359591394	0.98803931784467
H	-5.80486448415851	-1.40898214110026	-1.05042382164613

TS(XI˙→PH_3)

E= -676.82967765 Eh

im. freq.= 153.91 *i*

0 2

P	-4.83286364436697	-0.81274091081630	0.07511698377862
H	-5.24002803740576	-2.03453134030190	0.67931374234404
H	-4.73529291242464	-1.42254297281811	-1.20664002768500
H	-3.05708771556827	-1.44252121648449	0.34882847594792
Sn	-1.58981160346889	-2.53635505717155	0.34098036445976
H	-1.15432631333166	-2.39309069787126	-2.34259998561871
H	0.03012588214966	-1.11355943099413	2.00859647972255
H	-3.02873010313179	-4.72303765876699	-0.39833121873384
H	-2.81887762775863	-4.74125113894351	1.36208595150875
H	-0.88017165191006	-2.30101315607590	2.96284013432262
H	-0.14782583221895	-1.17850382958438	-1.53282441586200
C	-0.50829122219063	-2.20613261540409	-1.48431456964819
C	-0.33020565810384	-2.14191089134436	2.03538835309745
C	-2.31866071819350	-4.55384717879095	0.41163773330716
H	0.34630980597831	-2.88315075338983	-1.53324616440715
H	0.52712370257351	-2.81729178891511	2.01337513286781
H	-1.48933635062768	-5.25523936232681	0.30573303059820

PH_3

E= -343.01446629Eh

0 1

P	8.42936634074313	3.67709145784681	-3.03266937925800
H	9.82369998045064	3.43270048259611	-3.13961779057558
H	8.16866199131250	2.39548046574840	-2.48054200935607
H	8.17282168749374	3.24252759380868	-4.35959082081035

4.4.7.8 Alternative P–P cleavage steps

4.4.7.8.1 Alternative fifth P–P cleavage starting from VIIIa instead of VIIIc

IXe˙

E= -1350.82092032 Eh

0 2

P	-8.06836795546902	-1.71335839683136	-4.03181838644448
P	-6.37220477763271	-0.48364577978070	-3.54862151875334
Sn	-4.64907919429222	-2.15625734340544	-2.76184790968182
C	-3.57465405713612	-1.18420767578314	-1.17857280552176
C	-3.32480729281363	-2.58758407538163	-4.39195919292210
C	-5.59721594399744	-3.93739607839543	-2.04372772477759
H	-2.81454976028232	-1.67559284728395	-4.70270161943848
H	-3.86743578642157	-2.99406126945040	-5.24434981857090
H	-2.57999631886804	-3.31675889673496	-4.06866283695424
H	-3.12934892562043	-0.25711438183195	-1.53974323516474
H	-2.78238178276585	-1.83994082726377	-0.81378910829460
H	-4.25208203778928	-0.95602102507637	-0.35545570708381
H	-6.14896980898753	-3.71301705457364	-1.13063781708718
H	-4.84838660952882	-4.70216179703084	-1.83151381478544
H	-6.29612241699282	-4.31401868249862	-2.78985061041048
Sn	-7.18924490265631	-2.62458383969085	-6.20305712120610
C	-6.41962659144988	-4.61574403437447	-5.91645850853104
C	-5.68143158087419	-1.36284980942816	-7.06954151673946
C	-8.85991611867868	-2.75094946891114	-7.54487361378432
H	-9.64153105279268	-3.37764673178039	-7.11441580510292
H	-8.54375168188690	-3.18242666562118	-8.49587090337809
H	-9.26759951933066	-1.75594219080027	-7.72535938761970
H	-5.04803996562775	-0.92500866446864	-6.29896112098441
H	-6.16370572914659	-0.55599574820651	-7.62203138285648
H	-5.06230404432441	-1.94451627455576	-7.75411519103703
H	-6.03610544100580	-4.99377396443956	-6.86585624064774
H	-7.22136062671713	-5.27095836236035	-5.57400871239864
H	-5.61590510164859	-4.63232684246090	-5.18108730168352
H	-6.77771497526231	-0.12027127157947	-2.23365108813939

TS(IXe˙→Xe)

E= -1685.25400570 Eh

im. freq.= 868.44 *i*

0 2

P	-8.35483986930780	-0.28870128794962	-4.60720487899636
P	-6.31118426899988	0.30932234625928	-4.15702404556715
Sn	-5.28931280885310	-1.27361067103072	-2.48770989523015
C	-3.86908561101088	-0.09265954171358	-1.39020792406524
C	-4.26556222140239	-2.82312988464196	-3.56438459138111
C	-6.67716744550559	-2.15001842091143	-1.10581179798623
H	-3.53478821863650	-2.38294877026150	-4.24338416844266
H	-4.96693565617242	-3.42435948549257	-4.14257149717943
H	-3.74494065473673	-3.47453983946133	-2.86062851404754
H	-3.18718600674178	0.41329698360083	-2.07370135492646
H	-3.28996624418442	-0.73563758688580	-0.72528867003221
H	-4.38886208583228	0.65584884458175	-0.79165299844455
H	-7.37706096776047	-1.39522971362020	-0.74709881159014
H	-6.12900815895227	-2.56193879249264	-0.25618214621055
H	-7.23605982770909	-2.95047868155154	-1.58881259417234
Sn	-7.87449909449810	-2.27846027168633	-6.05717723236663
C	-7.83073397724662	-4.09171178693528	-4.89336265879627
C	-6.00825678982250	-2.05169763227374	-7.08641832339717
C	-9.49037282743052	-2.43316038539021	-7.46248075109676
H	-10.43156254250803	-2.18483261411264	-6.97234345769214
H	-9.55256232767331	-3.44975191150697	-7.85209812140969
H	-9.33473875872677	-1.74269810066180	-8.29102342792432
H	-5.19763230928232	-1.89635857777125	-6.37480015125958
H	-6.05409543824634	-1.19267902308316	-7.75560565490457
H	-5.80333169492695	-2.95088558866389	-7.66969421076790
H	-7.25790890366284	-4.85376189127518	-5.42488440262878
H	-8.84620385608557	-4.46084387471964	-4.74477293759668
H	-7.37261718861639	-3.92294111427605	-3.91904047158068
H	-6.63049293439420	1.29743474866405	-3.18580154356150
H	-8.93092985514992	-1.33017695719401	-3.36473199601370
Sn	-10.28165081686198	-2.36008646407045	-2.40358481092484
H	-11.92883284297738	-1.67127309281074	-4.46922998451317
H	-9.32868817338457	-4.93024386075608	-2.27517449641650
H	-11.21887612395766	-0.08448454918942	-1.22423433808769
H	-10.37349697929331	-1.06324468893935	-0.00865796323484
H	-9.19917884357999	-4.17706615204185	-0.67155712432722
H	-11.44321493278366	-3.36640902636570	-4.66628232178413
C	-11.76790710028998	-2.61452117117927	-3.94582423457612
C	-9.83331639270341	-4.29182771135842	-1.55054940489420
C	-11.06860899607375	-1.09651986111576	-0.84815933734659
H	-12.71252361384649	-2.93710635102452	-3.50404038982493
H	-10.77075047098011	-4.76632490187370	-1.25234725998891
H	-12.02473616919020	-1.49176640681716	-0.49959910481169

Xe

E= -1351.43353942 Eh

0 1

P	-8.14815783708573	-1.70433505878414	-4.07317698708880
P	-6.39677313217733	-0.45870820518254	-3.56263621895481

Sn	-4.70845357423903	-2.09327675107952	-2.67695127902459
C	-3.55686079082221	-1.06983995476654	-1.18221494006168
C	-3.39256014608347	-2.69707275922652	-4.26164666820816
C	-5.63396926845419	-3.82909087974625	-1.81841095214624
H	-2.88487194081827	-1.82524311732209	-4.67558453015361
H	-3.93731334241099	-3.19868338374414	-5.06116605403833
H	-2.64290379525114	-3.38445510560953	-3.86606893372704
H	-3.12083700821839	-0.16224673483809	-1.60061352602485
H	-2.75201522186514	-1.71696317589040	-0.82969200220487
H	-4.18893312172949	-0.79999302246551	-0.33587172874069
H	-6.38152247557591	-3.53460320056227	-1.08154407655036
H	-4.86921132775196	-4.43290466745105	-1.32659486354302
H	-6.11488351958048	-4.43346103979672	-2.58753292010009
Sn	-7.30577811120848	-2.59127115110669	-6.27722806093547
C	-6.54274179521605	-4.58437183112948	-6.01997721948162
C	-5.80433069665120	-1.28565661810602	-7.07433773913439
C	-8.97065266995655	-2.64925463380013	-7.62756600415571
H	-9.75784573320343	-3.28984981337721	-7.22870067226386
H	-8.65662588771321	-3.03768495807434	-8.59752575295280
H	-9.37278154481672	-1.64461197709365	-7.76216452665688
H	-4.91855721134681	-1.27950582868611	-6.44029950053240
H	-6.19449738351496	-0.26984972642327	-7.13700533976121
H	-5.52667427687923	-1.62474089728965	-8.07369852231414
H	-6.06628040880091	-4.92337213804513	-6.94143122375971
H	-7.36293732020907	-5.26154725740493	-5.77875686040885
H	-5.81161162317313	-4.61946045698213	-5.21245503725935
H	-6.85314453628686	-0.08680527670538	-2.26789952236755
H	-7.87024429895943	-2.90879037931053	-3.36869833744877

IXf˙

E= -1017.52670165 Eh

0 2

P	-8.89890213816106	-2.97020493113288	-4.52336309456754
P	-7.22914106012661	-3.56501250028977	-3.29201818567944
Sn	-7.54850317775030	-2.86810052661564	-6.64509502547368
C	-6.52709691897928	-4.72744153601072	-6.97883678016806
C	-6.10591636202898	-1.28791532624751	-6.47727457262520
C	-8.91742841705922	-2.49581602435221	-8.25191967143247
H	-9.63771285466757	-3.31083597305570	-8.32589973337091
H	-8.37115439647980	-2.42036273805892	-9.19328033477611
H	-9.45600221066357	-1.56393836213567	-8.07952875021014
H	-5.42416076766392	-1.50305695909175	-5.65420552769729
H	-6.60624281641055	-0.33954521674213	-6.28289510726816
H	-5.53529742857507	-1.20820538056631	-7.40382214174385
H	-5.66134168216593	-4.80861009462968	-6.32135889102883
H	-6.18673232445105	-4.77210462428564	-8.01467231774279
H	-7.19603178229344	-5.56766689662376	-6.79110159534378
H	-7.92436722756595	-4.22823942677221	-2.24930894820775
H	-6.77384843495760	-4.75020348338945	-3.92760932266393

TS(IXf˙→Xf)

E= -1351.96439809 Eh

im. freq.= 651.19 *i*

0 2

P	-8.88838269837942	-4.31238343691912	-3.91366998125796
P	-8.02019545593315	-2.93976799799059	-2.42589397933982
Sn	-8.31839156418412	-2.97440101887781	-5.96572696805225
C	-7.09891878226597	-4.22176712068977	-7.21699569760523
C	-7.26428220117906	-1.15771167469609	-5.51982002562126
C	-10.14498293888617	-2.50370203627208	-6.99733546158538
H	-10.77278170411654	-3.39154801309678	-7.07810010357414
H	-9.91782454554108	-2.13968017409945	-8.00063492201505
H	-10.69606955084538	-1.73061052999467	-6.46182931871578
H	-6.29414314035467	-1.37408906671572	-5.07259072042707
H	-7.84123759459517	-0.53852824393497	-4.83318250948442
H	-7.10633401494927	-0.60465724509413	-6.44736461450138
H	-6.11006832984666	-4.34109063328386	-6.77374180386994
H	-6.99360972054950	-3.76957162779458	-8.20446114092592
H	-7.55762012665183	-5.20496181934491	-7.32277118877619
H	-7.69418349472399	-3.92381058188936	-1.45522820607526
H	-6.69637494700075	-2.87784730642276	-2.93166650484700
H	-10.38149075240083	-3.40129100714656	-3.78690355779835
Sn	-11.62220859913463	-2.02962048697270	-3.30100374090033
H	-13.24913233469623	-2.08902235625767	-5.49145669936503
H	-12.42432212734975	-3.21314296380299	-0.97555571971535
H	-10.53689793187782	0.03143936888875	-4.74342466479726
H	-9.78198981190873	-0.04112836058249	-3.13569549071725
H	-11.10228134845331	-2.07752665730734	-0.63521233848025
H	-13.92517729263894	-3.15568663899070	-4.24463776603638
C	-13.45215254617897	-2.19026291366088	-4.42514606295450
C	-12.02446720071058	-2.22378413907438	-1.19786263913131
C	-10.72430257701134	-0.11142310632967	-3.67905356406602
H	-14.13762532004255	-1.39812144873276	-4.11757272028406
H	-12.75245236293265	-1.47007173864087	-0.89170746986033
H	-11.39528898465854	0.67696097572752	-3.33198441921839

(Me$_3$Sn)HP˙

E= -675.68135662 Eh

0 2

P	-2.04379445914334	1.02420699181242	-1.05586605321901
Sn	0.02017449621090	0.01765076694463	-0.03142632070508
C	-0.08876049093769	0.22964690246720	2.10049820108619
C	1.75847419366742	1.04342106938557	-0.76720497365601
C	0.14482498475284	-2.06337830198265	-0.55190878133248
H	1.69221949965412	2.10724944172850	-0.53887130700074
H	1.83934679582860	0.91810492725541	-1.84718939506377
H	2.65290946468595	0.63421241446371	-0.29458225208024
H	-0.13497387268385	1.28405898995917	2.37428145407432
H	0.79472345895238	-0.21488084591420	2.56133805643013
H	-0.97653803160648	-0.27259483290225	2.48577145474191
H	-0.70940304268924	-2.60532501799211	-0.14601920849694
H	1.06243568811034	-2.48942916993056	-0.14284539821437
H	0.15347177518984	-2.17770709554591	-1.63604382776817
H	-1.59464045999178	0.67751376025108	-2.36530164879572

4.4.7.8.2 Alternative fifth P–P cleavage starting from VIIIb instead of VIIIc

IXh˙

E= -1017.52727334 Eh

0 2

P	-3.30754552994930	-0.83943710609445	-1.47448329738396
P	-3.63644953355814	-1.20406969146510	0.63292490250261
H	-3.24212427630211	0.57489406608094	-1.33515497837332
Sn	-5.54435059753481	-2.83883838083351	0.39211121558630
C	-4.80799922820315	-4.42568781231388	-0.84068776519627
C	-6.03775842200333	-3.55498670843717	2.35229810202579
C	-7.21027455398281	-1.85291102037785	-0.52627905892980
H	-7.58696393325242	-1.06624781863406	0.12775747831395
H	-8.01175633920607	-2.56720449279909	-0.72123209801894
H	-6.88938080270985	-1.40865748328833	-1.46864969226952
H	-4.45292992316183	-4.02412802800950	-1.79002741168730
H	-5.60702058811394	-5.14255294295310	-1.03583754448454
H	-3.98577081727715	-4.93938456265959	-0.34231718829997
H	-5.15916226922056	-4.00842835251253	2.81148051335866
H	-6.83018695533195	-4.30222493173178	2.28727777268435
H	-6.37991480521916	-2.73188217052104	2.97995163008400
H	-4.40700142497338	-0.06352256344997	0.98197742008796

TS(IXh˙→Xf)

E= -1351.96166815 Eh

im. freq.= 838.16 *i*

0 2

P	-2.00543488971176	-1.35809150684505	-0.82582987589325
P	-3.09633421217662	-1.78341677904766	1.01045269490239
H	-1.41139429176642	-2.64819417393330	-0.88401016169315
Sn	-5.12190594873870	-3.06628953543571	0.23177144002863
C	-4.39585053124843	-4.86523476593358	-0.68479714380671
C	-6.26846676425063	-3.59329068009216	1.97054359021229
C	-6.33178681271392	-1.86431496284392	-1.07436326725644
H	-6.89490977091133	-1.14602122995220	-0.47761205246474
H	-7.02979144284148	-2.49185472704859	-1.62982343196186
H	-5.69970749207009	-1.32307163229801	-1.77762607261137
H	-3.64304632810611	-4.63743855627438	-1.43931523624030
H	-5.21653889256718	-5.41054949131838	-1.15291922683764
H	-3.94475462316325	-5.49826743847367	0.08016208815280
H	-5.65672407494879	-4.18217108742841	2.65448755098988
H	-7.13947427485449	-4.18165854758011	1.67752868807771
H	-6.60811452157882	-2.69495900770995	2.48673133544699
H	-3.75890040869719	-0.52804216106287	1.06504742029856
H	-3.01603811687000	-1.86042553256153	-2.15499782210972
Sn	-3.45258321444014	-2.58132485244400	-3.90225316033202
C	-3.32947926251551	-0.97042605893155	-5.32510924628962
H	-2.36100585947835	-0.47563140322339	-5.25278652748753
H	-4.11531771167086	-0.23821240232011	-5.13863573275768
H	-3.45082323803340	-1.36757613452773	-6.33476551539116
C	-1.86243310643533	-3.98188022378061	-4.28417622229024
H	-1.94716736334305	-4.36440662933893	-5.30316302887020
H	-1.91796952123214	-4.82050415914544	-3.58923288529289
H	-0.89412749616728	-3.49405607104193	-4.16998709521551
C	-5.34095128023137	-3.58613401405076	-4.16074103540044
H	-5.34868139481946	-4.06830777594687	-5.14051624932249
H	-6.16145709619252	-2.87077952862055	-4.11107739588910
H	-5.48054023822527	-4.34562893078864	-3.39256642269522

4.4.7.8.3 Alternative sixth P–P cleavage starting from Xf instead of Xb

TS(XIb˙→ Me$_3$SnPH$_2$)

E= -1010.11947952Eh

im. freq.= 205.28 *i*

0 2

P	-3.12780017274960	1.95348724569212	3.06368492654077
Sn	-1.25517676643077	0.69453657803857	1.97255099358905
H	-3.57071155870625	0.35660536829919	3.94268909558746
H	-4.05896963104449	1.52918109006933	2.07304143296819
C	0.16473465262885	2.06013190003995	1.11848490107878
H	0.57314039286771	2.70859748457549	1.89399287097186
H	-0.31401995770848	2.67985115322261	0.36014626318266
H	0.98128456079223	1.50178833609673	0.65729681825380
C	-0.25594572547912	-0.47764261436098	3.47455656426756
H	0.75815183057127	-0.71392383239857	3.14859329103657
H	-0.79379007735453	-1.41158923485632	3.64279677210441
H	-0.20397228599979	0.07292036391279	4.41448237971729

C	-2.00555773146134	-0.61733144966690	0.44824015898632
H	-1.19045832267552	-1.19836076831635	0.01375763162139
H	-2.48540388002988	-0.03736496345067	-0.34066396251414
H	-2.73741897696405	-1.30179973888535	0.87825460683925
Sn	-4.13177583109283	-1.21107771464319	4.72789807815267
C	-6.20699962413711	-0.98106719802947	5.23145652428073
H	-6.33444657177307	-0.14607337281899	5.92066471902736
H	-6.57862362805064	-1.89116429730819	5.70514790714676
H	-6.79127460413465	-0.78687999091286	4.33170876794868
C	-2.95927238700621	-1.54471225986519	6.49684695601555
H	-3.08663740834443	-0.71577621930409	7.19331735081943
H	-1.90396398184790	-1.62929011422157	6.23675985354569
H	-3.28015892774777	-2.46748173172329	6.98321172684143
C	-3.89060944016718	-2.86207169794071	3.37033051747426
H	-2.84485144558266	-2.97637260722223	3.08390341859219
H	-4.48752291850541	-2.70347641752321	2.47172796119028
H	-4.22412958186624	-3.78147329649866	3.85478147473356

4.4.7.8.4 Alternative sixth P–P cleavage starting from Xa instead of Xb

TS(XIf'→ $(Me_3Sn)_2PH$)

E= -1343.41596117 Eh

im. freq.= 362.61 *i*

0 2

P	-6.39713088193473	-0.96440402487073	-2.25276920469705
Sn	-4.26117986502652	-1.90557989273870	-3.14875952177375
C	-2.46648962087018	-0.99305606523870	-2.38871323958775
C	-4.27122669256438	-1.58365392600953	-5.27577530815166
C	-4.19717470100858	-4.00641831053256	-2.71034276628984
H	-4.17966276292648	-0.51743461072662	-5.48870344532504
H	-5.20104914534772	-1.94883808689354	-5.71206269984344
H	-3.43143404925059	-2.10473655547546	-5.73843577231800
H	-2.46256938953469	0.07356078204385	-2.61351441514755
H	-1.60120103383706	-1.45471496603936	-2.86827291234755
H	-2.38006938924939	-1.12829682842020	-1.31045484435391
H	-4.21178739399833	-4.15584498194023	-1.63027620334684
H	-3.28550497622894	-4.44703662628356	-3.11731185708431
H	-5.06136216491517	-4.50741184113205	-3.14650892075552
Sn	-5.59080527167440	-0.26824368214829	0.00928427124224
C	-4.61342998848821	-1.90590214211844	1.00498655256097
C	-4.23642745829942	1.40408003867386	-0.05145214649926
C	-7.32109614259082	0.32761471995890	1.13463210451828
H	-7.85614447827538	1.11179523492579	0.59754590184175
H	-7.02401841576116	0.70888699542035	2.11308428144029
H	-7.99148028776378	-0.52108429412133	1.27242763865457
H	-5.23309895791686	-2.80101492355263	0.94672109670109
H	-4.45121713361914	-1.65510825095699	2.05460646317929
H	-3.64895500713614	-2.11385635635081	0.54073247112507
H	-3.35741950425743	1.16545962491405	-0.64854854800685
H	-3.91878433294424	1.64726239632512	0.96422739349196
H	-4.73154581204629	2.27715062160513	-0.47781095745655
H	-5.89224901459772	0.66029097511499	-2.96135903960367
Sn	-5.49678731828305	2.28772287503072	-3.76366803794514
H	-2.99810934901749	2.69023638002664	-2.74096857005474
H	-5.63219971239308	1.46003330595564	-6.35561402352551
H	-6.17528683045350	3.90370669177765	-1.66759881462307
H	-7.61243347701058	3.59926614373383	-2.66134541666194
H	-7.25913623554248	1.89288313388971	-5.80002409518667
H	-2.85311736121005	1.93182024488634	-4.34065673008325
C	-3.38281642527874	2.68812043031806	-3.76069921507751
C	-6.21019434072336	2.18911841047564	-5.78727979396139
C	-6.54665954406663	3.82678055138513	-2.68968635677760
H	-3.19917156756074	3.66624279307712	-4.20917158718707
H	-6.11184289475820	3.16627170454518	-6.26348313434547
H	-6.40380107163773	4.78722231146599	-3.18809059673724

4.4.7.9 Structures calculated for NMR predictions

Bu_3SnPH_2

0 1

Sn	-0.28936279533172	-0.74590173721437	0.42060385502517
P	-0.41989079856249	-0.45426649810538	2.93594834251022
C	-2.18189869417144	-0.06863344005175	-0.39545739587389
C	-2.80098237659643	1.08483494232518	0.37770615010488
C	-4.12069487030108	1.56806175804944	-0.21038105728990
C	-4.73775895151376	2.71923512167119	0.56584467403688
C	0.04323837876774	-2.85563619668520	0.05344507106154
C	1.28861898699752	-3.38756963763665	0.74418713105456
C	1.54073690954485	-4.86820191405256	0.48811130775924
C	2.78664755072586	-5.39299839579792	1.18141701358977
C	1.34952670172139	0.42357879334052	-0.39168313261699
C	1.20537074427757	1.91394716271391	-0.13565870922484
C	2.37256304816423	2.73999062115570	-0.66181986098974
C	2.21850044731523	4.22860036680591	-0.39953880373925
H	0.98984512062614	-0.56724511334948	3.09533117941555
H	-0.36444014850531	0.96497007929655	2.85826083359345
H	-2.85809864374353	-0.92418353194774	-0.41406012821581
H	-2.00552794691642	0.21452772428127	-1.43475497038088
H	-2.10392151905392	1.92624199737342	0.42049531352072
H	-2.96499780889401	0.78737440021088	1.41692449937049
H	-4.82101486783053	0.72952537440201	-0.24665874271897
H	-3.95847269501561	1.86833059718928	-1.24898681017334
H	-4.93820311216174	2.43584317062739	1.59956192951401
H	-5.68009557160209	3.04126573248991	0.12384502035660
H	-4.07178797360593	3.58259711838183	0.58746541977812
H	0.10974797978338	-2.99959875133604	-1.02646863131384
H	-0.84439151310476	-3.39352342502458	0.38839887576138
H	1.21242290477472	-3.22531926150621	1.82299869864028
H	2.16623256695245	-2.81962087999852	0.42160196469126
H	1.62034071893240	-5.03409065619856	-0.58948468105251
H	0.66760916821902	-5.43813038433400	0.81599092245050
H	3.67811889897331	-4.86109006901478	0.84699481785792
H	2.94121100279732	-6.45273694697892	0.98106260327987
H	2.71872103837993	-5.26855587433617	2.26265287541469
H	1.40056102700356	0.21748734595103	-1.46265289943864
H	2.27265466061413	0.04243931836168	0.04668906410108
H	1.09899968322774	2.09746051342779	0.93723300045357
H	0.28073404296634	2.28079464826987	-0.59046721988801
H	2.47966448244206	2.56308326154952	-1.73524724734280
H	3.29704239902108	2.37809746030597	-0.20442536097749
H	1.31834750887762	4.62185112067545	-0.87336327073380
H	3.06662497553281	4.79414666262320	-0.78417906696895
H	2.14181622847236	4.43520405178996	0.66848429489789

$(Bu_3Sn)_2PH$

0 1

P	6.18264619950252	1.18217031078901	-0.10583371042508
Sn	3.88087546619954	2.16400731260384	0.24331692236538
Sn	5.65576694368287	-1.28038342770262	-0.19930867993347
C	2.96125312377423	1.55556644296313	2.11458674648960
C	4.17941757722979	4.32226267377374	0.15778277395513
C	2.67249591395247	1.49371753021214	-1.42821107631382
C	3.38269220722097	1.62276703112066	-2.76473221108864
C	2.56973212650336	1.08935637192471	-3.93666428944450
C	3.30105509735220	1.17741620448503	-5.26468775487289
C	3.17328587351453	5.08157887291839	-0.69288873450506
C	1.75564665564783	5.06500775667085	-0.14670594955108
C	0.76658088197500	5.82201400871753	-1.01511742704706
C	1.61936063781224	2.21931787265594	2.37234814181061
C	0.94346644572511	1.75191877633666	3.65594751705930
C	-0.39111128894949	2.43275107036737	3.90844284184801
C	4.71308170408044	-1.76127602993883	-2.09300376330791
C	4.79374708745384	-3.24179815631893	-2.43140884206591
C	4.14251059418582	-3.61819513113006	-3.76143238615865
C	2.63505882686788	-3.43309985754271	-3.79331728701812
C	7.57624472740528	-2.28806432046631	-0.04912419902459
C	7.46603280542192	-3.73369083689131	0.41155933714863
C	8.80095511044656	-4.47275914564558	0.49620753284149
C	9.75509075235785	-3.91644396763919	1.53943248584089
C	4.45050520179030	-2.02390776488738	1.44877204897161
C	5.04411956032883	-1.67367080946245	2.80325084808089
C	4.36740953926306	-2.35810611126807	3.98968950995244
C	2.92065613893629	-1.95116087098397	4.20762273887983
H	6.49138814724558	1.14901305259356	1.28541009520128
H	2.85380511419015	0.47324721821011	2.07723768763957
H	3.66438959183212	1.77237895569737	2.91933849549087
H	5.19022677402125	4.46007606193967	-0.22360145840558
H	4.17654015241853	4.69731357441475	1.18261636467252
H	2.40301210486079	0.45439991310665	-1.23373824919748
H	1.74020392488991	2.05975848200817	-1.42969034994692
H	3.63503072207970	2.66940894322770	-2.95406275126243
H	4.33925973874034	1.09659051476303	-2.73033925065141
H	2.30112316806360	0.04967602659424	-3.73469097858304
H	1.62540685510036	1.63708627493224	-3.99407325930887
H	2.69474464503426	0.79147170337898	-6.08358315842580
H	3.56248467941620	2.20856177069721	-5.50477087432186
H	4.22795946285780	0.60323138770449	-5.24200948684200
H	3.49486496536240	6.12453638241550	-0.78963831191870
H	3.16712035157866	4.68398383446545	-1.71110198847695
H	1.42015912592022	4.03149633271068	-0.03447338614894
H	1.75777161395374	5.48403558028231	0.86300185874866
H	-0.23932265587305	5.79161761440294	-0.59774300980407
H	1.05020028817799	6.86995483637113	-1.11650996981090
H	0.72058177070249	5.39803410451512	-2.01889356294839
H	1.74079201446784	3.30428654275226	2.41364123168253
H	0.94212938666241	2.03141221390051	1.53376936085150
H	0.80323458410503	0.66938369239339	3.61105438356480
H	1.61599238916489	1.93294517452681	4.49856600339309
H	-0.85327736562962	2.08090172170846	4.83024715726702
H	-0.27406121104223	3.51396282356104	3.99009693718022
H	-1.09149424975040	2.24124364442700	3.09469057883529
H	3.68071602040556	-1.42300786090893	-2.03282890758512
H	5.19461720384584	-1.16573552498294	-2.86891810620791
H	5.84119288604255	-3.55019237067818	-2.46128281562480
H	4.33198322485715	-3.83358239361084	-1.63497131705424
H	4.37871446328041	-4.66243987712545	-3.98187790181304
H	4.60200165023856	-3.02926359064331	-4.55989269548609
H	2.21537641644177	-3.77158243069012	-4.74002060634072
H	2.34919296025311	-2.38988455088685	-3.66963673103942
H	2.15298495547499	-4.00237561082019	-2.99709680818739

H	8.18525295942453	-1.69725361240104	0.63304727347832
H	8.05879860543071	-2.22816925592773	-1.02589640919967
H	6.80961867170643	-4.28711665192723	-0.26371845685213
H	6.98163022597177	-3.77519034736199	1.39100185535667
H	8.60286494369041	-5.52519146346485	0.71598809741390
H	9.28016242130477	-4.45402191257442	-0.48639277450724
H	10.66215011284099	-4.51642673414077	1.60555909622597
H	10.05792191144180	-2.89610672056659	1.30999895105515
H	9.29351458704403	-3.90824287554821	2.52817258079071
H	3.43651444584584	-1.64389081139084	1.33786034436015
H	4.39358797091615	-3.10721233926290	1.32230396426895
H	6.10434624338735	-1.93960914850457	2.81899968736806
H	5.01196735464175	-0.59092036374568	2.94611914073443
H	4.94140677305830	-2.13736598626782	4.89348842933141
H	4.42783463958864	-3.44141362815600	3.85248659757499
H	2.49595528045189	-2.45118678940363	5.07758708837818
H	2.29585882704031	-2.20287966935503	3.35157300801582
H	2.83639224714185	-0.87699766301626	4.37105217258406

$(Bu_3Sn)_3P$

0 1

P	-39.33005720086326	0.09268066038786	1.35220223463611
Sn	-37.32508756670529	1.00411286392173	0.14155377957442
Sn	-39.24641390006443	-2.30849692051389	0.63571041901404
Sn	-41.20333898776916	1.04813706634389	-0.01100088352548
C	-40.65617578126074	-3.39104803600061	1.88541794151324
C	-39.42587447513971	-2.73215880326428	-1.50020963573107
C	-37.27046799048431	-2.96588212875513	1.25655540896861
C	-37.02917174243383	-2.77335363559530	2.74323860453374
C	-35.61634559364475	-3.13800203695897	3.17984016812734
C	-35.36967198324076	-2.92217817661211	4.66277660650179
C	-40.22255719883998	-3.96715670657139	-1.89170048246323
C	-41.71797735166002	-3.89618269557645	-1.60875623364427
C	-42.43436148298901	-2.78263438389180	-2.35214323934040
C	-40.35695462261744	-4.88139202574357	1.93091094905163
C	-41.33010177830486	-5.69858101453220	2.77944620131053
C	-42.72212814051002	-5.81254883620014	2.18152988045606
C	-37.72506120496729	3.10761372682039	-0.23694009594932
C	-36.47765178077623	3.89705178053199	-0.59375119067495
C	-36.74666951914106	5.36976978359239	-0.87670438102667
C	-35.49417784611811	6.14627386148402	-1.24513007584256
C	-35.70539829456702	0.95157847966706	1.59508612735077
C	-34.31692713951394	0.93528740922681	0.97412116500780
C	-33.17800696774739	1.13840035490108	1.97189693705886
C	-33.05931931276963	0.04352289522008	3.01750762048473
C	-36.60697795505970	-0.11565292971884	-1.59436038318652
C	-37.31383231117599	0.07448541752322	-2.92471181454291
C	-37.19008887236994	1.46233209499244	-3.53852786575262
C	-35.77163551419430	1.85037573003725	-3.91927748602614
C	-41.43939998803628	3.08978222143618	0.70482283085759
C	-41.66296508910203	4.12253059264599	-0.38641490923046
C	-41.80512372055973	5.55601699736357	0.12387499853303
C	-40.54135974465456	6.11998817538484	0.75037924972183
C	-40.89464149783513	1.05493366644877	-2.16097216770406
C	-42.15669852142788	1.30870839278448	-2.96969506017397
C	-41.90994405911082	1.44141629722712	-4.47197589127589
C	-41.33897649741812	0.19374310849907	-5.12396656669535
C	-42.98552104803625	-0.07742636143829	0.51080863136559
C	-43.28712579918091	0.00574981504699	1.99832944817697
C	-44.59606534129087	-0.66101500637225	2.41637484265803
C	-44.60776768644963	-2.16970536826368	2.24643713492364
H	-40.58448855431409	-2.95123144422471	2.88081737980319
H	-41.66268882917588	-3.18761405513908	1.52912548813941
H	-38.39389333973645	-2.82968978715685	-1.83714456424025
H	-39.81612167956862	-1.84302672921598	-1.98637488880904
H	-37.15453926725830	-4.01405567985138	0.97427683339710
H	-36.53495408901426	-2.40684121872943	0.67682097682744
H	-37.22974755484899	-1.73490048262435	3.02000552488692
H	-37.74403451529217	-3.36848943607915	3.31841837826639
H	-35.41972877198477	-4.18137942280405	2.91912066051405
H	-34.90537333266702	-2.54514471502320	2.59985565743321
H	-34.34610859613829	-3.17199990068860	4.94046258081273
H	-35.54184435591308	-1.88254404303707	4.94302247513456
H	-36.03627072581924	-3.53705261692710	5.26859216224078
H	-40.08698027930151	-4.14657295885873	-2.96478806199899
H	-39.80873115232593	-4.84779122037546	-1.39507804250623
H	-42.16730678100686	-4.85480545134320	-1.87779772299908
H	-41.88372906004940	-3.78347711907147	-0.53699641120787
H	-43.50778892889755	-2.80982791613086	-2.16828962199621
H	-42.08207308655746	-1.79932970756024	-2.04866653425469
H	-42.27941351090756	-2.86516290061368	-3.42852831415899
H	-40.35065850481127	-5.29753522992204	0.91961796122288
H	-39.34574406848792	-5.03117320624160	2.31569953991808
H	-40.91777204874566	-6.70157894952881	2.91701912272795
H	-41.39010701009568	-5.25639967215370	3.77756488407294
H	-43.37195665354066	-6.42778110254984	2.80307042857295
H	-43.20054798886339	-4.84136900046003	2.07596694336896
H	-42.68502581084342	-6.26834526516789	1.19108821054194
H	-38.47975322180700	3.19260044703104	-1.01814580974978
H	-38.17920115616198	3.49791740830607	0.67406880204981
H	-35.74955694569350	3.82191516421836	0.21843401468533
H	-35.99070507520698	3.45904153402640	-1.46807302329428
H	-37.48004653299068	5.44680112676108	-1.68406916289599
H	-37.21716620444303	5.82035753835734	0.00271209070468
H	-35.71475763327988	7.19498447978992	-1.44181564693624
H	-34.75739885257117	6.10953046254343	-0.44198335962360
H	-35.02354421508009	5.73490525149201	-2.13891116639144
H	-35.86549228698572	0.08801205497859	2.23649573390457
H	-35.83498909010049	1.83349417526593	2.22584990707528
H	-34.23812193931538	1.71254004712888	0.20938335709332
H	-34.16282620082731	-0.01067640589707	0.44760315924330
H	-32.23752757348789	1.21229424272803	1.41923541896236
H	-33.31293454956248	2.10377304060625	2.46771969058697
H	-32.20467483241931	0.21263360407776	3.67177321741643
H	-33.94500501311558	-0.01278954709498	3.64774172352770
H	-32.92726653079583	-0.93315339083504	2.55004910061077
H	-35.54750138965030	0.12488240597242	-1.67452000363170
H	-36.65063454687799	-1.16113197420651	-1.29289795898380
H	-36.92225921206320	-0.65509758658648	-3.64311326850437
H	-38.36992169239833	-0.16570457148429	-2.81445572543459
H	-37.82338854446460	1.50626337229883	-4.42742604905199
H	-37.59741913028177	2.20237314390686	-2.84824677328279
H	-35.74162540713257	2.83611804836549	-4.38256831701207
H	-35.10965726633670	1.88099918617947	-3.05489263113010
H	-35.34739007012340	1.13858789262922	-4.62867312227416
H	-42.27347904924221	3.09083618122488	1.40827590447079
H	-40.54637145573112	3.30924110966128	1.28586884377559
H	-40.84132790633759	4.08879483507900	-1.10744329278803
H	-42.56308152557811	3.86906676797933	-0.95125387577377
H	-42.10611276768037	6.19489149118780	-0.71063114062969
H	-42.62467063091779	5.59589683756766	0.84651914612139
H	-40.67670864908442	7.15946572620844	1.04753552531101
H	-40.24505661197261	5.56493046864140	1.63913910918667
H	-39.70846245475490	6.08138499718782	0.04876340022994
H	-40.45537747366881	0.09513793784841	-2.41703647726946
H	-40.13899535097989	1.81019300659318	-2.37838433055118
H	-42.64640233591939	2.22025256967718	-2.62184329136721
H	-42.87315072550091	0.50149915479220	-2.79609102214821
H	-42.85241936522389	1.70377593086639	-4.95959086652692
H	-41.23549916037157	2.28474237276984	-4.64412616080053
H	-41.23172024373888	0.32520127829503	-6.20019723339480
H	-40.35600064612004	-0.05660530421967	-4.72852041935952
H	-41.98807812349997	-0.66698799209777	-4.96002780122003
H	-43.81497935968853	0.32367026846196	-0.07539814852293
H	-42.84287595878933	-1.10654583573190	0.18827588066813
H	-42.46238673074544	-0.43528932518454	2.56470615485477
H	-43.32565983447784	1.05360224681606	2.30556421121159
H	-44.79165841010703	-0.41954970891494	3.46434386371312
H	-45.41795694718190	-0.21893457176951	1.84628480126986
H	-45.54890159759649	-2.60211787409222	2.58476256815932
H	-44.47206113478926	-2.46386592540603	1.20617223157214
H	-43.80749343292550	-2.63011688800372	2.82604324039382

$(Ph_3Sn)PH_2$

0 1

Sn	0.15990070463911	0.23075402356736	-0.07811065536761
P	0.44359305920493	0.47495005457824	2.41489189447708
C	1.27477201674504	2.42822741760216	-1.93412887529737
C	1.35824086746445	3.67607721245483	-2.53856963739945
C	0.45572461739799	4.67417085324685	-2.20004012357628
C	-0.53012957975108	4.42277574406196	-1.25535806772184
C	-0.61047102426614	3.17565686262903	-0.65074265098182
C	0.29012858409182	2.16528513802701	-0.98424533096671
C	3.06267484024442	-0.80214260977908	-0.36193770967900
C	4.09875245821969	-1.58098181148961	-0.85967661254698
C	3.83726375483071	-2.56203607775835	-1.80646671072911
C	2.53881510783567	-2.76208672208513	-2.25374254288013
C	1.50377009131786	-1.98108054816757	-1.75586552321116
C	1.75550012382274	-0.99216524701221	-0.80700881783798
C	-2.51343693916017	-0.05094975857100	-1.59410813999945
C	-1.70871584095653	-0.65859346866982	-0.63275543213722
C	-2.12969784112560	-1.85860830238527	-0.06328588575171
C	-3.32996484116142	-2.44112209193476	-0.44647257802595
C	-4.12582155011243	-1.82595332632565	-1.40360705502502
C	-3.71646406081723	-0.63056342772252	-1.97706248683846
H	1.98400370953113	1.65628384750864	-2.20806631795135
H	2.12777653066448	3.86832388829357	-3.27514666696592
H	0.51952185750620	5.64683066224788	-2.67065784393542
H	-1.23622141026400	5.19874613646181	-0.98881317819174
H	-1.38724254292013	2.99567116404727	0.08385072664104
H	3.28121467384039	-0.04462882585732	0.38173188554981
H	5.10983826999080	-1.42432110988259	-0.50636735769671
H	4.64418072465155	-3.17058475337730	-2.19364729552986
H	2.33084936544425	-3.52785269572362	-2.99001413130186
H	0.49352139171445	-2.14926864736851	-2.10994962952754
H	-3.64510429603850	-3.37434692754189	0.00243488749194
H	-5.06280183402402	-2.27821449609943	-1.70158257784466
H	-4.33387859072924	-0.14816757449769	-2.72397629401002
H	-2.20403335287622	0.88192266828441	-2.05006434712658
H	-1.52082167694355	-2.35066581777520	0.68665353166938

H	-0.27988619647160	-0.72011665936187	2.68438494637299
H	-0.72038337423982	1.28501200947537	2.52859115190268

$(Ph_3Sn)_2PH$

0 1

Sn	2.01897960138033	-0.78965854744900	-0.71141138263333
Sn	-1.76810846410583	-1.14269251483552	-0.69165530939807
P	-0.00134570818548	0.44331320492660	0.12904912925234
C	2.78280324366052	-3.21399107461663	1.03089604771704
C	2.89593696886445	-4.54924752205524	1.39491791093354
C	2.42335537654129	-5.54209810696477	0.54889915121946
C	1.83854235829641	-5.19767400381181	-0.66114404871483
C	1.72843846490547	-3.86339814602760	-1.02297270102099
C	2.19810922441726	-2.85718351903674	-0.18245882068896
C	4.94568671724880	-0.42459960931475	0.21998769257935
C	6.04223090281596	0.21877971872683	0.77846377315260
C	5.90945385150561	1.50299632617472	1.28830008609058
C	4.67799892981944	2.14093480567688	1.23850353008821
C	3.58264346833716	1.49533566587797	0.67981888892749
C	3.70462597127227	0.20742937207486	0.16417542819550
C	2.64297768821793	-1.50329933559102	-3.65920955901262
C	2.59416965098499	-1.37689846829688	-5.04166454971086
C	1.85983864919873	-0.35155351846966	-5.61968071372152
C	1.17246261516692	0.54497210114607	-4.81426910479708
C	1.21980154172387	0.41487677070896	-3.43471042081489
C	1.95568710120703	-0.60868343842195	-2.84201235026317
C	-4.65982133956752	-1.20025979868765	0.39034285322385
C	-5.86780471442226	-0.69105846312101	0.84813138869016
C	-6.03911649792506	0.68022626420153	0.97970998869559
C	-4.99854652610544	1.54011725006616	0.65727425042554
C	-3.79012475061568	1.02847881313025	0.20209381213267
C	-3.61022183016025	-0.34556431681770	0.05985361858086
C	-2.64469107545498	-0.18718754288874	-3.48814822911592
C	-2.70041125597226	-0.15905300563000	-4.87576587538974
C	-1.97392250961507	-1.07816008688455	-5.61922362075880
C	-1.18995960759893	-2.02326930368926	-4.97326027413259
C	-1.13183818350310	-2.04547653676721	-3.58799916026221
C	-1.85660302916573	-1.12871756823454	-2.83039292615178
C	-2.08277065609339	-4.20544083457774	-0.78641579842210
C	-1.98663688067102	-5.51952111633311	-0.34550299572384
C	-1.35956606119004	-5.80319880508098	0.85868945942236
C	-0.82490659512535	-4.77273246094701	1.61929841751678
C	-0.92000207952938	-3.46249068157004	1.17645586744532
C	-1.55080585032716	-3.16482478078219	-0.02815736409732
H	-2.98043597363122	1.70982398923679	-0.03244293194207
H	-5.12592171098433	2.60978592159171	0.76476864289801
H	-6.98014393167163	1.07751483980729	1.33760916443517
H	-6.67495226124785	-1.36519533112836	1.10498199354280
H	-4.53644523045278	-2.27333508771225	0.30073034520658
H	-0.47979992458850	-2.67120276724958	1.77067930884328
H	-0.32017726608566	-4.99098854542178	2.55078243401260
H	-1.27890898180611	-6.82702222663310	1.20040162151656
H	-2.40242364077219	-6.32067868988182	-0.94335763862892
H	-2.57253948402899	-3.99905784660213	-1.73074693942061
H	-0.50589608781816	-2.78094489146759	-3.10036316626161
H	-0.61146702880642	-2.73434651113528	-5.54762457309722
H	-2.01485947379529	-1.05512144358764	-6.70057689895627
H	-3.31666329314305	0.57733716659015	-5.37576323703566
H	-3.23023411965650	0.52609258152046	-2.92004258312668
H	0.66383226648474	1.11374208235420	-2.82155315889035
H	0.58561558680437	1.33629355233893	-5.26105981866250
H	1.81615488990869	-0.25611848903374	-6.69690154400470
H	3.13249368810017	-2.07824420699432	-5.66657756153929
H	3.22176506277774	-2.30916238285349	-3.22350094833272
H	2.62594239997889	2.00379250074533	0.64908002389127
H	4.56946793426949	3.14190773589718	1.63612045406662
H	6.76363875323076	2.00469295917997	1.72426917812310
H	7.00079715500077	-0.28300002584530	0.81535384640311
H	5.06530292798238	-1.42985667188183	-0.16679669907563
H	3.16087206088539	-2.44917870368183	1.69891795137137
H	3.35339666393595	-4.81399040137727	2.33978848417209
H	2.50378113122165	-6.58272807648705	0.83525430270422
H	1.45549277365430	-5.96723032830412	-1.31803360769818
H	1.26839699217916	-3.61133155660437	-1.96947443836887
H	0.05889040894364	-0.13682947838648	1.42752942229597

$(Ph_3Sn)_3P$

0 1

Sn	1.58446054856098	1.37989328618921	3.33064980921104
Sn	3.33909711343256	-0.78261243170809	0.61403178258682
Sn	-0.49665069126447	-0.19574750244688	0.38424716787774
P	1.63917598575451	1.04654774293519	0.84584830308018
C	1.53785314212818	4.27007760133634	4.39194458876650
C	1.02618522974748	5.53441404818653	4.65643212389267
C	-0.24975014774683	5.87187040940535	4.22673185527730
C	-1.01167253247933	4.94278198694764	3.53115412885849
C	-0.49838772281200	3.68106811729737	3.26426237898286
C	0.78046595445629	3.33208231441694	3.69347887955245
C	4.64043610468654	1.91727393215221	3.33498107930698
C	5.94903712063151	1.83443076381529	3.79048452758996
C	6.22685897558392	1.17896700374008	4.98192540840011
C	5.19366986985654	0.61245196379758	5.71723486822373
C	3.88790321348598	0.68540685613388	5.25154421984185
C	3.59955900501925	1.33462713031769	4.05265910859831
C	0.68039835953886	-1.37921312367244	4.44277175741128
C	-0.01838478649718	-2.25066514750373	5.26804746293042
C	-0.92077560315542	-1.75538358830978	6.19892474704374
C	-1.11452817720823	-0.38418365503776	6.31027769514359
C	-0.41417753169191	0.48576792383511	5.48586437620990
C	0.48352353116087	-0.00505458585457	4.53915456106417
C	4.26596885993866	-2.05642973635903	3.26681582503802
C	4.28597792264292	-2.97790226793939	4.30470791546257
C	3.48734500013549	-4.11166355231242	4.24539705864663
C	2.66793883626465	-4.32185438006112	3.14459487644502
C	2.64258185699015	-3.39804796830079	2.10865812383553
C	3.43887466184731	-2.25431953422358	2.16232117389725
C	6.41125048341770	-0.45189012007689	0.84567682272738
C	7.64047464536308	0.18579911352934	0.74071654885096
C	7.71236683162443	1.48078974597828	0.24714368565713
C	6.55201349838378	2.13325599453319	-0.14769547554715
C	5.32508902426024	1.49276447989686	-0.04133742547231
C	5.24074725339647	0.19721279894530	0.46228525562832
C	3.17127301723664	-3.09536755559138	-1.45419203498591
C	2.81634462547593	-3.71403123158869	-2.64539946800290
C	2.17020354460256	-2.99179810335109	-3.64037661133505
C	1.89999664407520	-1.64366067743911	-3.45014625983253
C	2.26713634486036	-1.02680883184596	-2.26215243522157
C	2.88889193719236	-1.74716315971786	-1.24605552165247
C	-2.72406539462554	1.84772548864054	0.83183424760462
C	-3.71603843332850	2.56296051949801	1.48916329729066
C	-4.07001106130494	2.22731964198574	2.78879326471420
C	-3.43251785165820	1.17168463002641	3.42396044185471
C	-2.44095010589204	0.45724741708336	2.76519909894733
C	-2.07030786285002	0.78961067177045	1.46421346308196
C	-0.36719448310120	1.34105805085058	-2.30606864276053
C	-0.60580995366439	1.59084311736264	-3.65100234443212
C	-1.36790153653300	0.70236254215635	-4.39755694996438
C	-1.89738845186349	-0.42861727578830	-3.79183930215042
C	-1.65851118120378	-0.67354434937900	-2.44591837450752
C	-0.88483081185364	0.20393147328424	-1.69005775264733
C	-0.96022648574303	-2.92817946382540	1.80793220249136
C	-0.97196826482045	-4.30978915563318	1.93725056243617
C	-0.55421805364630	-5.11143629008972	0.88408780947655
C	-0.13081983318078	-4.52444453670448	-0.30004925354337
C	-0.11889273303355	-3.14186229209472	-0.42862808073875
C	-0.52622434193959	-2.32788716357625	0.62765665640954
H	1.37363009610534	-1.78548908030352	3.72134521899117
H	0.14610796669872	-3.31639823686528	5.17697624216587
H	-1.46763542300139	-2.43402126495123	6.84093478824666
H	-1.81350930698464	0.00766478045623	7.03828743008752
H	-0.58491543818092	1.55204649501999	5.56953859974361
H	3.09440742044836	0.21242010938676	5.81706846126520
H	5.40637372705504	0.10336997438643	6.64883539918145
H	7.24692644280035	1.10952639297539	5.33726267380623
H	6.74870252844845	2.26777412670242	3.20526083191997
H	4.44402904373820	2.42521495594888	2.40077431047906
H	2.53523800344962	4.01849112427240	4.73313453712254
H	1.62438907161211	6.25550717544621	5.19892975648032
H	-0.64883821861885	6.85673053986221	4.43330152545050
H	-2.00798077043745	5.19656001404148	3.19269519451076
H	-1.10756534868097	2.97208466297100	2.72210395405079
H	-1.94820019168476	-0.34499525650758	3.29309192064146
H	-3.69693447336401	0.90528783213157	4.43878289009567
H	-4.83838346924547	2.78830214215517	3.30479402487056
H	-4.21055403242701	3.38404401081742	0.98614142264273
H	-2.46085984146437	2.12049489589362	-0.18279303364755
H	0.22433198644273	-2.70671405919302	-1.35584860286786
H	0.20097820365846	-5.13874835400166	-1.12651664700148
H	-0.56050662763645	-6.18918360360392	0.98484454977895
H	-1.30574009590500	-4.75836345063460	2.86419623086724
H	-1.28003091253322	-2.32724279691064	2.64592876364272
H	-2.07270367537339	-1.56543299505646	-1.99161586333858
H	-2.49436636473809	-1.12346828102447	-4.36868223811581
H	-1.55113203938736	0.89275339239963	-5.44721009207279
H	-0.19423970965113	2.47696835612696	-4.11725840825927
H	0.24236395469428	2.03394183858180	-1.73725290715091
H	2.03966325299103	0.02175318192346	-2.12771208628294
H	1.38924654667402	-1.07342891240219	-4.21446656787920
H	1.87985222946717	-3.47850359620916	-4.56249514968804
H	3.03571744991428	-4.76392197134398	-2.79346244362066
H	3.65461397675847	-3.67859644658658	-0.67995554462101
H	4.42471660375567	2.01786669961232	-0.33948821310138
H	6.60287313835641	3.14157950760149	-0.53849654249706
H	8.66984238124351	1.97925174922489	0.16709298143207
H	8.54226261697551	-0.32805523177750	1.04844938415627
H	6.37330426751860	-1.46056440083997	1.23897857170372
H	4.88371260835439	-1.17229377878632	3.33682680357202
H	4.92208304742427	-2.80388988811106	5.16278773233091
H	3.49974161888513	-4.82719110351550	5.05755157887418
H	2.03696469698817	-5.19930194102050	3.09115564263498

H	1.98095184760168	-3.56617376600831	1.27090817854678

(*i*Pr$_3$Sn)PH$_2$

0 1

Sn	2.30988926595271	-1.61966966823679	-0.61236422837023
P	2.42588638623449	-1.81701510406494	-3.14441267850710
C	3.03493794983308	0.54856471810161	1.48713830620296
C	1.63806143057190	1.36294933216536	-0.45170918310836
C	5.19668170513159	-2.54376904215639	-0.18744301283141
C	3.61761223133884	-3.37305119858670	1.59868660996507
C	-0.07517374403551	-1.94952030815388	1.35069384979228
C	0.05185998983629	-3.67155642264755	-0.49237420912496
C	0.26682784400626	-2.21744621305195	-0.10591787838094
C	3.79680962300299	-3.04645909819580	0.12514662393614
C	2.75573042587160	0.43753501192191	-0.00281830694849
H	1.64234324785092	-0.64857855702125	-3.35971519730999
H	3.64978619179678	-1.09589977540368	-3.23431006773785
H	2.17394879485209	0.25282138941227	2.08649911668508
H	3.87654531569987	-0.06936736501268	1.79652805989673
H	3.27347625636351	1.58056366515185	1.76192485155642
H	3.66427864901813	0.68976848555801	-0.55316863159899
H	1.46933157876127	1.30930323025157	-1.52694713327915
H	0.69446180568654	1.12426253841253	0.04038252023248
H	1.86922352763085	2.40444102938131	-0.20974254197827
H	5.42048703780405	-1.61468818239284	0.33828244418086
H	5.95271561742379	-3.27267783879678	0.11887540283878
H	5.33894786262145	-2.35845822999567	-1.25178634563724
H	3.61049614107815	-3.94872337602739	-0.46063944562981
H	2.63790877760037	-3.79877969611702	1.81018602993620
H	4.36480393653278	-4.10104803543708	1.92871043675387
H	3.73417027122937	-2.49165566236636	2.22904323556580
H	0.56582677662434	-2.51298327350804	2.02851253888777
H	0.02021785502085	-0.89628896247809	1.61122699899270
H	-1.10589856419921	-2.24486311843364	1.56845178868421
H	-0.36555247485723	-1.58929205451511	-0.73683137523526
H	0.26280893126369	-3.85184005535173	-1.54577691872388
H	0.68923313649711	-4.34020065387719	0.08727914762408
H	-0.98210690574374	-3.97781359682785	-0.30810220642951

(*i*Pr$_3$Sn)$_2$PH

0 1

Sn	3.82701329202637	1.13206093717924	-3.53894110034339
Sn	2.35428936090204	-0.52193721107087	-0.20694021296438
P	1.66438326778981	0.39790240392210	-2.46146478375234
C	4.37117170583371	2.14041643130731	-6.43772903420057
C	2.26051659003806	3.03619992469796	-5.38793435627942
C	3.19830391242231	1.84840771236588	-5.51560522317107
C	3.51617756045880	3.62586592129132	-1.76715989500667
C	5.65460646773307	3.59760230812514	-3.09364199400068
C	4.64059089591717	2.76746925678153	-2.32257762561102
C	6.62959184615722	-0.11482447507657	-4.01459478621074
C	4.69288217001035	-1.46962345208932	-4.91281836094438
C	5.19476668045063	-0.56439831901343	-3.80167206078649
C	2.39978009808802	1.18590863627222	1.16241988630797
C	4.27442317081489	-1.58999142139932	-0.15188657997128
C	0.67266014748583	-1.86307110416167	0.23188475963710
C	0.74124876727644	-3.10135584314486	-0.64608164427790
C	0.54581034465209	-2.20805972029299	1.70601838035618
C	4.32310083526407	-2.59213363965257	0.99014704639395
C	5.43266005568432	-0.61063751224903	-0.08672504545721
C	1.05220633373892	1.88769361701145	1.15332646521516
C	2.83523948177232	0.79591574273796	2.56567432451734
H	4.99446782173598	2.95061137866647	-6.06031347239772
H	5.01477924543328	1.27336045426695	-6.57883619792046
H	4.01972207262097	2.44530642179807	-7.42850920945743
H	2.63573314059189	1.00508493315338	-5.92304658876619
H	1.42049588423575	2.82661351150207	-4.72678499966980
H	2.77688899457908	3.91374167657051	-4.99748599918946
H	1.85017760367868	3.31802936090964	-6.36255454692901
H	2.97660485836600	4.14205814075921	-2.56017549252085
H	2.78525494615251	3.04377647478421	-1.20973615855514
H	3.90720692784731	4.39290582328757	-1.09178620464005
H	5.15158331884126	2.27923503737843	-1.49060617709276
H	5.19428191661676	4.10318730137528	-3.94222192713303
H	6.08345252213677	4.37620941311681	-2.45538624526223
H	6.48099480899496	3.00077088976693	-3.47709121269562
H	7.00227891743481	0.47280154988535	-3.17600558188481
H	7.29643132637137	-0.97532087171370	-4.12842316189947
H	6.73842219443065	0.49149244784059	-4.91418705194626
H	5.13393687839894	-1.11064974527321	-2.86196558841981
H	3.67526234158010	-1.81533897730859	-4.72973908994664
H	4.69873006237456	-0.97066866633683	-5.88183114222932
H	5.32554946762107	-2.35736259590513	-5.00810739126827
H	-0.13586846597583	-3.73727667862465	-0.49272509845266
H	1.61742276520325	-3.71081260660659	-0.42196449667529
H	0.77816484479129	-2.85145286983114	-1.70587853034122
H	-0.19725130515697	-1.27478767185656	-0.06717115072094
H	-0.31447447337893	-2.86260170184523	1.87838137538917
H	0.40415153195835	-1.32237804635468	2.32336263042943
H	1.42355570256656	-2.73264279023136	2.08278348943074
H	4.21627228243073	-2.10707101715755	1.96067147351666
H	5.28185021970588	-3.12000407064778	1.00271690762074
H	3.54125089334512	-3.34538327950535	0.91415082096099
H	4.31793267315115	-2.13164961342888	-1.09824053609042
H	5.41420123325283	0.11095148182955	-0.90085394921613
H	6.39281916681937	-1.13257927173770	-0.14007685083360
H	5.42900211953647	-0.04537550585878	0.84518115342738
H	1.07367887004883	2.79014442891758	1.77185229389958
H	0.26420292676879	1.24727731121713	1.55200926993191
H	0.74901136724522	2.18501933117034	0.15014802718059
H	3.15051036990727	1.85761201789806	0.74255290025568
H	2.87331108285124	1.67402215074900	3.21779343135268
H	3.82479513244972	0.34135089443101	2.58135224128895
H	2.14528377406863	0.08966537483423	3.02629464385457
H	1.69245729205177	-0.88039971022618	-3.09209134943457

(*i*Pr$_3$Sn)$_3$P

0 1

Sn	0.54853241007887	-0.85973569378274	-4.02224060785990
Sn	2.65690303377349	-0.56915520747179	-0.41976908882829
Sn	4.44365653120812	0.77205183445949	-3.81266701585748
P	2.79772197292025	-0.90434264400518	-2.91521086220656
C	-1.45357548593132	0.39310322178447	-2.04598376897611
C	-0.47968540537709	2.04478246979549	-3.69615731994201
C	-0.96354382824193	0.62690548941228	-3.46239662618819
C	1.83665753410749	-1.76695496854305	-6.69302843446103
C	-0.38516756639063	-0.60477160890949	-6.95480488116631
C	0.91786854628877	-0.67384319614516	-6.17623775384973
C	0.62206086147292	-3.96483313281462	-3.88157386071920
C	-1.69327546823973	-2.99106202364344	-4.08438354190569
C	-0.29914253058149	-2.81861961217937	-3.50364332328694
C	2.78237610932451	1.33934951802917	1.99182416330291
C	1.07407718652303	2.04131976483517	0.29371184994587
C	5.69475142973182	-0.30786434439167	0.10983145788050
C	4.58001689515114	-2.00574239697704	1.58950595961257
C	0.61605404630979	-1.75438840199220	1.62085984647792
C	1.40509495094212	-3.35919660469549	-0.15683756116162
C	1.03223127774127	-1.92346537375475	0.16965991009890
C	4.61065864899832	-1.36727526529823	0.21070141759661
C	2.43945789563030	1.42102491916764	0.51215865661583
C	6.21282302926597	-0.53409825065362	-3.73396529112749
C	6.08465920848924	-1.60818895361445	-4.80082384921722
C	7.54201290985278	0.19672612196154	-3.78683570699933
C	4.63686017445115	2.57865197529668	-2.57390221685788
C	5.72582517060721	3.50565435217541	-3.08872743210715
C	3.30292838747673	3.29033403746460	-2.44586873593962
C	4.06682659176191	1.34575263232300	-5.90077872692443
C	3.04920954287321	2.46784718878375	-6.00882251889788
C	5.36106894077147	1.70596637700429	-6.61400364165538
H	-1.88253710128545	-0.60047515525973	-1.92083024401194
H	-0.64815175844942	0.49203964011090	-1.32154686886711
H	-2.22358941920337	1.11915709619805	-1.76730473287639
H	-1.78390268369235	0.41876241926731	-4.15457895158677
H	0.40025235713063	2.27538014927363	-3.09729511857651
H	-0.21497175401655	2.21744992269796	-4.73924374751745
H	-1.24964961095390	2.77607240680277	-3.43112282908456
H	2.13184487011405	-1.57387588731755	-7.72912954114161
H	2.74675083185537	-1.85828810513495	-6.10177076815181
H	1.34584227125046	-2.73933369754268	-6.67914362795669
H	1.42700618004410	0.28358646470155	-6.27238742876449
H	-1.03045005477290	0.20514529198401	-6.61526323525144
H	-0.19352365318314	-0.44066114920444	-8.01984024355679
H	-0.95297287335470	-1.53156675238160	-6.87485346105216
H	1.63903900003582	-3.81104141452139	-3.52399277330335
H	0.26178874306124	-4.91058103263530	-3.46552842492638
H	0.67553450538895	-4.09224170793039	-4.96234548102873
H	-0.37907914728894	-2.78307563236285	-2.41617797802004
H	-1.67222103646426	-3.03241885254993	-5.17346990782719
H	-2.14672369688603	-3.92610728689070	-3.74091722760685
H	-2.36770472608197	-2.18276146078483	-3.80193817841145
H	2.10247110251994	0.68504784006672	2.53570053803289
H	3.79374719056721	0.97937222522446	2.16691178250249
H	2.70904428200113	2.32829255647411	2.45545359672319
H	3.18999736172127	2.03607793650352	0.01777877906395
H	0.82697535163277	2.14191678156476	-0.76000182449736
H	0.28323823783722	1.45337910633682	0.75984617338334
H	1.02802922097187	3.04213882569544	0.73398670333730
H	5.52892299997784	0.51282158574361	0.80786972842338
H	6.67771580962314	-0.72893368260847	0.34253375512149
H	5.76077376995878	0.12453038648190	-0.88632153598152
H	4.80862222419410	-2.14151327768430	-0.53283140870209
H	3.85552111462568	-2.81504925201275	1.65616169520651
H	5.55834365032072	-2.42655572738323	1.84303380795570
H	4.33505187964364	-1.28510386120892	2.36913661107481
H	1.43543225517244	-1.96641824180782	2.30770048367362
H	0.26140294942133	-0.74705557780155	1.83320872556444
H	-0.19643468149641	-2.44313298648151	1.87305428890005
H	0.19737272235632	-1.62703041815917	-0.46647479474403
H	1.72792717692425	-3.47755634298529	-1.18858736156040
H	2.21364798208792	-3.71900090521542	0.47886663417885

H	0.55429289182806	-4.02895682923967	0.00130135422311
H	6.89309336995133	-2.34094648856342	-4.71666615051215
H	6.13467257062768	-1.19595292707398	-5.80875135002797
H	5.14328446388331	-2.14884654613820	-4.70894970108014
H	6.11709188297213	-1.02007127339766	-2.76242471874555
H	7.65995683311675	0.77397084292384	-4.70376439938737
H	8.37616552682111	-0.51113506771582	-3.74765917021997
H	7.66463594781696	0.88233263166962	-2.94894030087689
H	6.99901707587457	3.02140455856087	-3.14047138618306
H	5.83056808059640	4.37875772244050	-2.43713349930190
H	5.49398333894826	3.88252845590469	-4.08494851345395
H	4.93049153948832	2.20221954814790	-1.59266859094633
H	3.34748030085777	4.08474703418509	-1.69504281306358
H	2.50708151072165	2.60992863140186	-2.15493325532659
H	3.00387053691333	3.75284128942357	-3.38458397622617
H	2.76952581608121	2.64232473783639	-7.05232473239567
H	3.45435838399039	3.40579500976349	-5.63032342778136
H	2.13499558712900	2.26495646194456	-5.45427269831164
H	3.65820745146674	0.44712694297643	-6.36070813580675
H	5.16348817647905	1.96607548640989	-7.65868369824080
H	6.07682950923233	0.88694541396104	-6.61677060614864
H	5.85088236060479	2.56791991399558	-6.16092633341886

(TerMe$_2$Sn)PH$_2$

0 1

Sn	-0.93526340558298	0.71780191633318	-0.81179052163135
P	-1.44273741850548	2.84425184694364	0.47500720500339
C	0.86749700651909	1.17616561491009	-1.89418248558441
C	-2.46714825846335	0.70123875244590	-2.32895527051242
C	1.66565899721760	-2.59751437285670	-1.51858162022377
C	5.49768182879980	0.55145639927903	-0.74901300201665
C	1.63662478116720	0.50795340339185	2.44661093149240
C	-3.36242106471632	-2.71656255323360	-1.46118290496362
C	-7.21605936088794	0.39955334386005	-0.67437471218370
C	-3.40468443892697	0.29494910926071	2.57693436829245
C	-4.00866951998026	-1.64533721756597	-0.63749505290017
C	-5.25550074450010	-1.14360061649418	-0.99692258504301
C	-5.88695690333177	-0.15206663102034	-0.25817698802412
C	-5.24893255321338	0.31998857461156	0.88454337173833
C	-4.01231022106315	-0.16818242964778	1.28857443202790
C	-3.37449329180708	-1.13717326259839	0.50120544567425
C	2.31710055472582	-1.53405660853298	-0.68916208716243
C	3.55524585889872	-1.01740998918861	-1.05705502382588
C	4.17389680934824	-0.00997019469105	-0.32969044071300
C	3.52274271260981	0.47629530951379	0.79968824533413
C	2.29017184371177	-0.01954422415669	1.20623120502388
C	1.67890483457458	-1.02632637105695	0.44720425370544
C	0.37353161681369	-1.59296652204686	0.87447682758046
C	0.39656372493036	-2.70376261490612	1.71712482124419
C	-0.77877704168013	-3.29167255630118	2.15002191542931
C	-1.99241033787368	-2.76744031084558	1.73930023655048
C	-2.04144421817451	-1.65648302945827	0.90091233083480
C	-0.85285415995179	-1.05771555383908	0.45447096215726
H	-2.78283832431445	2.45652201677054	0.73804911936560
H	-0.98345915560286	2.37806085004408	1.73545556299957
H	-3.54638948638458	-0.45292185674661	3.35898957646657
H	-2.33397422104609	0.45437728326797	2.48948142149322
H	-3.86095411010687	1.22103338017007	2.91803281958321
H	-5.73301652985353	1.08180796501087	1.48526794378840
H	-7.59649223818623	-0.10269112809223	-1.56080527921122
H	-7.95839386036167	0.28764924243323	0.11626065221601
H	-7.14989929595133	1.46458557555148	-0.89937251972464
H	-5.73806756015400	-1.52741083991972	-1.88809658514457
H	-3.88225309111435	-2.85369830544385	-2.40629296273718
H	-2.31949495469446	-2.48876332719236	-1.67252251117445
H	-3.36499515277383	-3.67287811280296	-0.93672522825602
H	-2.92142089193158	-3.21495131101040	2.06951401137448
H	-0.74945050669338	-4.15314213495895	2.80446383069530
H	1.35409646233842	-3.10190300188010	2.02874911210648
H	2.29520742789671	-2.88602278273197	-2.35678007947493
H	0.70968248573434	-2.25674285315324	-1.91800908399345
H	1.44869891129286	-3.48945908600228	-0.93243743536125
H	4.04374444507199	-1.40618640585070	-1.94287029379008
H	5.89141126978268	0.03557635761522	-1.62170858650362
H	5.41704061193028	1.61008316914986	-0.99848344148638
H	6.23624339192882	0.46839904896333	0.04864813444885
H	3.98941898861186	1.26266861929242	1.38217322424137
H	1.59970697481988	-0.25199395952582	3.22762428170994
H	0.60690283759945	0.80806127162955	2.26383750267716
H	2.17490178045881	1.36701665525008	2.83911756555152
H	1.12734019720638	0.37291451833661	-2.57690791193329
H	1.70472000713810	1.35179034335026	-1.22922115912588
H	0.66780880301177	2.07843375211051	-2.46831185688844
H	-2.26492822218932	1.53140422021522	-3.00211880649142
H	-3.44948618076200	0.82349260060333	-1.88830243504094
H	-2.45127162535952	-0.22313510916288	-2.89895739588407

(TerMe$_2$Sn)$_2$PH

0 1

Sn	-1.52181921546428	5.54330271332078	1.84659221174780
Sn	-1.93267312892968	1.94501741940155	0.58955780553199
P	-2.59926793393810	3.38913400227282	2.56255528411275
C	-1.25527850531980	9.30794471009773	0.44736792696330
C	3.68745467412978	8.48904491320480	0.31530775404655
C	1.17070580262110	7.74386379906741	4.58266459219617
C	-0.01389098465788	8.81969841310914	1.13064109487433
C	1.20074122861475	8.83910016957321	0.45007105999275
C	2.39618361470972	8.50856856796950	1.07388264012705
C	2.35836294892043	8.17111589925861	2.42267821743380
C	1.16628465799409	8.11991647982555	3.13225462290742
C	-0.03457892519657	8.41850701366651	2.47211289038354
C	-7.62923155698566	3.30168441581967	3.74454797038073
C	-5.25697667795664	7.13519190886293	1.56719103465624
C	-3.42598942242395	5.10322635139325	5.80285693417228
C	-5.32652470666007	6.12619502172884	2.67248363907695
C	-6.34342655273213	5.17761143885292	2.68112248407360
C	-6.46212039630555	4.23875243721728	3.69817773951182
C	-5.49626495954842	4.23195469717318	4.69662395722067
C	-4.45809924294689	5.15616554883737	4.72013156651803
C	-4.38280356726227	6.12254168821094	3.70731952454979
C	-3.37914397504036	7.21722348880791	3.79290188090344
C	-3.72177975080788	8.30724191761146	4.59614401789613
C	-2.88460492734940	9.40193349509764	4.70916819544117
C	-1.68974870121088	9.41719419557259	4.01030639237012
C	-1.32302267079859	8.33993982738330	3.20877059470806
C	-2.16358346824995	7.21834803033108	3.09662756171948
C	0.56536697831885	5.11634773726778	2.13280027772536
C	-1.87746142151857	5.99731023512066	-0.24196309930788
C	-0.18684452240551	2.63868473692570	-0.47213838529806
C	-3.50446669016182	2.15263180323435	-0.87069387110567
C	1.40802370178577	-0.70166539789836	-0.33072481546821
C	4.25266185697174	2.85118796126689	1.78345083985956
C	0.10943426248427	1.27977055743278	4.11839741690465
C	-3.61430881385841	-1.64277070742281	-1.22453263277398
C	-8.00758334710296	0.64758868985821	-0.46048392992997
C	-4.63515147417098	0.46615883061594	3.24118442420936
C	-4.54022508379968	-0.89587697961946	-0.31415771330904
C	-5.80363838291613	-0.52329623393307	-0.75244076255954
C	-6.67449035152512	0.20027949935260	0.05546505388952
C	-6.25696464460064	0.52714233002092	1.33808279967638
C	-5.00559083753798	0.15697195784429	1.82299413111204
C	-4.13478510633742	-0.54226386536233	0.98068750184010
C	1.66286783034730	0.24549171913447	0.80131883479875
C	2.79785664344218	1.04935725408644	0.79945263566555
C	3.06333051402072	1.94259068891995	1.82923878879055
C	2.17200238330101	1.99563000630248	2.89486076253296
C	1.02691309325881	1.20909274632888	2.93717686359200
C	0.76029883492277	0.34373039034504	1.86659690974818
C	-0.45273253291596	-0.51384405660785	1.88886028492565
C	-0.33118661645989	-1.79102251944018	2.43439481400720
C	-1.42078641925956	-2.64133492269327	2.50086737059962
C	-2.64584064711047	-2.21340206698418	2.01964554279525
C	-2.79003590125881	-0.94259959560980	1.46721820042248
C	-1.68833279449900	-0.07707653430972	1.38762125992490
H	1.21097893897192	9.13488736348974	-0.59279374692126
H	3.95428813049189	7.47151831834576	0.02336492151178
H	3.62689745699646	9.08177769560709	-0.59508830740679
H	4.51035034486242	8.87480661392598	0.91531247479647
H	3.28259046316170	7.92131456118818	2.93127714689501
H	2.13050062265579	7.32512497397916	4.87621665831889
H	0.97825453987411	8.60970335460035	5.21700627809390
H	0.39303357637887	7.01855948961236	4.81437509244715
H	-1.02881397429029	10.27236715451980	4.07600839281230
H	-3.16576200555355	10.24224271012500	5.33064845657933
H	-4.66638776915405	8.28598039139069	5.12497632767683
H	-2.43984968581631	4.90809141978517	5.38112221002763
H	-3.64509952917657	4.31062730986318	6.51381949243628
H	-3.35800342273483	6.04406468494159	6.34688027587930
H	-5.55380800754715	3.49140518293530	5.48569633435741
H	-7.36611587010443	2.34512193086902	4.19245997179142
H	-8.43876945454039	3.72144190332185	4.34481158150739
H	-8.03213650750481	3.11373487028137	2.75130977418028
H	-7.07834709256383	5.19082042431119	1.88452389857716
H	-6.16106359628738	7.11974120915609	0.96315904971919
H	-4.41663943267307	6.93340098176190	0.90453677480587
H	-5.11584197218462	8.14422165804316	1.94988139594753
H	-2.23730355203256	5.11156074072516	-0.75443779284452
H	-0.94452578150768	6.31969868602751	-0.69728400100752
H	-2.61318071341114	6.78532643844157	-0.35880044426862
H	0.74519359924605	4.07234161846581	1.90578297720615
H	1.17115385060672	5.74029976767173	1.48476940792980
H	0.85448271131751	5.29673149967870	3.16229721254130
H	-2.14652816590618	8.79628114438302	0.79485707754898
H	-1.40534455455671	10.36929686666653	0.65456585240392
H	-1.18679183286402	9.19192161713324	-0.63171640172510
H	-3.88157627891824	3.65215828847325	2.01478275427465
H	-4.82878443992314	-0.39437404876995	3.88475077269204
H	-3.58282519008570	0.70844709774088	3.35069426366308
H	-5.20785702345148	1.30662017470488	3.62248506791656
H	-6.92410852707997	1.07920932126271	1.98675551335229

H	-8.47489926089201	-0.11608807697257	-1.08055165473309
H	-8.69106973846289	0.88727903191550	0.35165163857735
H	-7.90778683033751	1.54300819053575	-1.07694895026751
H	-6.11077503840320	-0.78839413235726	-1.75783840247168
H	-4.04312357993962	-1.75235540693156	-2.21774463046138
H	-2.65644067234838	-1.13189471344962	-1.32063526252638
H	-3.38993914879441	-2.63771616537149	-0.84083727169481
H	-3.51089009870814	-2.86266165266281	2.07237891067772
H	-1.31739475821472	-3.62899776602436	2.93137383856931
H	0.63268055920845	-2.10738006353792	2.81329473749671
H	2.12172792366318	-0.55169852311256	-1.13730964425474
H	0.40399898169886	-0.58095561817599	-0.73485655294460
H	1.48167335432557	-1.73976307344724	-0.00585129746170
H	3.48580477904064	0.98449453826228	-0.03567985114480
H	5.00344127512131	2.49540155961778	1.08088972210337
H	3.96052897440541	3.85570250245999	1.47107052735683
H	4.72216847560822	2.94628608169130	2.76161793263383
H	2.37193615622177	2.67260244448974	3.71709166779323
H	-0.04812220578924	0.29559619709677	4.55755498858079
H	-0.87452331929920	1.66005413208491	3.84643883229388
H	0.51224115176944	1.93627646893680	4.88601415780096
H	0.03749025098447	1.94290514047542	-1.27684898419054
H	0.68461890655062	2.72330861664745	0.16189468331655
H	-0.41295584246641	3.60847902124563	-0.90556531626023
H	-3.44809174060315	3.16266801981355	-1.27053601008885
H	-4.47647920062905	2.00289866843822	-0.41649509507997
H	-3.38140797552391	1.44720982632739	-1.68752531112081

1 (Ter(Me)$_2$Sn)$_2$P$_2$H$_2$-meso

0 1

Sn	-1.21024451699000	6.43092718315536	1.76694394771242
Sn	-1.89687654039984	1.06329839138541	-0.08160035510073
P	-2.49980898234210	4.29111645190349	1.32522118704870
P	-0.79805292637393	3.33239022665007	0.20563151122314
C	-0.82241447380865	10.40549939841748	1.26392552518245
C	4.00182711198185	9.70606567039816	2.44351542135940
C	0.42380713845108	8.00017832791553	5.51302958867930
C	0.21050879142979	9.81654939358413	2.17640650558309
C	1.56328649677955	9.99541632569256	1.90661864246699
C	2.55016368309656	9.54276964536376	2.77382601151464
C	2.15175645769364	8.91033215533936	3.94593167067497
C	0.81161141260588	8.69634401765520	4.24469783956981
C	-0.16523802815259	9.13252182190489	3.34033365453389
C	-7.12806964078758	3.66116172962550	1.00464448425809
C	-4.83110876781097	8.10543190115085	0.69040836676875
C	-4.12868723124103	5.17737646084580	4.72902986068947
C	-5.08661489913005	6.83673988700664	1.44520006873193
C	-5.93340311155541	5.86892277609020	0.91740803241082
C	-6.22701914444267	4.69693596598879	1.60125594071990
C	-5.63149677585372	4.49972073833135	2.84083061985479
C	-4.76887160916174	5.43567605823230	3.39925221963436
C	-4.50047090215495	6.61803993614248	2.69742557834626
C	-3.66533755063961	7.68216830372677	3.31257742047768
C	-4.30665293160576	8.58484220082470	4.16196894622340
C	-3.61405927486101	9.63228353403767	4.74273492936572
C	-2.26627731321415	9.79144351302917	4.46866712703764
C	-1.60424977015269	8.90159384881389	3.62696361545867
C	-2.29731643987341	7.82732888959439	3.04672090359538
C	0.70433251333069	5.84890545596387	2.56420844694691
C	-0.86116132389312	7.22472791527565	-0.20954523012501
C	-1.08931358871111	0.30574197102817	-1.93742124382266
C	-3.96856425018899	1.49685028636404	-0.46598467698430
C	1.18249300364690	-1.81237538868539	-0.36343092638521
C	4.19387026434075	2.19009174415392	-0.64242904652959
C	0.77025440015808	1.90706278223000	3.00632558708850
C	-3.85701720223862	-2.51240595733682	0.08438205139498
C	-8.16728582756309	-0.17378370612202	1.13138509902133
C	-4.02565060916716	1.00074924716371	3.69507059780455
C	-4.62017559540120	-1.52378713044643	0.91248108613250
C	-5.97747614664594	-1.32480696632795	0.68668527328574
C	-6.71537402607924	-0.40139849305347	1.41779345577386
C	-6.05817466571998	0.32623001081871	2.40153930240776
C	-4.70137296928709	0.16130272133453	2.65537381375728
C	-3.97749131826270	-0.77200090934837	1.90355241860865
C	1.59582858140544	-0.46892340997093	0.15616251842098
C	2.64694595457735	0.21840989320899	-0.44202162789124
C	3.09645723169732	1.43914680357866	0.04620688844074
C	2.47798871220572	1.96162104886622	1.17543830931481
C	1.41649201013161	1.31430450454099	1.79359057804266
C	0.95963196732974	0.09964580090446	1.26563256380543
C	-0.17902933706684	-0.59979189522470	1.91350057587639
C	0.09661327254192	-1.53908886959249	2.90342192620330
C	-0.92934025244756	-2.21337547221177	3.54381829066013
C	-2.24058773662859	-1.94508341688866	3.19444893038456
C	-2.54173155168953	-1.00654527280024	2.20658610974245
C	-1.50765390642249	-0.32529917847487	1.55141882169914
H	-1.33765716315695	3.71348592833557	-1.05968668168144
H	-2.10342783976160	3.74103086530344	2.57892560821700
H	1.85262987359816	10.51493299001135	1.00032461006111
H	4.38875714012471	8.82159103445934	1.93390708094852
H	4.16993197529739	10.55636556137275	1.78542035077025
H	4.60332602890289	9.84805126239216	3.33972895942841
H	2.90659157777463	8.55852273555328	4.63976400449760
H	1.28776813421964	7.54449507511967	5.99082033901148
H	-0.02478570384735	8.69324473667654	6.22530593049824
H	-0.31786334662663	7.22419648401005	5.33358760875688
H	-1.71284419083296	10.61578435086764	4.90057528337796
H	-4.12418533144464	10.32697391319623	5.39739400900827
H	-5.36461374495491	8.45733423691058	4.35422126717108
H	-3.04259653174434	5.24269736898177	4.66286596582870
H	-4.38342438146329	4.18833678261544	5.10113095230026
H	-4.43482868927781	5.91085409527549	5.47438918281848
H	-5.83511256096225	5.58663118026807	3.38627662831828
H	-6.54949216687498	2.85906672232700	0.54636066458047
H	-7.76572171509008	3.20191552242739	1.75840071649271
H	-7.76769467453919	4.08601039927326	0.23366197632802
H	-6.38410728321024	6.04184706263133	-0.05310376742944
H	-5.31905580721239	8.08877324885372	-0.28098926086348
H	-3.76744815776542	8.27151551735312	0.53106813613949
H	-5.19579453775958	8.97443662889942	1.23825487913835
H	-0.49594559553497	6.41407546634742	-0.83493821428768
H	-0.10621752831088	8.00368313871441	-0.17001751613109
H	-1.76945086927890	7.62460053624483	-0.65028094095832
H	1.03050169673783	4.98195634606522	1.99765376046641
H	1.42177085731974	6.65376433633789	2.44935104244087
H	0.62771043700747	5.58553491190352	3.61463697560682
H	-1.63254970438770	9.71165980884075	1.06013034232395
H	-1.27842405744941	11.28605802094362	1.71900442724406
H	-0.38468217893736	10.70960992622759	0.31624755430190
H	-3.36680524916523	0.41386864627769	4.33085013474302
H	-3.40840890600932	1.77078150138426	3.23045412384577
H	-4.75387522068631	1.50350108874093	4.32677373004210
H	-6.61650338726622	1.04340793970719	2.99119139083235
H	-8.65405627065611	-1.08062667724927	0.77711509051723
H	-8.70044754503743	0.17346810806080	2.01441209518904
H	-8.29745552448449	0.58572414905505	0.35823679617848
H	-6.47195130220794	-1.90974505412383	-0.08060706624236
H	-4.52720410926256	-3.11627667155468	-0.52251045778473
H	-3.16350174799874	-2.00993991918180	-0.59221492434923
H	-3.25574213962880	-3.17828427230484	0.70027936805657
H	-3.05450976614393	-2.46095932654760	3.68832967314046
H	-0.70778206522145	-2.94432198804294	4.31069554412906
H	1.12835376830654	-1.73472116963352	3.16720354280104
H	1.55253159650934	-1.97472763664598	-1.37319034020718
H	0.10215040182039	-1.93087467848661	-0.37119024989155
H	1.57764707533501	-2.61126344324291	0.26621434936405
H	3.12973259721691	-0.21517243684881	-1.31057450069106
H	4.83246847355859	1.52653937492939	-1.22234399518230
H	3.78464967829238	2.93183810890137	-1.33097441299074
H	4.81962943335291	2.72658575752906	0.06898706018184
H	2.81680157791825	2.90955256955161	1.57620261292670
H	0.86579288140497	1.24922770017765	3.87018995240095
H	-0.29764486296069	2.05868951809546	2.85403816711478
H	1.21158707447646	2.86712713714197	3.25574851132547
H	-1.35504871375205	-0.73741254933549	-2.08769964569704
H	-0.00908328467081	0.40171906865408	-1.94611546785236
H	-1.50813802920004	0.89311687473269	-2.75120712765029
H	-3.99684888488906	2.28899327384908	-1.21039459036625
H	-4.46000416149553	1.84520741746473	0.43307175916338
H	-4.48878322845163	0.62045686145025	-0.83797323768771

2 (TerMe$_2$Sn)$_2$P$_2$H$_2$ C$_2$

0 1

Sn	-1.24835712786472	6.42095757376946	1.67864264070311
Sn	-1.95513414793515	1.04752067613066	-0.13235810422187
P	-2.55106328341312	4.29277181552732	1.27338346284612
P	-1.05388054126114	3.39913138568502	-0.10738736859066
C	-0.77112775118489	10.39075258357352	1.28254234142498
C	4.05370185459960	9.58847347882264	2.38442439130339
C	0.48497585179653	7.85368075702566	5.45130395564165
C	0.26227518488246	9.76075011174621	2.16658847901746
C	1.61414434694562	9.92466574510654	1.88487215702683
C	2.60422794882638	9.43742672330209	2.73029335051188
C	2.20960066468213	8.78346516740148	3.89124399628874
C	0.86937777915576	8.58195621246892	4.20011336067517
C	-0.11069272867101	9.05526853025898	3.31894408028373
C	-7.16641785975458	3.69875721943805	1.02514694274625
C	-4.86513150283969	8.14301409727273	0.73970292014431
C	-4.10309025855567	5.15069004559154	4.72123277414852
C	-5.10956095869821	6.86296335216529	1.47883643858964
C	-5.96967758754721	5.90650833984592	0.95159213636368
C	-6.25546368325517	4.72547477288588	1.62264670947985
C	-5.64273474688123	4.50927076423367	2.85064852498301
C	-4.76502552572987	5.43209508901908	3.40678017314853
C	-4.50013721348236	6.62156862301689	2.71542981798814
C	-3.63759763773899	7.66531226633851	3.32733118627631
C	-4.24654769494783	8.56386276528693	4.20410229791266
C	-3.52469489660765	9.58901314422455	4.78886705953370
C	-2.17980686471450	9.72864900717837	4.49181471452266
C	-1.54923710421534	8.84252812519114	3.62217849178372

C	-2.27259900119511	7.79173412321539	3.03574209213464
C	0.70592038687742	5.84417336686462	2.38307031051796
C	-0.97941134872485	7.26126041410618	-0.28928017287683
C	-1.16567594080299	0.20216892046484	-1.95837722046101
C	-4.03446566049995	1.44051154074118	-0.51461917141750
C	1.24571203125913	-1.60054454887976	-0.31897054592035
C	4.14185698051589	2.49365983260299	-0.42931678693433
C	0.68979898611310	1.98538792849433	3.17078908523515
C	-3.81842477160566	-2.55981016466210	0.09697042766473
C	-8.18568200594176	-0.29328366182616	1.07413900782566
C	-4.08993877465276	1.00751437803465	3.64703715555696
C	-4.60856543874090	-1.57406544388880	0.90256862420660
C	-5.96896416352940	-1.40790721654603	0.66360820023798
C	-6.73105463207551	-0.48738532967610	1.37147504301507
C	-6.09701622807471	0.27194149007355	2.34776710190916
C	-4.74016011548150	0.13944661723701	2.61468145486266
C	-3.99008139609150	-0.79048305002663	1.88273516264822
C	1.59631591647280	-0.25296664849434	0.23405423587090
C	2.63612911399867	0.48294820987940	-0.32694644788383
C	3.05524911911152	1.69055776195447	0.21603532290045
C	2.42041600649810	2.14765244655932	1.36580518779782
C	1.36226266913291	1.45551904228671	1.94209506972823
C	0.92992391026397	0.25930078379728	1.35270113214511
C	-0.20113828389091	-0.48686461468235	1.96137174430619
C	0.08662487723100	-1.40725462234072	2.96591134885772
C	-0.92638923034058	-2.11815227089569	3.58627848992746
C	-2.23818344120955	-1.90043442749154	3.20601848931175
C	-2.55150437885371	-0.98193106116637	2.20317001440138
C	-1.52939188816111	-0.27040287858610	1.56026703865017
H	0.06096091023196	3.18420556906479	0.73328088287744
H	-2.15573728292325	3.68990161849689	2.50324229221166
H	1.90100824805344	10.46066982739126	0.98732705832432
H	4.38624515205869	8.77915183743692	1.73163350934723
H	4.24543634930401	10.52244685920499	1.85897950703968
H	4.68185994970920	9.56501629834976	3.27272227324205
H	2.96656489584781	8.40400170472469	4.56782456396520
H	1.35196336304892	7.39600164985285	5.92162497817672
H	0.02479184711969	8.52389248637393	6.17760515019694
H	-0.24741042169711	7.07379911714986	5.24986713042016
H	-1.60334056329733	10.53489682706972	4.92775249658080
H	-4.00972610461355	10.28157051110697	5.46451919895685
H	-5.30244546782179	8.45044775644034	4.41544789016107
H	-3.01753119628672	5.20040985170455	4.63477740228072
H	-4.36529549032179	4.16170096449514	5.08823566834106
H	-4.38378130482002	5.88073788990793	5.47982965383876
H	-5.84371358653812	3.59044622118398	3.38728252283272
H	-6.59465297294979	2.89235226834390	0.56562882124266
H	-7.80825649902659	3.24488004288497	1.77900858557381
H	-7.80238617528632	4.13006927447689	0.25485416666124
H	-6.43469243644068	6.09482596552399	-0.00916589572304
H	-5.35356751962120	8.13394769678425	-0.23149831562618
H	-3.80353587625627	8.32155129136702	0.58189243898210
H	-5.23859096546221	9.00144791530575	1.29851309260958
H	-0.72784619221594	6.44774286312321	-0.96424765452003
H	-0.16323473096474	7.97721048103089	-0.26996006032280
H	-1.87787203362433	7.75126535664395	-0.65125433372565
H	1.03766019611170	4.99875104398633	1.78806733480830
H	1.40423970776632	6.66483477939883	2.26425567121132
H	0.67497979167381	5.55045891173354	3.42761788130932
H	-1.60739434849415	9.72574898169091	1.08985965049722
H	-1.18805792720479	11.28063199873887	1.75670774523108
H	-0.34481644756588	10.69123146138433	0.32855800407776
H	-3.42333596578040	0.44333740880683	4.29523148399508
H	-3.48513526379699	1.78396606258436	3.17677034081150
H	-4.83307873977998	1.50239009535138	4.26729336604111
H	-6.67520582446537	0.98871230453145	2.91876760756683
H	-8.60634984513202	-1.15068355163211	0.55293686283900
H	-8.76354360771578	-0.13422454647903	1.98346895586902
H	-8.34052731749505	0.58179972841178	0.44043730465874
H	-6.44529888249510	-2.01611227882816	-0.09680181429913
H	-4.47128693374561	-3.19598747683251	-0.49564670472178
H	-3.14024921632967	-2.05317043662163	-0.59177071735661
H	-3.19869239873056	-3.19423732256828	0.72747594530260
H	-3.04395717117861	-2.43945469576811	3.68841565238912
H	-0.69476022945177	-2.83522019324286	4.36318145711342
H	1.11841589978120	-1.55804222500835	3.25772082418355
H	1.60420754227916	-1.71669845374441	-1.33912574002456
H	0.17494439738797	-1.78072732659623	-0.30875661542351
H	1.69977339194588	-2.38985601798767	0.28274118218319
H	3.13834611093164	0.09427228532473	-1.20540555238462
H	4.80930236731895	1.86732525228041	-1.01791444974967
H	3.72249062797740	3.24357431908755	-1.10264590650978
H	4.73924656391056	3.02573445181634	0.30919457309330
H	2.74688983463686	3.07676725005593	1.81804129589794
H	0.77664326613174	1.28922001814720	4.00437255757605
H	-0.37607779155284	2.13507579857017	3.00327860380002
H	1.11972950808595	2.93599607964454	3.47294959028287
H	-1.36851955469555	-0.86247599452455	-2.03738758539551
H	-0.09463467082592	0.36482369689478	-2.01724254537591
H	-1.64644613980942	0.71436307944881	-2.78832629998254
H	-4.07965994442322	2.22203489446523	-1.26951946392453
H	-4.52994172720626	1.79128188576420	0.38154846389322
H	-4.54248835106160	0.55247367371815	-0.87476020346881

3 ($TerMe_2Sn)_2P_3H$

0 1

Sn	-0.99807924651180	6.44394285303382	2.22749416686795
Sn	-2.10252401067938	1.23032383058459	0.28210903738148
P	-2.52489104187610	4.58860692093350	1.42219773752213
P	-2.53823442467742	3.19673570261216	3.12651580047888
P	-0.93128778116183	3.04619726384905	1.61100372930416
C	-0.88371938451161	10.22856485764594	0.17946055869691
C	4.03348822015934	9.89136683588571	1.09041925092347
C	0.75461410837570	9.07002492116368	4.80015680790285
C	0.23613812128466	9.96407856349640	1.13841193213962
C	1.55638460844722	10.07639731643050	0.72295266173950
C	2.62016612309192	9.81732509090490	1.58089943909729
C	2.33171403272814	9.46700347566336	2.89350457268075
C	1.02260655191011	9.36299791380526	3.35529300392625
C	-0.03142802847008	9.58700324960292	2.46159789942854
C	-6.50941765182001	3.24495559019083	3.47662338388185
C	-4.95935690186778	7.33048059126969	1.02529585715513
C	-3.36384195407355	6.43614207082910	5.72050296001118
C	-4.96947389476083	6.50212369853131	2.27194845607222
C	-5.73461240725725	5.34179014208785	2.33388522188255
C	-5.73990973016480	4.52726500228455	3.45602174067875
C	-4.95693672494537	4.90488608313312	4.54252632774831
C	-4.18141868325998	6.05720144748577	4.52353004125483
C	-4.18391700047130	6.85956282845085	3.37434587700097
C	-3.41335117310496	8.13041671823797	3.35358541245557
C	-4.05834071374627	9.27941368516683	3.81245830925571
C	-3.41022120813450	10.50181068406533	3.82749692146440
C	-2.10147618504993	10.58447628695577	3.38281352146667
C	-1.43730687000818	9.45104800236016	2.92178777958845
C	-2.09055025755354	8.20941219496743	2.89882525501525
C	0.31834378074565	5.71101264277810	3.77322257063175
C	0.21111922725533	6.73130575321706	0.46619690394327
C	-1.23521519943480	1.34780189647165	-1.69303796155866
C	-4.15691923800440	1.82673170125042	0.05267648161850
C	1.12601650302646	-1.02113548356274	-0.81954032909315
C	3.82678828059712	2.75051174540581	1.09538714185521
C	0.26344457000537	0.59461004867510	3.87593407235211
C	-3.74503989404928	-2.25766088682250	-1.31815490648447
C	-8.28765694490905	-0.50538491376117	-0.10794226133202
C	-4.59787042003015	-0.39022186362116	3.28293770003230
C	-4.66920498481047	-1.65309070309225	-0.30501581284322
C	-5.99409129794805	-1.38873152845577	-0.63338089224315
C	-6.87664191558790	-0.82360097977235	0.28033344459435
C	-6.40215870580045	-0.52849669304655	1.55176056540784
C	-5.08283907886184	-0.77092722658873	1.91824332415264
C	-4.21122561777598	-1.33630044608326	0.97968005782690
C	1.39815646997122	-0.06691798438286	0.30351773344251
C	2.42557947252921	0.86529128450158	0.19670005838989
C	2.76385732040160	1.70714022407409	1.24895226759804
C	2.05945242558406	1.58273524221180	2.43952412318130
C	1.00939973853882	0.68400659348124	2.57996089701331
C	0.66214931164396	-0.13052564573060	1.49286377200111
C	-0.47539653971001	-1.07710330076120	1.61681850614904
C	-0.23907278106609	-2.33514821554474	2.16436404314371
C	-1.27024890748406	-3.24770375864906	2.31170908079339
C	-2.54883392655324	-2.89840107742045	1.91513345327773
C	-2.80963321629368	-1.64290578512816	1.36571160169697
C	-1.76883982529166	-0.71975699369099	1.20362963936226
H	-1.80415281289362	3.95540487904595	4.08023768197831
H	1.76156262336188	10.35613659572533	-0.30405204512747
H	4.28611983744542	9.01602874851551	0.48948826289592
H	4.19295103523147	10.76604511558328	0.46116742518456
H	4.74186919892400	9.93605403356434	1.91480842908739
H	3.14688873884535	9.28092379610660	3.58324277081770
H	1.65130964338067	8.71878057339468	5.30500642460673
H	0.41037978596387	9.96722136324937	5.31641009005794
H	-0.02493714452376	8.32443777036665	4.92922780647963
H	-1.57894022683708	11.53287815481692	3.39161948389989
H	-3.92158054620844	11.38552597653836	4.18655253033259
H	-5.08136624840235	9.20047085414042	4.15843049350700
H	-2.32714651417887	6.63359486156103	5.45351005633497
H	-3.37759978835750	5.64825961791161	6.46958829407889
H	-3.73810656579771	7.34888420342418	6.18463978294041
H	-4.94343265656319	4.27721905055300	5.42614926002500
H	-5.84191543840818	2.40051292141076	3.30263297130420
H	-6.99349153380028	3.07965702476494	4.43836443214828
H	-7.27238516884046	3.22282141025651	2.70170459048519
H	-6.32210041331795	5.05584726254842	1.46985047851742
H	-5.70342027352552	6.97969368971371	0.31474504119824
H	-3.98627037152331	7.27925072303473	0.53361875063201
H	-5.14844750434338	8.38181580133037	1.23441589720260
H	0.51898092760349	5.74402315468327	0.13097191519692
H	1.08579669101873	7.33035724933736	0.69356109496710
H	-0.35307104817644	7.21243200531519	-0.32697565722734
H	0.54951647953014	4.67085926966487	3.56043761739208

H	1.23586229348881	6.29216097383629	3.73729444670129
H	-0.11542192914737	5.78897037986867	4.76465270175333
H	-1.61217991421972	9.41956747390292	0.18524351244006
H	-1.43052758376853	11.13374959652504	0.44453362091675
H	-0.51203188824779	10.34686263644399	-0.83540134365555
H	-4.02782077125743	-1.19071807599448	3.75016336332525
H	-3.93524064895327	0.47582060617261	3.23417707716859
H	-5.42743232267807	-0.13286364671088	3.93711419270306
H	-7.07601897027549	-0.09159115369546	2.27975827841322
H	-8.67207141176464	-1.21204867177357	-0.84136327099343
H	-8.95250513717603	-0.51697106437510	0.75369595557726
H	-8.35412142207910	0.48913097356431	-0.55349300675144
H	-6.34658912110046	-1.63069691188987	-1.62960937868141
H	-4.25969598532935	-2.44545310082135	-2.25728721658788
H	-2.89722405735828	-1.60444753724293	-1.52460022184740
H	-3.32441800569671	-3.19854813992082	-0.96538848769367
H	-3.36786628796798	-3.59733066720191	2.03004397847506
H	-1.07836157773086	-4.22467582721449	2.73612750971533
H	0.76602707596260	-2.59086713224848	2.47541065325824
H	1.59060495154514	-0.68660815581754	-1.74408513676409
H	0.06248562982164	-1.15207351552516	-0.99816845017927
H	1.52433174131901	-2.01001677283760	-0.58651148171367
H	2.98109336244600	0.92923712121164	-0.73201794061344
H	4.48409281301684	2.53305317547571	0.25605372854162
H	3.38194713038317	3.73146482197531	0.91759548048406
H	4.43910602572433	2.83545082107892	1.99211080962066
H	2.30894700494531	2.23008911304677	3.27207617549694
H	0.50953039982758	-0.32251541816138	4.41293735671534
H	-0.81296359964505	0.58423903004057	3.71966881720953
H	0.50259238787459	1.43631164865196	4.52105270887325
H	-1.47877756264120	0.47637914103443	-2.29523718141998
H	-0.15694357699554	1.44352339182608	-1.62448150125331
H	-1.64016564962307	2.23198739749521	-2.17938666162506
H	-4.16116700921589	2.79377664275338	-0.44135518809667
H	-4.65260901983698	1.92203693508385	1.01099024311076
H	-4.69227404343085	1.10100155280806	-0.54997845497131

4.5 References

[1] a) S. Havelange, N. Van Lierde, A. Germeau, E. Martins, T. Theys, M. Sonveaux, C. Toussaint, K. Schrödter, G. Bettermann, T. Staffel, F. Wahl, T. Klein, T. Hofmann, "Phosphoric Acid and Phosphates" *in Ullmann's Encyclopedia of Industrial Chemistry*, Wiley, Weinheim, **2022**; b) H. Diskowski, T. Hofmann, "Phosphorus" *in Ullmann's Encyclopedia of Industrial Chemistry*, Wiley, Weinheim, **2020**; c) W. Gleason, *JOM* **2007**, *59*, 17-19.

[2] a) J. Svara, N. Weferling, T. Hofmann, "Phosphorus compounds, organic" in *Ullmann's Encyclopedia of Industrial Chemistry*, Wiley, Weinheim, **2006**; b) G. Bettermann, W. Krause, G. Riess, T. Hofmann, "Phosphorus compounds, inorganic" in *Ullmann's Encyclopedia of Industrial Chemistry*, Wiley, Weinheim, **2006**.

[3] D. Corbridge, *Phosphorus: An Outline of its Chemistry, Biochemistry, and Technology*, Elsevier, New York, **1994**.

[4] a) L. Giusti, V. R. Landaeta, M. Vanni, J. A. Kelly, R. Wolf, M. Caporali, *Coord. Chem. Rev*. **2021**, *441*, 213927; b) C. M. Hoidn, D. J. Scott, R. Wolf, *Chem. Eur. J.* **2021**, *27*, 1886–1902; c) B. M. Cossairt, N. A. Piro, C. C. Cummins, *Chem. Rev.* **2010**, *110*, 4164-4177; d) M. Caporali, L. Gonsalvi, A. Rossin, M. Peruzzini, *Chem. Rev.* **2010**, *110*, 4178-4235; e) M. Scheer, G. Balázs, A. Seitz, *Chem. Rev.* **2010**, *110*, 4236-4256.

[5] For a recent review, see: D. J. Scott, *Angew. Chem. Int. Ed.* **2022**, *61*, e202205019; *Angew. Chem.* **2022**, *134*, e202205019.

[6] For selected significant examples, see: a) M. Bai, Y. Cao, J. Huang, Y. Liu, G. Tang, Y. Zhao, *CCS Chem.* **2024**, *6*, 91-99; b) Y. Chen, W. Liu, X. Huangfu, J. Wei, J. Yu, W.-X. Zhang, *Chem. Eur. J.* **2024**, *30*, e202302289; c) X. Huangfu, W. Liu, H. Xu, Z. Wang, J. Wei, W.-X. Zhang, *Inorg. Chem.* **2023**, *62*, 12009-12017; d) M. Donath, K. Schwedtmann, T. Schneider, F. Hennersdorf, A. Bauzá, A. Frontera, J. J. Weigand, *Nat. Chem.* **2022**, *14*, 384-391; e) Y. Mei, Z. Yan, L. L. Liu, *J. Am. Chem. Soc.* **2022**, *144*, 1517-1522; f) M. Till, V. Streitferdt, D. J. Scott, M. Mende, R. M. Gschwind, R. Wolf, *Chem. Commun.* **2022**, *58*, 1100-1103; g) S. Reichl, E. Mädl, F. Reidlberger, M. Piesch, G. Balázs, M. Seidl, M. Scheer, *Nat, Commun.* **2021**, *12*, 5774; h) P. B. Arockiam, U. Lennert, C. Graf, R. Rothfelder, D. J. Scott, T. G. Fischer, K. Zeitler, R. Wolf, *Chem. Eur. J.* **2020**, *26*, 16374-16382; i) U. Lennert, P. B. Arockiam, V. Streitferdt, D. J. Scott, C. Rödl, R. M. Gschwind, R. Wolf, *Nat. Catal.* **2019**, *2*, 1101-1106.

[7] These have been complemented by other recent reports showing improved methods for the preparation of P_4, or even for bypassing P_4 entirely. For example, see: a) J. F. Melville, A. J. Licini, Y. Surendranath, *ACS Cent. Sci.* **2023**, *9*, 373-380; b) T. Schneider, K. Schwedtmann, J. Fidelius, J. J. Weigand, *Nat.Synth.* **2023**, *2*, 972-979; c) T. Xin, C. C. Cummins, *ACS Cent. Sci.* **2023**, *9*, 1575-1580; d) F. Zhai, T. Xin, M. B. Geeson, C. C. Cummins, *ACS Cent. Sci.* **2022**, *8*, 332-339; e) M. B. Geeson, C. C. Cummins, *ACS Cent. Sci.* **2020**, *6*, 848-860; f) M. B. Geeson, P. Ríos, W. J. Transue, C. C. Cummins, *J. Am. Chem. Soc.* **2019**, *141*, 6375-6384; g) M. B. Geeson, C. C. Cummins, *Science* **2018**, *359*, 1383-1385.

[8] R. Rothfelder, V. Streitferdt, U. Lennert, J. Cammarata, D. J. Scott, K. Zeitler, R. M. Gschwind, R. Wolf, *Angew. Chem. Int. Ed.* **2021**, *60*, 24650-24658; *Angew. Chem.* **2021**, *133*, 24855-24863.

[9] D. J. Scott, J. Cammarata, M. Schimpf, R. Wolf, *Nat. Chem.* **2021**, *13*, 458-464.

[10] For more recent follow-up reports, see: a) J. Cammarata, D. J. Scott, R. Wolf, *Chem. Eur. J.* **2022**, *28*, e202202456; b) M. Till, J. Cammarata, R. Wolf, D. J. Scott, *Chem. Commun*. **2022**, *58*, 8986-8989.

[11] T. V. Rajanbabu, P. C. Bulman Page, B. R. Buckley, "Tri-*n*-butylstanne" *in Encyclopedia of Reagents for Organic Synthesis*, Wiley, Weinheim, **2004**.

[12] a) J. J. Weigand, N. Burford, "Catenated Phosphorus Compounds" in *Comprehensive Inorganic Chemistry II: From Elements to Applications*, Elsevier, New York, **2013**; b) K. B. Dillon, F. Mathey, J. F. Nixon, *Phosphorus: The Carbon Copy: From Organophosphorus to Phospha-organic Chemistry*, Wiley, Weinheim, **1998**.

[13] J. Schiller, M. Schimpf, D. J. Scott, R. Wolf, *unpublished results*.

[14] N. S. Simpkins, "Azobisisobtyronitrile" *in Encyclopedia of Reagents for Organic Synthesis*, Wiley, Weinheim, **2001**.

[15] The precise mechanism of initiation using light is currently uncertain and remains under investigation. Further (speculative) discussion can be found in the supplementary information of ref. [9].

[16] Given the similarity between butyl and methyl groups this is not expected to dramatically impact either the electronic or steric properties of the Sn centre.

[17] The calculated barrier for **I$^\bullet$ → II** is compounded by formation of **I$^\bullet$** from P_4 being endergonic while formation of the other P-centred radical intermediates *via* $Me_3Sn^\bullet$ attack is exergonic.

[18] M.-L. Y. Riu, M. Ye, C. C. Cummins, *J. Am. Chem. Soc.* **2021**, *143*, 16354-16357.

[19] A. Hirsch, Z. Chen, H. Jiao, *Angew. Chem. Int. Ed.* **2001**, *40*, 2834-2838; *Angew. Chem.* **2001**, *113*, 891-894.

[20] J. S. Sapsford, D. Csókás, R. C. Turnell-Ritson, L. A. Parkin, A. D. Crawford, I. Pápai, A. E. Ashley, *ACS Catal*. **2021**, *11*, 9143-9150.

[21] This should obviously disfavour $(i Pr_3Sn)_3P$ formation, but should also disfavour PH_3 formation, as any 'unused' P atoms will force the bulky $i Pr_3Sn$ moieties to occupy a smaller number of remaining P atoms, increasing steric clash.

[22] For Ter*Sn$(Me)_2$H formation of the intermediate singlet signals was only observed at slightly higher temperatures (60 °C). For full details see Section 4.4.4.3.

[23] V. Cappello, J. Baumgartner, A. Dransfeld, K. Hassler, *Eur. J. Inorg. Chem.* **2006**, 4589-4599.

[24] Intuitively, it seems unlikely that increased steric bulk would affect the regiochemical preference for formation of **IVa** shown in Figures 2 and 3, as the steps up to this point already keep the added R_3Sn moieties as separated as possible. However, subsequent $R_3Sn^\bullet$ attack to form an analogue of **Va$^\bullet$** would force two R_3Sn moieties onto the same P atom. Conversely, formation of an analogue of **Vh$^\bullet$**, which would then lead to **3**, would minimise steric clash by keeping the R_3Sn moieties as separated as possible. For a fuller discussion, see Section 4.4.4.2 and Scheme S1.

[25] This can also be understood in terms of Sn/H balance, as the total number of P–H and P–Sn bonds should remain equal throughout. This is true for the final equimolar mixture of R_3SnPH_2 and $(R_3Sn)_2PH$ but not for intermediate **3**, which contains more P–Sn than P–H bonds. To compensate for the presence of **3**, more P–H than P–Sn bonds must therefore exist elsewhere in the reaction mixture. Out of intermediates **1** and **2** and the final products, only R_3SnPH_2 is unbalanced in favour of P–H bonds and so only a relative excess of R_3SnPH_2 can achieve this.

[26] This criterion also appears to be satisfied by the well-known reaction of P_4 with I_2 to make PI_3. See: C. Mealli, A. Ienco, M. Peruzzini, G. Manca, *Dalton Trans.* **2018**, *47*, 394-408.

[27] K. Ruhlandt-Senge, J. J. Ellison, R. J. Wehmschulte, F. Pauer, P. P. Power, *J. Am. Chem. Soc.* **1993**, *115*, 11353-11357.

[28] S. Hino, M. M. Olmstead, J. C. Fettinger, P. P. Power, *J. Organomet. Chem*. **2005**, *690*, 1638–1644.

[29] M. Ito, D. Hashizume, T. Fukunaga, T. Matsuo, K. Tamao, *J. Am. Chem. Soc*. **2009**, *131*, 18024–18025.

[30] M. Olaru, S. Mebs, J. Beckmann, *Angew. Chem. Int. Ed.* **2021**, *60*, 19133-19138; *Angew. Chem.* **2021**, *133*, 19282-19287.

[31] G. R. Fulmer, A. J. M. Miller, N. H. Sherden, H. E. Gottlieb, A. Nudelman, B. M. Stoltz, J. E. Bercaw, K. I. Goldberg, *Organometallics*, **2010**, *29*, 2176-2179.

[32] C. Feldmeier, H. Bartling, E. Riedle, R. M. Gschwind, *J. Magn. Res*. **2013**, *232*, 39-44.

[33] F. Neese, F. Wennmohs, U. Becker, C. Riplinger, *J. Chem. Phys*. **2020**, *152*, 224108.

[34] F. Neese, *Wiley Interdiscip. Rev. Comput. Mol. Sci*. **2018**, *8*, e1327.

[35] R. A. Kendall, H. A. Früchtl, *Theor. Chem. Acc*. **1997**, *97*, 158–163.

[36] F. Neese, F. Wennmohs, A. Hansen, U. Becker, *Chem. Phys*. **2009**, *356*, 98–109.

[37] S. Grimme, J. Antony, S. Ehrlich, H. Krieg, *J. Chem. Phys.* **2010**, *132*, 154104.

[38] S. Grimme, S. Ehrlich and L. Goerigk, *J. Comput. Chem*. **2011**, *32*, 1456–1465.

[39] *Avogadro Chemistry*, **2016**, http://avogadro.cc/.

[40] a) B. M. Cossairt, C. C. Cummins, *New J. Chem.* **2010**, *34*, 1533-1536; b) D. H. R. Barton, R. A. Vonder Embse, *Tetrahedron* **1998**, *54*, 12475-12496; c) D. H. R. Barton, J. Zhu, *J. Am. Chem. Soc*. **1993**, *115*, 2071-2072.

[41] M. Janssen, S. Mebs, J. Beckmann, *Chem. Commun*. **2023**, *59*, 7267-7270.

[42] a) G. M. Sheldrick, *Acta Cryst. A* **2015**, *71*, 3-8; b) G. M. Sheldrick, *Acta Cryst. C* **2015**, *71*, 3-8.

[43] O. V. Dolomanov, L. J. Bourhis, R. J. Gildea, J. A. Howard, H. Puschmann, *J. Appl. Cryst*. **2009**, *42*, 339-341.

[44] V. Cappello, J. Baumgartner, A. Dransfeld, K. Hassler, *Eur. J. Inorg. Chem*. **2006**, 4589–4599.

[45] G. M. Sheldrick, SADABS, Bruker AXS, Madison, USA **2007**.

[46] SCALE3ABS, CrysAlisPro, Aglient Technologies Inc. Oxford, GB **2015**.

[47] L. J. Bourhis, O. V. Dolomanov, R. J. Gildea, J. A. K. Howard, H. Puschmann, *Acta Cryst.* **2015**, *A71*, 59-75.

[48] F. Kleemiss, O. V. Dolomanov, M. Bodensteiner, N. Peyerimhoff, L. Midgley, L. J. Bourhis, A. Genoni, L. A. Malaspina, D. Jayatilaka, J. L. Spencer, F. White, B. Grundkötter-Stock, S. Steinhauer, D. Lentz, H. Puschmann, S. Grabowsky *Chem. Sci*. **2021**, *12*, 1675-1692.

[49] R. A. Kendall, H. A. Früchtl, *Theor. Chem. Acc.* **1997**, *97*, 158–163.

[50] F. Neese, *Wiley Interdiscip. Rev. Comput. Mol. Sci.* **2012**, *2*, 73–78.

[51] F. Neese, *Wiley Interdiscip. Rev. Comput. Mol. Sci.* **2022**, *12*, e1606.

[52] J. W. Furness, A. D. Kaplan, J. Ning, J. P. Perdew, J. Sun, *J. Phys. Chem. Lett.* **2020**, *11*, 8208–8215.

[53] P. Pollak, F. Weigend, *J. Chem. Theory Comput.* **2017**, *13*, 3696−3705.

[54] J. G. Brandenburg, C. Bannwarth, A. Hansen, S. Grimme, *J. Chem. Phys.* **2018**, *148*, 064104.

[55] J. Tao, J. P. Perdew, V. N. Staroverov, G. E. Scuseria, *Phys. Rev. Lett.* **2003**, *91*, 146401.

[56] F. Weigend, R. Ahlrichs, *Phys. Chem. Chem. Phys.* **2005**, *7*, 3297-3305.

[57] J. D. Rolfes, F. Neese, D. A. Pantazis, *J. Comput. Chem.* **2020**, *41*, 1842–1849.

5 Hydrosilylation and Hydrogermylation of White Phosphorus[a]

Abstract:

The development of efficient, direct strategies for the transformation of white phosphorus (P_4) into useful monophosphorus compounds, as alternatives to the current wasteful and hazardous indirect processes, remains a significant challenge. Encouragingly, recent reports have shown that the reduction of P_4 with organotin hydrides and subsequent functionalisation with electrophiles allows for the efficient synthesis of an array of industrially relevant monophosphines in a 'one-pot' manner. However, despite the practical and conceptual simplicity of this method its appeal is limited by the inherent toxicity of most organotin derivatives. Here, we address this problem through experimental and computational studies of the reactivity of lighter and less toxic hydrogermane and hydrosilane homologues of organotin hydrides (R_3EH, E = Ge or Si) towards P_4. Upon optimisation, these hydroelementation reactions can also be employed to directly transform P_4 into useful monophosphorus compounds, in a simple 'one-pot' fashion similar to the original organotin-based systems.

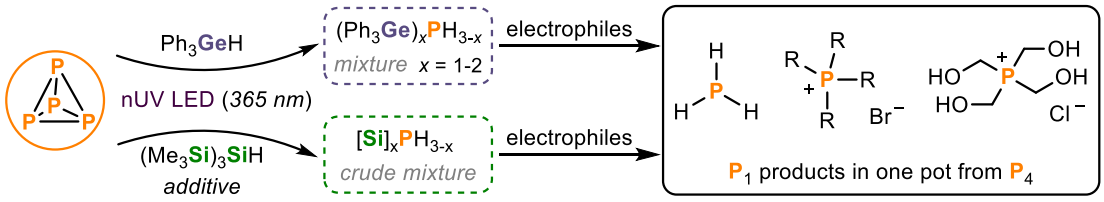

[a] Jose Cammarata and Daniel J. Scott together developed the hydrosilylation and hydrogermylation of white phosphorus (Sections 5.2.1 and 5.2.3). Maximilian Schimpf performed preliminary experiments for Section 5.2.1 as part of his MSc thesis. Jose Cammarata developed the functionalisation of the crude $[R_3E]_nPH_{3-n}$ mixtures (E = Si, Ge) and the procedures for product isolation and characterisation (Section 5.2.2 and 5.2.4). Jose Cammarata wrote the manuscript, which was reviewed and edited by Daniel J. Scott and Robert Wolf. Daniel J. Scott and Robert Wolf supervised and directed the project.

5.1 Introduction

White phosphorus, P_4, is by far the most reactive and industrially relevant allotrope of the element. It serves as the synthetic precursor for all commercially valuable and academically important organophosphorus compounds (OPCs).[1–4] Current industrial routes for converting P_4 into these useful OPCs involve indirect multi-step processes such as (oxy)chlorination reactions with chlorine gas (Cl_2) to produce phosphorus chloride intermediates (PCl_3/PCl_5/$POCl_3$), or disproportionation reactions under acidic or basic conditions to generate phosphine gas (PH_3). The desired OPCs are then obtained by functionalisation of these intermediates with nucleophiles or by hydrophosphination reactions of unsaturated organic compounds, respectively (Scheme 1a).[1–6] As a result, significant efforts have been made to develop alternative strategies for the functionalisation of P_4 that avoid the use of such hazardous reactants and intermediates.[7–11]

Notably, in recent years various strategies have been reported for converting P_4 *directly* into one or more P_1 products.[12–14] These remain at early stages of development, but include photocatalytic reactions,[15,16] electrochemical degradation,[17] and oxidative 'onioation' of P_4.[18] Among these new approaches, our group recently reported a simple method that can convert both white and red phosphorus (P_{red}) into stannyl phosphines $(Bu_3Sn)_xPH_{3-x}$ (x = 0–3) using the 'classical' radical reagent Bu_3SnH and initiation by light or a chemical radical initiator such as azobis(isobutyronitrile) (AIBN).[19,20] The resulting stannylphosphine mixture serves as a P^{3-} source, affording industrially relevant monophosphorus compounds upon treatment with various electrophiles in a 'one-pot' protocol (Scheme 1b). Moreover, simple procedures have been developed for the closed-loop recycling of the tin hydride reagent, thus minimising organotin waste.[19,20]

Unfortunately, the use of organotin compounds raises notorious, fundamental concerns around toxicity that cannot be fully mitigated, even by these recycling strategies. The replacement of R_3SnH with more benign options has long been an important goal for synthetic free-radical chemistry, and a multitude of alternative reagents have been proposed for a variety of chemical transformations.[21–24] Particularly appealing in the context of P_4 reduction would be close structural and chemical analogues of R_3SnH, in the expectation that they would also permit similar post-reduction functionalisation reactions. We have therefore recently turned our attention towards a fundamental study of the reactivity of P_4 with lighter Group 14 hydrides, which in other contexts are known to undergo hydroelementation reactions analogous to those of R_3SnH.[25]

Herein we describe the reactivity of the lighter and less toxic hydrogermanane and hydrosilane homologues of organotin hydrides (R_3EH, E = Ge or Si) towards P_4, promoted by LED light irradiation. Gratifyingly, these new hydroelementation reactions yield analogous $[E]_nPH_{3-n}$ mixtures that can also be converted into useful P_1 products upon reaction with electrophiles in a comparable, direct, one-pot manner (Scheme 1c).

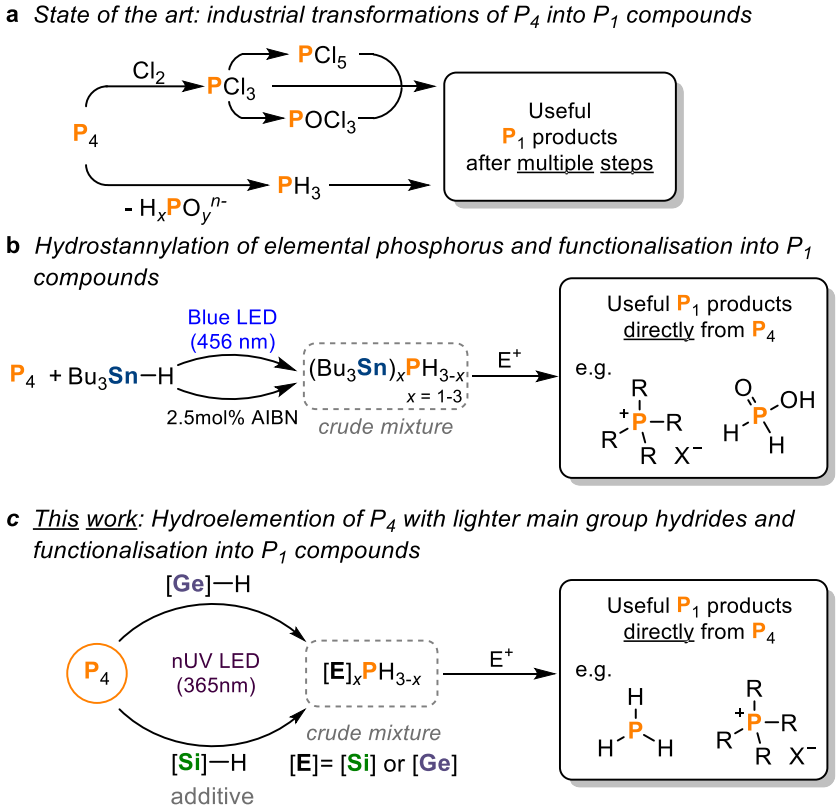

Scheme 1. a) Current state-of-the-art routes for the transformation of P_4 into P_1 products. b) Previously reported hydrostannylation of P_4 and subsequent treatment with electrophiles to afford P_1 compounds directly from P_4. c) Hydroelemention of P_4 with lighter main group hydrides, reported herein. E^+ represents a generic electrophile.

5.2 Results and Discussion

Inspired by the practical and conceptual simplicity of the hydrostannylation of P_4, we anticipated that this radical based activation of P_4 could be extended to the use of lighter R_3EH (E = Ge or Si). Building on our mechanistic studies on the degradation of white phosphorus with tin hydrides (see Chapter 4), computational investigations were performed at the outset of this project. DFT studies at the PBE-D3(BJ)/def2-TZVP level of theory were focused on the first P–P bond cleavage step of the reaction of P_4 with truncated model radicals $Me_3E^{\bullet}$ (E = Ge, Si), for comparison with the previous calculations using $Me_3Sn^{\bullet}$ (Figure 1a). Notably, this first step was found to be rate limiting for Me_3SnH. Interestingly, while the addition of $Me_3Sn^{\bullet}$ to P_4 is energetically uphill (2.2 kcal mol^{-1}), the same process is barrierless and downhill for both other $Me_3E^{\bullet}$ (E = Ge, Si), forming the 'butterfly' P_4 radical intermediates $(Me_3E)P_4^{\bullet}$. The subsequent hydrogen atom transfer (HAT) step to $(Me_3E)P_4^{\bullet}$ from another equivalent of Me_3EH then proceeds over activation barriers that are significantly higher for Si and Ge than for the heavier analogue Sn (23.4, 18.7 and 10.8 kcal mol^{-1}, respectively) consistent with expected differences in the E–H bond strengths (Figure 1b).[22,25–28] Nevertheless, all of these barriers should be easily accessible even at room temperature, suggesting that the desired hydroelementations should indeed be feasible.

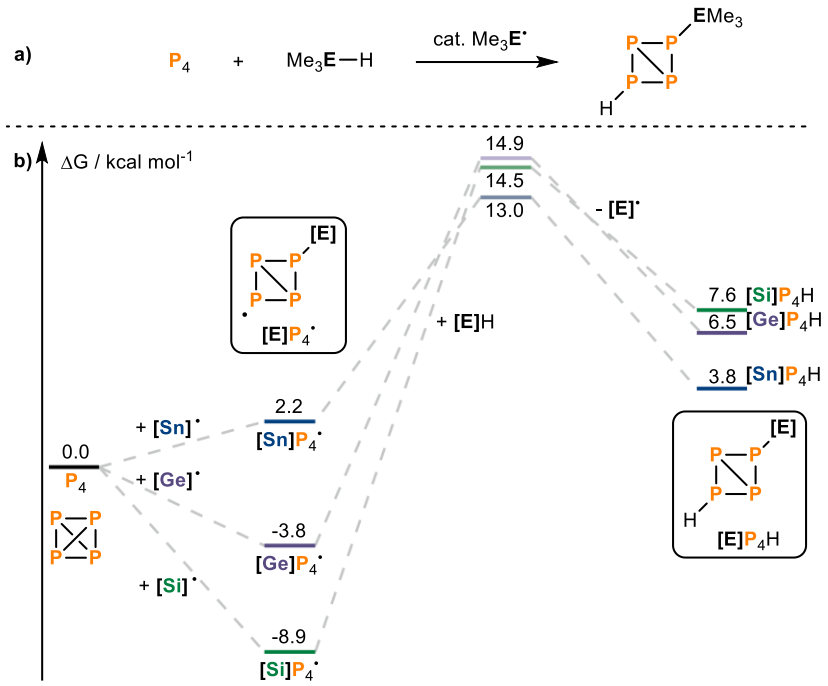

Figure 1. a) Model hydroelementation of the first P–P bond in P_4. b) Calculated mechanism, *via* attack of **[E]•** and subsequent HAT (relative free energies in kcal mol^{-1}). **[E]** = Me_3Si, Me_3Ge or Me_3Sn. For simplicity, stereochemistry is not shown.

5.2.1 Hydrogermylation of P_4

Our experimental studies began with investigation of the hydrogermylation of P_4. Notably, despite the stronger Ge–H bond, the commercially available organogermanes Bu_3GeH and Ph_3GeH have both been used as alternatives to replace organotin compounds in various radical reactions.[21,23,29] To provide the most direct comparison to the hydrostannylation of P_4 with Bu_3SnH, we first tested the reactivity of Bu_3GeH towards P_4 under the same reaction conditions. Thus, Bu_3GeH and P_4 were combined in a 6:1 molar ratio in PhMe and irradiated with blue LED light (455 nm) for one day. Unfortunately, and in sharp contrast to the efficient reaction of P_4 with R_3SnH, the $^{31}P\{^1H\}$ NMR spectrum of the reaction mixture showed only unconsumed P_4 at −521 ppm. Other attempts to achieve useful reactivity using Bu_3GeH also led to unsatisfactory results (for full details, see Section 5.4.2.1). However, when Ph_3GeH, which has a weaker Ge–H bond,[26] was used instead, additional minor resonances were observed at −240.5 and −248.0 ppm. Markedly, significant amounts of orange precipitate were observed at the end of the reactions with both Bu_3GeH and Ph_3GeH, suggesting the formation of red phosphorus or other insoluble polyphosphorus compounds (P_n).

Further investigations revealed that longer reaction times and irradiation with near UV LED light (365 nm) further favoured the conversion of P_4 into new species (Scheme 2a).[30] These can be assigned as the new products $(Ph_3Ge)_2PH$ (**1**; −240.5 ppm) and Ph_3GePH_2 (**2**; −248.0 ppm), both by analogy to the major products observed in the previous hydrostannylation reactions and by comparison with the chemical shifts reported for related Ge-substituted phosphines.[19,31] This

assignment is further supported by ^{1}H-coupled ^{31}P NMR spectra, where these resonances appear as a doublet ($^{1}J(^{31}P\text{-}^{1}H)$ = 185 Hz) and a triplet ($^{1}J(^{31}P\text{-}^{1}H)$ = 181 Hz), respectively (Scheme 2b). Corresponding doublets arising from coupling between ^{1}H and ^{31}P nuclei could also be observed in the ^{1}H NMR spectra (Figure S5). A single-crystal X-ray diffraction study further confirmed the identity of **1**, whose structure resembles the recently reported $(TerMe_2Sn)_2PH$ (Ter = 2,6-$Mes_2C_6H_3$; see Chapter 4). An additional, minor resonance was always also observed during these investigations, appearing as a small singlet at −125.8 ppm in the $^{31}P\{^{1}H\}$ NMR spectra. This signal splits into a doublet in the ^{1}H-coupled ^{31}P NMR spectrum ($^{1}J(^{31}P\text{-}^{1}H)$ = 199 Hz) and is attributed to $Ph_3GeP(H)Ph$ (**3**) forming as a minor side product (Scheme 2b).[32,33] Note that unlike with Bu_3SnH, no significant tertiary phosphine (i.e. $(Ph_3Ge)_3P$) or PH_3 products were observed.

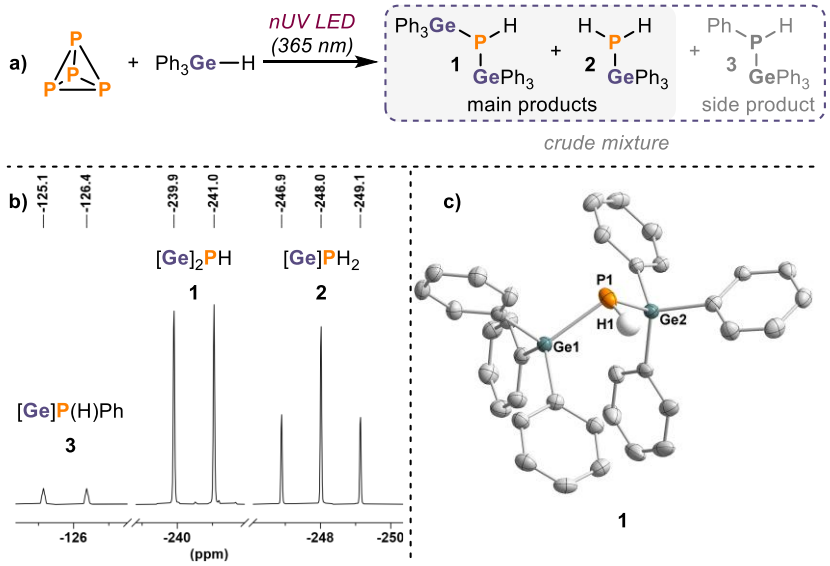

Scheme 2. a) Hydrogermylation of P_4 with Ph_3GeH promoted by near-UV LED irradiation (365 nm). b) Insets of the ^{31}P NMR spectrum for the reaction of P_4 (0.01 mmol) with Ph_3GeH (3 equiv. per P atom) driven by 365 nm LED irradiation. c) Single-crystal XRD structure of $[Ge]_2PH$ (**1**). [Ge] = Ph_3Ge. Thermal ellipsoids are shown at 50%. H atoms, except for the one bound directly to P, are omitted for clarity. C atoms are shown in grey, H is white, P in orange, and Ge in dark green.

Under these reaction conditions, the conversion to the main products (**1** and **2**) was still relatively limited (<54%), likely due to the continuing formation of the insoluble P_n compounds noted above. Gratifyingly, however, using an excess of Ph_3GeH and more concentrated reaction mixtures resulted in significantly improved reaction outcomes with conversions up to 87% (for **1** and **2**; 95% including **3**), reaction times reduced to 24 hours (see Scheme 3a and Table S1), and clear yellowish solutions with no observable precipitates at the end of the reaction. Interestingly, orange precipitates still form at the beginning of these reactions but later disappear,[34] which may suggest that the initially formed P_n compounds are in fact still available during the overall reaction course, serving as a source of P atoms in the formation of the final products, following a similar degradation process to that described for the reaction of P_{red} with Bu_3SnH.[20] Consistent with this suggestion, when Ph_3GeH was reacted with P_{red} instead of P_4, the hydrogermanylphosphines **1** and **2** were again formed, albeit with reduced conversion (39%, see Section 5.4.2.4). This result

also provides a proof-of-principle confirmation that bench-stable P_{red} can also be functionalised using germanium hydrides.

We propose that the hydrogermylation of P_4 follows a radical chain mechanism analogous to the hydrostannylation of P_4 and P_{red} (Scheme 3b).[35,36] This is also consistent with the calculations noted above. Nevertheless, the observation of significant formation of insoluble P_n is a clear point of contrast between R_3GeH and R_3SnH.

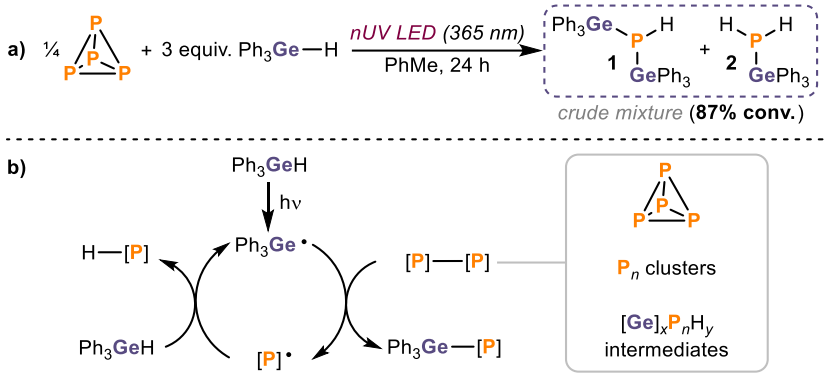

Scheme 3. a) Optimised conditions for the hydrogermylation of P_4 promoted by near-UV irradiation (365 nm). b) Proposed radical chain mechanism for P_4 hydrogermylation, where [P]–[P] represents a generic P–P bond.

To understand why this difference might occur, the aggregation of P_4 to form larger P_n moieties was considered computationally. For simplicity, calculations were limited to a single representative step: addition of further P_4 to the initial radical intermediate $(Me_3E)P_4^{\bullet}$, which was calculated for all three model systems, E = Sn/Ge/Si. This step would result initially in the formation of a P_8 "double butterfly" radical intermediate ($(Me_3E)P_8^{\bullet}$), *en route* to further aggregation and rearrangement steps (Scheme 4). Notably, for all three systems, this step was found to be *less* energetically demanding than the calculated HAT step that would lead to further hydroelementation (*cf.* Figure 1b), confirming that aggregation to larger P_n fragments is likely to be mechanistically relevant. However, for Me_3Sn the difference in activation barriers is relatively modest (2.2 kcal mol^{-1}; *cf.* Scheme 4 and Figure 1b or see Figure S1), whereas for Me_3Ge and especially Me_3Si it is much greater (10.6 kcal mol^{-1} and 13.0 kcal mol^{-1}, respectively). This is mostly due to differences in the HAT step, which is sensitive to changes in the E–H bond strength. In comparison, the identity of the Me_3E substituent has relatively little impact on the barrier to further P_4 addition since it is distant from the active radical site. Although care should be taken not to over-interpret these limited calculations, the results are consistent with the idea that for R_3SnH the desired hydrostannylation is sufficiently kinetically competitive with aggregation to prevent significant formation of large, insoluble P_n fragments. In contrast, for R_3GeH and R_3SiH there is a much stronger kinetic preference for aggregation, suggesting that large, insoluble P_n aggregates should be more prevalent and that precipitation should this limit the overall reaction rate, consistent with experimental observations. This problem should become more severe as E–H bond strength increases, consistent with the relative performance of Bu_3GeH and Ph_3GeH.

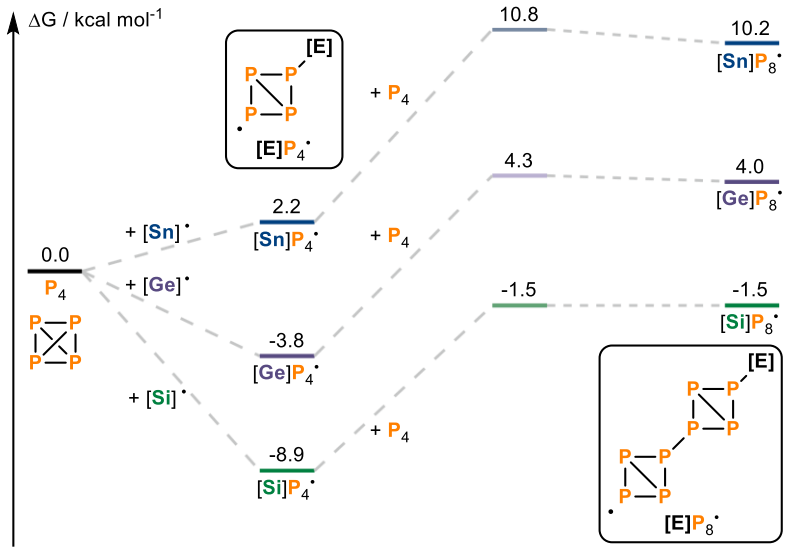

Scheme 4. Calculated aggregation between P_4 and the initial intermediate **[E]**$P_4^{\bullet}$ (relative free energies in kcal mol^{-1}). **[E]** = Me_3Si, Me_3Ge or Me_3Sn. For simplicity, stereochemistry is not shown.

5.2.2 Functionalisation of Ph_3GePH_2 and $(Ph_3Ge)_2PH$

After optimising the hydrogermylation of P_4, we next focused on the synthetic utilisation of the newly formed Ge-substituted phosphines **1** and **2** in a 'one-pot' fashion. Notably, simple acidification of the crude mixture with HCl (in 1,4-dioxane) prompted the cleavage of the P–Ge bonds, resulting in the formation of PH_3 (**4**, Scheme 5) with similar efficiency to that achieved using Bu_3SnH (≥50% conversion, *cf.* ≥56% *via* Bu_3SnH). Furthermore, treatment of the crude mixture with benzyl bromide (BnBr) or bromoethane (EtBr) in the presence of base yielded the phosphonium salts $[Bn_4P]Br$ (**5**) and $[Et_4P]Br$ (**6**), with the former being isolated at preparative scale in 77% yield (Scheme 5, *cf.* 80% *via* Bu_3SnH). These results confirm that the P–Ge bonds in the new P_1 intermediate mixture are sufficiently reactive to allow functionalisation into desirable P_1 compounds in a manner similar to $(Bu_3Sn)_xPH_{3-x}$.[19] However, it should be noted that these newer transformations require longer reaction times and higher temperatures to reach completion. Additionally, reactions of the crude mixture of **1** and **2** with other representative electrophiles that reacted successfully with $(Bu_3Sn)_xPH_{3-x}$, such as paraformaldehyde or acyl chlorides, have so far only resulted in low conversions and/or incomplete reactions (see Section 5.4.2.7), indicating that this equivalence is not universal, with the P–Ge bonds sometimes being less labile.

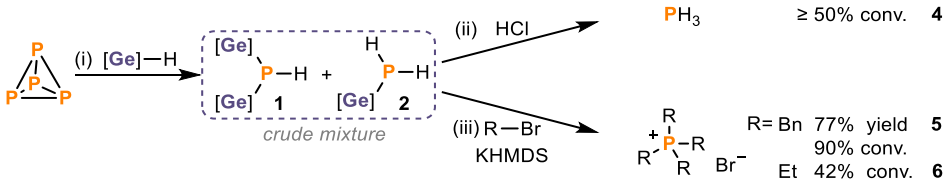

Scheme 5. Functionalisation of the crude mixture of **1** and **2** derived from P_4 directly into useful P_1 products. Equivalents are defined per P atom. (i) P_4 (0.25 equiv.), Ph_3GeH (3 equiv.), PhMe, 365 nm LEDs, RT, 24 h. (ii) Transformation of P_4 into PH_3 from crude mixture (**1** and **2**): 10 equiv. HCl (4.0M in 1,4-dioxane) RT, 1 h). (iii) Preparation of phosphonium salts $[R_4P]Br$ from crude mixture (**1** and **2**): 10 equiv. RBr (R = Bn or Et), 2.5 equiv. KHMDS, 100 °C, 3 d. [Ge] = Ph_3Ge.

5.2.3 Hydrosilylation of P_4

Having established successful hydrogermylation of P_4, focus was then shifted to the generally cheaper and more readily available hydrosilanes, R_3SiH (*cf.* the more specialised R_3GeH). Hydrosilanes, however, are known to be poor radical chain reagents due to their relatively strong Si–H bonds.[27,37] Moreover, the calculations discussed above imply that formation of insoluble P_n is likely to be an even greater problem for R_3SiH than for R_3GeH. And indeed, initial reactivity studies confirmed that the combination of R_3SiH (R = Ph, Et) with P_4 under the same conditions previously established for either R_3SnH or R_3GeH leads to either no reaction (see Section 5.4.3.1) or formation of insoluble P_n compounds only. Attention was then shifted to hypersilane, $(Me_3Si)_3SiH$, which is known to be a more reactive radical reagent due to hyperconjugation effect of the Me_3Si groups.[24,27,38] However, still only trace new resonances (and unreacted P_4) were observed in the $^{31}P\{^1H\}$ NMR spectra when it was reacted with P_4 (Scheme 6a).

To overcome similar problems in the radical hydrosilylation of unsaturated C=C bonds, organic chemists have developed the use of simple thiols as hydrosilylation catalysts.[39,40] The origin of this catalysis lies in the poor electronic compatibility between the hydrosilane and C-centred radical (both nucleophilic), and much better electronic match between these species and the thiyl radical and thiol (both electrophilic), respectively. Given the well-known, broad chemical similarity between P and C, and the fact that P is even slightly more electropositive than C, it was speculated that a similar thiol-assisted reaction could facilitate the key HAT process and enable the direct hydrosilylation of P_4 to $(R_3Si)_nPH_{3-n}$, as outlined in Scheme 6b.

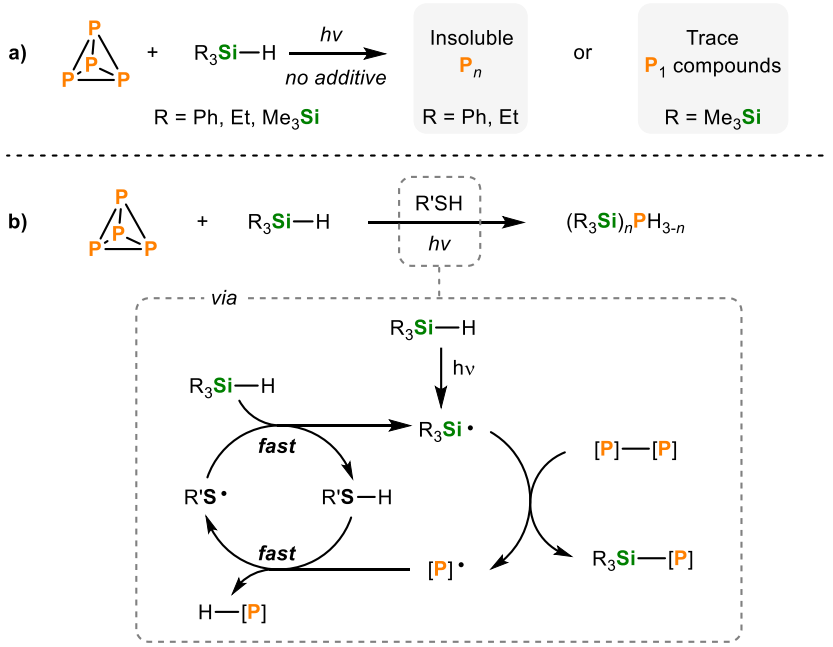

Scheme 6. a) Reactivity studies of silanes R_3SiH towards P_4 driven by LED irradiation (456 nm or 365 nm). b) Proposed thiol-assisted hydrosilylation of P_4, where [P]–[P] represents a generic P–P bond.

Gratifyingly, the reaction of $(Me_3Si)_3SiH$ and P_4 in the presence of an excess of a thiol such as iPr$_3$SiSH led to the full consumption of P_4 and the formation of a mixture of Si/H-substituted

monophosphorus products (Scheme 7), which appeared as singlets between *ca.* −210 and −280 ppm in the $^{31}P\{^{1}H\}$ NMR spectrum. The main species formed were identified after close examination of the $^{31}P\{^{1}H\}$ and ^{31}P NMR spectra (Scheme 7b and 7c, see also Figures S28 and S29) and comparison with reported spectroscopic data.[41,42] The major product was the primary phosphine $[(Me_3Si)_3Si]PH_2$ (**7**, −266.5 ppm), followed by $[(Me_3Si)_3Si]P(H)SiMe_3$ (**8**, −257.2 ppm), Me_3SiPH_2 (**9**, −236.5 ppm) and $(Me_3Si)_2PH$ (**10**, −236.3 ppm), which contain Me_3Si groups directly bound to the phosphorus atom, indicating Si–Si bond cleavage within the hypersilane motif. Whether this cleavage occurs primarily before or after the hydrosilylation is presently unclear. Satisfyingly, upon optimisation, hydrosilylation *via* this procedure yielded the major reduced P_1 products in almost 80% combined yield (Scheme 7d, see also Table S5). The hydrosilylation of P_4 was also achieved with other thiol derivatives, RSH (R = Cy, Ad, Ph, 4-MePh), and even with 1,4-cyclohexadiene (1,4-CHD; see Table S6 and Figures S30-35).[43,44] Optimisation studies revealed that the use of substoichiometric amounts of the hydrogen atom donor was detrimental to overall conversions. Additionally, other, less activated silanes R_3SiH (R = Ph, Et, Me_3SiO) were found to be ineffective, even when an excess of additive was used (see Table S7).

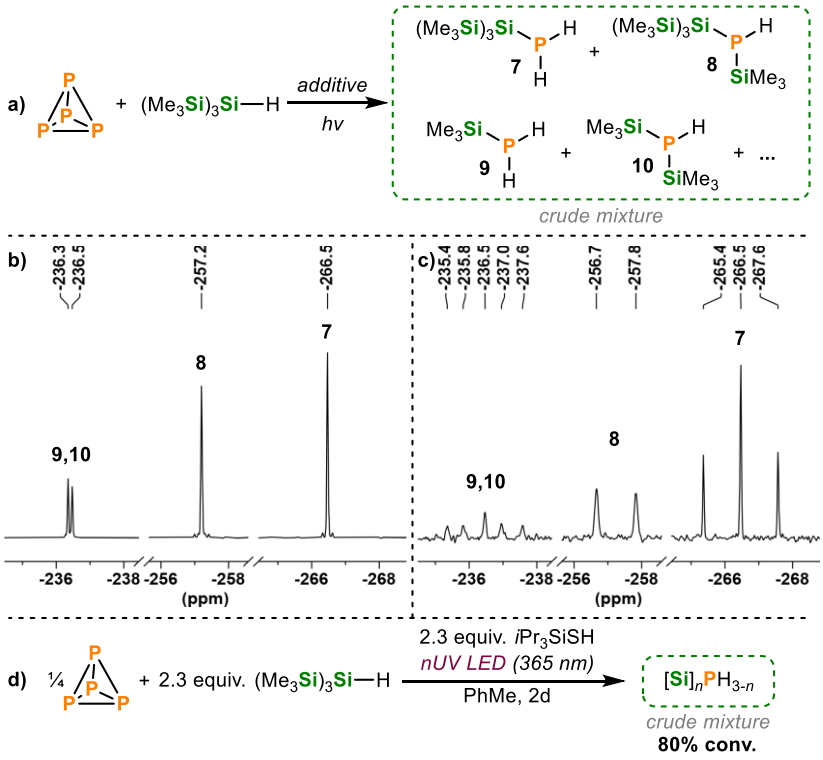

Scheme 7. a) Hydrosilylation of P_4 with $(Me_3Si)_3SiH$ in the presence of a hydrogen atom transfer donor, promoted by LED irradiation. Insets of the $^{31}P\{^{1}H\}$ (b) and ^{31}P (c) NMR spectra for the reaction of P_4 with $(Me_3Si)_3SiH$ (3.5 equiv. per P atom) and iPr$_3$SiSH (3.5 equiv. per P atom) in hexane and driven by 365 nm LED irradiation, see Figures S28 and S29 for the full version of the spectra. d) Optimised conditions for the hydrosilylation of P_4 in the presence of iPr$_3$SiSH, promoted by near-UV irradiation.

5.2.4 Functionalisation of crude $[Si]_nPH_{3-n}$ mixture

Finally, we examined the reactivity of the crude phosphine mixture obtained from the hydrosilylation of P_4 in the presence of a HAT donor to access monophosphosphorus compounds in 'one-pot' transformations. Simple acidification with HCl (in 1,4-dioxane) resulted in the efficient cleavage of the P–Si bonds and the selective formation of PH_3 (**4**) with good conversion (≥64%; Scheme 8, top). Additionally, various phosphonium salts including $[Bn_4P]Br$ (**5**, 73% conversion), $[Et_4P]Br$ (**6**, 54% conversion), and $[Bu_4P]Br$ (**11**, 40% conversion, marketed commercially as CYPHOS 442W) were also accessible directly from P_4 after reaction of the $[Si]_nPH_{3-n}$ mixture with the corresponding alkyl bromides and base (Scheme 8, middle). Furthermore, treatment of the hydrosilylphosphine mixture with paraformaldehyde in EtOH resulted in exclusive formation of the industrially relevant phosphonium salt THPC (tetrakis(hydroxymethyl)phosphonium chloride, **12**, 48% conversion) after quenching with HCl (Scheme 8, bottom). Although these new reactions generally require more forcing conditions than when starting from $(Bu_3Sn)_xPH_{3-x}$, they demonstrate that the $[Si]_nPH_{3-n}$ mixture has a similar potential to act as an efficient P_1 precursor and P^{3-} synthon.

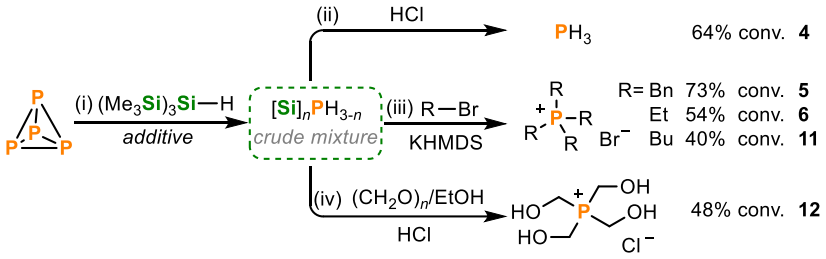

Scheme 8. Functionalisation of crude $[Si]_nPH_{3-n}$ mixture into useful P_1 products directly from P_4. Equivalents are defined per P atom. (i) P_4 (0.25 equiv.), $(Me_3Si)_3SiH$ (2.25 equiv.), iPr$_3$SiSH or 1,4-CHD (2.25 equiv.), PhMe, 365 nm LEDs, RT, 2 d. (ii) One-pot, selective transformation of P_4 into PH_3 from crude $[Si]_nPH_{3-n}$: 10 equiv. HCl (4.0M in 1,4-dioxane) RT, 1 h). (iii) Preparation of phosphonium salts $[R_4P]Br$ from crude $[Si]_nPH_{3-n}$: 10 equiv. RBr (R = Bn, Et or Bu), 2.5 equiv. KHMDS, 100 °C, 3 d. (iv) preparation of THPC from crude $[Si]_nPH_{3-n}$: EtOH, 12.5 equiv. paraformaldehyde, 50 °C, 3 d, then 10 equiv. HCl (4.0 M in 1,4-dioxane), RT, 2 h. [Si] = $(Me_3Si)_3Si$ or Me_3Si.

5.3 Conclusion

We have described herein our studies into the fundamental reactivity of lighter Group 14 hydrides, specifically hydrogermananes and hydrosilanes, towards P_4, as part of our mission to extend our previously reported P_4 hydrostannylation strategy and overcome safety concerns associated with the use of organotin compounds. Satisfyingly, the hydroelementation of P_4 is successful with both families of lighter homologues R_3EH. While our computational and experimental studies both reveal relevant differences in reactivity (which are related to the differing E–H bond strengths), these can be overcome through rational optimisation of the reaction conditions. Furthermore, these hydroelementation reactions yield similarly functionalisable $[E]_nPH_{3-n}$ mixtures which can serve as P_1 precursors for the formation of useful organophosphorus compounds in a 'one-pot' reaction. These results clearly show that the desired P_4 functionalisation is not limited to organotin derivatives and is in fact generalisable. Extrapolation from these results implies that extension to other known R_3SnH alternatives should be possible, many of which are known to compete well with R_3SnH in other contexts. Efforts in this direction are currently ongoing in our laboratories.

5.4 Supporting Information

General information

Unless stated otherwise, all reactions and manipulations were performed under an N_2 atmosphere (< 0.1 ppm O_2, H_2O) through use of MBraun Unilab and GS MEGA Line gloveboxes and standard Schlenk line techniques. All glassware was oven-dried (160 °C) overnight prior to use. PhH was distilled from Na/benzophenone and stored over molecular sieves (3 Å). MeCN was distilled from CaH_2 and stored over molecular sieves (3 Å). *n*-Hexane, PhMe, Et_2O and THF were purified using an MBraun SPS-800 system and stored over molecular sieves (3 Å). EtOH was degassed and dried by standing over at least three sequential batches of molecular sieves (3 Å). C_6D_6 was distilled from K and stored over molecular sieves (3 Å). CD_3CN, CD_3OD and D_2O were used without purification. All reagents and starting materials were purchased from major suppliers. Liquids were degassed (if not supplied under inert atmosphere) but were otherwise used as supplied, unless stated otherwise. 1,4-Cyclohexadiene was supplied containing 0.1% BHT as stabilizer and was used as received. BnBr, EtBr, BuBr, PhC(O)Cl and *t*BuC(O)Cl were distilled, degassed, and stored over molecular sieves (3 Å). Solids were dried under vacuum (with the exception of paraformaldehyde) but otherwise used as supplied, unless stated otherwise. Red phosphorus (≥97.0%) was purchased from Sigma-Aldrich.

NMR spectra were recorded at room temperature on Bruker Avance 400 spectrometers (400 MHz). Chemical shifts, δ, are reported in parts per million (ppm); ^{1}H NMR and ^{13}C NMR shifts are reported relative to $SiMe_4$ and were referenced internally to residual solvent peaks, while ^{31}P NMR and ^{119}Sn shifts were referenced externally to 85 % H_3PO_4 (aq.) and $SnMe_4$ (90% in C_6D_6), respectively. Except where stated otherwise, integrals for $^{31}P\{^{1}H\}$ and ^{31}P spectra are provided for the purposes of qualitative comparison only, and should not be considered quantitatively accurate. The abbreviations s, d, t, q, m are used to indicate singlets, doublets, triplets, quartets and multiplets, respectively.

Reactions driven by light were performed using apparatus that has been described in previous publications, in which reaction vessels are illuminated from beneath by LEDs while placed in a metal block through which cooling water is constantly circulated to maintain near-ambient temperature.[15]

LEDs used for the optimisation reactions:

- 365 nm, 3 W: 4.3 V, 700 mA, Osram OSLON SSL 80
- 365 nm, 10 W: 14 V, 700 mA, Osram OSLON SSL 80
- 390 nm, 40 W: Kessil PR160L
- 455 nm (±15 nm): 3.7 V, 700 mA, Osram OSLON SSL 80

5.4.1 Computational investigations

5.4.1.1 General methods

All calculations were carried out with the ORCA program package.[45,46] Unless stated otherwise, all calculations were carried out on isolated molecules (in the gas phase). Density fitting techniques, also called resolution-of-identity approximation (RI)[47], were used for GGA calculations and the RIJCOSX[48] approximation was used for hybrid-GGA DFT calculations. Atom-pairwise dispersion corrections with the Becke-Johnson damping (D3BJ)[49,50] were used for all DFT calculations. Pictures were rendered with the software Avogadro.[51] All geometries were obtained at the PBE-D3BJ/def2-TZVP level of theory.

5.4.1.2 Mechanisms of P_4 hydroelementation by Me_3EH (E = Si, Ge, Sn)

The calculated mechanisms for the hydroelementation of the first P–P bond in P_4 by $Me_3E^{\bullet}$ addition and subsequent HAT and the aggregation of P_4 with the initial intermediate $(Me_3E)P_4^{\bullet}$ are combined in Figure S1 for ease of comparison.

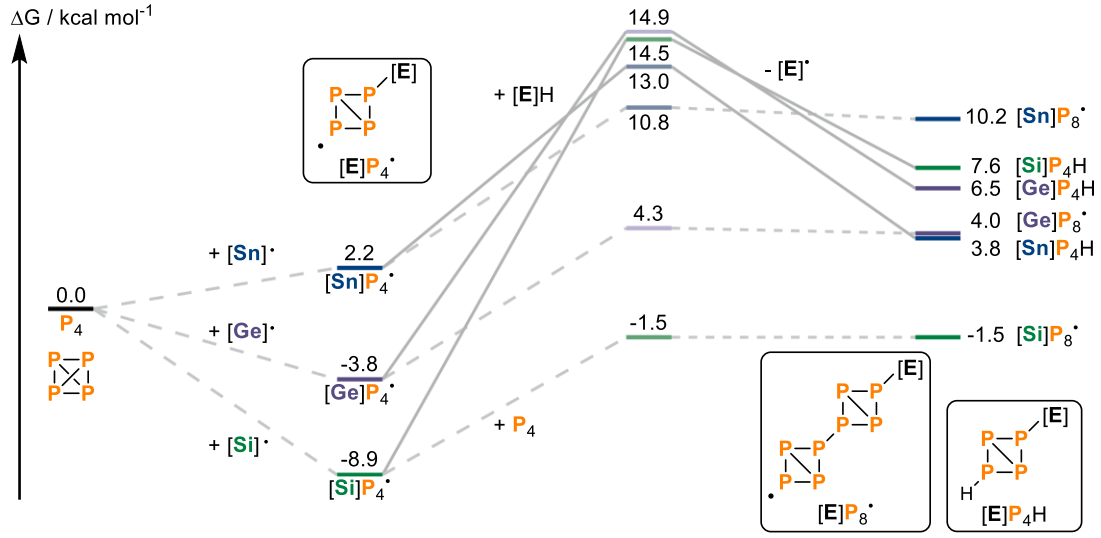

Figure S1. Calculated mechanisms for hydroelementation of the first P–P bond in P_4 and for agregation of further P_4 with the first P-centred radical intermediate (relative free energies in kcal mol^{-1}). **[E]** = Me_3Si, Me_3Ge or Me_3Sn.

5.4.2 Hydrogermylation of white phosphorus (P_4)

5.4.2.1 Hydrogermylation of P_4 using Bu_3GeH and LED irradiation (0.01 mmol scale)

Representative procedure:

To a 10 mL, flat-bottomed, stoppered tube were added P_4 (0.01 mmol, as a stock solution in 84.3 µL PhH), PhMe (500 µL), and Bu_3GeH (46.5 µL, 0.18 mmol). The tube was sealed, placed in a water-cooled block to maintain near-ambient temperature, and irradiated with UV light (365 nm, 14 V, 700 mA, Osram OSLON SSL 80) for 3 days. Ph_3PO (0.02 mmol, stock solution in benzene) was subsequently added to act as an internal standard. The resulting mixture was analysed by $^{31}P\{^1H\}$ and ^{31}P NMR spectroscopy, as shown in Figures S2-4 below.

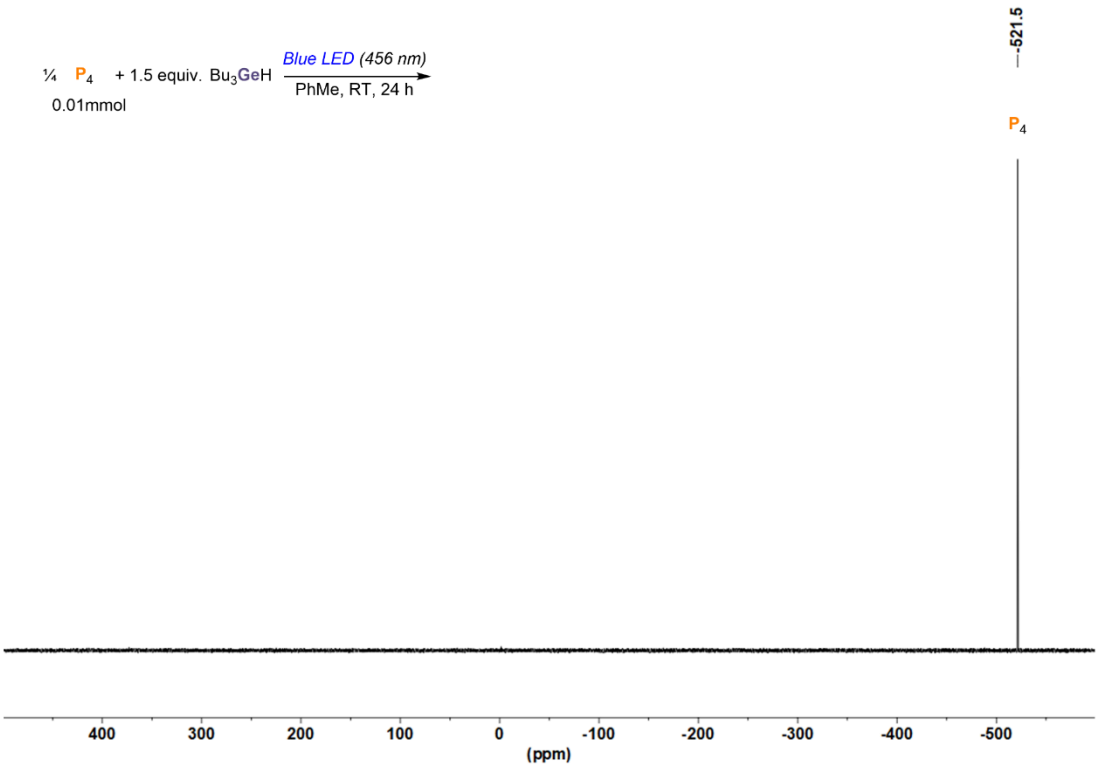

Figure S2. $^{31}P\{^{1}H\}$ NMR spectrum for the reaction of P_4 (0.01 mmol) with Bu_3GeH (0.06 mmol) in PhMe and driven by 456 nm LED irradiation for 24 h.

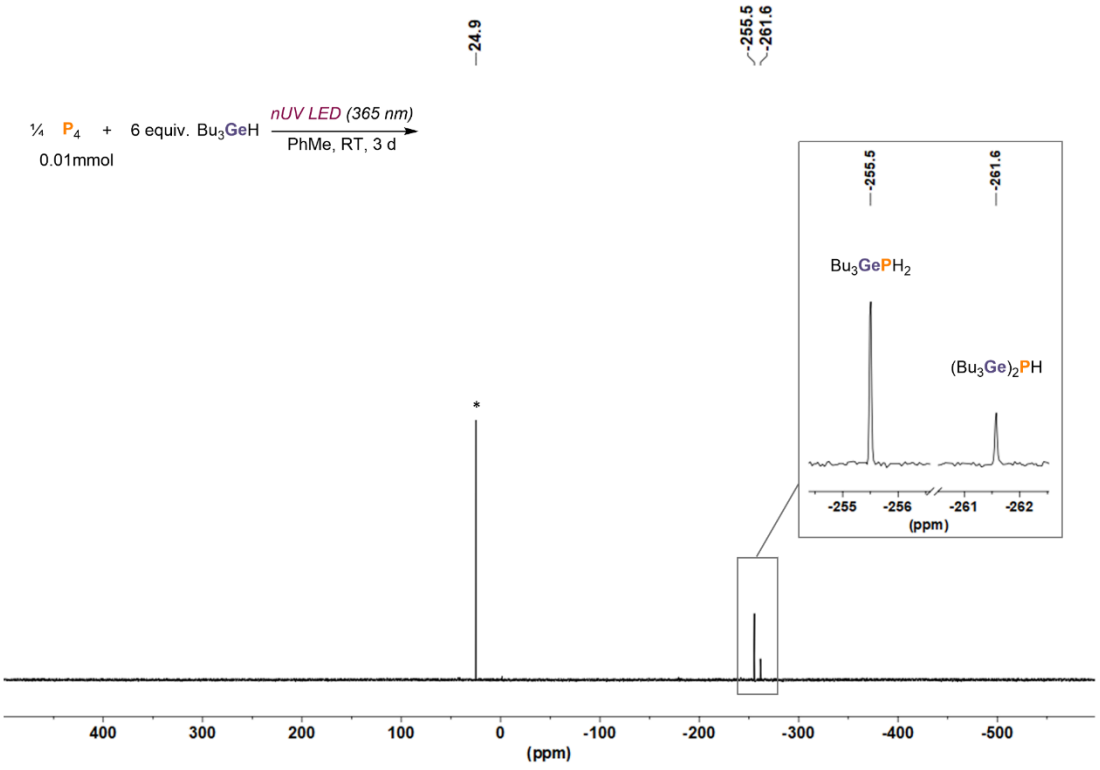

Figure S3. $^{31}P\{^{1}H\}$ NMR spectrum for the reaction of P_4 (0.01 mmol) with Bu_3GeH (0.18 mmol) in PhMe and driven by 356 nm, 10 W LED irradiation for 3 days. * marks the internal standard Ph_3PO.

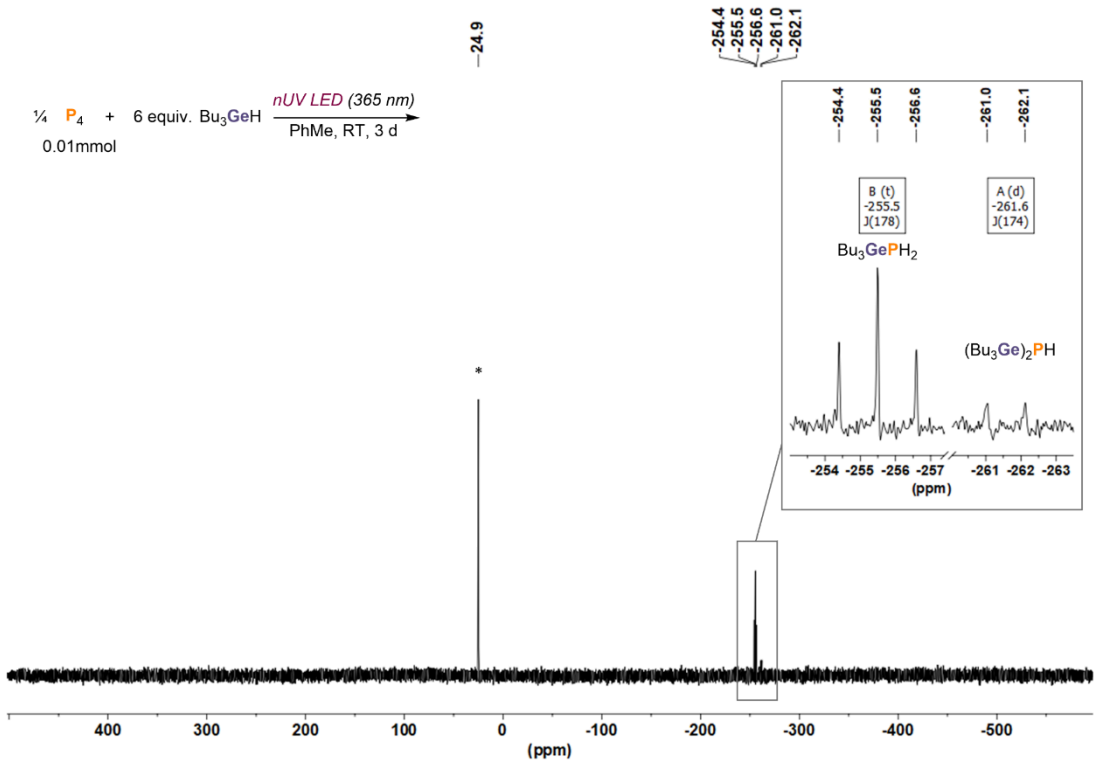

Figure S4. ^{31}P NMR spectrum for the reaction of P_4 (0.01 mmol)with Bu_3GeH (0.18 mmol) in PhMe and driven by 356 nm, 10 W LED irradiation for 3 days. The insets show expansions of the signals attributed to Bu_3GePH_2 and $(Bu_3Ge)_2PH$, highlighting their multiplicity due to $^1J(^{31}P\text{-}^1H)$ couplings. * marks the internal standard Ph_3PO.

5.4.2.2 General procedure and optimisation for the hydrogermylation of P_4 using Ph_3GeH and LED irradiation (0.01 mmol scale)

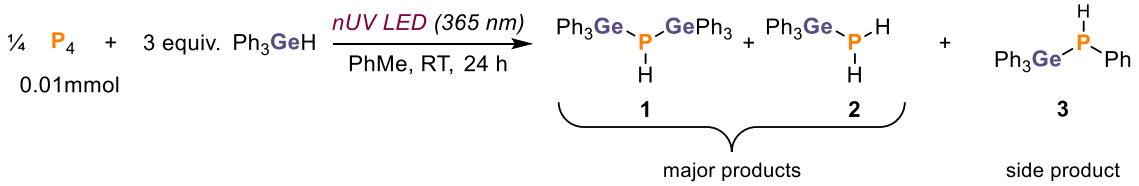

Representative procedure:

To a 10 mL, flat-bottomed, stoppered tube were added P_4 (0.01 mmol, as a stock solution in 84.3 µL PhH), PhMe (100 µL), and Ph_3GeH (36.6 mg, 0.12 mmol). The tube was sealed, placed in a water-cooled block to maintain near-ambient temperature, and irradiated with UV light (365 nm, 4.3 V, 700 mA, Osram OSLON SSL 80) for 24 hours. Ph_3PO (0.02 mmol, stock solution in benzene) was subsequently added to act as an internal standard. The resulting mixture was analysed by ^{1}H, ^{31}P{^{1}H}, and ^{31}P NMR spectroscopy, as shown in Figures S5-7, below. Compounds **1-3** have not been reported previously. However, the observed NMR data are consistent with those reported for similar compounds such as $(Me_3Ge)_2PH$[32] and $R_3Ge_2P(H)Ph$ (R = Me, Et).[33]

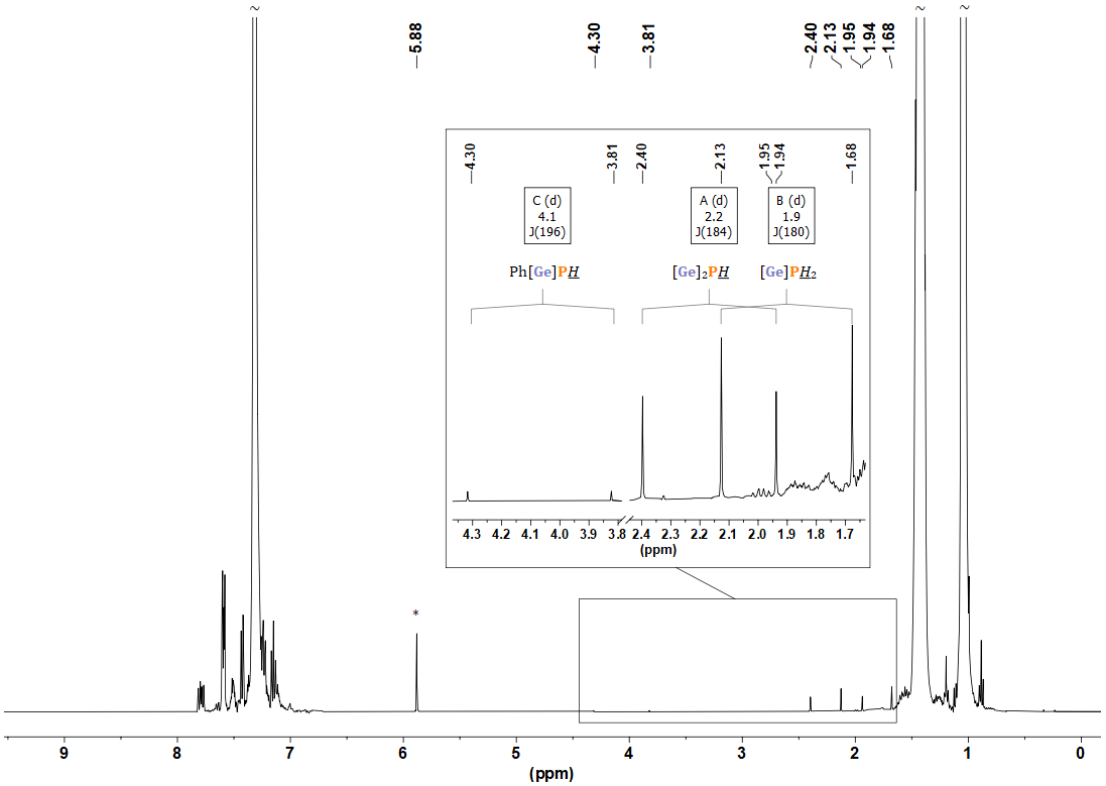

Figure S5. ^{1}H NMR spectrum for the reaction of P_4 with Ph_3GeH (0.12 mmol) in hexane and driven by 365 nm, 3 W LED irradiation for 3 d (Table S1, Entry 9). The inset shows expansions of the doublet resonances attributed to the P*H* moieties of $(Ph_3Ge)_2PH$ (**1**) and [Ge]P(H)Ph (**3**), and the PH_2 moiety of $(Ph_3Ge)PH_2$ (**2**). [Ge] = Ph_3Ge. * marks Ph_3GeH. ~ marks solvent resonances truncated for clarity.

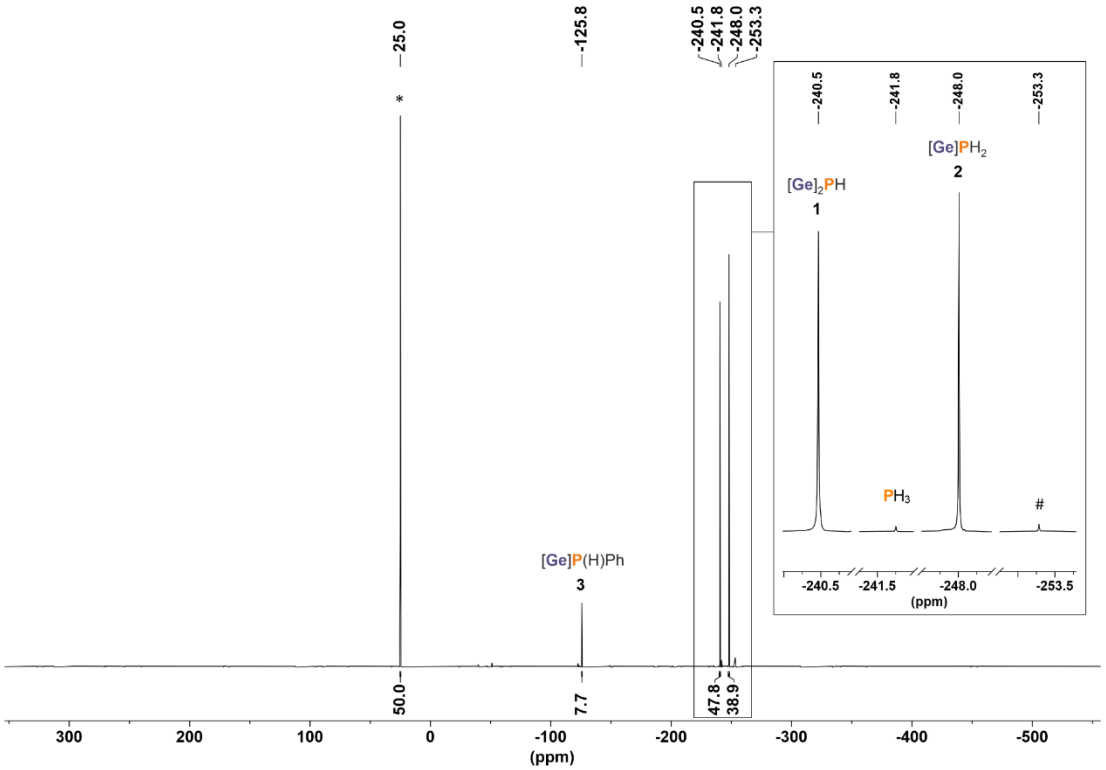

Figure S6. Quantitative $^{31}P\{^{1}H\}$ NMR spectrum (D1 = 40 s) for the reaction of P_4 with Ph_3GeH (0.12 mmol) in PhMe and driven by 365 nm, 3 W LED irradiation for 3 d (Table S1, Entry 9). [Ge] = Ph_3Ge. * marks the internal standard Ph_3PO (0.02 mmol). # marks an unknown side product.

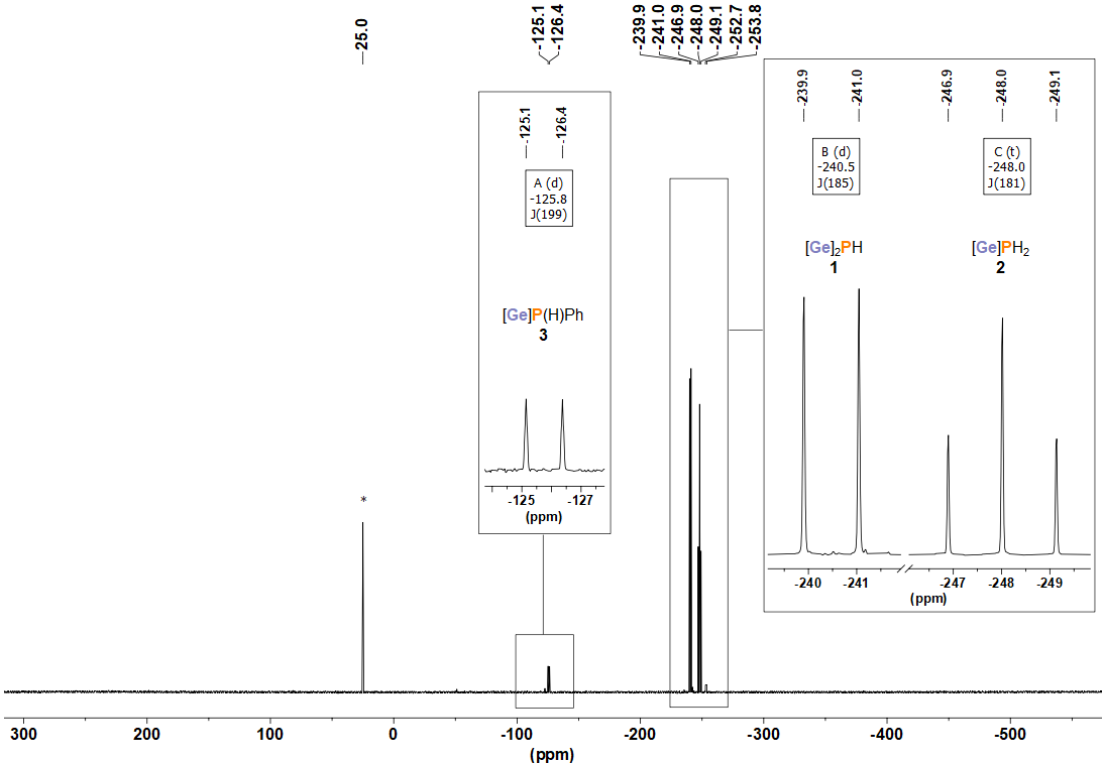

Figure S7. ^{31}P NMR spectrum for the reaction of P_4 with Ph_3GeH (0.12 mmol) in hexane and driven by 365 nm, 3 W LED irradiation for 3 d (Table S1, Entry 9). The insets show expansions of the signals attributed to $[Ge]_2PH$ (**1**), $[Ge]PH_2$ (**2**) and [Ge]P(H)Ph (**3**), highlighting their multiplicity due to $^1J(^{31}P\text{-}^1H)$ couplings. [Ge] = Ph_3Ge. * marks the internal standard Ph_3PO (0.02 mmol).

For reasons of experimental expediency, during the optimisation of the hydrogermylation of P_4, non-quantitative $^{31}P\{^1H\}$ NMR spectra was recorded to analyse each experiment and to assess the relative total conversion to **1-3**. Although this did not provide precise, quantitative conversions directly it did allow for meaningful, qualitative comparisons between experiments. Under the conditions highlighted in Table S1, entry 9, a quantitative $^{31}P\{^1H\}$ NMR spectrum was recorded using an inverse-gated decoupled pulse sequence (D1 = 40 s, Figure S6), and the conversion of P_4 to products **1-3** was determined. Thus, for ease of interpretation, the integrals measured for **1-3** for all optimisation experiments have been normalized relative to the value for this experiment (Table S1, entry 9) to provide the relative conversions indicated in Table S1.

Table S1. Optimisation of hydrogermylation of P_4 using Ph_3GeH and near-UV LED irradiation (365 nm).[a]

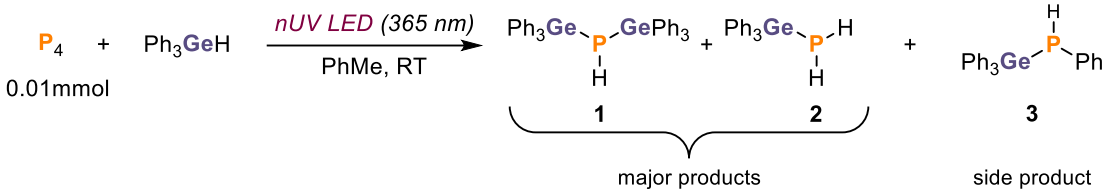

Entry	Ph_3GeH (mmol)	PhMe (µL)	Time (days)	Full conv. of P_4?	Relative conv. to **1** and **2** (%)	Relative conv. to **3** (%)
1[c]	0.06	500	1	X	traces	-
2[c]	0.06	500	3	✓	9	-
3	0.06	500	3	✓	46.7	10.0
4	0.06	500 (hexane)	3	✓	54.1	8.9
5	0.06	500 (THF)	3	✓	49.0	11.9
6	0.06	500 (EtOH)	3	X	4.7	-
7	0.06	500 (CH_3CN)	3	✓	7.9	-
6	0.09	500	4	✓	75.6	12.8
7	0.09	500 (hexane)	3	✓	70.2	7.6
8	0.12	500 (hexane)	3	✓	81.9	4.8
9	**0.12**	**500**	**3**	**✓**	**86.7**	**7.7**
10	0.12	100	3	✓	57.7	13.3
11	0.12	100	2	✓	77.9	12.0
12	**0.12**	**100**	**1**	**✓**	**87.4**	**7.8**

[a] The general procedure described in this section was modified to use the indicated amount of reactants and solvent. [b] Conversions were calculated by integration of the ^{31}P resonances of **1**-**3** relative to an internal standard, which was then normalized relative to entry 9 as described in the text above. [c] Blue LED (455 nm).

5.4.2.3 Crystallographic characterisation of $(Ph_3Ge)_2PH$ (1)

Single crystal X-ray diffraction data for $(Ph_3Ge)_2PH$ (**1**) were recorded on a Rigaku XtaLAB Synergy DW R (DW system, HyPix-Arc 150) diffractometer with microfocus Cu-Kα radiation (λ = 1.54184 Å). The crystal was selected under mineral oil, mounted on a micromount loop and quench-cooled using an Oxford Cryosystems open flow N_2 cooling device. Data processing, reduction and multi-scan absorption correction[52,53] was performed with the program CrysAlisPro (Rigaku Oxford Diffraction, 2021). Using Olex2,[54] the structure was solved with the SHELXT[55] structure solution program using Intrinsic Phasing and refined using SHELXL using Squares refinements on F^2.[56] $(Ph_3Ge)_2PH$ crystallizes in the monoclinic space group $P2_1$ with two molecules in the asymmetric unit. All non-hydrogen atoms were refined using anisotropic displacement parameters. All hydrogen atoms but the P bound hydrogen atoms were located in idealized positions and refined isotropically with a riding model. The P bound hydrogen atoms were located from the electron density map and had its positions and isotropic displacement parameters refined freely. The disorder of the P bound hydrogen atom (H2 at P2) was treated with a geometrical restraint.

Crystal and refinement data are collected in Table S2, and the structure itself is illustrated in Figure S8.

Table S2. Crystal data and structure refinement of **$(Ph_3Ge)_2PH$ (1)**.

	$(Ph_3Ge)_2PH$ (1)
Formula	$C_{36}H_{31}Ge_2P$
Formula weight, g mol^{-1}	639.76
Crystal system	123.0(1)
Crystal size, mm	monoclinic
Space group	$P2_1$
a, Å	9.67692(3)
b, Å	18.31240(5)
c, Å	17.49013(6)
α, °	90
β, °	105.3799(3)
γ, °	90
V, Å^3	2988.388(17)
Z	4
ρ_{calcd}, Mg m^{-3}	1.422
μ (Mo $K\alpha$), mm^{-1}	3.148
F(000)	1304.0
2θ range, deg	0.129 × 0.115 × 0.078
Index ranges	Cu Kα (λ = 1.54184)
	5.24 to 150.644
	-12 ≤ h ≤ 11, -22 ≤ k ≤ 22, -21 ≤ l ≤ 21
No. of reflns collected	174471
No. indep. Reflns	12237 [R_{int} = 0.0318, R_{sigma} = 0.0135]
No. refined params	12237/1/716
GooF (F^2)	1.040
R_1 (F) ($I > 2\sigma(I)$)	R_1 = 0.0168, wR_2 = 0.0426
wR_2 (F^2) (all data)	R_1 = 0.0172, wR_2 = 0.0427
Largest diff peak/hole, e Å^{-3}	0.25/-0.16

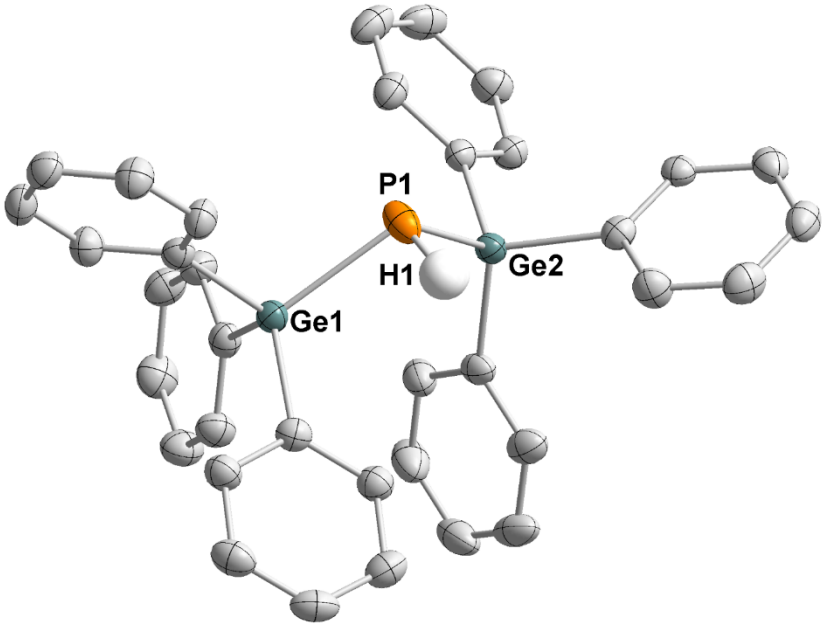

Figure S8. Single-crystal XRD structure of $(Ph_3Ge)_2PH$ (**1**). Thermal ellipsoids are shown at 50%. %. H atoms, except for the one bound directly to P, are omitted. C atoms are shown in grey, H in white, P in orange, and Ge in dark green.

5.4.2.4 Hydrogermylation of P_{red} using Ph_3GeH and LED irradiation (0.06 mmol scale)

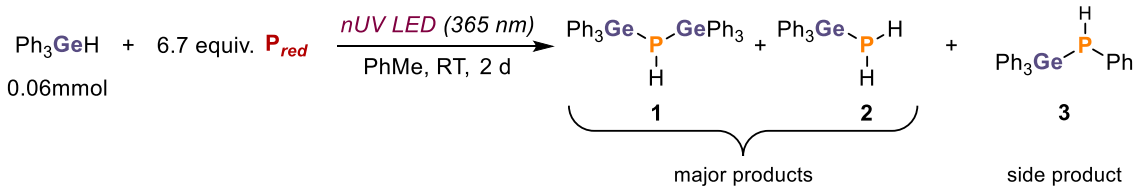

To a 10 mL, flat-bottomed, stoppered tube were added P_{red} (0.4 mmol, 12.4 mg), PhMe (250 µL), and Ph_3GeH (18.3 mg, 0.06 mmol). The tube was sealed, placed in a water-cooled block to maintain near-ambient temperature, and irradiated with UV light (365 nm, 14 V, 700 mA, Osram OSLON SSL 80) for 2 days. Ph_3PO (0.02 mmol, stock solution in benzene) was subsequently added to act as an internal standard. The resulting mixture was analysed by $^{31}P\{^1H\}$ NMR spectroscopy, as shown in Figure S9, below.

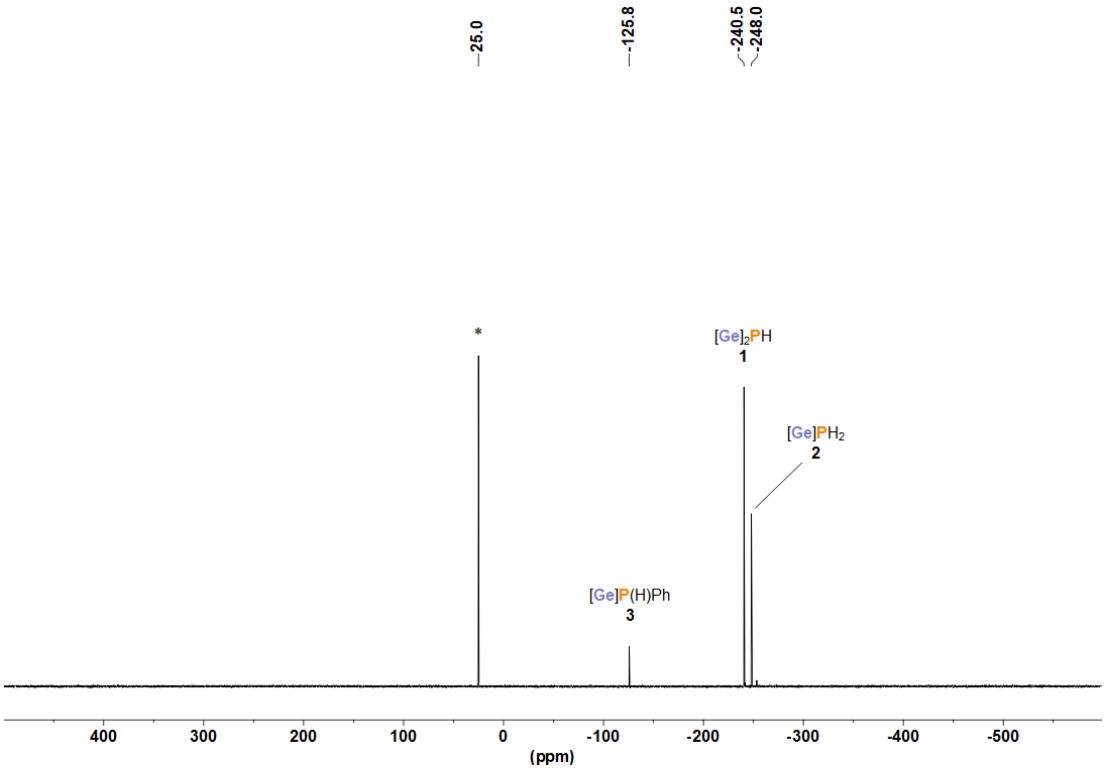

Figure S9. $^{31}P\{^{1}H\}$ NMR spectrum for the reaction of P_{red} with Ph_3GeH (0.06 mmol) in PhMe and driven by 356 nm, 10 W LED irradiation for 2 days. * marks the internal standard Ph_3PO. [Ge] = Ph_3Ge.

5.4.2.5 General procedure and optimisation for the hydrogermylation of P_4 using Ph_3GeH and chemical radical initiators (0.01 mmol scale)

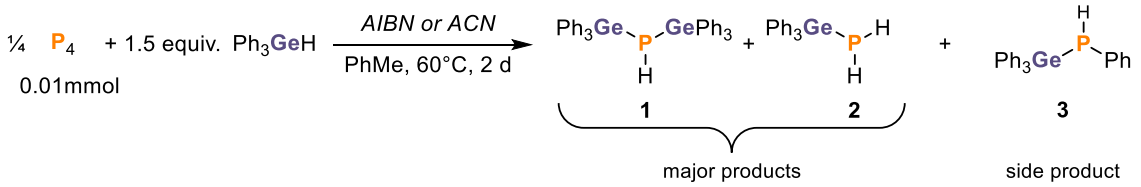

Representative procedure:

To a 10 mL, flat-bottomed, stoppered tube were added P_4 (0.01 mmol, as a stock solution in 84.3 µL PhH), PhMe (500 µL), AIBN (0.05 mmol, as a stock solution in PhH) and Ph_3GeH (18.3 mg, 0.06 mmol). The tube was sealed, wrapped in Al foil to exclude light, and heated to 60 °C for 2 days. Ph_3PO (14.0 mg, 0.0503 mmol) was subsequently added to act as an internal standard. The resulting mixture was analysed by $^{31}P\{^{1}H\}$ NMR spectroscopy, as shown in Figures S10 and 11, below.

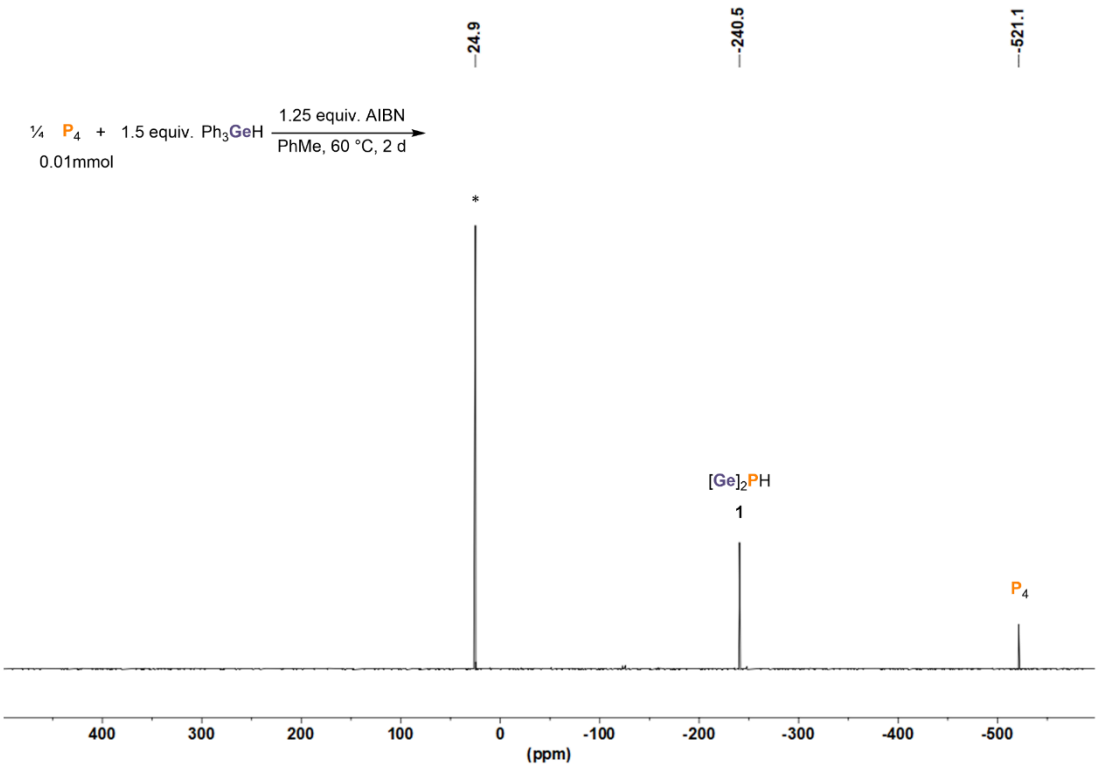

Figure S10. $^{31}P\{^{1}H\}$ NMR spectrum for the reaction of P_4 with Ph_3GeH (0.06 mmol) and AIBN (azobis(isobutyronitrile), 0.05 mmol) in PhMe, heated to 60 °C for 2 d (Table S3, Entry 4). * marks the internal standard Ph_3PO (0.0503 mmol). [Ge] = Ph_3Ge.

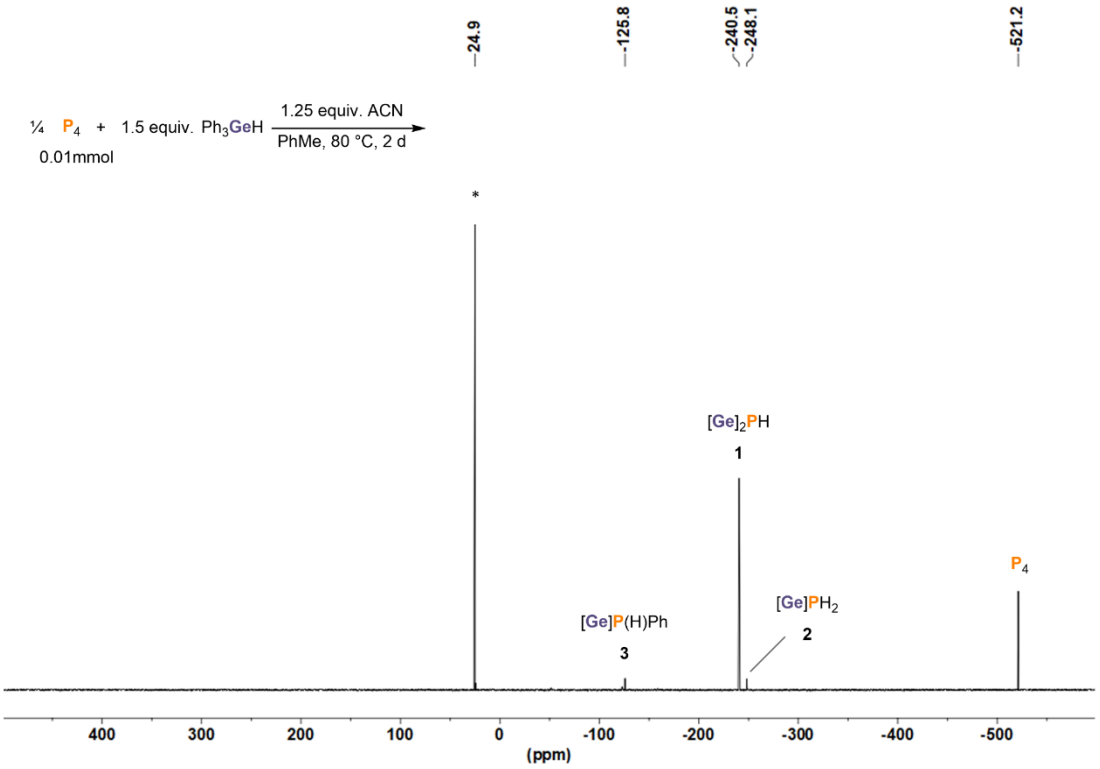

Figure S11. $^{31}P\{^{1}H\}$ NMR spectrum for the reaction of P_4 with Ph_3GeH (0.06 mmol) and ACN (1,1'-azobis(cyclohexanecarbonitrile), 0.05 mmol) in PhMe, heated to 80 °C for 2 d (Table S3, Entry 7). * marks the internal standard Ph_3PO (0.041 mmol). [Ge] = Ph_3Ge.

Table S3. Optimisation of hydrogermylation of P_4 using Ph_3GeH and chemical radical initiators.[a]

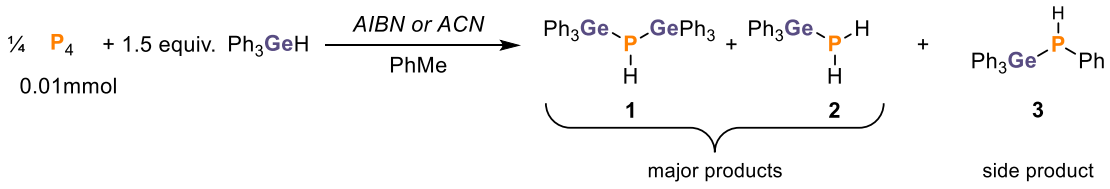

Entry	Radical initiator (mmol)	Temperature (°C)	Time (days)	Full conv. of $\mathbf{P_4}$?	Relative conv. to **1** and **2** (%)	Relative conv. to **3** (%)
1	AIBN (0.001)	60	1	X	traces	-
2	AIBN (0.001)	60	2	X	traces	-
3	AIBN (0.05)	60	1	X	<15	traces
4	AIBN (0.05)	60	2	X	27.6	traces
6	ACN (0.001)	80	1	X	traces	-
7	ACN (0.05)	80	2	X	21.7	traces
8	ACN (0.05)	100	2	X	<15	traces

[a] The general procedure described in this section was modified to use the indicated amount of reactant, temperature and time. [b] Conversions were calculated by integration of the ^{31}P resonances of **1**-**3** relative to an internal standard, which was then normalized relative to Table S1, entry 9 as described in section 5.4.2.2. AIBN = azobis(isobutyronitrile)). ACN = 1,1'-azobis(cyclohexanecarbonitrile).

5.4.2.6 Synthesis and quantification of PH_3 (4) via hydrogermylation of P_4 (0.01 mmol scale)

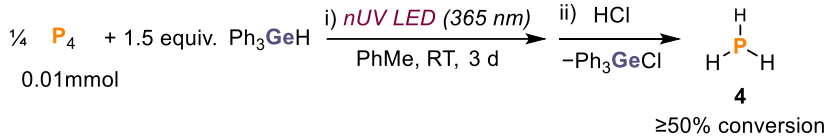

To an NMR tube fitted with a J. Young valve were added PhMe (500 µL), P_4 (0.01 mmol, as a stock solution in 97.7 µL PhH), Ph_3PO (11.5 mg, 0.0413 mmol) and Ph_3GeH (18.3 mg, 0.06 mmol). The NMR tube was sealed, placed in thermal contact with a water-cooled block to maintain near-ambient temperature (by placing in a water-filled, flat-bottomed glass tube, which was in turn placed in the block and wrapped in Al foil), and irradiated with UV light (365 nm, 4.3 V, 700 mA, Osram OSLON SSL 80) for 3 days. The resulting yellow suspension was frozen by placing the NMR tube in a bath of liquid nitrogen, and HCl (0.4 mmol, 4.0 M in 1,4-dioxane) was added (while still maintaining an inert atmosphere). The NMR tube was sealed and its contents were then thawed, agitated briefly, and analysed by ^{1}H, $^{31}P\{^{1}H\}$ and ^{31}P NMR spectroscopy. The resulting spectra indicated clean conversion of **1** and **2** to PH_3,[19] and the formation of $PhPH_2$ from **3** as shown in Figures S12-14, below.[57]

In order to accurately quantify the amount of PH_3 in solution, a proton-coupled ^{31}P spectrum was acquired with a 20 s delay between scans (which was confirmed to be > 5 x T_1), and the intensity of the PH_3 resonance was integrated relative to that of Ph_3PO (which had been added specifically to act as an internal standard). This indicated 50% of the theoretical maximum conversion to PH_3 (Figure S15), which provides a lower bound for the actual conversion (this value does not include any PH_3 present in the NMR tube headspace).

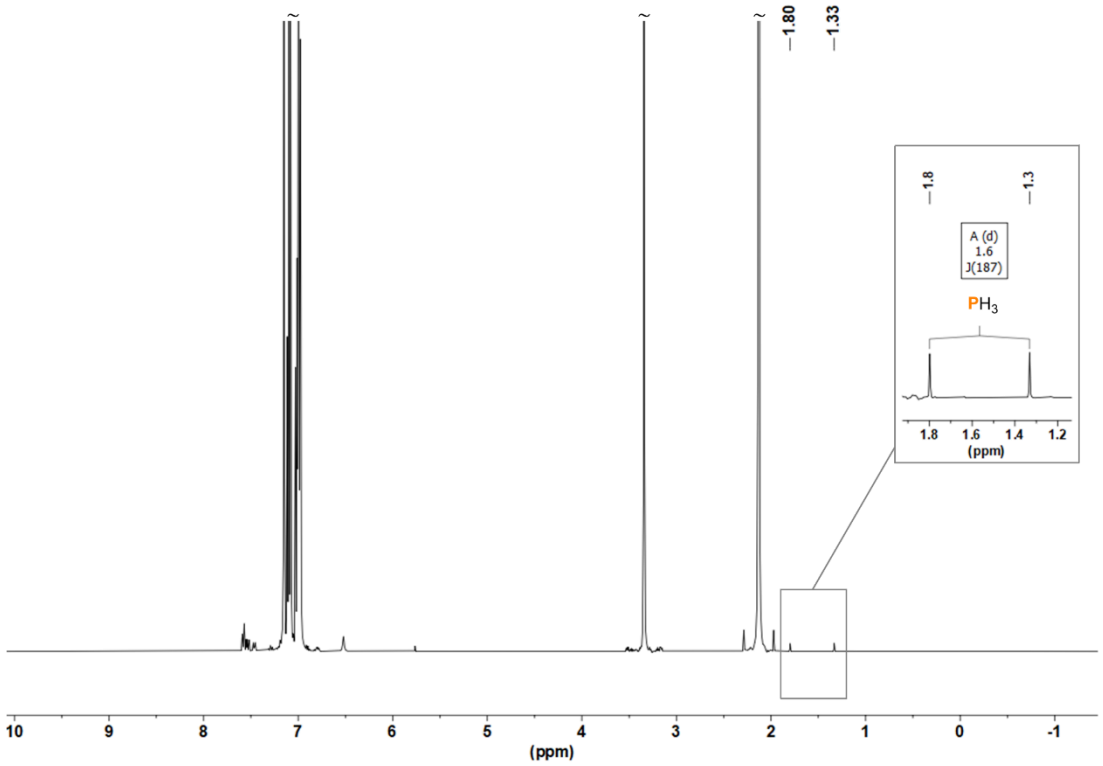

Figure S12. ^{1}H NMR spectrum of a solution of PH_3 (**4**) generated *via* hydrogermylation of P_4 in PhMe, followed by acidification. Solvent resonances (~) truncated for clarity.

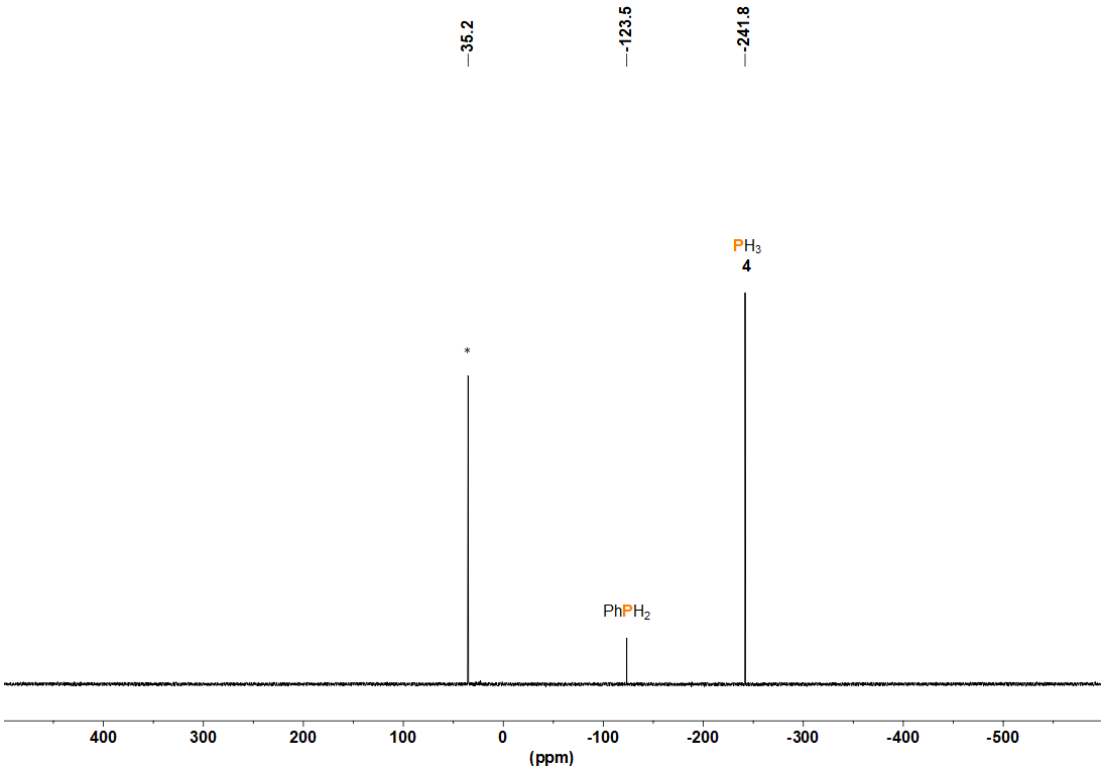

Figure S13. $^{31}P\{^{1}H\}$ NMR spectrum of PH_3 (**4**) generated *via* hydrogermylation of P_4 in PhMe, followed by acidification in the presence of Ph_3PO (*) as an internal standard.

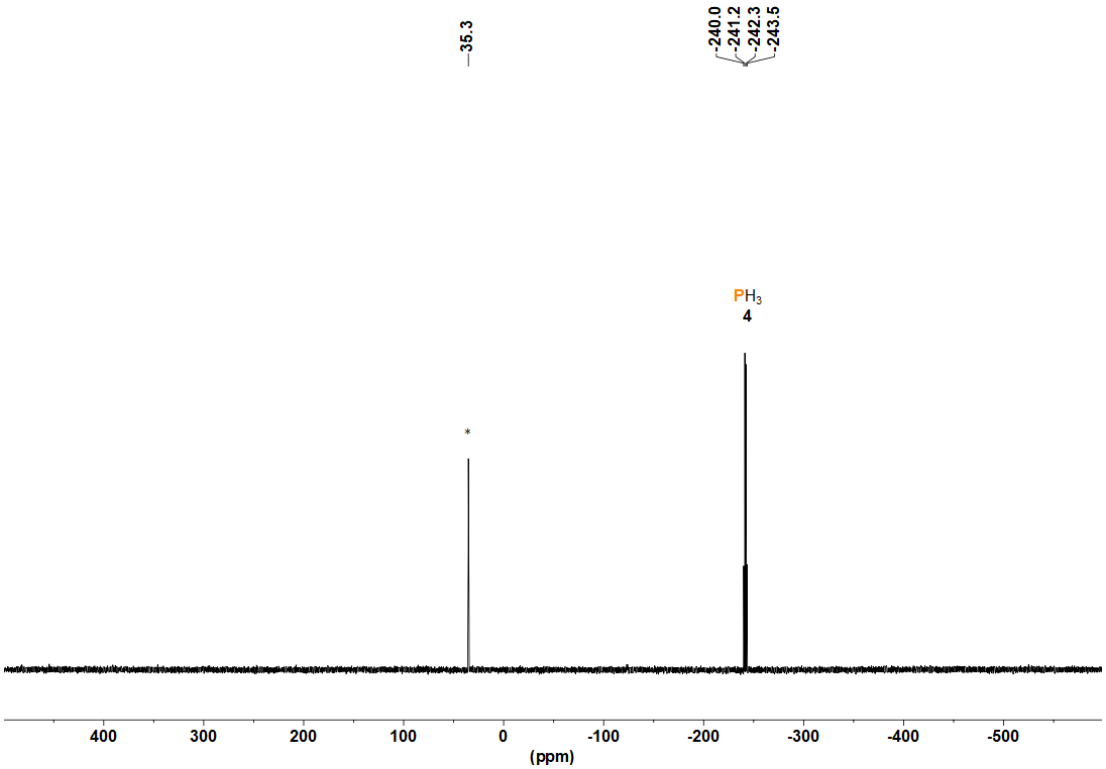

Figure S14. ^{31}P NMR spectrum of PH_3 (**4**) generated *via* hydrogermylation of P_4 in PhMe, followed by acidification in the presence of Ph_3PO (*) as an internal standard.

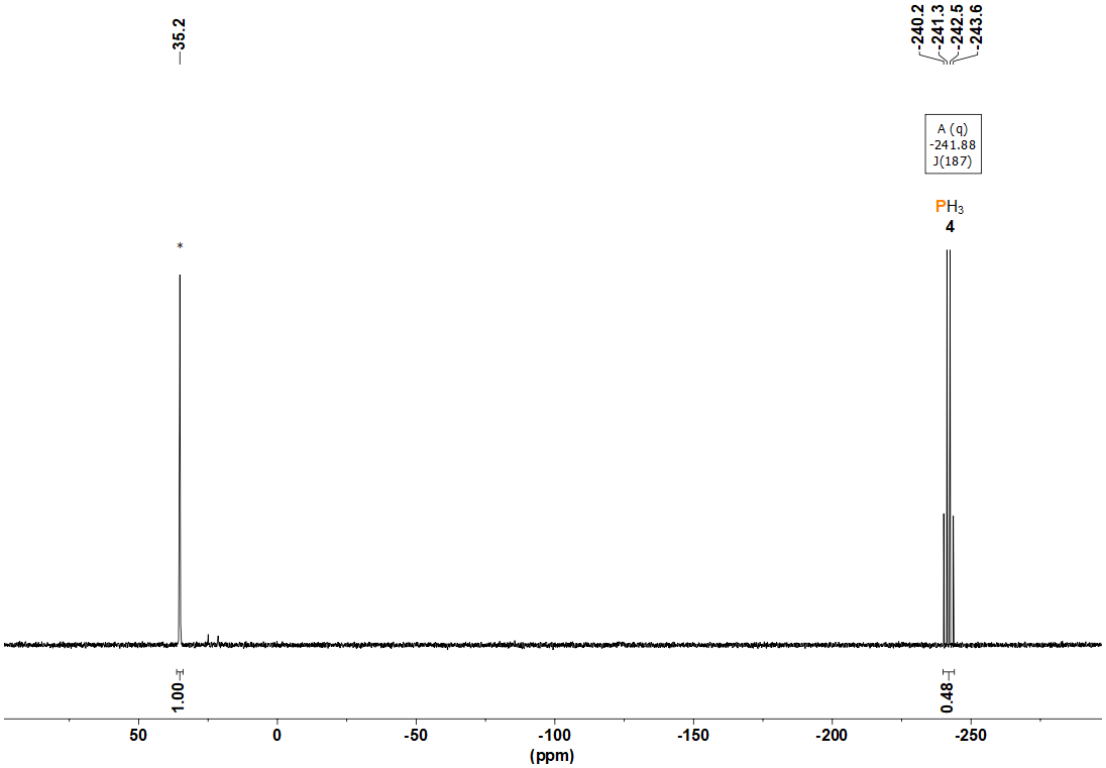

Figure S15. Quantitative ^{31}P NMR spectrum (D1 = 20 s) of PH_3 (**4**) generated *via* hydrogermylation of P_4 in PhMe, followed by acidification, in the presence of Ph_3PO (*) as an internal standard.

5.4.2.7 General procedure for the functionalisation of the mixture $(Ph_3Ge)_xPH_{3-x}$ (x = 1, 2)

The conversions of the products shown in this section were determined by a quantitative single scan inverse-gated $^{31}P\{^1H\}$ NMR (DS = 0, D1 = 2 s) methodology that we have described previously, and whose use to quantify tertiary phosphines and quaternary phosphonium salts has previously been validated.[15]

To a 10 mL, flat-bottomed, stoppered tube were added P_4 (0.01 mmol, as a stock solution in 84.3 μL PhH), PhMe (100 μL), and Ph_3GeH (36.6 mg, 0.12 mmol). The tube was sealed, placed in a water-cooled block to maintain near-ambient temperature, and irradiated with UV light (365 nm, 4.3 V, 700 mA, Osram OSLON SSL 80) for 24 hours (unless stated otherwise). The resulting clear yellowish solution was treated with the corresponding electrophiles as follows:

Reactivity towards benzyl bromide: Benzyl bromide (47.6 μL, 0.4 mmol) and KHMDS (19.9 mg, 0.1 mmol) were added to the yellowish solution, and heated to 100 °C with stirring for 3 days. After cooling to room temperature, Ph_3PO (0.02 mmol, stock solution in benzene) was subsequently added to act as an internal standard. Volatiles were removed under vacuum, and CH_3CN (0.5 mL) was then added. NMR analysis of the resulting mixture showed the formation of $[Bn_4P]Br$ (**5**) as the main product with 90 % conversion as shown in Figure S16.

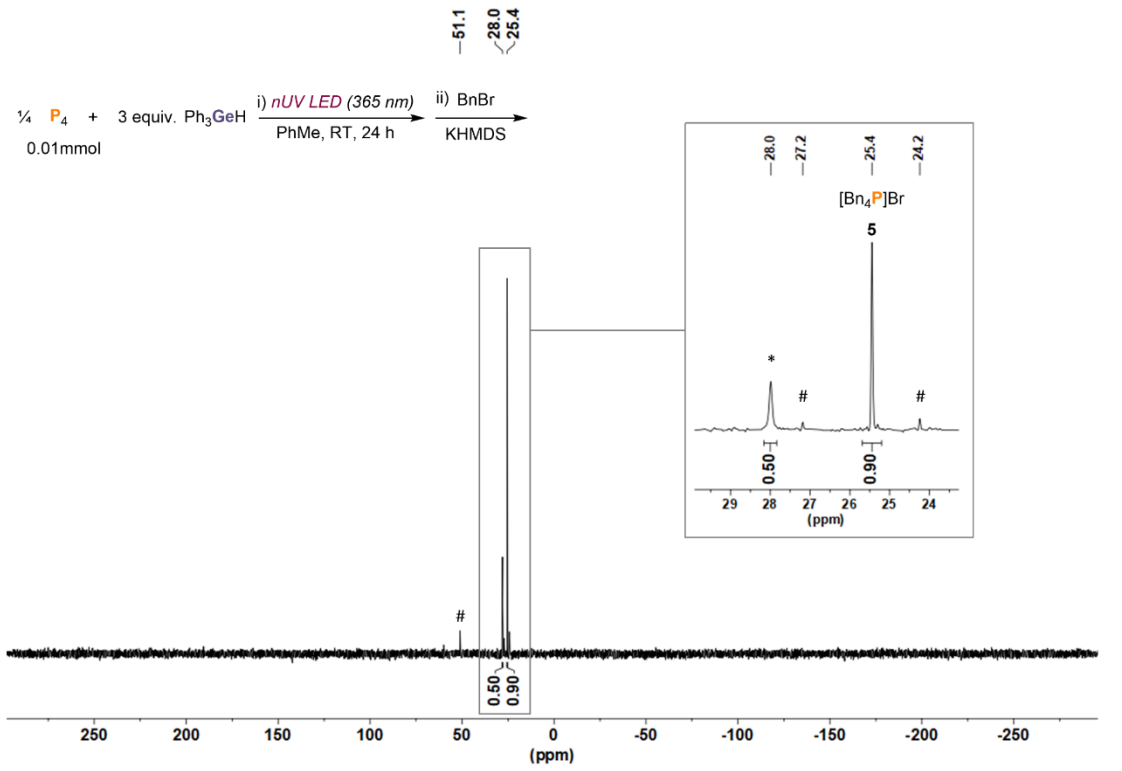

Figure S16. $^{31}P\{^1H\}$ NMR spectrum of $[Bn_4P]Br$ (**5**) generated *via* hydrogermylation of P_4 in PhMe, followed by treatment with benzyl bromide (0.4 mmol) and KHMDS (0.1 mmol), heated to 100 °C for 3 d. * marks the internal standard Ph_3PO (0.02 mmol). # marks unknown side products.

Reactivity towards bromoethane: Bromoethane (30 µL, 0.4 mmol) and KHMDS (19.9 mg, 0.1 mmol) were added to the yellowish solution, and heated to 100 °C with stirring for 3 days. After cooling to room temperature, Ph_3PO (0.02 mmol, stock solution in benzene) was subsequently added to act as an internal standard. Volatiles were removed under vacuum, and CH_3CN (0.5 mL) was then added. NMR analysis of the resulting mixture showed the formation of $[Et_4P]Br$ (**6**) as the main product with 42 % conversion as shown in Figure S17.

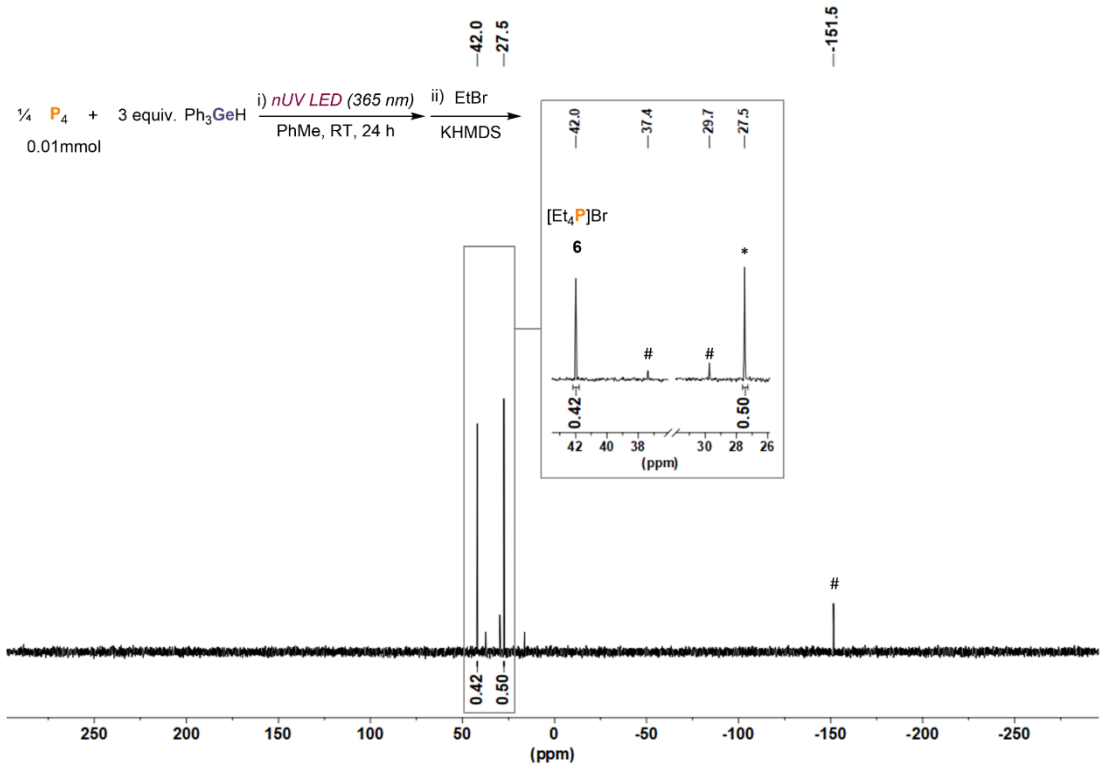

Figure S17. $^{31}P\{^1H\}$ NMR spectrum of $[Et_4P]Br$ (**6**) generated *via* hydrogermylation of P_4 in PhMe, followed by treatment with bromoethane (0.4 mmol) and KHMDS (0.1 mmol), heated to 100 °C for 3 d. * marks the internal standard Ph_3PO (0.02 mmol). # marks unknown side products.

Reactivity towards paraformaldehyde: Volatiles were removed under vacuum. EtOH (0.5 mL) and paraformaldehyde (15.0 mg, 0.5 mmol) were added to the oily solid residue, and the resulting suspension was heated to 50 °C with stirring for 2 days. After cooling to room temperature, the mixture was frozen in a liquid-nitrogen bath, and HCl (4.0 M in 1,4-dioxane, 100 µL, 0.4 mmol) was added. After thawing, the reaction mixture was stirred at room temperature for 2 hours. Ph_3PO (0.02 mmol, stock solution in benzene) was subsequently added to act as an internal standard. NMR analysis of the resulting mixture showed only traces of the desired product THPC (−27.6 ppm, <5% conversion), along with PH_3 (−242.7 ppm) and an unknown signal (−20.2 ppm), as shown in Figure S18.

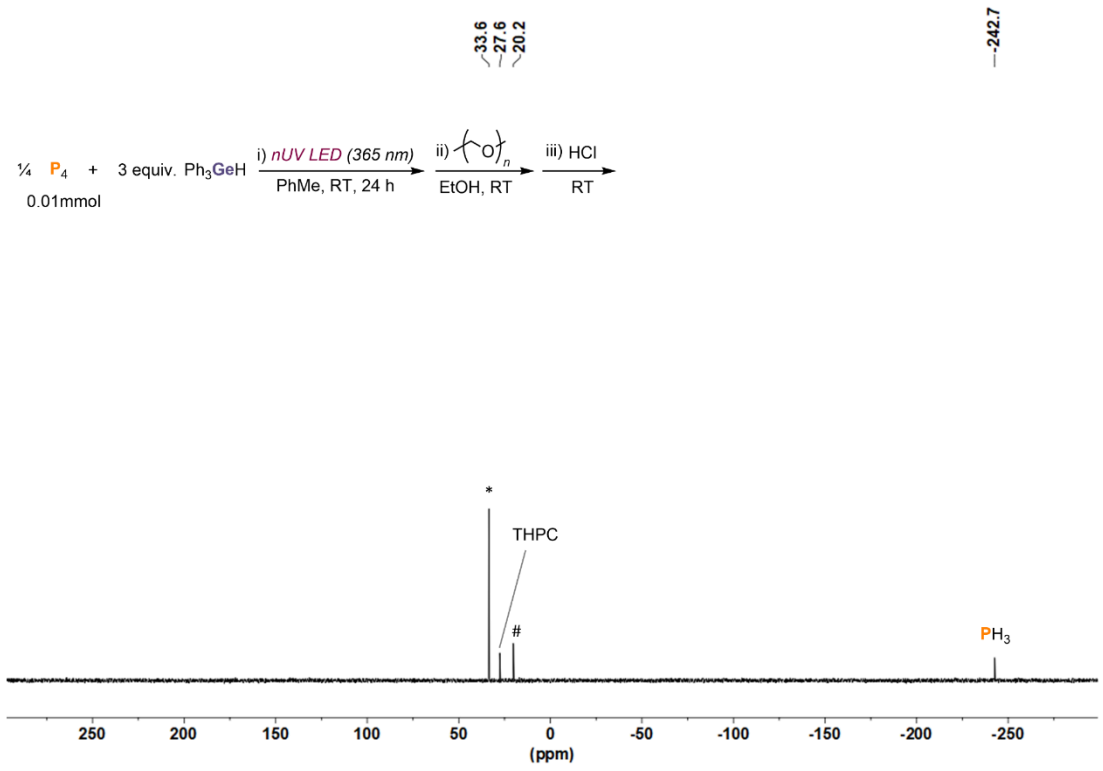

Figure S18. $^{31}P\{^{1}H\}$ NMR spectrum of THPC generated *via* hydrogermylation of P_4 in PhMe, followed by treatment with paraformaldehyde (0.5 mmol) in EtOH, heated to 50 °C for 2 d. Then, quenched with HCl (0.4 mmol).* marks the internal standard Ph_3PO (0.02 mmol). # marks unknown side products.

Reactivity towards benzoyl chloride: PhC(O)Cl (27.9 μL, 0.24 mmol) and KHMDS (19.9 mg, 0.1 mmol) were added to the yellowish solution, and stirred at room temperature for 24 hours. The resulting mixture was analysed by $^{31}P\{^{1}H\}$ and ^{31}P NMR spectroscopy as shown in Figure S19.

The spectra show the complete consumption of the crude **1**/**2** mixture and the formation of the desired product $P(C(O)Ph)_3$ at −54.1 ppm, albeit in trace amounts. Two other unidentified P-containing species were observed at −24.6 and −75.3 ppm, the latter being the main product of this reaction. Based on their chemical shifts and the absence of $^{1}J(^{31}P\text{-}^{1}H)$ splitting in the proton-coupled spectrum, these resonances are attributed to partially acylated species such as $Ph_3GeP(C(O)Ph)_2$ or $(Ph_3Ge)_2PC(O)Ph$ (or possibly $Ph_3GeP(Ph)C(O)Ph$, formed *via* acylation of side-product **3**). Similar outcomes were observed during experiments with higher temperatures and extended reaction times. Analogous experiments using fewer equivalents of PhC(O)Cl were also unsuccessful in our attempts to target these potential intermediates more selectively.

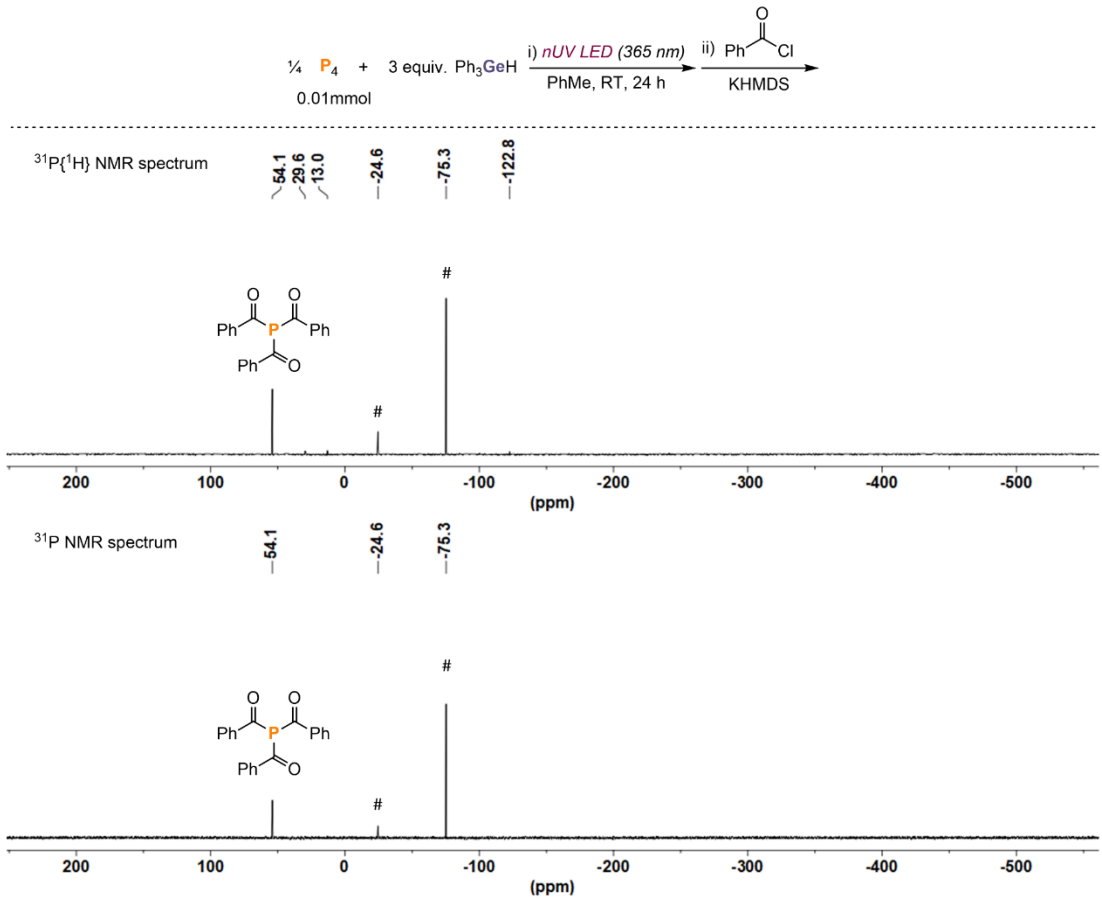

Figure S19. $^{31}P\{^{1}H\}$ and ^{31}P NMR spectra for the hydrogermylation of P_4 in PhMe, followed by treatment with benzoyl chloride (0.24 mmol) and KHMDS (0.1 mmol), stirred at room temperature for 24 h. # marks unknown species.

<u>*Reactivity towards pivaloyl chloride:*</u> *t*BuC(O)Cl (29.6 µL, 0.24 mmol) and KHMDS (19.9 mg, 0.1 mmol) were added to the yellowish solution, and heated to 60 °C with stirring for 24 hours. The resulting mixture was analysed by $^{31}P\{^{1}H\}$ and ^{31}P NMR spectroscopy as shown in Figure S20.

Similar to the reaction with benzoyl chloride, the $^{31}P\{^{1}H\}$ NMR spectrum shows only traces amounts of the desired product $P(C(O)tBu)_3$ (−51.9 ppm) along with a variety of other unknown species. The main product of this reaction appears as a singlet resonance at −117.1 ppm, which splits into a doublet in the ^{31}P spectrum ($^{1}J(^{31}P\text{-}^{1}H)$ = 200 Hz). Given the similarities on chemical shift and $^{1}J(^{31}P\text{-}^{1}H)$ coupling constant with analogous compounds ($Bu_3SnP(H)C(O)tBu$[19] and $Me_3SiP(H)C(O)tBu$[58]), this species was assigned as $Ph_3GeP(H)C(O)tBu$. Additional experiments using fewer equivalents of *t*BuC(O)Cl, in our attempts to target this potential intermediate more selectively, were unsuccessful. Moreover, similar outcomes were observed during experiments at higher temperatures and with longer reaction times.

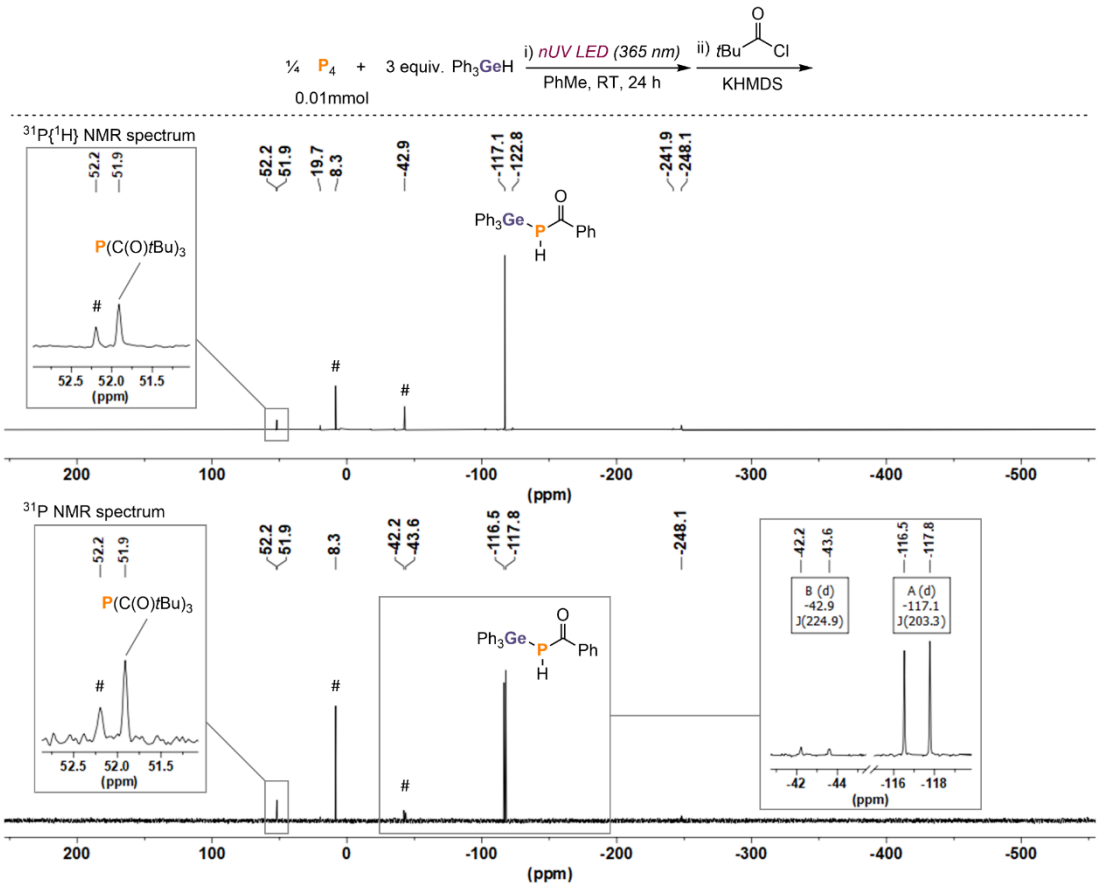

Figure S20. $^{31}P\{^{1}H\}$ and ^{31}P NMR spectra for the hydrogermylation of P_4 in PhMe, followed by treatment with benzoyl chloride (0.24 mmol) and KHMDS (0.1 mmol), heated to 60 °C for 24 h. # marks unknown species.

5.4.2.8 Synthesis and isolation of TBPB (5) via hydrogermylation of P_4 (0.1 mmol scale)

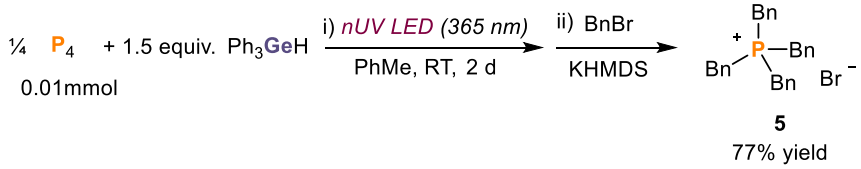

5

77% yield

To a 50 mL, flat-bottomed, stoppered tube were added P_4 (12.4 mg, 0.1 mmol), PhMe (2.0 mL), and Ph_3GeH (366.0 mg, 1.2 mmol). After stirring to obtain a homogeneous solution, the tube was placed in a water-cooled block to maintain near-ambient temperature, and irradiated with UV light (365 nm, 14 V, 700 mA, Osram OSLON SSL 80) for 2 days. To the yellowish solution benzyl bromide (476 µl, 4.0 mmol) and KHMDS (120 mg, 0.6 mmol) were added and the reaction mixture heated to 100 °C with stirring for 3 days. After cooling to room temperature the pale yellow suspension was filtered, and the remaining solid was washed with PhMe (3 x 6 mL) and extracted into acetonitrile (3 x 10 mL). Removal of volatiles under vacuum yielded the target product as a white solid (146 mg, 77 %).

^{1}H NMR (400 MHz, 300 K, CD_3CN): δ = 7.35 ppm (3H, m), 7.21 ppm (2H, m), 3.87 ppm (2H, d, $^{2}J(^{31}P\text{-}^{1}H)$ = 14.6 Hz). **$^{31}P\{^{1}H\}$ NMR** (121 MHz, 300 K, CD_3CN): δ = 25.8 ppm (s). **^{31}P NMR** (121 MHz, 300 K, CD_3CN): δ = 25.8 ppm (m). NMR data are consistent with our previous report.[19]

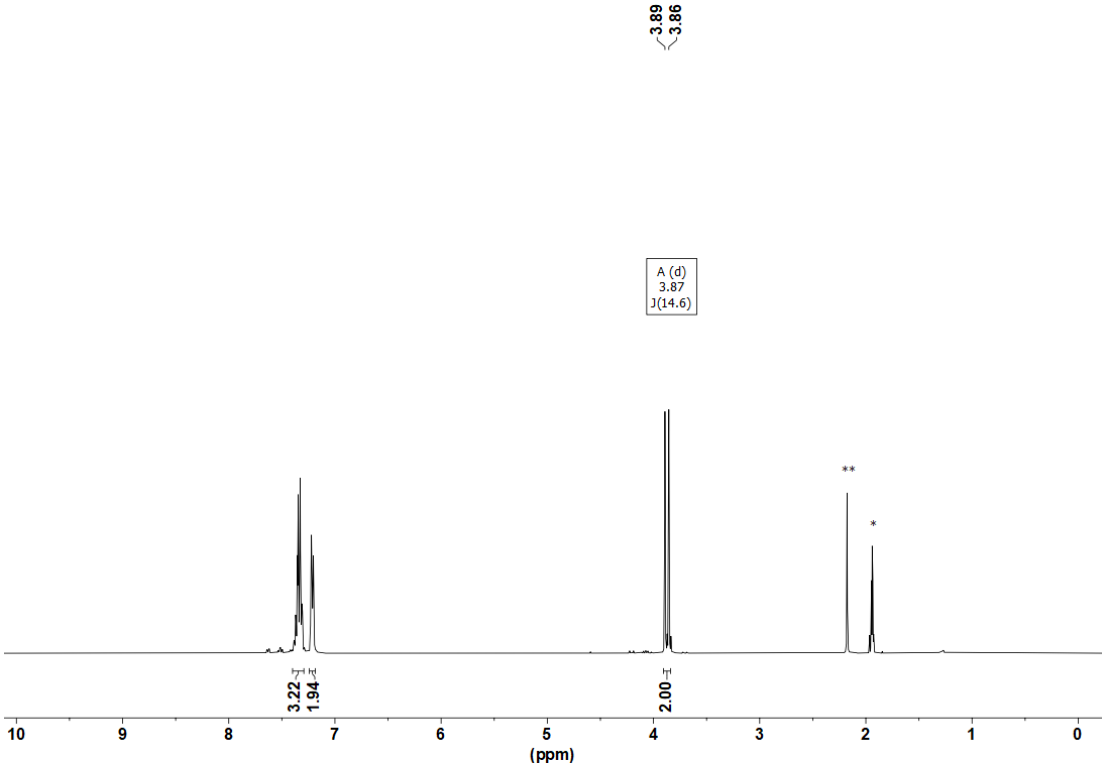

Figure S21. ^{1}H NMR spectrum of [Bn$_4$P]Br (**5**) in CD_3CN (*solvent, **H_2O).

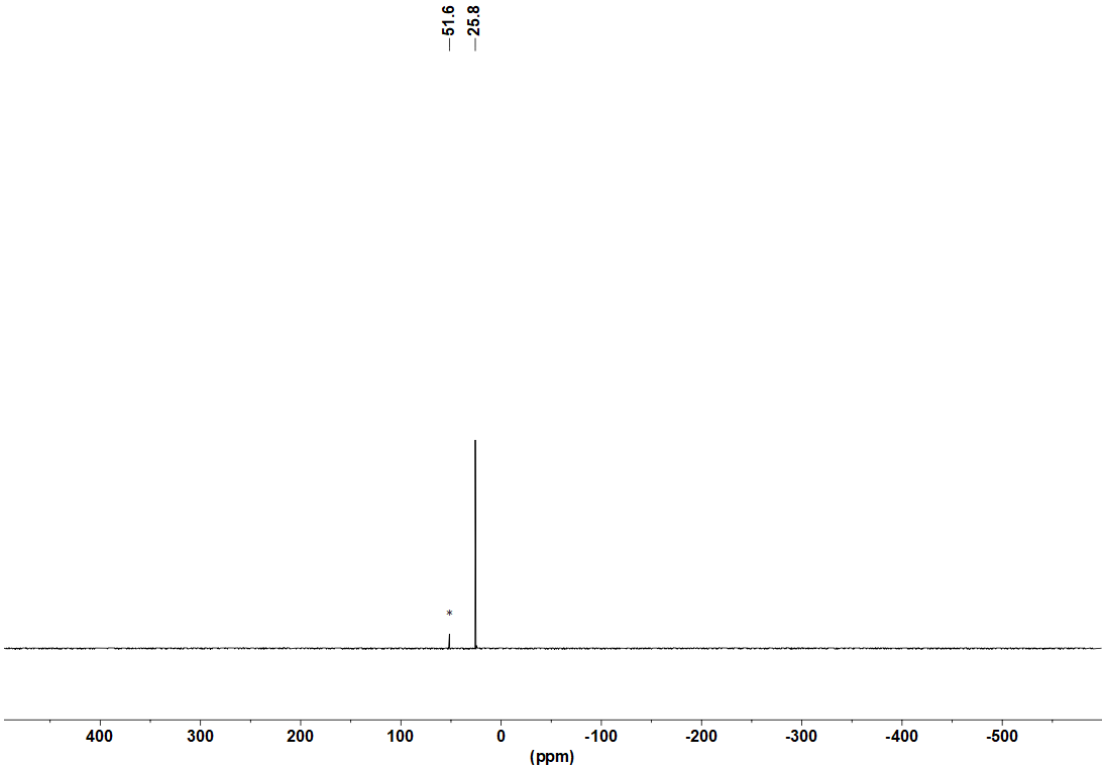

Figure S22. ^{31}P{^{1}H} NMR spectrum of [Bn$_4$P]Br (**5**) in CD_3CN. * maks an unknown side product.

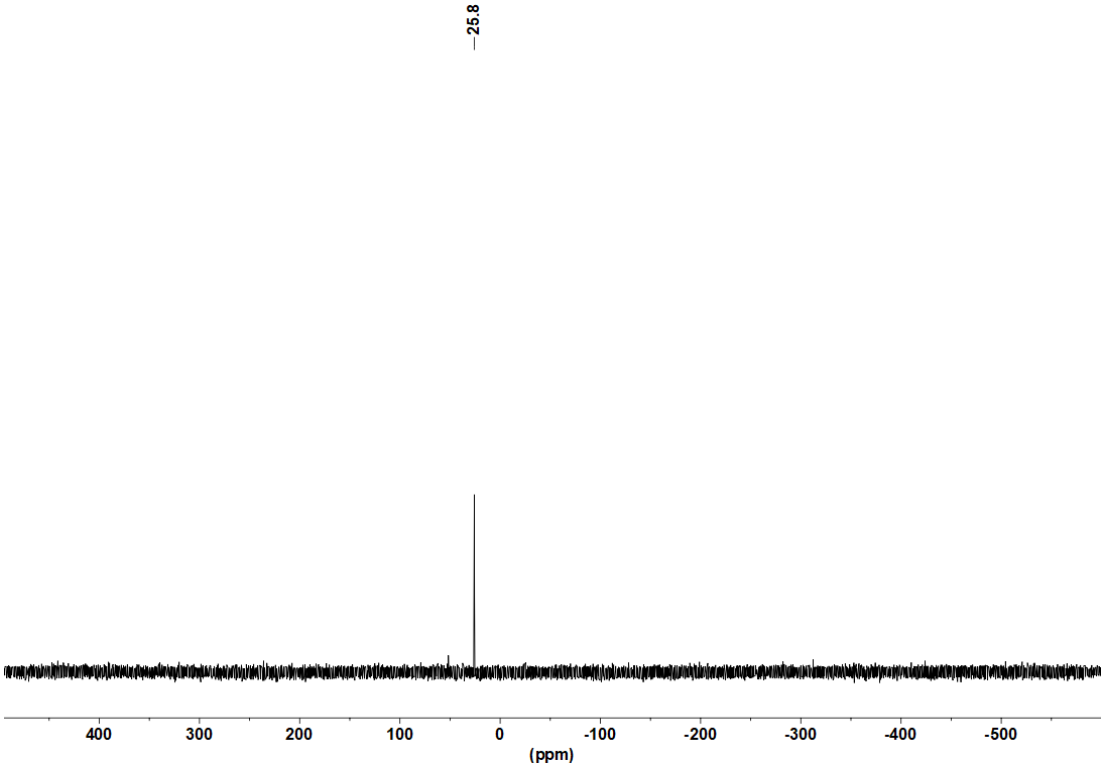

Figure S23. ^{31}P NMR spectrum of [Bn$_4$P]Br (**5**) in CD$_3$CN.

5.4.2.9 Hydrogermylation of P_4 using Ph_3GeH and HAT donors (0.01 mmol scale): general procedure and optimisation

The hydrogermylation of P_4 mediated by a HAT donor was also investigated. In summary, the outcomes of these reactions were found to be similar to those observed in the absence of additives, apart from different product distribution and the presence of PH_3 in the $^{31}P\{^1H\}$ and ^{31}P NMR spectra, in minor to considerable amounts. See Figures S24 and S25 for selected examples.

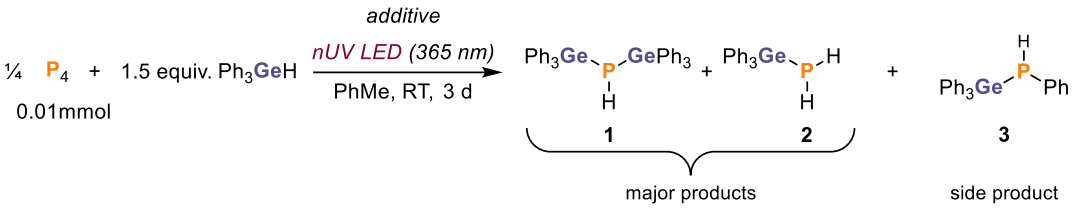

Representative procedure:

To a 10 mL, flat-bottomed, stoppered tube were added P_4 (0.01 mmol, as a stock solution in 84.3 µL PhH), PhMe (100 µL), Ph_3GeH (18.3 mg, 0.06 mmol) and 1,4-CHD (5.7 µL, 0.06 mmol). The tube was sealed, placed in a water-cooled block to maintain near-ambient temperature, and irradiated with UV light (365 nm, 4.3 V, 700 mA, Osram OSLON SSL 80) for 3 days (unless stated otherwise). Ph_3PO (0.02 mmol, stock solution in benzene) was subsequently added to act as an internal standard. The resulting mixture was analysed by ^1H, $^{31}P\{^1H\}$, and ^{31}P NMR spectroscopy.

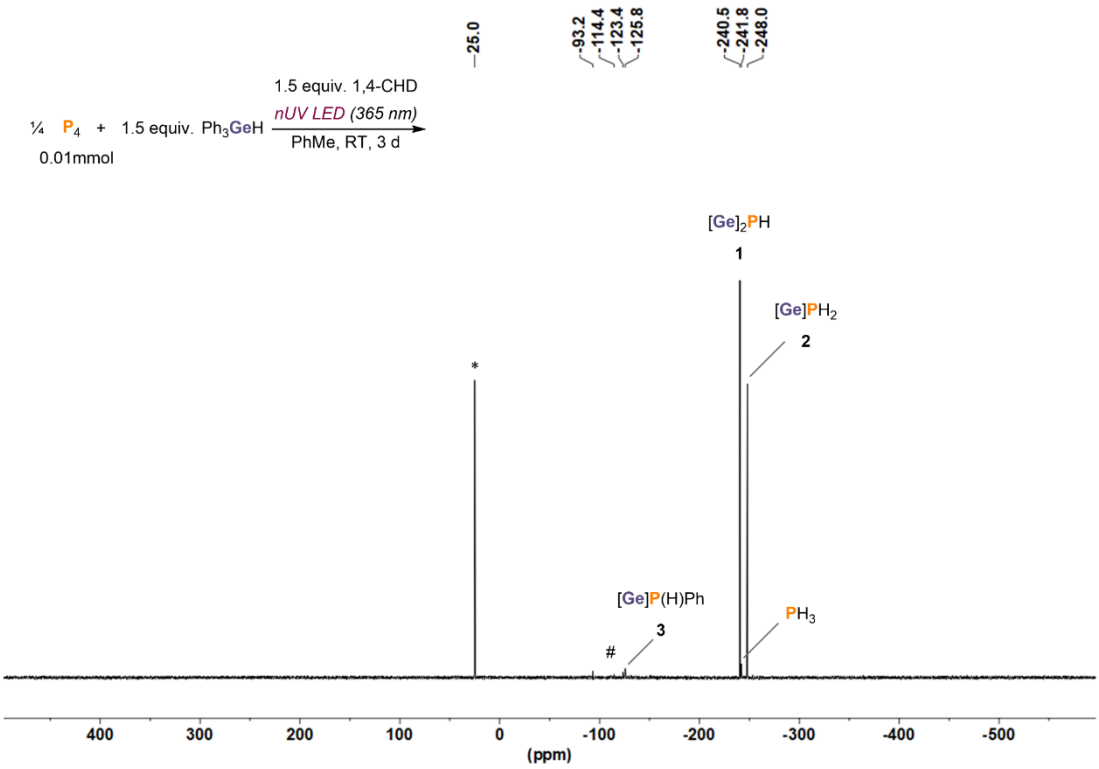

Figure S24. $^{31}P\{^{1}H\}$ NMR spectrum for the reaction of P_4 with Ph_3GeH (0.06 mmol) and 1,4-CHD (0.06 mmol) in PhMe and driven by 356 nm, 3 W LED irradiation for 3 d (Table S4, Entry 6). * marks the internal standard Ph_3PO. # marks unknown side products. [Ge] = Ph_3Ge.

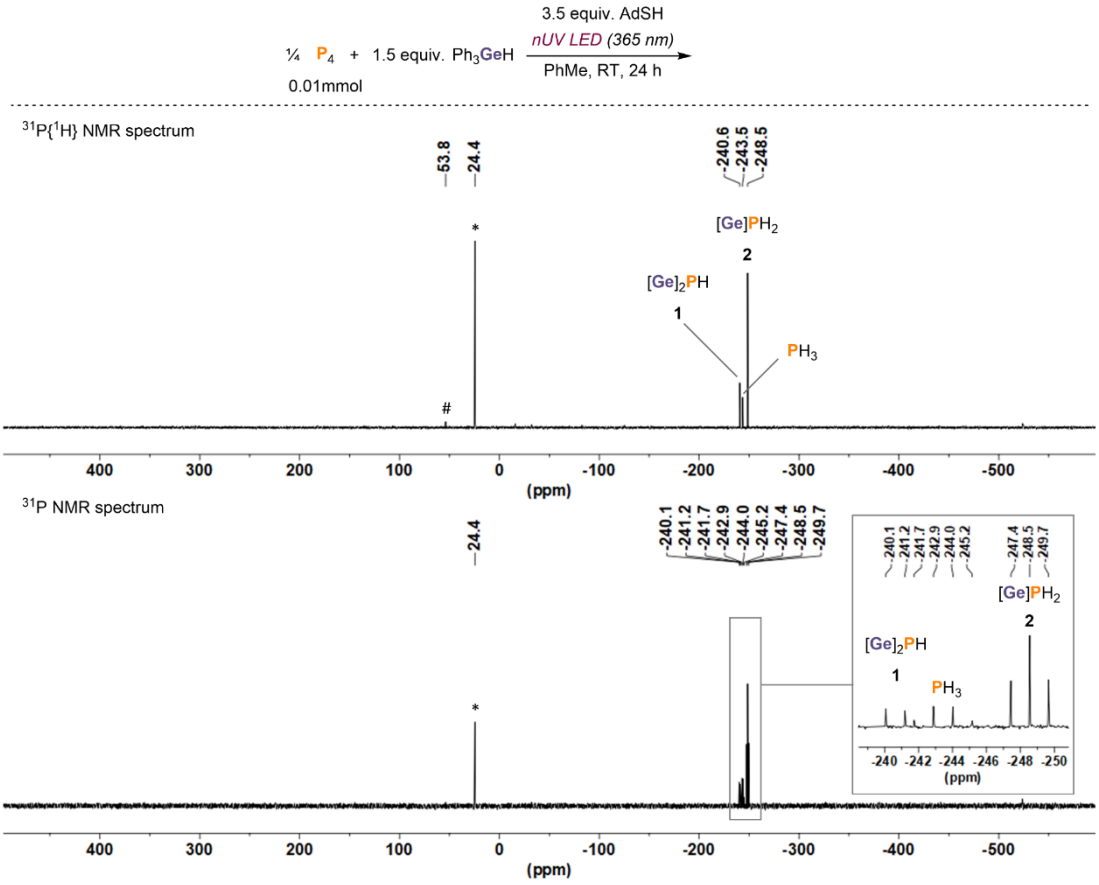

Figure S25. $^{31}P\{^{1}H\}$ and ^{31}P NMR spectra for the reaction of P_4 with Ph_3GeH (0.06 mmol) and AdSH (1-adamantanethiol, 0.14 mmol) in hexane and driven by 356 nm, 3 W LED irradiation for 3 d (Table S4, Entry 2). * marks the internal standard Ph_3PO. # marks unknown side products. [Ge] = Ph_3Ge.

Table S4. Optimisation of hydrogermylation of P_4 using Ph_3GeH in the presence of a HAT donor.[a]

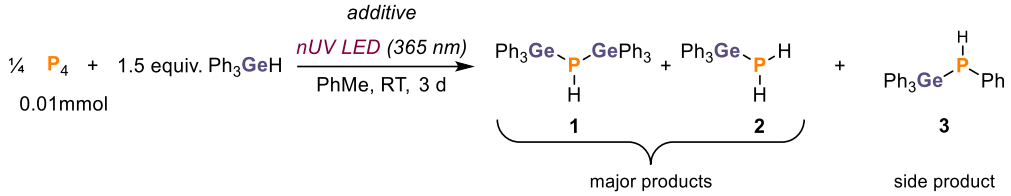

Entry	Additive (mmol)	PhMe (µL)	Time (days)	Full conv. of $\mathbf{P_4}$?	Relative conv. to **1** and **2** (%)[b]	Relative conv. to **3** (%)
1	AdSH (0.06)	500 (hexane)	3	✓	23.6	traces
2	AdSH (0.14)	500 (hexane)	3	✓	26.1	-
3	PhSH (0.01)	500	3	✓	49.4	traces
4	PhSH (0.06)	500	3	✓	19.3	traces
5	1,4-CHD (0.01)	100	3	✓	54.9	12.7
6	1,4-CHD (0.06)	100	3	✓	62.1	traces
7	*i*Pr_3SiSH (0.06)	500 (hexane)	3	✓	60.1	7.1

[a] The general procedure described in this section was modified to use the indicated amount of reactant and solvent. [b] Conversions were calculated by integration of the ^{31}P resonances of **1-3** relative to an internal standard, which was then normalized relative to Table S1, entry 9 as described in section 5.4.2.2. [b] The signal assigned to PH_3 was observed in the $^{31}P\{^1H\}$ and ^{31}P NMR spectra (see Figures S24 and S25 for selected examples).

5.4.3 Hydrosilylation of white phosphorus (P_4)

5.4.3.1 General procedure for reactivity studies of R_3SiH (R = Ph, Et) towards P_4 under LED irradiation (0.01 mmol scale)

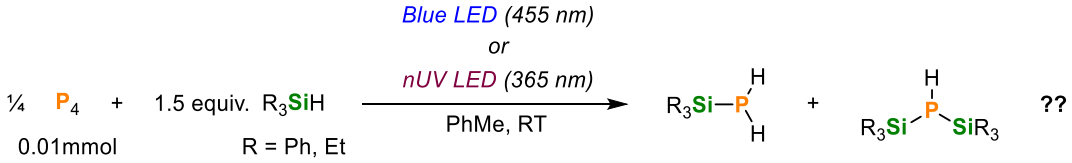

To a 10 mL, flat-bottomed, stoppered tube were added P_4 (0.01 mmol, as a stock solution in 84.3 µL PhH), PhMe (100 µL) and Ph_3SiH (15.6, 0.06 mmol) or Et_3SiH (18.5 µL, 0.06 mmol). The tube was sealed, placed in a water-cooled block to maintain near-ambient temperature, and irradiated with blue light (455 nm, 3.2 V, 700 mA, Osram OSLON SSL 80) or UV light (365 nm, 4.3 V, 700 mA, Osram OSLON SSL 80) for 3 days (unless stated otherwise). The resulting mixture was analysed by ^1H, $^{31}P\{^1H\}$, and ^{31}P NMR spectroscopy.

The $^{31}P\{^1H\}$ NMR spectra for the reaction of P_4 with R_3SiH (R = Ph, Et) only showed uncomsumed P_4. Figure S26 displays the $^{31}P\{^1H\}$ NMR spectrum for the reaction of P_4 with Ph_3SiH (0.06 mmol) in PhMe driven by 365 nm LED irradiation for 3 days as a selected example.

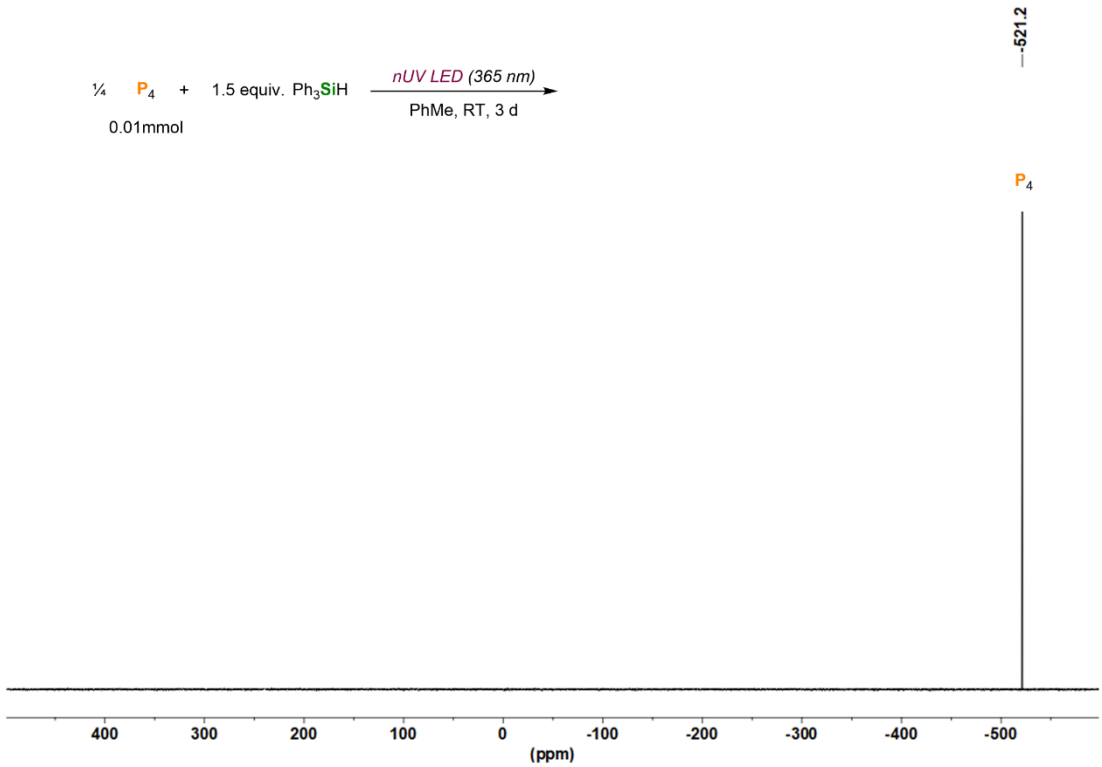

Figure S26. $^{31}P\{^{1}H\}$ NMR spectrum for the reaction of P_4 with Ph_3SiH (0.06 mmol) in PhMe and driven by 365 nm, 3 W LED irradiation for 3 d.

5.4.3.2 General procedure and optimisation for the hydrosilylation of P_4 using $(Me_3Si)_3SiH$ and iPr_3SiSH, under LED irradiation (0.01 mmol scale)

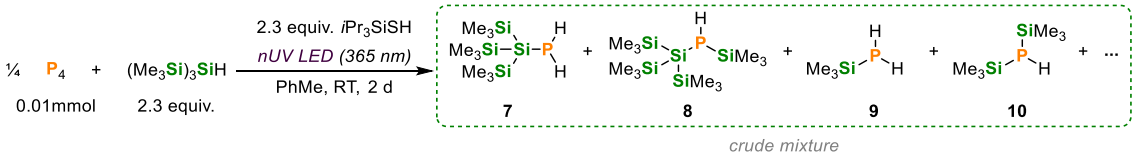

To a 10 mL, flat-bottomed, stoppered tube were added P_4 (0.01 mmol, as a stock solution in 84.3 µL PhH), PhMe (100 µL), $(Me_3Si)_3SiH$ (27.9 µL, 0.09 mmol), and iPr_3SiSH (19.3 µL, 0.09 mmol). The tube was sealed, placed in a water-cooled block to maintain near-ambient temperature, and irradiated with UV light (365 nm, 4.3 V, 700 mA, Osram OSLON SSL 80) for 2 days (unless stated otherwise). Ph_3PO (0.02 mmol, stock solution in benzene) was subsequently added to act as an internal standard. The resulting mixture was analysed by $^{31}P\{^{1}H\}$ and ^{31}P NMR spectroscopy, as shown in Figures S27-29, below.

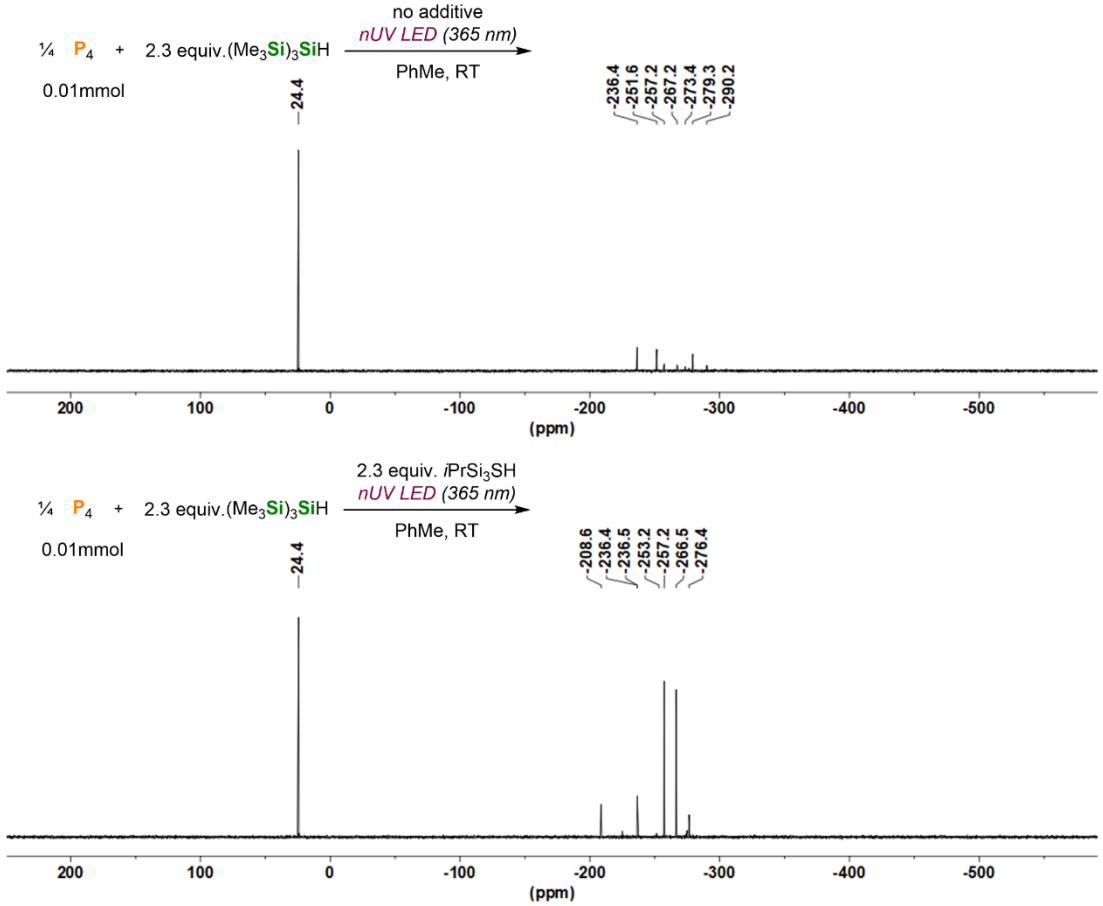

Figure S27. $^{31}P\{^{1}H\}$ NMR spectra for the reactions of P_4 with $(Me_3Si)_3SiH$ (0.14 mmol) and no additive (top) or in the presence of iPr$_3$SiSH (0.14 mmol) as additive (bottom), both in hexane and driven by 365 nm, 3 W LED irradiation for 3 or 1 days, respectively. * marks the internal standard Ph_3PO (0.02 mmol).

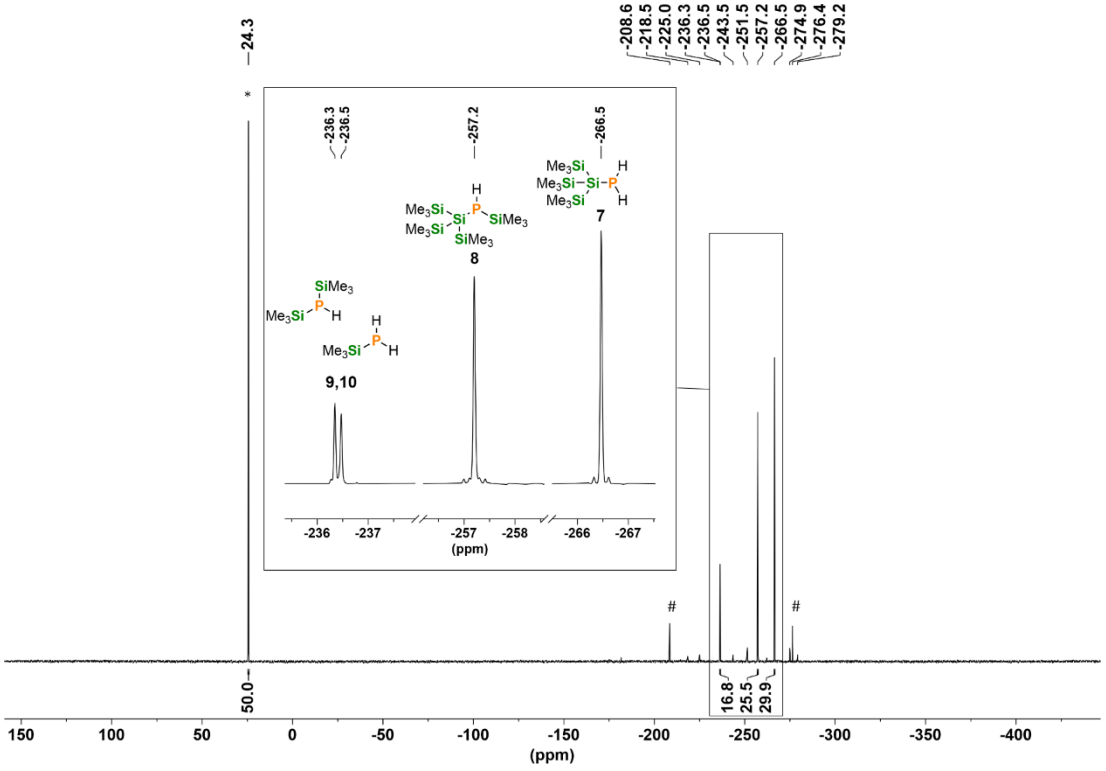

Figure S28. Quantitative $^{31}P\{^{1}H\}$ NMR spectrum (D1 = 40 s) for the reaction of P_4 with $(Me_3Si)_3SiH$ (0.14 mmol) and iPr$_3$SiSH (0.14 mmol) in PhMe and driven by 365 nm, 3 W LED irradiation for 24 h. * marks the internal standard Ph_3PO (0.02 mmol). # marks unknown side products. Assignments are consistent with previous reports.[41,42]

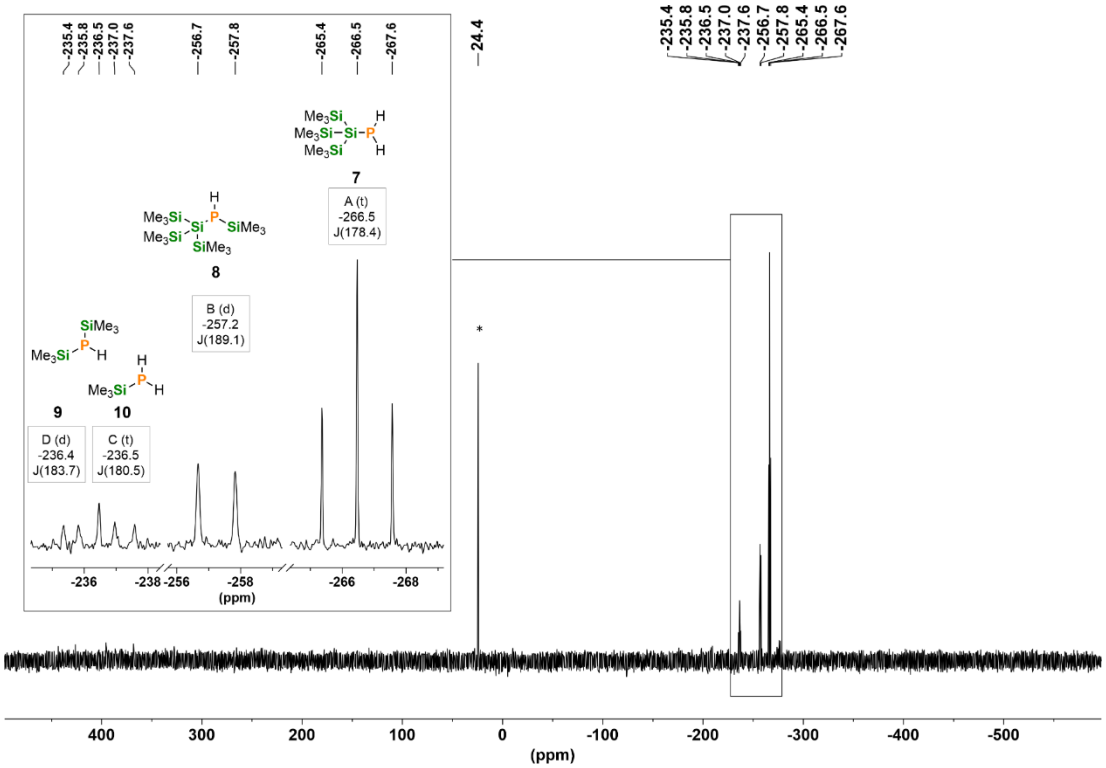

Figure S29. ^{31}P NMR spectrum for the reaction of P_4 with $(Me_3Si)_3SiH$ (0.14 mmol) and *i*Pr_3SiSH (0.14 mmol) in hexane and driven by 390 nm, 40W LED irradiation for 24 h. The insets show expansions of the signals attributed to $[(Me_3Si)_3Si]PH_2$ (**7**), $[(Me_3Si)_3Si]P(H)SiMe_3$ (**8**), Me_3SiPH_2 (**9**) and $(Me_3Si)_2PH$ (**10**), highlighting their multiplicity due to $^1J(^{31}P\text{-}^1H)$ couplings. * marks the internal standard Ph_3PO (0.02 mmol). Assignments are consistent with previous reports.[41,42]

For reasons of experimental expediency, during the optimisation of the hydrosilylation of P_4, acquisition of quick but non-quantitative $^{31}P\{^1H\}$ NMR spectra was used to analyse each experiment and to assess the relative total conversion to **7-10**. Although this did not directly provide precise, quantitative conversions it did allow for meaningful, qualitative comparisons between experiments. Under the conditions highlighted in Table S5, entry 4 a quantitative $^{31}P\{^1H\}$ NMR spectrum was recorded using an inverse-gated decoupled pulse sequence (D1 = 40 s, Figure S2), and the conversion of P_4 to products **7-10** was determined. Thus, for ease of interpretation, the integrals measured for **7-10** for all optimisation experiments have been normalized relative to the value for this experiment (Table S5, entry 4) to provide the relative conversions indicated in Table S5. However, additional integrations (of signals of as yet unidentified monophosphorus species) have not been taken into account, although they may contribute to the final yield in the formation of the desired end products (*e.g.* PH_3) after subsequent functionalisation with electrophiles.

Table S5. Optimisation of hydrosilylation of P_4 using $(Me_3Si)_3SiH$, *i*Pr_3SiSH, and near-UV LED irradiation (365 nm, 3 W).[a]

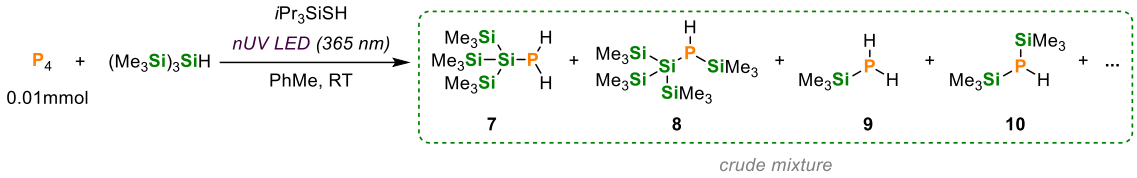

Entry	$(Me_3Si)_3SiH$ (mmol)	*i*Pr_3SiSH (mmol)	PhMe (µL)	Time (days)	Full conv. of $\mathbf{P_4}$?	Relative conv. to **7-10** (%)[b]
1[c]	0.06	-	500	1	✓	traces
2[d]	0.06	-	500	3	✓	traces
3[e]	0.14	-	500 (hexane)	3	✓	6.1
4[e]	0.14	0.14	500 (hexane)	1	✓	72.2
5	0.14	0.14	500 (hexane)	1	✓	73.4
6	**0.14**	**0.14**	**500**	**1**	**✓**	**77.5**
7	0.14	0.06	500	3	✓	69.8
8	0.14	0.01	500	3	✓	8.9
9	0.06	0.06	500	1	✓	42.4
10	0.06	0.06	500	2	✓	44.3
11	0.06	0.06	500	3	✓	49.9
12	0.09	0.09	500	4	✓	72.7
13	0.09	0.09	100	3	✓	67.0
14	**0.09**	**0.09**	**100**	**2**	**✓**	**67.4**
15	0.09	0.09	100	1	✓	55.0

[a] The general procedure described in this section was modified to use the indicated amount of reactants and solvent. [b] Conversions were calculated by integration of the ^{31}P resonances of **7-10** relative to an internal standard, which was then normalized relative to entry 4 as described in the text above. [c] 455 nm. [d] 365 nm, 10 W. [e] 390nm 40 W.

Table S6. Screening of additive for the hydrosilylation of P_4 using $(Me_3Si)_3SiH$ and near-UV LED irradiation (365 nm, 3 W).[a]

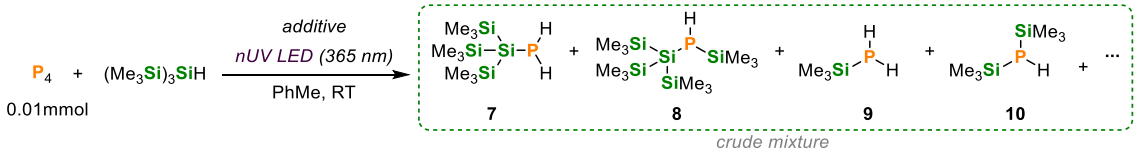

Entry	$(Me_3Si)_3SiH$ (mmol)	*additive* (mmol)	PhMe (µL)	Time (days)	Full conv. of $\mathbf{P_4}$?	Relative conv. to **7-10** (%)
1	0.06	CySH (0.06)	500	4	✓	21.0
2	0.14	AdSH (0.14)	500 (hexane)	1	✓	71.9
3	0.06	AdSH (0.06)	500 (hexane)	1	✓	35.9
4	0.14	PhSH (0.14)	500	1	✓	67.8
5	0.14	4-MePhSH (0.14)	500	1	✓	76.5
6	0.14	4-MePhSH (0.06)	500	1	✓	26.8
7	0.09	1,4-CHD (0.09)	100	3	✓	71.0
8[c]	0.09	1,4-CHD (0.09)	100	3	✓	50.3

[a] The general procedure described in this section was modified to use the indicated amount of reactants and solvent. [b] Conversions were calculated by integration of the ^{31}P resonances of **7-10** relative to an internal standard, which was then normalized relative to Table S5, entry 4 as described in the text above. [c] 455 nm.

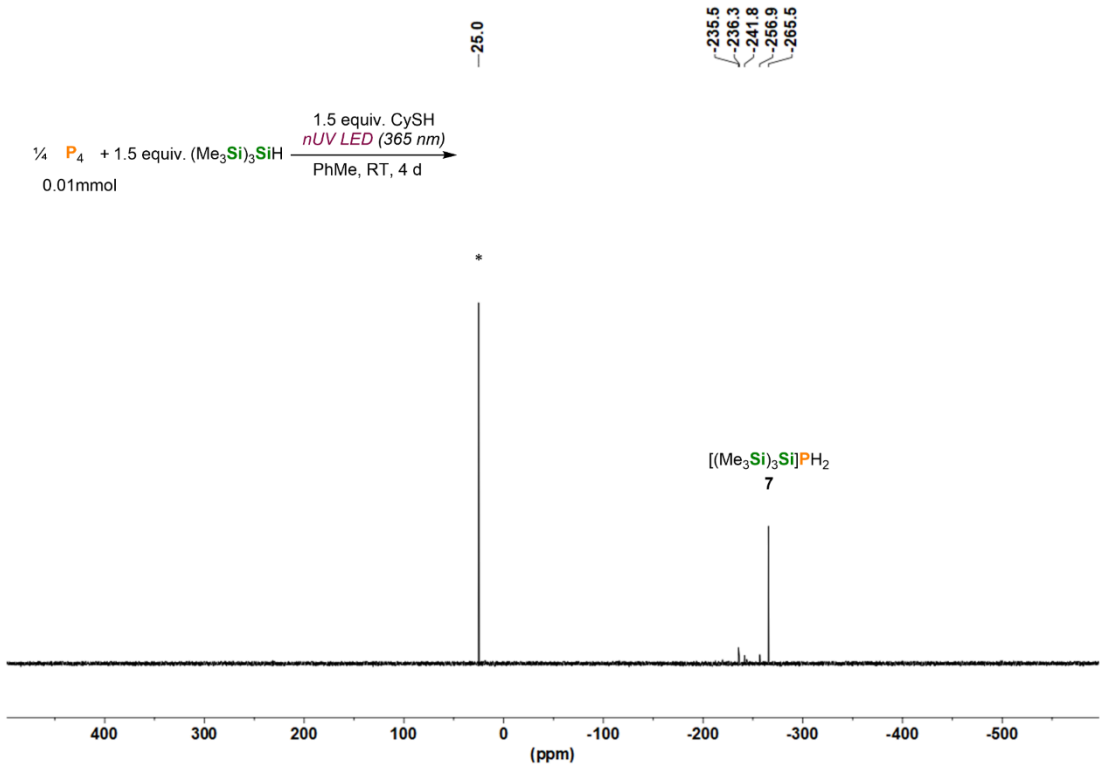

Figure S30. $^{31}P\{^{1}H\}$ NMR spectrum for the reaction of P_4 with $(Me_3Si)_3SiH$ (0.06 mmol) and CySH (0.06 mmol) in PhMe and driven by 365 nm, 3 W LED irradiation for 4 d (Table S6, Entry 1). * marks the internal standard Ph_3PO (0.02 mmol).

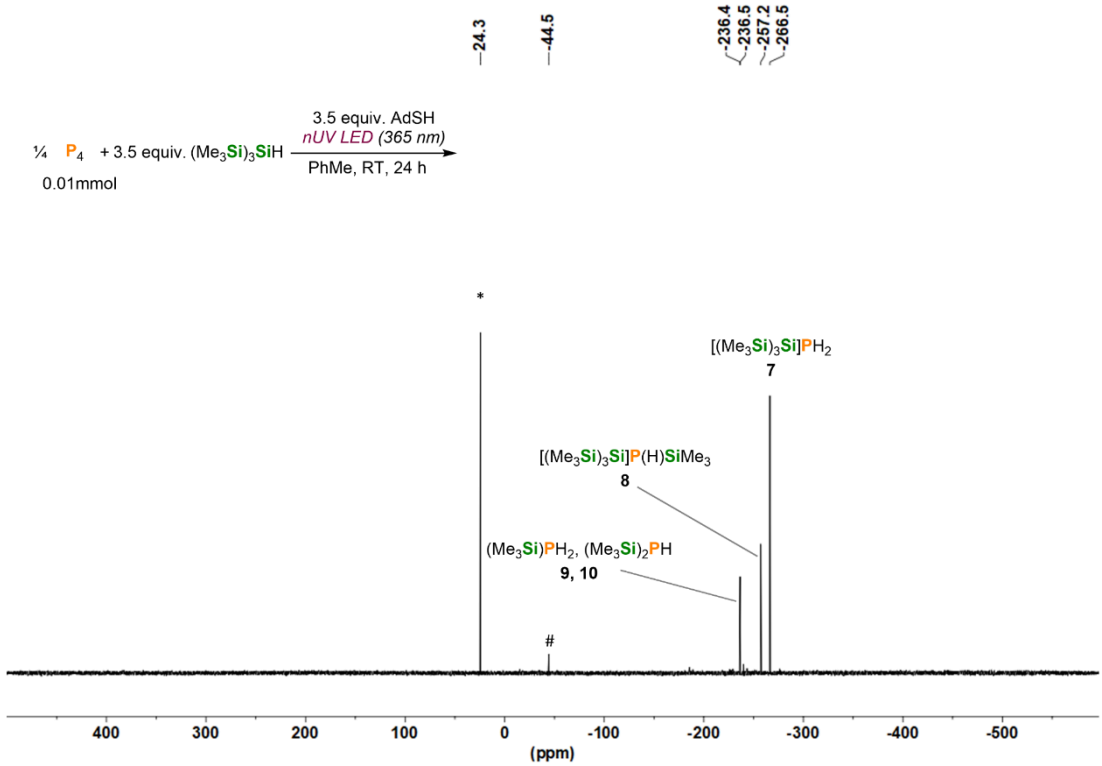

Figure S31. $^{31}P\{^{1}H\}$ NMR spectrum for the reaction of P_4 with $(Me_3Si)_3SiH$ (0.14 mmol) and AdSH (0.14 mmol) in hexane and driven by 365 nm, 3 W LED irradiation for 24 h (Table S6, Entry 2). * marks the internal standard Ph_3PO (0.02 mmol). # marks an unknown side product.

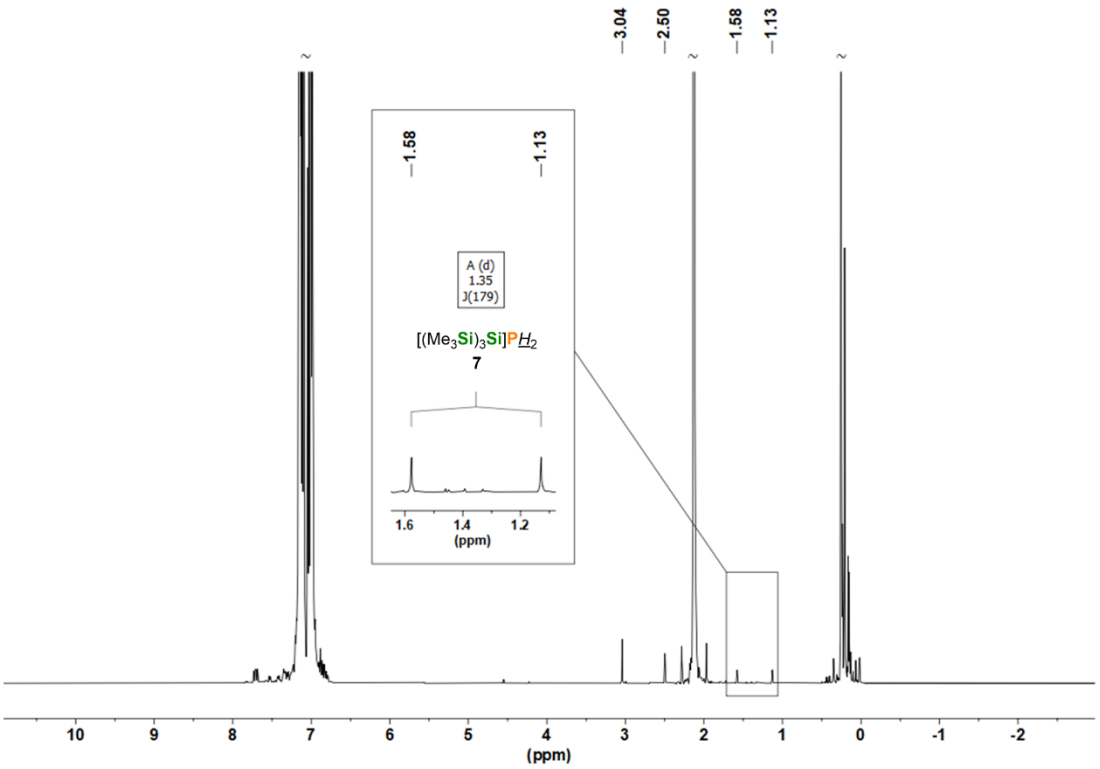

Figure S32. ^{1}H NMR spectrum for the reaction of P_4 with $(Me_3Si)_3SiH$ (0.14 mmol) and PhSH (0.14 mmol) in PhMe and driven by 365 nm, 3 W LED irradiation for 24 h (Table S6, Entry 4). The inset shows expansion of the doublet resonances attributed to the P*H*$_2$ moiety of $[(Me_3Si)_3Si]PH_2$ (**7**).~ marks solvent resonances truncated for clarity.

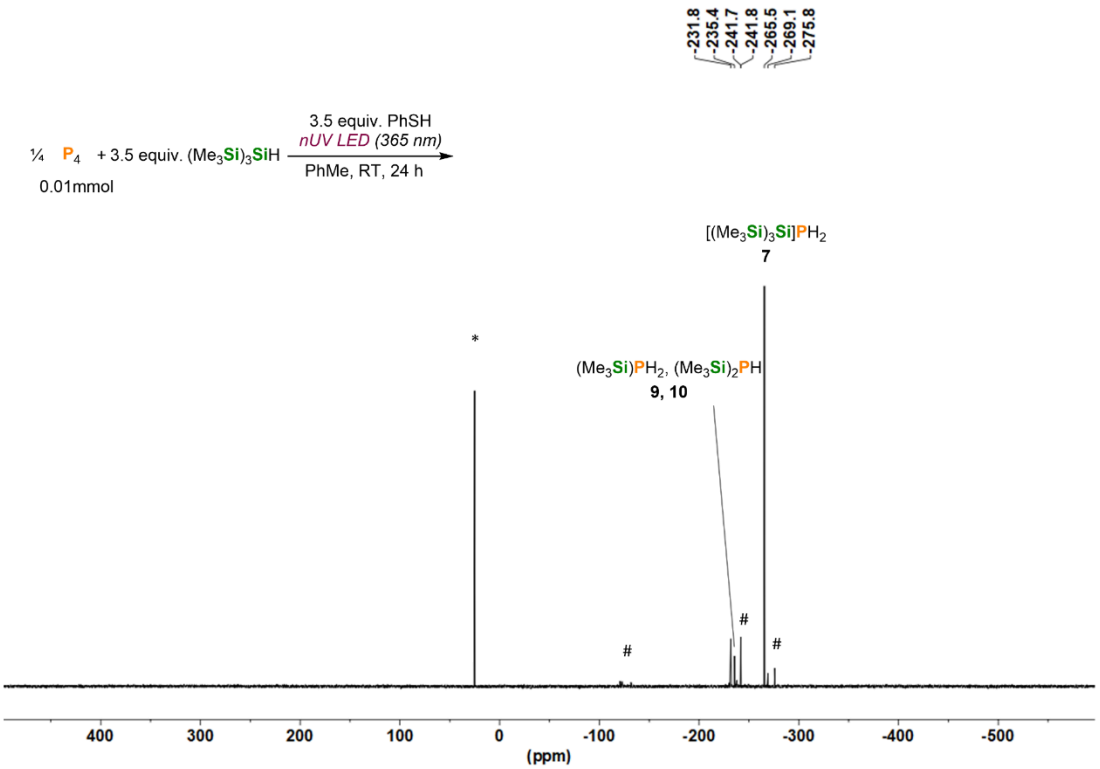

Figure S33. ^{31}P{^{1}H} NMR spectrum for the reaction of P_4 with $(Me_3Si)_3SiH$ (0.14 mmol) and PhSH (0.14 mmol) in PhMe and driven by 365 nm, 3 W LED irradiation for 24 h (Table S6, Entry 4). * marks the internal standard Ph_3PO (0.02 mmol). # marks unknown side products.

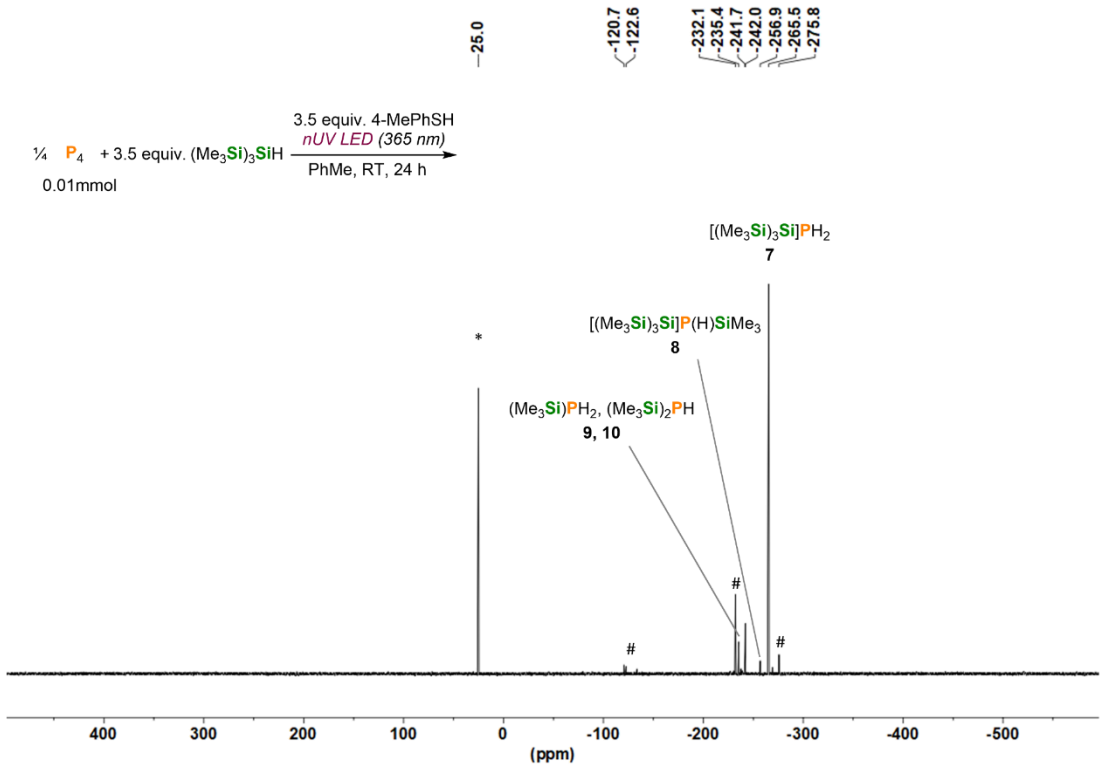

Figure S34. $^{31}P\{^{1}H\}$ NMR spectrum for the reaction of P_4 with $(Me_3Si)_3SiH$ (0.14 mmol) and 4-MePhSH (4-methylbenzenethiol, 0.14 mmol) in PhMe and driven by 365 nm, 3 W LED irradiation for 24 h (Table S6, Entry 5). * marks the internal standard Ph_3PO (0.02 mmol). # marks unknown side products.

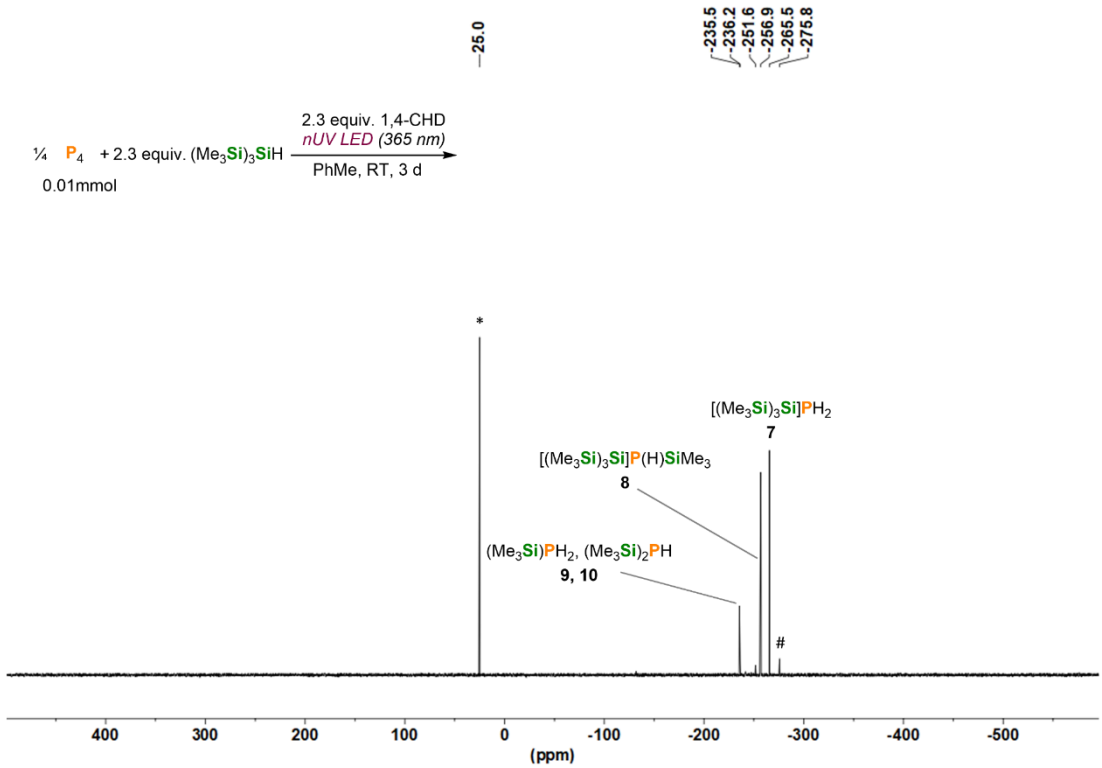

Figure S35. $^{31}P\{^{1}H\}$ NMR spectrum for the reaction of P_4 with $(Me_3Si)_3SiH$ (0.09 mmol) and 1,4-CHD (0.09 mmol) in PhMe and driven by 365 nm, 3 W LED irradiation for 3 d (Table S6, Entry 7). * marks the internal standard Ph_3PO (0.02 mmol).

Table S7. Screening of silanes for the hydrosilylation of P_4 using near-UV LED irradiation (365 nm, 3 W).[a]

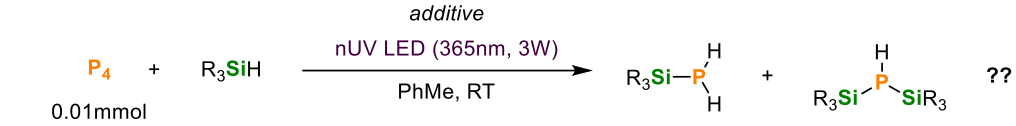

Entry	R_3SiH (mmol)	*additive* (mmol)	PhMe (µL)	Time (days)	Full conv. of $\mathbf{P_4}$?	Relative conv. to $\mathbf{P_1}$ compounds
1		-	500	3	X	-
2	Ph_3SiH	*i*Pr_3SiSH (0.14)	500	3	X	-
3	0.14	PhSH (0.14)	500	3	X	-[b]
4[c]		1,4-CHD (0.14)	100	2	X	-[b]
5		-	500	3	X	-
6	Et_3SiH	*i*Pr_3SiSH (0.14)	500	3	X	-
7	0.14	PhSH (0.14)	500	3	X	-[b]
8[c]		1,4-CHD (0.14)	100	2	X	-[b]
9[c]	$(Me_3SiO)_3SiH$	-	500	1	X	-
10[c]	0.09	*i*Pr_3SiSH (0.09)	500	1	X	-

[a] The general procedure described in this section was modified to use the indicated amount of reactants and solvent. [b] A small signal assigned to PH_3 was observed in the $^{31}P\{^1H\}$ and ^{31}P NMR spectra (see Figure S36 for a selected example). [c] 365 nm, 10 W.

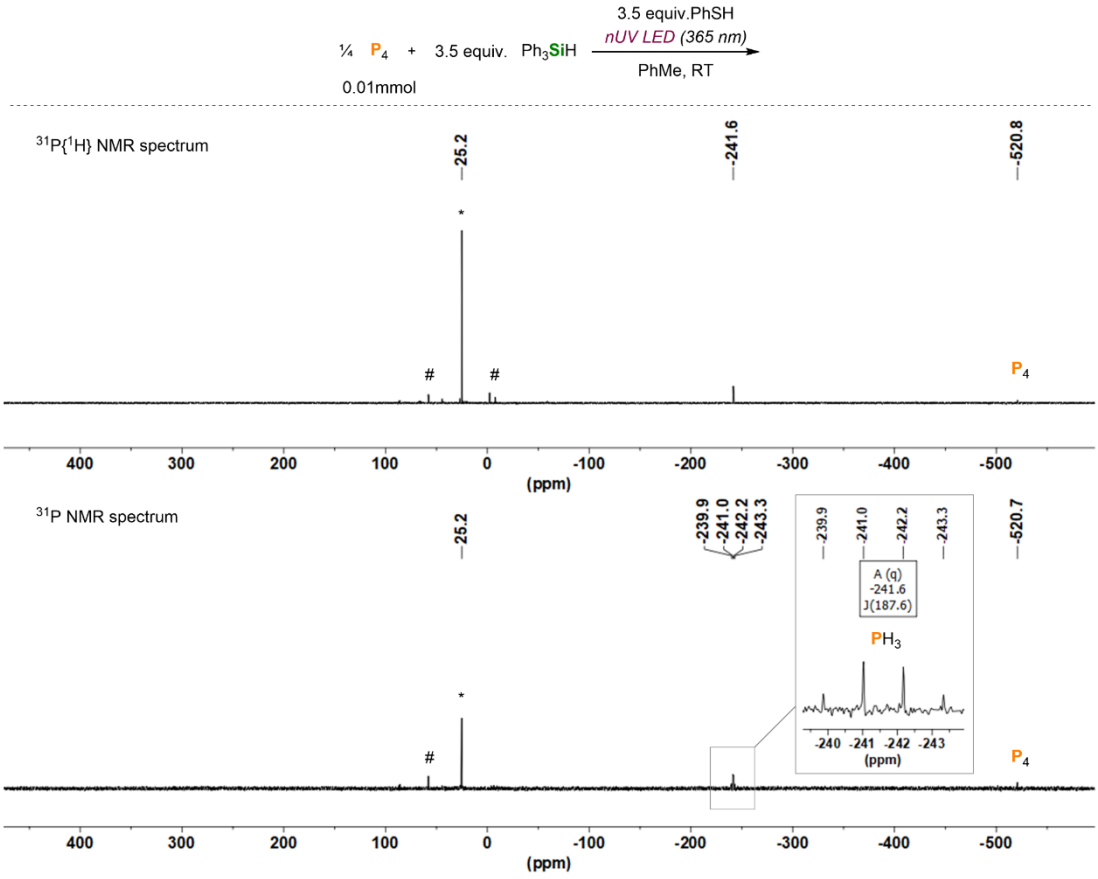

Figure S36. $^{31}P\{^1H\}$ and ^{31}P NMR spectra for the reaction of P_4 with Ph_3SiH (0.14 mmol) and PhSH (0.14 mmol) in PhMe and driven by 365 nm, 3 W LED irradiation for 3 d (Table S7, Entry 3). * marks the internal standard Ph_3PO (0.02 mmol). # marks unknown side products.

5.4.3.3 General procedure for the functionalisation of the hydrosilylphosphine mixture

The conversions of the products shown in this section were determined by a quantitative single-scan inverse-gated $^{31}P\{^{1}H\}$ NMR (DS = 0, D1 = 2 s) methodology that we have described previously, and whose use to quantify tertiary phosphines and quaternary phosphonium salts has previously been validated.[15]

To a 10 mL, flat-bottomed, stoppered tube were added P_4 (0.01 mmol, as a stock solution in 84.3 µL PhH), PhMe (100 µL), $(Me_3Si)_3SiH$ (27.9 µL, 0.09 mmol), and *i*Pr_3SiSH (19.3 µL, 0.09 mmol). The tube was sealed, placed in a water-cooled block to maintain near-ambient temperature, and irradiated with UV light (365 nm, 4.3 V, 700 mA, Osram OSLON SSL 80) for 2 days (unless stated otherwise). The resulting clear colourless solution mixture was treated with the corresponding electrophiles as follows:

Reactivity towards benzyl bromide: Benzyl bromide (47.6 µL, 0.4 mmol) and KHMDS (19.9 mg, 0.1 mmol) were added to the colourless solution, and heated to 100 °C with stirring for 3 days. After cooling to room temperature, Ph_3PO (0.02 mmol, stock solution in benzene) was subsequently added to act as an internal standard. Volatiles were removed under vacuum, and CH_3CN (0.5 mL) was then added. NMR analysis of the resulting mixture showed the formation of $[Bn_4P]Br$ (**5**) as the main product with 73 % conversion as shown in Figure S37.

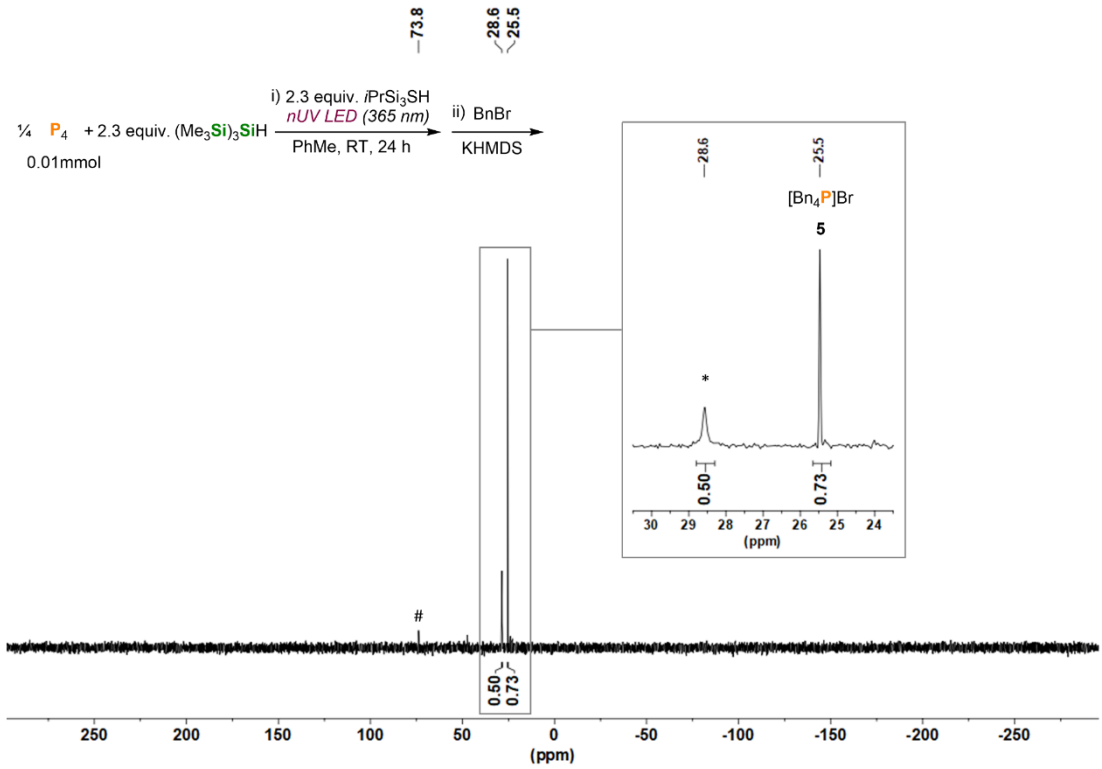

Figure S37. $^{31}P\{^{1}H\}$ NMR spectrum of $[Bn_4P]Br$ (**5**) generated *via* hydrosilylation of P_4 in PhMe, followed by treatment with benzyl bromide (0.4 mmol) and KHMDS (0.1 mmol), heated to 100 °C for 3 d. * marks the internal standard Ph_3PO (0.02 mmol). # marks an unknown side product.

Reactivity towards bromoethane: Bromoethane (30 µL, 0.4 mmol) and KHMDS (19.9 mg, 0.1 mmol) were added to the colourless solution, and heated to 100 °C with stirring for 3 days. After cooling to room temperature, Ph_3PO (0.02 mmol, stock solution in benzene) was subsequently added to act as an internal standard. Volatiles were removed under vacuum, and CH_3CN (0.5 mL) was then added. NMR analysis of the resulting mixture showed the formation of $[Et_4P]Br$ (**6**) as the main product with 54 % conversion as shown in Figure S38.

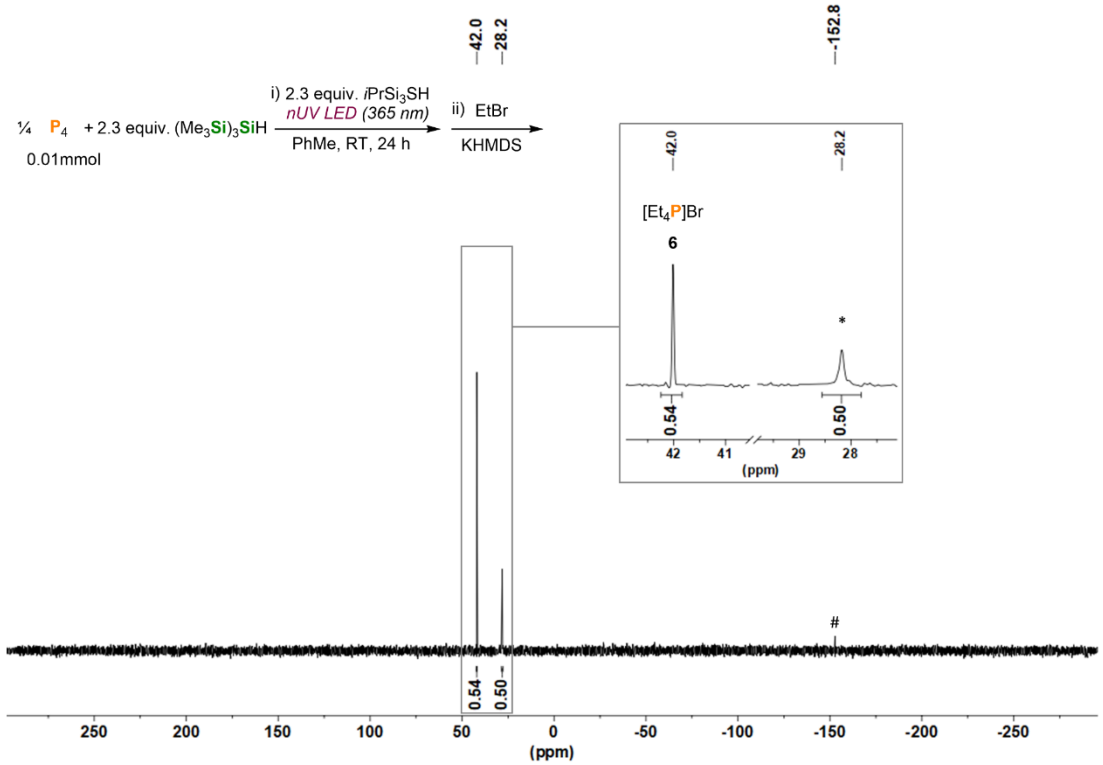

Figure S38. $^{31}P\{^1H\}$ NMR spectrum of $[Et_4P]Br$ (**6**) generated *via* hydrosilylation of P_4 in PhMe, followed by treatment with bromoethane (0.4 mmol) and KHMDS (0.1 mmol), heated to 100 °C for 3 d. * marks the internal standard Ph_3PO (0.02 mmol). # marks an unknown side product.

Reactivity towards 1-bromobutane: 1-bromobutane (43.2 µL, 0.4 mmol) and KHMDS (19.9 mg, 0.1 mmol) were added to the colourless solution, and heated to 100 °C with stirring for 3 days. After cooling to room temperature, Ph_3PO (0.02 mmol, stock solution in benzene) was subsequently added to act as an internal standard. Volatiles were removed under vacuum, and CH_3CN (0.5 mL) was then added. NMR analysis of the resulting mixture showed the formation of $[Bu_4P]Br$ (**11**) as the main product with 40 % conversion as shown in Figure S39.

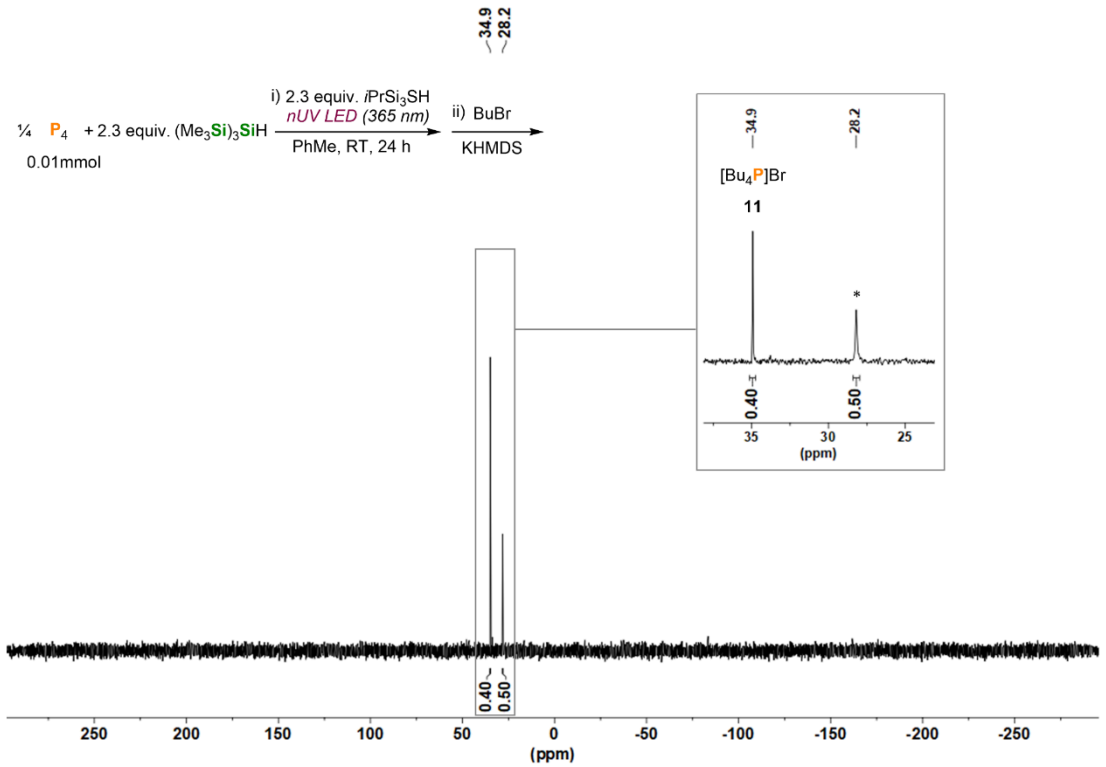

Figure S39. $^{31}P\{^{1}H\}$ NMR spectrum of $[Bu_4P]Br$ (**11**) generated *via* hydrosilylation of P_4 in PhMe, followed by treatment with 1-bromobutane (0.4 mmol) and KHMDS (0.1 mmol), heated to 100 °C for 3 d. * marks the internal standard Ph_3PO (0.02 mmol).

Reactivity towards paraformaldehyde: Volatiles were removed under vacuum. EtOH (0.5 mL) and paraformaldehyde (15.0 mg, 0.5 mmol) were added to the oily residue, and heated to 50 °C with stirring for 2 days. After cooling to room temperature, the mixture was frozen in a liquid nitrogen bath, and HCl (4.0 M in 1,4-dioxane, 100 µL, 0.4 mmol) was added. After thawing, the reaction mixture was stirred at room temperature for 2 hours. Ph_3PO (0.02 mmol, stock solution in benzene) was subsequently added to act as an internal standard. NMR analysis of the resulting mixture showed the formation of THPC (**12**) as the main product with 27% conversion, along with other unknown side products (<12%). Nevertheless, analogous reactivity studies of the crude $[Si]_nPH_{3-n}$ mixture generated in the presence of 1,4-CHD instead of iPr$_3$SiSH, resulted in the exclusive formation of THPC (**12**) with 48% conversion as shown in Figure S40.

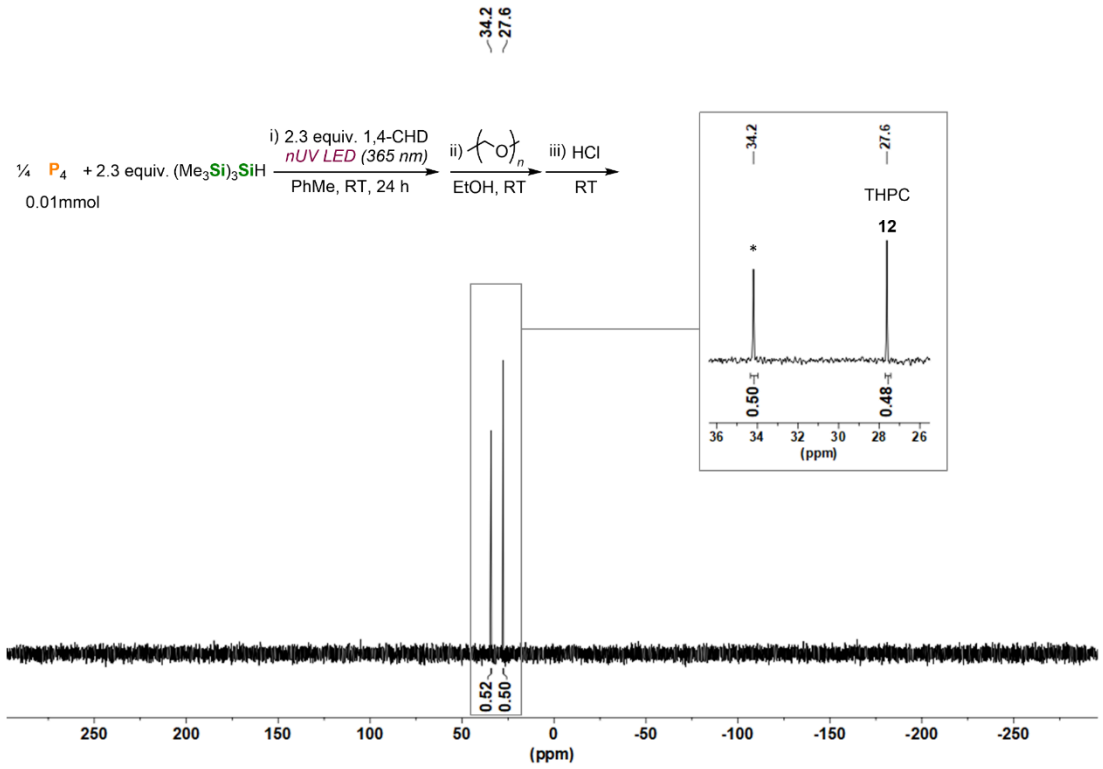

Figure S40. $^{31}P\{^{1}H\}$ NMR spectrum of THPC generated *via* hydrosilylation of P_4 in PhMe, followed by treatment with paraformaldehyde (0.5 mmol) in EtOH, heated to 50 °C for 2 d. Then, quenched with HCl (0.4 mmol). * marks the internal standard Ph_3PO (0.02 mmol).

Reactivity towards benzoyl chloride: PhC(O)Cl (27.9 μL, 0.24 mmol) and KHMDS (19.9 mg, 0.1 mmol) were added to the colourless solution, and stirred at room temperature for 24 hours. The resulting mixture was analysed by $^{31}P\{^{1}H\}$ and ^{31}P NMR spectroscopy as shown in Figure S41.

The $^{31}P\{^{1}H\}$ NMR spectrum showed only traces amounts of the desired product $P(C(O)tBu)_3$ (−54.1 ppm) along with a variety of other unknown species. The main product of this reaction appears as a singlet resonance at −114.6 ppm, which splits into a doublet in the ^{31}P spectrum ($^{1}J(^{31}P\text{-}^{1}H)$ = 208 Hz). Given the similarities on chemical shift and $^{1}J(^{31}P\text{-}^{1}H)$ coupling constant with analogous compounds ($Bu_3SnP(H)C(O)tBu$[19] and $Me_3SiP(H)C(O)tBu$[58]), this species was assigned to $R_3SiP(H)C(O)Ph$ (R = $SiMe_3$ or Me). Additional experiments using fewer equivalents of PhC(O)Cl, in our attempts to target this potential intermediate more selectively, were unsuccessful. Moreover, similar outcomes were observed during experiments at higher temperatures and longer reaction times.

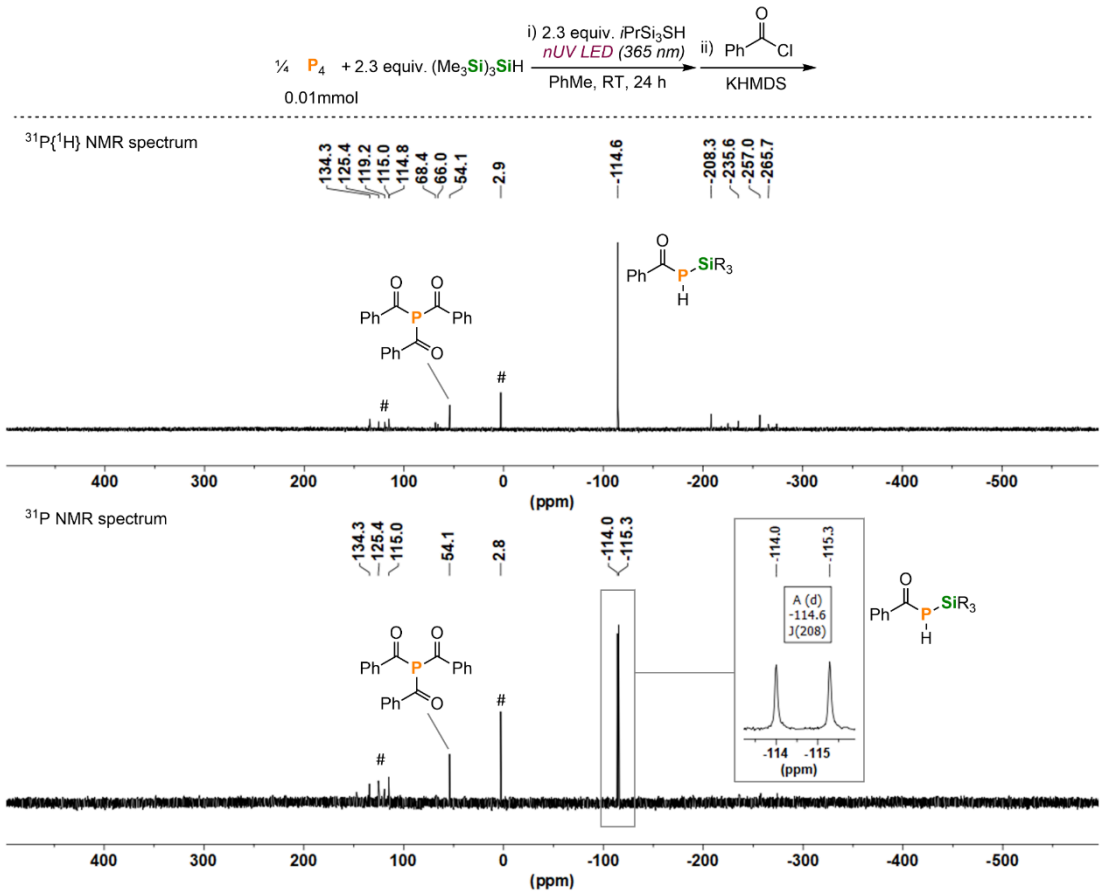

Figure S41. $^{31}P\{^{1}H\}$ and ^{31}P NMR spectra for the hydrosilylation of P_4 in PhMe, followed by treatment with benzoyl chloride (0.24 mmol) and KHMDS (0.1 mmol), stirred at room temperature for 24 h. # marks unknown species. R = $SiMe_3$, Me.

Reactivity towards pivaloyl chloride: *t*BuC(O)Cl (29.6 µL, 0.24 mmol) and KHMDS (19.9 mg, 0.1 mmol) were added to the colourless solution, and stirred at room temperature for 24 hours. The resulting mixture was analysed by $^{31}P\{^{1}H\}$ and ^{31}P NMR spectroscopy as shown in Figure S42.

Similar to the reaction with benzoyl chloride, the $^{31}P\{^{1}H\}$ NMR spectrum showed only trace amounts of the desired product $P(C(O)tBu)_3$ (−52.0 ppm) along with a variety of other unknown species. The main product of this reaction appears as a singlet resonance at −128.4 ppm, which splits into a doublet in the ^{31}P spectrum ($^{1}J(^{31}P\text{-}^{1}H)$ = 210 Hz). Given the similarities on chemical shift and $^{1}J(^{31}P\text{-}^{1}H)$ coupling constant with analogous compounds ($Bu_3SnP(H)C(O)tBu$[19] and $Me_3SiP(H)C(O)tBu$[58]), this species was assigned to $R_3SiP(H)C(O)tBu$ (R = $SiMe_3$ or Me). Aditional experiments using fewer equivalents of *t*BuC(O)Cl, in our attempts to target this potential intermediate more selectively, were unsuccessful. Moreover, similar outcomes were observed during experiments at higher temperatures and with longer reaction times.

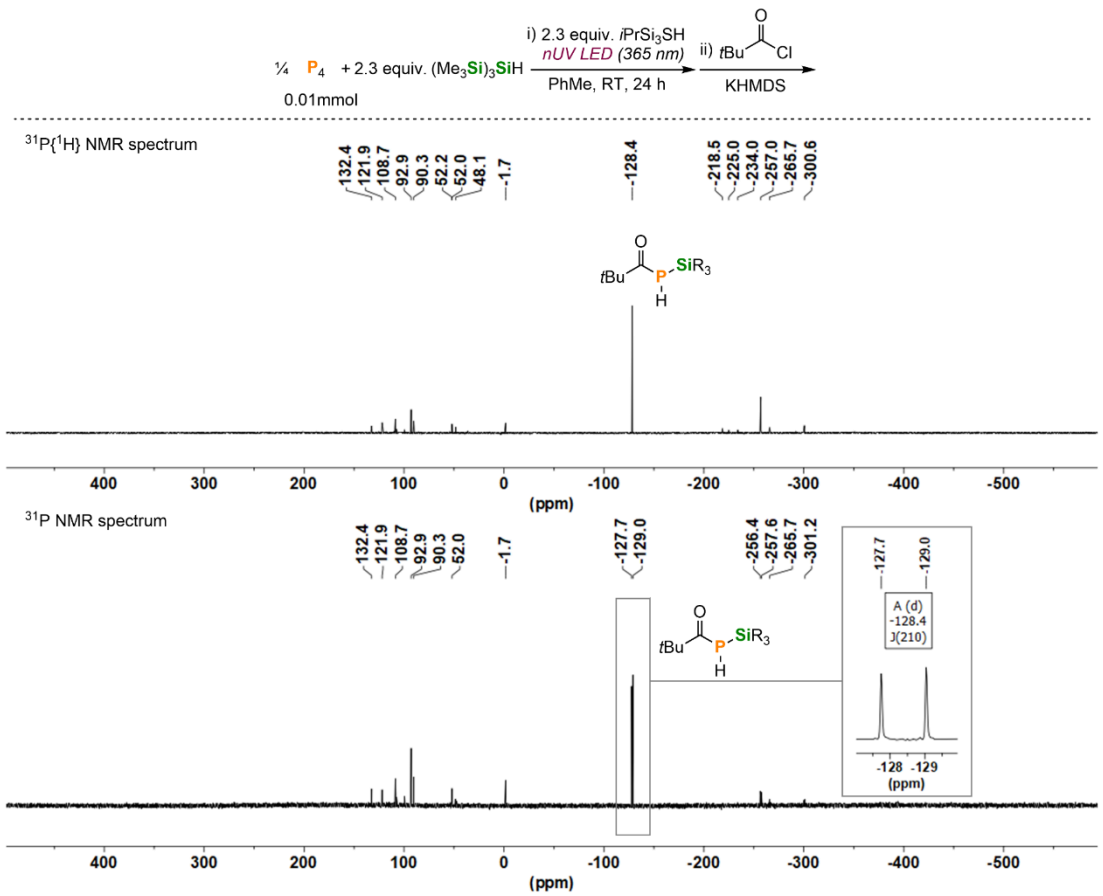

Figure S42. $^{31}P\{^{1}H\}$ and ^{31}P NMR spectra for the hydrosilylation of P_4 in PhMe, followed by treatment with pivaloyl chloride (0.24 mmol) and KHMDS (0.1 mmol), stirred at room temperature for 2 d. R = $SiMe_3$, Me.

5.4.3.4 Synthesis and quantification of PH_3 (4) via hydrosilylation of P_4 (0.01 mmol scale)

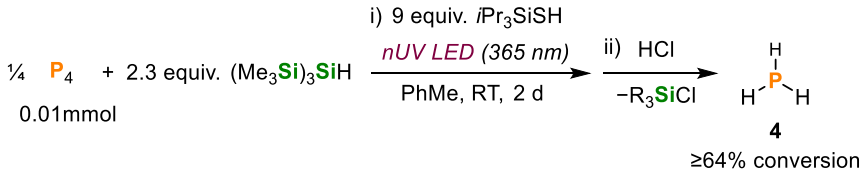

To a 10 mL, flat-bottomed, stoppered tube were added P_4 (0.01 mmol, as a stock solution in 84.3 µL PhH), PhMe (100 µL), $(Me_3Si)_3SiH$ (27.9 µL, 0.09 mmol), and iPr_3SiSH (19.3 µL, 0.09 mmol). The tube was sealed, placed in a water-cooled block to maintain near-ambient temperature, and irradiated with UV light (365 nm, 4.3 V, 700 mA, Osram OSLON SSL 80) for 2 days. Ph_3PO (0.02 mmol, stock solution in benzene) was subsequently added to act as an internal standard to the resulting clear colourless solution mixture and transferred to an NMR tube fitted with a J. Young valve. The mixture was frozen by placing the NMR tube in a bath of liquid nitrogen, and HCl (0.4 mmol, 4.0 M in 1,4-dioxane) was added (while still maintaining an inert atmosphere). The NMR tube was sealed and its contents were then thawed, agitated briefly, and analysed by ^{1}H, $^{31}P\{^{1}H\}$, and ^{31}P NMR spectroscopy. The resulting spectra indicated clean conversion to PH_3,[19] as shown in Figures S43-45, below.

In order to accurately quantify the amount of PH_3 in solution, a proton-coupled ^{31}P spectrum was acquired with a 20 s delay between scans (which was confirmed to be > 5 x T_1), and the intensity

of the PH_3 resonance was integrated relative to that of Ph_3PO. This indicated 64% of the theoretical maximum conversion to PH_3 (Figure S46), which provides a lower bound for the actual conversion (this value does not include any PH_3 present in the NMR tube headspace).

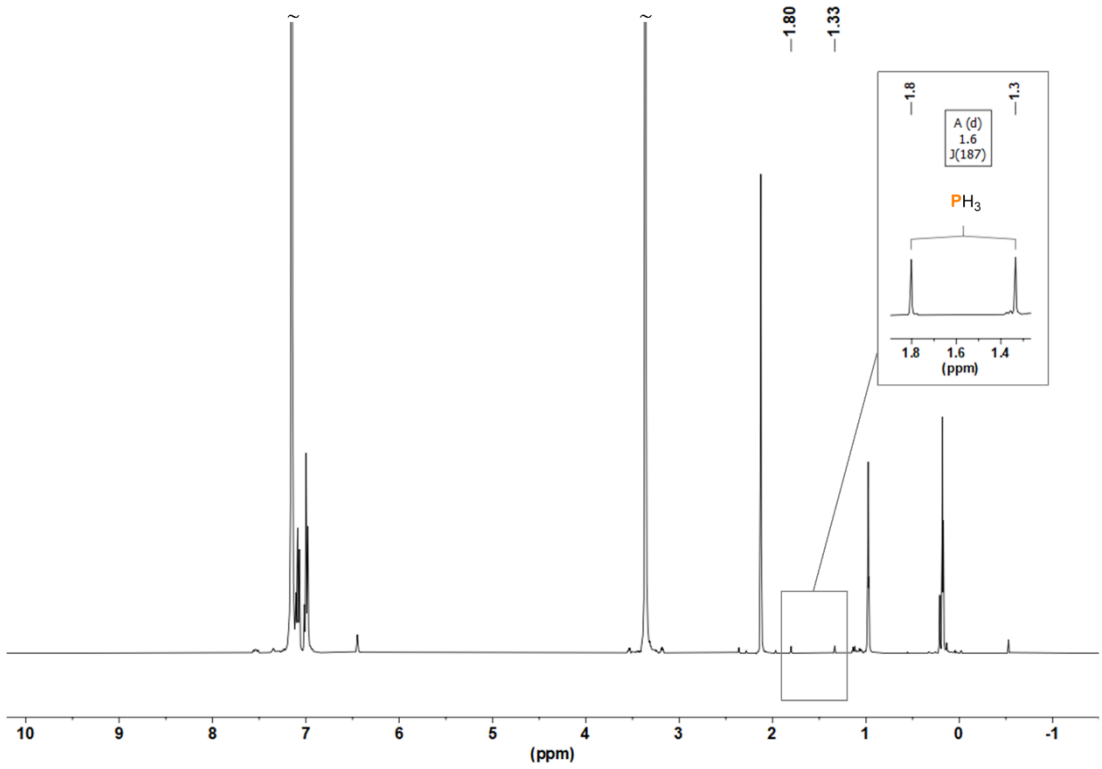

Figure S43. ^{1}H NMR spectrum of a solution of PH_3 (**4**) generated *via* hydrosilylation of P_4 in PhMe, followed by acidification. Solvent resonances (~) truncated for clarity.

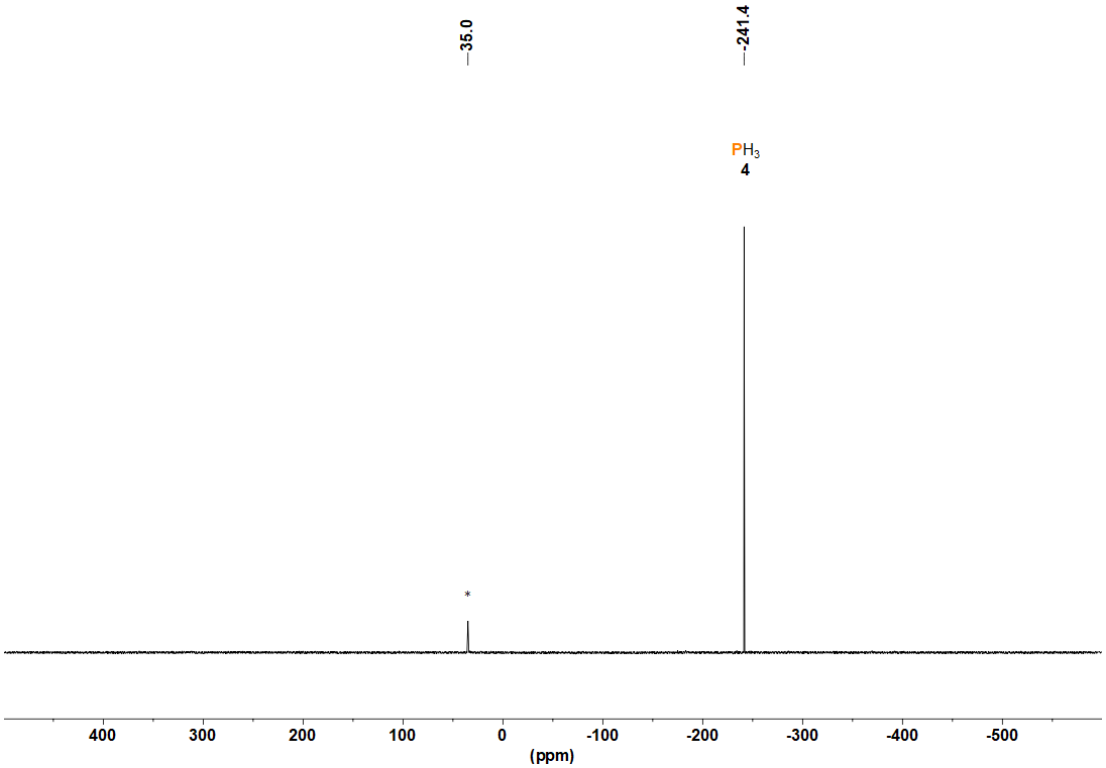

Figure S44. $^{31}P\{^{1}H\}$ NMR spectrum of PH_3 (**4**) generated *via* hydrosilylation of P_4 in PhMe, followed by acidification in the presence of Ph_3PO (*) as an internal standard.

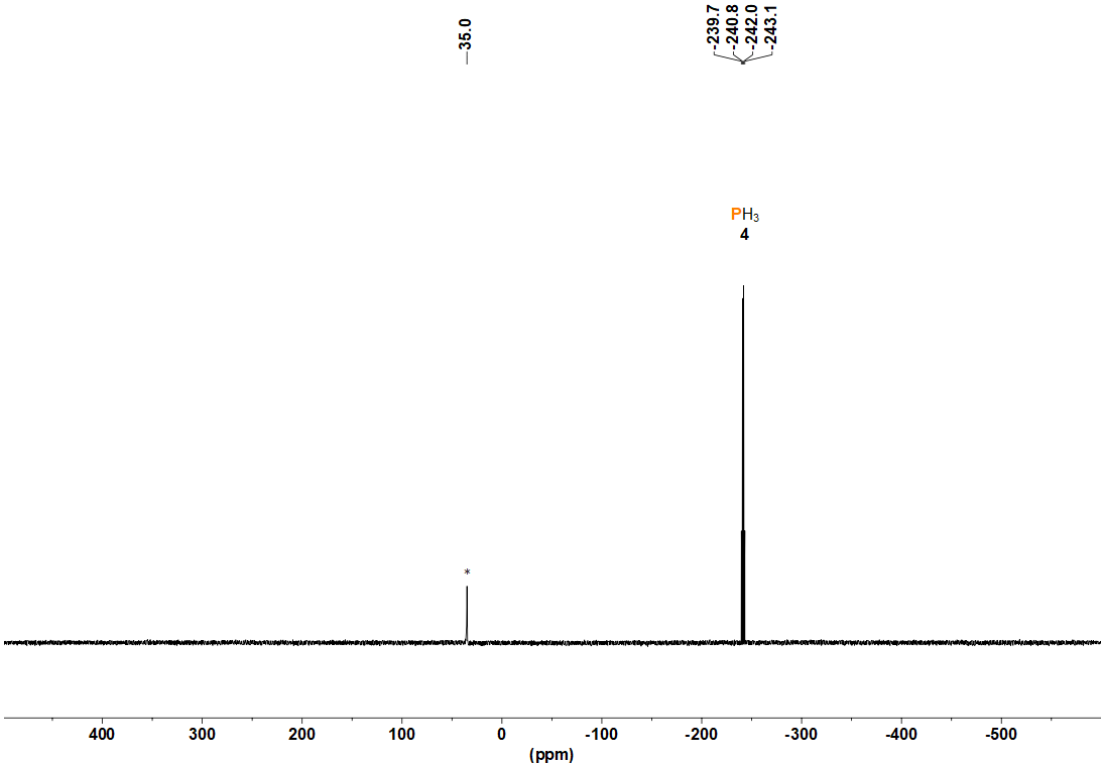

Figure S45. ^{31}P NMR spectrum of PH_3 (**4**) generated *via* hydrosilylation of P_4 in PhMe, followed by acidification in the presence of Ph_3PO (*) as an internal standard.

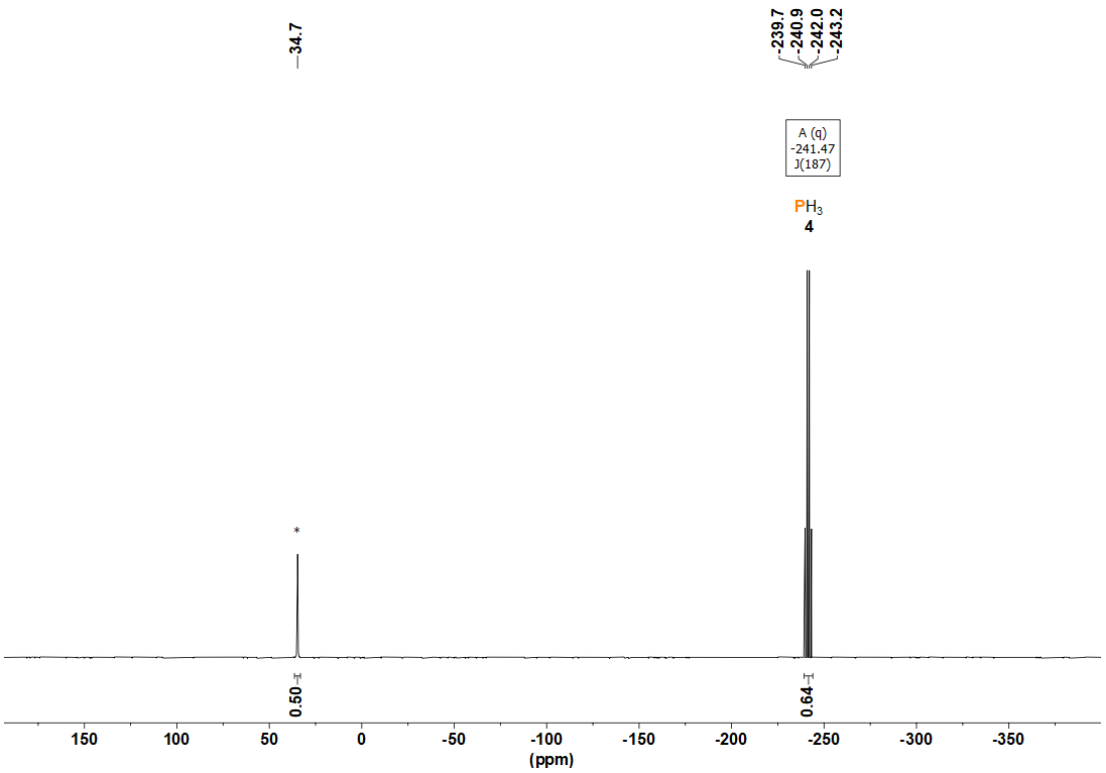

Figure S46. Quantitative ^{31}P NMR spectrum (D1 = 20 s) of PH_3 (**4**) generated *via* hydrosilylation of P_4 in PhMe, followed by acidification, in the presence of Ph_3PO (*) as an internal standard.

5.4.3.5 Hydrosilylation of P_{red} using using $(Me_3Si)_3SiH$, *i*Pr_3SiSH or 1,4-CHD and LED irradiation (0.06 mmol scale)

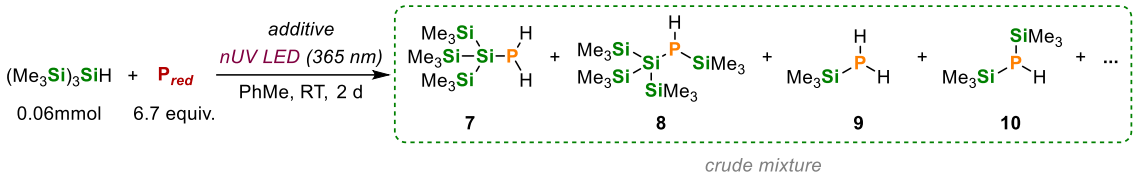

To a 10 mL, flat-bottomed, stoppered tube were added P_{red} (0.4 mmol, 12.4 mg), PhMe (250 µL), $(Me_3Si)_3SiH$ (18.5 µL, 0.06 mmol), and *i*Pr_3SiSH (12.9 µL, 0.06 mmol) or 1,4-CHD (5.7 µL, 0.06 mmol). The tube was sealed, placed in a water-cooled block to maintain near-ambient temperature, and irradiated with UV light (365 nm, 14 V, 700 mA, Osram OSLON SSL 80) for 2 days. Ph_3PO (0.02 mmol, stock solution in benzene) was subsequently added to act as an internal standard. The resulting mixture was analysed by $^{31}P\{^1H\}$ NMR spectroscopy, as shown in Figures S47 and S48, below.

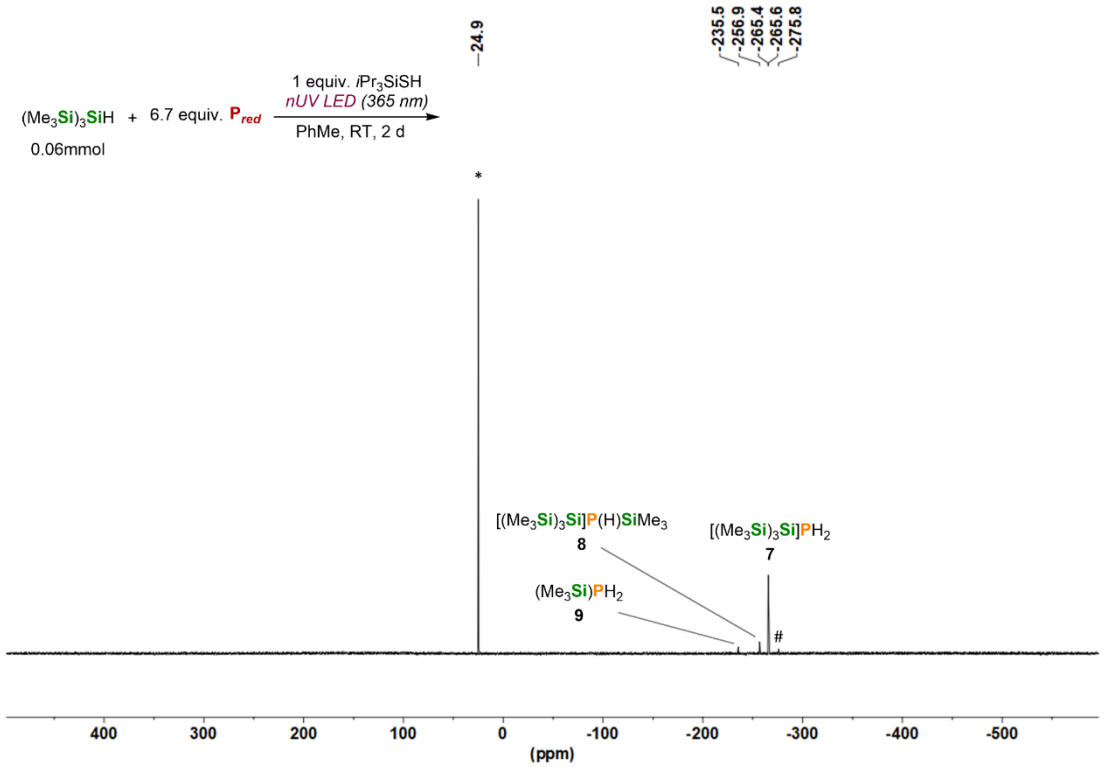

Figure S47. $^{31}P\{^1H\}$ NMR spectrum for the reaction of P_{red} with $(Me_3Si)_3SiH$ (0.06 mmol) and *i*Pr_3SiSH (0.06 mmol) in PhMe and driven by 365 nm, 10 W LED irradiation for 2 d. * marks the internal standard Ph_3PO.

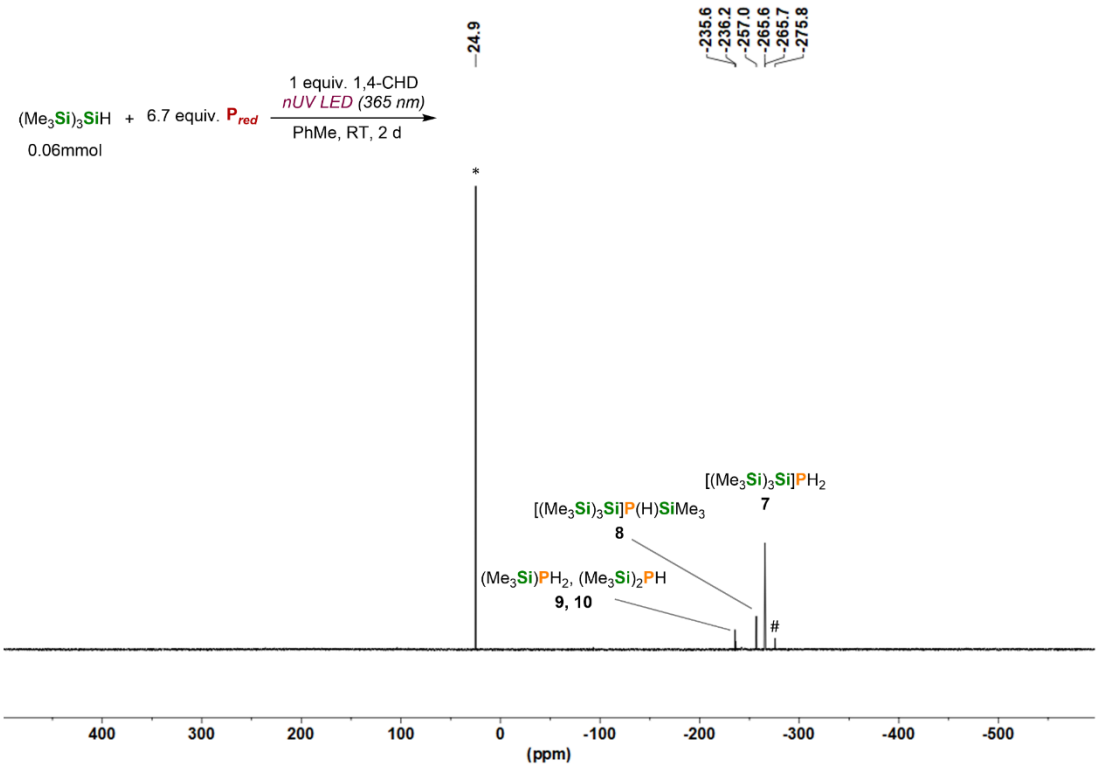

Figure S48. $^{31}P\{^{1}H\}$ NMR spectrum for the reaction of P_{red} with $(Me_3Si)_3SiH$ (0.06 mmol) and 1,4-CHD (0.06 mmol) in PhMe and driven by 365 nm, 10 W LED irradiation for 2 d. * marks the internal standard Ph_3PO.

5.4.3.6 General procedure for the hydrosilylation of P_4 using $(Me_3Si)_3SiH$, iPr_3SiSH and chemical radical initiators (0.01 mmol scale)

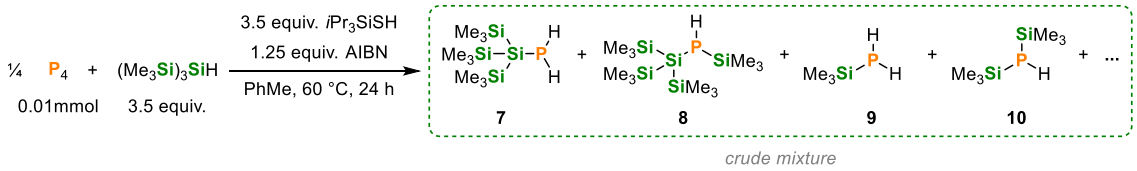

To a 10 mL, flat-bottomed, stoppered tube were added P_4 (0.01 mmol, as a stock solution in 84.3 µL PhH), PhMe (500 µL), AIBN (0.05 mmol, as a stock solution in PhH), $(Me_3Si)_3SiH$ (43.2 µL, 0.14 mmol), and iPr_3SiSH (30 µL, 0.14 mmol). The tube was sealed, wrapped in Al foil to exclude light, and heated to 60 °C for 24 hours (unless stated otherwise). Ph_3PO (0.02 mmol, stock solution in benzene) was subsequently added to act as an internal standard. The resulting mixture was analysed by $^{31}P\{^{1}H\}$ NMR spectroscopy, as shown in Figure S49, below.

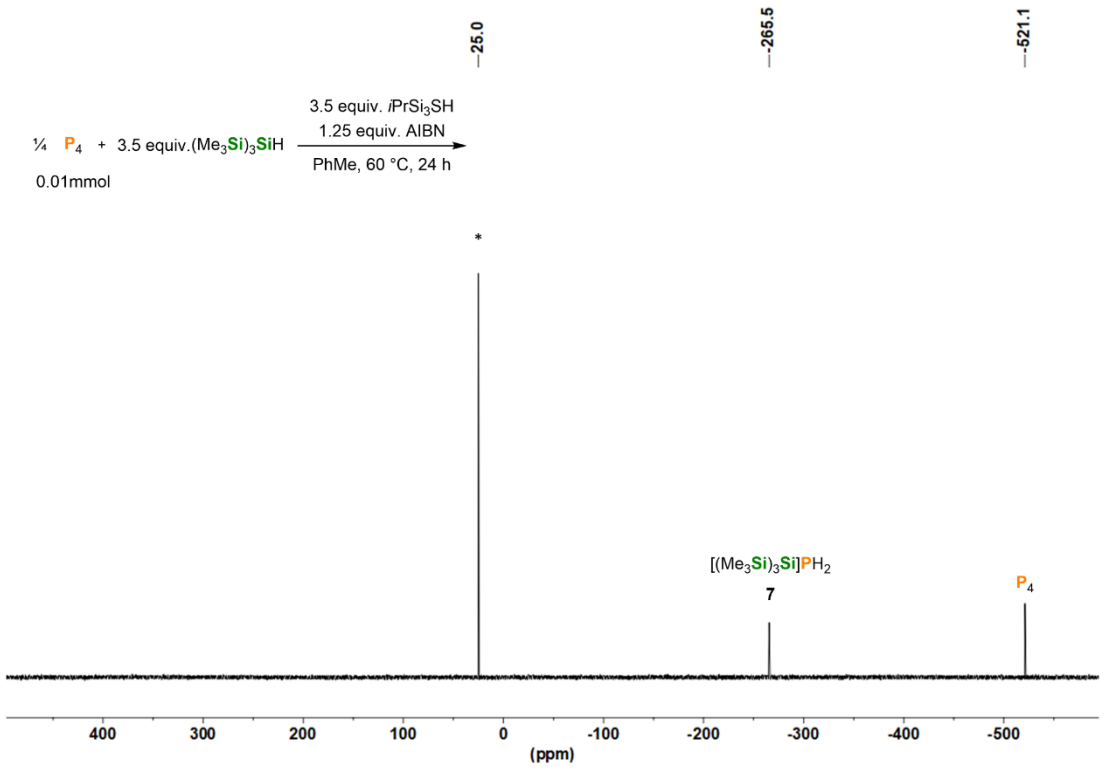

Figure S49. $^{31}P\{^{1}H\}$ NMR spectrum for the reaction of P_4 with $(Me_3Si)_3SiH$ (0.14 mmol), *i*Pr_3SiSH (0.14 mmol) and AIBN (0.05 mmol) in PhMe, heated to 60 °C for 24 h (Table S8, Entry 4). * marks the internal standard Ph_3PO (0.02 mmol).

Table S8. Optimisation of hydrosilylation of P_4 using $(Me_3Si)_3SiH$, HAT donor and chemical radical initiators.[a]

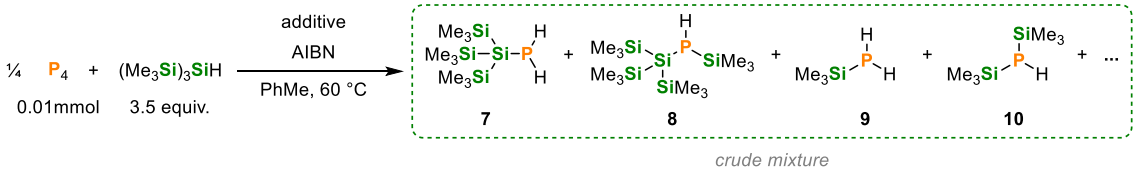

Entry	Additive (mmol)	Radical initiator (mmol)	Temperature (°C)	Time (days)	Full conv. of $\mathbf{P_4}$?	Relative conv. to **7-10** (%)
1	AdSH (0.14)	AIBN (0.05)	60	1	X	traces
2	*i*Pr_3SiSH (0.14)	AIBN (0.05)	60	1	X	traces
3	*i*Pr_3SiSH (0.14)	AIBN (0.14)	60	2	X	traces
4	1,4-CHD (0.14)	AIBN (0.14)	60	2	X	traces

[a] The general procedure described in this section was modified to use the indicated amount of reactant, temperature and time. [b] Conversions were calculated by integration of the ^{31}P resonances of **7-10** relative to an internal standard.

5.4.4 Cartesian coordinates of optimized structures

P_4
E= -1365.03900477 Eh
0 1

P	-8.63724066817835	1.73405756013613	0.95356065420993
P	-7.30344057381550	1.81815961948766	-0.77432824026063
P	-6.96619533814420	0.33677370507047	0.79516442354124
P	-8.68358341986195	0.14155911530574	-0.53970683749054

$Me_3Sn^{\bullet}$
E= -333.83773926 Eh
0 2

Sn	-0.04181811914409	-0.11771975225806	2.18561965993890
C	0.01624841845516	-0.03766963620385	0.02408622563928
C	1.95707088074064	-0.56728058815974	2.88224279632402
C	-0.55523065397075	1.85612096675477	2.90912231806715
H	0.34106820462594	-0.99425367785191	-0.38489706900594
H	0.72681657543460	0.73715997838795	-0.27485231550035
H	-0.96671998773747	0.20757913395128	-0.37752448186928
H	-1.54006851800091	2.15245397070418	2.54845420629491
H	0.18832079417249	2.56651605051999	2.53892030643005
H	-0.55323100757316	1.87485945633416	3.99882489447740
H	2.27918565815780	-1.54435600176422	2.52254509139057
H	1.99099649044407	-0.55860348753939	3.97155273552864
H	2.63847126439568	0.19588358712484	2.49769563228466

$[Sn]P_4^{\bullet}$
E= -1698.87329909 Eh
0 2

P	-1.95523966599795	-1.67253689686902	2.74605314937196
P	-4.46913481145529	-1.75104588972784	3.78802426030406
P	-3.64964678899596	-0.29707612212079	2.37015468200861
P	-2.81542757308502	-0.43707801362512	4.36931651554389
Sn	-0.07502888407850	-0.06570514227185	2.04485724530151
C	0.00879311068946	-0.06560143856404	-0.09861950975743
C	1.74654435191822	-0.82572726558248	2.88612211424798
C	-0.48175123769149	1.90665066206422	2.77896956639695
H	0.83447392423197	0.56515094414195	-0.43235579842360
H	-0.92378221563992	0.32562000100411	-0.50521193561982
H	0.16242055058868	-1.07789405977524	-0.47240897596584
H	-1.46724553645603	2.23853193473814	2.45265525883124
H	0.27268975288791	2.59356365941020	2.39124909644244
H	-0.44879161676758	1.91659140180575	3.86818390953441
H	2.58342993775571	-0.19270279932788	2.58655002116582
H	1.92775103073342	-1.84183155510255	2.53547485654537
H	1.67954567136235	-0.83277942019756	3.97409554407247

Me_3SnH
E= -334.45306553 Eh
0 1

Sn	-6.04471667208550	0.33284160579064	0.38585898860526
C	-7.71073127776283	-0.82831122829153	1.07102915111342
H	-7.40809971322585	-1.43674482176383	1.92467936063237
H	-8.06703535137819	-1.48923307853153	0.28038348036314
H	-8.52919079948289	-0.17654228763201	1.37822361613702
C	-4.49479454034692	-0.98497549741784	-0.28862299278680
H	-3.61978984365241	-0.41541993363825	-0.60385958039123
H	-4.84474622633764	-1.58366861053805	-1.13017019072076
H	-4.20148444456054	-1.65639892611004	0.51961102706190
C	-5.30862551989089	1.54303464840539	1.99503785789955
H	-6.07816567053497	2.23852704188395	2.33151435304507
H	-4.43742575389723	2.11525142695790	1.67425342800372
H	-5.02041604962666	0.90799357813743	2.83410633460966
H	-6.54115813721747	1.34597608274776	-0.91038483357233

TS($[Sn]P_4^{\bullet}$→$[Sn]P_4H$)
E= -2033.30911684 Eh
im. freq. = 771.71 *i*
0 2

H	0.06423181035575	-1.73612866467063	3.30241068825383
Sn	-0.20889869110693	-0.00204390311150	2.34204877368218
P	2.14953408882840	-2.62985782909297	6.79502752708436
P	0.57377560193294	-2.87782050273250	4.42838091071761
P	2.36010497775788	-1.65044831208672	4.81973330963943
P	0.56817678001534	-1.31073628529748	5.97583112593764
Sn	3.39345664481709	-0.82075258000473	8.10313762842307
C	2.67156601350831	1.12652783338235	7.55877446665433
C	5.47989741859054	-0.98037588984864	7.62234351453257
C	3.07403098652855	-1.16847994766599	10.19684985254107
H	2.73970662199042	1.27021447539667	6.48028876189557
H	3.27835294742562	1.88380077580779	8.05849278734947
H	1.63207068845080	1.24445352049963	7.86452605220644
H	3.62390732459128	-0.42954613041045	10.78181568131370
H	3.41987858782449	-2.16513919731435	10.47169273413654
H	2.01253664912419	-1.08633604478284	10.43152999218820
H	5.61866341980464	-0.85782730354501	6.54786373461452
H	5.86631657617706	-1.95540985461302	7.91942018339593
H	6.04039977564852	-0.20266808123123	8.14353225675101
C	0.77437304305083	1.62247735157282	3.36050967235314
H	1.84839295782703	1.44193547604309	3.39601127026933
H	0.39741716102985	1.70688404163896	4.37938120924122
H	0.58276377781308	2.55543478466263	2.82571809278882
C	0.59614159731586	-0.18734197178691	0.35166637906147
H	0.09581557022091	-0.99121866101514	-0.18838513477562
H	1.66415204387254	-0.40067182221209	0.39719213293675
H	0.44509818382991	0.74959369382293	-0.18854866801024
C	-2.32330748212930	0.39805420668573	2.22762646999092
H	-2.74646706000616	0.47819953260103	3.22890791137537
H	-2.83160982266577	-0.40301422413359	1.69076304260614
H	-2.48625819242375	1.33865151344217	1.69739764084497

$[Sn]P_4H$
E= -1699.48597461 Eh
0 1

P	2.60825079651189	-0.27852527900993	2.25044672203470
P	4.83618138677669	0.90114854014262	3.61294963869152
P	2.72930937079770	0.66783647939390	4.25216617051788
P	3.17430640760397	1.85064563304859	2.50069754164659
Sn	0.11767835233257	0.08158718528474	1.89492329543462
C	-0.47884956851307	2.02029042606585	2.58867641859464
C	-0.90658708668548	-1.44399803208477	3.00011104950728
C	-0.26247665066296	-0.12429133016896	-0.20608062449968
H	-0.15551634111142	2.16966592351333	3.61877548901145
H	-1.56665037597744	2.09482322070214	2.54211007348659
H	-0.04123314402378	2.79952592334858	1.96503170424256
H	0.24993368701561	0.66368396790055	-0.75828784086817
H	-1.33420845352469	-0.05088767232442	-0.39675450940367
H	0.09295656157647	-1.09217111849208	-0.56034463311294
H	-0.70608613549304	-1.32503104317873	4.06516545889515
H	-0.57060112492773	-2.43215906141740	2.68557342335666
H	-1.98166070287450	-1.36523508574272	2.83138429056076
H	5.11858302117921	2.03432132301868	4.44554633190407

TS($[Sn]P_4^{\bullet}$→$[Sn]P_8^{\bullet}$)
E= -3063.89939282 Eh
im. freq. = 100.14 *i*
0 2

P	-2.21003322683120	-1.90136616300394	2.54801167071202
P	-4.58995594469094	-2.42752452084971	3.94111640646466
P	-4.00653158811772	-0.62518548629350	2.82941040964135
P	-2.85201596664408	-1.23258221773813	4.55874473745784
Sn	-0.52993154069454	-0.00970127422268	2.17544671117925
C	-0.03146472974718	0.01251201257821	0.09012347761209
C	1.19233664424430	-0.48228574197601	3.36395902786457
C	-1.37905785297348	1.86449818948982	2.77895834461659
H	0.70917817633123	0.79000707172598	-0.10314331799110
H	-0.92118095409734	0.21541307134253	-0.50589343086431
H	0.38218584660922	-0.95102769238233	-0.20717021662121
H	-2.18760556060772	2.14732861144434	2.10486998832881
H	-0.60449492123789	2.63279506678443	2.74972183110074
H	-1.77338431752628	1.79515187424043	3.79274854344711
H	1.94523656723047	0.29914497108048	3.24957714059980
H	1.61883342558451	-1.43437177186465	3.04793658823939
H	0.90898640775024	-0.55088395934257	4.41435360995988
P	-7.49779783331619	-0.30623527418499	4.21005343607977
P	-7.76698655690785	0.13504014340855	6.33885486827557
P	-6.22082378513720	-1.48962118045098	5.52862193368994
P	-5.89848228922030	0.66690427021472	5.32611824020714

$[Sn]P_8^{\bullet}$
E= -3063.89957219 Eh
0 2

P	6.89148694749768	1.11570887185430	3.82048115990157
P	7.57080781414734	3.56223719836687	4.87391810295771
P	6.60537008018981	1.87548728955946	5.87402903164898
P	5.60202515492911	2.87315991350147	4.20956242397067
H	0.59365150584319	-0.04102484416759	0.46132195844439
P	3.85730307874197	0.19196847501584	2.49459688656549
C	-0.09825024708821	-0.61781540004384	1.07539034379769
H	1.28182422437636	2.19396349178298	3.19425259889989
H	-1.11305861950137	-0.25651224414088	0.90150218172150
H	-0.04141907596150	-1.66659452957893	0.78409844711898
P	5.42151872582528	-0.62804985648977	3.81986823078707
P	2.71200534542806	-1.42837409495145	3.47443499090614
C	0.44180369728059	1.69160070601011	3.67401733408055
Sn	0.40858074085498	-0.38600722842080	3.14678189078141
H	-0.48760425910361	2.15724298599206	3.34157287337379
P	3.57418088479375	0.25637664247679	4.64087761900586
H	0.53142163983356	1.80715287593786	4.75397775778859
C	-0.95125033310812	-1.46956981698081	4.40286855176961
H	-1.95255262568761	-1.04473374843718	4.31749568681963
H	-0.98595335018478	-2.51780701096958	4.10572293203903
H	-0.62873132910650	-1.40717967631692	5.44228899762143

$Me_3Ge^{\bullet}$
E= -2196.27911102 Eh
0 2

Ge	-6.03032719953612	0.30323244649022	0.42012632065943
C	-7.56354208901077	-0.75674867757626	1.04723080471239
H	-7.24933695643939	-1.38107096967147	1.88951262736187
H	-7.93662642644507	-1.40616646153573	0.25479950545397
H	-8.37416473998071	-0.10747445879040	1.37956270969865
C	-4.60513250651833	-0.90579213259089	-0.19168912386877
H	-3.73427082111365	-0.33926970587033	-0.52351139490647
H	-4.95224651126682	-1.52993975938974	-1.01570534938295
H	-4.30207077507694	-1.55690209854285	0.63399744024195
C	-5.35615022289328	1.41182021757530	1.89830815822001
H	-6.12802301586116	2.09476120984888	2.25461408455449
H	-4.49206497119805	1.99654398672809	1.58078173470203
H	-5.05388376465968	0.76516640332518	2.72789248255340

$[Ge]P_4^{\bullet}$
E= -3561.32408927 Eh
0 2

P	2.42558728149884	-0.25550882448982	2.25217185967132
P	4.69195391212326	0.81330550677054	3.49670748627093
P	2.63197416426256	0.71268616632875	4.23511882842292
P	3.08166274136950	1.85352097923624	2.43897677673396
Ge	0.10328307905216	0.09952894969010	1.92105057049387
C	-0.46483480968926	1.86201123697519	2.54411360513092
C	-0.82669753892190	-1.30562996086839	2.91513543784380
C	-0.20469542455597	-0.08657053815520	-0.00277063460256
H	-0.19325250271151	2.01291957199252	3.58950113476215
H	-1.55068735354438	1.93786972968373	2.45094655431498
H	-0.00678864274470	2.65212541985503	1.94834210179275
H	0.32876090456159	0.69218788954658	-0.54938505317920
H	-1.27109879630000	0.00186470871274	-0.22108971582520
H	0.14243146490425	-1.05892232541339	-0.35495518001395
H	-0.64262370331514	-1.19523232521587	3.98462620977393
H	-0.48489001304776	-2.29296233469123	2.60214960256393
H	-1.90207476294154	-1.23618384995752	2.73712041584547

Me_3GeH
E= -2196.90908050 Eh
0 1

Ge	-6.02484253113286	0.29233964428955	0.43396098170902
C	-7.55719281423406	-0.75637268264983	1.04819142270586
H	-7.26196208628080	-1.39314114038797	1.88474157459735
H	-7.93617358861047	-1.39366064841813	0.24789562918773
H	-8.36477764511334	-0.10227260916580	1.38052134201254
C	-4.60770933278757	-0.90502515072871	-0.18471008958487
H	-3.74256006393516	-0.33454914742391	-0.52649969814145
H	-4.95887208925337	-1.52724206900824	-1.00928455697813
H	-4.28851252301713	-1.55944994243157	0.62889604477255
C	-5.35708030830475	1.40540636350897	1.89709719798970
H	-6.13100446358158	2.09094513034933	2.24575906178828
H	-4.49696621901376	1.99386348362322	1.57364924913678
H	-5.04989046190243	0.77715012402210	2.73568934391907
H	-6.46789587283271	1.20298864442097	-0.73605750311443

TS($[Ge]P_4^{\bullet}$→$[Ge]P_4H$)
E= -5758.20342573 Eh
im. freq. = 131.50 *i*
0 2

P	3.07428885917582	-0.74811432365135	2.38897500515331
P	5.87863377854958	-0.48088139672441	2.88813527627351
P	4.14675247253712	0.24456213208272	4.05381155632408
P	4.43729399931663	0.96017919753545	2.03490202693636
Ge	1.04167121721564	0.44393401149729	2.45488143244306
C	1.17536634259464	2.11363278448522	3.46465002921999
C	-0.28241490125267	-0.73764477532669	3.27888298229168
C	0.55434516586656	0.81589047123786	0.59548662548154
H	1.39127140644483	1.91423217158455	4.51508969437364
H	0.22485915055828	2.64777377301852	3.39822698677184
H	1.96274991879479	2.75224380268855	3.06252568634665
H	1.29775208569062	1.46688296603921	0.13294654727026
H	-0.41763914819513	1.31250541535305	0.55487362491448
H	0.49669660076966	-0.10904624573060	0.02052988245954
H	-0.01688854493263	-0.94118076313201	4.31704506349240
H	-0.33682320556515	-1.68543029638552	2.74139738023884
H	-1.26768954668244	-0.26747745364713	3.25639811612034
H	9.58192282346799	2.79850619622769	3.02069792535177
H	6.62826990268200	4.09090113524281	2.44192558023745
H	9.62997168235085	3.68074142138670	4.55801439023358
C	9.31929008916926	2.74797814258621	4.07798924741110
H	6.68231140539183	4.93532279833854	4.00231224659700
C	6.40042196965027	4.00261942813594	3.50462040285360
H	9.86773265784496	1.92350108349798	4.53508885874602
Ge	7.38279707050351	2.50164224535820	4.30369222154366
H	5.32636294216179	3.85310034594753	3.61904956162050
H	6.77219515718480	0.63721867706682	3.41730593648693
H	7.26987634641221	3.21916650639399	6.74967968709026
C	6.93450782233008	2.32992703990926	6.20816631175023
H	7.42083566188356	1.45547496052001	6.64219226928830
H	5.85598881808050	2.22870854846354	6.33489744467788

$[Ge]P_4H$
E= -3561.93766778 Eh
0 1

P	2.41563134296158	-0.26310839398710	2.24078466387278
P	4.72410392445625	0.83367398481781	3.53158072244176
P	2.62479335240054	0.69871237925066	4.22499226513485
P	3.07829127033371	1.84065502673889	2.44568038027192
Ge	0.11191151540641	0.09934371392732	1.91889951575956
C	-0.46369437886685	1.86132248306837	2.54061581801322
C	-0.82258931115185	-1.30186997044448	2.91395552651133
C	-0.21086017235406	-0.08644506589942	-0.00196955182881
H	-0.19850098744781	2.01294634753757	3.58749887879574
H	-1.54918773787919	1.93340562071945	2.44133057769182
H	-0.00553851058479	2.65369487638344	1.94782947428334
H	0.31565812967733	0.69379524673330	-0.55331247534835
H	-1.27910398700370	-0.00108292256902	-0.21154074107830
H	0.13626464313080	-1.05757519505045	-0.35767283455303
H	-0.63609509234976	-1.19324126323113	3.98329116840890
H	-0.48559078236904	-2.29068591184082	2.60022988773978
H	-1.89789425725815	-1.22791719049873	2.73831393414492
H	5.06575103889859	1.96559623434434	4.34157278973857

TS($[Ge]P_4^{\bullet}$→$[Ge]P_8^{\bullet}$)
E= -4926.35020504 Eh
im. freq. = 105.96 *i*
0 2

P	2.57634092669917	-0.81423067389992	1.98602568749661
P	5.25389759013495	-0.25613965147818	2.64717775310880
P	3.41768201003514	0.27450514660820	3.72755337800731
P	3.74182072660894	1.05049385911874	1.72877460793962
Ge	0.40021362297731	0.11240610416707	2.01072641686715
C	0.39756936485301	1.95895825061705	2.64916071049511
C	-0.68119962661830	-1.02638861758345	3.17768525411737
C	-0.24541535472015	0.02254692931608	0.16641914406077
H	0.80397945591060	2.02593744563693	3.65886324476367
H	-0.62968670702691	2.33038133206199	2.66065161785609
H	0.99062807905314	2.59827100450931	1.99408995739302
H	0.37882076172339	0.63623230236875	-0.48463718542041
H	-1.27197185231062	0.39135429228312	0.11372829008988
H	-0.22565192117025	-1.00468989914829	-0.19973187509362
H	-0.30951852855707	-0.98368100351094	4.20215570882302
H	-0.65124964271932	-2.06236569568178	2.83800524766375
H	-1.71891187951537	-0.68631667099352	3.16810398251698
P	6.79413112139291	1.51268945117876	3.46679280841243
P	7.48573427633859	3.28588713985482	4.88594536382307
P	6.28284937025999	1.59538760380395	5.58889371219812
P	5.41738820665069	3.04364135077122	4.20832617488097

$[Ge]P_8^{\bullet}$
E= -4926.35080109 Eh
0 2

P	6.80794242672950	1.06336545571780	3.82513987519387
P	7.53860675230855	3.48454635334003	4.92610458823482
P	6.54063355107072	1.79646930323166	5.89180746817471
P	5.56033839030261	2.84428484877948	4.24334200605638
H	0.61080287841661	-0.02392590635154	0.61462616175226
P	3.75944467506537	0.27356468247069	2.48494211902891
C	-0.06258855160350	-0.59242209466097	1.25753287674895
H	1.17927088067082	2.09600938840511	3.03113808266267
H	-1.08306055858059	-0.24002590775149	1.09265516027423
H	-0.00861030785828	-1.64465404704312	0.97557100779901
P	5.29891002146424	-0.64163323232548	3.77780070391777
P	2.55650325964176	-1.33564521672988	3.40767448836278
C	0.42140672643137	1.55128799045201	3.59539974196802
Ge	0.42815437622619	-0.34921879013893	3.13608196193534
H	-0.55899182340478	1.96887897755684	3.35449859836052
P	3.48063638338620	0.27009353847783	4.63425579885958
H	0.60921269394913	1.69634387014246	4.65969910243827
C	-0.78355359192414	-1.34536967055900	4.30561501293049
H	-1.79925245259154	-0.95608559926557	4.20942060305677
H	-0.79023481857926	-2.40307301033589	4.03888638431218
H	-0.47241091112098	-1.25156093341202	5.34687825793238

$Me_3Si^{\bullet}$
E= -408.91880037 Eh
0 2

Si	-6.01402051526227	0.27061830776064	0.46188261231549
C	-7.49572177038263	-0.72928209931292	1.03987549331333
H	-7.20999313844297	-1.37485409559983	1.87868838845208
H	-7.88105082580489	-1.36723195801090	0.24179892912929
H	-8.30677872666042	-0.07987656429112	1.37610169639179
C	-4.65423753233380	-0.87250476273634	-0.14792647301809
H	-3.78453929170950	-0.30664987918378	-0.48886379525873
H	-4.99982067671912	-1.49485790967117	-0.97610006086427
H	-4.32757881798652	-1.53784494558140	0.65971261201179

C	-5.37642272184734	1.35504288780905	1.85706718820993
H	-6.14718924291025	2.04408102100073	2.20895832536620
H	-4.51508275436684	1.94608197754458	1.53842619346284
H	-5.06540398557342	0.73543802027247	2.70629889048834

[Si]P$_4$$^{\bullet}$
E= -1773.97201212 Eh
0 2

P	2.34947013291138	-0.25875155855258	2.23203374798272
P	4.64287752089734	0.78988328280609	3.47698857756903
P	2.57991826824500	0.71029281573002	4.21321975843626
P	3.04084471625620	1.84069561489277	2.41454919478782
Si	0.09881176169652	0.10820645615874	1.92403562195825
C	-0.44959584157801	1.79310502271836	2.51962980030735
C	-0.78369804831968	-1.24073493583690	2.87594868279375
C	-0.19613165027979	-0.07319651712265	0.08369236205008
H	-0.21188018917704	1.94712128585575	3.57432363818549
H	-1.53408198986518	1.88160839835441	2.40159761026664
H	0.01914472369145	2.59604138490059	1.94703611984932
H	0.33614146760016	0.69834725672018	-0.47731405548138
H	-1.26235300450979	0.01749805889459	-0.14383744056271
H	0.14325925229600	-1.04717535967083	-0.27668022604903
H	-0.60431711280528	-1.14120020242494	3.94894059158311
H	-0.44744780490449	-2.23313860554600	2.56720247948578
H	-1.86296220215478	-1.18161239787760	2.70638353683752

Me$_3$SiH
E= -409.55922044 Eh
0 1

Si	-6.01248331123423	0.26782889926965	0.46602798014279
C	-7.48855346046404	-0.73013459568590	1.04317364315214
H	-7.21259431195311	-1.37615306499274	1.88145080794240
H	-7.87375211982764	-1.36659962297267	0.24299268093057
H	-8.30081103755454	-0.07865747686688	1.37451537814760
C	-4.65690432196795	-0.87231024808338	-0.14127140546444
H	-3.78993052399976	-0.30468265685610	-0.48809688973143
H	-5.00495791262431	-1.49410340890456	-0.96964936335428
H	-4.32287928502732	-1.53771482366907	0.65971170322898
C	-5.37642313512936	1.34689306923911	1.85838846524285
H	-6.14748471167042	2.03882721315529	2.20585674630476
H	-4.51544827212018	1.93879592575456	1.53823551534058
H	-5.06576273840850	0.73579668618106	2.71050594586001
H	-6.44049485801863	1.14703410443163	-0.66389120774251

TS([Si]P$_4$$^{\bullet}$→[Si]P$_4$H)
E= -2183.49388392 Eh
im. freq. = 187.56 *i*
0 2

H	1.76785332166208	1.73192075453450	-0.74352556675964
P	5.26548175904519	1.57400204163037	0.44593987257250
C	1.41888243281266	0.69764885679241	-0.69952391982808
H	1.48794077398493	0.27571723064116	-1.70493255822981
H	0.36435626740824	0.70751884057105	-0.40914881547324
H	2.72152173980685	1.50289981516152	2.21905679621848
P	7.23129372702742	0.58670560754539	0.22214101631096
P	4.55784810420592	-0.38260342904176	-0.30988831320128
C	2.33596696123415	0.48106480099930	2.22410501193292
Si	2.42811498512531	-0.29885069111586	0.52488983724384
H	1.29236120083102	0.51412557799601	2.55164245033094
P	5.68723751237105	-0.20739785982348	1.59010784589570
H	2.90395935766787	-0.08961000730645	2.96184139407352
C	1.81822306163252	-2.06845147414236	0.58891405261393
H	1.86435931048357	-2.53644237214456	-0.39730456909300
H	0.78024959314093	-2.10508457569791	0.93176399347354
H	2.42242853207219	-2.66773520507423	1.27411865095924
H	6.17008741009510	3.38899185956549	4.89365058507193
H	7.57656389432358	5.26897175153512	2.71809265822366
H	9.31947205848223	3.56084754252580	4.76083998657407
C	6.20948089969268	2.58988308109948	4.14418273431479
C	7.58993419436337	4.40128785862589	2.04912459921795
C	9.29818664978982	2.74809728620655	4.02578344267518
Si	7.70567293573662	2.80847091729087	3.03321330045283
H	10.17178029613813	2.85788197386182	3.37948529956272
H	5.28669145814389	2.61892456426778	3.56161394670775
H	6.67675184458759	4.42334186137115	1.45008345834602
H	8.44100918080324	4.51033654357462	1.37319287737545
H	6.24348301988100	1.63349018813402	4.66993747500349
H	9.39315004821745	1.80418652680018	4.56672910774082
H	7.80266746923170	1.42645013361575	1.34539334969225

[Si]P$_4$H
E= -1774.58612818 Eh
0 1

P	2.34160725142255	-0.26015142346776	2.22923655084666
P	4.67547418971061	0.80810515159025	3.50735562410747
P	2.57584724317160	0.70686302135387	4.20876956630948
P	3.03865988421143	1.83428241275955	2.42393381692182
Si	0.10626585786440	0.10933683803006	1.92450299394151
C	-0.45041090319057	1.79363722083104	2.51817962649802
C	-0.77944640028840	-1.23813433873107	2.87609299102146
C	-0.19647533154646	-0.07172476442247	0.08538540143955
H	-0.21863712782384	1.94814933742902	3.57412194755100
H	-1.53435347360124	1.87900689486086	2.39394772161822
H	0.01920275572997	2.59825637155943	1.94849654654072
H	0.33243725914831	0.70070708103751	-0.47772598479367
H	-1.26343848267232	0.01693208127468	-0.13853387173446
H	0.14394225102503	-1.04493569207092	-0.27625274639312
H	-0.59992800326494	-1.13903226224294	3.94918743423886
H	-0.44334683818464	-2.23072034223980	2.56755911008737
H	-1.85852546944850	-1.17850552334198	2.70670624120257
H	5.03445533773700	1.93913793579068	4.31110703059651

TS([Si]P$_4$$^{\bullet}$→[Si]P$_8$$^{\bullet}$)
E= -3138.99921989 Eh
im. freq. = 101.26 *i*
0 2

P	6.80930377065385	1.31257592157288	3.97650312244923
P	7.58148297273131	3.23878324693308	5.06573963322217
P	6.57453563818840	1.60792622097576	6.12593314380650
P	5.45142484967171	2.85191127235550	4.73130573080480
H	0.39469323040173	-0.18143663740558	0.56769085214903
P	3.70432564299016	0.51068575614294	2.48605309822503
C	-0.21047792634541	-0.68460084278552	1.32519659425797
H	1.03213929355579	2.05778989538455	2.63848419472026
H	-1.24202384960440	-0.33490930682332	1.22362864293390
H	-0.19534287549680	-1.75629529070821	1.11343749462599
P	5.24411332885430	-0.61815003062887	3.57819949468350
P	2.53061970644032	-1.25348673862987	3.12828395731171
C	0.43405488835684	1.51646546580289	3.37449297677182
Si	0.43176079306204	-0.32504733803216	3.04651373989537
H	-0.59233918735693	1.89212857896968	3.31715671746463
P	3.45057248842806	0.12892113693711	4.60403926202759
H	0.82442533892916	1.75349680539972	4.36632367083483
C	-0.58585641784556	-1.22514254059766	4.33449897371637
H	-1.62575210341447	-0.88697973447153	4.30247023004516
H	-0.57722206477507	-2.30398366168832	4.16315160451386
H	-0.20127751742521	-1.03943217870310	5.33997686553992

[Si]P$_8$$^{\bullet}$
E= -3138.99919594 Eh
0 2

P	6.77027283155221	1.04974892229513	3.82668057190752
P	7.51090745474446	3.45862374009500	4.95528289769527
P	6.50554709174998	1.76314066105081	5.90104793902137
P	5.53165674734286	2.83346854494524	4.26302514278594
H	0.61662664890327	-0.02195070932587	0.67430379695746
P	3.71442836007537	0.31026000653690	2.48370763597252
C	-0.04709260996760	-0.58251204792616	1.33660665746047
H	1.14424278198834	2.04932681993334	2.96390790671796
H	-1.06991566222461	-0.23407077212283	1.16600643453481
H	0.00194148537523	-1.63610446168719	1.05231969895078
P	5.25129763455232	-0.64444229818586	3.75200124017370
P	2.49608893259533	-1.30640309172119	3.37405978315460
C	0.42376815087547	1.48520820304494	3.56009919945864
Si	0.43342710187942	-0.33525680302538	3.12940222397278
H	-0.57170680933178	1.89498808805727	3.36251264897932
P	3.44134907416976	0.26352114068074	4.63265001756066
H	0.65303374410620	1.65297473603823	4.61445933207992
C	-0.71210869741062	-1.28743409539801	4.26363999847774
H	-1.73663011623462	-0.91527954756804	4.17291911999094
H	-0.71684815688385	-2.35163904874104	4.01680660099509
H	-0.40712598785745	-1.18494798697608	5.30764115315196

5.5 References

[1] D. E. C. Corbridge, *Phosphorus. Chemistry, Biochemistry and Technology*, Elsevier, **2000**.

[2] J. Svara, N. Weferling, T. Hofmann, *Ullmann's Encycl. Ind. Chem.* **2012**, *27*, 20–50.

[3] H. Diskowski, T. Hofmann, *Ullmann's Encycl. Ind. Chem.* **2012**, *26*, 725–746.

[4] N. Weferling, S. M. Zhang, C. H. Chiang, *Procedia Eng.* **2016**, *138*, 291–301.

[5] G. Bettermann, W. Krause, G. Riess, T. Hofmann, *Ullmann's Encycl. Ind. Chem.* **2012**, *27*, 1–18.

[6] A. R. Jupp, S. Beijer, G. C. Narain, W. Schipper, J. C. Slootweg, *Chem. Soc. Rev.* **2021**, *50*, 87–101.

[7] J. E. Borger, A. W. Ehlers, J. C. Slootweg, K. Lammertsma, *Chem. Eur. J.* **2017**, 11738–11746.

[8] N. K. Gusarova, B. A. Trofimov, *Russ. Chem. Rev.* **2020**, *89*, 225–249.

[9] B. M. Cossairt, N. A. Piro, C. C. Cummins, *Chem. Rev.* **2010**, *110*, 4164–4177.

[10] M. Caporali, L. Gonsalvi, A. Rossin, M. Peruzzini, *Chem. Rev.* **2010**, *110*, 4178–4235.

[11] M. Scheer, G. Balázs, A. Seitz, *Chem. Rev.* **2010**, *110*, 4236–4256.

[12] D. J. Scott, *Angew. Chem. Int. Ed.* **2022**, *61*, e2022050.

[13] J. Hu, W. Liu, W. X. Zhang, *Phosphorus, Sulfur Silicon Relat. Elem.* **2022**, *197*, 398–407.

[14] Y. Liu, X. Chen, B. Yu, *Chem. Eur. J.* **2023**, *29*, e202302142.

[15] U. Lennert, P. B. Arockiam, V. Streitferdt, D. J. Scott, C. Rödl, R. M. Gschwind, R. Wolf, *Nat. Catal.* **2019**, *2*, 1101–1106.

[16] P. B. Arockiam, U. Lennert, C. Graf, R. Rothfelder, D. J. Scott, T. G. Fischer, K. Zeitler, R. Wolf, *Chem. Eur. J.* **2020**, *26*, 16374–16382.

[17] Y. Mei, Z. Yan, L. L. Liu, *J. Am. Chem. Soc.* **2022**, *144*, 1517–1522.

[18] M. Donath, K. Schwedtmann, T. Schneider, F. Hennersdorf, A. Bauzá, A. Frontera, J. J. Weigand, *Nat. Chem.* **2022**, *14*, 384–391.

[19] D. J. Scott, J. Cammarata, M. Schimpf, R. Wolf, *Nat. Chem.* **2021**, *13*, 458–464.

[20] J. Cammarata, D. J. Scott, R. Wolf, *Chem. Eur. J.* **2022**, *28*, e2022024.

[21] P. A. Baguley, J. C. Walton, *Angew. Chem. Int. Ed.* **1998**, *37*, 3072–3082.

[22] B. C. Gilbert, A. F. Parsons, *J. Chem. Soc. Perkin Trans.* **2002**, *2*, 367–387.

[23] W. R. Bowman, S. L. Krintel, M. B. Schilling, *Org. Biomol. Chem.* **2004**, *2*, 585–592.

[24] C. Chatgilialoglu, *Chem. Eur. J.* **2008**, *14*, 2310–2320.

[25] C. Chatgilialoglu, M. Newcomb, *Adv. Organomet. Chem.* **1999**, *44*, 67–112.

[26] C. Chatgilialoglu, M. Ballestri, *Organometallics* **1999**, *18*, 2395–2397.

[27] C. Chatgilialoglu, *Chem. Rev.* **1995**, *95*, 1229–1251.

[28] For comparison of the E–H bond strength and the rate constants for H-abstraction with carbon-centred radicals (e.g. alkyl radicals) from R_3EH (E = Si, Ge, Sn), see refs: 22, 25, 27 and 28.

[29] H. Yorimitsu, K. Oshima, *Inorg. Chem. Commun.* **2005**, *8*, 131–142.

[30] Analogous resonances were also observed in the reaction with Bu_3GeH under these conditions, although with lower conversions. For full details see section 5.4.2.1.

[31] D. M. Schubert, A. D. Norman, *Inorg. Chem.* **1985**, *24*, 1107–1109.

[32] J. Escudié, C. Couret, *J. Satgé, Recl. des Trav. Chim. des Pays-Bas.* **1979**, *98*, 461–466.

[33] Similar side/decomposition products have been observed in our previous study of the P_4 hydrostannylation system, in the form of $R_3SnP(H)R$, though in much smaller amounts.

[34]. During the optimisation of the reaction, no signals corresponding to soluble polyphosphorus intermediates were observed in the $^{31}P\{^{1}H\}$ NMR spectra.

[35] Proof-of-concept results have also been achieved using chemical radical initators such as AIBN instead of LED irradiation. However, for these systems we have thus far only been able to achieve low conversions (<28 % **1** and **2**). For full details see section 5.4.2.5.

[36] Irradiation with LED light is proposed to induce the formation of an initial $R_3Ge^{\bullet}$ or $R_3Si^{\bullet}$ radical which initiates the chain reaction. However, the precise details of this initiation are currently unclear and remain under investigation.

[37] C. Chatgilialoglu, *Organosilanes in Radical Chemistry*, John Wiley & Sons Ltd, **2004**.

[38] C. Chatgilialoglu, J. Lalevée, *Molecules* **2012**, *17*, 527–555.

[39] H. S. Dang, B. P. Roberts, *Tetrahedron Lett.* **1995**, *36*, 2875–2878.

[40] B. P. Roberts, *Chem. Soc. Rev.* **1999**, *28*, 25–35.

[41] V. Cappello, J. Baumgartner, A. Dransfeld, K. Hassler, *Eur. J. Inorg. Chem.* **2006**, 4589–4599.

[42] K. X. Bhattacharyya, S. Dreyfuss, N. Saffon-Merceron, N. Mézailles, *Chem. Commun.* **2016**, *52*, 5179–5182.

[43] I. Chatterjee, M. Oestreich, *Angew. Chem. Int. Ed.* **2015**, *54*, 1965–1968.

[44] H. Bauer, K. Thum, M. Alonso, C. Fischer, S. Harder, *Angew. Chem. Int. Ed.* **2019**, *58*, 4248–4253.

[45] F. Neese, F. Wennmohs, U. Becker, C. Riplinger, *J. Chem. Phys.* **2020**, *152*, 224108.

[46] F. Neese, *Wiley Interdiscip. Rev. Comput. Mol. Sci.* **2018**, *8*, e1327.

[47] R. A. Kendall, H. A. Früchtl, *Theor. Chem. Acc.* **1997**, *97*, 158–163.

[48] F. Neese, F. Wennmohs, A. Hansen, U. Becker, *Chem. Phys.* **2009**, *356*, 98–109.

[49] S. Grimme, J. Antony, S. Ehrlich, H. Krieg, *J. Chem. Phys.* **2010**, *132*, 154104.

[50] S. Grimme, S. Ehrlich and L. Goerigk, *J. Comput. Chem.* **2011**, *32*, 1456–1465.

[51] *Avogadro Chemistry*, **2016**, http://avogadro.cc/.

[52] G. M. Sheldrick, SADABS, Bruker AXS, Madison, USA **2007**.

[53] SCALE3ABS, CrysAlisPro, Aglient Technologies Inc. Oxford, GB **2015**.

[54] O. V. Dolomanov, L. J. Bourhis, R. J. Gildea, J. A. Howard, H. Puschmann, *J. Appl. Cryst.* **2009**, *42*, 339–341.

[55] G. M. Sheldrick, *Acta Cryst. A*, **2015**, *71*, 3–8.

[56] G. M. Sheldrick, *Acta Cryst. C*, **2015**, *71*, 3–8.

[57] T. M. Horsley-Downie, M. F. Mahon, J. P. Lowe, R. M. Bailey, D. J. Liptrot, *ACS Catal.* **2022**, *12*, 8214–8219

[58] G. Becker, M. Roessler, W. Uhl, *ZAAC*, **1981**, *473*, 7–19.

6 Summary and Conclusion

Chapter 1. *Organofunctionalisation of Elemental Phosphorus: Recent Advances in Direct and Catalytic P–C Bond Formation*

Organophosphorus compounds are of enormous industrial and academic interest due to their wide range of applications, including pharmaceuticals, agrochemicals, photoinitiators, flame retardants, ligands for catalysis, and many others. In essentially all cases, these compounds are ultimately prepared using white phosphorus (P_4) as their common P atom source. However, current industrial production relies on wasteful multi-step processes, that involve the use of hazardous, toxic and/or corrosive reactants and intermediates. Consequently, dedicated academic efforts have been made to develop strategies that could overcome such limitations.

Chapter 1 provides an overview of key recent academic reports on the organofunctionalisation of P_4, highlighting direct transformations into monophosphorus compounds, and approaches that could facilitate the preparation of these compounds in a 'one-pot' manner. This introductory chapter describes alternative methodologies for the preparation of P_1 compounds, including the direct nucleophilic functionalisation of P_4, electrochemical approaches, and transition-metal-mediated transformations. Of particular relevance to this thesis is the radical-mediated degradation of P_4, which has emerged as a promising avenue for the preparation of organophosphorus compounds. Unfortunately, these systems have previously required elaborate strategies involving highly complex mechanisms to access the necessary radical intermediates, thereby restricting their practicality and potential scope of implementation. These limitations provided the central motivation for the development of efficient methods for the preparation of P_1 compounds directly from elemental phosphorus, *via* the radical-mediated hydroelementation reactions described in this thesis.

Chapter 2. *Synthesis of Monophosphines Directly from White Phosphorus*

This chapter describes the simple and effective 'one-pot' synthesis of a wide range of organic and inorganic monophosphorus compounds directly from P_4, mediated by the triorganotin(IV) moiety Bu_3Sn^+. Remarkably, the efficient degradation of P_4 was achieved using the inexpensive, classical radical reagent tri-*n*-butyltin hydride (Bu_3SnH), in a mild and versatile process compatible with either photoinitiation or common chemical radical initiators, resulting in the formation of stannyl-substituted monophosphines $(Bu_3Sn)_xPH_{3-x}$ (x = 0–3). Significantly, it was demonstrated that the crude hydrostannylphosphine mixture could serve as a "P^{3-}" synthon, which can be treated with various electrophiles to directly afford industrially relevant monophosphorus compounds in a 'one-pot' fashion. This transformation allowed the synthesis of valuable monophosphorus products, including acyl phosphines, alkyl phosphonium salts, and

hydroxymethyl phosphines, among others, in good to excellent isolated yields directly from P_4. Furthermore, simple procedures were developed for the closed-loop recycling and ultimately even catalytic use of the key Bu_3Sn moiety, thus minimising the formation of stoichiometric Sn-containing waste (Scheme 1). The conceptual simplicity of this radical-mediated method would permit later extrapolation to other radical sources, including those based on other p-block elements, as discussed in Chapter 5.

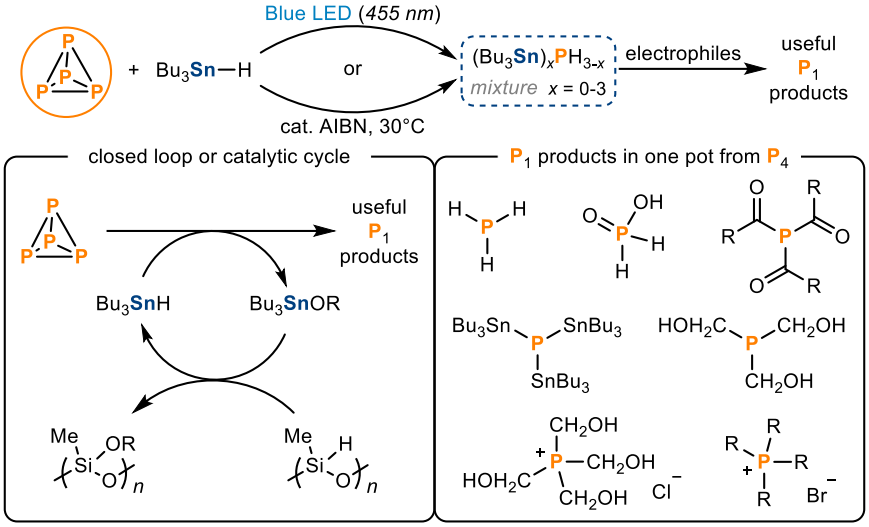

Scheme 13. 'One-pot' hydrostannylation and subsequent electrophilic functionalisation of P_4.

Chapter 3. *Hydrostannylation of Red Phosphorus: A Convenient Route to Monophosphines*

Although P_4 remains as the principal industrial precursor for the preparation of organophosphorus compounds, in most other contexts its notoriously pyrophoric character and significant toxicity render it highly undesirable. An alternative P atom source for academic and other laboratory-scale chemistry would be the bench-stable allotrope *red* phosphorus (P_{red}).

Chapter 3 describes the preparation of a variety of monophosphorus compounds directly from P_{red} (Scheme 2), following a methodology largely inspired by the direct and simple hydrostannylation of P_4 (Chapter 2). Notably, despite the relative inertness of P_{red}, these transformations can be achieved without the need for especially powerful or elaborate reagents, or extremely rigorous inert atmosphere techniques, making it an unusually accessible approach for the preparation of P_1 compounds from elemental phosphorus in a typical laboratory setting. In this regard, the fully stannylated phosphine $(Bu_3Sn)_3P$, accessible directly from P_{red}, proved to be an attractive intermediate for the preparation of P_1 compounds, as an alternative to the more complex, PH_3-containing mixture $(Bu_3Sn)_xPH_{3-x}$ (x = 0–3).

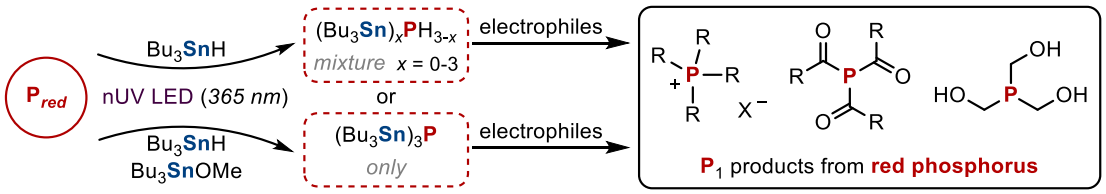

Scheme 14. (Hydro)stannylation and subsequent electrophilic functionalisation of red phosphorus (P_{red}).

Chapter 4. *Unravelling White Phosphorus: Experimental and Computational Studies Reveal the Mechanisms of P_4 Hydrostannylation*

While the scope and practicality of the hydrostannylation of P_4 as a viable route for the preparation of monophosphorus compounds have been established (Chapter 2), many aspects of its radical-mediated mechanism remained unclear.

Chapter 4 provides comprehensive mechanistic insights into the hydrostannylation of P_4, obtained through a cooperative effort that combined DFT calculations and *in situ* ^{31}P NMR reaction monitoring, including the kinetic trapping of previously unobservable intermediates with bulky tin hydrides (Scheme 3). Notably, the studies showed a sequence of elementary bond cleavage steps through which the breakdown of the P_4 tetrahedron can occur. However, it was also demonstrated that numerous competing pathways are available, all of which ultimately lead to the same set of products $(R_3Sn)_xPH_{3-x}$. Additionally, while in principle each P–P bond cleavage represents a distinct mechanistic step, the studies suggest that these steps are mechanistically and energetically analogous, characterised by a common sequence of $R_3Sn^{\bullet}$ radical attack and H atom transfer, all with similar activation barriers (Scheme 3). These results provide useful guidelines to aid in the development of future P_4 functionalisation reactions.

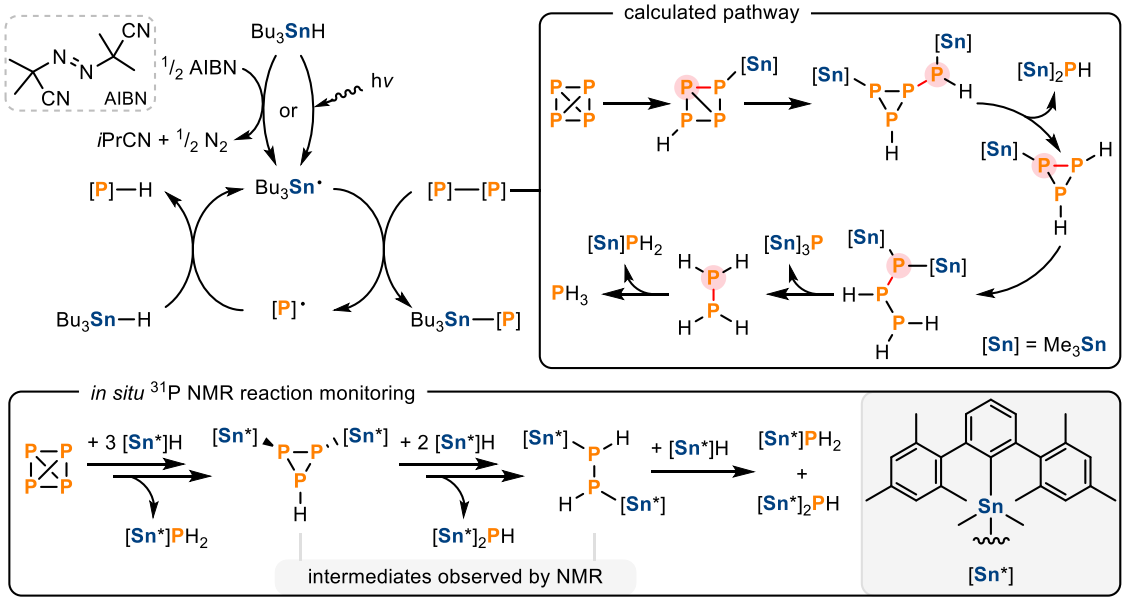

Scheme 15. Mechanistic insights into the hydrostannylation of P_4, obtained from DFT calculations and *in situ* ^{31}P NMR reaction monitoring.

Chapter 5. *Hydrosilylation and Hydrogermylation of White Phosphorus*

Previous chapters have focused on the reactivity of the readily available classical reducing agent Bu_3SnH for the radical-mediated degradation of P_4 (Chapter 2) and P_{red} (Chapter 3), and demonstrated the practical and conceptual simplicity of this method for the preparation of monophosphorus compounds. However, the toxicity of the organotin derivatives represents a significant limitation.

Chapter 5 describes experimental and computational studies of the reactivity of lighter and less toxic hydrogermane and hydrosilane homologues of organotin hydrides (R_3EH, E = Ge or Si) towards P_4. Gratifyingly, although marked reactivity differences were observed, related to the differing E–H bond strengths, the hydroelementation of P_4 was successfully achieved with both families of the lighter homologues (R_3EH, E = Ge or Si) upon optimisation. Additionally, these new hydroelementation reactions yield analogous Ge- or Si-substituted monophosphine mixtures ($(R_3E)_nPH_{3-n}$) that can also be converted into useful P_1 products upon reaction with electrophiles in a comparable, direct, 'one-pot' manner. The outcomes of this study demonstrate the broader applicability of this radical-mediated methodology for the functionalisation of P_4, extending beyond organotin derivatives.

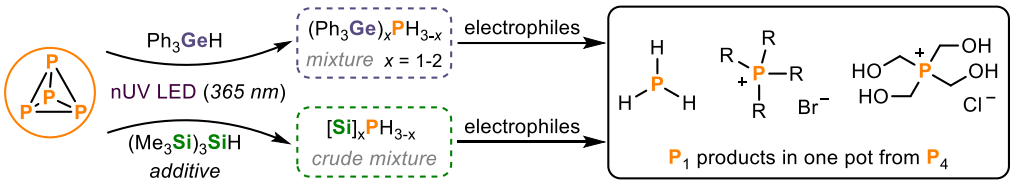

Scheme 16. Hydroelemention of P_4 with lighter main group hydrides and subsequent functionalisation into P_1 compounds.

Conclusion

This doctoral thesis highlights the potential of the radical-mediated functionalisation of P_4 as a direct and simple approach for the synthesis of industrially relevant monophosphorus compounds. Particularly, it was demonstrated that hydroelementation reactions can be employed as a viable method for the efficient degradation of P_4 into P_1 intermediates that can undergo subsequent transformation to furnish desirable monophosphorus compounds. Although this methodology remains at a proof-of-principle stage and the replacement of current industrial procedures is still a distant goal, the results discussed here represent a significant step forward in the development of new direct and even catalytic methods for the efficient functionalisation of P_4. Future investigations could extend the scope of this strategy, exploring the reactivity of a broader range of radical precursors, with the aim of identifying more efficient transformations. Furthermore, particular attention should be directed towards the development of more reliable catalytic P_4 functionalisation procedures, which remain exceedingly rare to date. In addition, new procedures should also target closed-loop strategies that could avoid the generation of stoichiometric waste.

7 Acknowledgements

This work was only possible thanks to the support of numerous people.
Firstly, I would like to thank Prof. Dr. Robert Wolf for his supervision and guidance over the last few years and for giving me the wonderful opportunity to work on and develop these exciting projects. Thank you for all your support.

I would like to thank Prof. Dr. Manfred Scheer (second examiner), Prof. Dr. Frank-Michael Matysik (third examiner) and Prof. Dr. Marcel Schorpp (chairman) for their willingness to be part of the examination board.

My special thanks to Dr. Daniel J. Scott, for not only being an excellent supervisor, who supported me in all aspects of this thesis, but also a great friend throughout this journey. Thanks a lot Dan, you are the best!

In addition, many collaborators have made important contributions to this work. Many thanks to Dr. Peter Coburger (TU München), Franz F. Westermair, Prof. Dr. Ruth M. Gschwind (Universität Regensburg), Daniel Duvinage, Marvin Janssen and Prof. Dr. Jens Beckmann (Universität Bremen) for their valuable contributions, their high level of commitment and the interesting discussions.

I would also like to thank the staff of the central analytics and workshops for their support over the years, in particular Tuan Anh Nguyen, Annette Schramm, Fritz Kastner, Veronika Scheidler and Dr. Ilya Shenderovich (NMR department), Josef Kiermaier and Wolfgang Söllner (Mass spectrometry department), Sabine Stempfhuber, Birgit Hischa and Florian Meurer (X-ray structure analysis), Barbara Baumann and Helmut Schüller (elemental analysis), Markus Lindner, Carl-Heinz Hierl, Helena Ackermann (glass blowing), Peter Fuchs and Andreas Gruber (electronics workshop).

In addition, I would like to thank all the former and current members of the Wolf's group for creating such a great work environment, making this a rather enjoyable journey. Specially, I would like to thank my lab-mates from Lab 25/04, it was always a pleasure come to work and have you there to have fruitful discussions, watching cool videos, listening to good music, dancing and laughing.

Many thanks to my boys! Martin, John and Felix, for being such amazing friends, for all the laughs, the weird questions, the debates, the support, the drinks, the games, the hugs, the good times.

Ahora quiero agradecer a la familia que me regaló Regensburg. Jose, Erika, Jeimy, Karol y Jhoa :) Muchísimas gracias por acogerme y apoyarme en absolutamente todo. Gracias por siempre tanto cariño, por los rones, las comidas, los bailes y las risas. Soy afortunado de haberlos conocido. Especialmente a los amigos/hermanos/padres/familia que Regensburg me dio, Jose y Erika. Gracias por escucharme y entenderme.

Así mismo, a mi amigo y hermano José Miguel. No solo por mostrarme el video que me hizo venir a Alemania xD también por literalmente acompañarme en esta aventura, siendo un apoyo incondicional. Muchas gracias bro, por supuesto que lo vamos a lograr.

Me gustaría también agradecer a mi hermanita querida María Angélica, por siempre traer luz y felicidad a mi vida. Me inspiras y das fuerza para seguir, te quierocito. También un agradecimiento especial a mi tía Zule. Gracias tía, eres la mejón :)

A mi hermano Gaspar, por ser un ejemplo de esfuerzo y dedicación, y por hacer el camino más fácil para mí.

A mis abuelos por tanto amor y cariño, esto es para ustedes.

Y bueno, a mis queridos padres, Judith del Carmen y Rosario (pelao), siempre gracias :D Soy lo que soy por y para ustedes, y me encanta. Que lujo tenerlos como padres, y poder compartir esta etapa tan especial en mi vida con ustedes, así como todas las demás. Gracias papi por tu ejemplo, esfuerzo, apoyo y por tu amor incondicional. Gracias mami, por ser tan especial, alegre, amable, cariñosa, por enseñarme tanto. Gracias a ambos por enseñarme tanto. Me inspiran cada día. ¡Los amo!

Finally, I would like to thank my amazing partner. Thank you for making all my days lovely ones. Thank you so much for all your support and all the beautiful moments along this journey. I look forward to many more of those. Thank you my love ♥ you are the best!

8 Curriculum Vitae

Education

Since 06/2020	Ph.D. student in the group of Prof. Dr. Robert Wolf University of Regensburg – Regensburg, Germany.
10/2017 – 04/2020	M.Sc. "Advanced Synthesis and Catalysis" within the Elite Network of Bavaria, University of Regensburg – Regensburg, Germany.
10/2010 – 12/2016	B.Sc. in Chemistry – *Cum Laude* Distinction. University of Los Andes (ULA) – Mérida, Venezuela.

Training

06/2022 – 09/2022	**Research stay** - University of Oxford – Oxford, United Kingdoms. Supervisor: Dr. Daniel J. Scott.
09/2018 - 10/2018	**External module, Internship -** Max-Planck-Institut für Kohlenforschung (MPI KOFO) – Mülheim an der Ruhr, Germany. Supervisor: Dr. Josep Cornella.
08/2015 - 12/2016	**Assistant Student** - Venezuelan Institute of Scientific Research (IVIC). Supervisors: Dr. Yomaira Otero and Dr. Juan Garcia.
07/2014 - 08/2014	**Visiting Student** - Venezuelan Institute of Scientific Research (IVIC). Supervisor: Dr. Yomaira Otero.

Recognitions

09/2023	Poster prize at the GDCh Science Forum of Chemistry 2023 (WiFo 2023) – Leipzig, Germany.
12/2016	*Cum Laude* Distinction. University of Los Andes – Mérida, Venezuela.
2010 - 2015	Recognitions granted by the Science Faculty of the University of Los Andes – Mérida, Venezuela. For having occupied the top places among the best students of the Chemistry Career during seven lecture periods.
11/2011	Recognition granted by the Directorate of Student Affairs "DAES" at the University of Los Andes, for excellent academic performance in the semester A-2011 in the career of Chemistry – Mérida, Venezuela.
11/2011	Order "Luis María Ribas Dávila" for having obtained the highest academic performance of the Chemistry School, Sciences Faculty. Awarded by the University of Los Andes – Mérida, Venezuela.

Conference Contributions

09/2023	**Poster presentation** at the GDCh Science Forum of Chemistry 2023 (WiFo 2023) – Leipzig, Germany.
04/2023	**Poster presentation** at the Europe Workshop on Phosphorus Chemistry (EWPC) – San Sebastian, Spain.
03/2023	**Oral presentation** at the International Conference on Phosphorus, Boron and Silicon (PBSi 2023) – Berlin, Germany.
09/2022	**Oral presentation** at the Europe Workshop on Phosphorus Chemistry (EWPC) – Rostock, Germany.
07/2021	**Online poster presentation** at the 23rd Iinternational Conference on Phosphorus Chemistry (ICPC23).
05/2021	**Online poster presentation** at the Online Workshop on Phosphorus Chemistry (OWPC).
09/2020	**Online poster presentation** at the Online-Vortragstagung für Anorganische Chemie der Fachgruppen Wöhler-Vereinigung und Festkörperchemie & Materialforschung. German Chemical Society (GDCh).

Skills

- Synthesis under inert gas (Schlenk and glovebox techniques).
- Analytical techniques, such as heteronuclear NMR and IR.
- Quantum Chemical Calculations (DFT).
- Oral and written scientific communication.
- Supervision of research projects (bachelor's and master's theses).

Languages

Spanish (native speaker, C2), **English** (fluent, C1), **German** (basic, A2).

Hobbies

Softball, swimming, cooking.

9 List of Publications

7) J. Cammarata, F. F. Westermair, P. Coburger, D. Duvinage, M. Janssen, M. K. Uttendorfer, J. Beckmann, R. M. Gschwind, R. Wolf, and D. J. Scott, "Unravelling White Phosphorus: Experimental and Computational Studies Reveal the Mechanisms of P_4 Hydrostannylation", *Angew. Chem. Int. Ed.* **2024**, e202408423.

6) J. Cammarata, D. J. Scott and R. Wolf, "Hydrostannylation of Red Phosphorus: A Convenient Route to Monophosphines", *Chem. Eur. J.* **2022**, *28*, e202202456.

5) M. Till, J. Cammarata, R. Wolf, D. J. Scott, "Photocatalytic Stannylation of White Phosphorus", *Chem. Commun.* **2022**, *58*, 8986–8989.

4) R. Rothfelder, V. Streitferdt, U. Lennert, J. Cammarata, D. J. Scott, K. Zeitler, R. M. Gschwind, R. Wolf, "Photocatalytic Arylation of P_4 and PH_3: Reaction Development Through Mechanistic Insight", *Angew. Chem. Int. Ed*. **2021**, *60*, 24650–24658.

3) D. J. Scott, J. Cammarata, M. Schimpf, R. Wolf, "Synthesis of monophosphines directly from white phosphorus", *Nat. Chem*. **2021**, *13*, 458–464.

2) Y. Ma, J. Cammarata, J. Cornella, "Ni-Catalyzed Reductive Liebeskind–Srogl Alkylation of Heterocycles", *J. Am. Chem. Soc.* **2019**, *141*, 1918–1922.

1) J. Cammarata, R. Rivera, F. Fuentes, Y. Otero, E. Ocando, A. Arce, J. M. Garcia, "Single and double A^3-coupling (aldehyde-amine-alkyne) reaction catalyzed by an air stable copper(I)-phosphole complex", *Tetrahedron Lett.* **2017**, *58*, 4078–4081.

Eidesstattliche Erklärung

Ich erkläre hiermit an Eides statt, dass ich die vorliegende Arbeit ohne unzulässige Hilfe Dritter und ohne Benutzung anderer als der angegebenen Hilfsmittel angefertigt habe; die aus anderen Quellen direkt oder indirekt übernommenen Daten und Konzepte sind unter Angabe des Literaturzitats gekennzeichnet. Die Arbeit wurde bisher weder im In- noch im Ausland in gleicher oder ähnlicher Form einer anderen Prüfungsbehörde vorgelegt.

Jose Ricardo Cammarata Paredes